

**Copyright by**  
**Neil Adam Smith**  
**2011**

The Dissertation Committee for Neil Adam Smith certifies that this is the approved  
version of the following dissertation:

**Systematics and evolution of extinct and extant Pan-Alcidae  
(Aves, Charadriiformes): combined phylogenetic analyses, divergence estimation,  
and paleoclimatic interactions.**

Committee:

---

Julia A. Clarke, Supervisor

---

Christopher J. Bell

---

David C. Cannatella

---

Timothy B. Rowe

---

James Sprinkle

**Systematics and evolution of extinct and extant Pan-Alcidae  
(Aves, Charadriiformes): combined phylogenetic analyses, divergence estimation,  
and paleoclimatic interactions.**

**by**

**Neil Adam Smith B.S.**

**Dissertation**

Presented to the Faculty of the Graduate School of

The University of Texas at Austin

in Partial Fulfillment

of the Requirements

for the Degree of

**Doctor of Philosophy**

The University of Texas at Austin

August, 2011

To my mother who has always provided loving support in every aspect of my life, my father who inspired my lifelong passion and respect for the natural world, and to my wife who has assisted me in every aspect of achieving this goal.



## **Acknowledgments**

Special thanks to my advisor Julia A. Clarke for providing me with the opportunity to pursue graduate work and for skillfully guiding me through this process. I am also very grateful for the guidance provided by my committee members at UT, Christopher J. Bell, David C. Cannatella, Timothy Rowe, and James Sprinkle. I also thank my former committee members at NCSU, Lonnie Leithold, Mary Schweitzer, and Brian Wiegmann, for their guidance during the early stages of my graduate experience.

I thank my undergraduate advisor Frederick Siewers for his creative teaching and mentoring that inspired me to pursue graduate work in a field I am passionate about.

I thank Vince Schneider, Paul Brinkman and Becky Desjardins at the North Carolina Museum of Natural Sciences for providing me with beneficial field and preparation experiences.

I thank Paul Brinkman, Matt Brown, Maggie Carrino, Robert Chandler, Sandra Chapman, Terry Chesser, Joel Cracraft, James Dean, Becky Desjardins, Tom Deméré, Mark Florence, Leah Fuller, Gary Graves, John Gerwin, Ned Gilmore, Mark Goodwin, Pat Holroyd, Richard Hulbert, Makoto Manabe, Marcial de la Cruz Martín, Hiroshige Matsuoka, Sam McLeod, C. Mourer-Chauviré, Lyn Murray, Storrs Olson, Kesler Randall, Chisako Sakata, Vince Schneider, John Stewart, and Howell Thomas for collections assistance, access to specimens, specimen preparation, and for providing photographs of specimens.

I thank Dave and Tammy Abbott, Heather Ahrens, Anna Behrensmeyer, Matt

Bertone, Robert Boessenecker, David Bohaska, Clint Boyd, Marty Buzas, Kerin Claeson, Tim Cleland, Matt Colbert, Alma Colmenero, Katie Criswell, Aj DeBee, Eric Eckdale, Drew Eddy, Alexei Drummond, Nancy Elder, Rania Eldham, Steve Emslie, John Everette, Christian George, Kaitlyn Gray, Jeremy Greene, Kim Greene, Lee-Ann Hayek, Ron Ison, Helen James, Liz Johnson, Rich Ketcham, Mary Martha Kidd, Daniel Ksepka, Dan Lawver, Zhiheng Li, Ernie Lundelius, Jessie Maisano, Gerald Mayr, Kevin Middleton, Carl Mehling, Cecile Mourer-Chauvire, Paul Murdoch, Sterling Nesbitt, Mark Norell, Jen Olori, Rich Olsen, Curtis Ormond, George Powell Jr., Doug Pratt, Bob Purdy, Charlie Rankin, Clayton Ray, Dale Russell, The Samples, Antonio Sanchez-Marco, Brian Schmidt, Paul Scofield, Jake Smith, Scott Snyder, Tom Stidham, Michelle Stocker, J. Thorne, Chris Torres, Takanobu Tsuihji, Erik Wijnker, Kyle Womack, Pat Young, and Dick Zusi for productive conversations and/or other assistance with this project.

I thank Carlo Rosales Fernandez, Tom Hess, Gary Howell, Effie Jarrett, David Spindler, and Scott Wall for technical assistance, and I thank the JGB staff, MEAS staff, NSCM staff, UT library staff, NCSU library staff, and all of the other people I have forgotten to include.

I gratefully acknowledge financial support from The Ernest L. and Judith W. Lundelius Scholarship in Vertebrate Paleontology; The Francis L. Whitney Endowed Presidential Scholarship; The Frank M. Chapman Memorial Fund, Section of Ornithology, American Museum of Natural History; The Geological Society of America; The Jackson School of Geosciences, The University of Texas at Austin; The National Science Foundation; The North Carolina Fossil Club; North Carolina State University

Department of Marine Earth and Atmospheric Sciences; The Smithsonian Institution Office of Fellowships; and The Society of Vertebrate Paleontology. This project was also funded in part by NSF Grant DEB 0949897 to J. A. Clarke "Collaborative Research: Wings to Flippers - Phylogenetics, character acquisition, and feather biomechanics in the evolution of wing-propelled diving".

## **Preface**

This dissertation combines a variety of data and analytical methods to explore the systematics, evolution, and biogeography of Pan-Alcidae (Aves, Charadriiformes).

Because each of the chapters following the introduction are formatted to be published as independent works, there is some repetition with respect to introductory statements and materials and methods sections. Although figures and tables are imbedded throughout the text of the dissertation, the reader is frequently referred to a wealth of information contained in the appendices that follow directly after the text of the final chapter.

References included in each chapter and the appendices have been combined into a single literature cited section. All photographs were taken by the author.

**Systematics and evolution of extinct and extant Pan-Alcidae  
(Aves, Charadriiformes): combined phylogenetic analyses, divergence estimation,  
and paleoclimatic interactions.**

Neil Adam Smith, Ph.D.

The University of Texas at Austin, 2011

Supervisor: Julia A. Clarke

Although the ecological interactions and ethology of the wing-propelled diving seabirds known as the Alcidae (Aves, Charadriiformes) have been intensively studied, systematic studies of the clade have been overwhelmingly limited to extant taxa. Pan-Alcidae have the richest fossil record among Charadriiformes, with specimens representing more than 35 million years of evolutionary history. Morphometric and apomorphy-based taxonomic revision of previously named extinct pan-alcids along with description of new species of extinct pan-alcids facilitated refined estimates of species richness. Combined phylogenetic analyses of morphological and molecular sequence data including pan-alcid fossils elucidated the poorly understood evolutionary history of the clade. Divergence estimation analysis for Charadriiformes placed previously hypothesized episodes of pan-alcid radiation and extinction in context with proposed paleoclimatic drivers of alcid evolution.

## TABLE OF CONTENTS

INTRODUCTION.....	1
CHAPTER 1 - Phylogeny of the extant Alcidae (Aves, Charadriiformes): comparisons of individual and combined analyses of morphological and molecular data.....	10
INTRODUCTION .....	11
<i>Previous hypotheses regarding the position of Alcidae and relationships among alcids</i> .....	12
<i>Rationale for combining data in phylogenetic analyses</i> .....	23
MATERIALS AND METHODS.....	29
<i>Institutional Abbreviations</i> .....	36
PHYLOGENETIC RESULTS.....	37
DISCUSSION.....	67
CONCLUSIONS .....	74
CHAPTER 2 - Alphataxonomic revision of <i>Alca</i> (Aves, Alcidae): a combined morphometric and phylogenetic approach.....	77
INTRODUCTION .....	78
MATERIALS AND METHODS.....	85
<i>Institutional Abbreviations</i> .....	86
<i>Comparative skeletal material used for phylogenetic analysis</i> .....	86
MORPHOMETRIC ANALYSES .....	87
PHYLOGENETIC ANALYSIS .....	92
RESULTS.....	96
MORPHOMETRIC RESULTS.....	96
PHYLOGENETIC RESULTS.....	107
SYSTEMATIC PALEONTOLOGY .....	111
DISCUSSION.....	156
CONCLUSIONS .....	166
CHAPTER 3 - The fossil record and phylogeny of the flightless Mancallinae (Charadriiformes, Pan-Alcidae).....	170
INTRODUCTION .....	171
<i>Review of the Mancallinae fossil record</i> .....	174
<i>Geologic setting</i> .....	184
MATERIALS AND METHODS.....	187

<i>Institutional abbreviations</i> .....	191
SYSTEMATIC PALEONTOLOGY .....	192
PHYLOGENETIC RESULTS .....	224
DISCUSSION .....	230
<i>Referral of fossils to species level</i> .....	233
<i>Flightlessness and convergence</i> .....	234
<i>Geological and phylogenetic context for Pan-Alcidae</i> .....	240
CONCLUSIONS .....	246
CHAPTER 4 - The fossil record and phylogeny of the puffins (Pan-Alcidae, Fraterculini)	
.....	249
INTRODUCTION .....	250
<i>Review of the Fraterculini fossil record</i> .....	252
MATERIALS AND METHODS .....	265
<i>Institutional abbreviations</i> .....	268
PHYLOGENETIC RESULTS .....	269
SYSTEMATIC PALEONTOLOGY .....	280
DISCUSSION .....	289
CONCLUSIONS .....	298
CHAPTER 5 - The fossil record and phylogeny of the auklets (Pan-Alcidae,	
Aethiini) .....	301
INTRODUCTION .....	302
<i>The fossil record of auklets</i> .....	304
MATERIALS AND METHODS .....	308
<i>Institutional abbreviations</i> .....	311
PHYLOGENETIC RESULTS .....	311
SYSTEMATIC PALEONTOLOGY .....	313
DISCUSSION .....	329
CONCLUSIONS .....	335
CHAPTER 6 - The fossil record and phylogeny of the guillemots (Pan-Alcidae,	
Cepphini) .....	339
INTRODUCTION .....	340
<i>A Review of the fossil record of guillemots</i> .....	343
MATERIALS AND METHODS .....	346
<i>Institutional abbreviations</i> .....	351
PHYLOGENETIC RESULTS .....	352
SYSTEMATIC PALEONTOLOGY .....	358
DISCUSSION .....	365

CONCLUSIONS .....	368
CHAPTER 7 - The fossil record and phylogeny of the murrelets (Pan-Alcidae, Alcinae)	
.....	373
INTRODUCTION .....	374
<i>The fossil record of murrelets</i> .....	376
MATERIALS AND METHODS.....	383
<i>Institutional abbreviations</i> .....	386
PHYLOGENETIC RESULTS.....	386
SYSTEMATIC PALEONTOLOGY .....	393
DISCUSSION .....	404
CONCLUSIONS .....	408
CHAPTER 8 - The systematics and evolution of the Pan-Alcidae (Aves, Charadriiformes) inferred through combined phylogenetic analysis and divergence estimation.....	
.....	412
INTRODUCTION .....	413
<i>Previous phylogenetic hypotheses of charadriiform relationships</i> .....	420
<i>Previous estimates of charadriiform divergence times</i> .....	421
MATERIALS AND METHODS.....	428
<i>Anatomical terminology, measurements, and taxonomy</i> .....	428
<i>Taxon and character sampling</i> .....	431
<i>Phylogeny estimation</i> .....	433
<i>Divergence time estimation</i> .....	435
<i>Charadriiformes fossil calibration</i> .....	436
<i>Institutional abbreviations</i> .....	446
RESULTS .....	446
<i>Phylogenetic results</i> .....	446
<i>Morphological character optimization</i> .....	467
<i>Divergence estimation results</i> .....	484
DISCUSSION .....	488
<i>Phylogeny of Pan-Alcidae</i> .....	488
<i>Divergence time estimates and inferred relationships between paleoclimatic events and charadriiform evolution</i> .....	494
<i>Pan-Alcidae paleodiversity</i> .....	515
<i>Pan-Alcidae origination area and dispersal</i> .....	518
<i>Potentially biasing factors in divergence time analyses</i> .....	521
<i>Limitations of current phylogenetic and divergence estimation software</i> .....	525
CONCLUSIONS .....	526



Appendix 1. Extant comparative material.....	530
Appendix 2. Morphological character list.....	536
Appendix 3. Morphological character matrix.....	602
Appendix 4. Molecular sequence authorship.....	627
Appendix 5. Extant osteological measurement data.....	630
Appendix 6. Fossil measurement data.....	646
Appendix 7. Rejected and revised charadriiform fossil calibrations.....	694
Appendix 8. Phylogenetic classification of Pan-Alcidae.....	698
Literature Cited.....	708

## List of Tables

Table 1.1- Previous analyses of extant alcid relationships.....	18
Table 1.2- Character incompleteness by taxon.....	30-31
Table 1.3- Details of sampled molecular sequences and morphological characters.....	31
Table 1.4- Summary of phylogenetic analyses, parameters, and results.....	39
Table 1.5- Apomorphies supporting clade monophyly.....	64
Table 2.1- Previously published extinct <i>Alca</i> holotype material.....	82
Table 2.2- Summary of morphometric analyses and results.....	99
Table 2.3- Comparison of size variation in alcids.....	100
Table 2.4- Measurements of <i>Alca</i> humeri (in mm).....	103
Table 2.5- Apomorphies supporting clade monophyly .....	108
Table 2.6- Measurements of associated <i>Alca</i> holotype specimens.....	136
Table 3.1- Summary of Mancallinae holotype material and taxonomic revision.....	173
Table 3.2- Measurements of Mancallinae holotype humeri.....	199
Table 3.3- Measurements of new associated Mancallinae holotype specimens.....	201
Table 3.4.- Apomorphies supporting clade monophyly .....	228
Table 4.1- Previously published specimens referred to Fraterculini.....	253
Table 4.2- Apomorphies supporting clade monophyly .....	277
Table 4.3- Measurements of puffin humeri.....	290
Table 4.4- Summary of Fraterculini taxonomic revision.....	292
Table 4.5- Geographic and temporal distribution of Fraterculini.....	294

Table 5.1- Previously published auklet fossil remains.....	306
Table 5.2- Apomorphies supporting clade monophyly .....	313
Table 5.3- Measurements of auklet humeri and <i>Bisulca demerei</i> .....	325
Table 5.4- Summary of Aethiini taxonomic revision.....	333
Table 6.1- Previously published guillemot fossil remains.....	344
Table 6.2- Apomorphies supporting clade monophyly .....	358
Table 6.3- Measurements of Cepphini humeri.....	363
Table 6.4- Summary of Cepphini taxonomic revision.....	366
Table 7.1- Previously published murrelet fossil remains.....	378
Table 7.2- Apomorphies supporting clade monophyly .....	388
Table 7.3- Summary of taxonomic revision of previously published murrelet fossil remains.....	407
Table 8.1- Age range of pan-alcid species based on published fossil material .....	417-418
Table 8.2- Cenozoic fossil pan-alcid species based on taxonomic revisions .....	420
Table 8.3- Previous estimates of the basal divergence among crown Charadriiformes..	423
Table 8.4- Critique of calibrations used by Baker et al. (2007).....	429
Table 8.5- Critique of calibrations used by Pereira and Baker (2008).....	430
Table 8.6- Fossil calibrations used in the divergence time analysis.....	438
Table 8.7- Apomorphies supporting taxonomic referrals of fossil used as calibrations for divergence estimation.....	451
Table 8.8- Morphological apomorphies with a CI = 1.0 supporting clade monophyly in the resultant phylogenetic tree.....	458

Table 8.9- Mass, dive depth, and feeding ecology of extant charadriiforms.....	478-479
Table 8.10- Estimated divergence times, 95% posterior density, prior ages based on fossil data, and posterior probabilities for each node recovered.....	487-488

## List of Figures

Figure 1.1- World map depicting the geographic distribution of extant Alcidae.....	11
Figure 1.2- Results of previous phylogenetic analyses of alcid relationships.....	20
Figure 1.3- Results of previous phylogenetic analyses of alcid relationships.....	22
Figure 1.4- Graphical representation of morphological character sampling.....	34
Figure 1.5- Parsimony-based results from the separate analysis of the ND2 data.....	40
Figure 1.6- Bayesian results from the separate analysis of the ND2 data.....	41
Figure 1.7- Parsimony-based results from the separate analysis of the ND5 data.....	42
Figure 1.8- Bayesian results from the separate analysis of the ND5 data.....	43
Figure 1.9- Parsimony-based results from the separate analysis of the ND6 data.....	44
Figure 1.10- Bayesian results from the separate analysis of the ND6 data.....	45
Figure 1.11- Parsimony-based results from the separate analysis of the COI data.....	46
Figure 1.12- Bayesian results from the separate analysis of the COI data.....	47
Figure 1.13- Parsimony-based results from the separate analysis of the <i>cyt-b</i> data.....	48
Figure 1.14- Bayesian results from the separate analysis of the <i>cyt-b</i> data.....	49
Figure 1.15- Parsimony-based results from the separate analysis of the 12S data.....	50
Figure 1.16- Bayesian results from the separate analysis of the 12S data.....	51
Figure 1.17- Parsimony-based results from the separate analysis of the 16S data.....	52
Figure 1.18- Bayesian results from the separate analysis of the 16S data.....	53
Figure 1.19- Parsimony-based results from the separate analysis of the RAG1 data.....	54
Figure 1.20- Bayesian results from the separate analysis of the RAG1 data.....	55

Figure 1.21- Parsimony-based topology resulting from the combined analysis of the molecular data.....	57
Figure 1.22- Bayesian results from the combined analysis of the molecular data.....	58
Figure 1.23- Parsimony-based topology resulting from the separate analysis of the morphological data.....	60
Figure 1.24- Bayesian topology resulting from the separate analysis of the morphological data.....	61
Figure 1.25- Parsimony-based strict consensus cladogram resulting from the combined analysis of the molecular and morphological data.....	65
Figure 1.26- Bayesian topology resulting from the combined analysis of the molecular and morphological data.....	66
Figure 2.1- Maps depicting the modern range of the extant Razorbill Auk <i>Alca torda</i> , and <i>Alca</i> fossil localities.....	79
Figure 2.2- Comparison of <i>Alca</i> and <i>Pinguinus</i> humeri in anterior view.....	83
Figure 2.3- Flowchart depicting a simplified explanation of the combined morphometric and morphologic method used to refer specimens to species.....	89
Figure 2.4- Example phenogram depicting the results of cluster analysis of extant alcid species based on humeral measurements.....	97
Figure 2.5- Graphical representation of results from discriminant function analysis of <i>Alca</i> humeri.....	102
Figure 2.6- Cladogram of Alcini relationships resulting from parsimony-based analysis.....	109
Figure 2.7- Comparison of <i>Alca</i> skulls.....	117
Figure 2.8- <i>Alca grandis</i> referred associated specimen (USNM 215454).....	121
Figure 2.9- <i>Alca grandis</i> referred associated specimen (USNM 336379).....	122
Figure 2.10- Distal view of <i>Alca</i> and <i>Pinguinus</i> humeri.....	123

Figure 2.11- <i>Alca ausonia</i> referred left humerus (USNM 446692).....	127
Figure 2.12- <i>Alca stewarti</i> referred associated specimen (USNM 242238).....	130
Figure 2.13- Holotype specimen of <i>Alca carolinensis</i> (NCSM 13734) after preparation from matrix.....	134
Figure 2.14- Holotype and referred specimens of <i>Alca minor</i> .....	144
Figure 2.15- Holotype specimen of <i>Alca olsoni</i> (USNM 454590).....	147
Figure 2.16- Type specimens of <i>Pinguinus impennis</i> and <i>Pinguinus alfrednewtoni</i> .....	154
Figure 2.17- Holotype specimen of <i>Uria brodkorbi</i> (UF-PB 7690).....	156
Figure 2.18- Latitudinal ranges of extant alcids.....	164
Figure 3.1- Map depicting Mancallinae fossil localities.....	174
Figure 3.2- Previously recognized Mancallinae holotype humeri.....	175
Figure 3.3- Skull of Mancallinae (SDSNH 25236).....	183
Figure 3.4- Holotype specimen of <i>Mancalla lucasi</i> (SDSNH 25237).....	196
Figure 3.5- <i>Mancalla</i> referred humeri in anterior view.....	197
Figure 3.6- Line drawings for comparison of Mancallinae proximal humeri.....	198
Figure 3.7- Comparison of sternal facet curvature in charadriiform left coracoids.....	202
Figure 3.8- Holotype specimen of <i>Mancalla vegrandis</i> (SDSNH 77399).....	206
Figure 3.9- Holotype specimen of <i>Mancalla vegrandis</i> (SDSNH 77399).....	207
Figure 3.10- Comparison of charadriiform and sphenisciform sternebrae.....	211
Figure 3.11- Holotype specimen of <i>Miomancalla howardi</i> (SDSNH 68312).....	215
Figure 3.12- Photograph and line drawing of the skull of <i>Miomancalla howardi</i> compared with the skull of <i>Pinguinus impennis</i> .....	216
Figure 3.13- Referred left humerus of <i>Miomancalla howardi</i> (SDSNH 24584).....	217

Figure 3.14- Results of primary phylogenetic analysis.....	225
Figure 3.15- Results of secondary parsimony analysis of Mancallinae inter-relationships.....	231
Figure 3.16- Wing elements of flightless and volant auks.....	238
Figure 3.17- Comparison of carpometacarpal.....	239
Figure 4.1- World map depicting published Fraterculini fossil localities and the extant distribution of Fraterculini.....	252
Figure 4.2- Holotype specimen of <i>Cerorhinca dubia</i> Miller 1925 (UCMP 26546).....	255
Figure 4.3- Holotype specimen of <i>Cerorhinca minor</i> Howard 1971 (LACM 15408)....	256
Figure 4.4- Holotype specimen of <i>Cerorhinca reai</i> Chandler 1990 (SDSNH 25319)...	258
Figure 4.5- Holotype specimen of <i>Fratercula dowi</i> (LACM 127813).....	260
Figure 4.6- Fossilized egg of <i>Fratercula dowi</i> (LACM 127814).....	261
Figure 4.7- NHMUK PV A 9034 in ventral view.....	261
Figure 4.8- Map of eastern USA indicating the locality of PCS Phosphate mine.....	262
Figure 4.9- Comparison of Fraterculini humeri in posterior view.....	263
Figure 4.10- Proximal ends of <i>Cerorhinca</i> sp. right humeri.....	264
Figure 4.11- Phylogenetic position of <i>Cerorhinca dubia</i> .....	271
Figure 4.12- Phylogenetic position of LACM 18274.....	272
Figure 4.13- Phylogenetic position of LACM 18275.....	273
Figure 4.14- Phylogenetic position of SDSNH 23079.....	274
Figure 4.15- Phylogenetic position of NHMUK PV A 9034.....	275
Figure 4.16- Parsimony-based topology depicting Fraterculini relationships.....	278



Figure 4.17- Bayesian hypothesis of Fraterculini relationships.....	279
Figure 5.1- World map depicting published auklet fossil localities and their extant distribution.....	304
Figure 5.2- Holotype specimen of <i>Ptychoramphus tenuis</i> (UCMP 45562).....	305
Figure 5.3- Holotype specimen of <i>Aethia rossmoori</i> (LACM 18948).....	305
Figure 5.4- Aethiini sp. partial humerus (LACM 107031) in anterior view.....	307
Figure 5.5- Strict consensus cladogram of 14 MPT's showing the sister taxon relationship between <i>Ptychoramphus tenuis</i> and <i>Ptychoramphus aleuticus</i> .....	314
Figure 5.6- Strict consensus cladogram of two MPT's showing the unresolved phylogenetic position of <i>Aethia rossmoori</i> in Alcidae.....	315
Figure 5.7- Strict consensus cladogram showing the systematic positions of extinct auklets.....	316
Figure 5.8- Phylogenetic positions recovered for LACM 107031 and SDSNH 63195..	317
Figure 5.9- Holotype specimen of <i>Aethia barnesi</i> .....	321
Figure 5.10- Holotype specimen of <i>Aethia storeri</i> .....	326
Figure 5.11- Comparison of extant auklet humeri.....	327
Figure 5.12- Holotype specimen of <i>Bisulca demerei</i> .....	330
Figure 6.1- World map depicting guillemot fossil localities and the range of extant guillemot species.....	341
Figure 6.2- Holotype specimen of <i>Cepphus storeri</i> .....	344
Figure 6.3- Holotype specimen of <i>Cepphus olsoni</i> .....	347
Figure 6.4- Holotype specimen of <i>Pseudoepphus teres</i> .....	348
Figure 6.5- Systematic position of <i>Cepphus storeri</i> .....	353
Figure 6.6- Strict consensus cladogram of 11 MPT's resulting from the phylogenetic analysis of the character data of Wijnker and Olson (2009).....	356

Figure 6.7- Strict consensus cladogram showing the placement of <i>Pseudocepheus teres</i> .....	357
Figure 6.8- Comparison of extant <i>Cephus humeri</i> .....	364
Figure 7.1- World map depicting previously published murrelet fossil localities and extant distribution.....	378
Figure 7.2- Holotype specimen of <i>Brachyramphus pliocenium</i> (LACM 2119).....	379
Figure 7.3- Specimens referred to <i>Synthliboramphus</i> by Howard (1971).....	380
Figure 7.4- Holotype specimen of <i>Brachyramphus dunkeli</i> (SDSNH 24573).....	381
Figure 7.5- Holotype specimen of <i>Synthliboramphus rineyi</i> (UCMP 61590).....	382
Figure 7.6- Strict consensus cladogram showing the unresolved systematic positions of murrelet species and previously referred specimens.....	389
Figure 7.7- Strict consensus cladogram of the resultant phylogenetic tree for <i>Synthliboramphus</i> and <i>Brachyramphus</i> murrelets.....	390
Figure 7.8- Strict consensus cladogram showing the unresolved systematic position of LACM 15426 in Alcinae.....	391
Figure 7.9- Strict consensus cladogram showing the unresolved systematic position of LACM 26571 in <i>Synthliboramphus</i> .....	392
Figure 7.10- Left humeri of extant brachyramphine murrelets in posterior view.....	396
Figure 7.11- <i>Brachyramphus</i> sp. referred coracoid (SDSNH 24865).....	398
Figure 7.12- <i>Brachyramphus</i> sp. referred coracoid (SDSNH 24866).....	400
Figure 7.13- Left humeri of extant synthliboramphine murrelets in posterior view.....	404
Figure 7.14- Optimization of body mass for extant alcids.....	410
Figure 8.1- Map of extant alcid geographical range and pan-alcid fossil localities.....	416
Figure 8.2- Earliest known pan-alcid fossil (GCVP 5690) from the Hardie Mine in Gordon Georgia, USA.....	442

Figure 8.3- Strict consensus cladogram indicating the placement of <i>Boutersemia belgica</i> in Jacanidae.....	452
Figure 8.4- Strict consensus cladogram indicating the placement of <i>Nupharanassa bulotorum</i> in Jacanidae.....	453
Figure 8.5- Strict consensus cladogram indicating the placement of <i>Larus elegans</i> in Laridae.....	454
Figure 8.6- Strict consensus cladogram indicating the unresolved placement of <i>Numenius antiquus</i> in Charadriiformes.....	455
Figure 8.7- Strict consensus cladogram indicating the unresolved placement of <i>Jiliniornis huadianensis</i> in Charadriiformes.....	456
Figure 8.8- Parsimony-based results of the combined phylogenetic analysis.....	457
Figure 8.9- Charadriiform relationships recovered in the Bayesian analysis.....	465
Figure 8.10- Charadriiform relationships recovered in the Bayesian analysis.....	466
Figure 8.11- Charadriiform cladogram indicating the distribution of variation of the width of the tricipital sulci of the distal humerus.....	471
Figure 8.12- Charadriiform cladogram indicating the distribution of the presence of an m. supracoracoideus nerve foramen of the procoracoid process.....	473
Figure 8.13- Positive relationship between maximum body mass and estimated maximum dive depth for extant alcids.....	480
Figure 8.14- Bayesian topology estimated for extant taxa.....	485
Figure 8.15- Chronogram of charadriiform relationships with estimated divergence times and associated error bars.....	486
Figure 8.16- Comparison of divergence estimates for Charadriiformes with geologic epochs and major paleoclimatic events.....	501
Figure 8.17- Minimum cladogram fit to the fossil record.....	505
Figure 8.18- Graphical representation of alcid diversity through time.....	517

Figure 8.19- Distribution of extant Alcidae compared with distribution of modern cold-water upwelling locations and Pan-Alcidae fossil localities.....519

## INTRODUCTION

The extant auks, auklets, murres, murrelets, guillemots, and puffins are pelagic birds collectively known as the clade Alcidae (Aves, Charadriiformes). Extant diversity within Alcidae includes twenty-three species of exclusively Holarctic distribution (del Hoyo et al, 1996); however, the most well known species is the recently extinct alcid, the Great Auk *Pinguinus impennis*. Perhaps the recency of its demise (~1844; Fuller, 1987), the perceived helplessness of this flightless bird, or the fact that man played a pivotal role in its extinction plays a part in its popularity (Dingus and Rowe, 1998). Even the name ‘penguin’, to which we now ascribe to a clade of southern hemisphere birds with widespread public popularity (i.e., Spheniscidae), is a term coined in reference to the Great Auk and only later applied to the birds we now regard as penguins (Fuller, 1987; Olson and Lund, 2007). Prized by collectors of natural history specimens and immortalized as the symbol of the American Ornithologist’s Union, the Great Auk’s connection to man, as a commodity, as an advertising tool, and as a symbol of extinction continue more than 160 years after its disappearance, owing in part to the lack of knowledge regarding this enigmatic bird (Fuller, 1987).

Just as the biology of the Great Auk has remained a topic of speculation due to an almost complete lack of scientific study of this species while it was extant, the systematics of the clade to which it belongs, the Alcidae (Aves, Charadriiformes), has also remained in flux throughout the history of its study. The uncertainty concerning systematic placement of Alcidae with respect to other charadriiforms, and of the placement of species and clades within Alcidae stems from at least three causes. First, as

pelagic seabirds that spend the majority of their lives on the open ocean, alcids are notoriously hard to observe in the wild (Sealy, 1990), thus making potentially phylogenetically informative observations of their biology difficult to obtain. Although technological developments have begun to reveal long sought-after information about alcids while diving and at sea (Benvenuti et al., 1998; Whitworth et al., 2000; Johansson and Aldrin, 2002; Watanuki et al., 2003; Watanuki et al., 2006), historically, most information about living alcids was gathered while they were on land during the breeding season. However, even the breeding habits of one secretive species, the Marbled Murrelet *Brachyramphus marmoratus*, were not discovered until quite recently (Binford, et al., 1975). Secondly, the derived morphology of alcids as a clade (with respect to other charadriiforms), as well as the morphological similarity between sub-clades of Alcidae, has a long history of misleading non-phylogenetic-based attempts at classifying them (e.g., Linnaeus, 1758; Gmelin, 1789; Vigors, 1825; Bonaparte, 1831; Huxley, 1867; Coues, 1868; Dawson, 1920; Salomonsen, 1944; Verheyen, 1958). Thirdly, previous phylogenetic studies of Charadriiformes (Strauch, 1978; Sibley & Ahlquist 1990; Chu 1995; Thomas et al., 2004) and of alcids in particular (Strauch, 1985; Chandler, 1990a; Moum et al., 1994; Friesen et al., 1996; Moum et al. 2002) have neglected to include extinct taxa, which can affect resulting hypotheses of relationships (Gauthier et al., 1988; Donoghue et al., 1989; Huelsenbeck, 1991).

The goal of this study was to assess the relationships among all pan-alcids, both extinct and extant, through analyses of a variety of data including osteological morphology, oological, myological, integumentary, ethological, and molecular sequence

data. Taxonomic revision and description of published and unpublished fossil material resulted in refined estimates of alcid paleodiversity, and evaluation of the largest morphological data-matrix yet assembled for alcids, in combination with published molecular sequence data, allowed for the timing and pattern of alcid diversification to be assessed. Knowledge of the systematic position of extinct alcids clarifies previously contentious relationships between extant alcids, and also informs hypotheses regarding alcid biogeography. These results contribute to our understanding of avian evolution in response to Cenozoic global climate change, and may inform our interpretations of present day shifts in pelagic avian population ranges in response to the current global warming trend.

The dissertation is divided into eight chapters, each with a different taxonomic, geographic, or methodological focus. The first chapter deals only with extant alcids, their interrelationships, and the relationship of Pan-Alcidae to the rest of Charadriiformes. Because of the great quantity of material referred to *Alca*, a chapter is devoted to that taxon, *Pinguinus*, and other related fossil taxa known from the Atlantic Ocean basin. Likewise, the large quantities of material referred to the morphologically distinctive flightless Mancallinae from the Pacific Ocean basin are treated in a separate chapter. The fossil record and phylogeny of puffins (Alcidae, Fraterculini) from the Atlantic and Pacific Ocean basin constitute the fourth chapter. The fossil record and phylogeny of the smaller, Pacific Ocean endemic auklets (*Aethia* and *Ptychoramphus*) are the topic of the fifth chapter. The fossil record and phylogeny of the Cepphini are described in the sixth chapter. Although not a monophyletic group, the fossil record and phylogeny of the

smaller, primary planktivorous, Pacific Ocean endemic murrelets (*Brachyramphus* and *Synthliboramphus*) are the topic of the seventh chapter. The eighth and final chapter entails a combined phylogenetic analysis of extinct and extant Pan-Alcidae, divergence estimation for Pan-Alcidae, and assesses potential paleoclimatic drivers of pan-alcid evolution.

The first chapter focuses on analyses of extant Alcidae, details previous phylogenetic hypotheses for the clade, and includes a discussion of issues related to combined phylogenetic analyses, and rationale for model choice and data included. Analyses of extant taxa in the first chapter provide context for additional phylogenetic analyses including fossils that follow in successive chapters.

In addition to the description of three new species of extinct *Alca* from the Pliocene of North Carolina, the second chapter examines the taxonomy and systematic position of other closely related extinct species of alcids known from the Atlantic Ocean basin (i.e., *Pinguinus*, *Uria*, *Miocepheus*, *Alle*). The range of size variation among extant alcids is statistically assessed, and a combined morphometric and phylogenetic approach is used to evaluate the diversity represented by fragmentary remains of the alcid taxon *Alca* during the Pliocene. These analyses resulted in increased knowledge of Atlantic alcid paleodiversity, and facilitated assessment of extinct Atlantic alcid species in phylogenetic analyses. The phylogenetic context provided by these analyses help to clarify the patterns of radiation and extinction, which have resulted in the modern diversity of Atlantic Ocean Alcidae.



The third chapter is a taxonomic revision of the extinct Mancallinae based upon a phylogenetic analysis of that clade. In addition to descriptions of three new flightless alcid species from the Miocene and Pliocene of California, the third chapter examines the taxonomy of all previously described Mancallinae (Aves, Pan-Alcidae), and investigates the relationships of these species to one another and to the rest of Alcidae. This is the first phylogenetic analysis to include any extinct Pacific Ocean pan-alcids at the species level. Accordingly, the results of this analysis affected interpretations of pan-alcid evolutionary history, and allowed for the investigation of hypotheses concerning the origins of extant alcid diversity in the Pacific Ocean.

The fourth chapter entails a review of the fossil record of puffins (Alcidae, Fraterculini) and estimates the systematic relationships of extant and extinct puffins in a phylogenetic analysis. Additionally, description of fossil puffin remains referable to *Cerorhinca* provides the first record of this clade from the Atlantic Ocean basin.

The fifth chapter includes a review of the fossil record of auklets (*Aethia* and *Ptychoramphus*) and murrelets (*Brachyramphus* and *Synthliboramphus*), description of new fossil material referable to these taxa, and phylogenetic analysis including these taxa. More nuanced understanding of the fossil record and evolution of these clades facilitated comparisons with diversity and ecological interactions of extant species in this clade.

The sixth chapter entails phylogenetic analysis of living and extinct guillemots (Cepphini). Although no new material referable to this taxon is described, fossil records of guillemots are reviewed and fossil remains that were previously assigned to another taxon are referred to Cepphini based upon the results of the phylogenetic analyses.

The seventh chapter includes a review of the fossil record of the murrelets (*Brachyramphus* and *Synthliboramphus*), description of new fossil material referable to these taxa, and phylogenetic analysis including extant species and fossil referred to these taxa. This represents the first time that fossil murrelets have been included in a phylogenetic analysis.

The final chapter entails a combined phylogenetic analysis and divergence estimates for extinct and extant Pan-Alcidae. These analyses represent the most inclusive, (with respect to character variety) combined phylogenetic analyses for Pan-Alcidae and also for Charadriiformes. The final chapter also includes a discussion of the biogeographical implications of the phylogenetic results of the combined analysis and divergence estimates, in the context of paleoclimatic records, and reviews the evolution of ecological attributes of Pan-Alcidae in light of the new phylogenetic hypothesis.

The ranked hierarchy of the Linnaean taxonomic system as defined by the International Code of Zoological Nomenclature (ICZN, 2000; e.g., Family Alcidae) is not based on evolutionary principles (e.g., monophyly) and is not adopted in this dissertation. However, with the exception of this dissertation being published in a widely available format, new species descriptions do meet all other ICZN requirements for the establishment of new species names. New species descriptions will be subsequently published in peer-reviewed journals. With the exception of species names (e.g., *Fratercula arctica*), all taxonomic designations (e.g., *Fratercula*) are intended as clade names as defined by the International Code of Phylogenetic Nomenclature (i.e., The PhyloCode v.4c; Cantino and de Queiroz, 2010), regardless of use of italics or previous

recognition of rank by other authors, and are not intended to convey rank under the Linnaean system of nomenclature. Several previously used taxon names are converted to phylogenetically defined clade names (e.g., Alcini), and some new clade names (e.g., Pan-Alcidae) are defined herein for the first time. Clade names are defined as stem-based, apomorphy-based, or node-based names, and will be registered after the publication of those clade names in peer-reviewed journal articles based upon chapters of this dissertation. The PhyloCode recommendation that all scientific names be italicized (PhyloCode v.4c; Cantino and de Queiroz, 2010; Recommendation 6.1A) was not followed here. Only species names are italicized herein. Pursuant to Article 21.2 of the PhyloCode (Cantino and de Queiroz, 2010), the first word of species names are considered prenomens, not genus names (see also Dayrat et al., 2008).

Because several major clade names are used throughout this dissertation but are not formally defined until the final appendix, I have chosen to informally define several clade names here to clarify their usage throughout the dissertation. Aves Linnaeus, 1758 is used for the last common ancestor of all living birds and all of its descendents (*sensu* Gauthier and de Queiroz, 2001). Charadriiformes Huxley, 1867 is used for the charadriiform crown clade. Pan-Alcidae *nomen cladi novum* is used for the clade composed of crown clade and stem alcids, and is defined as the most inclusive clade containing *Alca torda* Linnaeus, 1758, *Fratercula arctica* (Linnaeus, 1758), and *Mancalla californiensis* Lucas, 1901, but not *Stercorarius longicaudus* Vieillot, 1819, *Charadrius vociferus* Linnaeus, 1758 or *Larus marinus* Linnaeus, 1758. Alcidae Leach, 1820 refers to the alcid crown clade, and is defined as the most recent common ancestor

of *Alca torda* and *Fratercula arctica* Linnaeus, 1758 and all of its descendants.

Throughout the dissertation, the common name ‘alcid’ is applied to species in the crown clade, Alcidae, and the common name ‘pan-alcid’ is used to refer to the clade composed of stem and crown clade species.

Internal and external clade specifiers were chosen based on previous phylogenetic hypotheses and with the possibility of plausible future taxonomic changes taken into consideration. *Alca torda* and *Fratercula arctica* were chosen to represent the two major clades that have been consistently recovered in recent phylogenetic analyses of alcids (Friesen et al., 1996; Thomas et al., 2004; Baker et al., 2007; Pereira and Baker, 2008), those clades being the Alcinae and the Fraterculinae respectively. *Stercorarius longicaudus* was chosen as an external specifier owing to the hypothesized sister taxon relationship between Alcidae and Stercorariidae recovered in recent analyses of molecular sequence data (Baker et al., 2007; Pereira and Baker, 2008). *Charadrius vociferus* was chosen an external specifier because of its hypothesized basal position in Charadriiformes and in reference to previous hypotheses that placed Alcidae as the sister taxon to all other Charadriiformes (Strauch, 1978; Björklund, 1994; Chu, 1995). *Larus marinus* was chosen based on the close affinity hypothesized between alcid and larids (Thomas et al., 2004; Baker et al., 2007; Livezey, 2009, 2010; Mayr, 2011).

With regard to taxonomic revisions, holotype specimens that could not be distinguished from other previously named species (i.e., operational equivalents) are considered nomen dubium (ICZN, 2000). Based upon phylogenetic results, specimens that were previously referred to a taxon but not named as distinct species (e.g., *Cephus*

sp.), and that cannot be distinguished from previously named species are considered *insertae sedis* with respect to the least inclusive taxon in which they are recovered (ICZN, 2000; Cantino and de Queiroz, 2010). Likewise, previously named species that are morphologically distinct but that are of uncertain placement based upon phylogenetic results are considered *incertae sedis* with respect to the least inclusive taxon in which they are recovered (ICZN, 2000; Cantino and de Queiroz, 2010).

## CHAPTER 1.

Phylogeny of the extant Alcidae (Aves, Charadriiformes):  
comparisons of individual and combined analyses  
of morphological and molecular data

## INTRODUCTION

Alcidae Leach, 1820 (Aves Linnaeus, 1758, Charadriiformes, Huxley, 1867) are pelagic, wing-propelled divers with extant diversity consisting of twenty-three species of exclusively Holarctic distribution (Fig. 1.1; del Hoyo et al, 1996). Alcid diversity includes birds commonly known as auks, auklets, puffins, guillemots, murre, and murrelets. The restriction of alcids to the northern hemisphere has resulted in the common perception of them as the northern ecological equivalent of penguins from the southern hemisphere (Storer, 1960). While the ecological interactions and ethology of Alcidae have been intensely studied, systematic hypotheses regarding the clade have a long history of fluctuation.

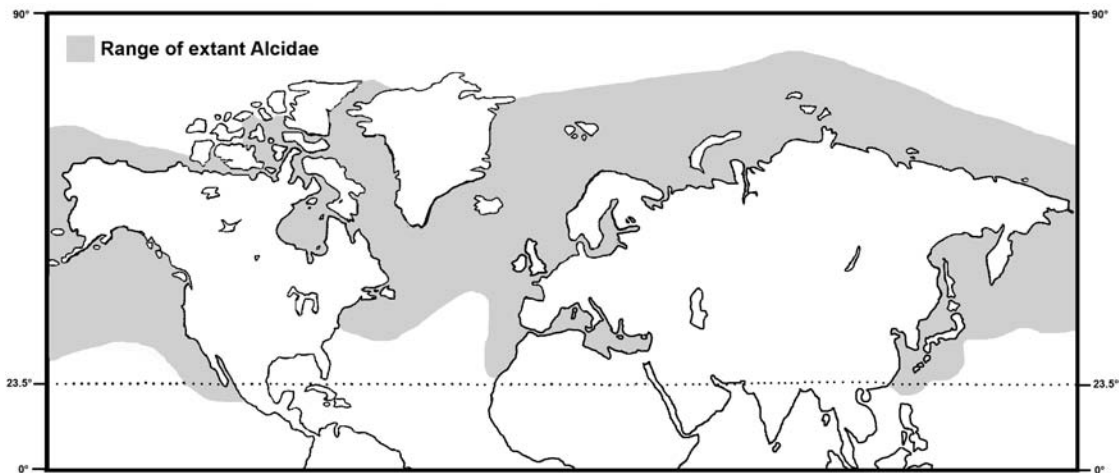


Figure 1.1- World map depicting the geographic distribution of extant Alcidae (altered from del Hoyo et al., 1996).

Alcidae was originally systematically grouped with penguins (i.e., Spheniscidae) by Linnaeus (1758) and that currently unsupported viewpoint lingered among at least one

worker well into the 20<sup>th</sup> Century (see Verheyen, 1958). Nineteenth century classifications placed alcids either in Natatore along with penguins, loons, grebes, and ducks (Vigors, 1825; Brandt, 1837; Swainson, 1837; Coues, 1868), or in Pygopodes with loons and grebes (Bonaparte, 1831; American Ornithologists' Union, 1895). The earliest classifications to group Alcidae with other charadriiforms were those of Gadow (1892), Fürbringer (1888), and Beddard (1898), who correctly surmised close affinity between alcids and other charadriiforms, specifically gulls (i.e., Laridae). There is consensus among more recent classifications on the placement of Alcidae in a monophyletic Charadriiformes (Shufeldt, 1901; Ridgway, 1919; Storer, 1960; Sibley and Ahlquist, 1972; Strauch, 1978; Sibley and Ahlquist, 1990; Björklund, 1994; Chu, 1995; Ericson et al., 2003; Paton et al., 2003; Thomas et al., 2004; Baker et al., 2007; Livezey and Zusi, 2006, 2007; Livezey, 2009, 2010; Mayr, 2011). Previous studies of charadriiform relationships also support the monophyly of Alcidae (Strauch, 1978; Björklund, 1994; Chu, 1995; Thomas et al., 2004; Baker et al., 2007). However, previous analyses addressing the evolutionary relationships of extant alcids (Figs. 1.2 & 1.3; Strauch, 1985; Watada et al., 1987; Chandler 1990a; Moum et al. 1994; Friesen et al., 1996; Chu, 1998; Moum et al. 2002; Thomas et al., 2004; Baker et al., 2007; Pereira and Baker, 2008) lack consensus regarding species relationships within and among sub-clades of Alcidae.

***Previous hypotheses regarding the position of Alcidae and relationships among alcids:*** The Charadriiformes (shorebirds and allies) are a morphologically and ecologically diverse clade (del Hoyo et al., 1996). Previous phylogenetic analyses based on a variety of types of character data including protein electrophoresis, morphology, DNA-DNA hybridization, and mitochondrial and nuclear DNA sequence data have



established the monophyly of Alcidae within a monophyletic Charadriiformes (Strauch, 1978; Sibley and Ahlquist, 1990; Chu, 1995; Ericson et al., 2003; Paton and Baker, 2006; Baker et al., 2007). However, early classifications placed Alcidae in a variety of systematic positions and the contents of 'Alcidae' varied from that of modern classifications (e.g., AOU, 1998; reviewed by Coues, 1868). Alcids were grouped with other diving birds or waterbirds including anseriforms, podicipediforms, gaviiforms, sphenisciforms, pelicaniforms, and some other charadriiforms in the Order Natatore by Linnaeus (1758). Although Linnaeus (1758) included species of auks, murres, guillemots, puffins, and auklets, he did not propose a hypothesis of relationships among alcids. As early as 1837, the classification of Brandt correctly divided Alcidae into two groups, the first including auks, murres, murrelets, and guillemots, and the second including auklets and puffins. Coues (1872) recognized 12 Alcidae genera, *Alca* (Great Auk), *Utamania* (Razorbill Auk), *Fratercula* (Atlantic Puffin, Tufted Puffin, and Horned Puffin), *Ceratorhina* (Rhinoceros Puffin), *Phaleris* (Parakeet Auklet), *Simorhynchus* (Crested Auklet and Least Auklet), *Ptychoramphus* (Cassin's Auklet), *Mergulus* (Dovekie), *Synthliboramphus* (Ancient Murrelet and Xantus' Murrelet), *Brachyramphus* (Marbled Murrelet and Kittlitz's Murrelet), *Uria* (Black Guillemot and Pigeon Guillemot), and *Lomvia* (Common Murre and Thick-billed Murre). The current AOU classification (AOU, 1998) also includes *Alca*, *Fratercula*, *Ptychoramphus*, *Synthliboramphus*, *Brachyramphus*, and *Uria*. However, the Great Auk is placed in *Pinguinus* rather than *Alca*, the Razorbill Auk is placed in *Alca* rather than *Utamania*, the Parakeet auklet is placed in *Aethia* rather than *Phaleris*, the Dovekie is placed in *Alle* rather than *Mergulus*, the guillemots are placed in *Cepphus* rather than *Uria*, and the murres are placed in *Uria*

rather than *Lomvia*. The rationale for the changes adopted by the AOU were largely based on the works of Storer (1945a, b, 1960) and Strauch (1985) and were reviewed by Sibley and Ahlquist (1990).

The pioneering study by Sibley and Ahlquist (1972) examined egg white proteins using electrophoresis and recovered alcids as most closely related to the Laridae and Sternidae (i.e., gulls and terns) among their taxonomic sample. Interestingly, the results of that early biomolecular study are congruent with that of recent analyses of multi-gene molecular sequences (e.g., Ericson et al., 2003; Baker et al., 2007).

The morphological study by Strauch (1978) placed Alcidae as the sister taxon to all other Charadriiformes. Although Strauch included 227 charadriiform species, those taxa were scored for only 70, primarily osteological characters that were analyzed using the method of character compatibility (Estabrook et al., 1976). The appropriateness of compatibility analysis as a method of phylogeny estimation has been criticized (see Mickevich and Parenti, 1980; Churchill et al., 1984). However, subsequent parsimony-based re-analyses of Strauch's (1978) data set by Mickevich and Parenti (1980), Björklund (1994), and Chu (1995) all recovered Alcidae as the sister taxon to all other Charadriiformes.

The DNA-DNA hybridization study by Sibley and Ahlquist (1990) recovered Alcidae nested within Charadriiformes as the sister to all other larids (including *Stercorarius*), a result that was consistent with the results of their previous study based on egg-white proteins (Sibley and Ahlquist, 1972). Both studies by Sibley and Ahlquist (1972, 1990) included a dense sample of charadriiforms. Relationships among major charadriiform clades recovered by Sibley and Ahlquist (1990) differ from more recent

multi-gene analyses (e.g., Baker et al., 2007) in that the Charadrii (e.g., plovers) were not recovered as monophyletic, and some Charadrii subclades (e.g., Charadriidae) are placed closer to Alcidae than the Scolopacidae (e.g., curlews and sandpipers).

Other systematic studies with comparatively dense taxonomic sampling of Charadriiformes include those by Cracraft et al. (2004) and Fain and Houde (2007). The mitochondrial sequence-based (*cyt-b*, COI, COII, COIII) study by Cracraft et al. (2004) recovered Alcidae as sister to Laridae (*Stercorarius* not included). The nuclear sequence-based study of Fain and Houde (2004) also recovered Alcidae as sister to Laridae with Stercorariidae recovered as an outgroup to that clade.

A growing consensus regarding the systematic placement of Alcidae stems from many recent molecular sequence-based phylogenetic hypotheses that have recovered Alcidae nested within Charadriiformes as the sister taxon to the Stercorariidae (i.e., skuas and jaegers). Single-gene analyses of the nuclear RAG-1 gene (Ericson et al., 2003; Paton et al., 2003) and the mitochondrial cytochrome-*b* gene (Thomas et al., 2004) recovered Alcidae as the sister taxon to Stercorariidae. Alcidae and Stercorariidae were also recovered as sister taxa in the results of an analysis that included fourteen mitochondrial genes (Paton and Baker; 2006) and subsequent multi-gene (i.e., nuclear, mitochondrial, and ribosomal RNA) analyses (Baker et al., 2007; Fain and Houde, 2007). An Alcidae + Stercorariidae clade is consistently recovered as the sister taxon to a clade comprising Laridae, Sternidae, and Rynchopidae in the results of recent molecular-based analyses (Ericson et al., 2003; Paton et al., 2003; Paton and Baker; 2006; Baker et al., 2007; Fain and Houde, 2007). Although Alcidae was not included in the avian genomic study of Hackett et al., (2008; ~32 kb), charadriiform relationships in those results are congruent

with the most inclusive previous molecular phylogeny of Charadriiformes (Baker et al., 2007; ~5 kb).

In contrast to molecular-based results, the results of the phylogenetic analysis of morphological characters by Livezey and Zusi (2006, 2007) and Livezey (2009, 2010) recovered Alcidae as the sister taxon to a clade that comprised Stercorariidae, Rynchopidae, and Laridae. However, taxon sampling for Alcidae was limited to *Uria* in the analysis by Livezey and Zusi (2006, 2007), and Alcidae was included as a single, supraspecific terminal in the analyses of Livezey (2009, 2010) and Mayr (2011). The morphology-based hypothesis of Mayr (2011) placed Alcidae in a polytomy with Dromadidae, Stercorariidae, and a clade that comprised Laridae, Sternidae, and Rynchopidae.

There have been several systematic studies with dense taxonomic sampling of Alcidae (Table 1.1). The first phylogenetic analysis of the clade was that by Strauch (1985). An outgrowth of Strauch's previous (1978) work on Charadriiformes, the analysis consisted of a small number ( $n = 33$ ) of osteological, integumentary, and natural history characters analyzed by character compatibility analysis, and did not include any outgroup taxa. Although Strauch (1985) also performed a parsimony-based phylogenetic analysis, he did not publish the full results of that analysis. The results of Strauch's analysis (Fig. 1.2A) are largely incongruent with more recent molecular sequence-based hypotheses of alcid relationships.

Alcid phylogeny was estimated by Watada et al. (1987) using data from 24 protein loci, but that analysis included a limited number of species ( $n = 12$ ). Although the topology recovered by Watada et al. (1987) with respect to the auklets (*Aethia* and

*Ptychoramphus*) and puffins (*Fratercula* and *Cerorhinca*) is congruent with recent hypotheses (Fig. 1.2B), the hypothesized paraphyly of *Uria* Pontoppidan, 1763 was not supported by any previous or subsequent molecular-based analysis.

A parsimony approach was used by Chandler (1990a) to analyze 106 morphological characters. That analysis recovered relationships between several clades (e.g., *Cepphus* Moehring, 1758 and *Alle* Link, 1806 clustered with the puffins and auklets; Fig.1.2C) that were not supported by any previous or subsequent analysis. However, Chandler (1990a) was the first to include the extinct flightless Mancallinae (Charadriiformes, Pam-Alcidae) of the Pacific Ocean in a phylogenetic analysis, albeit in the form of a supraspecific terminal. The Mancallinae were recovered as the sister taxon to all other Alcidae in the results of Chandler's (1990a) analysis, a hypothesis congruent with the sub-family Linnean rank given to 'Mancallidae' by Brodkorb (1967). The paraphyly of *Uria* recovered by Chandler (1990a) is congruent with the results obtained by Watada et al. (1987), and like all subsequent analyses, *Alca* and *Pinguinus* were recovered as sister taxa. However, outgroup taxa, which can be important for polarization of character states, were limited to a hypothetical ancestor terminal.

The analyses of mitochondrial DNA (ND6) and ribosomal RNA (12S) for a subset of living alcids ( $n = 19$  species) by Moum et al. (1994) recovered trees (Fig. 1.2D) that agree in many respects with the hypothesis of alcid relationships presented by Strauch (1985). However, 12S sequences were not analyzed for three of the four species of *Synthliboramphus* Brandt, 1837 and *Synthliboramphus antiquus* was recovered as the sister taxon to all other Alcidae in the parsimony-based analysis of the combined 12S and ND6 data. That position for *Synthliboramphus* is not supported by subsequent analyses

Table 1.1- Previous analyses of alcid relationships. Number of taxa refers only to alcids included in analyses. The following abbreviations are used to indicate multiple methods of phylogenetic inference: (B) Bayesian (ML) maximum likelihood, (ME) minimum evolution, (NJ) neighbor-joining, (P) parsimony, (QP) quartet puzzling. Note that the analysis by Pereira and Baker (2008) included 25 extant alcids owing to the inclusion of subspecies (*Alle alle alle*, *Alle alle polaris*, *Uria aalge aalge*, and *Uria aalge inornata*).

Reference	Data type	# of taxa	Analysis method
Strauch, 1985	morphological	23	compatibility
Watada, 1987	protein loci	12	electrophoresis
Chandler, 1990	morphological	24	parsimony
Moum et al., 1994	12S, ND6	19	likelihood
Friesen et al., 1996	cyt- <i>b</i> , allozyme loci	22	ML, NJ, P
Chu, 1998	morphological	6	parsimony
Moum et al., 2002	ND5, ND6, cyt- <i>b</i> , 12S	5	likelihood
Thomas et al., 2004	cyt- <i>b</i>	21	B, ME, QP
Baker et al., 2007	ND2, cyt- <i>b</i> , 12S, RAG1	12	Bayesian
Pereira & Baker, 2008	ND2, COI, cyt- <i>b</i> , 12S, 16S, RAG1	25	B, ML, P

(Friesen et al., 1996; Thomas et al., 2004; Baker et al., 2007; Pereira and Baker, 2008) with denser taxonomic sampling that have resulted in the placement of *Synthliboramphus* as the sister taxon to Alcini (contents of Alcini include *Uria* + *Alca* + *Pinguinus* + *Alle* + *Miocepphus*). The results of the likelihood-based analysis by Moum et al. (1994) recovered *Synthliboramphus* as the sister taxon to *Brachyramphus*. However, the variability with respect to the positions recovered for *Synthliboramphus* raises some

doubt about the hypothesized relationship of *Synthliboramphus* as the sister taxon to *Brachyramphus*.

The analysis by Friesen et al. (1996) was the first to combine both morphological and molecular data for all extant species of alcids in a single analysis. Mitochondrial DNA (cytochrome-*b*) and allozyme loci data were combined with the morphological characters used by Strauch (1985), and all data were analyzed using parsimony methods. Although Friesen et al. (1996) briefly discussed the effect of adding Strauch's (1985) morphological characters to their analysis, they did not publish those results. The molecular-based results obtained by Friesen et al. (1996) are congruent, yet less resolved than more recent multi-gene molecular-based hypotheses of alcid relationships (Thomas et al., 2004; Baker et al., 2007; Pereira and Baker, 2008; Fig. 1.3A).

The morphology-based charadriiform phylogeny proposed by Chu (1998) included six alcid species; however, the results of that analysis with respect to alcid phylogeny are incongruent with recent molecular-based hypotheses (Fig. 1.2E). A sister group relationship between *Aethia pusilla* and *Brachyramphus marmoratus* was not supported in subsequent analyses.

Although Moum et al. (2002) made an important contribution to alcid systematics by sequencing mitochondrial DNA of the recently extinct Great Auk *Pinguinus impennis*, their analysis included only four other closely related alcid species (*Uria aalge*, *Uria lomvia*, *Alle alle*, *Alca torda*), and thus, comparisons between the results of that analysis (Fig. 1.2F) and other analyses of alcid relationships are limited. However, subsequent molecular-based analyses (Baker et al., 2007; Pereira and Baker, 2008) and previous

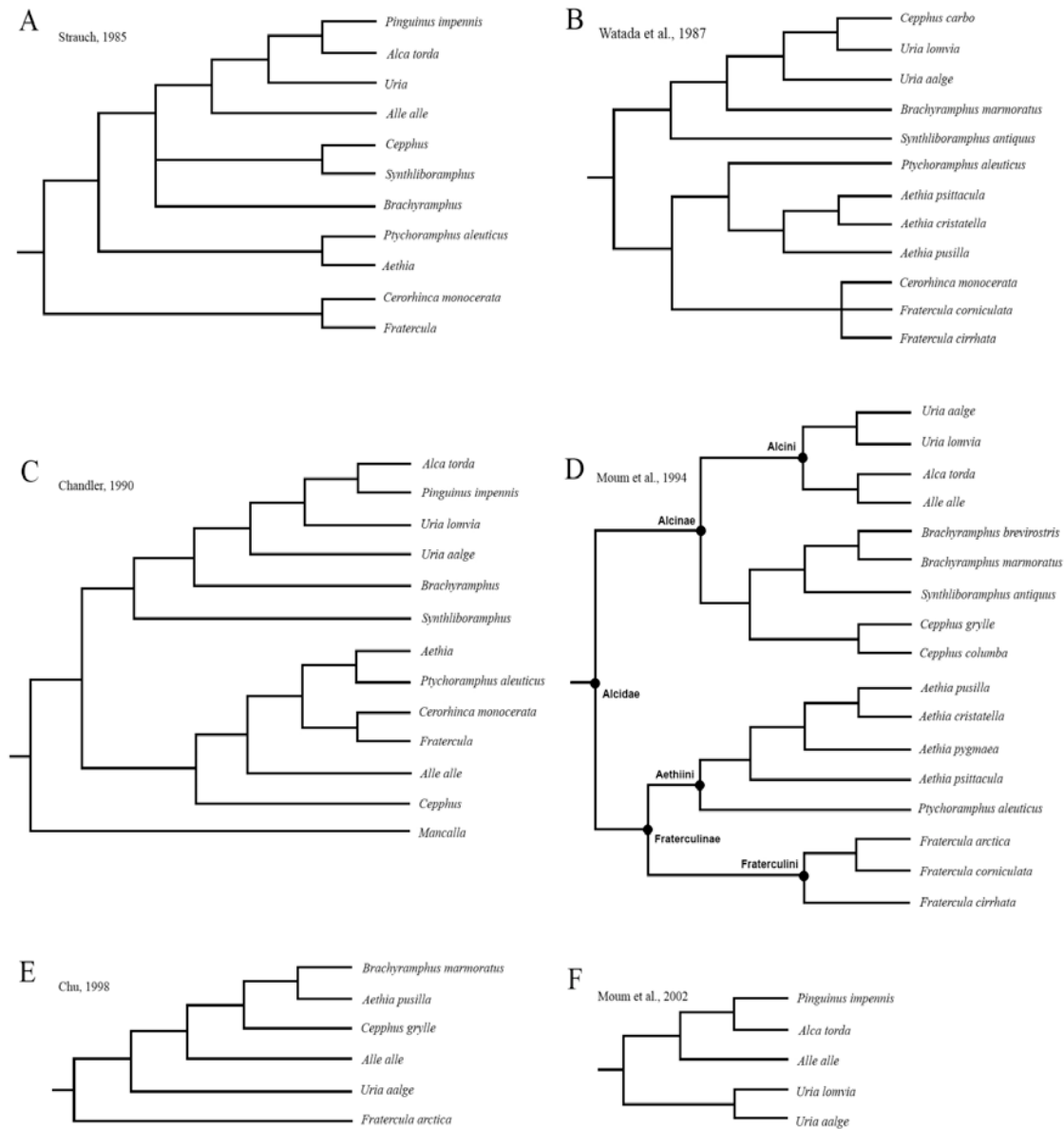


Figure 1.2- Results of previous phylogenetic analyses of alcid relationships. Modified from: **A.** Strauch (1985; Fig.18); **B.** Watada et al. (1987); **C.** Chandler, 1990a; **D.** Moum et al. 1994; **E.** Chu, 1998; **F.** Moum et al. 2002.



morphology-based analyses (Strauch, 1985; Chandler, 1990a; Smith, 2011; Smith and Clarke, in press) all support the sister taxon relationship between *Alca* and *Pinguinus* recovered by Moum et al. (2002).

Mitochondrial DNA sequence data (cytochrome-*b*) for 21 alcid species were analyzed by Thomas et al. (2004) using four different phylogeny estimation methods (parsimony, Bayesian, minimum evolution, and quartet puzzling). Each method produced a different hypothesis of relationships within Alcidae. *Brachyramphus* was recovered as the sister taxon to all other Alcidae in the Bayesian and parsimony-based analyses, a result not recovered by previous analyses. The topology shown in Fig. 1.3B is based upon the Bayesian analysis.

The primary goal of this study was to assess the relationships among all 23 extant species of alcids and the recently extinct Great Auk by synthesizing information from a variety of potentially phylogenetically informative sources including morphological character data (osteological, oological, myological, integumentary, ethological) and all previously published molecular sequence data (mitochondrial, ribosomal, nuclear). Another focus of this study is the exploration of potential effects on resultant topologies owing to inclusion of different types of data (i.e., molecular or morphological) and different methods of phylogeny estimation (i.e., parsimony and Bayesian). Furthermore, the development of morphological characters for Alcidae facilitates inclusion of extinct alcid taxa in future phylogenetic analyses that will provide phylogenetically analyzed fossil taxa for use as calibration points in divergence-time analyses. Hence, the results of this study will serve as a basis of comparison for results of analyses including species

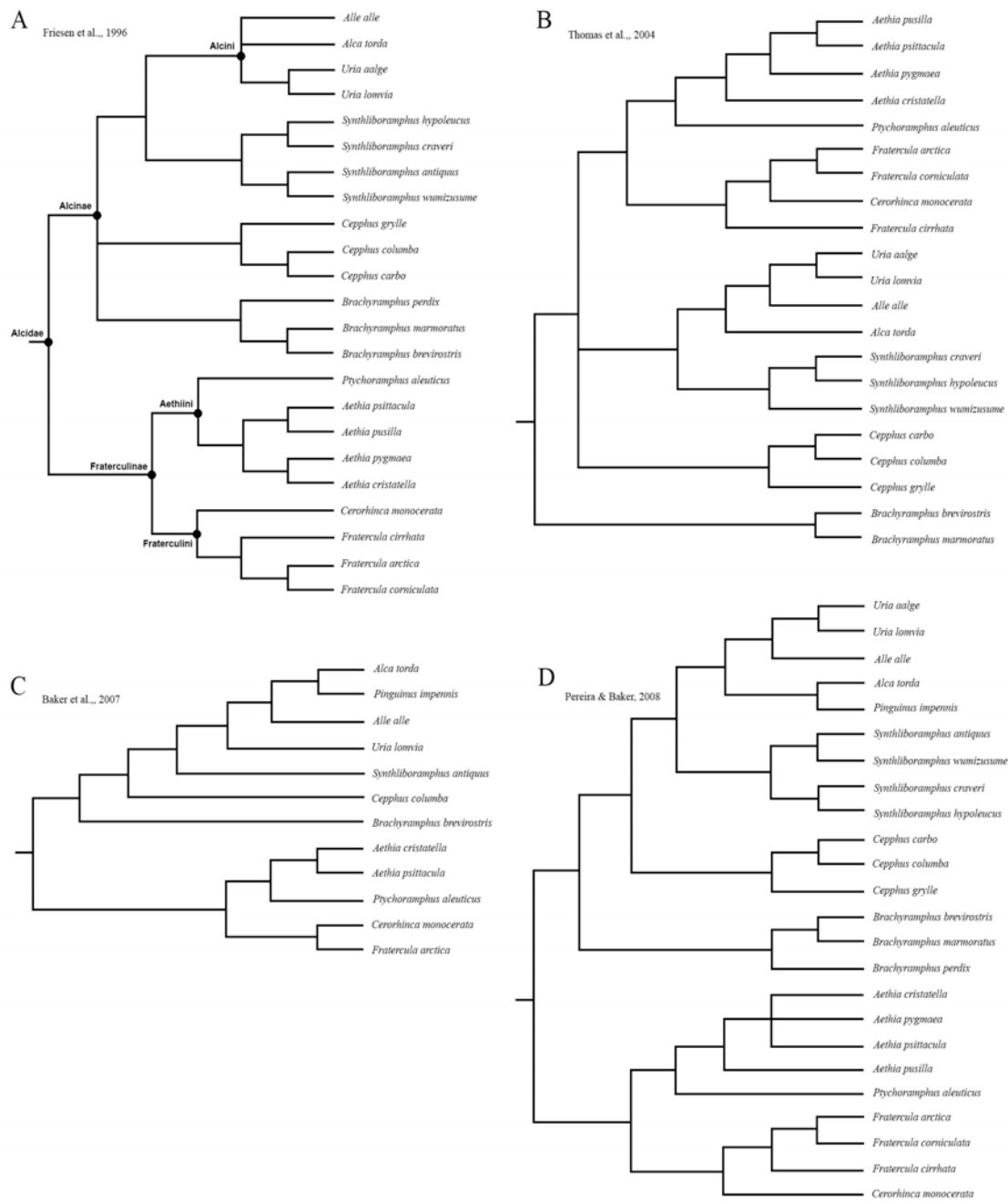


Figure 1.3- Results of previous phylogenetic analyses of alcid relationships. **A.** Friesen et al. 1996; **B.** Thomas et al. 2004; **C.** Baker et al. 2007; **D.** Pereira and Baker 2008.

known from incompletely preserved fossils, the inclusion of which may have effects on topological resolution and systematic hypotheses of alcid relationships.

***Rationale for combining data in phylogenetic analyses:*** A combined approach of phylogeny estimation was used to obtain phylogenetic hypotheses for extant Alcidae. Simulations show that the combination of molecular and morphological data often provide a more accurate estimate of phylogeny owing to increased character sampling (Wiens, 2009). Termed the total evidence, combined, or character-congruence approach (Kluge, 1989; de Queiroz, 1993), the practice of combining and simultaneously analyzing different types of data to produce a hypothesis of systematic relationships was questioned by some authors (e.g., de Queiroz, 1993; Bull et al., 1993; de Queiroz et al., 1995). These authors expressed concern regarding heterogeneity of data, and its potential to produce misleading or inaccurate hypotheses of relationships. Although the combination of all available molecular sequence data, and even genomic analysis, has become an accepted practice (e.g., Hackett et al., 2008), some systematists are more hesitant to embrace the combination of molecular and morphological data. However, the same arguments that eventually led to the widespread acceptance of combined analyses of molecular data also apply to the combined analysis of molecular and morphological data. “The total evidence approach can be justified philosophically and statistically” (Huelsenbeck et al., 1996:152). It has been said that the best hypothesis is the one that explains all of the data simultaneously, because the exclusion of data may represent a form of *a priori* assumption regarding any phylogenetic signal contained in those data (Huelsenbeck et al., 1996). The results of previous research by Rokas et al. (2003) suggests that combination of multiple genes can account for conflicting signals that are potentially

present in different genes. Although this argument assumes that more data are more likely to lead to a more accurate phylogenetic hypothesis, the true phylogeny will never be known for most clades because taxon sampling affects resulting topologies. Furthermore, most taxa that have ever existed are extinct, and because of the vagaries of the fossil record, the vast majority of species are unknown to science. No matter how strongly supported, there is effectively no way to know if our hypotheses of organismal relationships are correct for most clades. Therefore, theoretically at least, combined analyses offer the best option to systematists focused on producing the most inclusive and potentially accurate systematic hypothesis for any clade. Although the advent of so-called ‘homoplasy free’ molecular markers provide a promising new opportunity with respect to the resolution of deep divergences among vertebrates (i.e., micro RNA methods; Heimberg et al., 2008), similar ‘homoplasy-free’ markers for species-level phylogenetic analysis have yet to be discovered. Phylogenetic hypotheses will, therefore, continue to be associated with caveats regarding the potential effect of homoplasy and the effect of potentially incorrect assessments of homology.

Although it could be argued that there exists no reliable metric with which one might decide between incongruent hypotheses based upon different sets of data, debate continues regarding the separate or combined analysis of different types of data (Mickey, 1978; de Queiroz 1993; Bull et al., 1993; Huelsenbeck et al., 1996; Wiens, 1998). Proponents of taxonomic congruence advocated the prior agreement approach, which states that data that have produced incongruent yet strongly supported hypotheses of relationships should not be combined because of the potential for the incongruence between sets of data to produce hypotheses of relationships not supported by any

individual set of data (i.e., misleading or inaccurate results). Methods such as differential weighting were proposed to deal with the combination of potentially incongruent sets of data (Chippendale and Wiens, 1994). However, character weighting requires *a priori* knowledge of evolutionary processes, which often are the original focus of the investigation, creating logical circularity with respect to evolutionary inferences. Equal weighting of character data allows the data to drive the outcome of the analysis without preloaded assumptions.

Consensus methods that combine the phylogenetic results from different sets of data were also proposed as an alternative to simultaneous analysis of different types of data. However, those methods (e.g., supertree methods) are prone to the loss of data from the original sources with respect to competing phylogenetic hypotheses (Sanderson et al., 1998). Additionally, because nodes recovered in multiple separate analyses also are likely to be strongly supported when those data are combined, there seems to be little advantage to separately analyzing data and then combining the results. “Misleading characters should (overall) be outnumbered by characters that reflect the true organismal relationships” (Wiens and Chippendale, 1994:566). Combination of slowly evolving genes with quickly evolving genes can, for example, contribute to the resolution of the tree at different levels (i.e., deep and shallow nodes). That the addition of relatively small quantities of morphological characters can affect resultant topologies when combined with much larger molecular sets of data was also demonstrated (Swofford et al., 1990; Nylander et al., 2004; Sole et al., 2007). Increased taxon sampling has demonstrated potential to increase phylogenetic accuracy (Wheeler, 1992; Zwickl and Hillis, 2002; Heath et al., 2008). Likewise but potentially to a lesser degree, increased sampling of data

can also increase phylogenetic accuracy (Huelsenbeck et al., 1996). The combination of data may increase phylogenetic accuracy by maximizing the number of characters available for an analysis and may result in hypotheses of relationships that would not have been recovered in separate analyses (Chippendale and Wiens, 1994). Therefore, incongruence between phylogenetic hypotheses does not provide a sound argument against the combination of data from different sources, providing that appropriate models are applied to all partitions of data so that differential rates of evolution between sets of data are encompassed. Just as there is no logical basis for excluding characters, there is no basis for choosing between separately produced phylogenetic trees, and combination of types of data provides a logical alternative (Kluge, 1998) that can potentially reconcile competing hypotheses based upon different types of data.

One objection to combined analyses was the potential for character non-independence to negatively affect the accuracy of estimated phylogenetic relationships (de Queiroz, 1993). Methods to evaluate potential character dependence include the independent contrasts test of Felsenstein (1985), the correlation method of Pagel (1994), and the pairwise comparison test of Maddison (2000). However, with the exception of poorly conceived morphological characters (see Hawkins et al., 1997), character independence is frequently difficult to assess (Clarke and Middleton, 2008), and does not provide a compelling reason to refrain from combining data.

The advent of maximum likelihood and Bayesian phylogeny estimation approaches (Rannala and Yang, 1996; Yang and Rannala, 1997; Huelsenbeck et al., 2001) that allow partitioning of data, and that allow each partition to have a separate evolutionary model, accounts for heterogeneity of data and alleviates the potential need

for differential weighting that was proposed in the context of parsimony analyses of combined data. Introduction of the Mk model (Lewis 2001a) facilitated the combined analysis of discrete morphological and molecular data in a maximum likelihood or Bayesian framework. The complexity of evolutionary models available with likelihood and Bayesian approaches make them an attractive alternative to parsimony methods that apply the same ‘model’ to all data (Huelsenbeck et al., 2002).

Although molecular characters generally far outnumber morphological characters available for analysis, the inclusion of small numbers of morphological characters can positively influence tree topology (Nylander et al., 2004). The potential for molecular data to ‘swamp’ morphological signal was not supported in empirical studies of combined analyses (Nylander et al., 2004; Wiens, 2009; Wiens et al., 2010).

The inclusion of incomplete taxa can result in an increase in the number of most parsimonious trees (MPT’s) and decreased phylogenetic resolution (Huelsenbeck, 1991; Wheeler, 1992; Nixon and Wheeler, 1992; Zwickl and Hillis, 2002; Wiens, 2003). However, lack of resolution is an issue of phylogenetic precision, and is unrelated to degree of phylogenetic accuracy (Kearney, 2002; Kearney and Clark, 2003). Increased numbers of characters and taxa can increase the accuracy of phylogeny estimation (Zwickl and Hillis, 2002; Wiens, 2003; Heath et al., 2008), and even incomplete fossils can help break up long branches that contribute to long-branch attraction in parsimony and Bayesian phylogenetic analyses (Swofford et al., 1990; Wiens, 2005). Many fully resolved topologies for extant taxa contain numerous examples of ‘missing data’ entries in the form of morphological characters that have no homologues (e.g., teeth in extant birds) or the absence of particular genes or portions of genes (i.e., indels). Accordingly,

incomplete taxa were not *a priori* pruned from these analyses. Additionally, because all of the taxa in this analysis are extant, missing data are not a critical issue with respect to osteological, integumentary and natural history characters.

The extant taxa included in this analysis ranged from 3.7% - 92.0% incomplete (including molecular gaps and missing morphological character scorings; Tables 1.2 and 1.3). Myological data published by Hudson et al. (1969) included scorings for only 17 of the 53 taxa included in this analysis and feather microstructure data published by Dove (2000) included scorings for only 29 taxa included in this analysis. Analyses with the myological and feather microstructure partitions removed (results not shown) did not result in significant topological changes or changes in tree support values. Therefore, those characters were included in all of the morphological and combined analyses so that character state distributions could be evaluated on the resulting trees. All but 15 of the 53 extant taxa sampled are > 75% complete with respect to morphological scorings (Table 1.2). All but 4 taxa are > 90% complete with respect to morphological scorings if the myological scorings from Hudson et al. (1969) and the feather microstructure characters from Dove (2000) are not considered.

With respect to molecular sequence availability, data for 23 of the 53 sampled taxa were > 50% incomplete (Table 1.2). Taxonomic sampling was comparatively high for ND2, COI, Cyt-*b*, 12S, and RAG1, with sequence data available for 40 or more of the 53 sampled taxa (Table 1.3; Appendix 4). The majority of missing molecular sequence data stems from the unavailability of ND5 and ND6 sequences. ND5 sequence data was available for only 14 taxa, and ND6 sequence data was available for only 21 taxa (Table 1.3; Appendix 4). Inclusion of ND5 and ND6 sequences did not negatively affect the



resolution of the combined analyses and so ND5 and ND6 sequences, albeit rather incomplete, were not excluded on the basis of incomplete taxon sampling. The taxon with the greatest quantity of missing data was *Charadrius wilsonia*, because only COI molecular sequence data was available for this species and myological (Hudson et al., 1969) and feather microstructure characters (Dove, 2000) were also not scored for this species. However, *Charadrius wilsonia* was consistently recovered as the sister taxon to *Charadrius vociferus* in the results of the phylogenetic analyses. Thus, although very incomplete, its inclusion did not negatively affect the resolution or topology of resulting cladograms. Full details of molecular sequence availability for included taxa are provided in Appendix 4 and are further detailed in Tables 1.2 and 1.3.

## MATERIALS AND METHODS

Included in the combined analyses are all 23 species of extant alcids, the recently extinct Great Auk *Pinguinus impennis*, and twenty-nine charadriiform outgroup taxa. Species level taxonomy of extant North American Charadriiformes follows the 7th edition of the Checklist of North American Birds (American Ornithologists' Union, 1998).

All taxa were scored into a matrix consisting of 353 morphological characters. Comparative material is listed in Appendix 1. Character descriptions are provided in Appendix 2, and character scorings are provided in Appendix 3. Description of anatomical features primarily follows the English equivalents of the Latin osteological

Table 1.2- Character incompleteness by taxon (% missing data). Totals include gaps and morphological characters not scored owing to absence. (Table continued on next page).

Taxa	Molecular Sequence Data	Morphological Data	Combined Data
<i>Aethia cristatella</i>	32.6	25.2	32.4
<i>Aethia psittacula</i>	32.4	12.5	31.8
<i>Aethia pusilla</i>	31.7	11.6	31.1
<i>Aethia pygmaea</i>	31.7	24.6	31.5
<i>Alca torda</i>	30.5	3.1	29.7
<i>Alle alle</i>	26.9	11.0	26.5
<i>Anous tenuirostris</i>	58.0	27.2	57.1
<i>Bartramia longicauda</i>	49.4	13.0	48.3
<i>Brachyramphus brevirostris</i>	32.1	24.9	31.9
<i>Brachyramphus marmoratus</i>	31.7	5.4	30.9
<i>Brachyramphus perdix</i>	36.2	26.1	35.9
<i>Cepphus carbo</i>	36.3	25.2	36.0
<i>Cepphus columba</i>	22.5	3.4	22.0
<i>Cepphus grylle</i>	71.2	16.7	69.5
<i>Cerorhinca monocerata</i>	37.3	3.4	36.3
<i>Charadrius vociferus</i>	7.5	11.6	7.6
<i>Charadrius wilsonia</i>	93.7	26.3	92.0
<i>Chlidonias leucoptera</i>	56.2	27.2	55.4
<i>Creagrus furcatus</i>	57.9	15.3	56.7
<i>Cusorius temminckii</i>	7.4	33.1	8.2
<i>Fratercula arctica</i>	3.7	3.1	3.7
<i>Fratercula cirrhata</i>	31.7	3.4	30.9
<i>Fratercula corniculata</i>	31.7	16.4	31.3
<i>Glareola maldivarum</i>	78.9	33.4	77.6
<i>Gygis alba</i>	55.1	17.3	53.9
<i>Hydrophasianus chirurgus</i>	52.5	28.3	51.8
<i>Larosterna inca</i>	52.9	13.9	51.8
<i>Larus argentatus</i>	84.1	7.4	81.9
<i>Larus marinus</i>	46.6	24.1	45.9
<i>Numenius minutus</i>	55.6	32.6	54.9
<i>Pagophila eburnea</i>	50.3	15.9	49.3
<i>Phaetusa simplex</i>	52.7	16.4	51.6
<i>Pinguinus impennis</i>	76.3	25.8	74.8
<i>Ptychoramphus aleuticus</i>	32.6	4.8	31.8
<i>Rhinoptilus chalcopterus</i>	56.3	19.3	55.3
<i>Rhodostethia rosea</i>	51.2	15.9	50.1
<i>Rissa tridactyla</i>	7.5	12.7	7.6
<i>Rynchops niger</i>	7.4	8.2	7.4
<i>Stercorarius longicaudus</i>	49.3	11.9	48.2

Taxa	Molecular Sequence Data	Morphological Data	Combined Data
<i>Stiltia isabella</i>	55.7	13.3	54.5
<i>Sterna anaethetus</i>	70.3	26.9	69.0
<i>Sterna maxima</i>	53.6	19.3	52.6
<i>Sterna nilotica</i>	46.7	9.1	45.6
<i>Sternula superciliaris</i>	55.6	31.2	54.9
<i>Synthliboramphus antiquus</i>	17.0	4.2	16.6
<i>Synthliboramphus craveri</i>	36.3	24.6	36.0
<i>Synthliboramphus hypoleucus</i>	80.7	24.9	79.1
<i>Synthliboramphus wumizusume</i>	31.8	26.3	31.6
<i>Tryngites subruficollis</i>	50.1	14.4	49.0
<i>Uria aalge</i>	21.4	4.2	20.9
<i>Uria lomvia</i>	27.1	17.3	26.8
<i>Xema sabini</i>	50.1	15.3	49.0

Table 1.3- Details of sampled molecular sequences and morphological characters. Number of characters and percent missing data totals include gaps.

Gene	# of taxa	Sequence length	% missing data	# of parsimony informative characters
ND2	48	1041	0.0 – 11.5	493
ND5	14	1815	0.0 – 93.7	316
ND6	21	540	3.3 – 3.9	226
COI	40	1551	0.0 – 57.9	397
Cyt- <i>b</i>	53	1143	0.0 – 38.8	433
12S	50	1053	1.2 - 55.2	242
16S	27	1636	2.1 – 38.9	376
RAG1	45	2871	0.0 – 17.3	266
Morph.	53	353	3.1 - 33.4	317
Total	53	11954	0.0 – 93.7	3066

nomenclature summarized by Baumel and Witmer (1993). The terminology proposed by Howard (1929) is followed for features not treated by Baumel and Witmer (1993). All osteological and adult integumentary characters were evaluated by direct observation. Whenever available, five or more specimens of each species including both sexes, were evaluated to account for intraspecific character variation and sexual dimorphism respectively. Only adult specimens, assessed based on degree of ossification (Chapman, 1965), were evaluated for osteological characters, and when available, specimens from multiple locations within the geographic range of extant species (i.e., subspecies) were examined to account for geographic variation within species. Reproductive, chick integument, dietary, and some myological characters were scored from published sources (see Appendix 2).

Morphological characters include osteological ( $n = 232$ ), integumentary ( $n = 32$ ), ethological ( $n = 16$ ), myological ( $n = 24$ ) and feather microstructure ( $n = 52$ ; Fig. 1.4). One hundred and sixty-four characters were newly identified for this analysis. The other 189 characters were drawn from the work of Hudson et al. (1969;  $n = 24$ ), Strauch (1978, 1985;  $n = 39$ ), Chandler (1990a;  $n = 63$ ), Chu (1998;  $n = 11$ ), and Dove (2000;  $n = 34$ ; Fig. 1.4).

Regarding previously published characters, only those characters that varied in the taxa sampled for this study were sampled. Only 34 of the 38 characters identified by Dove (2000) varied in the taxa examined in this study. Of the 34 used in this analysis, eighteen were modified (i.e., split into 2 separate characters) to distinguish absence of a feature from character variation (see Hawkins et al., 1997), resulting in a total of 52

feather microstructure characters. For example, character #17 (nodal spines) of Dove (2000) originally contained four states: (a) absent; (b) present at nodes all along the barbule; (c) present mainly at basal to mid-nodes on the barbule; (d) some nodes with spines and some nodes on other barbules at the same location without spines. That character was split into two characters (characters 322 and 323) in the combined matrix. Character 322 is scored for the absence or presence of nodal spines and character 323 is scored for the position of nodal spines in taxa that possess those spines.

The cladistic matrix also includes a maximum of 11,601 base pairs scored for sampled taxa (15.9 - 96.3 % complete; average sequence completeness = 38.6 %). See Appendix 4 for full details of sequence availability and sequence authorship. Molecular sequence data (mitochondrial: ND2, ND5, ND6, COI, *cyt-b*; ribosomal RNA: 12S, 16S; and nuclear: RAG1) were downloaded from GenBank. Preliminary sequence alignments for each gene were obtained using ClustalX v2.0.6 (Thompson et al., 1997) and then manually adjusted using Se-Al v2.0A11 (Rambaut, 2002). The general time reversible model with invariant sites and gamma distribution (GTR+i+g) was estimated as the best nucleotide substitution model for each gene partition and for the concatenated molecular data including all eight genes by MrModeltest v.2.3 (Nylander, 2008). In the Bayesian analyses the Mk model (Lewis, 2001a) was applied to morphological data.

Parsimony and Bayesian phylogeny estimation approaches were explored, because Bayesian methods allow incorporation of complex models of nucleotide substitution not available with parsimony methods (Lewis, 2001a, 2001b; Huelsenbeck, 2001, 2002; Holder and Lewis, 2003; Nylander et al., 2004). A total of 22 separate

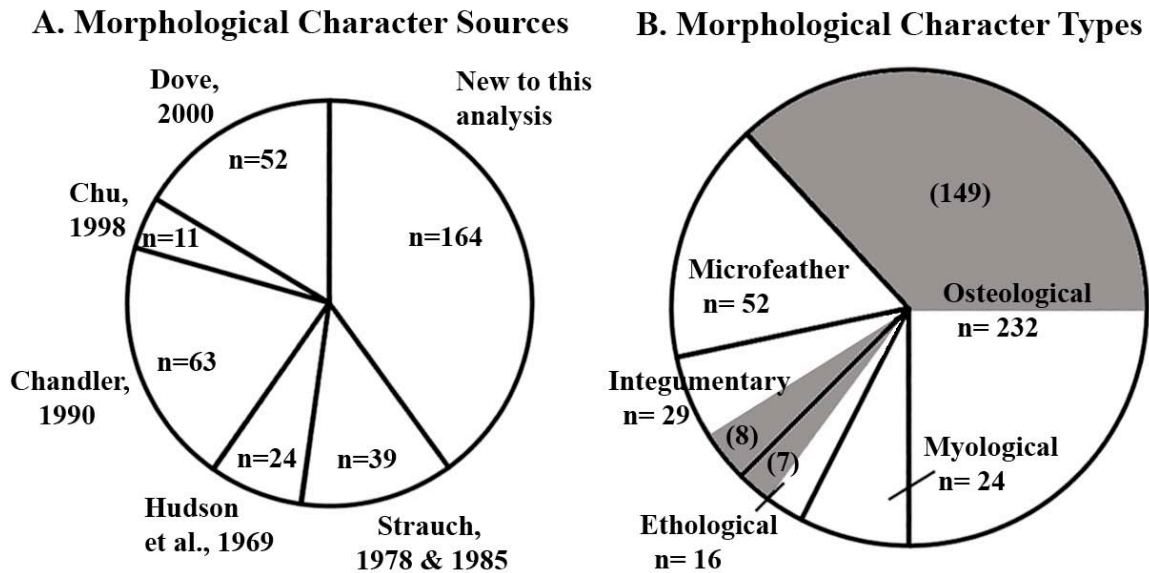


Figure 1.4- Graphical representation of morphological character sampling: **A.** quantities and sources of morphological characters; **B.** quantities and types of morphological characters. Grey shaded area and corresponding quantities in parentheses represents newly identified characters.

phylogenetic analyses were conducted. Combined analyses were conducted using parsimony and Bayesian approaches to evaluate potential differences between the results of these different phylogeny estimators. Additionally, to explore the effects of different types of data on the resulting phylogenetic hypotheses, parsimony and Bayesian analyses were also conducted on the morphological and molecular data separately. Furthermore, parsimony and Bayesian analyses were conducted for each of the eight genes to assess potential phylogenetic signal contributed by each gene partition.

Parsimony-based analyses employed the parsimony criterion of phylogenetic inference as implemented in PAUP\* v4.0b10 (Swofford, 2002). Parsimony tree search criteria are as follows: heuristic search strategy; 10,000 random taxon addition sequences; tree bisection-reconnection branch swapping; random starting trees; all characters equally

weighted; minimum length branches = 0 collapsed; multistate (e.g., 0&1) scorings used only for polymorphism. Bootstrap values and descriptive tree statistics (i.e., CI, RI, RC) were calculated using PAUP\* v4.0b10 (Swofford, 2002). Bootstrap value calculation parameters included 1,000 heuristic replicates and 100 random addition sequences per replicate. All other settings were the same as the primary analysis. Bremer support values were calculated using a script generated in MacClade v4.08 (Maddison and Maddison, 2005) and analyzed with PAUP\* v4.0b10 (Swofford, 2002). Based on the results of previous phylogenetic analyses of charadriiform relationships (Strauch, 1978; Sibley and Ahlquist, 1990; Chu, 1995; Ericson et al., 2003; Paton et al., 2003; Thomas et al., 2004; Baker et al., 2007), resultant trees were rooted with an exemplar of *Charadrius vociferus*, except for the results of the analysis of the ND6 sequence data which were rooted with *Charadrius alexandrinus* because ND6 sequence data for *Charadrius vociferus* and *Charadrius wilsonia* were unavailable. Tree graphics were produced in MacClade v4.08 (Maddison and Maddison, 2005) and FigTree v1.3.1 (Rambaut, 2009).

Bayesian phylogenetic analyses of morphological, molecular, and combined data were performed using the program Mr. Bayes v3.1.2 (Ronquist and Huelsenbeck, 2003). MrBayes parameters were as follows: two simultaneous independent runs with one cold and five heated chains each, starting trees random, MCMC samples taken every 1000 generations, nine partitions in the combined analyses (1 morphological and 8 gene partitions), all parameters (e.g., branch lengths, topology, rate) unlinked across partitions, all fully resolved topologies considered equally likely, branch lengths unconstrained (i.e., molecular clock not enforced), exponential (10.0), substitution rate flat Dirichlet (1, 1, 1, 1), state frequencies flat Dirichlet (1, 1, 1, 1), standard deviation of split frequencies

<0.01 considered evidence of convergence of MCMC chains, nodes with  $\geq 0.95$  posterior probability considered strongly supported. Log likelihoods were evaluated to determine burn-in with Tracer v1.4 (Rambaut and Drummond, 2009), and the resulting consensus of retained trees was plotted using FigTree v1.3.1 (Rambaut, 2009). *Charadrius alexandrinus* was used to root the tree resulting from analysis of the ND6 sequence data because corresponding sequences for *Charadrius vociferus* and *Charadrius wilsonia* were unavailable through Genbank. All other trees were rooted with *Charadrius vociferus*. The number of Markov Chain Monte Carlo (MCMC) generations varied between analyses (Table 1.1). Individual gene analyses (e.g., analysis of RAG1 sequences only) and the concatenated molecular data were run for ten million MCMC generations and the first half of retained trees were discarded as burn-in. Preliminary Bayesian analyses of the morphological data were run for 10 and then 20 million MCMC generations but the Markov Chains did not converge. Subsequently, the morphological data were run for 50 million MCMC generations and the first 35 thousand trees (i.e., 70%) were discarded as burn-in. The combined data were run for 20 million MCMC generations and first half of retained trees were discarded as burn-in.

***Institutional Abbreviations:*** AMNH—American Museum of Natural History, New York, NY, USA; NCSM—North Carolina Museum of Natural Sciences, Raleigh, NC, USA; NSM PO—National Museum of Nature and Science Paleontology Osteological Collection, Tokyo, Japan; SDSNH—San Diego Natural History Museum, San Diego, CA, USA; UMMZ—University of Michigan Museum of Zoology, Ann Arbor, MI, USA; USNM—National Museum of Natural History, Smithsonian Institution, Washington, D.C., USA.



## PHYLOGENETIC RESULTS

Analyses of individual genes produced widely varying results and degrees of resolution using parsimony and Bayesian estimation methods (Table 1.4; Figs. 1.5–1.20). Separate analyses of ND2, ND6, COI, 16S, and RAG1 using a parsimony approach produced trees with relatively resolved nodes in deep and shallow positions (Figs. 1.5, 1.9, 1.11, 1.17, 1.19). Parsimony-based analyses of *cyt-b* and 12S produced trees that have poor resolution for deep nodes, but that have fairly resolved relationships within sub-clades (e.g., *Aethia* monophyly supported but its position with respect to other Alcidae unresolved; Figs. 1.13 & 1.15). The parsimony-based analysis of the ND5 sequence data resulted in a poorly resolved consensus tree. However, the resultant tree placed the larids, alcids, and *Stercorarius* in a clade to the exclusion of other more basal charadriiforms, confirming that some phylogenetic signal is present in these data.

The Bayesian analyses of separate genes produced trees with relatively resolved nodes in deep and shallow positions based on the ND2, ND6, COI, *cyt-b*, 16S, and RAG-1 data (Figs. 1.6, 1.10, 1.12, 1.14, 1.18, 1.20) and recovered relatively well-resolved relationships between closely related species in analyses of the 12S data (Figs. 1.16). The results of the Bayesian analysis of the ND5 data were congruent yet more resolved than the parsimony-based results (Fig. 1.8), with Alcinae species *Alca torda*, *Pinguinus impennis*, *Uria aalge*, *Uria lomvia*, and *Cepphus grylle* recovered as a clade. *Alle alle* and *Synthliboramphus antiquus* were not placed with the other Alcinae species, but the two *Uria* species were recovered as sister taxa.

The only previous single-gene analysis with comparably dense taxonomic sampling of Alcidae to the single-gene analyses presented here are the cytochrome-*b*-based analyses by Thomas et al. (2004) who performed analyses using four different phylogeny estimation methods (parsimony, Bayesian, minimum evolution, and quartet puzzling). The parsimony results presented by Thomas et al. (2004) were more resolved than the results presented here (e.g., Alcidae monophyly recovered), possibly owing to differences in taxon sampling or sequence alignment. The Bayesian results from the analysis of the cytochrome-*b* data presented herein are largely congruent with the Bayesian results presented by Thomas et al. (2004). *Brachyramphus* was placed in a novel position as the sister taxon to all other Alcidae in the results obtained by Thomas et al. (2004). *Brachyramphus* is recovered as the sister to all other Alcinae in the Bayesian topology presented herein, a position congruent with other previous molecular-based hypotheses for the position of this taxon (Baker et al., 2007; Pereira and Baker, 2008).

Recovery of Alcidae monophyly was variable in the individual gene analyses. Alcidae monophyly was supported in the parsimony-based results of the ND2, ND6, and RAG1 data, and in the Bayesian analysis results of the ND2, ND6, *cyt-b*, 12S, and RAG-1 data (Table 1.4). Alcidae monophyly was not recovered in the parsimony-based results of the separate analyses of the ND5, COI, *cyt-b*, 12S, and 16S data, or in the Bayesian results from the analysis of the ND5, COI, and 16S data (Table 1.4).

Unexpected topological results also include the placement of *Stercorarius skua* in a clade that otherwise includes only alcid taxa in the parsimony-based analysis of the 16S data (Fig. 1.17). Furthermore, the parsimony-based analysis of the COI data placed the auklets and puffins outside of a clade composed of an otherwise monophyletic Alcidae

plus Laridae (Fig. 1.11). Despite these potential phylogenetic inconsistencies, all of the individual genes displayed recognizable phylogenetic signal and were retained for combination into a concatenated molecular set of data.

Table 1.4- Summary of phylogenetic analyses, parameters, and results. Note that tree length and number of most parsimonious trees (MPTs) are not applicable to Bayesian analyses and that number of Markov Chain Monte Carlo (MCMC) generations is not applicable to parsimony analyses.

<b>Data types</b>	<b># of taxa</b>	<b># of characters</b>	<b>Phylogenetic estimator</b>	<b># of MPTs</b>	<b>Treelength</b>	<b># of mcmc gens.</b>	<b>Alcidae monophyly</b>
<b>ND2</b>	48	1041	parsimony	11	3310	n/a	yes
<b>ND2</b>	48	1041	Bayesian	n/a	n/a	10M	yes
<b>ND5</b>	14	1815	parsimony	13	1167	n/a	no
<b>ND5</b>	14	1815	Bayesian	n/a	n/a	10M	no
<b>ND6</b>	21	522	parsimony	8	1282	n/a	yes
<b>ND6</b>	21	522	Bayesian	n/a	n/a	10M	yes
<b>CO1</b>	40	1551	parsimony	1	2170	n/a	no
<b>CO1</b>	40	1551	Bayesian	n/a	n/a	10M	no
<b>cyt-<i>b</i></b>	52	1143	parsimony	39	2912	n/a	no
<b>cyt-<i>b</i></b>	52	1143	Bayesian	n/a	n/a	10M	yes
<b>12S</b>	50	1053	parsimony	633	1163	n/a	no
<b>12S</b>	50	1053	Bayesian	n/a	n/a	10M	yes
<b>16S</b>	27	1636	parsimony	11	1548	n/a	no
<b>16S</b>	27	1636	Bayesian	n/a	n/a	10M	no
<b>RAG1</b>	45	2871	parsimony	144	993	n/a	yes
<b>RAG1</b>	45	2871	Bayesian	n/a	n/a	10M	yes
<b>Molecular</b>	53	11601	parsimony	1	14125	n/a	yes
<b>Molecular</b>	53	11601	Bayesian	n/a	n/a	10M	yes
<b>Morphol.</b>	53	350	parsimony	2	1645	n/a	yes
<b>Morphol.</b>	53	350	Bayesian	n/a	n/a	50M	yes
<b>Combined</b>	53	11951	parsimony	2	15912	n/a	yes
<b>Combined</b>	53	11951	Bayesian	n/a	n/a	20M	yes

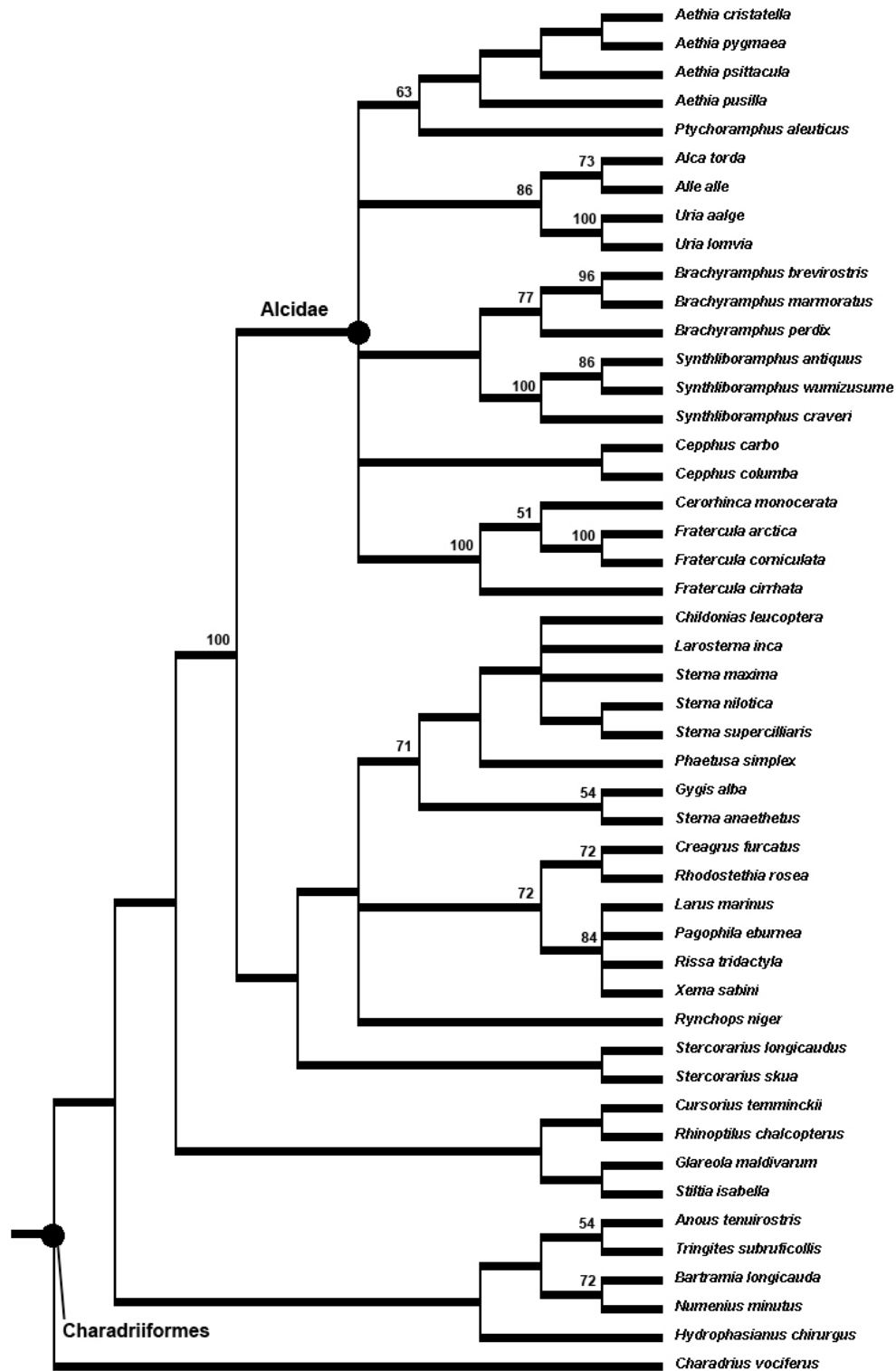


Figure 1.5- Strict consensus cladogram of 11 MPTs from the separate analysis of the ND2 data. Bootstrap values appear above nodes that received greater than 50% support.

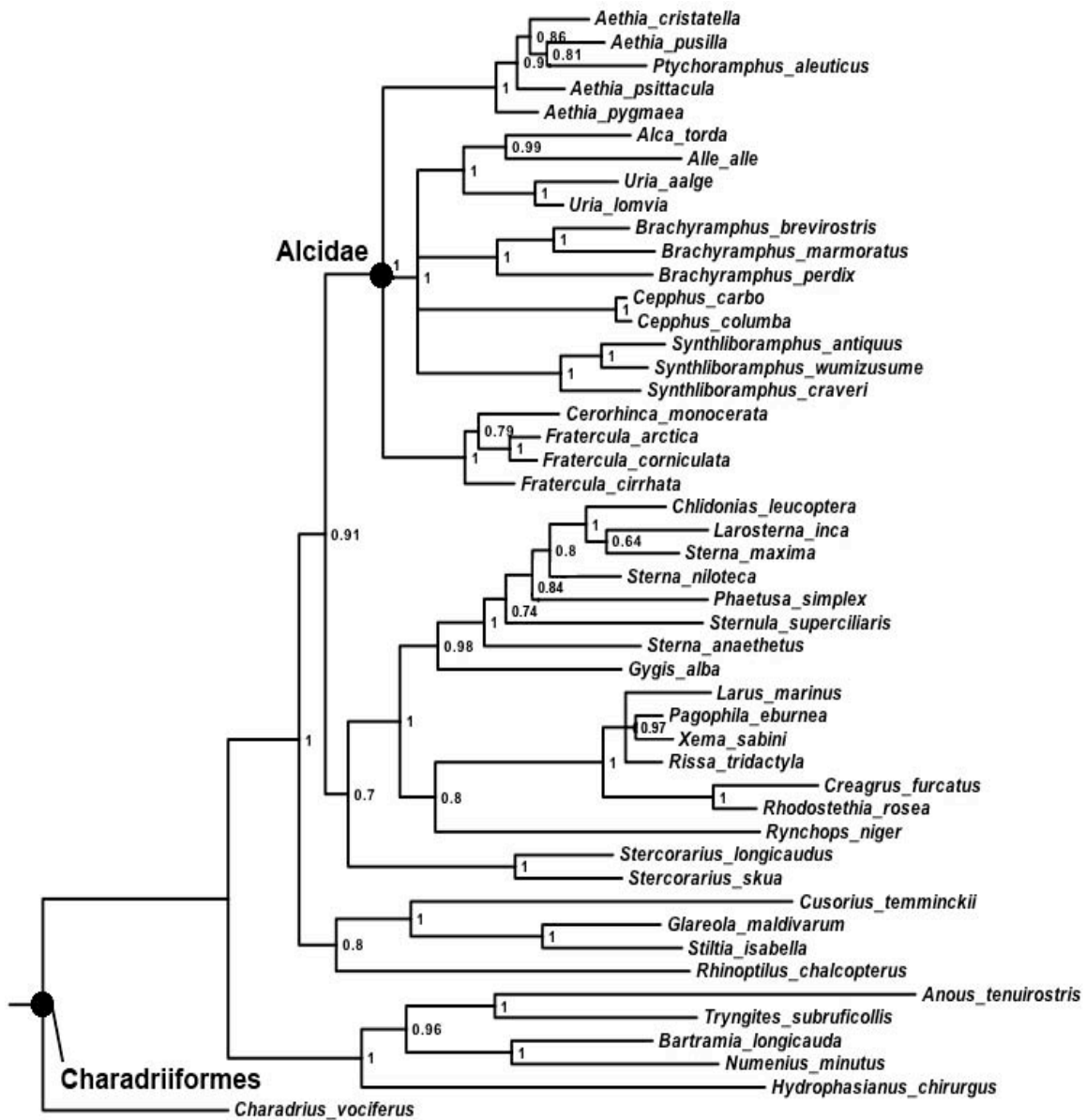


Figure 1.6- Bayesian results from the separate analysis of the ND2 data. Posterior probability values are provided beside nodes.

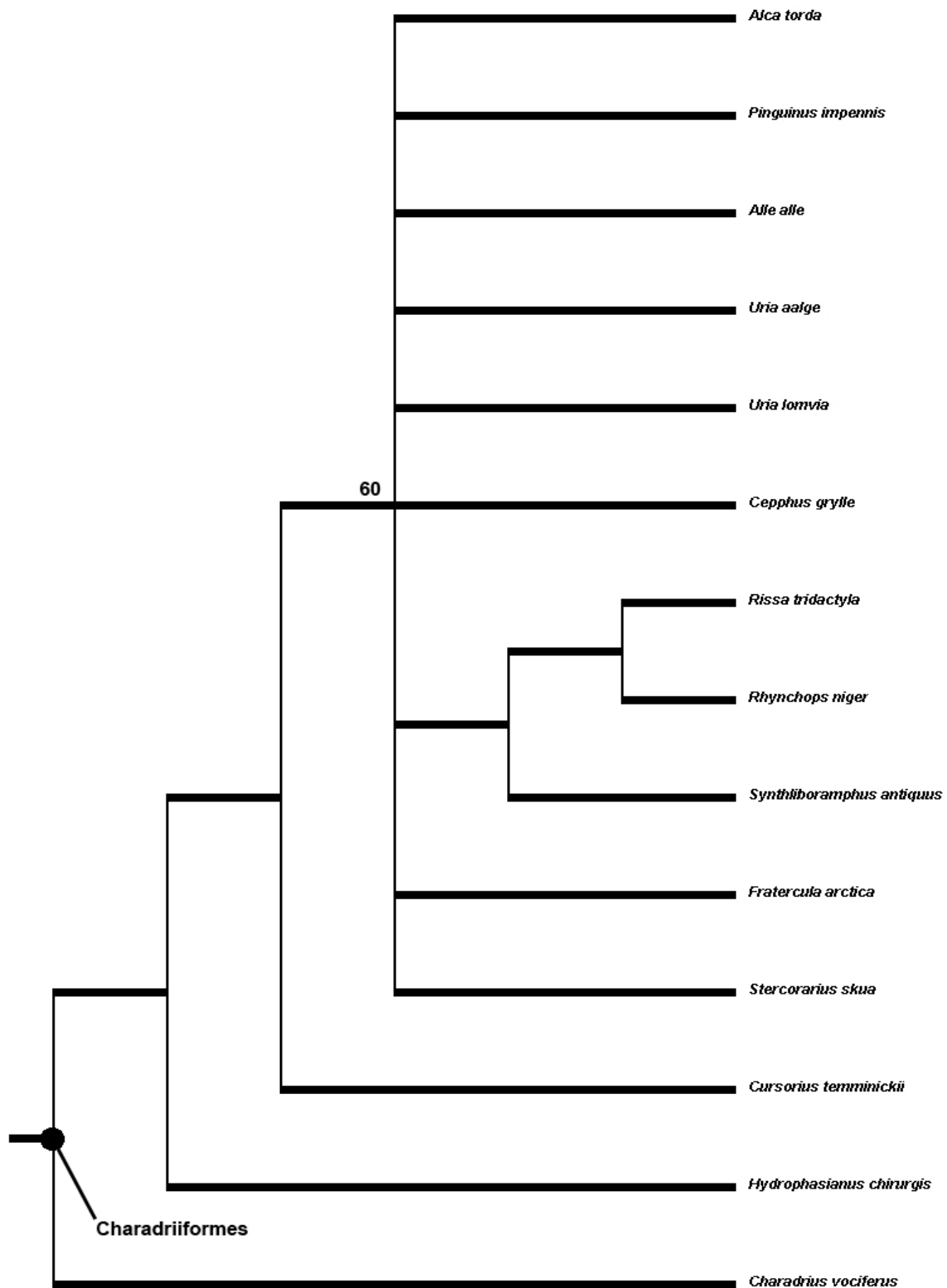


Figure 1.7- Strict consensus cladogram of 13 MPTs from the separate analysis of the ND5 data. Bootstrap values appear above nodes that received greater than 50% support.

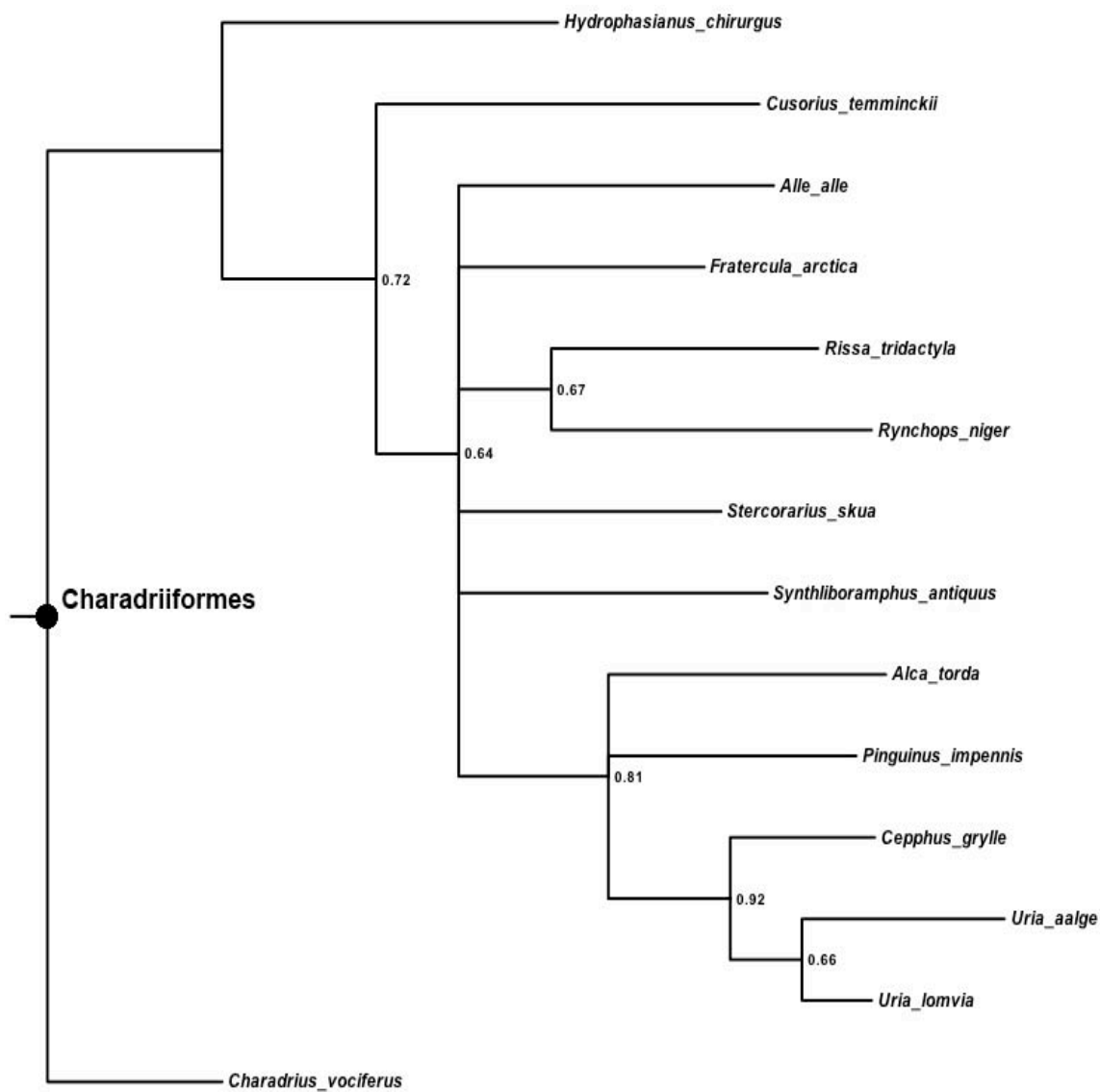


Figure 1.8- Bayesian results from the separate analysis of the ND5 data. Posterior probability values are provided beside nodes.

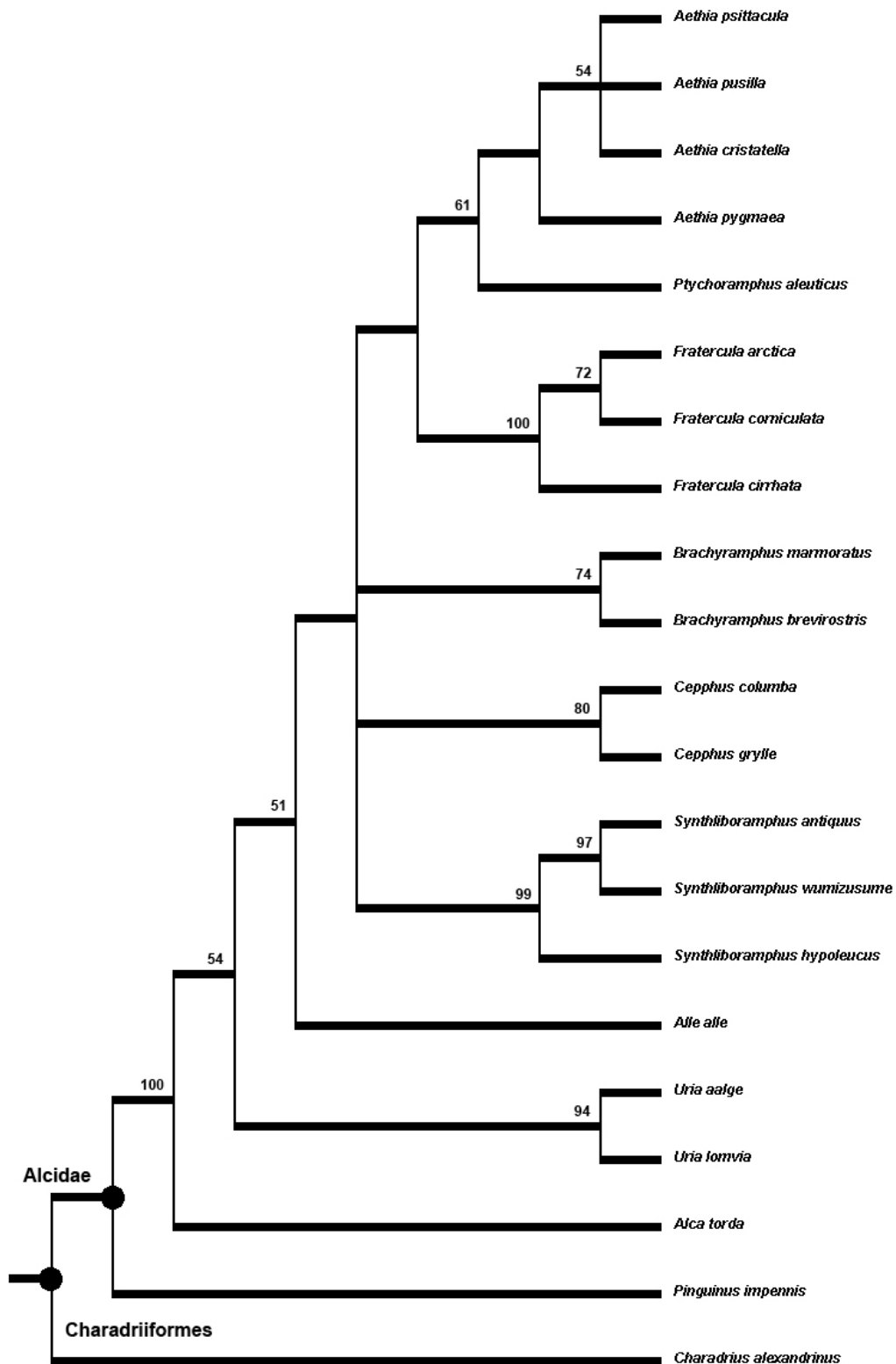


Figure 1.9- Strict consensus cladogram of 8 MPTs from the separate analysis of the ND6 data. Bootstrap values appear above nodes that received greater than 50% support.



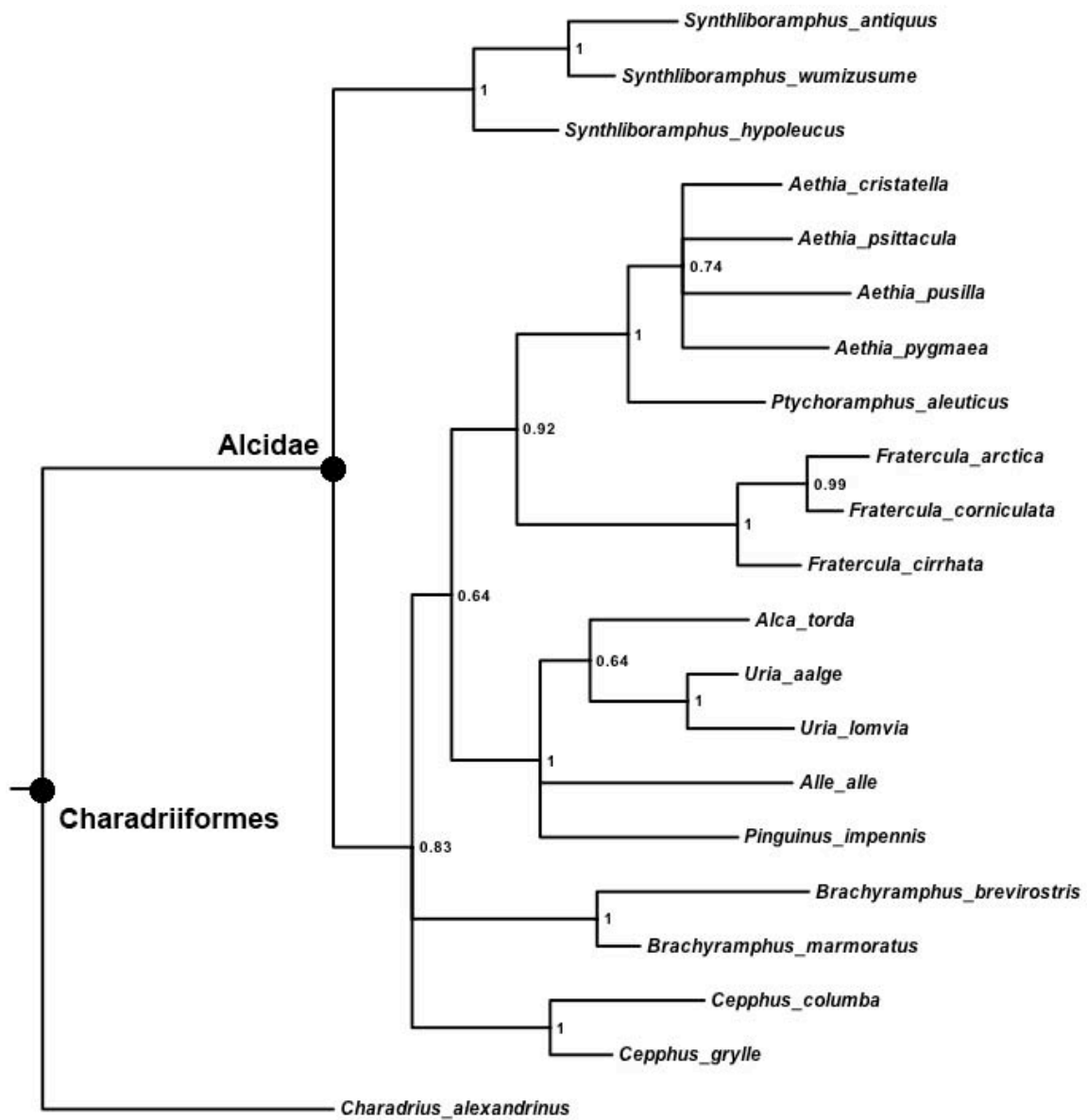


Figure 1.10- Bayesian results from the separate analysis of the ND6 data. Posterior probability values are provided beside nodes.

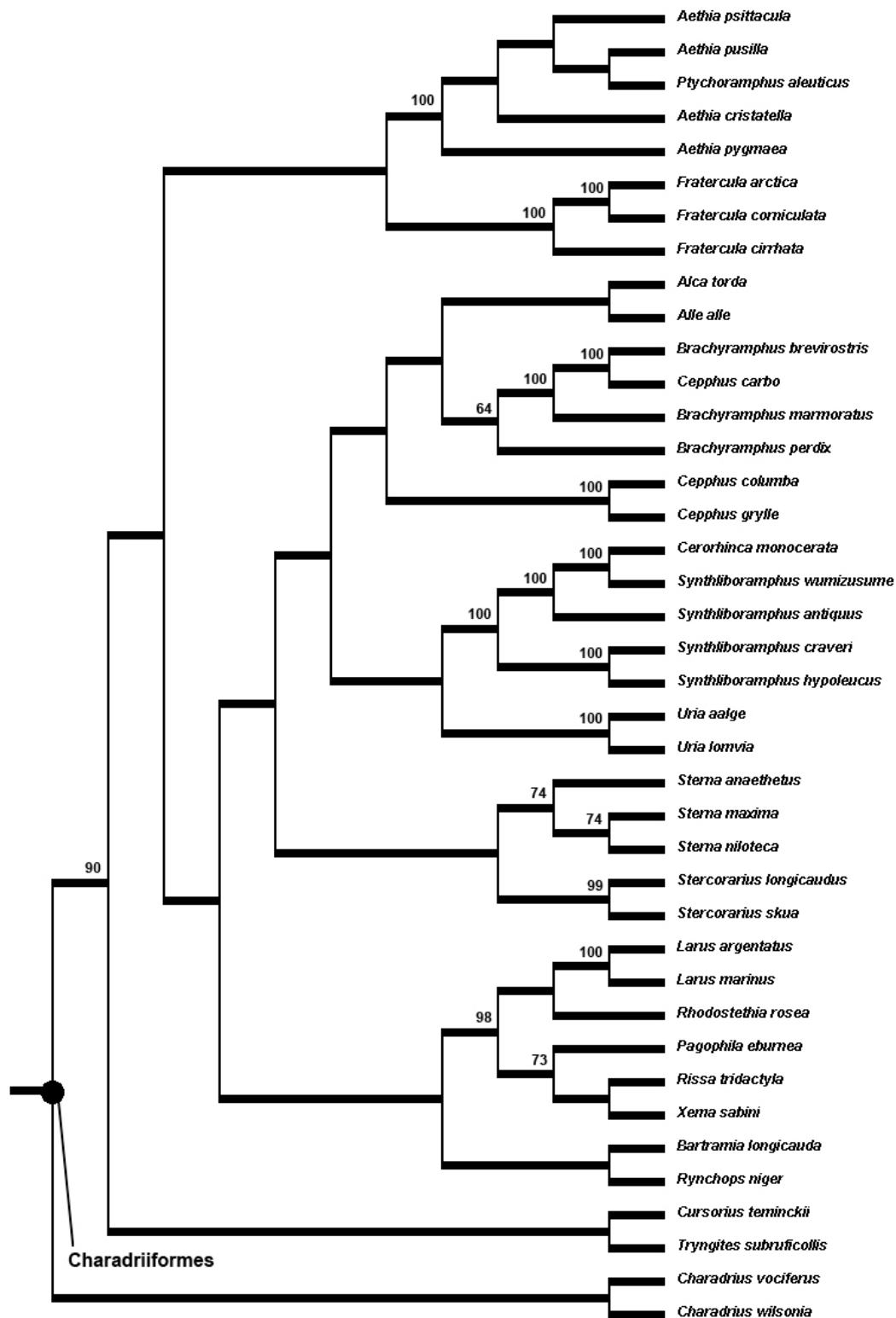
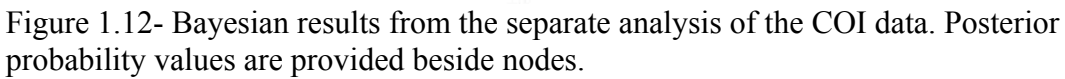


Figure 1.11- Single MPT resulting from the separate analysis of the COI data. Bootstrap values appear above nodes that received greater than 50% support.



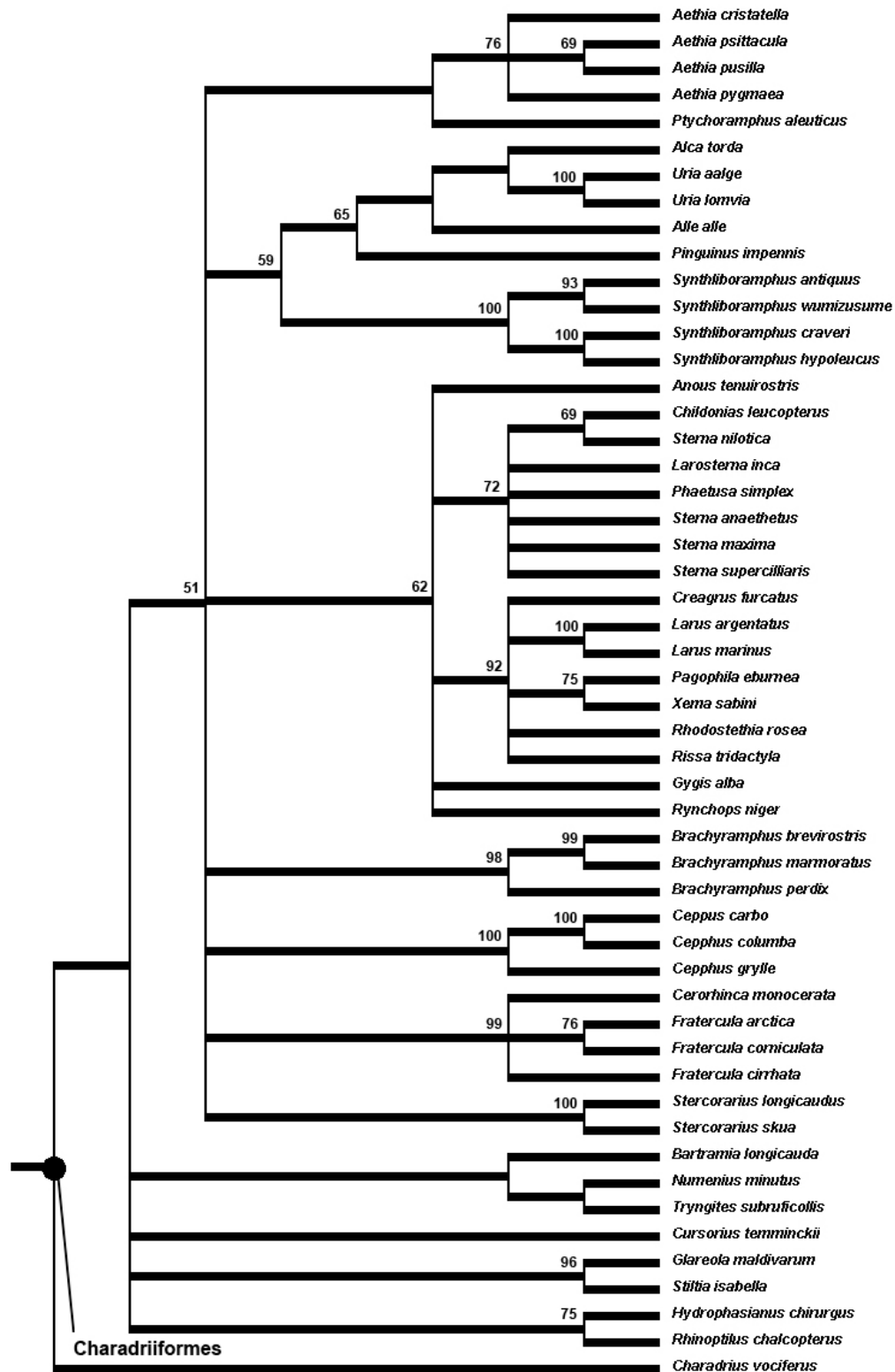


Figure 1.13- Strict consensus cladogram of 39 MPTs from the separate analysis of the *cyt-b* data. Bootstrap values appear above nodes that received greater than 50% support.

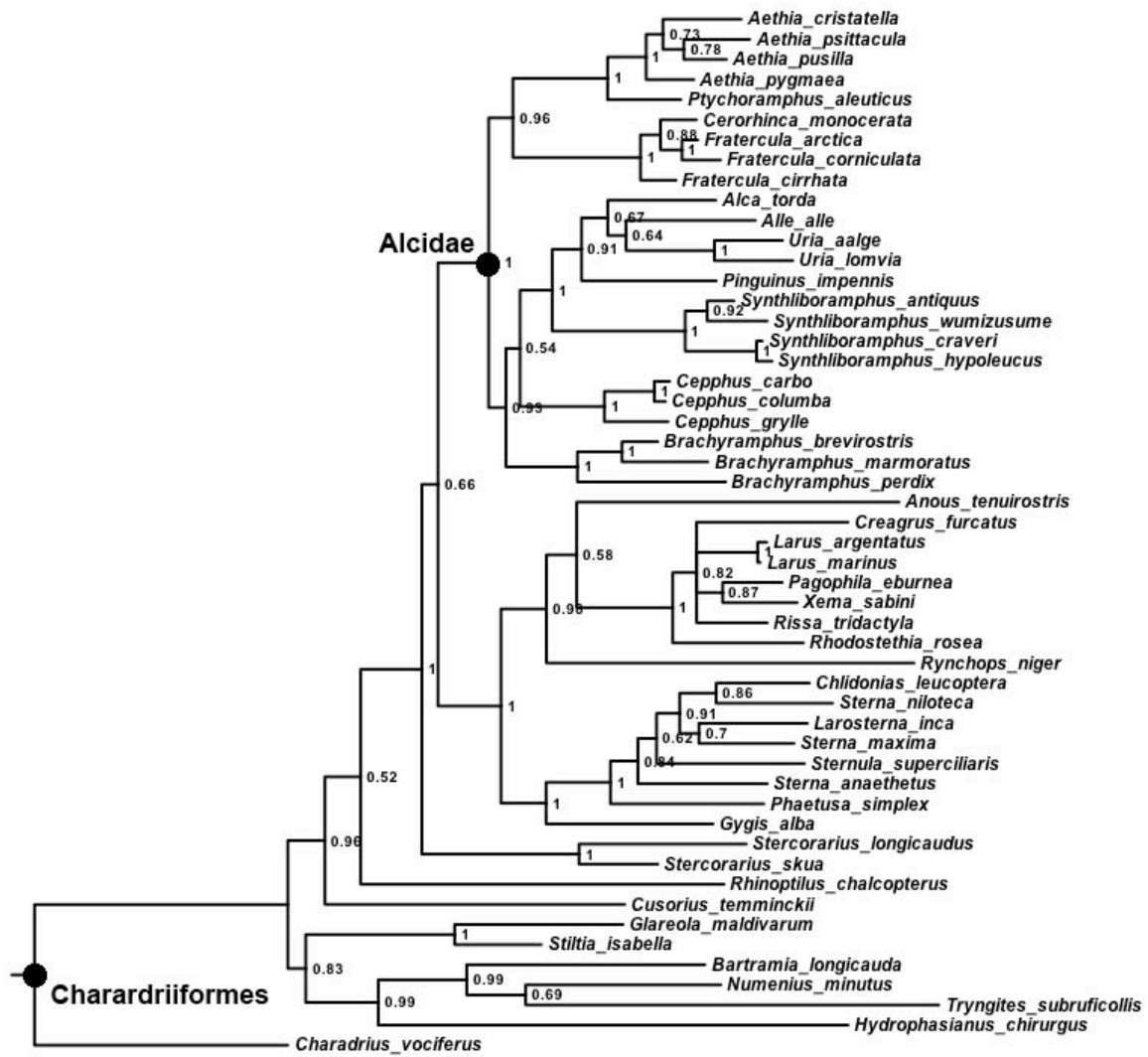


Figure 1.14- Bayesian results from the separate analysis of the *cyt-b* data. Posterior probability values are provided beside nodes.

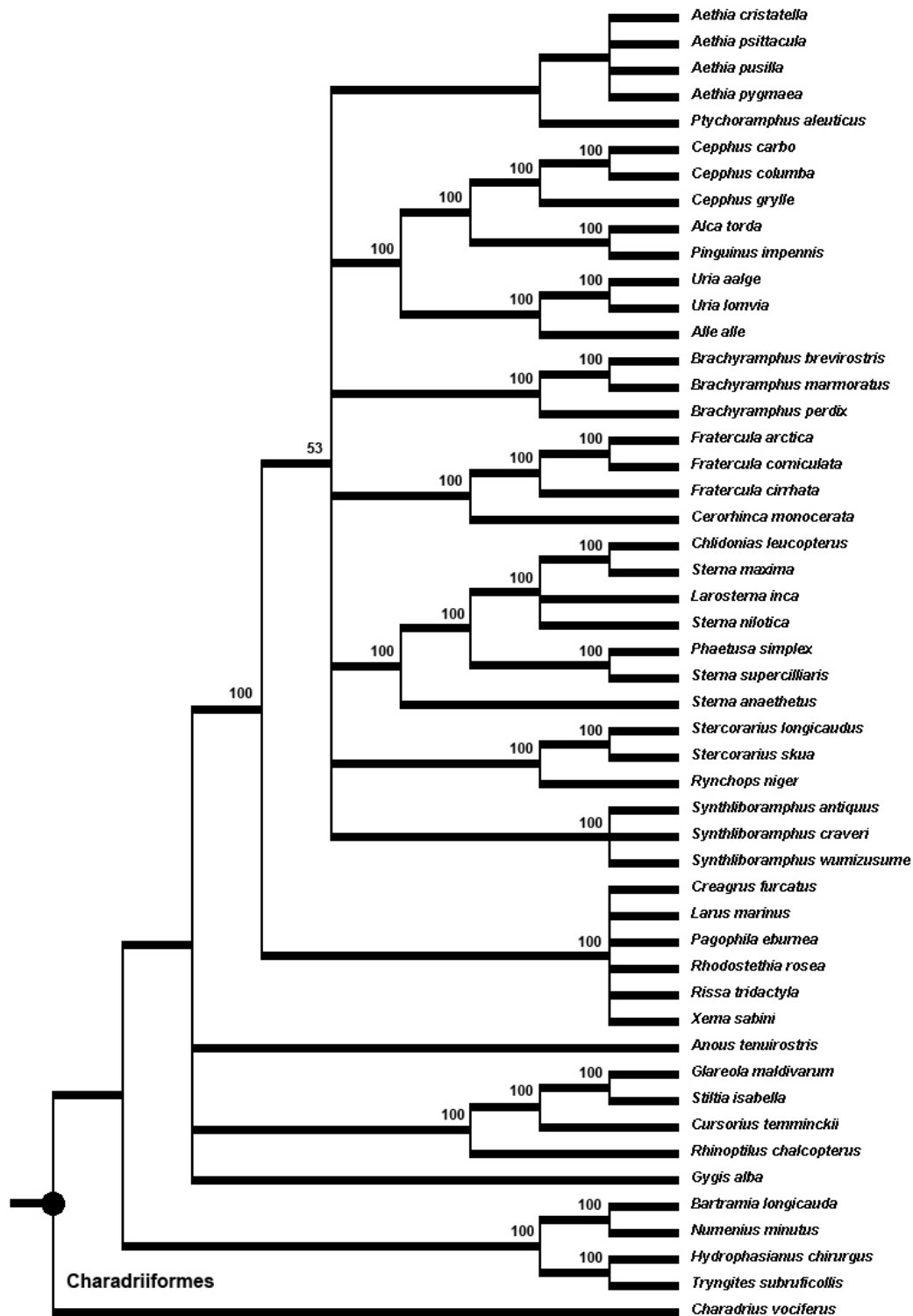


Figure 1.15- Strict consensus cladogram of 633 MPTs from the separate analysis of the 12S data. Bootstrap values appear above nodes that received greater than 50% support.

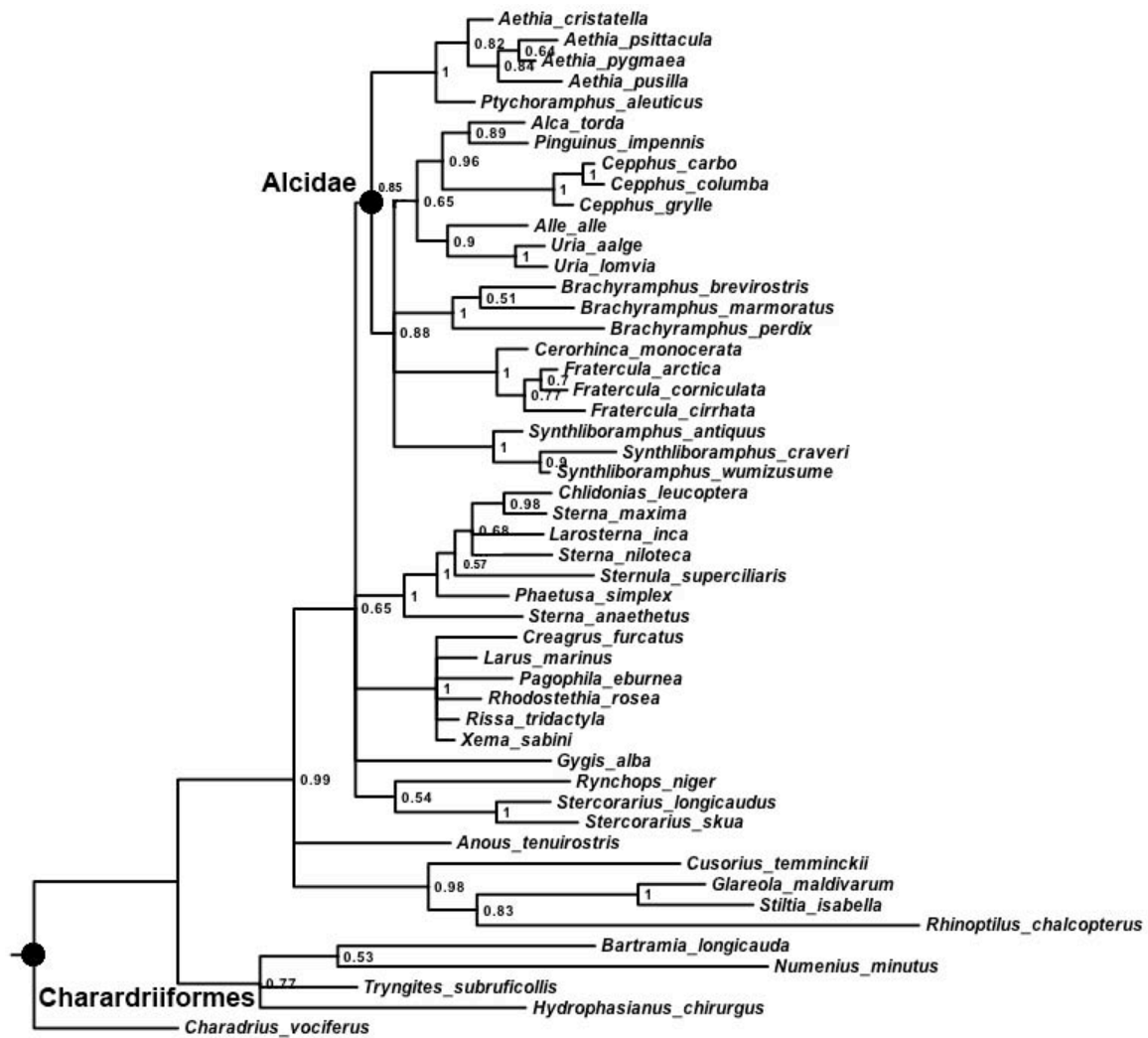


Figure 1.16- Bayesian results from the separate analysis of the 12S data. Posterior probability values are provided beside nodes.

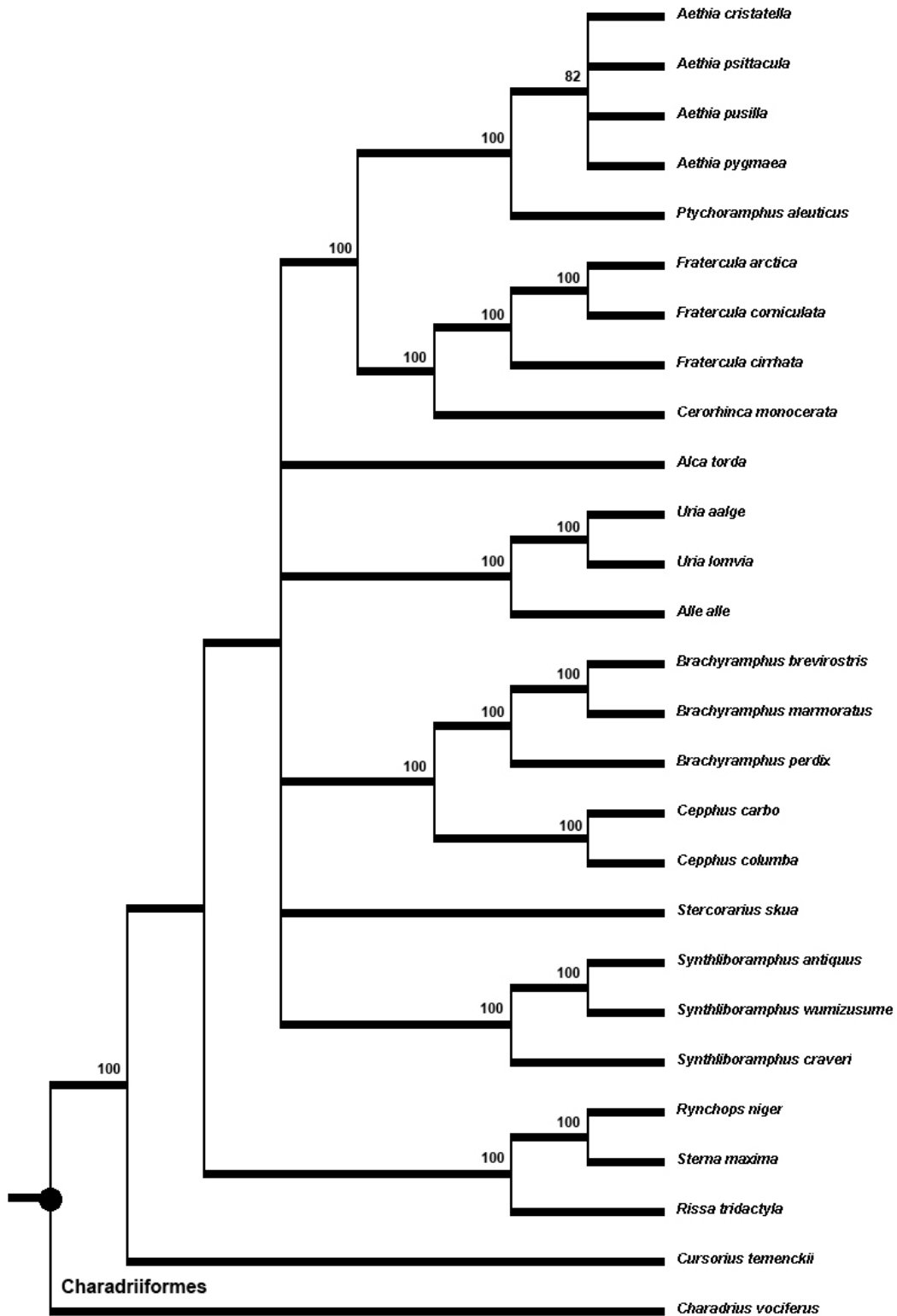


Figure 1.17- Strict consensus cladogram of 11 MPTs from the separate analysis of the 16S data. Bootstrap values appear above nodes that received greater than 50% support.





Figure 1.18- Bayesian results from the separate analysis of the 16S data. Posterior probability values are provided beside nodes.

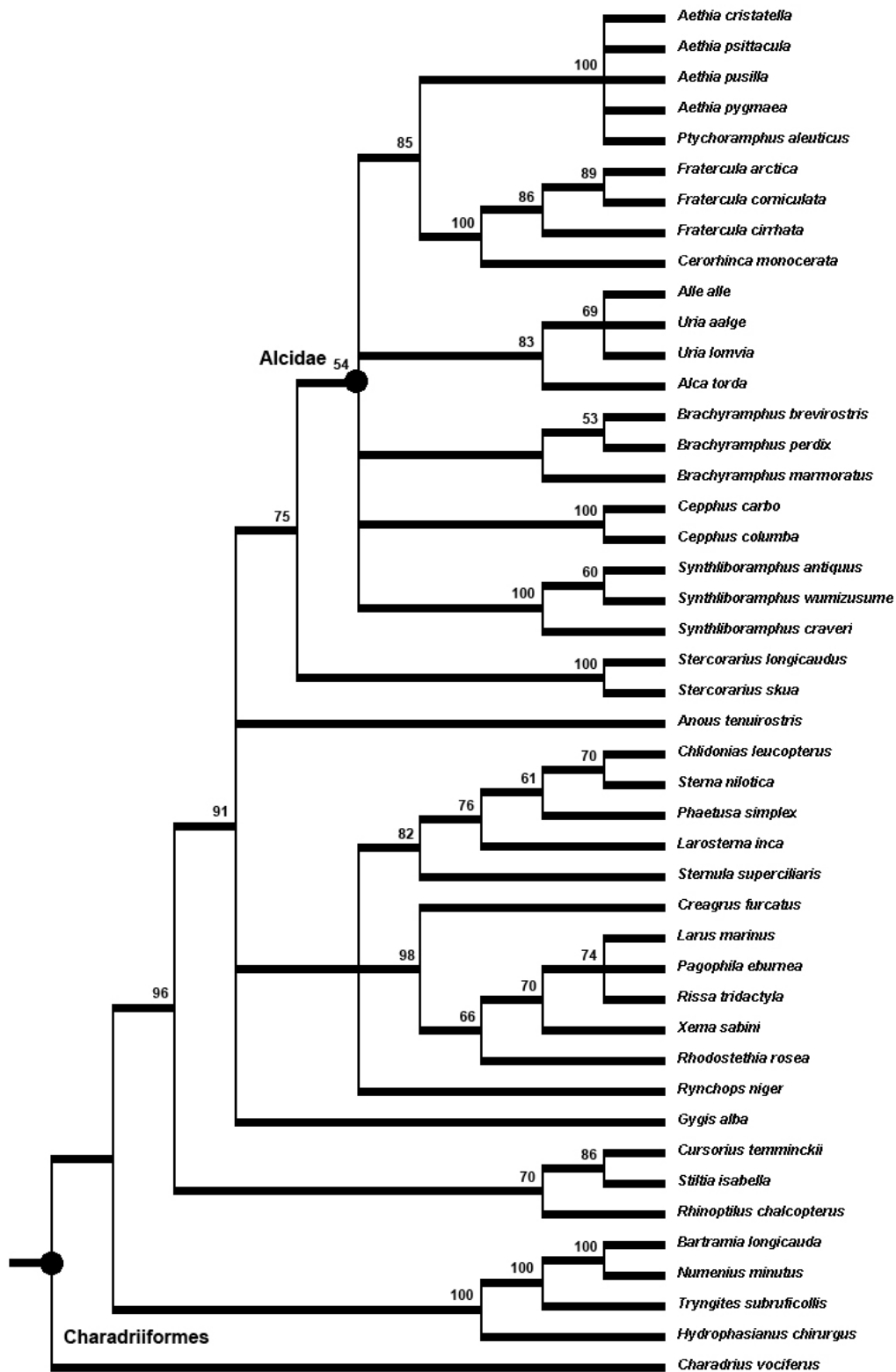


Figure 1.19- Strict consensus cladogram of 144 MPTs from the separate analysis of the RAG1 data. Bootstrap values appear above nodes that received greater than 50% support.

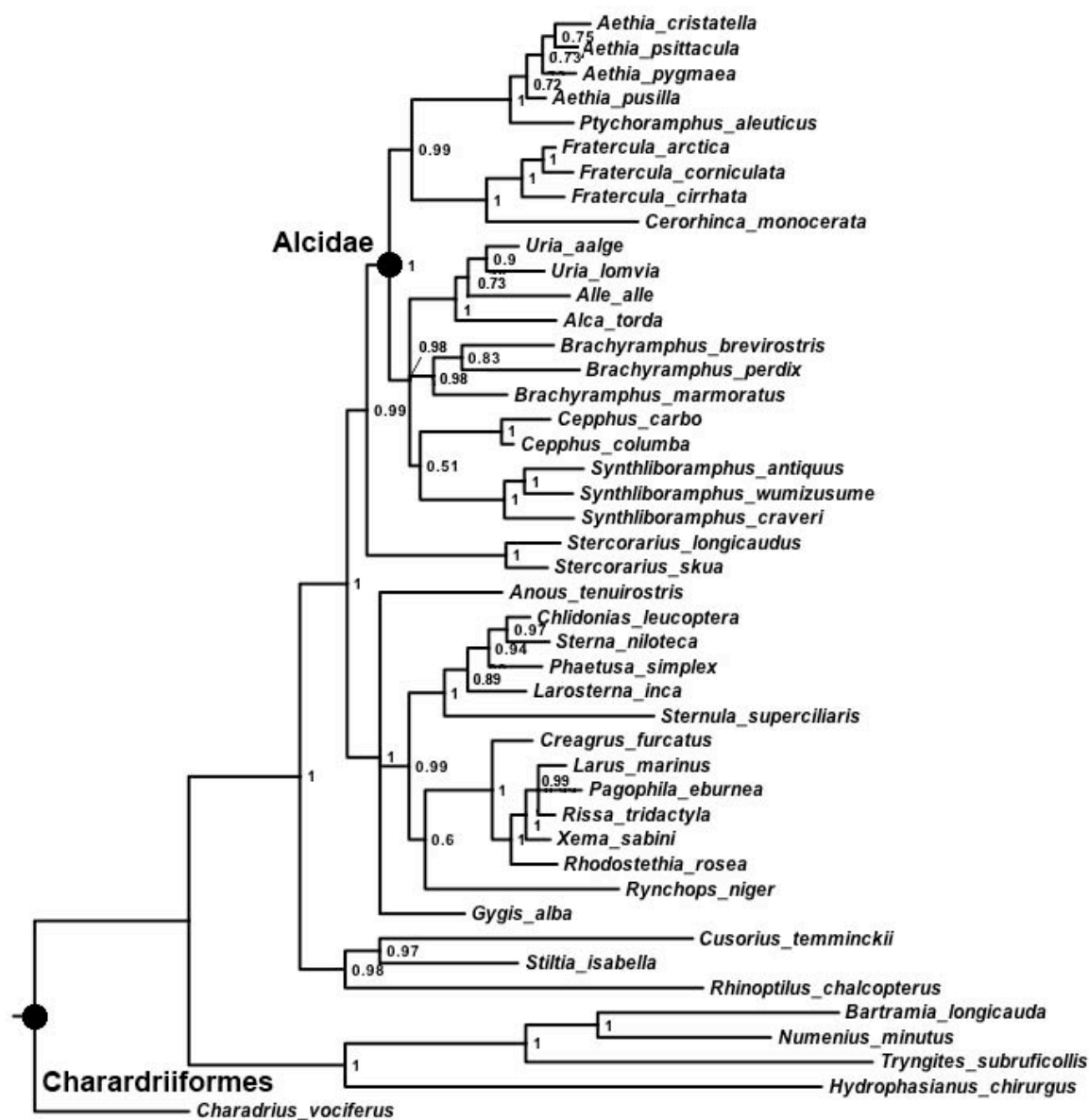


Figure 1.20- Bayesian results from the separate analysis of the RAG1 data. Posterior probability values are provided beside nodes.

Results of the combined analysis of the concatenated molecular data (ND2, ND5, ND6, COI, *cyt-b*, 12S, 16S, RAG1) using parsimony and Bayesian estimation approaches recovered fully resolved trees with relationships that are consistent with other recent molecular-based hypotheses for alcid and outgroup charadriiform relationships (Baker et al., 2007; Pereira and Baker, 2008; Table 1.4; Figs. 1.21 & 1.22). The parsimony-based topology received relatively high levels of bootstrap and Bremer support (Fig. 1.21), and the Bayesian topology was also supported by relatively high posterior probabilities (Fig. 1.22). Alcidae was recovered as monophyletic in both analyses. One significant topological difference between the Bayesian and parsimony-based topologies is the placement of *Synthliboramphus*. In the parsimony-based tree *Synthliboramphus* is placed as the sister taxon to the remainder of Alcinae (Fig. 1.21), whereas in the Bayesian topology *Synthliboramphus* is placed in a more derived position as the sister taxon to Alcini (Fig. 1.22). These placements for *Synthliboramphus* also were recovered in two equally-most-parsimonious topologies in the results obtained by Pereira and Baker (2008). Furthermore, in the parsimony-based topology, *Brachyramphus* and *Cepphus* form a clade that is the sister to Alcini (Fig. 1.21). In the Bayesian topology *Cepphus* and *Brachyramphus* are placed in successively basal positions to an Alcini + *Synthliboramphus* clade (Fig. 1.22). Additionally, the position of *Alle alle* varies from sister to *Alca torda* + *Pinguinus impennis* in the parsimony-based topology (Fig. 1.21), to sister to *Uria* in the Bayesian topology (Fig. 1.22).

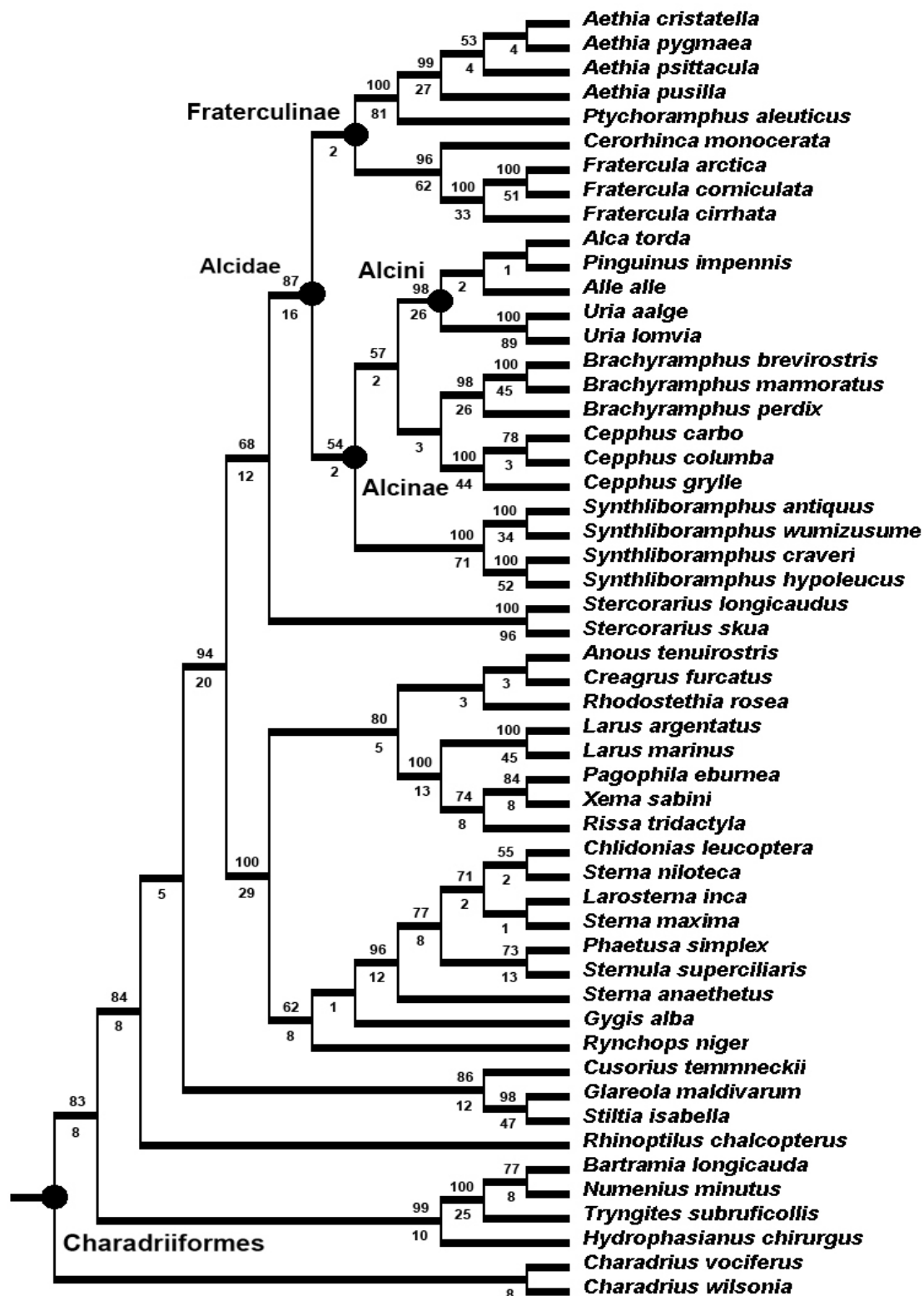


Figure 1.21- Single MPT resulting from the combined analysis of the molecular data. Bootstrap (>50) and Bremer support values appear above and below nodes respectively.

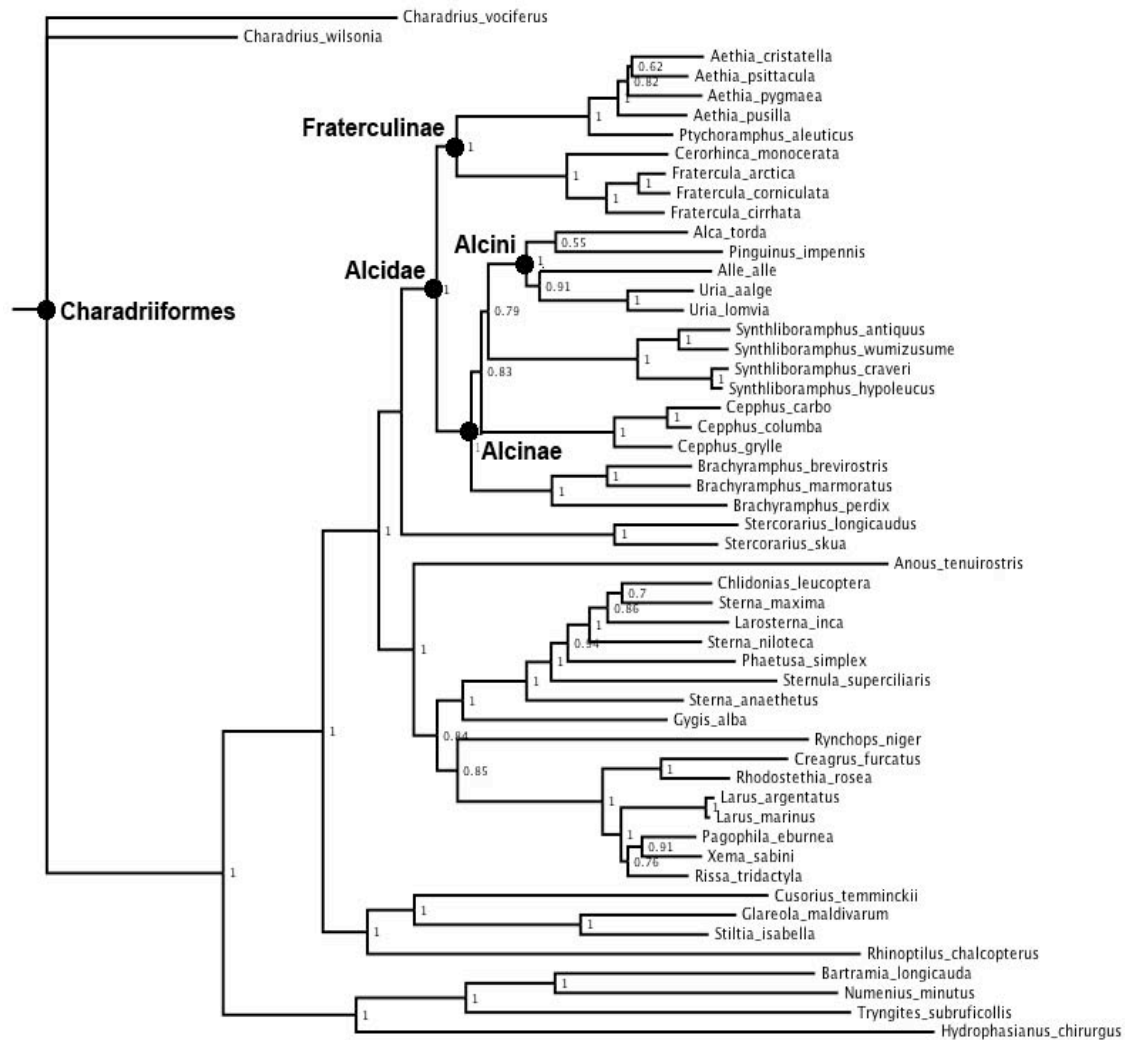


Figure 1.22- Bayesian results from the combined analysis of the molecular data (ND2, ND5, ND6, CO1, CYTB, 12S, 16S, RAG1). Posterior probability values are provided beside nodes. Note that Alcidae monophyly is recovered and that Stercorariidae is recovered as the sister taxon to Alcidae.

The results of the Bayesian and parsimony-based analyses of the morphological data contrasted with respect to hypotheses of relationships, degree of resolution, and levels of tree support. The parsimony-based topology was fully resolved but received relatively low levels of bootstrap support (Fig., 1.23). However, Bremer support values for nearly all nodes are quite high. Whereas the results of both analyses support Alcidae monophyly, relationships among the outgroup taxa in the Bayesian topology are largely unresolved and posterior probability values are low (Fig. 1.24).

Hypothesized relationships resulting from the parsimony-based analysis of the morphology-only data are congruent with the parsimony-based analysis of the molecular data except for the relative placement of *Brachyramphus*, *Synthliboramphus*, and *Cepphus* relative to Alcini (Fig., 1.23). Additionally, in contrast with the parsimony-based combined molecular analysis results, *Stercorarius* is not placed as the sister taxon to Alcidae. Instead, *Stercorarius* is placed as the sister taxon to a Laridae + Sternidae + *Rynchops* + *Anous* clade, a result which is largely consistent with previous morphology-based analyses of charadriiform relationships (Chu, 1995; Livezey, 2009, 2010). The potentially aberrant placement of *Ptychoramphus aleuticus* nested within *Aethia*, rather than as the sister taxon to *Aethia*, is not supported by the results of other previous analyses (Strauch, 1985; Chandler, 1990a; Thomas et al., 2004; Pereira and Baker, 2008).

The Bayesian analysis of the morphological data produced results that are inconsistent with previous estimates of alcid relationships in that *Brachyramphus*, *Synthliboramphus*, and *Aethia* all are recovered as paraphyletic assemblages (Fig. 1.24). Additionally, the placement of *Numenius minutus* as the sister taxon to Alcidae is a novel hypothesis for the systematic position of that taxon.

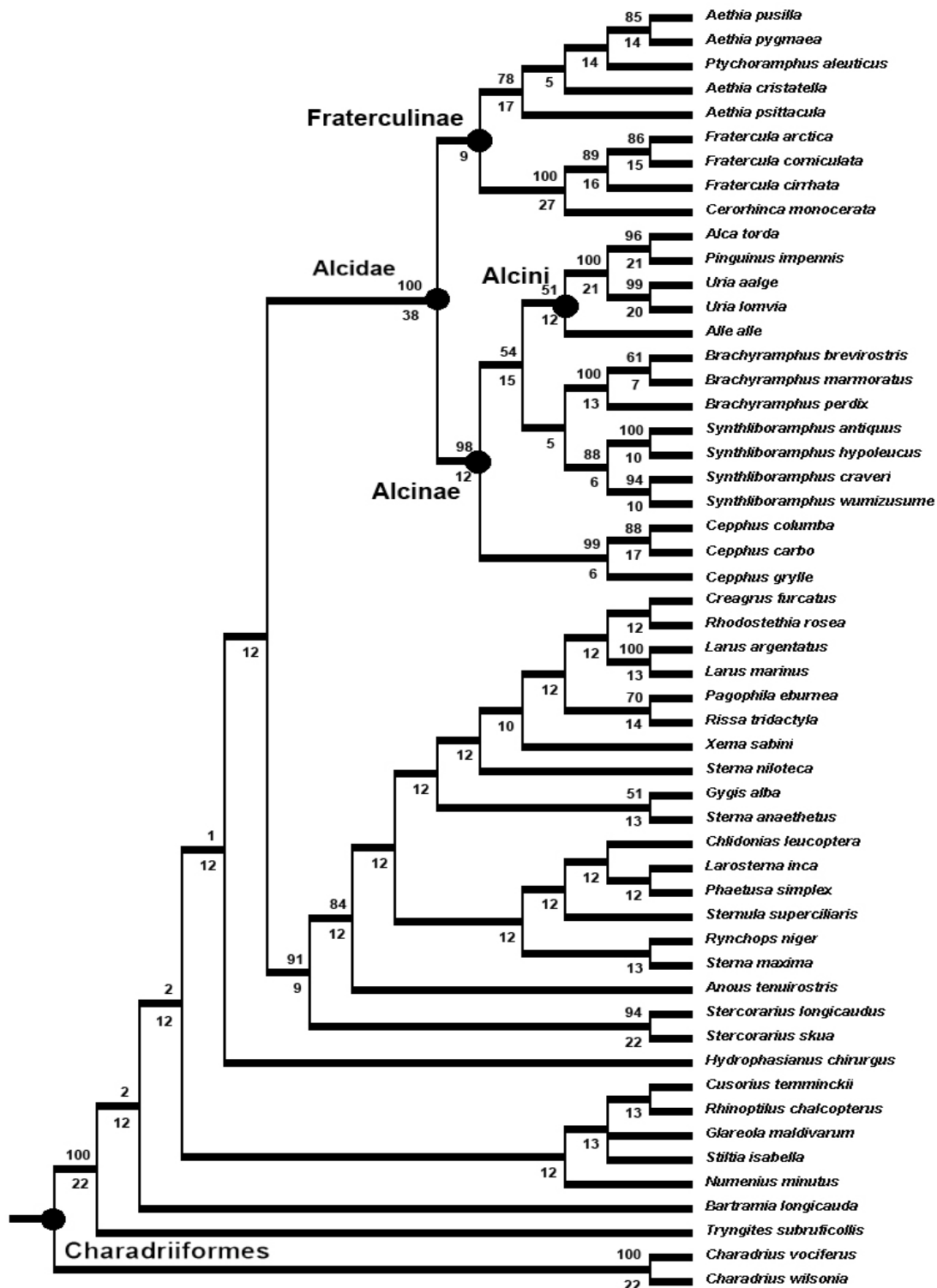


Figure 1.23- Strict consensus cladogram of 2 MPTs resulting from the separate analysis of the morphological data. Bootstrap (>50) and Bremer support values appear above and below nodes respectively.



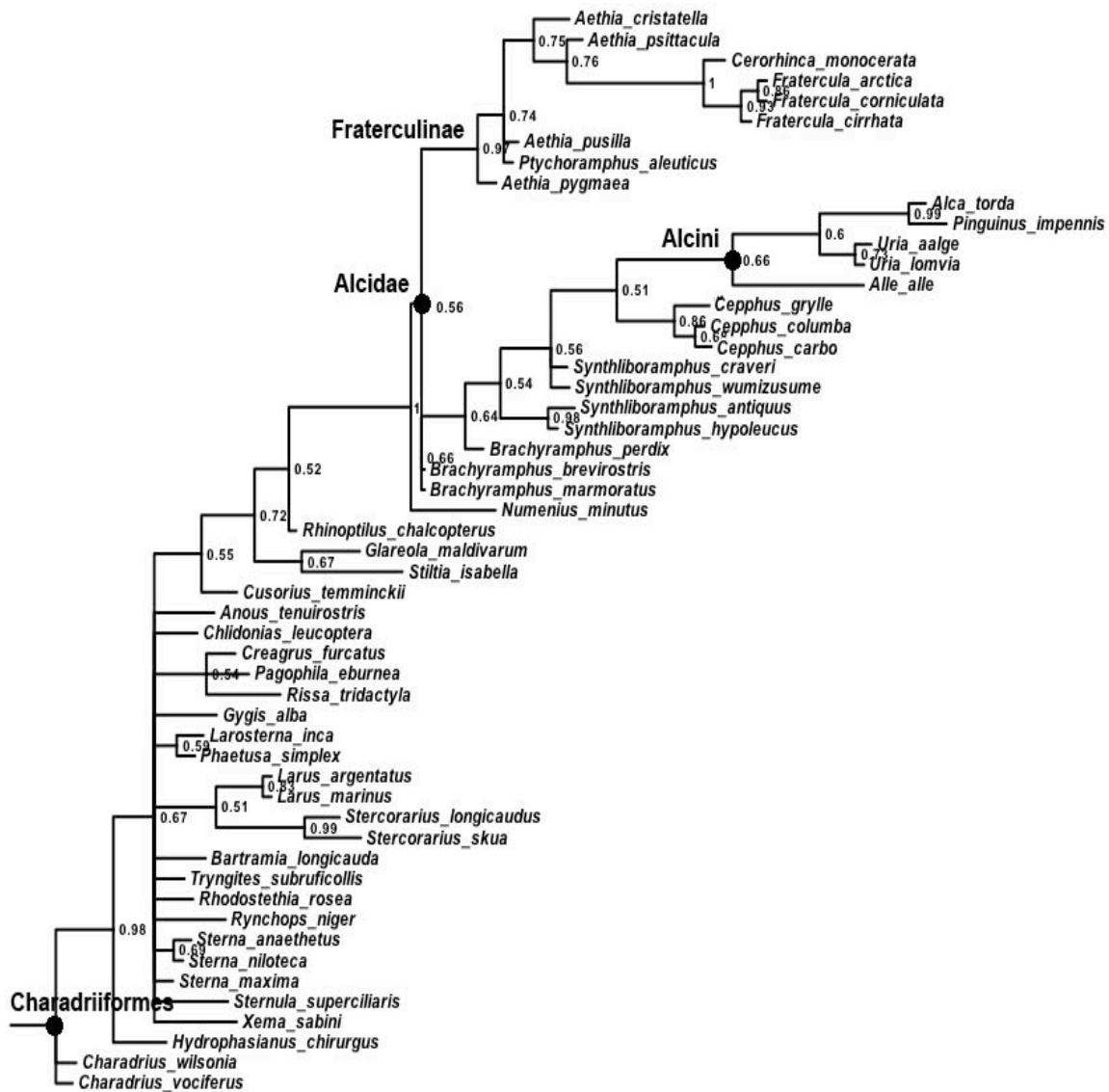


Figure 1.24- Bayesian topology resulting from the separate analysis of the morphological data. Posterior probability values are provided beside nodes.

The parsimony-based and Bayesian combined analyses the morphological and molecular data resulted in trees that are largely congruent with one another and with recent molecular-based hypotheses of charadriiform relationships (Baker et al., 2007; Pereira and Baker, 2008; Figs. 1.25 & 1.26). These results do, however, contrast with previously published morphology-based results that placed Alcidae as the sister taxon to a Stercorariidae + Rynchopidae + Laridae clade (Livezey, 2010), or as the sister taxon to all other Charadriiformes (Strauch, 1978; Björklund, 1994; Chu, 1995). The parsimony-based and Bayesian topologies are resolved, with relatively high levels of bootstrap and Bremer support values, and posterior probabilities respectively. Alcid monophyly is supported by the results of both analyses.

With respect to alcid relationships, topological differences between the parsimony-based and Bayesian combined analysis topologies are relatively limited. However, *Cepphus* is placed as the sister to Alcini (*Alca* + *Pinguinus* + *Alle* + *Uria*) in the parsimony-based topology (Fig. 1.25), whereas *Cepphus* is placed as the sister to all other Alcinae (Alcini + *Brachyramphus* + *Sythliboramphus*) in the Bayesian topology (Fig. 1.26). Although *Alle alle* is recovered as the sister taxon to all other Alcini in the Bayesian topology, the position of *Alle alle* remains unresolved within Alcini in the parsimony-based topology. Finally, *Aethia pygmaea*, rather than *Ptychoramphus*, is the sister to the other Aethiini in the Bayesian results.

Outgroup charadriiform relationships differ in the positions of two taxa. *Rynchops niger* is placed as the sister taxon to *Gygis alba* in the parsimony-based topology, whereas *Rynchops niger* is recovered as the sister taxon to the Laridae in the Bayesian topology, a position that is congruent with its position in recent molecular-based analyses

(Paton et al. 2003, Baker et al. 2007). *Rhinoptilus chalcopterus* is placed as the sister taxon to the rest of the Glareolidae in the Bayesian topology (Fig. 1.26); however, it is placed outside of Glareolidae as the sister taxon to Glareolidae plus the rest of Charadriiformes in the parsimony-based analysis (Fig. 1.25).

*Anous minutus* was recovered as the sister taxon to Sternidae + Laridae + *Rynchops*. Glareolidae, Scolopacidae, and Charadriidae (represented only by *Charadrius*) are placed in successively more basal positions to Alcidae and relatives in the parsimony-based and Bayesian topologies. *Anous* is placed in Sternidae in recent classifications (American Ornithologists' Union, 1998) and this placement was supported by the results of a previous phylogenetic analysis (Bridge et al., 2005).

The monophyly of extant Alcidae is supported by 12 unambiguously optimized apomorphies with a consistency index (CI) of 1.0: quadrate apneumatic (39:1) as opposed to the pneumatized quadrates of other charadriiforms; pygostyle with relatively straight dorsal margin rather than dorsally expanded as in other charadriiforms (58:0); furcula sharply curved proximal to the coracoidal facet and distal extremity (78: 1) rather than gently sloping as in other charadriiforms; scapular tuberosity of furcula separate from and anterior to the coracoidal facet (80:1) rather than contacting the coracoidal facet; ventral condyle of the humerus anteriorly flattened (157:1) rather than rounded; bicipital tubercle of radius rounded (166:1) rather than distally elongated; dorsal cotylar process of the ulna projects farther anteriorly than that of other charadriiforms (176:1); ulnar quill knobs reduced to impressions (181:1) rather than distinct raised knobs; barbule base length continuous with pennulum (307:2); barbule base cells not visible (308:0); proximal node shape straight (318:3); midsection node shape straight (319:3). Note, however, that

feather microstructure characters 307, 308, 318, and 319 were only scored for 30 of 53 taxa.

Table 1.5- Apomorphies supporting clade monophyly in the resultant Bayesian and parsimony-based combined analysis topologies (Figs. 1.25 & 1.26). Character numbers from Appendix 2 are followed by character state symbols (e.g., 23:0 = character 23, state 0). ‘\*’ represents locally optimized apomorphies with a CI < 1.0. All other apomorphies have a CI = 1.0.

Clade	Character numbers and states that support monophyly
Alcidae + Stercorariidae	324:1; 352:1.
Alcidae	39:1; 58:0; 78: 1; 80:1; 157:1; 166:1; 176:1; 181:1; 307:2; 308:0; 318:3; 319:3.
Alcinae	50:1; 279:1.
Fraterculinae	61:1.
Fraterculini	30:1; 41:1; 115:0; 295:1; 296:1.
Aethiini	8:1; 11:1; 89:0.
Alcini	21:1; 191:1; 246.
<i>Alca</i> + <i>Pinguinus</i>	122:0.
<i>Uria</i>	*35:0; *97:0; *101:1; *106:0; *205:0; *233:2.
<i>Cepphus</i>	184:1.
<i>Brachyramphus</i>	98:1; 158:1.
<i>Synthliboramphus</i>	*15:1; *216:0; *230:1; *231:0; *273:1; 275:1.
<i>Fratercula</i>	259:1.

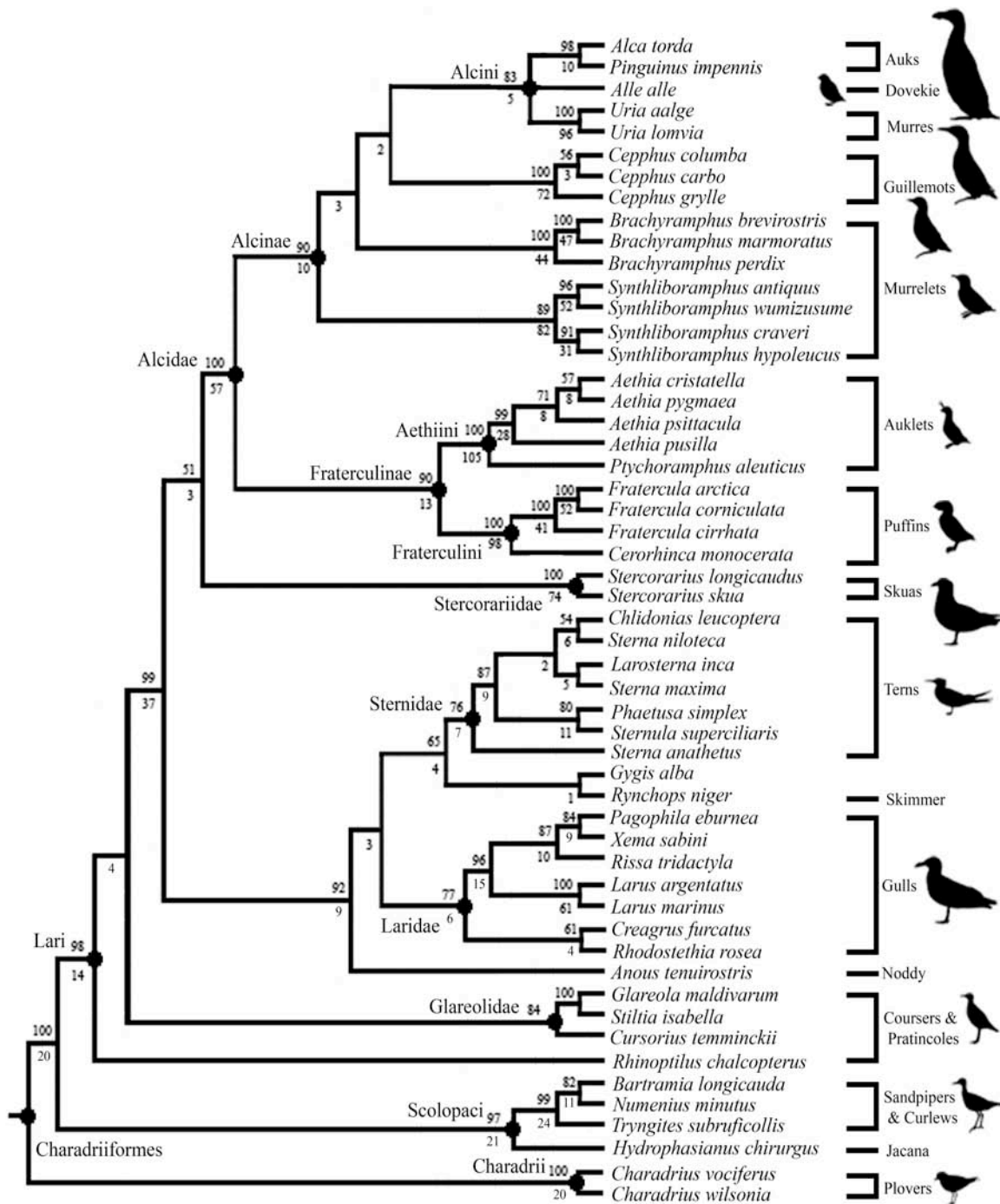


Figure 1.25- Parsimony-based strict consensus cladogram resulting from the combined analysis of molecular and morphological data (2 MPT's, L:15912; CI:0.38; RI:0.50; RC:0.19). Bootstrap (>50) and Bremer support values appear above and below nodes respectively.

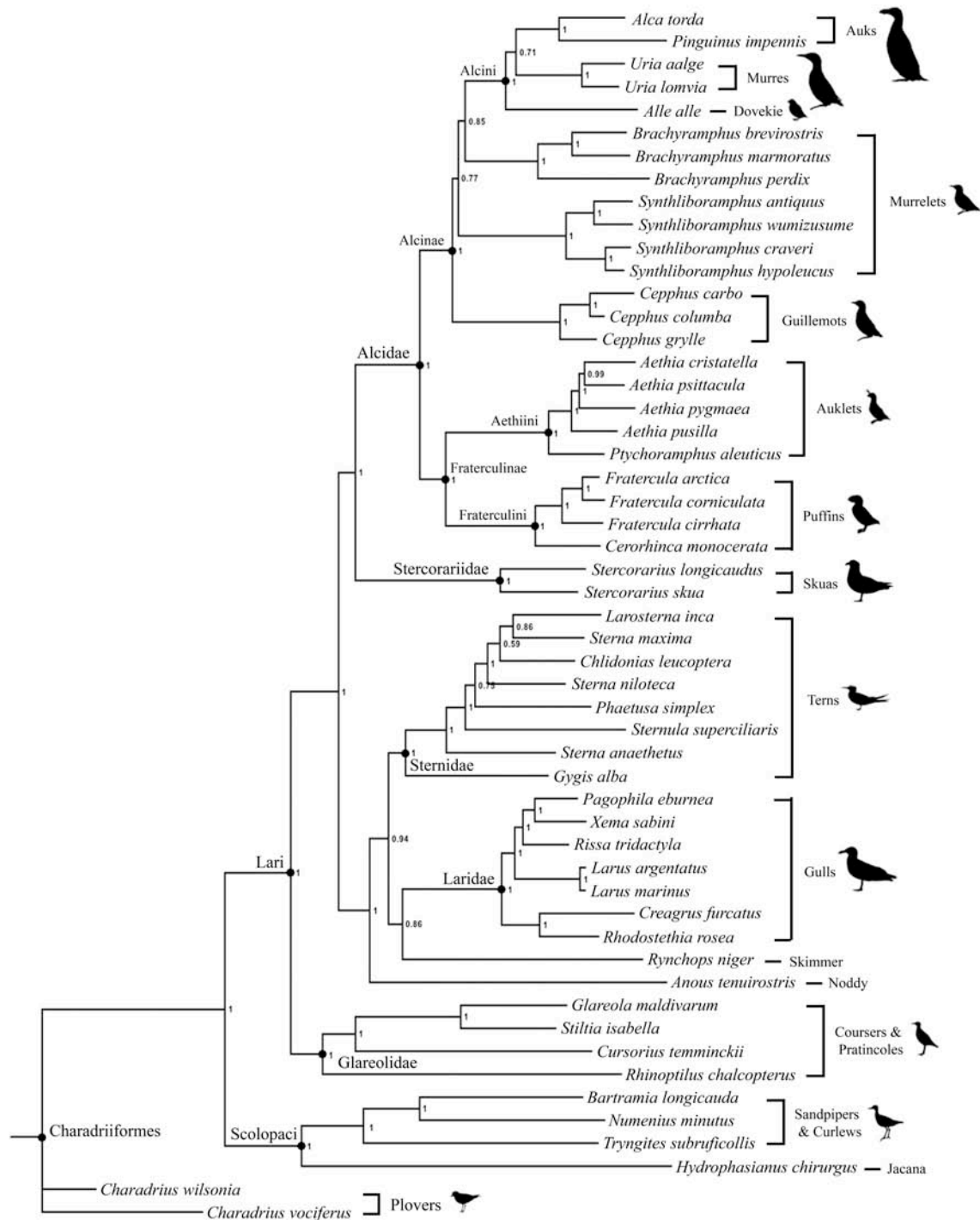


Figure 1.26- Bayesian topology resulting from the combined analysis of molecular and morphological data. Posterior probability values are provided beside nodes.

## DISCUSSION

Based on the relative resolution of deep and shallow nodes in recovered trees, individual genes appear to have contributed unequally to resolution at different levels of the combined tree. Visual examination of the resultant single-gene trees revealed that deep nodes (i.e., relationships between major alcid clades such as *Cepphus* and *Brachyramphus*) were relatively well resolved in the parsimony-based analyses of the COI tree and in the Bayesian COI, RAG-1 and *cyt-b* trees. Shallower nodes (i.e., species relationships within sub-clades such as *Aethia*) were relatively more resolved than deeper nodes in the results of the parsimony-based analyses of the ND2 and ND6 data, and in the Bayesian analysis results of the ND2, 12S, and 16S data. This may be a reflection of potential rate heterogeneity among the different genes analyzed; however, the different phylogenetic estimation methods applied may also be a contributing factor to this disparity.

Aethiini relationships (*Aethia* and *Ptychoramphus*) were unresolved in the results of the parsimony-based analyses of the *cyt-b*, 12S, 16S, and RAG-1 data, and in the results of the Bayesian analyses of the ND6 and COI data. It has been suggested that ancestral DNA polymorphism or incomplete lineage sorting may be responsible for the variable placements recovered for *Aethia* species in previous phylogenetic analyses (Walsh and Friesen, 2003; Walsh et al., 2005). In contrast, *Ptychoramphus* was consistently recovered as the sister taxon to the other auklets (i.e., *Aethia*; Watada, 1987; Chandler 1990a; Moum et al., 1994; Friesen et al., 1996; Thomas et al., 2004; Baker et al., 2007; Pereira and Baker, 2008). *Ptychoramphus* was recovered as the sister taxon to

*Aethia* in the parsimony-based results of the analysis of the *cyt-b*, 12S, and 16S data, and in the Bayesian results from the analysis of the ND6 data.

The strict consensus cladogram resulting from the parsimony-based analysis of the morphological data was resolved (Fig. 1.23) with the exception of a single outgroup polytomy (2 MPTs). In contrast, the Bayesian topology resulting from the morphology-only analysis is considerably less resolved. The lack of resolution in the Bayesian topology is puzzling given the well-resolved parsimony-based topology. Although a more detailed assessment would be needed to draw conclusions with any certainty, the lack of resolution in the results of the Bayesian analysis of morphology (Fig. 1.24) is potentially indicative of limits of the Mk model (Lewis, 2001a) in the context of large, complex morphological sets of data with relatively large amounts of missing data (Table 1.2). Additionally, the Bayesian results did not support *Brachyramphus*, *Synthliboramphus*, and *Aethia* monophyly, a result that is inconsistent with previous analyses of alcid relationships (e.g., Pereira and Baker, 2008). Given that the morphological data matrix was constructed primarily to account for morphological variation in Alcidae, the amount of resolution in the outgroup to Alcidae and the congruence with previous hypotheses of charadriiform relationships is noteworthy. However, basal nodes in Alcidae (e.g., relationships among Alcinae) were poorly supported in parsimony-based and Bayesian results (Figs. 1.23 and 1.24).

As in previous morphology-based analyses of charadriiform relationships (Strauch, 1978; Björklund, 1994; Chu 1995; Livezey, 2010), Alcidae and Stercorariidae were not recovered as sister taxa in the results of the Bayesian or parsimony-based analyses of the morphological data. The positions recovered for Alcidae and



Stercorariidae are unresolved in the results of the recent morphology-based analysis of Mayr (2011). Congruence between morphology-based results suggests that the molecular data are responsible for the sister taxon hypothesis between Alcidae and Stercorariidae.

The combined analysis of the concatenated molecular sequence data produced well-resolved trees with limited amounts of topological differences between the parsimony-based and Bayesian hypotheses (Figs. 1.21 and 1.22). These topological differences reflect the potential for these different methods of phylogeny estimation to recover different hypotheses of relationships based upon analysis of the exact same data. The only major topological difference (i.e., not referring to positions of individual taxa) between the results of these two methods is with respect to the position of *Synthliboramphus*. *Synthliboramphus* was recovered in a relatively derived position as the sister to Alcini in previous Bayesian molecular-based analyses of alcid relationships (Thomas et al., 2004; Baker et al., 2007; Pereira and Baker, 2008), whereas parsimony-based results have consistently placed *Synthliboramphus* at or near the base of Alcinae (Strauch, 1985; Watada, 1987; Chandler, 1990a; Moum et al., 1994). The only previous parsimony-based analysis to recover *Synthliboramphus* as the sister to Alcini was that by Friesen (1996; Fig. 1.3A). However, the parsimony analysis by Pereira and Baker (2008) also recovered *Synthliboramphus* at the base of Alcinae in one of two most-parsimonious topologies. Given that different sets of data and different methods of phylogeny estimation were used in the analyses mentioned above, it is intriguing that *Synthliboramphus* has been recovered in only two positions relative to other Alcidae. Perhaps additional sequence data might resolve the conflict between these two competing hypotheses.

The parsimony-based and Bayesian phylogenetic analyses of the combined morphological and molecular sequence data recovered Alcidae as the sister to Stercorariidae, a result that is congruent with the results of previous molecular-based analyses (Ericson et al., 2003; Paton et al., 2003; Thomas et al., 2004; Paton and Baker, 2006; Baker et al., 2007), but conflicts with previous morphology-based analyses that placed Alcidae at or near the base of Charadriiformes (Strauch, 1978; Björklund, 1994; Chu, 1995, 1998; Chu et al., 2009). As in the analysis that was restricted to the molecular data (i.e., 8 gene partitions), the combined analysis (i.e., molecules and morphology) estimates of relationships among crown clade Alcidae are congruent with the results of recent analyses of molecular sequence data (Thomas et al., 2004; Paton et al., 2003; Baker et al., 2007; Pereira and Baker, 2008), except that *Cepphus* is placed at the base of Alcinae in the Bayesian topology (Fig. 1.26), rather than as the sister to Alcini as in the parsimony-based topology (Fig. 1.25). The positions of other species (e.g., *Alca* + *Pinguinus*), and sub-clades in Alcidae (e.g., Fraterculinae + Alcinae) are consistent with the results of recent molecular-based analyses (Baker et al. 2007, Pereira and Baker 2008) with dense taxonomic sampling for Alcidae. The only prior morphology-based analyses of Alcidae with sufficient taxonomic sampling for comparison to these results, those by Strauch (1985) and Chandler (1990a), resulted in topologies that strongly conflict with more recent hypotheses of alcid relationships in that they do not support a traditional Fraterculinae (i.e., monophyly of Fraterculini + Aethiini). The Aethiini (i.e., *Ptychoramphus* + *Aethia*) are placed basal to the Alcinae (*Alca* + *Pinguinus* + *Cepphus* + *Brachyramphus* + *Synthliboramphus*), rather than as sister to the Fraterculini (i.e., *Cerorhinca* + *Fratercula*) in the topology presented by Strauch (1985). Although the

work by Chandler (1990a) represented an increase in the number of characters scored for Alcidae, the results of that analysis placed *Alle alle* and *Cephus* in a clade with the Fraterculini, rather than in Alcinae. The combined analysis presented herein, and other previous analyses (Watada, 1987; Moum et al., 1994; Friesen et al., 1996; Thomas et al., 2004; Baker et al., 2007; Pereira and Baker, 2008) are congruent in support of the monophyly of a Fraterculinae clade consisting of *Ptychoramphus*, *Aethia*, *Cerorhinca*, and *Fratercula*, and the sister-group relationship between Fraterculinae and Alcinae as defined here (Figs. 1.25 & 1.26).

The systematic position of *Alle alle* remained unresolved at the base of Alcini in the parsimony-based topology (Fig. 1.25). Consistent with recent molecular-based analyses (Thomas et al., 2004; Pereira and Baker, 2008), *Alle alle* was recovered as the sister taxon to *Uria* in the Bayesian analysis. The systematic position of *Alle alle* is one of the most contentious issues in alcid systematics because *Alle alle* has been recovered as the sister to *Alca* + *Pinguinus* (Moum et al., 1994, 2002; Baker et al., 2007), sister to *Alca* + *Pinguinus* + *Uria* (Strauch, 1985), sister to *Uria* (Thomas et al., 2004; Pereira and Baker, 2008), sister to Fraterculinae (Chandler 1990a), and sister to *Cephus* + *Aethia* + *Brachyramphus* (Chu, 1998). Although *Alle* shares characters with other extant Alcini taxa (i.e., *Uria* and *Alca*) and the recently extinct taxon *Pinguinus*, each to the exclusion of the other, *Alle* also has characteristics that are not present in other extant Alcidae (e.g., scapulotricipital sulcus of humerus broader than humerotricipital sulcus; 152:2). This issue is addressed in the context of a comprehensive analysis of alcid relationships including dense taxonomic sampling of extinct Alcini (see Chapter 2).

The hypotheses of charadriiform outgroup relationships based on the combined analyses are largely congruent with prior molecular-based analyses of the clade, which is not surprising given the inclusion of those same molecular data. *Larus* and *Hydrophasianus* (i.e., gulls and jacanas) are recovered as more closely related to one another than either are to *Charadrius* (i.e., plovers), as in the results obtained by Hackett et al. (2008). Also consistent with the results of prior molecular analyses (Ericson et al., 2003; Paton et al., 2003; Paton and Baker, 2006; Baker et al., 2007), an Alcidae + Stercorariidae clade is placed as the sister to a Laridae + Sternidae + Rynchopidae clade. The results of the combined analyses are congruent with recent molecular-based analyses that place Lari (e.g., alcids, gulls, and pratincoles) as the sister to Scolopaci (e.g., sandpipers, jacanas, and curlews), and place Charadrii (e.g., plovers), at the base of Charadriiformes.

The combined analysis results (Figs. 1.25, 1.26) do not support previously published morphology-based results that place Charadrii nested in Charadriiformes rather than at its base (Strauch, 1978; Chu, 1995; Livezey, 2010; Mayr, 2011). This hypothesis contrasts with the morphology-based results obtained by Björklund (1994) and Chu (1995), which were the result of parsimony-based re-analyses of the compatibility analysis of Strauch (1978). In the topology recovered by Björklund (1994) the Charadrii and Scolopaci are placed in an unresolved polytomy basal to the Lari, whereas the Lari and Charadrii are placed in an unresolved polytomy basal to the Scolopaci in the results presented by Chu (1995). The contents of Charadrii, Scolopaci, and Lari estimated by the combined analyses are, however, consistent with the composition of those clades recovered in prior molecular-based analyses (Sibley and Ahlquist, 1990; Paton et al.,

2003; Ericson et al., 2003; Paton and Baker, 2006; Baker et al., 2007), supporting the monophyly of Charadrii, Lari, and Scolopaci. Scolopaci is placed as an outgroup to sister taxa Charadrii and Lari in the results of the morphology-based analyses by Mayr (2011) and Livezey and Zusi (2006, 2007). The incongruence between different morphology-based hypotheses is contrasted by the relative congruence between molecular hypotheses based on mitochondrial and nuclear genes (RAG-1, Paton et al., 2003; *cyt-b*, Thomas, 2004).

Also of interest is the placement of the Black Skimmer *Rynchops niger*. In the results of the Bayesian combined analysis and recent molecular sequence-based analyses (Paton et al., 2003; Baker et al., 2007) *Rynchops* is recovered as the sister to Laridae, whereas other molecular sequence-based analyses have recovered this taxon as the sister to Sternidae (Paton and Baker, 2006). The morphology-based analyses by Chu (1995, 1998) placed *Rynchops* as the sister to a Sternidae + Laridae + Stercorariidae clade. The results of the parsimony-based combined analysis placed *Rynchops* as the sister taxon to the White Tern *Gygis alba*. Considering the currently accepted placement of *Gygis alba* in Sternidae (AOU, 1998; Brigde et al., 2005), this result would suggest Sternidae paraphyly as the clade is currently defined. Although, this result is not entirely novel because an alternative hypothesis also places *Gygis* outside Sternidae as the sister to a Laridae + Sternidae clade (Baker et al., 2007). However, denser taxonomic sampling of Rynchopidae, Sternidae, and other Charadriiformes may resolve this issue in the future.

*Anous* (i.e., noddies) was recovered as the sister to a Sternidae + Laridae + *Rynchops* clade in the results of the parsimony and Bayesian combined analyses, a placement consistent with the molecular-based results reported by Baker et al. (2007),

and in conflict with the morphology-based results obtained by Chu (1998), which placed *Anous* as the sister to Stercorariidae. The only study with dense taxonomic sampling of terns and noddies (Bridge et al., 2005) included only a single larid (*Larus delawarensis*) as an outgroup taxon, but placed *Anous* basally in Sternidae. *Anous* was not included in a recent analysis by Livezey (2009, 2010) and Sternidae was represented by a single terminal in the analysis of Mayr (2011). Resolution of the systematic affinities of *Anous* will likely require denser taxonomic and character sampling for *Anous*, similar to that employed by Bridge et al. (2005) for other terns, and combination of those data with large molecular and morphological sets of data for other closely related charadriiforms such as Laridae and Rynchopidae. Species-level sampling for all of Charadriiformes would be ideal, but admittedly ambitious given the ~350 currently recognized species.

## CONCLUSIONS

The 22 phylogenetic analyses presented herein provide a case study involving the potential effects of analyzing data separately and in combination. Furthermore, the similarities and contrasts between the results from parsimony and Bayesian analyses of these data provide some insight into the potential advantages and limitations of these different methods of phylogeny estimation. Whereas the generally higher level of resolution associated with the parsimony results is attractive in that it allows for more detailed conclusions regarding evolution, the generally higher level of ambiguity in the Bayesian results presents a more conservative estimate based on methods that are

arguably more sophisticated because they are based on evolutionary theory, albeit subject to their own biases.

The combined analysis hypothesis of relationships presented here simultaneously considers the largest quantity of phylogenetically informative data for alcids and other charadriiforms to date. These results do not support morphology-based hypotheses of alcid relationships previously proposed by Strauch (1985) and Chandler (1990a), but are largely congruent with recent molecular-based hypotheses for the clade proposed by Baker et al. (2007) and Pereira and Baker (2008). Considering that many of the data analyzed herein were drawn from those previous studies, it is intriguing that the combined analysis produced novel results.

The placement of *Cepphus* at the base of Alcinae in the Bayesian topology is a novel result that was, otherwise, only recovered in the parsimony-based analysis of the morphological data (Fig. 1.23). Although there are other strongly supported placements for *Cepphus* within Alcidae (Pereira and Baker, 2008), this position for *Cepphus* is supported by apomorphies shared by species of *Cepphus* to the exclusion of all other Alcinae (e.g., humeral and ulnar shafts less dorsoventrally compressed than other alcids; 147:1; 184:1).

More than half of known alcid diversity is extinct (reviewed by Olson, 1985). The inclusion of additional taxa can increase phylogenetic accuracy (Wheeler, 1992; Zwickl and Hillis, 2002; Heath et al., 2008), and therefore, dense taxonomic sampling for extinct Alcidae will likely affect the topology of recovered trees. The morphological data matrix for Alcidae developed herein for the combined analyses of extant Alcidae forms the basis for future analyses including Alcidae fossils and additional charadriiform fossils that will

provide calibration points for divergence time estimation analyses. Among extinct pan-alcids, only the recently extinct Great Auk *Pinguinus impennis*, and the flightless Mancallinae have been included in previous phylogenetic analyses (Strauch, 1985; Chandler, 1990a; Moum et al., 2002; Baker et al., 2007; Pereira and Baker, 2008; Smith, 2011). The systematic positions of fossils used as calibration points by Pereira and Baker (2008) have yet to be evaluated in a phylogenetic analysis. Therefore, recent inferences regarding the biogeography of Alcidae based purely upon extant alcid data and in the absence of reliable divergence estimates for Alcidae (Pereira and Baker, 2008) should be viewed with caution.

These analyses strongly support Stercorariidae as the sister taxon to a monophyletic Alcidae. Extant Alcidae is divided into two sister clades. Alcinae includes *Cepphus*, *Brachyramphus*, *Synthliboramphus* and the Alcini. Fraterculinae includes the Fraterculini and the Aethiini. However, levels of support are relatively low for the recovered placement of clades including *Synthliboramphus*, *Brachyramphus*, and *Cepphus*. Additional taxon and character sampling may resolve this issue in subsequent analyses.



## CHAPTER 2.

Taxonomic revision of *Alca* (Aves, Alcidae):  
a combined morphometric and phylogenetic approach.

## INTRODUCTION

With respect to other charadriiforms, Alcidae have a comparatively rich fossil record along northern coastlines of both the Atlantic and Pacific Oceans (Olson, 1985). Specimens referred to the taxon *Alca* are most numerous (Olson and Rasmussen, 2001). The geographic range of the only extant species of *Alca*, the Razorbill Auk *Alca torda*, and all known *Alca* fossils are restricted to the northern Atlantic Ocean basin (Brodkorb, 1967; Olson, 1985; though see Howard, 1968 and discussion below; Fig. 2.1). Extinct *Alca* have been described from Miocene deposits in Virginia (Olson and Rasmussen, 2001; Wijnker and Olson, 2009), and Pliocene deposits in Italy, Florida, North Carolina, Spain, Belgium, and Morocco (Portis 1888, 1891; Brodkorb, 1955; Olson and Rasmussen, 2001; Martin et al., 2001; Sanchez-Marco, 2003; Dyke and Walker, 2005; Mourer-Chauvire and Geraads, 2010; Fig. 2.1).

The richest of these deposits is the Early Pliocene Yorktown Formation, a shallow marine deposit geologically linked with cold-water upwelling (Gibson, 1967; Snyder, 2001) that is exposed at the PCS Phosphate mine in Aurora, North Carolina (formerly known as the Lee Creek Mine; Ray, 1983; Olson and Rasmussen, 2001; Fig. 2.1). Although approximately 8000 fossils from this locality, consisting primarily of ulnae, humeri, and coracoids, have been referred to *Alca*, a recent re-evaluation of this material indicates that only ~3% of these specimens are represented by undamaged skeletal elements (e.g., complete humeri), and only 23 specimens consist of associated material (18 of the 23 associated specimens are >90% incomplete; Smith, 2007).

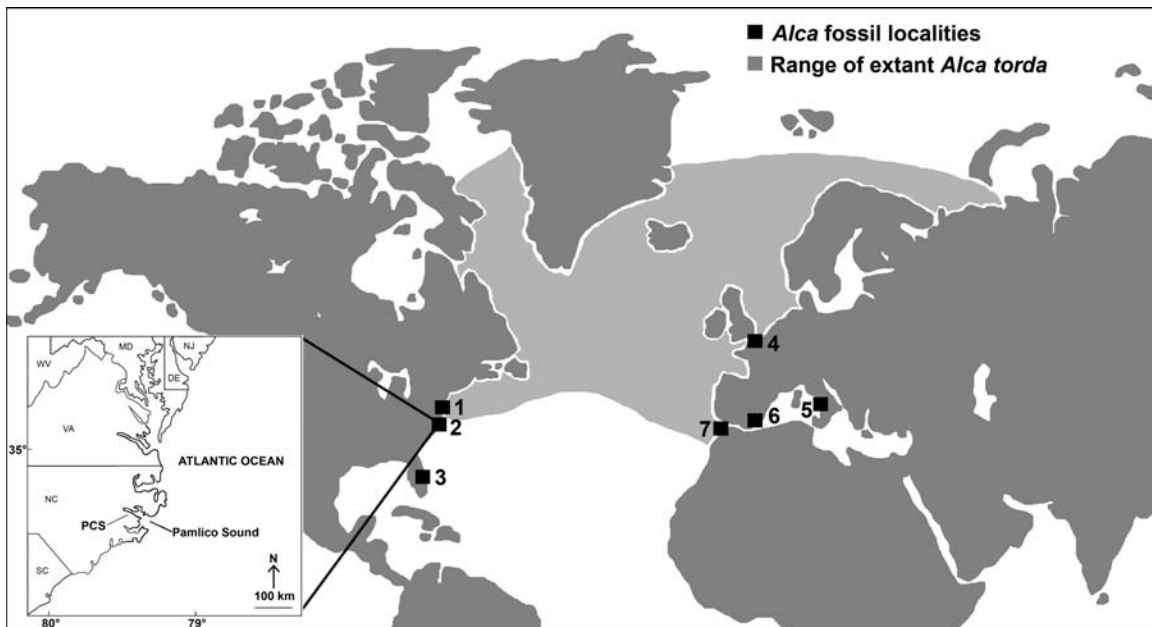


Figure 2.1- Maps indicating the geographic range of the extant Razorbill Auk *Alca torda*, and *Alca* fossil localities. **1.** Eastover Fm., Virginia, USA; **2.** Yorktown Fm., North Carolina, USA; **3.** Bone Valley Fm., Florida, USA; **4.** Kallo Sands Fm., Belgium; **5.** Oriano Pisano, Italy (Fm. unknown); **6.** Puerto de Mazarron Fm., Murcia, Spain. **7.** Ahl al Oughlam Quarry, Casablanca, Morocco. Inset map of the eastern USA indicates the locality of PCS Phosphate mine near Aurora, NC where the holotype specimens of *Alca carolinensis*, *Alca minor*, and *Alca olsoni* were collected. Shaded area on inset map denotes the subsurface extent of the Yorktown Formation. Range map altered from del Hoyo et al., 1996; inset map altered from Gibson, 1983.

Previously recognized alcid diversity from the Yorktown Fm. comprises *Miocepphus mcclungi*, *Miocepphus bohaski*, *Miocepphus mergulellus*, *Fratercula cirrhata*, *Fratercula arctica*, *Alca torda*, *Alca ausonia*, *Alca grandis*, *Alca stewarti*, *Pinguinus alfrednewtoni*, and *Cerorhinca* sp. (Olson, 1977; Martin et al., 2001; Olson and Rasmussen, 2001; Smith et al., 2007). The addition of three new species of *Alca* described herein increases the number of *Alca* known to seven, and the total number alcids known from this locality to fourteen. Microfaunal analysis has confirmed the Pliocene Yorktown Fm. provenience of many avian fossils from this locality (Gibson,

unpublished data *in* Olson and Rasmussen, 2001). However, the lack of associated sediments leaves the probable provenience of many fossils from this locality in question (Olson and Rasmussen, 2001; Smith et al., 2007; Wijnker and Olson, 2009).

PCS Phosphate Mine is located along the southern shore of the Pamlico River (Fig. 2.1) and exposes sediments of Miocene, Pliocene, and Pleistocene age (Gibson, 1983). The Pliocene Yorktown Fm. unconformably overlies the Miocene Pungo River Formation, and is composed primarily of clay-rich sands (i.e., marls), with the basal-most unit containing reworked phosphate pebbles from the underlying Pungo River Fm. (Gibson, 1983). An age of  $4.4 \pm 0.2$  Ma (Early Pliocene) was assigned to the Yorktown Fm. at PCS Phosphate Mine based on K/Ar dating of the *Orionina vaughani* assemblage zone and correlated with planktonic foraminifera Zone N19 (Hazel, 1983). Yorktown Fm. sediments from the PCS Phosphate Mine are interpreted to be the result of moderate depth (~150 m) outer neritic marine deposition at the southwestern end of the Aurora Embayment (Popenoe, 1985, Snyder, 2001). The Aurora Embayment was a deep depression that allowed cold waters to upwell ~100 kilometers west of the margin of the Pliocene continental shelf (Riggs, 1984). This upwelling resulted in a nutrient-rich marine environment interpreted as “a marine vertebrate high-use feeding area” by Purdy et al. (2001:188). As noted above, distribution of extant alcids also coincides with cold-water upwelling zones (Prince and Harris, 1988; del Hoyo et al., 1996), suggesting that the environmental preferences of alcids have remained relatively stable since the Early Pliocene. The Yorktown Fm. contains abundant remains of marine vertebrates (e.g., Chondrichthyes, Osteichthyes, Cetacea, Sirenia, Pinnipedia, Testudines, and Crocodylia;

Ray, 1983, 1987; Ray and Bohaska, 2001, Ray et al., 2008) and invertebrates (e.g., Echinodermata, Hexagonaria, Porifera, Mollusca, and Foraminifera; Ray, 1983, 1987). In addition to the taxa listed above, the remains of a diverse avifauna representing ~100 other avian species are known from this location (Storer, 2001; Olson and Rasmussen, 2001; Smith et al., 2007).

The paucity of associated fossil specimens, incomplete preservation of the overwhelming majority of specimens, and morphological similarity of *Alca* species combined to complicate previous referrals of *Alca* fossils to species-level (Olson and Rasmussen, 2001). Further compounding the difficulties of referring additional elements to species, the holotype and paratype material of all three previously described extinct *Alca* species are isolated skeletal elements (*Alca grandis*; *Alca ausonia*; *Alca stewarti*; Table 2.1; Fig. 2.2). Osteologically distinguishing between modern species in a species-rich or sub-species-rich taxon can be difficult or impossible (Stewart, 2002, 2007). Previous researchers (Olson and Rasmussen, 2001) assigned *Alca* specimens to species based on humeral size classes determined through principal components analysis (PCA) in conjunction with a modified version of the phenetic technique proposed by Warheit (1992a). Because PCA does not account for co-varying character complexes (i.e., principal axes not orthogonal), a method for differentiating species was developed to account for the non-independence of osteological variables, while allowing for the analysis of fragmentary material. This method is an improvement on previous methods that rely solely on measurement data to differentiate between species, because it

Table 2.1- Previously published extinct *Alca* holotype material.

Taxa	Material	Provenience	Age	Reference
<i>Alca ausonia</i>	Distal humerus	Italy	Middle Pliocene	Portis, 1888
<i>Alca grandis</i>	Humerus	USA	Early Pliocene	Marsh, 1870
<i>Alca stewarti</i>	Ulna	Belgium	Early Pliocene	Martin et al., 2001

additionally employs intra-group and inter-group morphological analysis of morphometrically determined clusters and allows for identification of discrete morphological characters with utility for phylogenetic analysis.

Interspecific size variation has been successfully used to differentiate between extant and extinct avian species (Livezey, 1988, 1989; Warheit, 1992a), and knowledge of interspecific size variation has a long history of use as a criterion for estimating diversity among fossil material (reviewed by Warheit, 1992a). However, the application of interspecific size-based models to distinguish proposed size classes of fossil specimens assumes that phylogenetic data are conserved in the relative size dimensions of different species (Warheit, 1992a). Thus, referral of fossil specimens solely on the basis of size data is not recommended. This does not mean that morphometric data, including size, cannot play a role in the identification of fossils; instead, morphometric data should be used in conjunction with discrete morphological characters in a phylogenetic context.

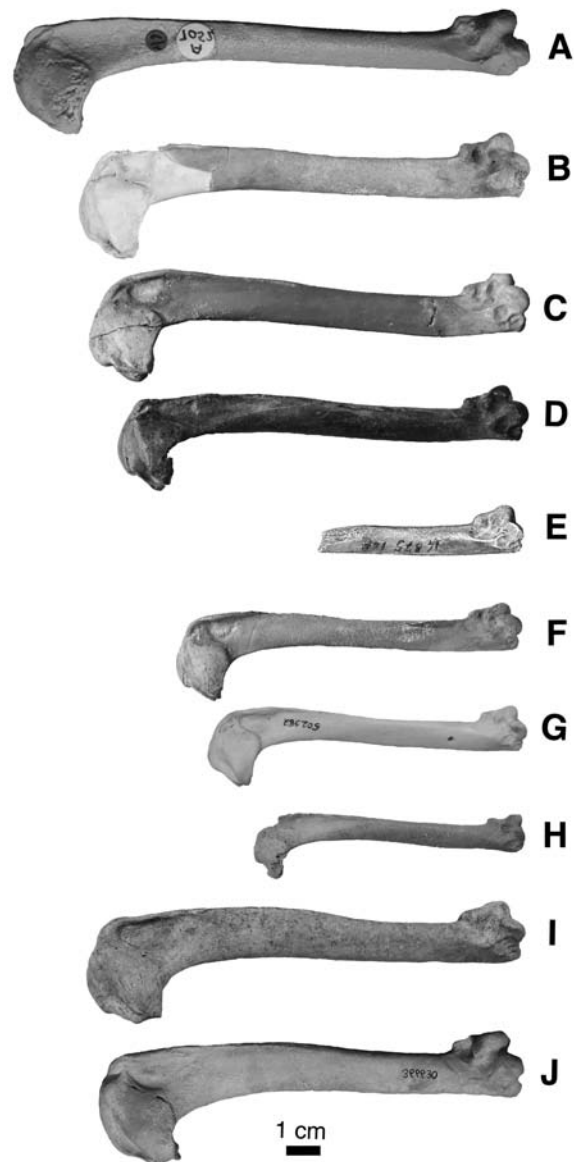


Figure 2.2- Comparison of *Alca* and *Pinguinus* humeri in anterior view. **A.** paratype cast of *Alca stewarti* (BMNH A 7052; specimen image reversed for comparison); **B.** holotype humerus of *Alca olsoni* (USNM 454590); **C.** holotype humerus of *Alca carolinensis* (NCSM 13734); **D.** holotype specimen of *Alca grandis* (ANSP 13357); **E.** cast of *Alca ausonia* holotype specimen (IGF 14875); **F.** referred specimen of *Alca ausonia* (USNM 446692); **G.** *Alca torda* (USNM 502382); **H.** holotype specimen of *Alca minor* (USNM 302324); **I.** *Pinguinus impennis* (USNM 623465); **J.** *Pinguinus alfrednewtoni* (USNM 366630; specimen image reversed for comparison).

The ability to quantify the diversity represented by fossil assemblages known from fragmentary taxa is a tool that holds potential to inform both paleoecological trends and paleobiogeographic patterns that are currently understudied or undescribed. Long recognized as one of the dominant groups of seabirds during the Pliocene (Olson, 1985), increasing knowledge of extinct alcid diversity, relative abundance of species, and estimates of species longevity will clarify our presently poor understanding of alcid paleobiogeographical patterns. Additionally, evaluation of extinct species diversity with respect to latitudinal gradients will allow for comparisons with extant latitudinal distribution of alcid species, and insights gained through more detailed evaluation of the alcid fossil record will result in a more nuanced understanding of the extent to which previously hypothesized (Warheit, 1992b; Emslie, 1998; Olson and Rasmussen, 2001; Smith et al., 2007; Pereira and Baker, 2008) paleoclimatic drivers contributed to radiations and extinctions in Alcidae.

Although analyses of recently sequenced molecular data have resulted in strongly supported phylogenetic hypotheses of extant alcid relationships (Moum et al., 1994; Friesen et al., 1996; Moum et al., 2002; Thomas et al., 2004; Baker et al., 2007; Pereira and Baker, 2008), extinct alcid species have been largely ignored in analyses of morphological data (Strauch, 1985; Chandler, 1990a; Chu, 1998). Analyses of morphological (Strauch, 1985; Chandler, 1990a) and molecular sequence data (Moum et al., 2002; Baker et al., 2007; Pereira and Baker, 2008) place the extant Razorbill Auk *Alca torda* as the sister taxon to the recently extinct Great Auk *Pinguinus impennis*. *Alca* and *Pinguinus* are part of Alcini, which also includes *Uria*, *Alle*, and *Miocepphus*. Extinct



*Alca* species, *Pinguinus alfrednewtoni* Olson 1977, and *Miocepphus* species have never been included in a phylogenetic analysis. This study is the first to include all known extant and extinct Alcini in a combined phylogenetic analysis of morphological (i.e., osteological) and molecular sequence data.

To assess the monophyly of *Alca* and to evaluate the relationships among all Alcini, osteological variation among the thousands of fossils that have been referred to *Alca* was investigated. Estimates of species-diversity resulting from this investigation form a more complete picture of morphological variation between *Alca* species, and between *Alca* and *Pinguinus*. The discovery of an associated partial *Alca* skeleton (the most complete fossil exemplar of *Alca* presently known) from the Pliocene Yorktown Fm. of North Carolina prompted an extensive review of the *Alca* fossil record, and a re-examination of *Alca* diversity that resulted in the recognition of three new species. Descriptions of these new species and amended diagnoses for previously recognized *Alca* species are presented along with species referrals for 203 isolated specimens and phylogenetic analysis of Alcini relationships.

## MATERIALS AND METHODS

Description of anatomical features primarily follows the English equivalents of the Latin osteological nomenclature proposed by Baumel and Witmer (1993). The terminology of Howard (1929) is followed for features not described by Baumel and Witmer (1993). Taxonomy of extant North American Charadriiformes follows that of the

7th edition of the American Ornithologists' Union Checklist of North American Birds (1998). Measurements follow those of Von den Driesch (1976). All measurements were taken using digital calipers and rounded to the nearest tenth of a millimeter. Ages of geologic time intervals are based on the International Geologic Timescale (Gradstein et al., 2004; Ogg et al., 2008).

***Institutional Abbreviations:*** Alam—Asociación Cultural Paleontológica Murciana, Murcia, Spain; ANSP—Academy of Natural Sciences of Philadelphia, PA, USA; BMNH—Natural History Museum, London, England; GCVP—Georgia College Vertebrate Paleontology Collection, Milledgeville, GA, USA; IGF—Museo di Storia Naturale, Firenze, Italy; LACM—Natural History Museum of Los Angeles County, Los Angeles, CA., USA; NCSM—North Carolina Museum of Natural Sciences, Raleigh, NC, USA; UCMP—University of California Museum of Paleontology, Berkeley, CA, USA; UF/PB—Florida Museum of Natural History/Pierce Brodkorb Collection, Gainesville, FL, USA; USNM—Smithsonian Institution, National Museum of Natural History, Washington, D.C., USA.

***Comparative skeletal material used for phylogenetic analysis:*** *Alca torda* Razorbill Auk NCSM 20058, 20502; USNM 18062, 347946, 501644, 502378, 502382, 502387, 502388, 502389, 502549, 555666, 555668; *Alle alle* Dovekie NCSM 18374; USNM 344740, 344748, 499471, 560929; *Cepphus columba* Pigeon Guillemot NCSM 18094, 18095, 18096, 18097; *Pinguinus impennis* Great Auk USNM 346387 (composite), 557975 (composite), 623465 (composite), additional series of disarticulated USNM material from the Lucas expedition (Lucas, 1890); *Uria aalge* Common Murre

NCSM 17822, 18116, 18117, 18118, 18234; *Uria lomvia* Thick-billed Murre NCSM 18114, 19414; USNM 344435, 561265.

## MORPHOMETRIC ANALYSES

Measurements of 66 osteological variables (e.g., greatest length of humerus) were taken from 67 skeletons representing 12 extant alcid species and the recently extinct Great Auk *Pinguinus impennis* (Appendix 5). Inclusion of measurement data from extant auklets (i.e., *Aethia* and *Ptychoramphus*) provided a test of the robustness of this method with respect to differentiating between members of a single clade, the monophyly of which is supported by analyses of both morphological (Strauch, 1985; Chandler, 1990a) and molecular data (Friesen et al., 1996; Pereira and Baker, 2008).

Owing to relative incompleteness of associated *Alca* fossils, it was necessary to evaluate not only how this method performed when utilizing measurements from complete skeletons of extant alcids, but more importantly how the method performed when more limited sets of data were available. Additional analyses were conducted using subsets of measurement data (e.g., distal humeri data only) from extant alcids to gauge how this method might perform when applied to isolated and fragmentary fossils.

A hierarchical cluster analysis employing single linkage, nearest neighbor joining, and Euclidean distance was performed on measurement data using the statistical software package SPSS 16 (Inc. SPSS, 2007). Resulting phenogram topology was evaluated to infer potential clusters of specimens (i.e., clusters of measurement data). Statistical support for cluster membership was determined by conducting discriminate function

analyses on raw measurement data assigned to categories based on phenogram topology (Fig. 2.3).

Measurement data from extant alcids were also used to determine the typical range of intraspecific size variation of extant alcid species so that this metric could be applied as an additional criterion in the acceptance or rejection of clusters of *Alca* fossils. As suggested by Warheit (1992a), this procedure provided a phylogenetic context for the estimation of average size for extinct *Alca*. Whenever available, specimens from multiple locations within the geographic range of extant species (e.g., extant *Alca torda* specimens from the eastern and western Atlantic) were used to calculate the intraspecific size variation values that were used as a criterion to evaluate the size ranges of clustered fossils. This value was calculated by assessing the difference between the median of measurements of the greatest length of sampled humeri, and the length of the longest and shortest specimens for each extant species. Comparing the differences between the known ranges of variation between closely related extant alcids (e.g., auklets) with the range in size of statistically supported clusters of fossils provided an additional criterion with which to evaluate support for clustered groups of fossils (Warheit, 1992a). Only clusters with a size range of specimens not significantly exceeding that of the predetermined range of intraspecies size variation for Alcidae were accepted. Although in practice this method mistakenly assumes that no two fossil species fall within the same size range, morphological comparison of statistically clustered specimens guarded against the possibility of underestimating the number of species represented by a single size class. However, this assumes that no two species represented by the mensural data are

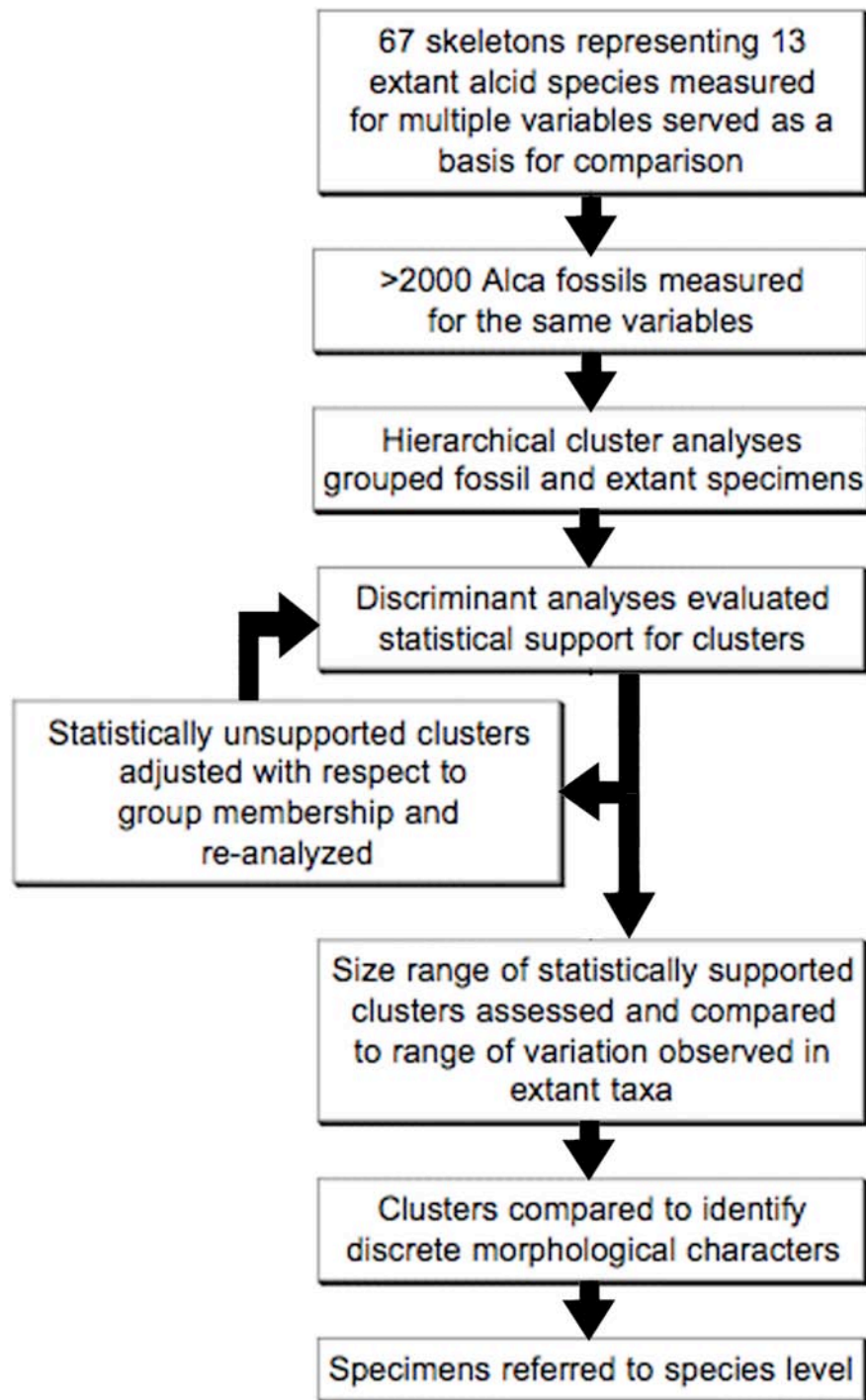


Figure 2.3- Flowchart depicting a simplified explanation of the combined morphometric and morphology-based method used to refer *Alca* specimens to species.

the exact same size and morphologically indistinguishable.

The same procedure as described above was applied to raw mensural data from 203 *Alca* humeri including the type specimens of all previously described species of *Alca*, and additional *Alca* humeri from both eastern and western Atlantic fossil localities (Appendix 6A). Although 944 *Alca* fossil humeri were examined and measured (Appendix 6B), only specimens in which a minimum of at least three of the six humeral variables could be measured, and that preserved diagnostic morphological details were included in the final analysis. The holotype or paratype specimens of all three previously described species of extinct *Alca* are humeri (Table 2.1; Fig. 2.2), and humeri are the second most frequently represented skeletal element amongst collections of fossil *Alca*. Although ulnae are more abundant, this element lacks morphologically distinguishing characters as compared to *Alca* humeri. Additional analyses of ulnar measurement data (Appendix 6C), carpometacarpus measurement data (Appendix 6D), and coracoid measurement data (Appendix 6E) were also performed.

As with extant specimens, cluster membership of fossil specimens was determined by visually evaluating phenogram topology resulting from cluster analyses and grouping topologically adjacent specimens. Statistical support values (i.e., number of cases correctly classified) obtained from canonical discriminant function analysis of extant alcids were used as a metric to accept or reject clusters of fossils. Clusters receiving <90% statistical support (the lowest support resulting from analysis of extant taxa) were rejected. A caveat to this method is that as the number of specimens being analyzed increases, the interpretation of phenogram topology into distinct clusters (i.e.,

categorization of fossils) becomes increasingly complicated. For example, even though analysis of the distal humeri of extant alcids showed that this metric accurately clusters specimens into species groups, analysis of 621 distal humeri produced a phenogram with such a complex topology that clusters could not be reliably inferred. The largest number of successfully analyzed specimens in this analysis was 146, although numbers of specimens included for analysis were more commonly limited by completeness of the fossil specimens themselves (e.g., only 66 complete fossil *Alca* humeri) rather than by complexity of interpretation of data. Data analyzed using this method cannot contain any missing entries (i.e., values not measured due to incompleteness or damage to fossils). However, limiting the quantities of specimens analyzed using this method should not present a significant problem, as the method itself is not biased by small sample sizes. However, the possibility that a small sample size may represent individuals that are skewed towards one size extreme or another within a species (e.g., only three complete *Alca stewarti* humeri available for analysis) should be considered.

The results of analyses that contained clusters of fossils that were rejected based on the criteria outlined above (i.e., statistical support and range of size variation as compared with extant alcids) were discarded. Phenogram topology was then re-evaluated and outliers (i.e., smallest or largest specimens within a cluster) were re-assigned to topologically adjacent clusters and the entire data set was then re-analyzed to determine if an alternative clustering scheme would receive stronger statistical support (Fig. 2.3). When re-assigning specimens to different categories, only adjacently placed specimens and groups of specimens (i.e., those specimens with linked Euclidean distances) were

combined into new potential categories. No specimens with Euclidean distance values intermediate between those of specimens placed adjacently in phenogram topology were excluded.

Statistically supported clusters of fossils were compared to identify shared intra-group morphological characters and inter-group morphological differences, which could be used to differentiate species of *Alca* and facilitate referral of specimens to species. Additionally, the morphology of specimens clustered with the holotype or paratype specimens of previously recognized species were compared to those name-bearing type specimens to identify previously unrecognized morphological variation and to document characteristics not visible in the type specimens owing to damage. The range of size variation within fossil clusters was compared to values obtained from extant alcid taxa as described above. Intraspecific size variation within alcid species owing to latitude are well documented (Storer, 1952; Spring, 1971; Moen, 1991; Burness and Montevicchi, 1992). Additional analyses of measurement data collected from *Alca* fossils deposited in a single stratigraphic layer (Early Pliocene Yorktown Fm.) exposed at a single geographic locality (Aurora, North Carolina) were performed to address this issue.

#### PHYLOGENETIC ANALYSIS

Whenever possible, five or more specimens of each extant species, and both sexes were evaluated to account for intraspecific character variation and potential sexual dimorphism respectively. Only adult specimens, assessed based on degree of ossification (Chapman, 1965), were included, and whenever possible specimens from multiple



locations within the geographic range of extant species (i.e., sub-species) were examined to account for geographic variation.

Morphological characters were scored for 18 taxa (five extant and thirteen extinct alcids). See Appendix 2 for morphological character descriptions and Appendix 3 for morphological character scorings used in the phylogenetic analysis.

The primary goal of this study was to accurately evaluate diversity within *Alca* so that all species within Alcini could be included in a combined phylogenetic analysis. Owing to the isolated preservation of all but four extinct Alcini holotype specimens (i.e., associated holotype specimens of *Miocepphus blowi*, *Mioceppus bohaski*, *Alca carolinensis*, and *Alca olsoni*) resolution of systematic relationships was facilitated by combination of all available referable specimens into supraspecific terminals, thus decreasing the amount of missing data in the phylogenetic analysis. Taxonomic referrals of all holotype and previously referred specimens were re-evaluated using an apomorphy-based approach. Characters for all extinct taxa were coded from direct observation. Characters for *Pinguinus alfrednewtoni* were scored from the hypodigm of that species (USNM specimen #'s: 179226, 179277, 192497, 193101, 193334, 206362, 275780, 366630, 430935, 430943, 430947, 459391; Olson and Rasmussen, 2001). Characters for *Alca grandis* were scored from the holotype specimen as well as two previously referred specimens (USNM 215454, USNM 336379; Olson and Rasmussen, 2001) and one specimen referred herein (USNM 236802,). Characters for *Alca ausonia* were scored from 2 high quality casts of the holotype retained in the USNM and UF/PB collections as well as a representative specimen referred herein (USNM 446692). Characters for *Alca*

*stewarti* were scored from the holotype (BMNH A 7050), the paratype humerus (BMNH A 7052; Martin et al., 2001), and previously referred specimens (USNM 242238, USNM 446650; Olson and Rasmussen, 2001). Characters for *Alca carolinensis* sp. nov. and *Alca olsoni* sp. nov. were scored from the holotype specimens of those species, while *Alca minor* sp. nov. was scored from the hyodigm of that species (USNM 302324, 192879, 495600). *Miocepphus* species were scored directly from the holotype specimens representing those taxa.

*Pseudocepphus teres* Wijnker and Olson, 2009 was not included in the phylogenetic analysis because results of a comprehensive analysis including all extinct and extant Alcidae place this species outside Alcini. Additionally, recent re-evaluation of the holotype specimen of *Uria paleohesperis* Howard, 1982 (UCMP 88704) failed to identify any apomorphies that support its referral to *Uria*. Contra Howard (1982), the size of UCMP 88704 is consistent in all dimensions with the holotype specimen of *Uria brodkorbi* Howard, 1981 (UF/PB 7690). Additionally, UCMP 88704 and *Uria brodkorbi* share a concave sternal margin of the procoracoid process of the coracoid. This margin is convex in both *Uria aalge* and *Uria lomvia*. Furthermore, the Late Miocene (~6.7-10 Ma) age of the San Luis Rey River Local Fauna of the San Mateo Formation from which UCMP 88704 was discovered is consistent with the Late Miocene age assigned to the Sisquoc Formation from which the holotype of *Uria brodkorbi* was recovered (Domning and Deméré, 1984; Dumont and Barron, 1995). The possibility that *Uria paleohesperis* may be a junior synonym of *Uria brodkorbi* should be considered further upon recovery of additional remains.

Previously published molecular sequence data (mitochondrial: ND2, ND5, ND6, CO1, CYTB; ribosomal RNA: 12S, 16S; and nuclear: RAG1) were acquired from GenBank (<http://www.ncbi.nlm.nih.gov/genbank>; see Appendix 4 for sequence authorship). ND5 sequence data for *Cepphus columba*, as well as ND2, CO1, 16S, and RAG-1 sequence data for *Pinguinus impennis* were not included because these data are currently unavailable through GenBank. Preliminary sequence alignments were obtained using the program ClustalX v2.0.6 (Thompson et al., 1997), and then aligned by eye using the program Se-Al v2.0A11 (Rambaut, 2002). Alignment and concatenation of sequence data resulted in a final molecular matrix of 11601 base pairs. Molecular sequence data were combined with morphological characters for a matrix of 11,954 characters.

The phylogenetic analysis employed a branch and bound search strategy in PAUP\* v4.0b10 (Swofford, 2002). All characters were equally weighted, minimum length branches = 0 were collapsed, and multistate scorings represent polymorphism. Bootstrap values and descriptive tree statistics (e.g., CI, RI, RC) were calculated using PAUP\* v4.0b10 (Swofford, 2002). Bootstrap value calculation parameters included 1,000 replicates with 100 random addition sequences per replicate. All other settings were the same as the primary analysis. Bremer support values were calculated using a script generated in MacClade v4.08 (Maddison and Maddison, 2005) and implemented in PAUP\* v4.0b10 (Swofford, 2002). The tree was rooted with *Cepphus columba* based upon the placement of this taxon outside of Alcini in the results of previous phylogenetic

analyses (Strauch, 1985; Chandler, 1990a; Moum et al., 1994; Baker et al., 2007; Pereira and Baker, 2008).

## RESULTS

### MORPHOMETRIC RESULTS

***Extant Alcidae:*** Results of the morphometric analysis including all 66 osteological variables taken from the entire skeleton indicate that osteological measurement data can be used to discern between different species of closely related extant alcids (Fig. 2.4). Cluster analyses correctly classified all 67 extant skeletal specimens into distinct species groups in 100% of cases (Table 2.2). When subjected to discriminant function analysis, group membership of specimen clusters representing extant species received 100% statistical support (i.e., 100% of cases correctly classified).

Additional analyses of single skeletal elements (e.g., only humeri) and partial elements (e.g., proximal ends of humeri only) of extant alcids had variable results (Table 2.2). Although analyses of coracoids, and complete and partial humeri resulted in correctly classified and statistically supported clusters, analyses of ulnae and carpometacarpi resulted in statistically significant percentages of incorrectly classified specimens. In addition to providing measures of statistical support for groups of measurement data categorized by cluster analysis, discriminant function analysis identifies the variables that have the most influence on the resulting classification. Discriminant analysis of extant alcid measurement data identified the medial length of the

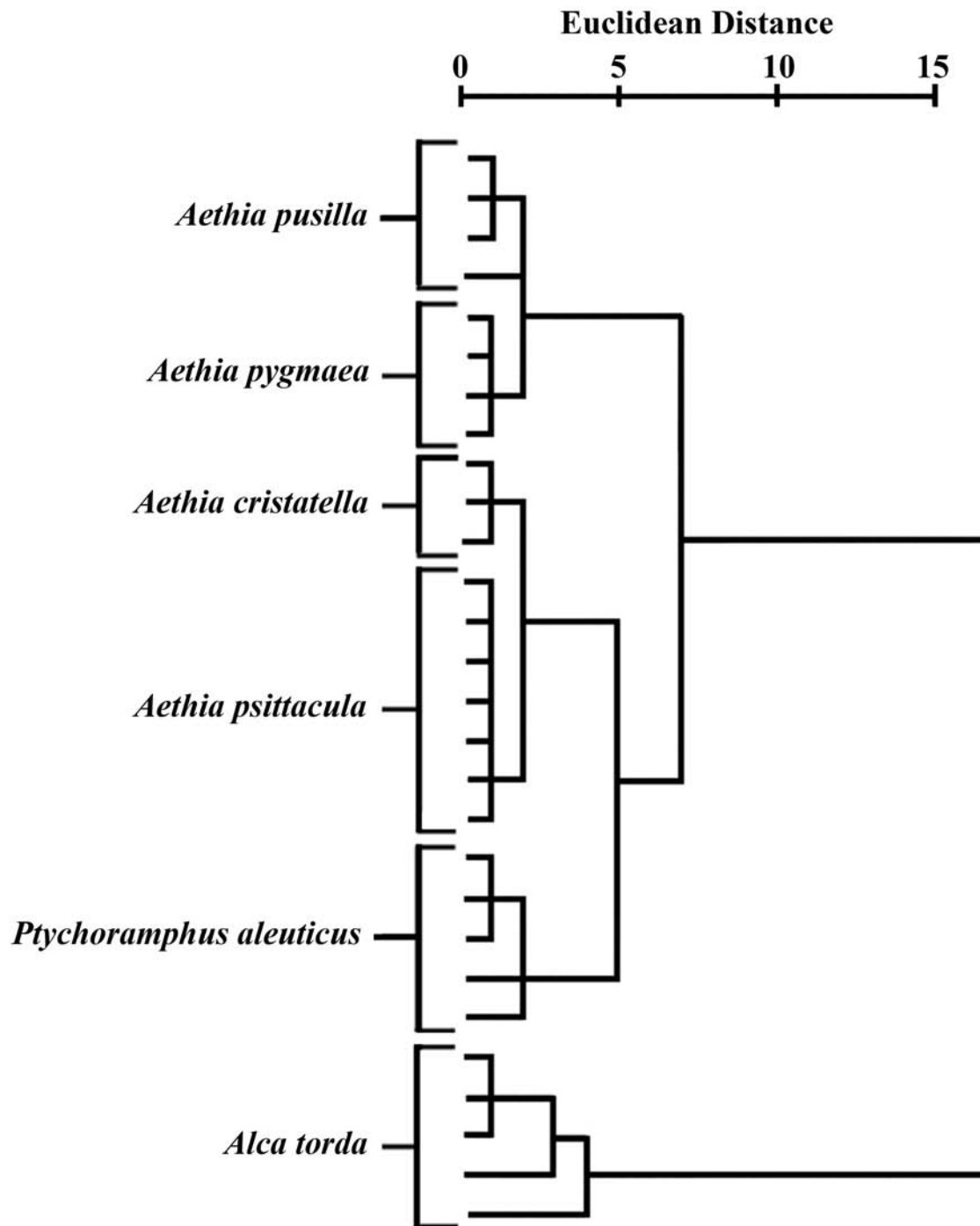


Figure 2.4- Example phenogram from cluster analysis results of extant alcid species based on humeral measurements. Each terminal represents a separate specimen of a particular species. Note, species relationships shown reflect size similarity, not phylogeny.

coracoid as the most informative classificatory variable included in the analysis, followed in order of decreasing utility by the greatest length of the humerus.

The range of intraspecific size variation among extant alcids (based on the median value of greatest length of humeri for each species) varied from  $\pm 1.1\%$  in *Uria lomvia* to  $\pm 6.2\%$  in *Alca torda* (Table 2.3). The calculated range of size differences between species of auklets varied from  $\pm 0.3\%$  from the median between *Aethia pusilla* and *Aethia psittacula*, to  $\pm 2.8\%$  between *Aethia pygmaea* and *Ptychoramphus aleuticus*.

**Extinct *Alca*:** After the robustness of this method for differentiating between extant species of alcids was evaluated, the same procedure (Fig. 2.3) was applied to mensural data collected from *Alca* fossils (Appendix 6). As with living species of alcids, morphometric analyses of measurement data from fossil ulnae (Appendix 6C) and carpometacarpi (Appendix 6D) did not result in distinctly clustered or statistically supported groups of fossils (Table 2.2). Analysis of coracoid measurement data (Appendix 6E) resulted in seven well-supported clusters of fossils (Table 2.2), which likely correspond to the seven species of *Alca*. Although *Alca* coracoids do not display sufficient inter-specific morphological differences to allow differentiation of all species within the clade, the coracoids of *Alca stewarti*, *Alca carolinensis*, *Alca torda*, and *Alca olsoni* can be differentiated by morphological and meristic means. Although there are no associated specimens of *Alca ausonia* or *Alca minor* that would allow for confident referral of coracoids to these species, the smallest *Alca* coracoids from the Yorktown Fm. are likely representative of *Alca minor*, and the size class of coracoids that are larger than *Alca torda* yet smaller than *Alca grandis* likely represent *Alca ausonia*.

Table 2.2- Summary of morphometric analyses and results. Taxon categories include the following species: Extant Alcidae = taxa listed in Appendix 1; Extant Atlantic = *U. aalge*, *U. lomvia*, *A. torda*, *C. grylle*, *A. alle*, *P. impennis*, and *F. arctica*; Auklets and *Alca* = *A. cristatella*, *A. psittacula*, *A. pusilla*, *A. pygmaea*, *P. aleuticus*, and *A. torda*; *Alca* fossils = fossils referred to *Alca* from both eastern and western Atlantic localities as well as extant *Alca torda* specimens utilized as a control group of specimens with known species identity. Note that accuracy of inclusion is only applicable for analyses of known (i.e., extant) taxa.

Alcid taxa	# of species	# of specimens	# of variables	Data type	# of clusters recovered	Accuracy of inclusion	Statistical support
Extant Alcidae	13	61	4	carpo-metacarpi	4-10	73%	<90%
Extant Alcidae	13	67	6	complete ulnae	5-9	69%	<90%
Extant Atlantic	8	40	66	entire skeleton	8	100%	100%
Extant Atlantic	8	40	6	complete humeri	8	92%	97%
Auklets & <i>Alca</i>	6	28	53	entire skeleton	6	100%	100%
Auklets & <i>Alca</i>	6	28	6	complete humeri	6	96%	96%
Auklets & <i>Alca</i>	6	28	3	proximal humeri	6	82%	94%
Auklets & <i>Alca</i>	6	28	3	distal humeri	6	93%	90%
<i>Alca</i> fossils	?	121	4	carpo-metacarpi	5-7	NA	<90%
<i>Alca</i> fossils	?	116	6	complete ulnae	4-7	NA	<90%
<i>Alca</i> fossils	?	58	1	medial coracoids	7	NA	97%
<i>Alca</i> fossils	?	79	6	complete humeri	6	NA	93%
<i>Alca</i> fossils	?	146	3	proximal humeri	6	NA	92%
<i>Alca</i> fossils	?	117	3	distal humeri	6	NA	93%

Table 2.3- Comparison of alcid humeral size variation. All data are from greatest length of the humerus except for data for *Australca*, which are measurements of the greatest width of the distal humerus. Integer values are in mm and have been rounded to the nearest tenth.

Taxa	Size range	Median value	Variation from median value
<i>Alca torda</i> (extant)	9.9	77.9	6.0%
<i>Pinguinus impennis</i>	4.5	104.1	2.1%
<i>Uria aalge</i>	7.3	85.6	4.5%
<i>Uria lomvia</i>	1.9	88.5	1.1%
<i>Alle alle</i>	3.1	41.9	3.8%
<i>Cephus grille</i>	3.9	59.8	3.4%
<i>Cephus columba</i>	4.2	66.7	3.3%
<i>Fratercula arctica</i>	7.7	65.1	5.6%
<i>Ptychoramphus aleuticus</i>	3.8	45.4	9.2%
<i>Aethia psittacula</i>	2.3	54.4	2.1%
<i>Aethia pusilla</i>	1.7	34.8	2.4%
<i>Aethia cristatella</i>	3.7	52.5	3.4%
<i>Aethia pygmaea</i>	0.9	37.9	1.2%
<i>Alca torda</i> (fossils)	12.3	77.4	8.6%
<i>Alca grandis</i>	15.2	92.0	7.6%
<i>Alca carolinensis</i>	1.8	101.9	0.9%
<i>Alca ausonia</i>	2.8	105.4	1.3%
<i>Alca stewarti</i>	0.8	111.6	0.4%



Analyses of complete, proximal, and distal ends of humeri all resulted in clusters of fossils with high degrees of statistical support (Table 2.2) and distinct morphologies. Cluster and discriminant analyses of complete, proximal and distal ends of humeri recovered six statistically supported size-based groups of fossils (Fig. 2.5; Table 2.2). The holotype and paratype humeri of *Alca grandis*, *Alca stewarti*, *Alca torda*, *Alca minor*, and *Alca ausonia* were recovered in separate statistically supported clusters (Fig. 2.5). The similarly proportioned *Alca olsoni* and *Alca carolinensis* clustered together. Although *Alca carolinensis* and *Alca olsoni* can be differentiated based on characteristics of the coracoid, ulna, radius, and furcula, the humeri of these species are morphologically similar, and are comparable in greatest humeral length. Although *Alca olsoni* is slightly more robust with respect to other proportions (Table 2.4), greatest length of the humerus was identified as the second most informative measurement in the discriminant analysis, therefore explaining how six size classes could represent seven different species. Rather than trying to separate humeri representing these two species based upon statistically insignificant size differences, referrals of isolated humeri to these species were left ambiguous (Appendix 6A). Adding further support to the hypothesis that six distinct size classes are represented by the proximal and distal humeri measurement data, iterative analyses with fossil measurement data clustered into two, three, four, five, seven, and eight clusters did not receive strong (i.e., >90%) statistical support.

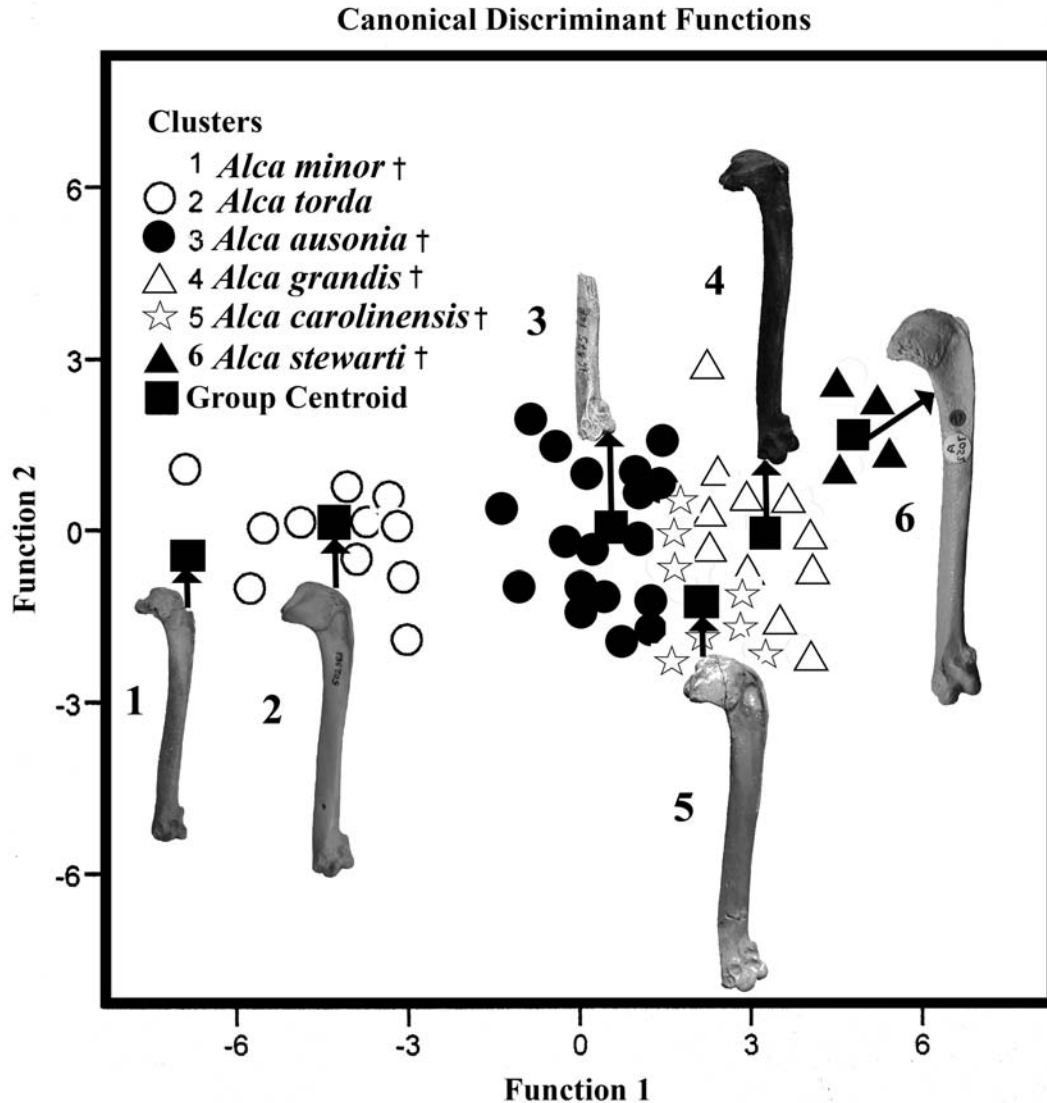


Figure 2.5- Graphical representation of results from the discriminant function analysis of *Alca* humeri. Plot shows *Alca* species clusters and representative humeri: **1.** *Alca minor* holotype specimen (USNM 302324); **2.** *Alca torda* (USNM 502382); **3.** *Alca ausonia* cast of holotype specimen (IGF 14875); **4.** *Alca grandis* holotype specimen (ANSP 13357); **5.** *Alca carolinensis* (NCSM 13734); **6.** *Alca stewarti* cast of paratype specimen (BMNH 7052). *Alca olsoni* not shown owing to overlap in size range with *Alca carolinensis*. Note that *Alca minor* is represented only by a centroid because only one complete humerus is known for that taxon. Values on vertical and horizontal axes represent the coefficients of the variables of the discriminant axes, where discriminant function 1 represents the maximum amount of variation in the data.

Additional morphometric analyses were conducted including measurement data from extant *Alca torda* specimens in order to identify which clusters of fossils are referable to that species, and to further test the validity of previously recovered clusters containing the holotype specimens of other *Alca* species. Extant *Alca torda* specimens were recovered in a single cluster that did not contain the holotype or paratype specimens of any other *Alca* species, allowing for potential identification of Pliocene examples of this taxon. Pliocene examples of this taxon were slightly larger on average than extant examples (Table 2.4), but are otherwise morphologically identical to the extant sample with respect to humeral morphology.

Table 2.4- Measurements of *Alca* humeri in mm (measurements based on von den Driesch, 1976). Abbreviations: **Bd**, breadth of the distal end; **Bp**, breadth of proximal end; **Dd**, distal diagonal; **Dip**, diagonal of proximal end; **Gl**, greatest length; **Sc**, smallest dorsoventral breadth of corpus (shaft). Extant *Alca torda* specimen numbers listed in Appendix 1.

Taxa	Specimen #	Bd	Bp	Dd	Dip	Gl	Sc
<i>Alca ausonia</i>	IGF 14875	12.4	-	9.2	-	-	7.5
<i>Alca carolinensis</i>	NCSM 13734	14.9	20.8	10.4	21.0	102.4	9.2
<i>Alca grandis</i>	ANSP 13357	13.9	19.7	9.4	18.8	97.2	8.2
<i>Alca minor</i>	USNM 302324	-	13.8	-	-	63.7	5.7
	USNM 192879	-	13.2	-	-	-	-
	USNM 495600	9.1	-	7.0	-	-	5.8
<i>Alca olsoni</i>	USNM 454590	15.4	22.8	11.0	21.7	104.0	8.8
<i>Alca stewarti</i>	BMNH A 7052	15.5	22.8	12.1	21.8	111.2	8.9
<i>Alca torda</i> (extant)	average (n=13)	11.2	16.4	8.1	15.7	78.4	7.0
<i>Alca torda</i> (fossils)	average	11.5 (n=14)	16.5 (n=44)	8.4 (n=14)	15.5 (n=43)	78.8 (n=17)	6.8 (n=44)

Adding further support to the hypothesis that at least six species of *Alca* are represented by the measured fossils, the range of size variation based upon greatest length of the humerus within five of the six clusters is congruent with the size range established based on extant alcids (Table 2.3). Only values for *Alca stewarti* showed a significantly different range than observed in other alcids, and this may be an artifact because only three complete humeri are known from this taxon. Values of size variation calculated using measurements from distal humeri referred to *Alca stewarti* ( $n = 10$ ) vary 5.3% from the median, a value similar to estimates of size variation for other extinct *Alca* and extant *Alca torda* (Table 2.3).

Morphological comparison of the six clusters of fossils revealed previously undocumented morphological variation that allowed for referral of three associated *Alca* specimens to species. Clusters of humeri corresponding to *Alca carolinensis* and *Alca olsoni* could not be separated based on morphological differences. *Alca* diversity would therefore be underestimated if it were not for the association of other elements (e.g., ulnae) in the holotype specimens of those species, which display distinct morphological differences between those two species. Combination of holotype and referred specimens into supraspecific terminals decreased the amount of missing data for *Alca* species terminals and facilitated phylogenetic analysis.

Additional analyses performed on a subset of mensural data collected from the Early Pliocene Yorktown Fm. also recovered six statistically supported clusters of complete and partial humeri. Morphological evaluation of specimens from this locality

confirms that all seven species of *Alca* were present in North Carolina during the Pliocene.

Specimens from the Early Pliocene Bone Valley Fm. of southern Florida (i.e., ‘*Australca grandis*’ *sensu* Brodkorb, 1955) were assigned to three distinct size classes and displayed a large range of size variation (based on measurements of distal humeri; 14.5%), suggesting that more than one species is represented by this assemblage. The principal components analysis by Olson and Rasmussen (2001) obtained a similar result. Only one complete humerus (GCVP 5691) is known from this location. That specimen was recovered with specimens representing *Alca grandis*. However, analysis of 45 proximal and distal humeri from that location resulted in placement of ‘*Australca*’ specimens in clusters corresponding to *Alca grandis*, *Alca torda*, and *Alca ausonia* (Appendix 6A).

Strong statistical support for morphometrically-clustered groups of fossils, and congruence between those groups and morphological-based assessment of those groups, allow for referral of 203 *Alca* humeri to species (Appendix 6A). Additionally, specimens were consistently clustered together based upon analysis of multiple subsets of data. For example, the holotype humerus of *Alca carolinensis* was clustered along with the same specimens in analyses of complete humeri, proximal humeri, and distal humeri. Nineteen complete humeri (e.g., USNM 446692; Appendix 6A) can now be confidently referred to *Alca ausonia*, which was previously known only from the holotype specimen, a distal humerus. Two associated specimens (USNM 336379, USNM 215454) are referred to *Alca grandis*, greatly increasing the number of characters available for phylogenetic

analysis of that taxon. An additional associated specimen (USNM 242238) is referred to *Alca stewarti*.

The referral of *Alca humeri* through the combined morphometric and phylogenetic analysis approach allowed for calculation of tentative estimates of relative species abundance from the Yorktown Formation. The most frequently represented taxon is likely *Alca grandis* (25.7%), because humeri representing *Alca carolinensis* and *Alca olsoni* (27.6%) were combined owing to the morphological similarity of the humeri of those species. Remains of *Alca minor* (3.9%) and *Alca stewarti* (2.0%) are the least frequently represented. The remainder of the sample was composed of the remains of *Alca ausonia* (18.4%) and *Alca torda* (22.4%). These estimates of relative species abundance assume that all seven species lived contemporaneously and that the Yorktown Fm. is not significantly time-averaged. Chronological evaluation of *Alca* species diversity within the Yorktown Fm. will require direct sampling of in-situ *Alca* fossils. Exposures of the Yorktown Fm. outside the PCS Phosphate Mine are rare, and permission to sample directly from in-situ strata at the PCS Mine has not been obtained.

The possibility of the existence of a Pliocene alcid even larger than *Alca stewarti* was mentioned by Olson and Rasmussen (2001), and Dyke and Walker (2005). The specimen mentioned by Olson and Rasmussen (2001; USNM 181090) was evaluated and found to be within the statistically supported size range of *Alca stewarti*. A very large premaxilla (BMNH A 9033) with the mediolateral compression and dorsal expansion characteristic of *Alca* and *Pinguinus* premaxillae was reported by Dyke and Walker (2005). Given the very large sample size of Pliocene *Alca* fossils, and the lack of

statistical support for a species of *Alca* larger than *Alca stewarti*, it seems likely that this specimen represents the first record of *Pinguinus* from the Early Pliocene Kallo Sands Formation of Belgium. Although fragmentary, the curvature and size of BMNH A 9033 agrees more with specimens of *Pinguinus* than with those known for *Alca*.

## PHYLOGENETIC RESULTS

Phylogenetic analysis of the combined matrix resulted in a single most parsimonious tree (L: 1931; CI: 0.80; RI: 0.47; RC: 0.38; Fig. 2.6). An additional analysis performed with all characters unordered did not result in topological differences, or an increase in the number of MPTs recovered. Bootstrap and Bremer support values were highest for clades with higher proportions of extant taxa and thus available molecular data (i.e., *Pinguinus* and *Uria*), and were fairly low for clades including abundant extinct taxa with significant amounts of missing data (i.e., *Alca* and *Miocepphus*). Optimized morphological characters that support recovered clades are listed in Table 2.5.

As with the results previous studies of alcid relationships (Strauch, 1985; Chandler, 1990a; Moum et al., 2002; Baker et al., 2007; Pereira and Baker, 2008), this study recovered strong support for a clade composed of *Alca* and *Pinguinus*, although relationships between *Alca* species remained partially unresolved. *Alca torda* and *Alca minor* were recovered as sister taxa, and *Alca stewarti*, *Alca carolinensis*, and *Alca olsoni* were recovered as successive outgroups to this clade. The positions of *Alca grandis* and *Alca ausonia* remain unresolved at the base of *Alca*. Although the sister relationship of *Pinguinus impennis* and *Pinguinus alfrednewtoni* is strongly supported by these results,

Table 2.5- Apomorphies supporting clades in the resultant phylogenetic tree (Fig. 2.15). Character numbers from Appendix 2 are followed by character state symbols (e.g., 23:0 corresponds with character 23, state 0). Characters followed by ‘\*’ are locally optimized apomorphies with a CI <1.0. All other apomorphies have a CI = 1.0.

Clade	Character numbers and states that support monophyly
Alcini:	(17:0); (69:0); (94:0); (100:0); (110:0); (116:0); (117:0); (130:0); (136:0); (139:0); (145:0); (160:1); (182:1); (184:0); (191:1); (202:1); (204:1); (206:1); (226:1).
<i>Alca</i> + <i>Pinguinus</i> :	(26:1); (42:1); (113:1); (201:0).
<i>Alca</i> :	(213:0)*.
<i>Pinguinus</i> :	(107:1); (170:1); (212:0); (217:0).
Miocepphini:	(9:1); (34:0); (45:1); (48:0); (174:1).
<i>Uria</i> :	(169:1)*; (183:1)*; (196:1)*.
<i>Miocepphus</i> + <i>Alle</i> :	(101:1); (168:0).
<i>Alle</i> + <i>Miocepphus mergulellus</i> :	(114:1)*; (127:0)*.
<i>A. torda</i> + <i>A. minor</i> + <i>A. stewarti</i> + <i>A. carolinensis</i> + <i>A. olsoni</i> :	(75:1); (183:1)*.
<i>A. torda</i> + <i>A. minor</i> + <i>A. stewarti</i> :	(105:0)*; (122:0)*; (171:1)*.
<i>A. torda</i> + <i>A. minor</i> :	(118:1)*.



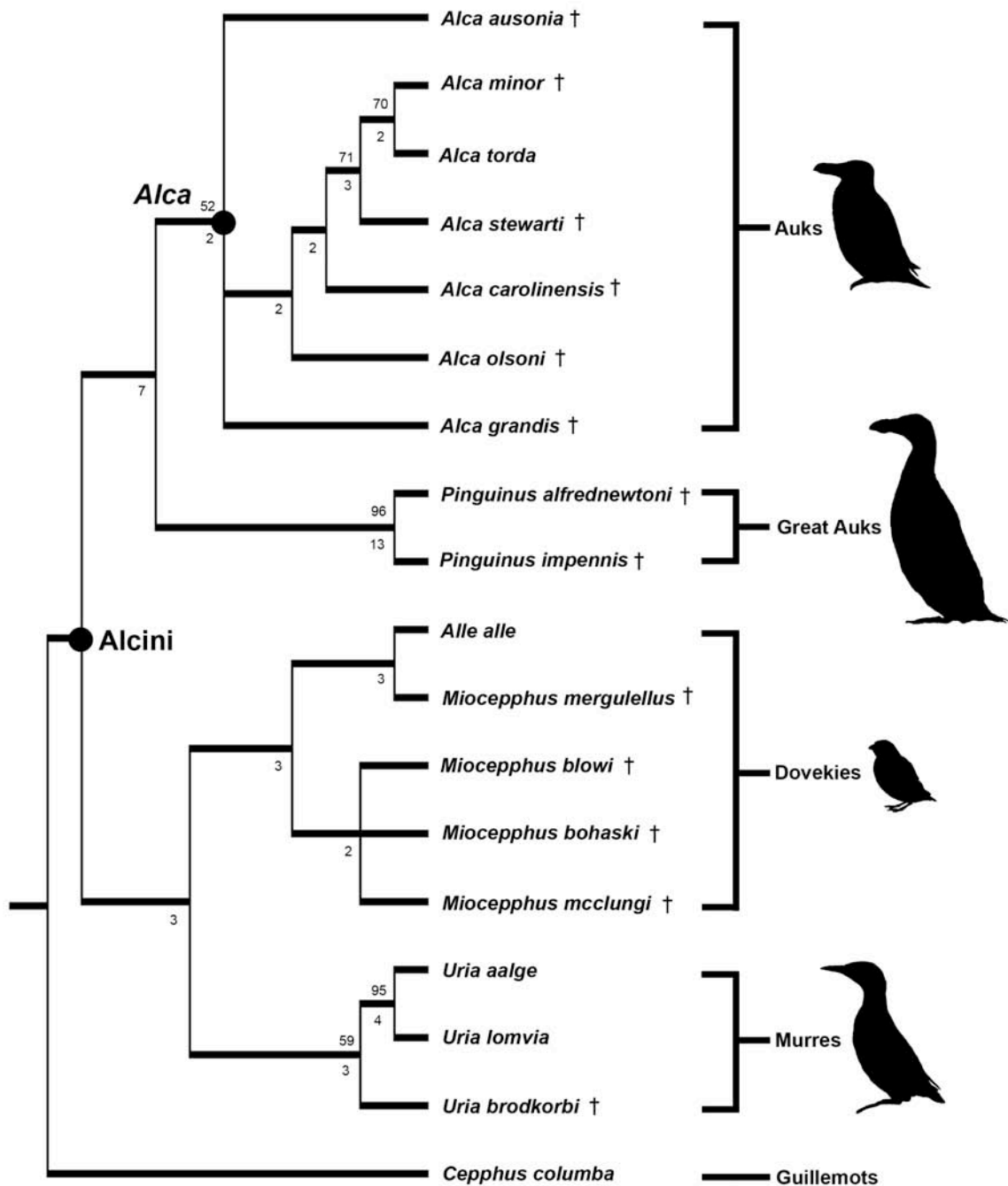


Figure 2.6- Cladogram of Alcini relationships resulting from parsimony-based analysis of the combined data (1 MPT, L: 1931; CI: 0.80; RI: 0.48; RC: 0.38). Bootstrap support values >50% are presented above and Bremer support values are presented below the node they refer to.

the monophyly of *Alca* with respect to *Pinguinus* is weakly supported. This study identified four unambiguously optimized morphological synapomorphies that unite *Alca* and *Pinguinus*, but only a single locally optimized character that supports the monophyly of *Alca* (Table 2.5). Further clarification of the systematic relationship between *Alca* and *Pinguinus*, and support for *Alca* monophyly will require discovery of additional associated *Alca* fossil specimens referable to species. Although there are documented integumentary differences between *Alca torda* and *Pinguinus impennis* (Strauch, 1985; Chandler, 1990a), there are no known fossils that preserve integumentary details of additional extinct *Alca* and *Pinguinus* species that might provide these missing data, data that might clarify the relationship between *Alca* and *Pinguinus*.

The clade comprising *Alca* and *Pinguinus* was recovered as the sister to the clade that includes *Uria*, *Miocepphus*, and *Alle*. *Uria* was recovered as monophyletic, with *Uria brodkorbi* placed as an outlier to extant sister taxa *Uria aalge* and *Uria lomvia*. *Uria* is placed as the sister taxon to a clade composed of *Miocepphus* + *Alle*. *Alle alle* is placed as the sister taxon to *Miocepphus mergulellus*. *Alle alle* and *Miocepphus mergulellus* were recovered as the sister taxon to an unresolved clade composed of the other *Miocepphus* species (i.e., *Miocepphus blowi*, *Miocepphus bohaski*, and *Miocepphus mcclungi*).

Because this was the first phylogenetic analysis to include all 17 Alcini species, 12 of which had not been previously phylogenetically analyzed, comparisons between these results and the results of previous analyses are somewhat limited. *Alca torda* has been recovered as the sister taxon to *Pinguinus impennis* in every analysis that has

included both taxa (Strauch, 1985; Chandler, 1990a; Moum et al., 2002; Baker et al., 2007; Pereira and Baker, 2008). However, extinct *Alca* species and *Pinguinus alfrednewtoni* have not been previously included in a phylogenetic analysis. The sister relationship between *Alca* plus *Pinguinus*, and *Uria* is also strongly supported by the results of previous analyses (Strauch, 1985; Chandler, 1990a; Moum et al., 2002; Baker et al., 2007; Pereira and Baker, 2008).

The systematic position of *Alle alle* is perhaps the most contentious issue within alcid systematics, because it has been recovered as the sister to *Alca* (Moum et al., 1994), outgroup to *Alca* and *Pinguinus* (Moum et al., 2002; Baker et al., 2007), sister to *Alca* and *Pinguinus* plus *Uria* (Strauch, 1985), sister to *Uria* (Thomas et al., 2004; Pereira and Baker, 2008), sister to Fraterculinae (Chandler, 1990a), and sister to *Cepphus*, *Aethia*, and *Brachyramphus* (Chu, 1998). The nested placement of *Alle* along with *Miocepphus* species supports the hypothesized affinity between these taxa (Wijnker and Olson, 2009). The placement of *Alle* and *Miocepphus* as the sister taxon to *Uria* is also congruent with the molecular-based results of Pereira and Baker (2008) and Thomas et al. (2004), in which *Alle alle* was placed as the sister to *Uria*.

## SYSTEMATIC PALEONTOLOGY

AVES Linnaeus, 1758

CHARADRIIFORMES Huxley, 1867

ALCIDAE Leach, 1820

*Remarks*—Originally spelled ‘Alcadae’ the earliest usage of this name is often credited to Leach (1820). However, the authorship of this document is not precisely known (ICZN, 1977). In 1977 the ICZN voted to suppress the name ‘Alcadae’ and replace it with Alcidae, for which the earliest usage was that by Bonaparte (1831). For a detailed nomenclatural and classificatory history of alcids see Coues (1868) and Sibley and Ahlquist (1990).

ALCINI Storer, 1960

(contents include *Alca*, *Pinguinus*, *Uria*, *Alle*, and *Miocepphus*)

*ALCA* Linnaeus, 1758

*Diagnosis*—*Alca* is referable to Alcidae based on dorsoventral compression of the humerus (145:0), radius, and ulna (182:0). The shafts of these elements are more rounded in cross-section in all other Charadriiformes. The humeral, radial, and ulnar shafts of *Cephus* and *Pseudocepphus teres* are intermediate with respect to shaft-roundness (145:1; 182:1) as compared to all other Alcidae and Charadriiformes systematically placed outside of Alcidae. As in all Alcidae except Mancallinae Brodkorb, 1967, the dorsal cotylar process of the ulna is anteriorly expanded to a degree exceeding that of other Charadriiformes. As in all alcids, the sternum is elongated in comparison with the relatively shorter sterni of other Charadriiformes. *Alca* is referable to Alcini (contents = *Alca* + *Pinguinus* + *Uria* + *Alle* + *Miocepphus*) based on anterior flattening of the extensor process of the carpometacarpus (191:1). *Alca* is differentiated from *Pinguinus*

by the restriction of the deltopectoral crest to the proximal half of the humeral shaft (107:0). The coracobrachial nerve sulcus of *Alca* and *Pinguinus* is a closed duct (113:1), rather than an open sulcus (113:0) as in other Alcini. *Alca* and *Pinguinus* are differentiated from *Uria*, *Alle*, and *Miocepphus mergulellus* based on the equal width of the tricipital sulci of the distal humerus (151:1). The humerotricipital sulcus is wider than the scapulotricipital sulcus in *Uria* (151:0) and *Miocepphus mergulellus*. The scapulotricipital sulcus is wider than the humerotricipital sulcus in *Alle* (151:2).

*Remarks*—Despite a long history of study, no osteological apomorphies of *Alca* have been identified. The lack of osteological distinction from *Pinguinus* calls into question the monophyly of *Pinguinus* with respect to *Alca*. *Alca* (*sensu* Linnaeus, 1758) originally contained the Great Auk, which was then known as *Alca impennis*. Both Strauch (1985) and Chandler (1990a) recommended that *Pinguinus* be synonymized with *Alca*; however, both the American and British Ornithologists' Unions have followed the recommendations of Salomonsen (1944) and Olson (1977) in maintaining the generic status of *Pinguinus*. Although *Pinguinus impennis* is characterized by many apomorphies with respect to *Alca torda*, the monophyly of *Alca* to the exclusion of *Pinguinus* is weakly supported by current osteological data. However, knowledge of the skeletal anatomy of extinct *Alca* that might bolster support for *Alca* monophyly is currently incomplete for most species in the clade.

*Alca* Linnaeus, 1758 was originally included as a member of the Order Natatore (anseriforms, podicipediforms, gaviiforms, sphenisciforms, pelicaniforms, and

charadriiforms), which was defined by “the backward position of the legs, which are thrown entirely behind the equilibrium of their body, and with wings considerably shorter, and less covered with feathers than those of any other birds” (Vigors, 1825:497). Family ‘Alcidae’ (sensu Vigors, 1825) was differentiated and later separated from other Natatore (sensu Linnaeus, 1758) based on the ‘tri-dactyl’ configuration of the feet (i.e., absence of a hallux), and differentiated from sphenisciforms by the mediolateral compression of the bill. Close relationship of alcids with penguins was a common misconception (e.g., Linnaeus, 1758; Verheyen, 1958; Gysels and Rabaey, 1964). Originally, *Alca* (sensu Linnaeus, 1758) included six species: *A. impennis*, *A. torda*, *A. pica*, *A. arctica*, *A. lomvia*, and *A. alle*. *Alca pica*, upon further study, turned out to be *Alca torda* in winter plumage (Coues, 1868). The other five species are still recognized, though only *torda* is placed within *Alca* in modern classifications.

Unlike the preceding classifications, that of Gadow (1892) considered osteological and ethological characters in making distinctions between avian taxa. Alcidae was placed along with Laridae in Suborder Gaviae of the Order Charadriiformes based upon 5 characters: aquatic lifestyle, complex coloration of down in nestlings, ossified supraorbital rims, and hypotarsus with 2 grooves (Gadow, 1892). Among Gaviae, Gadow (1892) diagnosed Alcidae on the basis of five additional characters: Palearctic (i.e., Holarctic) distribution, coracoids not fused, dorsal supracondylar process absent (this feature is not absent but merely reduced in alcids relative to larids), presence of a procoracoid process, and sternum with only two notches posteriorly (i.e., medial sternal notches absent; contra Gadow 1892, medial sternal notches are present in puffins).

*Alca* (including *Pinguinus*) was further distinguished from other Alcidae by Beddard (1898) on the basis of three characters: foramen at the anterior end of the supra-orbital groove, lack of a medial notch of the sternum (in contrast with puffins), two ‘brevis’ tendons (i.e., brachialis muscle with two heads) which pass over the extensors and insert on the ulna. The oological study of Dawson (1920) differentiated *Alca* and *Uria* from other alcids on the basis of four characters: single egg clutches, ovate shape, dull luster, and granular texture. In a study of Alcidae hind limb osteology, Storer (1945a) united *Alca*, *Pinguinus*, and *Uria* and cited the following characteristics: long and narrow post-acetabular ilium; narrow, tapering posterior ischium; leg of medium length, with thick joints; moderately heavy toes with short, broad claws; especially heavy tarsometatarsus with a groove on its upper surface.

More recent osteological studies (Strauch, 1985; Chandler, 1990a) have resulted in an increasing suite of proposed diagnostic characters for *Alca* and *Pinguinus*. The compatibility analysis by Strauch (1985) identified an *Alca torda* + *Pinguinus impennis* clade that was defined by the presence of a coracoidal foramen, a flat extensor process of the carpometacarpus, first tendinal canal of the hypotarsus a narrow groove, completely feathered nostrils, one incubation patch, intermediate post-hatching development pattern, nesting in the open, and pointed retrices. The phylogenetic analysis of Chandler (1990a) identified five additional apomorphies that unite *Alca* and *Pinguinus*: enlarged premaxilla, nasal bar extending beneath premaxilla, internal cotyla of the ulna with a lateral crest that is separate from the anterior articular ligament scar, and a crest that extends from the shaft of the femur to the lateral edge of the internal cotyla.

The earliest known fossil referred to Alcidae was also proposed to have affinities with *Alca*. This specimen (GCVF 5690) is from the Late Eocene (34.2-36 Ma) Clinchfield Formation of Wilkinson County Georgia, USA (Chandler and Parmley, 2002), and consists of an isolated and weathered distal humerus. The equal width of the tricipital sulci is consistent with the morphology of *Alca* and *Pinguinus*. However, due to the weathered and fragmentary nature of this isolated specimen, it cannot be confidently referred at this time. It is best considered Alcidae *incertae sedis*.

Two specimens from Late Miocene deposits in Laguna Hills, California, USA were tentatively referred to *Alca* by Howard (1968). These specimens consist of a fragment of coracoid (LACM 18282) and a weathered distal humerus (LACM 18283). Recent re-examination of these specimens failed to identify any characters that would support referral to any Alcini taxon. Furthermore, no additional material has been referred to *Alca* from Pacific localities in the intervening 40 years. Thus, *Alca* affinities of these specimens are considered unreliable, and these fossils are identified as Alcidae *incertae sedis*.

Although previously referred *Alca* cranial material is largely restricted to bills (Olson and Rasmussen, 2001; Dyke and Walker, 2005), two fossilized skulls from Pliocene age deposits have been referred to *Alca* (Fig. 2.7). The first specimen (Alam 0001) is housed in the collections of the Asociación Cultural Paleontológica Murciana, Murcia Spain, and was described by Sanchez-Marco (2003). Recent re-examination of this specimen confirms its referral to *Alca* based upon the mediolaterally compressed and dorsoventrally expanded premaxilla, and deeply incised nasal salt gland fossae. The



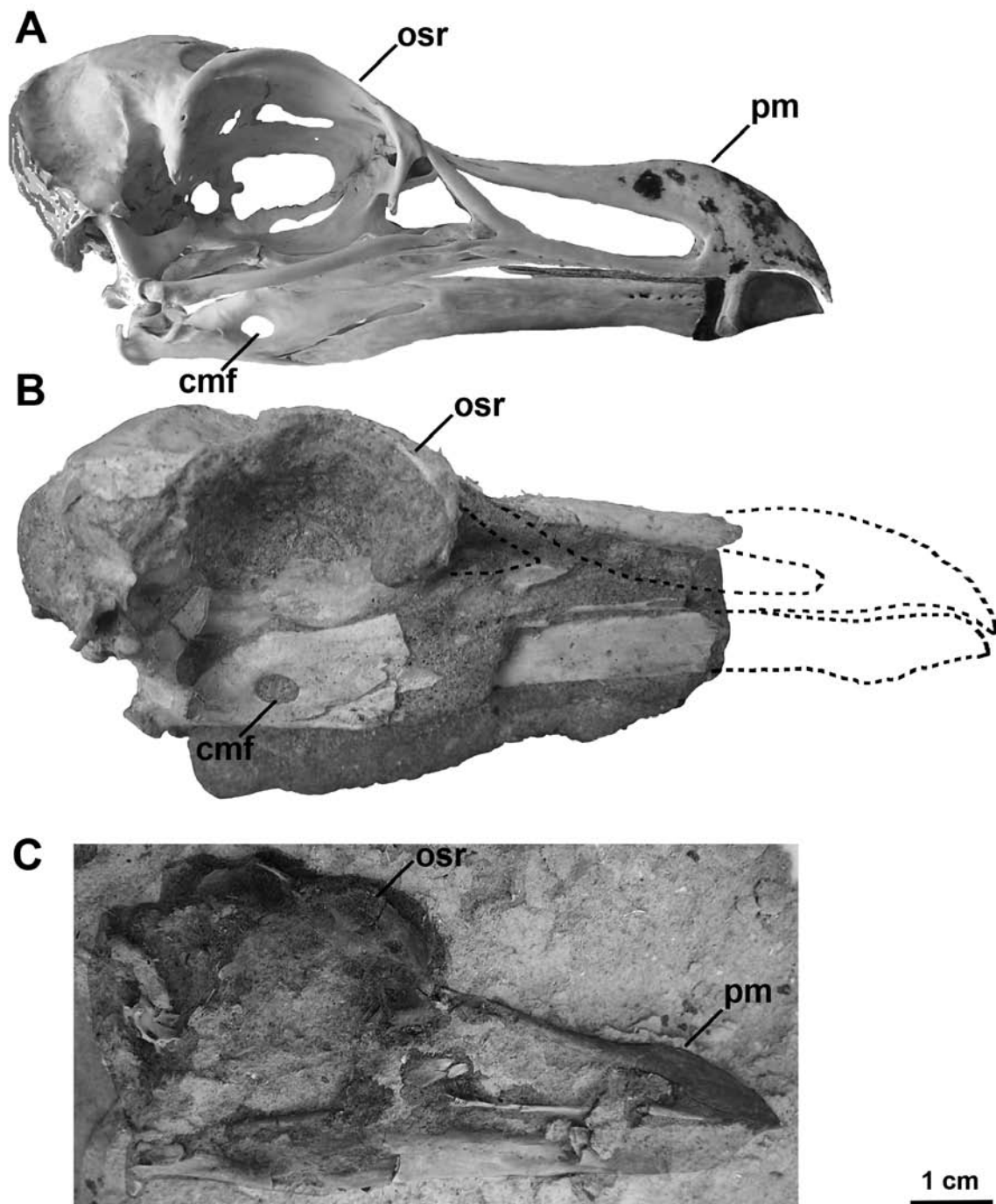


Figure 2.7- Comparison of skulls referred to *Alca* in right lateral view. **A.** *Alca torda* NCSM 20058; **B.** Alam-001; **C.** NCSM 24139. Anatomical abbreviations: (**cmf**) caudal mandibular fenestra; (**osr**) ossified supraorbital rim; (**pm**) dorsally expanded premaxilla.

second skull (NCSM 24139) was recovered from the Yorktown Fm. exposed at Aurora, North Carolina, and is reported herein for the first time (Fig. 2.7). These two skulls are both comparable in size and morphological characteristics to *Alca torda*, although these skulls lack any associated post-crania, preventing referral of these specimens to species at this time. There is currently only a single associated *Alca* fossil specimen with both cranial and postcranial elements preserved (USNM 336380; Olson and Rasmussen, 2001) that might allow diagnosis of cranial characters for extinct *Alca* species. The only cranial element preserved by USNM 336380 is the premaxilla, and no discrete morphological variation was identified between that specimen, the two skulls described above, and extant *Alca torda* specimens.

### ***ALCA TORDA* Linnaeus, 1758**

*Diagnosis*—*Alca torda* is differentiated from other species of *Alca* by the following characteristics of the humerus: distal margin of posterior humeral head rounded as in *Alca stewarti*, and *Alca minor*, (105:0; pointed in *Alca olsoni*, *Alca stewarti*, *Alca ausonia*, and *Alca grandis*); dorsal margin of the primary pneumotricipital fossa (i.e., crus dorsale fossae; Baumel and Witmer, 1993) of *Alca torda* and *Alca minor* extends further distally (118:1) than in all other *Alca*; primary pneumotricipital fossa rounded as in *Alca minor* and *Alca stewarti* (122:0; oval in all other *Alca*); distal edge of the primary pneumotricipital fossa straight as in *Alca carolinensis*, *Alca grandis*, *Alca olsoni*, and *Alca stewarti* (129:1; concave in *Alca minor* and *Alca ausonia*). The size of *Alca torda* is

intermediate between that of the smaller *Alca minor* and the larger *Alca ausonia* (Table 2.4; Fig. 2.2).

*Remarks*—Remains of at least four species of *Alca* from Early Pliocene deposits in North Carolina (*Alca* aff. *torda*, *Alca ausonia*, *Alca grandis*, *Alca* sp.) were reported by Olson and Rasmussen (2001). Among these fossils are specimens that are consistent in both size and morphological characteristics with the extant Razorbill Auk *Alca torda* (Fig. 2.2). Furthermore, Miocene aged (5-10 Ma) specimens from deposits in Maryland and Virginia, USA, were recently referred to *Alca* cf. *torda* by Wijnker and Olson (2009). Although estimates of the average geologic longevity of species are variable (May et al., 1995), the existence of *Alca torda* throughout the last 10 Ma would constitute an example of extreme species-longevity. Although the extension of the temporal range of an extant species into the Miocene prompts questions about both the longevity and diagnosability of species (Stewart, 2002, 2007), no discrete differences in size or morphology between Miocene and Pliocene fossils attributed to *Alca* aff. *torda* and extant *Alca torda* specimens were noted in specimens examined. Furthermore, Miocene *Alca* specimens provide a calibration point for the divergence between *Alca* and *Pinguinus*.

### ***ALCA GRANDIS* (Marsh, 1870)**

*Holotype*—left humerus (ANSP 13357; Figs. 2.2 & 2.5).

*Referred material*—right coracoid, right distal humerus (USNM 215454; specimen referred to *Alca grandis* by Olson and Rasmussen, 2001; Fig. 2.8); partial sternum, right distal humerus, right proximal radius, right ulna, right distal carpometacarpus, right digit I phalanx 1, right digit II phalanx 1, right digit II phalanx 2, partial pelvis, right femur, right proximal tibiotarsus (USNM 336379; specimen referred to *Alca grandis* by Olson and Rasmussen, 2001; Fig. 2.9). See Appendix 6A for referral of isolated humeri.

*Original diagnosis*—Originally described by Marsh (1870:213-214) as *Cataractes antiquus* (see Olson, 2007) and diagnosed relative to *Uria lomvia* based upon the following humeral characteristics: humeral head more obtusely rounded; tricipital grooves of approximately equal width; small posterodorsally projecting tubercle on the posterodistal margin of the ventral tubercle (Fig. 2.10); ventral condyle anteroposteriorly narrow.

*Amended diagnosis*—*Alca grandis* is characterized by a small posterodorsally projecting tubercle on the posterodistal margin of the ventral tubercle of the humerus (156:1). This tubercle is absent in all other *Alca* species, but is present in *Pinguinus* (Fig. 2.10). As in all *Alca*, restriction of the deltopectoral crest to the proximal half of the humeral shaft (107:0) differentiates *Alca grandis* from *Pinguinus*. *Alca grandis* is further differentiated from other species of *Alca* by the following characteristics: dorsal margin of the medial sternal process of coracoid notched (103:1) as in *Alca torda* and *Alca*

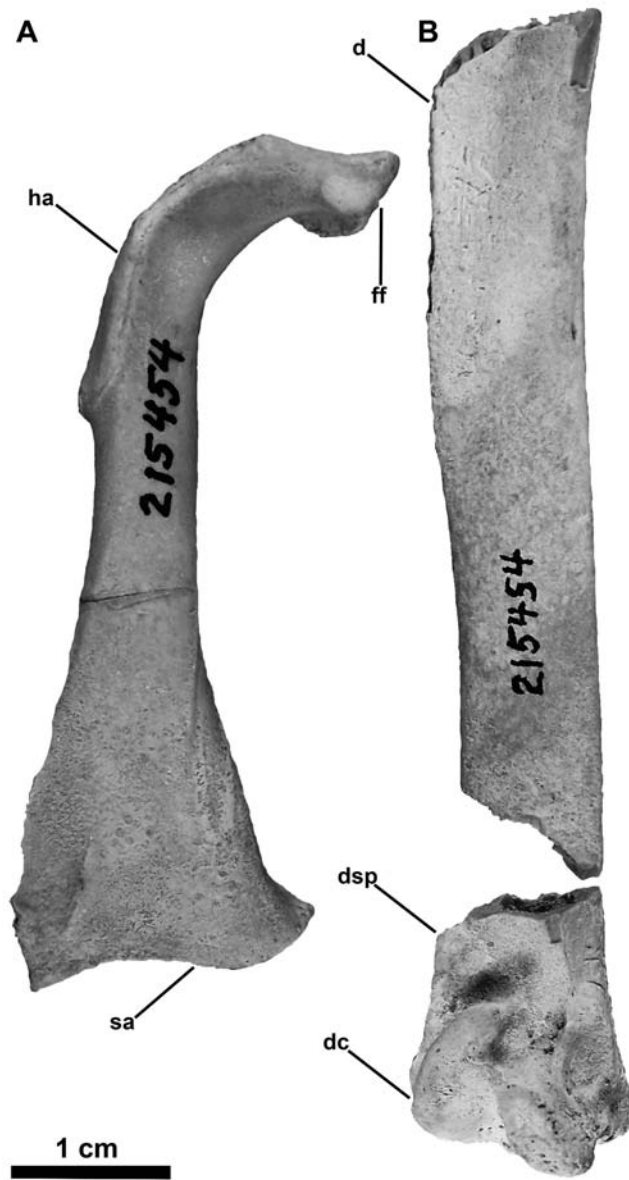


Figure 2.8- Associated specimen (USNM 215454) referred to *Alca grandis*. **A.** right coracoid, (mediolateral view); **B.** distal left humerus in two pieces (anterior view). Anatomical abbreviations: (**d**) deltopectoral crest; (**dc**) dorsal condyle; (**dsp**) dorsal supracondylar process; (**ff**) furcular facet; (**ha**) humeral articulation facet; (**sa**) sternal articular surface of coracoid.

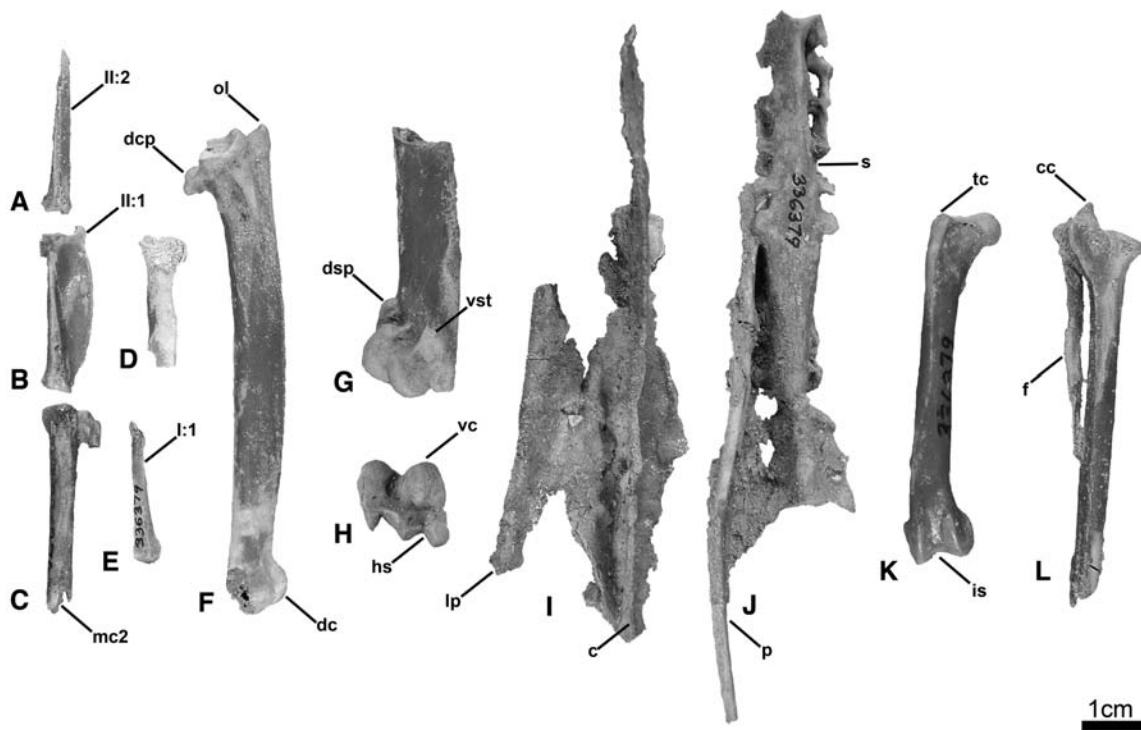


Figure 2.9- Associated specimen (USNM 336379) referred to *Alca grandis*. Specimen prepared from matrix since original description (see Olson and Rasmussen, 2001, Fig. 13). **A.** digit II phalanx 2 (dorsal view); **B.** digit II phalanx 1 (dorsal view); **C.** right distal carpometacarpus (ventral view); **D.** right proximal radius (ventral view); **E.** digit I phalanx 1 (dorsal view); **F.** right ulna (ventral view); **G.** distal right humerus (anterior view); **H.** right humerus (distal view); **I.** partial sternum (ventral view); **J.** partial pelvis (ventral view); **K.** right femur (anterior view); **L.** right proximal tibiotarsus and fibula (anteromedial view). Anatomical abbreviations: (**I:1**) manual phalanx I:1; (**II:1**) manual phalanx II:1; (**II:2**) manual phalanx II:2; (**c**) carina; (**cc**) cnemial crest; (**dc**) dorsal condyle; (**dcp**) dorsal cotylar process; (**dsp**) dorsal supracondylar process; (**f**) fibula; (**hs**) humerotricipital sulcus; (**is**) intercondylar sulcus; (**lp**) lateral process; (**mc2**) metacarpal two; (**ol**) olecranon process; (**p**) pubis; (**s**) sacrum; (**tc**) trochanteric crest; (**vst**) ventral supracondylar tubercle; (**vc**) ventral condyle.

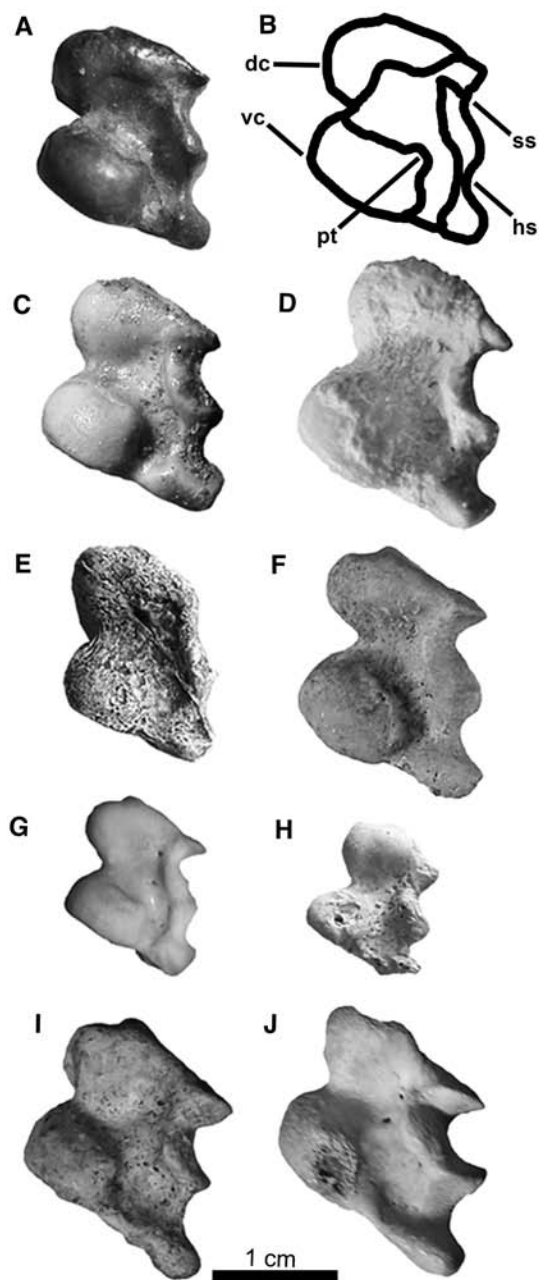


Figure 2.10- *Alca* and *Pinguinus* humeri in distal view: **A.** *Alca grandis* (ANSP 13357); **B.** line drawing of *Alca grandis*; **C.** *Alca carolinensis* (NCSM 13734); **D.** *Alca stewarti* (BMNH A 7052); **E.** *Alca ausonia* (IGF 14875); **F.** *Alca olsoni* (USNM 454590); **G.** *Alca torda* (USNM 502382); **H.** *Alca minor* (USNM 495600); **I.** *Pinguinus impennis* (USNM 623465); **J.** *Pinguinus alfrednewtoni* (USNM 366630). Anatomical abbreviations: (**dc**) dorsal condyle; (**hs**) humerotricipital sulcus; (**pt**) proximodistal tubercle; (**ss**) scapulotricipital sulcus; (**vc**) ventral condyle.

*carolinensis* (absent in other *Alca* for which the coracoid is known; i.e., *Alca stewarti* and *Alca olsoni*); distal margin of posterior humeral head pointed (105:1; rounded in *Alca stewarti*, *Alca minor*, and *Alca torda*); primary pneumotricipital fossa of humerus oval (122:1) as in *Alca ausonia*, *Alca carolinensis*, and *Alca olsoni* (rounded in other *Alca*); olecranon curves posteriorly (171:0) as in *Alca carolinensis* and *Alca olsoni* (curves anteriorly in *Alca stewarti* and *Alca torda*); anterior margin of dorsal cotylar prominence of ulna rounded (175:0) as in *Alca carolinensis* and *Alca torda* (margin straight in *Alca olsoni* and *Alca stewarti*); dorsal condyle of ulna rounded (183:0) as in *Alca olsoni* (angled in *Alca torda* and *Alca stewarti*); distal tendinal groove of carpometacarpus a sulcus (195:0) as in *Alca torda* (a closed canal in *Alca carolinensis*). The size of *Alca grandis* is between that of the smaller *Alca ausonia* and the larger *Alca carolinensis* (Table 2.4; Fig. 2.2).

*Remarks*—‘*Catarractes antiquus*’ was described by Marsh in 1870 based upon a left humerus with minor damage to the bicipital crest from Pliocene deposits in North Carolina (Fig. 2.2). Characteristics of this fossil prompted Olson and Rasmussen (2001) to create a new combination for this species, *Alca antiqua* (Marsh, 1870). *Alca antiqua* became *Alca grandis* (Marsh) 1870, as the previous name was “a secondary homonym preoccupied by *Alca antiqua* Gmelin, 1789, a basionym of the extant Ancient Murrelet *Synthliboramphus antiquus*, and was therefore unavailable for the fossil species” (Olson, 2007:225). The species name *grandis* stems from *Australca grandis* Brodkorb, 1955, which was recognized as a junior synonym of *Alca antiqua* by Olson and Rasmussen



(2001). The morphology and size of the coracoid referred *Alca grandis* herein (USNM 215454) are comparable to that of the holotype specimen of *Australca grandis* (UF/PB 141). These data support the synonymy of *Australca grandis* Brodkorb, 1955 and *Alca antiqua* Marsh, 1870 by Olson and Rasmussen (2001). Numerous examples of *Alca grandis* are known from Yorktown Fm. deposits at PCS Phosphate Mine (Olson and Rasmussen, 2001) and it has also been reported from the Pliocene of Belgium (Dyke and Walker, 2005).

### ***ALCA AUSONIA* (Portis, 1888)**

*Holotype*—right distal humerus (IGF 14875; Figs. 2.2 & 2.5).

*Referred material*—left humerus (USNM 446692; specimen previously referred to *Alca grandis* by Olson and Rasmussen, 2001; Figs. 2.2 & 2.11; Table 2.4). See Appendix 6A for referral of additional isolated specimens.

*Original diagnosis*—Originally described as *Uria ausonia* by Portis in 1888. The original description and subsequent publication (Portis, 1891) did not list diagnostic characteristics relative to other Alcini taxa.

*Amended diagnosis*—Although no autapomorphic characters are present in the humerus of *Alca ausonia*, this taxon can be differentiated from other species of *Alca* by

the presence of a unique combination of characteristics. Owing to lack of associated specimens referable to *Alca ausonia*, only humeri can be confidently referred to this species. The humeral shaft of *Alca ausonia* is relatively more gracile than that of other *Alca* (ratio of greatest width at midshaft to greatest distal width = 1.65 *Alca ausonia*; 1.69 *Alca torda* fossils; 1.70 *Alca grandis*). The coracobrachial sulcus forms the dorsal and lateral margin of the bicipital surface, and the point at which the sulcus curves ventrally is variable in *Alca*. This area of curvature of the coracobrachial sulcus is located more dorsally in *Alca ausonia* and *Alca grandis* (114:0; positioned ventrally in other *Alca*). The shape of the distal edge of the primary pneumotricipital fossa is concave (129:0) in *Alca minor* and *Alca ausonia* (straight in other *Alca*). As in *Alca carolinensis*, *Alca grandis*, and *Alca olsoni*, the posteriorly overturned portion of the humeral head is distally pointed (105:1; i.e., ~triangular) in *Alca ausonia*, whereas the profile of this feature is more rounded in *Alca stewarti*, *Alca minor*, and *Alca torda*. The size of *Alca ausonia* falls between the smaller *Alca torda* and the larger *Alca grandis* (Table 2.4, Fig. 2.2).

*Remarks*—A distal humerus (IGF 14875) from the Pliocene of Italy was described by Portis (1888, 1891). This fragmentary specimen (Fig. 2.2) was designated as the holotype of a new taxon *Uria ausonia* Portis, 1888. *Uria ausonia* was diagnosed with respect to *Uria aalge*, based solely on size (Portis, 1888). Although a more complete description of this specimen followed (Portis, 1891), the poor preservation of IGF 14875

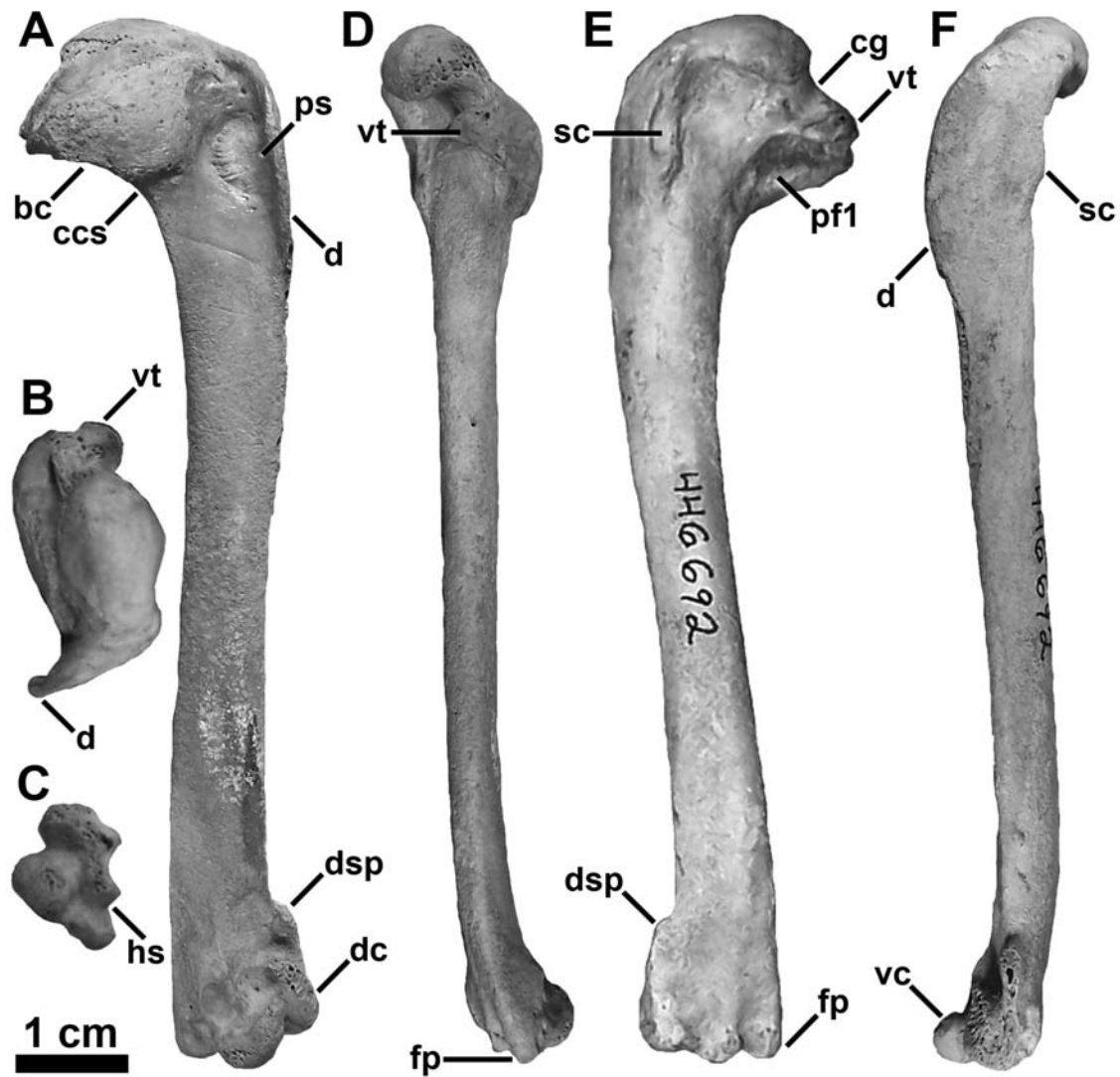


Figure 2.11- Left humerus (USNM 446692) referred to *Alca ausonia*. **A.** anterior view; **B.** proximal view; **C.** distal view; **D.** ventral view; **E.** posterior view; **F.** dorsal view. Anatomical abbreviations: (**bc**) bicipital crest; (**ccs**) coracobrachial sulcus; (**cg**) capital groove; (**d**) deltopectoral crest; (**dc**) dorsal condyle; (**dsp**) dorsal supracondylar process; (**fp**) flexor process; (**hs**) humerothoracic sulcus; (**pf1**) primary pneumatic fossa; (**ps**) pectoralis scar; (**sc**) m. supracoracoideus scar; (**vc**) ventral condyle; (**vt**) ventral tubercle.

prevented character-based diagnosis relative to other closely related alcids (e.g., *Alca torda*, *Uria aalge*). Olson and Rasmussen (2001) referred this specimen to *Alca*. Those authors (Olson and Rasmussen, 2001) noted that the holotype specimen of *Alca ausonia* agrees with characters that Marsh (1870) used to diagnose *Alca grandis*, and that its size range falls between the smaller *Alca torda* and the larger *Alca grandis* (Fig. 2.2).

Additional material from Italy representing this species is not known, although, specimens of *Alca ausonia* (Portis) 1888 are common within the Early Pliocene Yorktown Fm. exposed at PCS Phosphate Mine in Aurora, North Carolina, and have been reported from the Pliocene of Belgium (Dyke and Walker, 2005). Recently, remains from Late Pliocene deposits in Morocco were referred to *Alca ausonia* based on size (Mourer-Chauviré and Geraads, 2010).

#### ***ALCA STEWARTI* Martin et al., 2001**

*Holotype*—left ulna (BMNH A 7050).

*Paratype*—cast of right humerus (BMNH A 7052; Figs. 2.2 & 2.5).

*Referred material*—partial sternum, left coracoid, right humerus, right radius, right ulna, (USNM 242238; Fig. 2.12; specimen previously reported by Olson 1984, 1985; Olson and Rasmussen, 2001; Wijnker and Olson, 2009). See Appendix 6A for referral of isolated specimens.

*Original diagnosis*—Proposed diagnostic characteristics cited in the original description of *Alca stewarti* included: deltopectoral crest less rounded; ventral tubercle more ventrally deflected; crus dorsale fossa positioned more obliquely; dorsal supracondylar process narrow, and extends further proximally; scapulotricipital sulcus narrower than humerotricipital sulcus.

*Amended diagnosis*—Although missing data for other *Alca* species (e.g., *Alca ausonia*) prevents the unambiguous optimization of all the characters listed below, examination of the holotype, paratype, and additional referred material (USNM 242238, USNM 446650) identified the following unique suite of characteristics in which *Alca stewarti* differs from other species of *Alca*: notch in medial sternal process of coracoid absent (103:0) as in *Alca olsoni*; sternocoracoidal facet of coracoid angled  $\sim 135^\circ$  (104:1) as in *Alca carolinensis*; dorsal humeral shaft between deltopectoral crest and dorsal tubercle slightly concave (109:0); capital incisure of humerus broader, and expanded farther ventrally (141:0); ventral tubercle of humerus more ventrally deflected than in other *Alca*. Contra Martin et al. (2001), the tricipital sulci of the distal humerus are roughly equal in width, as in other *Alca*. *Alca stewarti* is larger (e.g., greatest length of humerus longer; Table 2.4; Fig. 2.2) than all other known *Alca*.

*Remarks*—*Alca stewarti* was described from Early Pliocene deposits of Belgium by Martin et al. (2001). Although *Alca stewarti* was originally diagnosed relative to *Alca torda* and Pliocene ‘*Australca*’ (i.e., Pliocene *Alca*), Martin et al. (2001) made no

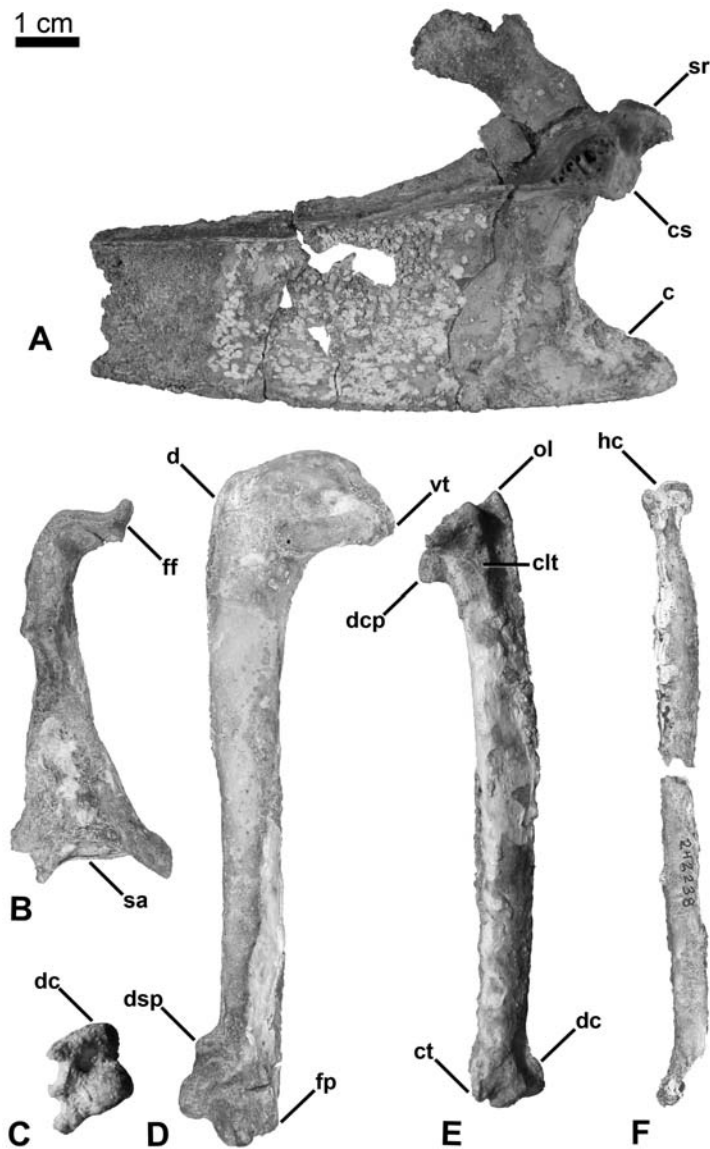


Figure 2.12- Associated specimen (USNM 242238) referred to *Alca stewarti*. **A.** partial sternum (right lateral view); **B.** left coracoid (posteromedial view); **C.** right humerus (distal view) **D.** right humerus (posterior view); **E.** right ulna (ventral view); **F.** right radius (dorsal view). Anatomical abbreviations: (**c**) carina; (**clt**) ventral collateral ligament tubercle; (**cs**) coracoidal sulcus; (**ct**) carpal tubercle; (**d**) deltopectoral crest; (**dc**) dorsal condyle; (**dcp**) dorsal cotylar process; (**dsp**) dorsal supracondylar process; (**ff**) furcular facet; (**fp**) flexor process; (**hc**) humeral cotyla of radius; (**ol**) olecranon process; (**sa**) sternal articular surface of coracoid; (**sr**) sternal rostrum; (**vt**) ventral tubercle.

mention of fossil comparative material examined; nor are there any references to previously published figures of Pliocene species of *Alca*. At the time of its description, the ulna designated as the holotype specimen of *Alca stewarti* (BMNH A 7050) by Martin et al. (2001) was not directly comparable to the holotype specimens of previously described extinct species of *Alca*, all of which were humeri. Additionally, there were no associated *Alca* specimens referred to species based on any criteria other than size (Olson and Rasmussen, 2001), that would allow for comparisons between holotype and additional fossil material referred to *Alca stewarti* by Dyke and Walker (2005). None of the alcid remains described by Martin et al. (2001) or Dyke and Walker (2005) were associated, thus referrals of elements other than ulnae to *Alca stewarti* were based only on size, locality, and age. However, the humerus designated as the paratype specimen of *Alca stewarti* (Fig. 2.2) by Martin et al. (2001) is diagnosably distinct from those of other *Alca*. Additionally, an associated specimen (USNM 242238) is referable to *Alca stewarti* on the basis of both size and diagnostic morphology. This specimen was previously documented but not referred to species by Olson, 1984, 1985; Olson and Rasmussen, 2001). In a recent review of Miocene Alcidae known from the Western North Atlantic Ocean, Wijnker and Olson (2009) referred this specimen to *Alca stewarti* based upon its larger size in comparison with other known *Alca*. This specimen is comprised of multiple associated elements including a humerus and an ulna, and therefore allows for confirmation of the validity of ulnae and humeri referred to *Alca stewarti* by Martin et al. (2001) and Dyke and Walker (2005), and for description of additional skeletal elements representing this taxon. Furthermore, the specimen (USNM 242238; Fig. 2.12) from the

Late Miocene Eastover Fm. of Virginia is the earliest known occurrence of *Alca* (Wijnker and Olson, 2009).

***ALCA CAROLINENSIS*, sp. nov.**

*Holotype*—NCSM 13734: a partial postcranial skeleton including the following elements: furcula, sternum, ribs, left coracoid, right and left scapulae, right and left humeri, right and left ulnae, right radius, left radius missing proximal tip, partial right ulnare, right carpometacarpus, and right manual phalanx I:1 (Figs. 2.2, 2.5, & 2.13). Although discovered partially articulated, all elements were prepared from the matrix to allow for detailed examination, description, and measurement of osteological features (Tables 2.4 & 2.6). The holotype specimen of *Alca carolinensis* (NCSM 13734) was collected by Vince and Judy Schneider from the spoil piles at the PCS Phosphate Mine in Aurora, North Carolina during a 1996 field expedition of the North Carolina Museum of Natural Sciences.

*Etymology*—The species name *carolinensis* reflects the provenience of the holotype specimen, Aurora, North Carolina.

*Locality & Horizon*—Beaufort County, Aurora, North Carolina, USA; PCS Phosphate Mine (35°23'N; 76°47'30"W; Fig. 2.1), Rushmere Member of the Yorktown Formation, Lower Pliocene (Berggren et al., 1995; Woodburne and Swisher, 1995).



Sedimentary characteristics of the matrix surrounding NCSM 13734, such as grain size, mineralogical composition, degree of induration, color, abundance of echinoderm remains, and lack of phosphate nodules, are consistent with the sedimentology of the Rushmere Member of the Yorktown Fm. (Snyder, 2001). Independent analysis of the foraminiferal assemblage identified the presence of *Elphidium* species and absence of *Parafissurina bidens*, and also supports the referral of this specimen to the Rushmere Member (S. Snyder, pers. com.).

*Diagnosis*—Proposed autapomorphies of *Alca carolinensis* include the presence of a dorsally projecting tubercle on the posterior apophysis of the furcula (76:1), and bicipital tubercle of the proximal radius positioned distal to and separated from the proximal ligamental papilla (167:1; *sensu* Howard, 1929). These features are not known in any other extant alcid, or in any extinct alcid for which these elements are known. However, among other *Alca*, furculae are known only from *Alca torda* and *Alca olsoni*, and radii are known only from *Alca torda*, *Alca olsoni*, and *Alca stewarti*. *Alca carolinensis* can be differentiated from *Alca olsoni* by the presence of a distinct ridge that borders the m. brachialis scar on the ventral surface of the proximal ulna. Like *Alca torda* and *Alca grandis*, the ulna of *Alca carolinensis* has a rounded anterior margin of the dorsal cotylar prominence (175:0), rather than a straight margin as in *Alca olsoni* and *Alca stewarti*. The intercondylar sulcus is less deeply incised than in *Alca olsoni*, *Alca stewarti*, *Alca grandis* and *Alca torda* (185:1). *Alca carolinensis* is further differentiated from *Alca grandis* by the lack of a posterodorsally projecting tubercle on the distal

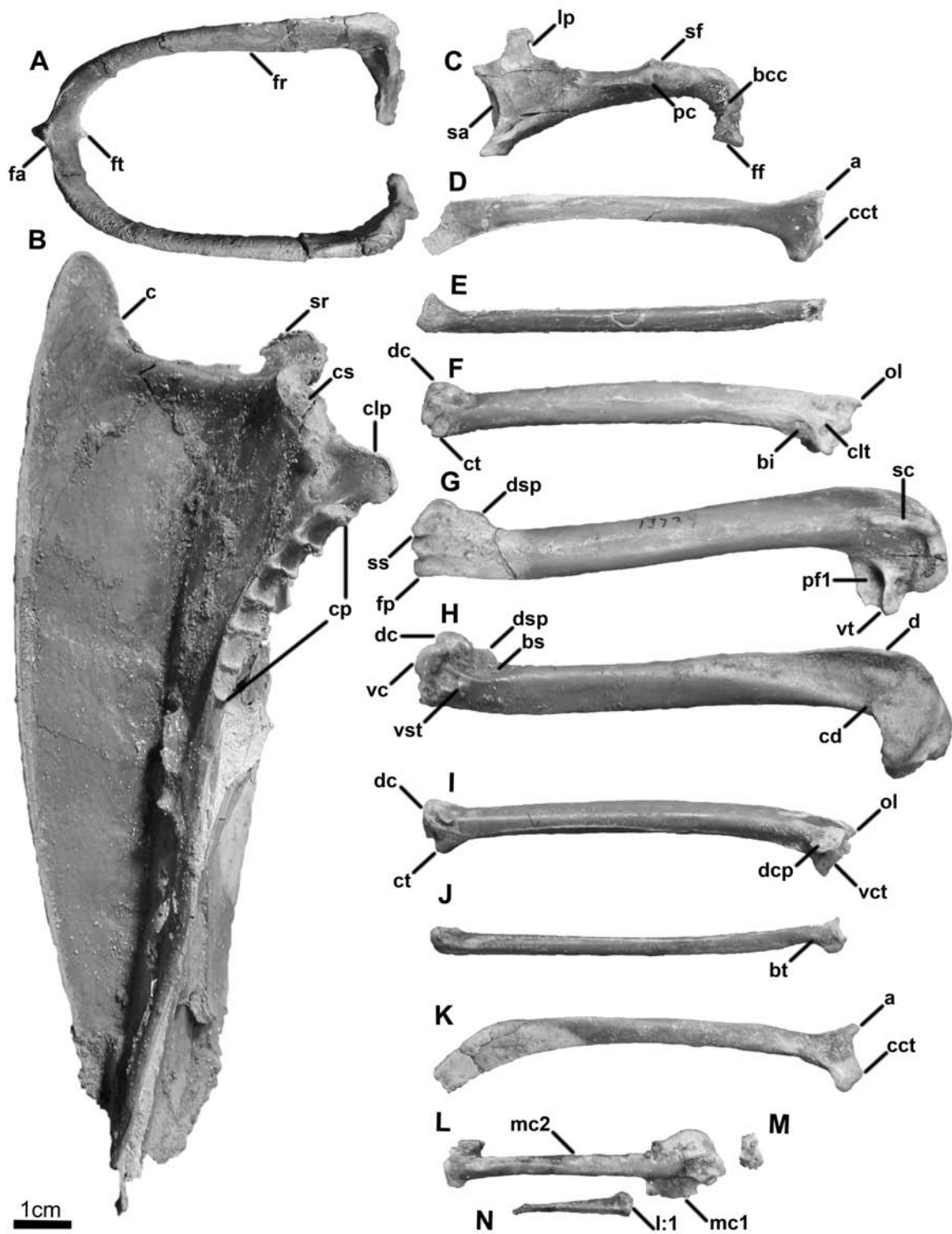


Figure 2.13- Holotype specimen of *Alca carolinensis* (NCSM 13734). **A.** furcula (anterior view); **B.** sternum (left lateral view); **C.** left coracoid (caption continued on next page;

posteromedial view); **D.** left scapula (medial view); **E.** left radius missing proximal end (ventral view); **F.** left ulna (ventral view); **G.** left humerus (posterior view); **H.** right humerus (anterior view); **I.** right ulna (dorsal view); **J.** right radius (dorsal view); **K.** right scapula (lateral view); **L.** right carpometacarpus (dorsal view); **M.** right ulnare (distal view); **N.** right digit 1:phalanx 1 (dorsal view). Anatomical abbreviations: **(I:1)** manual phalanx I:1; **(a)** acromion; **(bcc)** bicipital crest of coracoid; **(bi)** brachial impression; **(bs)** brachialis scar; **(bt)** bicipital tubercle; **(c)** carina; **(cct)** coracoidal tubercle; **(cd)** m. coracobrachialis duct; **(clp)** craniolateral process; **(clt)** ventral collateral ligament tubercle; **(cp)** costal processes of sternum; **(cs)** coracoidal sulcus; **(ct)** carpal tubercle; **(d)** deltopectoral crest; **(dc)** dorsal condyle; **(dcp)** dorsal cotylar process; **(dsp)** dorsal supracondylar process; **(fa)** furcular apophysis; **(ff)** furcular facet; **(fp)** flexor process; **(fr)** furcular ramus; **(ft)** furcular tubercle; **(lp)** lateral process; **(ol)** olecranon process; **(pc)** procoracoid process; **(pfl)** primary pneumotricipital fossa; **(mc1)** metacarpal one; **(mc2)** metacarpal two; **(sa)** sternal articular surface of coracoid; **(sc)** m. supracoracoideus scar; **(sf)** scapular facet; **(sr)** sternal rostrum; **(ss)** scapulotricipital sulcus; **(vc)** ventral condyle; **(vct)** ventral cotyla; **(vst)** ventral supracondylar tubercle; **(vt)** ventral tubercle.

surface of the ventral condyle (156:0; Fig. 2.10). *Alca carolinensis* is further differentiated by the concave ventral/sternal margin of the procoracoid process of the coracoid (95:0). This margin is convex in *Alca torda*, *Alca stewarti*, *Alca olsoni*, and *Alca grandis*. Associated specimens that would allow for referral of coracoids to *Alca ausonia* and *Alca minor* are not known. The dorsal margin of the primary pneumotricipital fossa (i.e., crus dorsale fossae; Baumel and Witmer, 1993) of *Alca carolinensis* and other *Alca* except *Alca torda* and *Alca minor* ends proximal to the junction of the bicipital crest with the humeral shaft (118:0). The ventral margin of the primary pneumotricipital fossa (i.e., crus ventrale fossae; Baumel and Witmer, 1993) of *Alca carolinensis* and other *Alca* except *Alca minor* and specimens referred to *Alca ausonia* is straight rather than concave (129:1). With the exception of *Alca olsoni* with which it shares similar proportions, *Alca carolinensis* can be differentiated from other *Alca* based upon size (Table 2.4; difference

Table 2.6- Measurements of newly described associated *Alca* holotype specimens (in mm). '-' = missing data due to damage or lack of comparable element. '~' = approximate measurement due to damage.

Measurements	<i>Alca olsoni</i> USNM 454590	<i>Alca carolinensis</i> NCSM 13734
<b>STERNUM</b>		
Medial length	-	~137.0
Dorsal length	-	126.0
Medial length of rostrum sterni	10.0	11.0
Length of carina	-	~144.0
Smallest width between costal processes	-	5.4
<b>FURCULA</b>		
Dorsoventral height of apophysis	7.5	9.2
Length of omal extremity	-	29.3
<b>CORACOID</b>		
Greatest length	48.5	48.8
Medial length	46.8	46.5
Basal breadth	-	26.1
Breadth of sternal articulation	20.3	20.9
<b>SCAPULA</b>		
Greatest proximal height	-	14.8
<b>HUMERUS</b>		
Greatest length	104.0	102.4
Breadth of proximal end	21.7	20.8
Breadth of shaft	8.8	9.2
Breadth of distal end	15.3	14.9
<b>RADIUS</b>		
Greatest length	77.0	79.2
Breadth of proximal end	6.5	6.7
Breadth of shaft	5.0	4.6
Breadth of distal end	6.8	7.1
<b>ULNA</b>		
Greatest length	87.5	83.0
Breadth of proximal end	16.4	16.0
Breadth of shaft	7.0	7.9
Breadth of distal end	11.1	10.8
<b>CARPOMETACARPUS</b>		
Greatest length	-	53.4
Length of metacarpal one	-	9.7

between greatest length of humeri: ~61%> *Alca minor*; ~30.6%> *Alca torda*; ~15.1%> *Alca ausonia*; 5.3%> *Alca grandis*; 8.6%< *Alca stewarti*).

*Anatomical Description*—The sternum is the most complete known for extinct *Alca* (Fig. 2.13). Complete *Alca* sterni are known only from extant *Alca torda*; however, partial sterni are known from *Alca grandis*, *Alca stewarti*, and *Alca olsoni*. As in all Alcidae, the sternum is long and narrow, although the width of the sternum immediately distal to the costal processes is relatively narrower than that of *Alca torda*. The dorsally directed sternocoracoidal processes are rounded, rather than pointed as in *Alca torda*. The carinal apex projects anterior to the mediolaterally-compressed rostrum sterni, which is more ventrally expanded than in extant *Alca torda*, and is characterized by a ventrally projecting spine. The dorsal and ventral rostral spines are fused, and separate the anteroposteriorly-broad coracoidal sulci. As in *Alca torda* there are seven costal processes. Two complete vertebral ribs, and three sternal ribs are preserved.

The furcula was recovered in five pieces and subsequently repaired. It is the first complete furcula known for extinct *Alca* (Fig. 2.13). Comparisons of *Alca* furculae are limited to extant *Alca torda* and the partial furcula (apophysis and adjacent portions of rami; omal extremities not preserved) of the holotype specimen of *Alca olsoni*. As with all Alcidae for which the furcula is known, and many other Charadriiformes (e.g., *Larus argentatus*), the omal ends of the furcular rami are mediolaterally compressed posterior to the coracoidal facet. The posterior omal extremity is elongate compared with most other charadriiforms (e.g., *Larus marinus*) and surveyed specimens of *Alca torda*.

Additionally, the distance from the furcular apophysis to the coracoidal facet is relatively longer than that of *Alca torda*. The furcular apophysis expands anteriorly, posteriorly, and ventrally, to form a semicircular projection. Both anterior and posterior extensions of the apophysis bear a dorsally projecting tubercle. The posterior tubercle is absent in all other alcids from which the furcula is known, although an anterior tubercle is present in *Alca torda*. Cristae are present along the anterior shafts of the rami dorsal to the apophysis, and are less distinct than those of *Alca torda*.

The scapulae are missing only their distal tips, with the right scapula preserving slightly more of the original length of this element (Fig. 2.13). Associated specimens of other extinct *Alca* that would allow for referral of isolated scapulae are not currently known. As in specimens of extant *Alca torda*, the tip of the acromion is rounded and directed anterodorsally. However, the acromion projects further dorsally and contacts the shaft of the scapula at a more acute angle than in *Alca torda*. The scapular blade is mediolaterally-compressed along its entire length, unlike the more rounded condition in some charadriiforms (e.g., *Larus argentatus*). The scapular blade broadens distally towards the ventrally deflected distal extremity, which is dorsoventrally-narrower in *Alca torda*.

The left coracoid is complete (Fig. 2.13) and is characterized by a rounded scapular cotyla, triangular procoracoid process with a concave sternal margin (convex in other *Alca*), and a distinctly ovoid m. supracoracoideus nerve foramen. The lateral process is dorsoventrally-broad with an anterodorsally directed “hook” along its dorsal margin. As in *Alca torda* the medial end of the sternal articular surface curves posteriorly

and broadens anteroposteriorly to form an approximately 90° angle in proximal view. This angle is less acute (i.e., ~135°) in some other Alcidae (e.g., *Cepphus* and *Synthliboramphus*), and more acute (i.e., ~75°) in some Alcidae (e.g., *Aethia* and *Ptychoramphus*). As in all *Alca* except *Alca olsoni*, the brachial tuberosity of the coracoid is not deeply undercut or pneumatized. The medial sternal process of the coracoid of *Alca carolinensis*, *Alca torda*, and *Alca grandis* is notched, rather than smooth as in *Alca olsoni* and *Alca stewarti*.

Before preparation both humeri (Fig. 2.13) were preserved in articulation with the radii and ulnae. The humeral head is smoothly rounded in comparison with that of *Uria aalge*. As in *Alca grandis*, the distal margin of the humeral head in posterior view is slightly pointed, whereas this feature is more rounded in *Alca torda*. The m. coracobrachialis impression is small compared to charadriiforms such as *Larus argentatus*, triangular, and separated from a well-defined m. pectoralis scar that is comparatively shallower in *Alca grandis*. The deltopectoral crest is prominent, slightly undercut dorsally by the m. pectoralis scar, and unlike the condition in *Pinguinus*, is restricted to the proximal half of the shaft. The deltopectoral crest merges smoothly with the anterior surface of the dorsal tubercle, which is separated from the humeral head in proximal view only by a slight notch. In posterior view, the dorsal tubercle is distally elongated into what Fürbringer (1888; see Baumel and Witmer, 1993:98) termed a supracoracoidal crest. The capital groove is less deeply incised than in *Alca torda*. The posterior surface of the ventral tubercle is more flattened and laterally deflected in *Alca grandis*, and mediolaterally-broader in *Alca torda*. The primary pneumotricipital fossa is

shallower in *Cepphus*, *Cerorhinca*, and *Fratercula*. The primary pneumotricipital fossa is round in shape, rather than oval as in *Alca torda* and *Alca minor*. Like other Alcini, *Alca carolinensis* has a weakly developed secondary pneumotricipital fossa (i.e., absent). The capital incisure is relatively narrow compared to that of *Alca stewarti*. The ventral tubercle is robust, with a well-developed pit for insertion of the m. subcoracoideus at the junction of the distal margin of the ventral tubercle and the ventral margin of the primary pneumotricipital fossa. The width of the shaft just distal to the deltopectoral crest is broader than that of *Alca stewarti*. The morphology of the distal humerus agrees with other *Alca* in having tricipital grooves of equal width. The m. brachialis scar extends proximal to the dorsal supracondylar process, while it is more distally restricted in *Alca ausonia*. Like all alcids other than Mancallinae, the anterior surface of the ventral condyle is flattened (Smith, 2011), although more rounded and anteriorly projected than in specimens here referred to *Alca ausonia*. The distal margin of the dorsal condyle lies proximal to that of the ventral condyle. The proximal tip of the dorsal condyle is narrower and more anteriorly deflected than that of *Alca grandis*. The dorsal epicondyle and dorsal supracondylar tubercle are continuous, forming an anteroposteriorly-compressed crest along the dorsal margin of the shaft. The dorsal supracondylar tubercle projects less than in some specimens of *Alca torda*. The distal margin of the ventral epicondyle is level with that of the ventral condyle, while this margin is distal to the ventral condyle in *Pinguinus*.

The right radius is complete, whereas the left radius is missing the distal end (Fig. 2.13). Radii are also known from *Alca torda*, *Alca olsoni*, and *Alca stewarti*. Compared to



the radial shaft of *Pinguinus*, which is strongly bowed and dorsoventrally-compressed to a degree exceeding that of volant alcids, the radial shaft in *Alca carolinensis* is comparably straight and less compressed, although more compressed than in *Alca torda*. The proximal end below the humeral cotyla adjacent to the capital tuberosity is more excavated than in *Alca torda*. Unlike all other alcids for which the radius is known, the bicipital tubercle is separated from the ligamental papilla and positioned more distally. A distinct intramuscular line is present along the entire length of the radial shaft and the distal end of the radius is relatively broader than in *Alca torda*.

Both ulnae are complete (Fig. 2.13). *Alca* ulnae are also known from *Alca torda*, *Alca stewarti*, *Alca olsoni*, and *Alca grandis*. The olecranon is prominent, pointed, and deflected slightly ventrally. As in *Alca torda* and *Alca grandis*, the dorsal cotylar prominence has a rounded anterior margin that borders the dorsal cotyla (straight in *Alca stewarti* and *Alca olsoni*) and partially bounds the proximal radial depression. The ventral collateral ligament tubercle is anteroposteriorly-broader than in *Alca stewarti* and more distally extended than that of *Alca torda*. The anterior shaft is characterized by a distinct intramuscular line that extends the length of the ulnar shaft and the posterior shaft displays distinct feather papillae. As in *Alca stewarti* and *Alca torda*, the anterior margin of the dorsal condyle is straight. The intercondylar sulcus is only slightly depressed relative to other *Alca*.

The holotype specimen of *Alca carolinensis* (NCSM 13734) preserves the second known manual phalanx I:1 (also present in *Alca grandis* specimen USNM 336379; Fig. 2.9), and the first known partial ulnare from an extinct *Alca* species (Fig. 2.13). Like the

carpometacarpus, these elements are larger but otherwise morphologically indistinguishable from those of *Alca torda*. The right carpometacarpus of NCSM 13734 lacks most of the shaft of metacarpal III (Fig. 2.13). Metacarpal I is elongate with the anteriorly-flattened extensor process characteristic of all Alcini. The ventral margin of the carpal trochlea extends posterior to the dorsal trochlear margin. The infratrochlear fossa is well defined and bordered distally by a distinct and anteriorly deflected pisiform process. The intermetacarpal spatium extends proximal to the distal extent of metacarpal I. Metacarpal II and III are equal in distal extent, and the anteriorly projecting tuberosity of metacarpal II (*sensu* Howard, 1929) is rectangular in shape.

***ALCA MINOR*, sp. nov.**

*Holotype*—USNM 302324: a left humerus (Figs. 2.2, 2.5, & 2.14; Table 2.4) missing the dorsal tubercle and the proximal-most section of the deltopectoral crest. The holotype specimen was collected by Peter J. Harmatuk from the spoil piles at the PCS Phosphate Mine in Aurora, North Carolina and donated to the Smithsonian Institution National Museum of Natural History in 1979.

*Etymology*—The species name *minor* reflects the diminutive size of this species compared to other known species of *Alca*.

*Locality & Horizon*—Beaufort County, Aurora, North Carolina, USA; PCS Phosphate Mine (35°23'N; 76°47'30"W; Fig. 2.1), Yorktown Formation, Lower Pliocene (Berggren et al., 1995; Woodburne and Swisher, 1995). No associated sediment was recovered with USNM 302324 that might permit microfaunal analysis. The color and lack of phosphatic patina of this specimen agrees with the preservation of other Pliocene Yorktown Fm. specimens; however, the possibility that this specimen is from the underlying Miocene Pungo River Fm. cannot be entirely ruled out.

*Referred specimens*—USNM 192879 (proximal right humerus; Fig. 2.14); USNM 495600 (distal right humerus; Fig. 2.14).

*Diagnosis*—Although this smallest known species of *Alca* (Table 2.4) can be morphologically differentiated from other known species of *Alca*, there are no autapomorphic characters preserved in the three specimens herein referred to this species. Unlike all other *Alca*, and similar to the condition observed in *Uria*, the m. coracobrachialis nerve appears to be transmitted in a sulcus rather than in a closed canal or duct (113:0); however, the possibility that the m. coracobrachialis nerve passage was exposed owing to weathering cannot be ruled out. The holotype (USNM 302324) and referred specimens (USNM 192879 & USNM 495600) of *Alca minor* were previously referred to ‘*Miocepphus* undescribed species’ (Olson and Rasmussen, 2001). *Alca minor* is differentiated from *Miocepphus* by the equal width of the tricipital sulci (151:1), and by the relative robustness of the humerus (average dorsoventral height of proximal

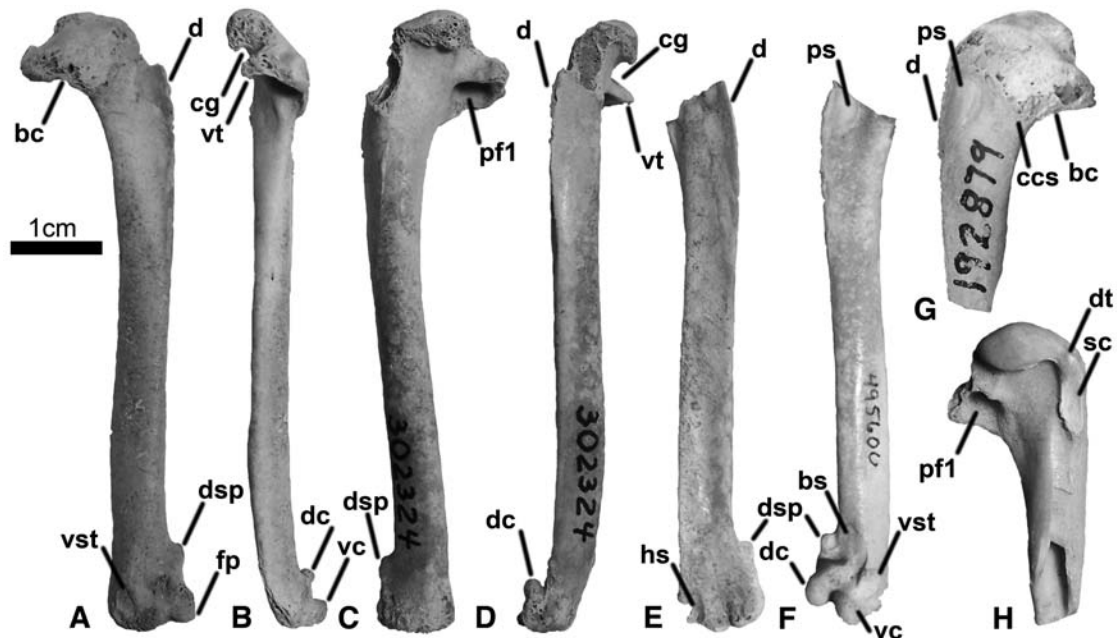


Figure 2.14- *Alca minor* holotype and referred specimens. Holotype left humerus USNM 302324 **A.** anterior view; **B.** ventral view; **C.** posterior view; **D.** dorsal view; Referred distal right humerus USNM 495600 **E.** posterior view; **F.** anterior view; Referred right proximal humerus USNM 192879 **G.** anterior view; **H.** posterior view. Anatomical abbreviations: (**bc**) bicipital crest; (**bs**) brachialis scar; (**ccs**) m. coracobrachialis sulcus; (**cg**) capital groove; (**d**) deltopectoral crest; (**dc**) dorsal condyle; (**dsp**) dorsal supracondylar process; (**dt**) dorsal tubercle; (**fp**) flexor process; (**hs**) humero-tricipital sulcus; (**pf1**) primary pneumatic fossa; (**ps**) pectoralis scar; (**sc**) m. supracoracoideus scar; (**vc**) ventral condyle; (**vst**) ventral supracondylar tubercle; (**vt**) ventral tubercle.

humerus 2.33 times wider than shaft; average dorsoventral height of distal humerus 1.57 times wider than shaft). The tricipital sulci of *Miocepphus* are of different widths. The humeral shaft is thicker, and the proximal and distal ends of the humerus are dorsoventrally-expanded (average dorsoventral height of proximal humerus 2.68 times wider than shaft; ratio derived from measurements of *M. blowi* and *M. mergulellus*; average dorsoventral height of distal humerus 1.75 times wider than shaft; ratio derived from measurements of *Miocepphus* holotype specimens). *Alca minor* is differentiated

from *Alle alle*, the smallest member of the Alcini, by its larger size, equal width of the tricipital sulci (151:1), and dorsally curving ventral margin of the distal humerus (*Alle* characterized by ~52% shorter greatest length, scapulotricipital sulcus wider than humerotricipital sulcus; ventrally flared ventral margin of distal humerus). *Alca minor* is differentiated from similarly sized *Synthliboramphus* and *Brachyramphus* by the rounded shape (122:0) and shallow depth of the primary pneumotricipital fossa (121:0). Due to the fragmentary nature of the holotype specimen of *Alca ausonia* (IGF 14875; Fig. 2.2), discernable differences between this taxon and *Alca minor* are limited to size. The greatest width of the humeral shaft at midpoint of *Alca minor* is ~32% smaller than that of *Alca ausonia* (Table 2.4). This is significantly outside the range of intraspecific variation documented for other alcids (Moen, 1991; Burness and Montevecchi, 1992). *Alca minor* is further differentiated from *Alca grandis* by the lack of a posteriodorsally-projecting tubercle on the posterior margin of the ventral condyle (156:0; Fig. 2.10). In contrast to other *Alca* in which the primary pneumotricipital fossa is deeper and more ovoid, the primary pneumotricipital fossa of *Alca minor* is relatively shallower and more rounded. As in *Alca ausonia* the distal margin of the primary pneumotricipital fossa is concave (129:0) rather than straight as in other *Alca*. *Alca minor* is differentiated from all other species of *Alca* by its overall smaller size (Table 2.4; greatest length of humerus: ~75% < *Alca stewarti*; ~63% < *Alca olsoni*; ~61% < *Alca carolinensis*; ~53% < *Alca grandis*; ~27% < *Alca torda*).

*Anatomical Description*—The dorsal surface of the proximal end of the holotype humerus proximal to the scar for attachment of m. pectoralis is missing (Fig. 2.14). The posterior surface of the head, the ventral tubercle, and the condyles on the distal end of the humerus are abraded, obscuring fine morphological details in these areas. The referred proximal right humerus (USNM 192879; Fig. 2.14) is broken at approximately mid-shaft, has minor abrasions on the anterior bicipital surface, and is missing the ventral tubercle. The referred distal humerus (USNM 495600; Fig. 2.14) is broken proximal to the m. pectoralis attachment scar, and the flexor process is missing.

The humerus of *Alca minor* is smaller in all dimensions than that of extinct and extant specimens of *Alca torda* (Fig. 2.2; Table 2.4). As in other *Alca* the humeral head is proximally rounded and overhangs the shallowly excavated secondary pneumotricipital fossa. The m. coracobrachialis nerve is transmitted in a sulcus rather than in a closed canal. The deltopectoral crest merges smoothly with the humeral shaft proximal to midshaft. The m. latissimus dorsi scar is prominent, extends distally from the m. supracoracoideus scar, is restricted to the proximal shaft, confined to the anterior surface of the shaft, and does not curve onto the dorsal surface of the humerus as in *Cepphus*. As in other *Alca*, the tricipital sulci are of equal width and the dorsal supracondylar process is a rounded dorsally projected tubercle (less dorsally projected in *Uria*).

***ALCA OLSONI*, sp. nov.**

*Holotype*—USNM 454590: a partial postcranial skeleton including the following elements: partial furcula, partial sternum, left coracoid, left humerus, distal right humerus, right ulna, and right radius. (Figs. 2.2, 2.6, & 2.15; Tables 2.4 & 2.6). The holotype specimen of *Alca olsoni* (USNM 454590) was collected by Reginald Titmas from the spoils piles at the PCS Phosphate Mine in Aurora, North Carolina, USA and donated to the Smithsonian Institution, National Museum of Natural History in 1992.

*Etymology*—This new species is named in honor of Storrs L. Olson and in recognition of his many contributions to the systematics of extinct Alcidae.

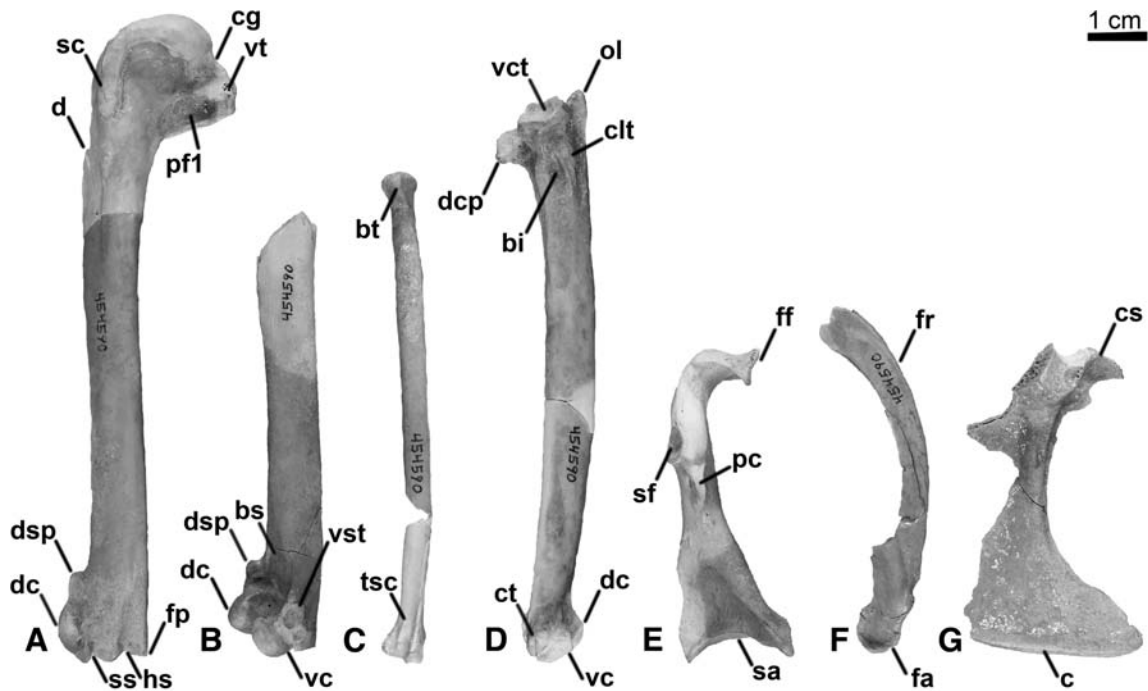


Figure 2.15- *Alca olsoni* holotype specimen (USNM 454590). **A.** left humerus (posterior view); **B.** right distal humerus (anterior view); **C.** right radius (dorsal view); **D.** right ulna (ventral view); **E.** left coracoid (posteromedial view); **F.** partial furcula (right lateral view); **G.** partial sternum (right lateral view). Anatomical abbreviations: (**bi**) brachial

impression; (**bs**) brachialis scar; (**c**) carina; (**cg**) capital groove; (**clt**) ventral collateral ligament tubercle; (**cs**) coracoidal sulcus; (**ct**) carpal tubercle; (**d**) deltopectoral crest; (**dc**) dorsal condyle; (**dcp**) dorsal cotylar process; (**dsp**) dorsal supracondylar process; (**fa**) furcular apophysis; (**ff**) furcular facet; (**fp**) flexor process; (**fr**) furcular ramus; (**hs**) humerotricipital sulcus; (**ol**) olecranon process; (**pc**) procoracoid process; (**pfl**) primary pneumotricipital fossa; (**sa**) sternal articular surface of coracoid; (**sc**) m. supracoracoideus scar; (**sf**) scapular facet; (**sr**) sternal rostrum; (**ss**) scapulotricipital sulcus; (**tsc**) tendinal sulcus crest; (**vc**) ventral condyle; (**vct**) ventral cotyla; (**vst**) ventral supracondylar tubercle; (**vt**) ventral tubercle.

*Locality & Horizon*—Beaufort County, Aurora, North Carolina, USA; PCS Phosphate Mine (35°23'N; 76°47'30"W; Fig. 2.1), Yorktown Formation, Lower Pliocene (Berggren et al., 1995; Woodburne and Swisher, 1995). No associated sediment was recovered with USNM 454590 that might allow for microfaunal analysis. The color and lack of phosphatic patina of this specimen agrees with the preservation of other Pliocene Yorktown Fm. specimens; however, the possibility that this specimen is from the underlying Miocene Pungo River Fm. cannot be entirely ruled out.

*Diagnosis*—*Alca olsoni* is diagnosed from all other species of *Alca* in which the ulna is known (i.e., *Alca torda*, *Alca stewarti*, *Alca carolinensis*, *Alca grandis*) by the presence of a distinct ridge that borders the m. brachialis scar on the ventral surface of the proximal end of the ulna. Associated specimens of *Alca minor* and *Alca ausonia* that would allow for referral of ulnae to these taxa, and evaluation of this proposed autapomorphy, are not known. The ventral extension of this ridge along the m. brachialis scar makes the brachialis scar appear as a deep pit rather than a shallow scar (Fig. 2.15). An additional proposed autapomorphy of *Alca olsoni* is a furcular apophysis that is expanded ventrally but is anteroposteriorly-narrow (Fig. 2.15). This feature is not seen in



any extant Alcidae, or in any extinct Alcidae for which these elements are known (i.e., *Alca torda* and *Alca carolinensis*). Although the ulnae of *Alca olsoni* and *Alca carolinensis* are morphologically distinct, the humeri of these species are similar in both size and morphological characteristics (Table 2.4). However, *Alca olsoni* is differentiated from *Alca carolinensis* by the curvature of the sternal margin of the procoracoid process of the coracoid, which is convex (95:1) in *Alca olsoni* but concave in *Alca carolinensis*. The brachial tuberosity is less deeply undercut than that of *Alca stewarti* and *Alca torda* (88:1), and as in *Alca torda* and *Alca grandis*, the medial end of the sternal articular surface of the coracoid curves posteriorly to form a  $\sim 90^\circ$  angle in sternal view (104:2;  $\sim 135^\circ$  in *Alca stewarti* and *Alca carolinensis*). Based on the greatest length of the humerus, *Alca olsoni* is larger than *Alca grandis* ( $\sim 7\%>$ ), *Alca torda* ( $\sim 32\%>$ ), and *Alca minor* ( $\sim 63\%>$ ), and smaller than *Alca stewarti* ( $\sim 6.5\%<$ ; Table 2.4). The width of the humeral shaft of *Alca ausonia* is  $\sim 17\%$  smaller than that of *Alca olsoni*.

*Anatomical Description*—The furcular apophysis and left furcular ramus distal to the omal extremity are preserved (Fig. 2.15). As in all other Alcidae and many other Charadriiformes (e.g., *Larus argentatus*) the furcular ramus is mediolaterally-compressed. Unlike other *Alca* species for which the furcula is known (i.e., *Alca torda*, *Alca carolinensis*), the apophysis lacks either an anterior or posterior tubercle and is expanded further ventrally than in other *Alca*. These features were not observed to vary in specimens of extant *Alca torda* examined.

The proximal sternum comprising the right coracoidal sulcus, medial section of the left coracoidal sulcus, rostrum sterni, and anterior carina are preserved (Fig. 2.15). The posterior margins of the coracoidal sulci are bordered by a distinct ridge. This ridge is less distinct in *Alca torda* and *Alca carolinensis*. As in *Alca stewarti* and *Alca carolinensis* the coracoidal sulci broaden medially and nearly contact the sternal rostrum. The left coracoid lacks only the lateral process (Fig. 2.15) and is characterized by a rounded scapular cotyla, a triangular procoracoid process (square in *Alle*), and an ovoid m. supracoracoideus nerve foramen.

The complete left humerus and distal right humerus are preserved (Fig. 2.15). The left humerus was collected in two pieces and repaired. A portion of the deltopectoral crest is missing. The depth of the m. coracobrachialis impression on the proximal humerus is shallower than that of *Alca stewarti*, and the attachment scar of m. subcoracoideus on the posterior surface of the ventral tubercle is deeper than in *Alca stewarti*. The distal margin of the humeral head in posterior view is slightly pointed, rather than rounded as in *Alca torda*. The posterior tip of the ventral tubercle of *Alca olsoni* is not ventrally deflected as in *Alca stewarti*. All other morphological features of the humerus agree with those of *Alca carolinensis*.

The right ulna is complete (Fig. 2.15). As in *Alca stewarti* the anterior margin of the dorsal cotylar prominence is straight rather than rounded as in *Alca torda* and *Alca carolinensis*. A distinct ridge borders the m. brachialis scar on the anterior surface of the proximal ulna, which gives the m. brachialis scar a narrow, ‘eye-shaped’ appearance and makes this feature appear as a deep pit (i.e., a fovea) rather than a shallow scar. This

conformation is not seen in any other *Alca* from which the ulna is known (e.g., *Alca torda*, *Alca stewarti*, *Alca carolinensis*). The ridge along the anterior margin of the m. brachialis scar is as wide as the muscle scar itself, and results in an anteriorly curving bulge along the length of the m. brachialis scar. Interestingly, this condition resembles that of *Mancalla emlongi* Olson, 1981, a flightless alcid that is not closely related to *Alca* (Chandler, 1990a, Smith, 2011). As in other *Alca*, the shaft of the ulna is dorsoventrally compressed. The posterior margin of the dorsal condyle just distal to its contact with the ulnar shaft is rounded, whereas the contact with the shaft is more angular in *Alca torda* and *Alca stewarti*. The intercondylar sulcus is more deeply incised than that of *Alca carolinensis*.

The right radius is complete (Fig. 2.15). Unlike the condition in *Alca carolinensis*, the bicipital tubercle contacts the ligamental papilla. As in other alcids, the shaft of the radius is dorsoventrally compressed and tapered to a distinct crest along the anterior margin. The distal tendinal sulcus is divided lengthwise into two distinct sulci by a distinct crest, a character shared by all Alcini taxa except *Alle*.

#### *PINGUINUS* Bonaterre, 1790

*Diagnosis*—deltopectoral crest extends distally past the midpoint of the humeral shaft (107:1); olecranon shorter than other Alcidae (170:1), except Mancallinae in which the olecranon does not extend proximally past the level of the cotylae; cnemial crests ‘T’ shaped in proximal view (212:0); supratendinal bridge not ossified (217:0).

***PINGUINUS IMPENNIS* (Linnaeus, 1758)**

*Hypotype*—right ulna (USNM 326589; Fig. 2.16A).

*Diagnosis*—differentiated from *Pinguinus alfrednewtoni* by: ventral margin of brachial tubercle of coracoid convex (90:0); neck of coracoid long (91:0); distal margin of humeral head rounded (105:0); coracobrachial impression of humerus deeper (110:0); m. subcoracoideus scar of humerus not deeply excavated (128:0); secondary pneumotricipital fossa divided by a crest beneath humeral head (132:1); tricipital sulci of distal humerus equal in width (151:1); m. pronator sublimis scar positioned at proximal point of ventral supracondylar tubercle of humerus (164:0); posterior side of distal radius not notched (169:0); brachial impression of ulna narrower (178:1); ulnar quill knobs absent (180:0); femoral trochanter straight (210:1); notch in lateral margin of medial condyle of tibiotarsus (215:1); anterior groove of tarsometatarsus shallower (225:1).

***PINGUINUS ALFREDNEWTONI* Olson, 1977**

*Holotype*—left ulna (USNM 193334; Fig. 2.16B).

*Original diagnosis*—differentiated from *Pinguinus impennis* by: shaft of ulna more curved and less compressed; ventral cotyla wider and more rounded; dorsal cotyla wider and less excavated; olecranon more robust, protruded further proximally; groove

between olecranon and dorsal cotylae deeper; distal tendinal groove more perpendicular; articular surface to shaft; proximal radial depression narrower; intermuscular line less distinct; carpal tubercle and distal tendinal groove wider; anterior articular ligament scar positioned more proximally.

*Additional diagnostic characteristics*— differentiated from *Pinguinus impennis* by: ventral margin of brachial tubercle of coracoid concave (90:1); neck of coracoid short (91:1); distal margin of humeral head pointed (105:1); m. coracobrachialis impression of humerus shallower (110:1); m. subcoracoideus scar of humerus more deeply excavated (128:1); secondary pneumatic foramen not divided by a crest beneath humeral head (132:0); humerotricipital sulcus of distal humerus wider than scapulotricipital sulcus (151:0); m. pronator sublimis scar does not contact ventral supracondylar tubercle of humerus (164:2); posterior side of distal radius notched (169:1); m. brachialis impression of ulna wider (178:0); ulnar quill knobs present (180:1); femoral trochanter convex (210:0); notch in lateral margin of medial condyle of tibiotarsus absent (215:0); anterior groove of tarsometatarsus deeper (225:0).

*Remarks*—Although there are no known associated specimens of *Pinguinus alfrednewtoni*, skeletal elements of *Pinguinus* can be distinguished from those of *Alca*, and there is no statistical support for more than one species of *Pinguinus* in the Yorktown Formation. Therefore, the phylogenetic analysis and the diagnosis for this taxon are based upon the holotype of *Pinguinus alfrednewtoni*.

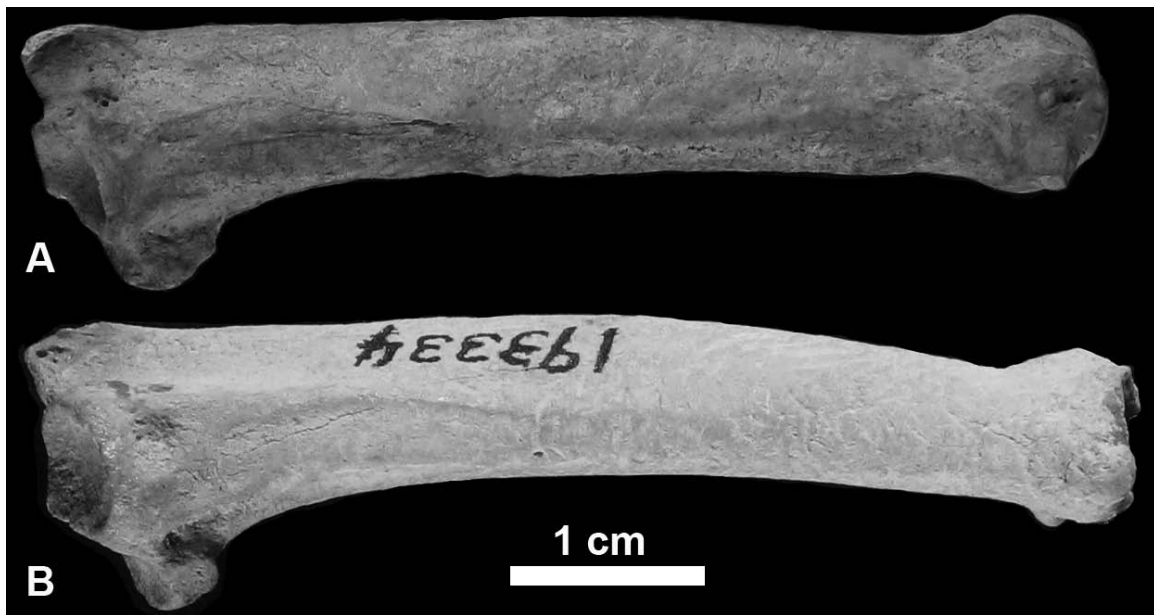


Figure 2.16- Hypotype specimen of *Pinguinus impennis* (USNM 326589) in ventral view (A; specimen image vertically flipped for comparison), and holotype specimen of *Pinguinus alfrednewtoni* (USNM 193334) in ventral view (B).

*MIOCEPPHUS* Wetmore, 1940

*Diagnosis*—presence of a crest on the lateral edge of the coracoid positioned omally to the lateral process (101:1); absence of a crest dividing the distal tendinal sulcus of the radius (168:0).

*Remarks*—This diagnosis above also applies *Alle alle*, which is nested within Miocepphus in the phylogenetic hypothesis presented here.

*URIA* Brisson, 1760

*Diagnosis*—notch in posterior margin of distal radius (169:1); dorsal condyle of ulna rounded (183:1); articulation facet of digit 2 phalanx 1 proximal to articulation facet of digit 3 phalanx 1 (196:1).

***URIA BRODKORBI* Howard, 1981**

*Holotype*—associated partial skeleton (UF-PB 7960 A & B; two slabs; Fig. 5.17).

*Original diagnosis*—differentiated from extant species *Uria aalge* and *Uria lomvia* by: premaxillary symphysis shorter; height of mandible at angular greater; sternum with broadly curved anterior margin; tip of carina more truncated; anterior carinal margin more protruded anteriorly; lateral process of coracoid with upturned tip; scapular facet of coracoid more excavated and rounder; glenoid facet broader; humeral head narrower; latissimus dorsi scar longer and angled more posteriorly; distal metacarpal symphysis of carpometacarpus with metacarpal III sloping rather than angled distally.

*Additional diagnostic characteristics*—differentiated from extant species *Uria aalge* and *Uria lomvia* by: posterolateral processes of atlas angled laterally (54:1); sternum with six costal processes rather than seven as in extant *Uria* (62:1); neck of coracoid shorter (91:0); ventral trochlea extends level with distal extent of metacarpal III (193:1).

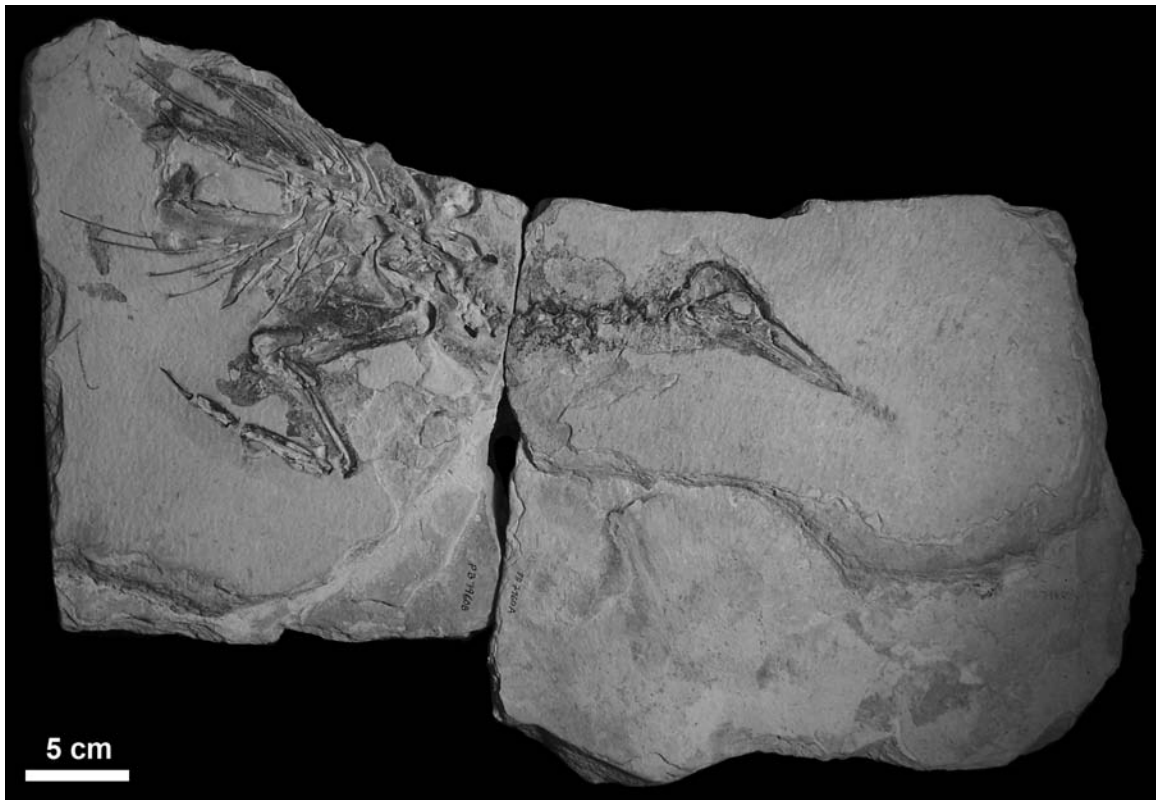


Figure 2.17- Holotype specimen of *Uria brodkorbi* (UF-PB 7690).

## DISCUSSION

The identification of three new species of *Alca* brings the total number of *Alca* species known from the western Atlantic Ocean to seven, making *Alca* the most speciose clade of Atlantic alcids, and the most species-rich clade of Pliocene Atlantic seabirds currently known. Analytical results indicate that material referred to ‘*Australca grandis*’ from the early Pliocene Bone Valley Fm. represents at least three species of *Alca* (*Alca grandis*, *Alca torda*, and *Alca ausonia*) and that *Alca* fossil material from the eastern Atlantic Ocean represents at least four distinct species (*Alca ausonia*, *Alca grandis*, *Alca*



*stewarti*, and *Alca carolinensis* or *Alca olsoni*). However, *Alca minor* may also be present in the Pliocene of the Netherlands (E. Wijnker, personal communication). The inclusion of extinct *Alca* species and additional extinct Alcini species in a combined phylogenetic analysis calls in to question the monophyly of *Alca* with respect to *Pinguinus*, and also supports placement of *Alle alle* nested within *Miocepphus*. Additionally, assessment of *Alca* paleodiversity with respect to latitude reveals an apparent trend of higher *Alca* diversity at higher latitudes that is consistent with distribution of extant alcids.

Known diversity of extinct Atlantic alcids now approaches that of extinct Pacific alcids (~16-19 species ranging from Miocene-Pleistocene age). Hypotheses concerning Pacific ancestral origination of alcids based upon proposed greater Pacific species diversity should accordingly be re-evaluated. Extant alcid diversity in the Pacific Ocean may be a poor indicator of origination area, and the two oldest known alcid fossils are both from Atlantic Ocean deposits (Wetmore, 1940; Chandler and Parmley, 2002; Wijnker and Olson, 2009). Regardless of the ancestral area of the clade, similarly diverse lineages of alcids inhabited the eastern and western coasts of North America during the Pliocene, as at least six species of the flightless Mancallinae (Aves, Alcidae) lineage are known from approximately coeval Early Pliocene deposits in California (Smith, 2011). In comparison, the five species of auklets (*Aethia cristatella*, *Aethia pusilla*, *Aethia psittacula*, *Aethia pygmaea*, and *Ptychoramphus aleuticus*) are the most speciose clade of extant alcids, and are restricted to the Pacific Ocean (del Hoyo et al., 1996).

The possibility that all seven *Alca* species from North Carolina contemporaneously shared overlapping geographic ranges is consistent with data on the

distribution of extant alcids (e.g., auklets; del Hoyo et al., 1996). Depositional duration of the Yorktown Fm. is estimated at approximately one million years (3.7-4.8 Ma; Hazel, 1983), but there is little information on the relative stratigraphic occurrence of *Alca* material within the deposit. Considering that the only *Alca* fossils from Pleistocene and younger deposits are referred to the living species *Alca torda* (Harrison and Stewart, 1999), extinction of the other six species of *Alca* is inferred to have taken place during the last two million years of the Pliocene (i.e., sometime between the end of Yorktown Fm. deposition and the beginning of the Pleistocene). However, whether there is unrecognized *Alca* diversity among Pleistocene fossils merits further investigation. At least one species of the flightless Pacific taxon *Mancalla* survived until the Pleistocene (Howard, 1976), and *Pinguinus*, the sister taxon of *Alca*, was driven to extinction by man less than 200 years ago (Bengston, 1984). Middle and Late Pliocene records of *Alca* and *Pinguinus* that would potentially elucidate whether decreases in diversity were gradual or abrupt (owing to paleoclimatic changes in the Late Pliocene), are currently limited to the reported presence of *Alca ausonia* from the Late Pliocene (~2.5 Ma) of Morocco (Mourer-Chauvire and Geraads, 2010).

The new method described here encompasses analyses of complete skeletons, complete elements, and partial elements, and estimates statistical support for inferred species clusters at all of these levels of inclusiveness. Comparisons between results based on different subsets of data allow for evaluation of congruence between subsets of data and identification of systematically informative and uninformative measurements. With regards to number of *Alca* species inferred, the results of this combined morphometric

and morphological analysis are largely congruent with the results of the PCA analysis of distal *Alca* humeri by Olson and Rasmussen (2001).

Potential biases including sample size, collection bias, ontogeny, sexual dimorphism, and intraspecific size variation were considered. Sample size does not present a potential bias because the morphometric method described herein is not negatively affected by small sample size. Although larger specimens are more likely to be seen and collected, the unusually large sample size utilized in this study, in conjunction with specimens having been sampled from the North Carolina locality for over a ~30 year period, should negate any potential effect of collection bias. Ontogeny is not a complicating factor with respect to this analysis because only specimens assessed to be adult based on degree of ossification (Chapman, 1965) were included in this study. Extant alcids do not display statistically significant degrees of sexual dimorphism in their size, plumage, or osteological morphology (Storer, 1952; Nettleship and Birkhead, 1985; Szekely et al., 2000). Thus, it can be reasonably assumed that extinct alcids were also not sexually dimorphic as the proposed sister taxon of all alcids, the Stercorariidae (Ericson et al., 2003; Thomas et al., 2004; Baker et al., 2007; Pereira and Baker, 2008), as well as the closely related Laridae are also not sexually dimorphic.

Small degrees of intraspecific size variation within alcid species due to latitude have been well documented (Storer, 1952; Spring, 1971; Moen, 1991; Burness and Montevecchi, 1992). However, as noted by Olson and Rasmussen (2001), the possibility that the Aurora, NC locality might have served as a wintering ground for multiple geographic races (i.e., subspecies with geographically variable size) cannot be ruled out.

Although there are clear differences in size between *Alca* species, size alone is not a sufficiently robust criterion to diagnose species. Rather, statistically determined size classes were examined to determine shared morphological characteristics that could be used to diagnose or differentiate species of *Alca*. Additionally, the ranges of size documented for statistically supported clusters of fossils is consistent with that estimated for extant alcids. Inherent in this statement is the assumption that range of size variation within *Alca* species has not evolved.

Although partially unresolved, the relationships recovered among *Alca* in the results of the phylogenetic analysis suggest that moderate body-size would be optimized at the base of *Alca*, with more derived (i.e., much larger and much smaller) forms such as *Alca stewarti* and *Alca minor* nested deep within the clade. Among *Alca*, fossils representing *Alca stewarti* and *Alca minor* are the most rare. The small population sizes that might be inferred from this are suggestive of niche-specialization. However, the possibility that these species that represent extremes of body-size may have been more common in other localities should be considered.

The systematic position of *Uria brodkorbi* as the sister taxon to the living species *Uria aalge* and *Uria lomvia* is consistent with the Miocene age of *Uria brodkorbi* and the lack of other more recent fossils referable to this clade. Additionally, *Uria affinis* Marsh, 1872 (ANSP 13358) from the Pleistocene of Maine, lacks any characters that differentiate it from modern *Uria*, and may represent a Pleistocene occurrence of one of these modern forms.

The systematic placement of *Alle alle* nested within *Miocepphus* as the sister taxon to *Miocepphus mergulellus* may provide an explanation for the widely varying previous hypotheses regarding the systematic affinities of *Alle*. Based on the age of *Miocepphus bohaski* Wijnker and Olson, 2009, the split between the lineages leading to *Uria* and *Alle* occurred at least 20 mya, and provides a calibration point for the divergence between *Alle* and *Uria*. Much like *Alca torda*, *Alle alle* is the only surviving member of a clade including at least four additional extinct species. The inclusion of these extinct congeners (i.e., *Miocepphus*) results in a phylogenetic hypothesis that partially explains the unique suite of characters present in *Alle* and *Miocepphus* with respect to other Alcini. These characters, which may have misled previous analyses, and the systematic position of *Alle* can now be viewed in evolutionary context.

When Pliocene *Alca* diversity is evaluated with respect to latitude, it is noted to decline in more southerly localities. Yorktown Fm. deposits from North Carolina (~35°23'N latitude; Fig. 2.1) record the presence of all seven species of *Alca*, whereas the similarly sampled deposits from the Bone Valley Fm. of Florida (~27°45'N latitude) record the presence of only three species. Although age estimates for the Bone Valley Fm. of Florida, USA are slightly older (4.5-5.2 Ma) than those for the Yorktown Fm. (Emslie, 1998), whether the decreased diversity represented by the Bone Valley assemblage is a function of the different age of the deposits, the geographical range of *Alca* paleospecies, or a latitudinal species-diversity gradient is not known. Although *Alca* fossil localities in Europe are not as heavily sampled as those in North America, the same apparent pattern is observed in the Eastern Atlantic. Four species of *Alca* are known from

deposits in Belgium (Martin et al., 2001; Dyke and Walker, 2005; 51°15'N latitude), while only a single species has been reported from deposits in Italy and Morocco (Portis, 1888; Mourer-Chauvire and Garaads, 2010; ~43°N latitude). The apparent pattern of lower *Alca* diversity in southerly latitudes observed in the occurrence of fossil *Alca* is consistent with the latitudinal distribution of extant alcids (Fig. 2.18). Only four of the 23 extant alcid species have ranges that extend below the Tropic of Cancer (i.e., below 23.5° N latitude). The ranges of *Cepphus carbo* and *Synthliboramphus antiquus* in the Western Pacific Ocean extend south to the Ryuku Islands, whereas the ranges of *Synthliboramphus hypoleucus* and *Synthliboramphus craveri* in the Eastern Pacific Ocean extend just south of the southern tip of Baja California (del Hoyo et al., 1996). Confirmation of this same trend of higher diversity in northern latitudes among other extinct alcids will require further study. Just as extant alcid distribution is closely associated with nutrient-rich cold-water upwelling ocean systems, the apparent latitudinal diversity trend observed in *Alca* may represent changes in the abundance of feeding opportunities at different geographic locations at different points in geologic time.

Pelagic seabirds such as alcids are an excellent proxy for the study of interactions between the marine and terrestrial environments because they depend on the ocean for sustenance but must return to shore to reproduce. Changes in climate that effect sea level have potential to impact the availability of suitable breeding sites, and changes in ocean temperatures have potential to impact the distribution and availability of food. As such, radiations and extinctions of pelagic seabirds often have been hypothesized to be linked with climatic changes that are commonly the result of large-scale geologic processes.

Potential environmental drivers of alcid evolution have been extensively discussed (Warheit, 1992b; Emslie, 1998; Olson and Rasmussen, 2001; Smith et al., 2007; Pereira and Baker, 2008; Smith, 2011), and include: (1) the Mid-Miocene Climatic Optimum (MMCO; ~11-16mya) that may have been a factor in radiation of Alcidae; (2) reorganization of ocean currents after the final emergence of the Panamanian Isthmus (~2.6 mya) that resulted in changes in salinity, temperature, and pelagic invertebrate fauna that may have negatively impacted Pliocene alcid diversity (Warheit, 1992b; Bartoli et al., 2005; Head et al., 2008; Sarnthein et al., 2009); (3) periods of Pleistocene glaciation and environmental change possibly affecting distribution and diversity in Alcidae (Emslie, 1998; Warheit, 1992b). El Niño Southern Oscillation (ENSO) events also have a documented record of impacts on extant seabird populations (Hatch, 1987; Duffy et al., 1988; Hyrenbach and Veit, 2003), and recent research indicates that ENSO-like conditions may have existed in the Pliocene (Ravelo et al., 2006). However, evidence of short-term oceanic disturbances is rare in the fossil record (Emslie and Morgan, 1994; Emslie et al., 1996) and presently known alcid deposits do not appear to be death assemblages. Comparison of alcid evolutionary history with the timing of the MMCO, and the changes in sea level relative to the Panamanian Isthmus will require resolution of phylogenetic relationships of extinct alcid taxa, and estimation of clade origins based upon reliably dated and phylogenetically evaluated alcid and other charadriiform fossils. Unfortunately, the fossil record of the clade so far lacks sufficient resolution to test hypotheses on the scale of glacial cycles and ENSO events.

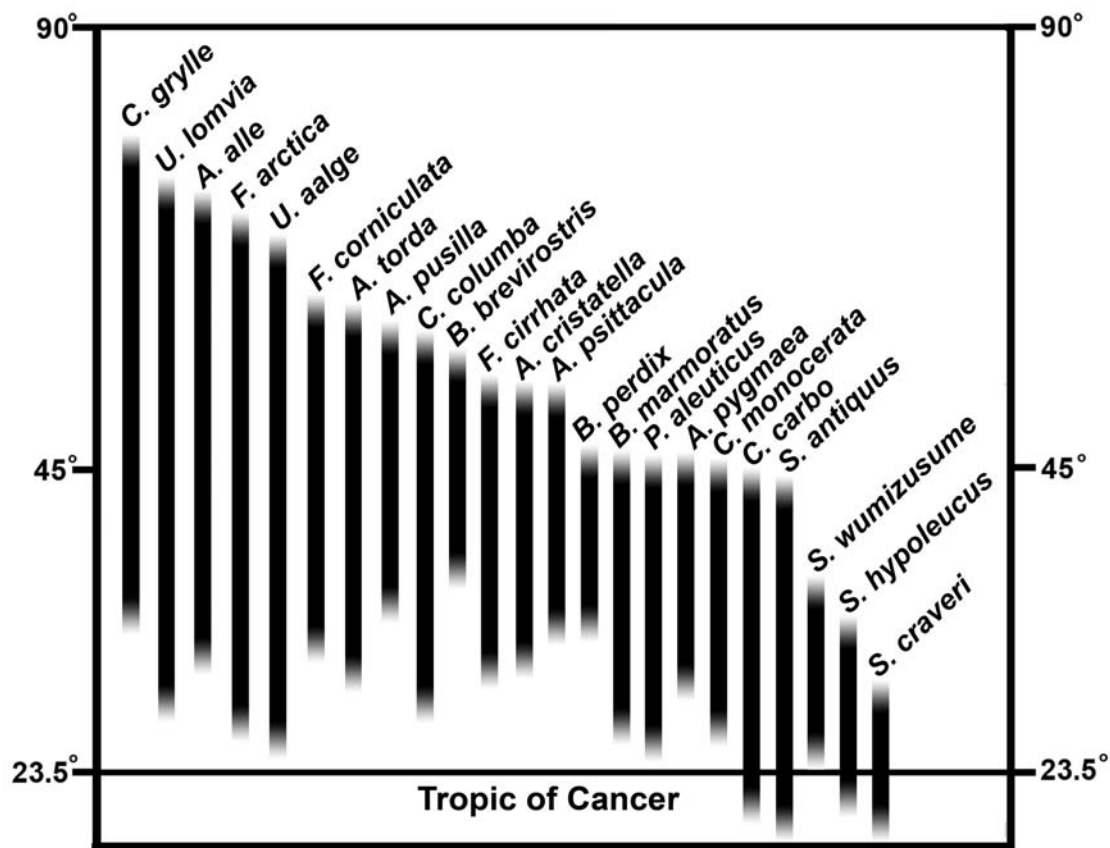


Figure 2.18- Latitudinal ranges of extant alcids (ranges based on del Hoyo et al., 1996). Note that the ranges of only four species cross the Tropic of Cancer and that overall species diversity decreases in higher and lower latitudes.

However, the absence of *Alca* from Pliocene Pacific Ocean deposits may not be linked to geologic or paleoclimatic factors. Colonization of the Pacific Ocean basin by *Alca* may have been prevented by the occupation of wing-propelled diving niches (Volterra, 1926; Hardin, 1960; Levin, 1970) by other relatively diverse clades of alcids (e.g., *Mancalla*, *Uria*; Howard, 1976, 1981, 1982) regardless of the potential for dispersal



through ocean passages. Although potential drivers of alcid radiation may be difficult to identify, the profound worldwide cooling that accompanied the final emergence of the Panamanian Isthmus (Sarnthein et al., 2009) offers a potential explanation for the significant decrease in Pliocene *Alca* diversity. The effect of this climatic transition on other marine organisms has been well documented (Versteegh, 1997; Bartoli et al., 2005; Kameo and Sato, 2000). The extant Razorbill Auk *Alca torda* is recognized as the only survivor of a once diverse lineage of seabirds with a fossil record extending back into the Miocene. The timing and pattern of radiation, extinction, range retraction, and the absence of *Alca* in the Pacific Ocean warrant further investigation.

Body size in extant alcids has been correlated with dive depth and feeding ecology (Prince and Harris, 1988; Watanuki and Burger, 1999) and moderate body size in living Alcidae has been associated with more generalist feeding strategies (e.g., moderately sized *Cephus* commonly prey on both vertebrates and invertebrates; Bradstreet and Brown, 1985). Thus, the size range observed in extinct *Alca* species may indicate a similar partitioning of resources related to differences in prey items available at varying depths. In a recent study, Gaston and Woo (2008) proposed that *Alca torda* is capable of rapidly adapting to environmental changes that affect its food supply by expanding and contracting its breeding and foraging range. Compared with smaller (i.e., *Alca minor*) and larger (e.g., *Alca stewarti*) congeners, the moderate body size of *Alca torda* may be linked to its apparently enhanced ability to respond to environmental changes both past and present. The presence of three moderately-sized species of *Alca* from the southernmost known *Alca* fossil locality (i.e., *Alca torda*, *Alca ausonia*, and

*Alca grandis* from the Bone Valley Fm.) and the absence of larger and smaller congeners (e.g., *Alca minor* and *Alca stewarti*) in that locality may also be a reflection of adaptive advantage of moderately sized *Alca*.

The geographical ranges and feeding ecology of extant seabirds that are changing rapidly in response to the current global warming trend (Kitaysky and Golubova, 2000; Hyrenbach and Veit, 2003; Gaston and Woo, 2008) may be best contextualized by insight from the past. Knowledge of extinct seabird diversity can have direct influence on our interpretation of the severity of these changes in extant seabird populations. Additional investigation of changes in modern seabird populations can facilitate a more nuanced understanding of the processes that may have affected seabird paleodiversity. Increased global warming and its future effects on seabird diversity might be used as a corollary for conditions experienced by extinct alcids. Declines in seabird populations related to ocean-warming have already been documented (Hyrenbach and Veit, 2003). The combination of an evermore detailed understanding of extant avian ecology with new paleontological discoveries offers the potential for new insights into the effects of climate change on avian evolution and seabird conservation.

## CONCLUSIONS

This study represents the largest statistical analysis of fragmentary avian material to date, and an initial attempt at developing a combined morphometric and morphology-based method of referring large quantities of isolated material to species. The resolution

of phylogenetic relationships is facilitated by the referral of previously unknown skeletal elements to species, making this method a potentially valuable tool when traditional morphology-only based methods of specimen referral are complicated by large quantities of isolated, or fragmentary, or morphologically similar specimens. However, the application of this method to fossil data is predicated on the identification of statistically robust recovery of species groups based on measurements of extant analogs, and determination of phylogenetically contextualized size variances in extant analogs. Although the application of this combined morphometric and morphologic method to fossils without extant analogs (e.g., non-avian dinosaurs) is not recommended, application of this method to other fossil remains with extant analogs (e.g., turtles, crocodilians, mammals, squamates) may provide a refined assessment of diversity in those clades. Additionally, the ability to accurately cluster small numbers of specimens may be of use when dealing with fossil taxa known from limited quantities of material.

The combined morphometric and morphologic method provides quantification of previously hypothesized (Olson and Rasmussen, 2001) high diversity in *Alca*. Additionally, the measurement data reported herein from both extant and extinct *Alca* is a resource that might be used to explore additional morphometric parameters (e.g., allometry) in Alcidae. The application of this method to other speciose clades within Alcidae (e.g., *Mancalla*), or other birds, may also provide new insights into the diversity of those clades.

The phylogenetic hypothesis of Alcini relationships presented herein represents the most inclusive sampling of this clade to date and provides evolutionary context for

future studies involving ecological interactions between Alcini species, other alcids, other seabirds, and other marine organisms. The results of the combined phylogenetic analysis of morphological and molecular sequence data demonstrate the value of fossils in resolving systematic relationships among both extant and extinct organisms. The reduction in species diversity in both *Alca* and *Miocepphus*, which has left only a single living representative of each of these clades, may provide compelling examples of extinction related to climatic changes that could have bearing on the plight of seabirds in the face of current global warming and pressures from over-fishing. Evaluation of the potential relationship between alcid extinctions and paleoclimatic changes will require divergence estimation for Alcidae utilizing rigorously dated and phylogenetically analyzed fossils, such as *Alca carolinensis*.

Detailed evaluation of fossil Pan-Alcidae has resulted in estimates of species diversity that continue to increase (Warheit, 2002; Olson and Rasmussen, 2001; Wijnker and Olson, 2009; Smith, 2011). Diverse assemblages of alcids are now known from the Pliocene of the Atlantic (Olson and Rasmussen, 2001), the Miocene of the Atlantic (Wijnker and Olson, 2009), and the Pliocene of the Pacific (Howard, 1982; Smith, 2011). Recent evaluation of fossil Alcidae from the Miocene of the Pacific also indicates that undescribed species diversity was present (Smith, 2008, 2011). The relative species diversity of fossil Alcidae from numerous localities at different points in geologic history (Warheit, 2002) and the relatively high species diversity of extant Alcidae ( $n = 23$  species) may reflect a pattern of high species diversity through time. Heavily sampling and thorough evaluation of alcid fossil localities continue to result in recognition of new

species. However, study of additional alcid fossil-producing localities from under-sampled temporal spans is needed to determine if these ‘snapshots’ of alcid species diversity reflect a real trend in alcid population dynamics or if this apparent trend is the result of sampling bias.

## CHAPTER 3.

The fossil record and phylogeny of the flightless Mancallinae

(Charadriiformes, Pan-Alcidae)

## INTRODUCTION

Pan-Alcidae taxon nov. is a clade of pelagic wing-propelled-diving Charadriiformes including 23 living species with an exclusively northern hemisphere distribution (del Hoyo et al., 1996). The fossil record indicates that alcid diversity during the Late Miocene and Early Pliocene equaled or exceeded extant alcid diversity (Olson, 1985; Olson and Rasmussen, 2001; Smith et al., 2007), although systematic evaluation of fossils referred to Alcidae is needed to refine estimates of paleodiversity in the clade. Analyses of morphological (Strauch, 1985; Chandler, 1990a) and molecular data (Baker et al., 2007; Pereira and Baker, 2008) support the monophyly of extant Alcidae, although the systematic position of most extinct species referred to Alcidae have yet to be evaluated in a phylogenetic analysis.

Although all living alcid are volant, two lineages of extinct flightless alcid are known. These flightless auks superficially resemble penguins, and share many morphological features convergent with those southern hemisphere wing-propelled divers. During the Miocene and Pliocene a diverse assemblage of alcid including the flightless Great Auk *Pinguinus* Bonnaterre, 1790, and other volant auks such as *Alca* Linnaeus, 1758 and *Miocepphus* Wetmore, 1940 were present in the Atlantic Ocean (Olson and Rasmussen, 2001; Wijnker and Olson, 2009). Similarly, during the Miocene and Pliocene the Pacific was inhabited by a lineage of flightless alcid known as the Mancallinae Brodkorb, 1967. Although Mancallinae (contents = *Mancalla* Lucas, 1901 +

*Praemancalla* Howard, 1966; sensu Brodkorb, 1967, Olson, 1985) and *Pinguinus* share several morphological characteristics related to extreme adaptation for wing-propelled diving and the subsequent loss of aerial flight, phylogenetic results indicate that these taxa are not closely related within Pan-Alcidae (Chandler, 1990a; Smith, 2008).

*Pinguinus* is consistently recovered as the sister taxon to *Alca* (Chandler, 1990a; Smith, 2008; Pereira and Baker, 2008).

Fossil records of Mancallinae are restricted to the northern Pacific Ocean basin. Miocene and Pleistocene aged fossils have been reported from Japan (Hasegawa et al., 1988; Kohno, 1997; Fig. 3.1), although these remains have not been systematically described or figured in publication. In contrast to the sparse record of the clade from the western Pacific Ocean, approximately four thousand mostly isolated specimens are known from California, USA and northern Baja California, Mexico (Miller and Howard, 1949; Howard, 1966, 1968, 1970, 1971, 1976, 1978, 1981, 1982; Chandler, 1990b; Fig. 3.2) and range in age from Late Miocene to Pleistocene (Table 3.1). The northernmost occurrence is in Humboldt County California (Howard, 1970; Kohl, 1974) and the southernmost occurrence is in Baja California, Mexico (Howard, 1971).

Discovery of an articulated partial skeleton referable to Mancallinae (SDSNH 68312) from the Early Pliocene Capistrano Formation of Orange County California prompted a re-evaluation of diversity and morphological variation within Mancallinae. Previously reported Mancallinae remains are reviewed below, and the results of an extensive survey of Mancallinae remains are reported. Three new species of Mancallinae



are described and the systematic placement of Mancallinae within Alcidae, as well as the inter-relationships of Mancallinae species is evaluated in phylogenetic analyses.

Table 3.1. Summary of Mancallinae holotype material and taxonomic revision.

Taxon	Holotype Material	Provenience	Age	Reference	Taxonomic Status
<i>Mancalla californiensis</i>	Humerus	Los Angeles, CA	Early Pliocene	Lucas 1901	<i>Mancalla californiensis</i>
<i>Mancalla diegensis</i>	Femur	San Diego, CA	Early Pliocene	Miller 1937	nomen dubium
<i>Praemancalla lagunensis</i>	Distal Humerus	Laguna Hills, CA	Late Miocene	Howard 1966	nomen dubium
<i>Alcodes ulnulus</i>	Ulna	Laguna Hills, CA	Middle Miocene	Howard 1968	Pan-Alcidae incertae sedis
<i>Mancalla milleri</i>	Femur	San Diego, CA	Early Pliocene	Howard 1970	nomen dubium
<i>Mancalla cedrosensis</i>	Partial Skeleton	Baja Calif., Mexico	Late Miocene	Howard 1971	<i>Mancalla cedrosensis</i>
<i>Praemancalla wetmorei</i>	Humerus	Laguna Niguel, CA	Late Miocene	Howard 1976	<i>Miomancalla wetmorei</i>
<i>Mancalla emlongi</i>	Ulna	San Diego, CA	Early Pliocene	Olson 1981	Mancallinae incertae sedis
<i>Miomancalla howardi</i>	Partial Skeleton	San Diego, CA	Late Miocene	Smith 2011	<i>Miomancalla howardi</i>
<i>Mancalla lucasi</i>	Partial Skeleton	San Diego, CA	Early Pliocene	Smith 2011	<i>Mancalla lucasi</i>
<i>Mancalla vegrandis</i>	Partial Skeleton	San Diego, CA	Early Pliocene	Smith 2011	<i>Mancalla vegrandis</i>

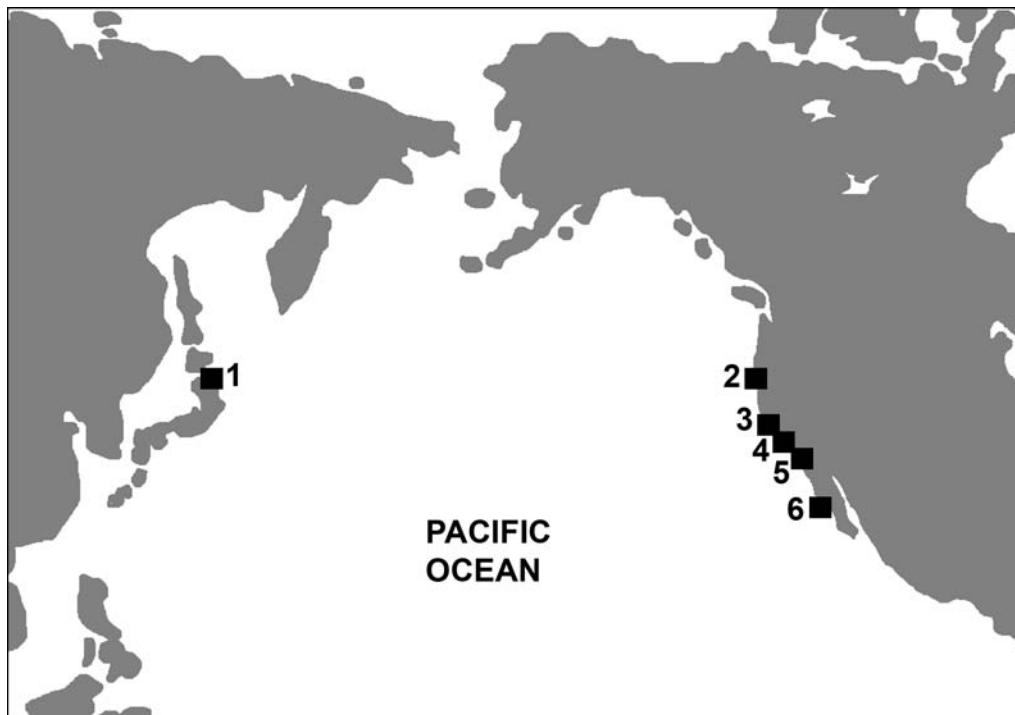


Figure 3.1- Map indicating Mancallinae fossil localities: **1.** Shiriya, Honshu, Japan; **2.** Humboldt County, CA, USA; **3.** Los Angeles, CA, USA; **4.** Laguna Hills, and Laguna Niguel, CA, USA; **5.** San Diego, CA, USA; **6.** Cedros Island, Baja California, Mexico.

***Review of the Mancallinae fossil record:*** Due to the identification of several Mancallinae species based upon non-diagnostic material, the systematics of Mancallinae required extensive revision (Table 3.1). The following review of the Mancallinae fossil record is presented to clarify the systematic position of previously named species and referred fossil material, and to justify the exclusion of some previously named species from the phylogenetic analysis.

Although greater than 100,000 avian fossils are currently known from sediments in California (Miller, 1946; Brodkorb, 1967; Olson, 1985), the first avian fossil from that state was not reported until 1901 when F. A. Lucas described a nearly complete left

humerus from what were thought to be Late Miocene sediments of Los Angeles. That specimen (USNM 4976; Fig. 3.2) represented the first of approximately four thousand fossils that are now referred to the flightless alcid taxon *Mancalla* (Smith, personal observation). *Mancalla californiensis* Lucas, 1901 was the first of seven flightless alcid species recognized between 1901 and 1981 (Table 3.1).

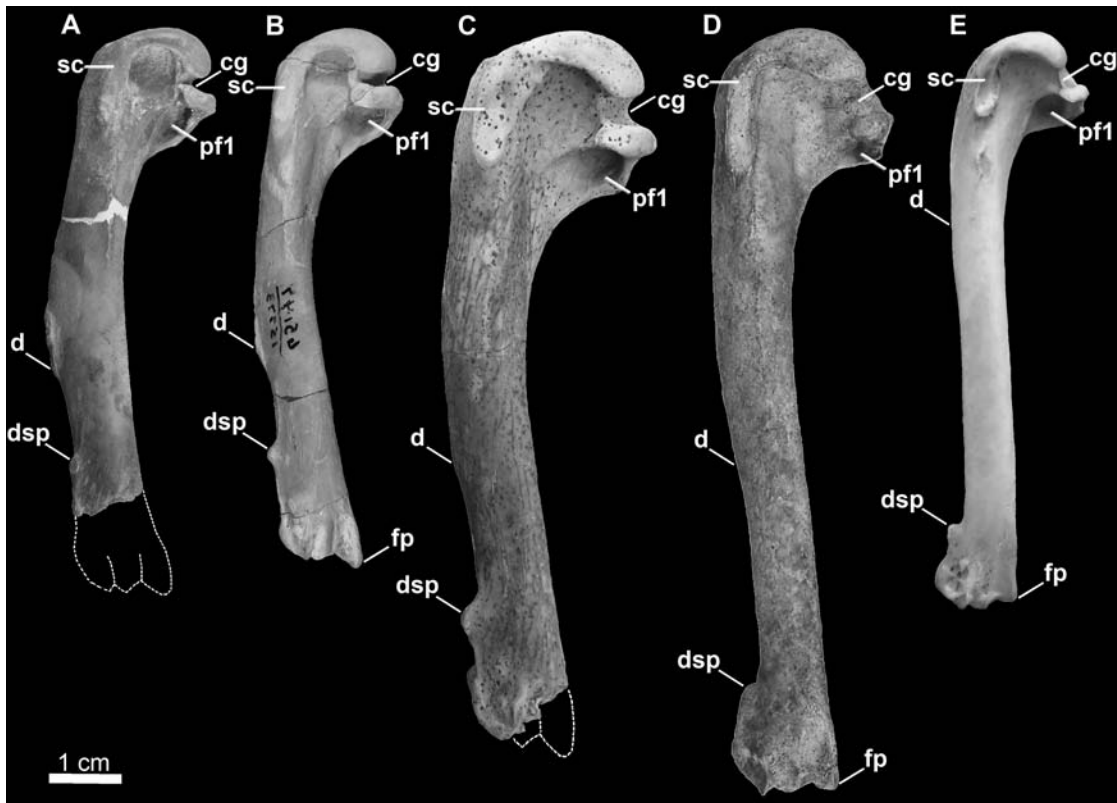


Figure 3.2- Previously recognized Mancallinae holotype humeri in posterior view along with examples of *Pinguinus impennis* and volant *Alca torda* humeri for comparison (dotted lines represent reconstructed parts of humeri). **A.** Holotype specimen of *Mancalla californiensis* (USNM 4976; **B.** Holotype humerus of *Mancalla cedrosensis* (LACM 15373); **C.** Holotype specimen of *Miomancalla wetmorei* (LACM 42653); **D.** *Pinguinus impennis* (USNM 623465); **E.** *Alca torda* (NCSM 20058). Anatomical abbreviations: (**cg**) capital groove; (**d**) deltopectoral crest; (**dsp**) dorsal supracondylar process; (**fp**) flexor process; (**pf1**) primary pneumotricipital fossa; (**sc**) m. supracoracoideus scar.

The second report of *Mancalla* remains (humerus; catalog # uncertain) was from the Early Pliocene San Diego Formation exposed in San Diego, California (Miller, 1933). The Early Pliocene age of the material reported by Miller (1933) was congruent with the revised age estimate for the holotype locality of *Mancalla californiensis* in Los Angeles (Arnold, 1906). An additional specimen, a complete right femur (UCMP 33409) from the San Diego Fm., was reported by Miller in 1937. Based on characteristics of that specimen Miller (1937) considered it a Pliocene example of a puffin (i.e., '*Lunda*', *Fratercula*, and *Cerorhinca*), and designated the specimen as the holotype of a new taxon, *Pliolunda diegensis* Miller, 1937. Additional *Mancalla* remains (LM 2218) were reported by Miller (1946), who discussed the possibility that *Pliolunda* was a synonym of *Mancalla* and erected the Family Mancallidae, separating *Mancalla* from Alcidae. The rank of Mancallidae later became subfamily Mancallinae (sensu Brodkorb, 1967), systematically reuniting *Mancalla* and *Praemancalla* with other Alcidae.

Mounting evidence that more than one species of *Mancalla* was extant during the Early Pliocene came from Howard in 1949. At that time approximately 118 specimens representing *Mancalla* were known, including two size classes of carpometacarpi from localities in Los Angeles, San Diego, and Corona del Mar, California. Although no associated remains were known, carpometacarpi were referred to *Mancalla* based upon characters such as an elongated first metacarpal, a morphology considered convergent with that of penguins (i.e., Spheniscidae) by Howard (1949). Humeri of *Mancalla* were well known and also display characteristics correlated with extreme specialization for wing-propelled diving considered by Miller (1946) to be convergent with those of

penguins, thus, prompting the referral of carpometacarpi exhibiting ‘penguin-like’ features.

The growing number of specimens from the San Diego Fm. prompted a review known *Mancalla* remains (Miller and Howard, 1949) that resulted in the recognition of *Pliolunda* as a junior synonym of *Mancalla*. However, additional remains other than humeri were referred solely on the basis of size, provenience, and osteological characteristics correlated by those authors with flightlessness. No associated *Mancalla* remains were known at the time that would allow for referral of femora to *Mancalla californiensis*, nor to facilitate comparisons between *Mancalla californiensis* and the holotype specimen of *Mancalla diegense*. The species name *Mancalla diegense* was amended to *Mancalla diegensis* by Brodkorb (1967) to reflect correct latinization of the place name San Diego. Although my recent re-examination of *Mancalla* material in the collections of UCMP, LACM, and SDSNH identified several associated specimens within the size range of *Mancalla diegensis* as reported by Howard (1970), and that correspond with characters described for that taxon by Howard (1970), no associated specimens referable to *Mancalla californiensis* that preserved femora were identified. The holotype femur of *Mancalla diegensis* is, therefore, not presently comparable to *Mancalla californiensis*. Furthermore, my survey of the femora of all known alcid species revealed that the morphology of the femur is remarkably conserved in alcid taxa, potentially explaining Miller’s (1937) original proposal, that UCMP 33409 represented an extinct species of puffin. No characteristics were identified that would allow for

confident referral of isolated femora to *Mancalla*, and *Mancalla diegensis* is, therefore, considered a nomen dubium.

In 1966 Howard described a new Mancallinae taxon from the Late Miocene based upon isolated elements including a distal humerus, carpometacarpi, a partial coracoid, the proximal end of a scapula, and the articular portion of a mandible. *Praemancalla lagunensis* Howard, 1966 was considered by that author to be less specialized with respect to features associated with flightlessness, and the possibility that *Praemancalla* might represent a less derived ancestor of *Mancalla* was proposed. All elements referred to *Praemancalla lagunensis* were isolated so only the holotype distal humerus (LACM 15288) can be compared with previously recognized taxa to evaluate the taxonomic status of this species. The holotype specimen of *Praemancalla lagunensis* is weathered smooth, obscuring many fine morphological details. Although LACM 15288 is referable to Mancallinae based upon the rounded anterior surface of the ventral condyle (153:0), all of the characteristics that Howard (1966) proposed as diagnostic for this species may be an artifact of weathering, or also are found in *Mancalla*. *Praemancalla lagunensis* is, therefore, considered a nomen dubium.

Another species of alcid with characteristics interpreted as “progressing towards flightlessness” (Howard, 1968:19) was described by Howard in 1968 from reportedly Miocene sediments of Laguna Hills, California. *Alcodes ulnulus* Howard, 1968 was described based on isolated elements including a complete left ulna, additional ulnar fragments, and a partial carpometacarpus (Howard, 1968). Additional material representing this taxon was recovered from the Middle Miocene Topanga Formation

along Oso Creek in Orange County, California (Howard and Barnes 1987), confirming the Miocene age of this species. Ulnae of *Alcodes* are differentiated from those of *Mancalla* by their more gracile and rounded shafts, and projection of the olecranon more posteriorly. Although associated humeri and ulnae of *Mancalla* (e.g., holotype specimen of *Mancalla cedrosensis* LACM 15373) demonstrate that *Alcodes* is distinct from *Mancalla*, the lack of associated *Praemancalla* specimens with ulnae raises the possibility that *Alcodes* is congeneric with *Praemancalla*. Until additional material is recovered that would allow comparison with other recognized alcid taxa, the systematic affinities of *Alcodes* in Pan-Alcidae remain uncertain, and *Alcodes* is, therefore, considered Pan-Alcidae *incertae sedis*.

Although the review by Howard (1970) expanded the known geographic range of Mancallinae, and greatly increased knowledge of character- and size-related differences in the taxon, the description of *Mancalla milleri* Howard, 1970 based upon isolated material further complicated the taxonomy of the clade. Comparisons between the holotype femur of *Mancalla diegensis* and the holotype femur of *Mancalla milleri* (LACM 2185) provide limited morphological data because neither of those elements are directly comparable to the isolated holotype humerus of *Mancalla californiensis*. Additionally, my recent re-examination of the ~4,000 fossils referred to *Mancalla* indicates that femoral characters cited by Howard (1970) are more variable within proposed size classes of *Mancalla* than previously recognized (Smith, personal observation). Furthermore, as stated above, femoral morphology is remarkably conserved in Alcidae. Although characteristics of humeri indicate that multiple species of *Mancalla* are represented by *Mancalla* material

from the San Diego Fm., the species to which the holotype femora of *Mancalla diegensis* and *Mancalla milleri* belong will likely never be determined. *Mancalla milleri* is, therefore, considered a nomen dubium.

*Mancalla cedrosensis* Howard, 1971 was the first species of *Mancalla* described from associated remains, and was also the first holotype specimen that was directly comparable to *Mancalla californiensis* (Howard, 1971). The holotype specimen (LACM 15373; Fig. 3.2) and additional referred specimens were recovered from Early Pliocene deposits on Cedros Island off the coast of Baja California, Mexico (Howard, 1971). The associated remains of *Mancalla cedrosensis* provided the first reliable assessment of inter-element osteological proportions for *Mancalla*, proportions that supported earlier size-based estimates of diversity among material from the San Diego Fm. proposed by Howard (1970).

*Praemancalla wetmorei* Howard, 1976 was described based upon a humerus with minor damage to the distal end (LACM 42653; Fig. 3.2) from Late Miocene sediments in Laguna Niguel, California. Several features distinguish this species from other *Mancalla* (see diagnoses below). An associated specimen (LACM 107028) was tentatively referred to *Praemancalla wetmorei* by Howard (1982) on the basis of overall resemblance between the ulna of that specimen and the paratype ulna of *Praemancalla wetmorei*. Because the paratype ulna (LACM 32429) is not associated with the holotype humerus, and was referred only on the basis of its occurrence within the same deposit, the affinities of that specimen remain uncertain. Likewise, the affinities of additional non-humeral material (e.g., LACM 53907, 37637, 52216) referred to *Praemancalla wetmorei* by



Howard (1976) are uncertain, because those specimens are not comparable to the holotype, and therefore not referable to species at this time. As stated above, the name-bearing specimen of *Praemancalla* (i.e., *Praemancalla lagunensis* Howard, 1966) is a nomen dubium. Based upon phylogenetic results and apomorphies shared with *Miomancalla howardi* sp. nov., *Praemancalla wetmorei* is referred to *Miomancalla*, and becomes *Miomancalla wetmorei*.

*Mancalla emlongi* was described based on a complete ulna from Early Pliocene San Diego Fm. in San Diego, California, USA (Olson, 1981). In the original description, comparisons were made between the holotype specimen of *Mancalla emlongi* (USNM 243765) and ulnae referred to *Mancalla californiensis*, *Mancalla diegensis*, *Mancalla milleri*, and *Mancalla cedrosensis*. As stated above, size and provenience alone do not in my opinion constitute strong evidence that material is referable to a taxon previously known from a particular locality or geologic formation. *Mancalla diegensis* and *Mancalla milleri* are nomen dubia, and there are no known associated specimens that would allow for referral of ulnae to *Mancalla californiensis*. Although the holotype ulna of *Mancalla emlongi* can be differentiated from ulnae of *Mancalla cedrosensis*, the possibility exists that *Mancalla emlongi* is synonymous with another species of Mancallinae (e.g., *Mancalla californiensis*). *Mancalla emlongi* is, therefore, considered Mancallinae *incertae sedis*.

Additional material from the San Diego Fm. including a well-preserved skull and mandible (SDSNH 25236; Fig. 3.3) was tentatively referred to *Mancalla emlongi* by

Chandler (1990b) on the basis of size. SDSNH 25236 and an additional skull (SDSNH 23753) are referable to Alcidae based upon the strongly protruding cerebellar prominence (35:0), and deeply incised temporal fossae (31:1) and deep salt gland fossae (20:1). Although no cranial apomorphies of Mancallinae have thus far been identified, the cranium of Mancallinae can be differentiated from the skulls of all other known Alcidae: differentiated from Fraterculinae (*Aethia*, *Ptychoramphus*, *Cerorhinca*, and *Fratercula*) by the dorsal position and extension of the temporal fossae; differentiated from *Brachyramphus*, *Synthliboramphus*, *Alle*, *Miocepphus*, *Alca*, *Pinguinus*, *Cerorhinca* and *Aethia* by the lack of supraoccipital foramina; differentiated from *Cepphus* by protrusion of the cerebellar prominence farther posteriorly (condition resembles that in *Uria*), and deeper interhemispherical furrow along midline of skull; differentiated from *Uria* by depth of nasal fossae (deeper, distinctly bordered posteriorly, and laterally incised in *Uria*). Although these specimens cannot be referred to species at this time, two associated specimens comprising associated cranial and postcranial material (LACM 103940 *Mancalla* sp. and SDSNH 68312 *Miomancalla howardi* sp. nov.) allow for comparison of SDSNH 25236 with known cranial morphology of Mancallinae. All three of the aforementioned specimens possess two small caudal mandibular fenestrae (46:1; Fig. 3.3D), a characteristic otherwise known only in the Fraterculini (i.e., *Fratercula* and *Cerorhinca*) among crown clade Alcidae, and also in the proposed sister taxon of Pan-

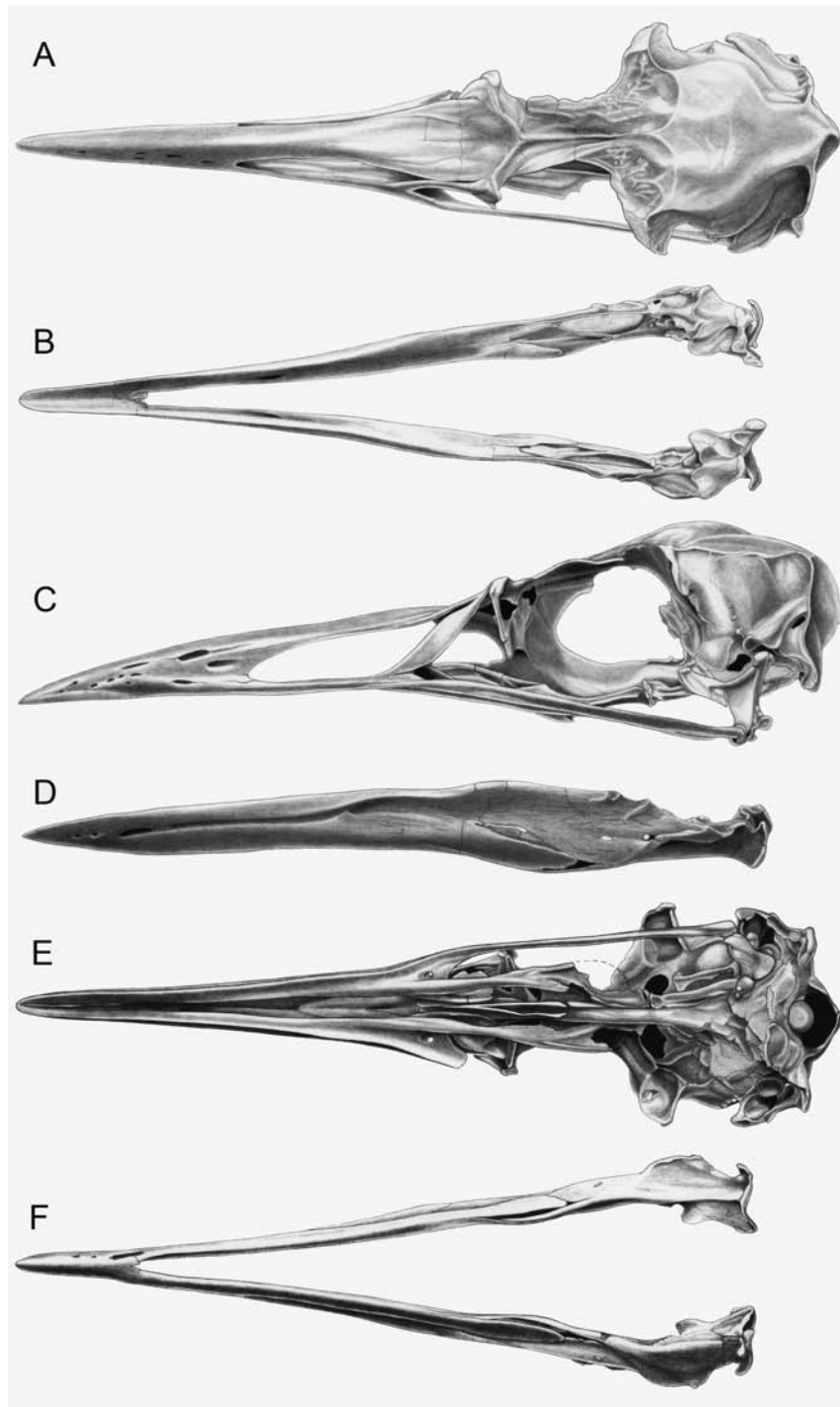


Figure 3.3- Skull of Mancallinae (SDSNH 25236). **A.** Dorsal view of skull; **B.** Dorsal view of mandible; **C.** Left lateral view of skull; **D.** Left lateral view of mandible; **E.** Ventral view of skull; **F.** Ventral view of mandible (sketches by Michael Emerson).

Alcidae, the Stercorariidae. SDSNH 25236 is differentiated from Fraterculini by the lack of dorsoventral expansion of the premaxilla and mandible (2:0), and by the less acute angle formed between the jugal and the proximo-ventrally descending bar of the nasal (6:0). SDSNH 25236 is consistent in size and morphological characteristics with the skull and mandible of LACM 103940, which is the only known *Mancalla* specimen with both cranial and postcranial elements preserved. Additionally, SDSNH 25236 lacks the dorsoventrally expanded mandible of *Miomancalla howardi*, suggesting systematic placement within *Mancalla*.

*Mancalla* remains were reported from Pleistocene sediments in Shiriya, Japan (Hasegawa et al. 1988). However, that material was never described, figured, nor systematically evaluated. My recent reexamination of the fossils confirms referral to Mancallinae. The presence of *Mancalla* in Japan provides a considerable range extension, and based upon the age of the material, also confirms that *Mancalla* survived into the Pleistocene in the eastern and western Pacific Ocean (Howard, 1970; Kohl 1974).

**Geologic setting:** The Mancallinae fossil remains described herein come from four Miocene and Pliocene aged marine deposits (Domning and Deméré, 1984; Ingle, 1979; Wagner et al., 2001). Congruent with the habitat of extant alcids (del Hoyo et al., 1996), three of these deposits (San Mateo Formation, Niguel Formation, San Diego Formation) are interpreted as the result of shallow to moderate depth marine facies (Vedder, 1960; Kern and Wicander, 1974; Vedder, 1972; Ingle, 1979; Wagner et al., 2001) associated with cold-water upwelling ocean systems. The upper siltstone facies of the Capistrano Formation, from which Mancallinae fossils have been recovered, contains

transported remains of neritic mollusks and microfossils that are mixed with the remains of bathyal species (Kern and Wicander, 1974), suggesting a shallow water origin for Mancallinae fossils from the Capistrano Formation. As with other vertebrate fossil assemblages from nutrient-rich cold-water systems (e.g., Pliocene Yorktown Formation assemblage; Ray, 1987; Ray and Bohaska, 2001), a diverse assemblage of vertebrates including marine mammals and seabirds are documented from marine deposits such as the Pliocene San Diego formation in southern California (Barnes et al., 1981).

**San Mateo Formation:** The San Mateo Formation is composed of sandstones, siltstones, and conglomerates that interfinger with the latest Miocene and earliest Pliocene aged member of the Capistrano Formation (Tan and Kennedy, 1996), and has been interpreted as the result of shallow marine deposition (Vedder, 1972). The San Mateo Formation is exposed in natural and quarried exposures near Lawrence Canyon in San Diego County, California, and has yielded two distinct vertebrate assemblages including sharks, fish, birds, and marine and terrestrial mammals (Barnes et al., 1981, Domning and Deméré, 1984; Howard, 1982).

The vertebrate assemblages of the San Mateo Fm. were discussed by Barnes et al. (1981), who designated the lower assemblage the San Luis Rey River Local Fauna (SLRRLF), and the upper assemblage the Lawrence Canyon Local Fauna (LCLF). Based on correlation of marine vertebrate and terrestrial mammal remains, the age of the younger LCLF has been proposed to be latest Miocene or earliest Pliocene (~5.0Ma), and correlative with the Late Hemphillian North American Land Mammal Age (NALMA; Domning and Deméré 1984). Mancallinae fossils, including the humerus (SDSNH

24584) referred to *M. howardi*, have been recovered from the older SLRRLF. Age estimates for the SLRRLF based upon terrestrial mammal and marine bird fossils range from approximately 6.7-10.0 Ma (i.e., Late Miocene or Turtonian equivalent; Barnes et al. 1981, Domning and Deméré, 1984).

Capistrano Formation: The Capistrano Fm. is composed of sandstones and siltstones that are correlated with the upper portions of the San Mateo Fm. in northern San Diego County (Elliot, 1975; Domning and Deméré, 1984), and have been interpreted as the result of marine deep-sea fan deposition on the basis of microfaunal analysis and abundant turbidites (Ingle, 1979; Vedder, 1972). The Capistrano Fm. spans the Late Miocene-Early Pliocene boundary (Deméré and Berta, 2005), and has accordingly been subdivided into upper and lower units. The age of the lower unit is estimated at 5.6-6.4Ma (i.e., Late Miocene or Late Messinian; Barron, 1986). Although no refined estimates are known for the uppermost siltstone unit from which the holotype of *Miomancalla howardi* was recovered, microfaunal analysis of the Capistrano Fm. has identified diatoms with ages as young as 4.9Ma (Early Pliocene or Early Zancian; Deméré and Berta, 2005).

Niguel Formation: The Niguel Formation is composed of a mixed sequence of marine and non-marine siltstones, sandstones, and conglomerates (Ingle, 1979). Analysis of microfaunal and molluscan fossils indicated deposition at a relatively shallow depth (i.e., <200m; Vedder, 1960) during the Late Pliocene and Pleistocene (Late Piacenzian-Early Calabrian; Vedder, 1960; Ingle, 1979) with sea-surface temperatures similar to

those offshore southern California today (i.e., nutrient rich cold-water system; Ingle, 1979).

San Diego Formation: The San Diego Formation predominantly consists of Pliocene and Pleistocene marine sandstones with minor amounts of conglomerates and claystones, which have been interpreted as shore-face and relatively shallow depth shelf facies deposits (Deméré, 1983; Wagner et al., 2001). Based upon microfaunal analysis and correlation with mammalian and molluscan assemblages of known age, the age of San Diego Fm. sediments are estimated to range from 3.6-1.5Ma (i.e., Middle Pliocene to Pleistocene; Piacenzian-Early Calabrian; Deméré, 1982; Wagner et al., 2001). The San Diego Fm. was divided into 7 stratigraphic sub-units by Wagner et al. (2001). *Mancalla* fossils occur throughout the San Diego Fm. (T. Deméré, personal communication). Paleomagnetic analysis indicates that sub-unit two can be correlated with the Gilbert Chron C2Ar and Gauss Chron C2An.3n boundary, which has been assigned an age of 3.6Ma (Wagner et al., 2001). The distribution of *Mancalla* species with respect to sub-units within the San Diego Fm. has not been evaluated.

## MATERIALS AND METHODS

Description of anatomical features primarily follows the English equivalents of the Latin osteological nomenclature proposed by Baumel and Witmer (1993). The terminology of Howard (1929) is followed for features not described by Baumel and

Witmer (1993). Taxonomy of extant North American Charadriiformes follows the 7th edition of the Checklist of North American Birds (American Ornithologists' Union, 1998). Measurements follow those proposed by Von den Driesch (1976). All measurements were taken using digital calipers and rounded to the nearest tenth of a millimeter. Ages of geologic time intervals are based on the International Geologic Timescale (Gradstein et al., 2004; Ogg et al., 2008).

All extinct taxa were evaluated by direct observation of holotype and referred specimens. Whenever available, five or more specimens of each extant species (Appendix 1), and both sexes, were evaluated to account for intraspecific character variation and sexual dimorphism respectively. Only adult specimens, assessed based upon degree of ossification (Chapman, 1965), were evaluated for osteological characters, and when available, specimens from multiple locations within the geographic range of extant species (i.e., subspecies) were examined to account for geographic variation within species. Reproductive, chick integument, dietary, and some myological characters were scored from published sources (Appendix 2). Descriptions of anatomical characteristics are followed by character numbers and character state designations from Appendix 2 (e.g., 23:0 = character number 23, state 0).

The analysis includes 72 terminals scored for a maximum of 353 morphological characters (293 binary; 60 multistate; 15 ordered). All twenty-three extant alcids, the recently extinct Great Auk *Pinguinus impennis*, eighteen Mancallinae specimens, and a Mancallinae supraspecific terminal are included in the matrix. Twenty-nine other extant charadriiforms constitute the remainder of the taxa analyzed, and provide a dense



outgroup taxonomic sample to test the monophyly of Pan-Alcidae with respect to other charadriiforms. Morphological characters include osteological ( $n = 232$ ), integumentary ( $n = 32$ ), reproductive ( $n = 11$ ), dietary ( $n = 2$ ), myological ( $n = 24$ ) and micro-feather ( $n = 52$ ). One hundred and sixty-four characters were developed for this analysis. The other 189 characters were drawn from the work of Hudson et al. (1969;  $n = 24$ ), Strauch (1978, 1985;  $n = 39$ ), Chandler (1990a;  $n = 63$ ), Chu (1998;  $n = 11$ ), and Dove (2000;  $n = 34$ ). Only 34 of the 38 characters identified by Dove (2000) varied in the taxa examined in this study. Of the 34 used in this analysis, eighteen were modified (i.e., split into 2 separate characters) according to the philosophy of character independence proposed by Hawkins et al. (1997), resulting in a total of 52 microfeather characters.

The cladistic matrix also includes a maximum of 11,601 base pairs from eight DNA sequence types. See Appendix 4 for details of sequence availability, inclusion for each species, and sequence authorship. Molecular sequence data (mitochondrial: ND2, ND5, ND6, CO1, CYTB; ribosomal RNA: 12S, 16S; and nuclear: RAG1) were downloaded from GenBank. Preliminary sequence alignments for each gene were obtained using the program ClustalX v2.0.6 (Thompson et al., 1997), and then manually adjusted using the program Se-Al v2.0A11 (Rambaut, 2002).

A combined approach of phylogeny estimation was used to evaluate the systematic position of Mancallinae species. Simulations show that the combination of molecular and morphological data often provides a more accurate estimate of phylogeny with respect to both extant and extinct organisms (Wiens, 2009). Parsimony-based phylogenetic analyses were conducted using PAUP\* v4.0b10 (Swofford, 2002).

Parsimony tree search criteria are as follows: heuristic search strategy; 10,000 random taxon addition sequences; tree bisection-reconnection branch swapping; random starting trees (primary analysis only); all characters equally weighted; minimum length branches =0 collapsed; multistate (e.g., 0&1) scorings used only for polymorphism. Bootstrap values and descriptive tree statistics (e.g., CI, RI, RC) were calculated using PAUP\* v4.0b10 (Swofford, 2002). Bootstrap value calculation parameters included 1,000 heuristic replicates, 100 random addition sequences per replicate. Bremer support values were calculated using a script generated in MacClade v4.08 (Maddison and Maddison, 2005) and analyzed with PAUP\* v4.0b10 (Swofford, 2002). Based on the results of previous phylogenetic analyses of charadriiform relationships (Strauch, 1978; Sibley and Ahlquist, 1990; Chu, 1995; Ericson et al., 2003; Paton et al., 2003; Thomas et al., 2004; Baker et al., 2007) resultant trees were rooted with the clade represented by exemplars of *Charadrius vociferus* and *Charadrius wilsonia*.

Owing to the incomplete and fragmentary preservation of most Mancallinae specimens referable to species, preliminary analysis of the systematic relationships of Mancallinae resulted in an unresolved polytomy among Pan-Alcidae sub-clades (i.e., relationships between Mancallinae, *Cepphus* Moehring, 1758, *Brachyramphus* Brandt, 1837, *Synthliboramphus* Brandt, 1837, Alcini Storer, 1960, and Fraterculinae (contents = Fraterculini Storer, 1960 + Aethiini Storer, 1960) unresolved at the base of Pan-Alcidae). Two additional phylogenetic analyses were performed to investigate the position of Mancallinae within Charadriiformes, and the interrelationships of Mancallinae species. The primary phylogenetic analysis included a Mancallinae supraspecific terminal (SST)

constructed by combining scorings from 19 Mancallinae specimens (including all holotype material; Appendix 3). The referral of all Mancallinae specimens used to construct the SST was evaluated based upon the unambiguously optimized apomorphies listed in the diagnosis section for Mancallinae below. Note that due to damage or missing elements in Mancallinae holotype specimens, five of the specimens used to construct the Mancallinae supraspecific terminal preserve morphological data not preserved by the holotype specimens, thus providing a more complete picture of morphological variation in Mancallinae than if only the holotype specimens were analyzed. The results of the first analysis were used to constrain the topology of trees accepted during a secondary tree search in which the species-level relationships of Mancallinae were evaluated.

***Institutional abbreviations:*** AMNH—American Museum of Natural History, New York, NY, USA; GCVP—Georgia College and State University Vertebrate Paleontology Collection, Milledgeville, GA, USA; IVPP—Institute of Vertebrate Paleontology and Paleoanthropology, Beijing, China; LACM—Natural History Museum of Los Angeles County, Los Angeles, CA., USA; LM—Loye Miller Collection, location presently unknown; NSM PO—National Museum of Nature and Science Paleontology Osteological Collection, Tokyo, Japan; NCSM—North Carolina Museum of Natural Sciences, Raleigh, NC, USA; SDSNH—San Diego Natural History Museum, San Diego, CA, USA; TMM—Texas Natural Science Center Vertebrate Paleontology Laboratory, Austin, TX, USA; UCMP—University of California Museum of Paleontology, Berkeley, CA, USA; USNM—Smithsonian Institution, National Museum of Natural History, Washington,

D.C., USA.

## SYSTEMATIC PALEONTOLOGY

AVES Linnaeus, 1758

CHARADRIIFORMES Huxley, 1867

PAN-ALCIDAE taxon nov.

Pan-Alcidae is defined as the most inclusive clade containing *Alca torda* Linnaeus, 1758 but not *Stercorarius longicaudus* Vieillot, 1819 or *Larus marinus* Linnaeus, 1758. This branch-based definition is adopted so that alcids outside of the crown clade (e.g., *Mancalla* Lucas, 1901) and potential discoveries of stem Alcidae taxa will not require alteration of the definition of this clade definition for Pan-Alcidae. Although the monophyly of Pan-Alcidae is strongly supported, the sister taxon of Pan-Alcidae is an issue of contention (Pereira and Baker, 2008; Chu et al., 2009). Accordingly, *Stercorarius longicaudus* and *Larus marinus* are both specified as outgroup taxa to maintain stability of this clade definition of Pan-Alcidae. The monophyly of Pan-Alcidae is supported by five unambiguously optimized morphological characters: strongly protruding cerebellar prominence (36:0); quadrate apneumatic (39:1); furcula sharply curved or angled at distal extremity (78:1); coracoidal tuberosity of furcula positioned anterior to coracoidal facet (80:1); bicipital tubercle of radius rounded rather than elongate (166:1).

## MANCALLINAE Brodkorb, 1967

Mancallinae (contents = *Mancalla* + *Miomancalla* new taxon) is referable to Alcidae based on the dorsoventral compression of the humeral shaft (145:2). The humeral shaft is less compressed in all other Charadriiformes. Mancallinae is differentiated from all other alcids on the basis of the following unambiguously optimized humeral apomorphies: deltopectoral crest extends past the midway point of the humeral shaft rather than restricted to the proximal half of the humeral shaft (107:2); presence of a muscle scar extending distally from the primary pneumatic fossa (123:1); capital groove communicates with transverse ligament sulcus resulting a notched rather than rounded appearance of ventral margin of the humeral head in anterior view (140:2); humeral head rotated anterodorsally rather than in-line with humeral shaft (143:1); humeral shaft arched rather than sigmoidal (144:1); presence of fossae in tricipital sulci (154:1); anterior surface of the ventral condyle rounded rather than flattened (157:0). Additional proposed apomorphies of Mancallinae are distal elongation (190:1) and anterior flattening of the first metacarpal (191:1). These characteristics are present in *Mancalla cedrosensis* Howard, 1971, *Miomancalla howardi* sp. nov., and two additional associated specimens referable to Mancallinae (SDSNH 77966 and LACM 107028). Although these two characters are also diagnostic for Alcini, the clade composed of *Alca*, *Pinguinus*, *Alle* Link, 1806, and *Uria* Brisson, 1760, the degree of distal elongation and anterior flattening in *Mancalla* exceeds that observed in Alcini.

*MANCALLA* Lucas, 1901

*Original diagnosis* (sensu Lucas, 1901)—Referred to Alcidae based upon dorsoventral compression of the humeral shaft. Differs from other alcids in the following characteristics: humerus short, with arced rather than sigmoid lengthwise curvature; anterior rotation of the humeral head; ventral margin of m. brachialis scar a distinct ridge.

*Emended diagnosis*—*Mancalla* is differentiated from *Miomancalla* on the basis of the following humeral characteristics: m. supracoracoideus scar (i.e., distally elongated dorsal tubercle) does not broaden proximally (116:2); distal margin of the primary pneumotricipital fossa convex rather than concave (129:0); ventral margin of the ventral tubercle narrow and ventrally expanded (i.e., convex) rather than wide and deeply grooved (137:0); capital groove constricted rather than wide (141:1). Additional proposed apomorphies which are present in *Mancalla cedrosensis* and two additional associated specimens (SDSNH 77966 and LACM 128870) referable to *Mancalla* but not to species include: ulna shorter than carpometacarpus (186:1); ulna more dorsoventrally compressed than other alcids; extension of the dorsal ulnar condyle farther distally to the ventral ulnar condyle than in other alcids (188:0); pisiform process of carpometacarpus reduced or absent (194:1).

***MANCALLA LUCASI*, sp. nov.**

*Holotype*—SDSNH 25237: a partial postcranial skeleton including the following elements: right scapula, left scapula, partial sternum, right and left humeri, left femur (Fig. 3.4; Tables 3.1, 3.2, & 3.3). The holotype specimen was collected by H. M. Wagner in April, 1980.

*Etymology*—This new species is named in recognition of Frederic A. Lucas who described the first known remains of *Mancalla*.

*Locality and Horizon*—Late Pliocene or Pleistocene (Zanclean or Calabrian) Niguel Formation of Orange County, California. Latitude, longitude, and elevation data are on file at SDSNH (locality 3202). Details of the geologic setting are provided above.

*Referred specimen*—SDSNH 59049: a complete left humerus from the Middle Pliocene to Pleistocene San Diego Formation (SDSNH locality 3506; Fig. 3.5E).

*Differential Diagnosis*—Scar extending into primary pneumotricipital fossa is raised in relief to the floor of the primary pneumotricipital fossa and the humeral shaft as in *Mancalla cedrosensis*, rather than an excavated pit as in *Mancalla vegrandis* sp. nov. and *Mancalla californiensis* Lucas, 1901 (124:1; Fig. 3.6); dorsal edge and ventral edge of the scar extending into primary pneumotricipital fossa taper to a point as in *Mancalla*

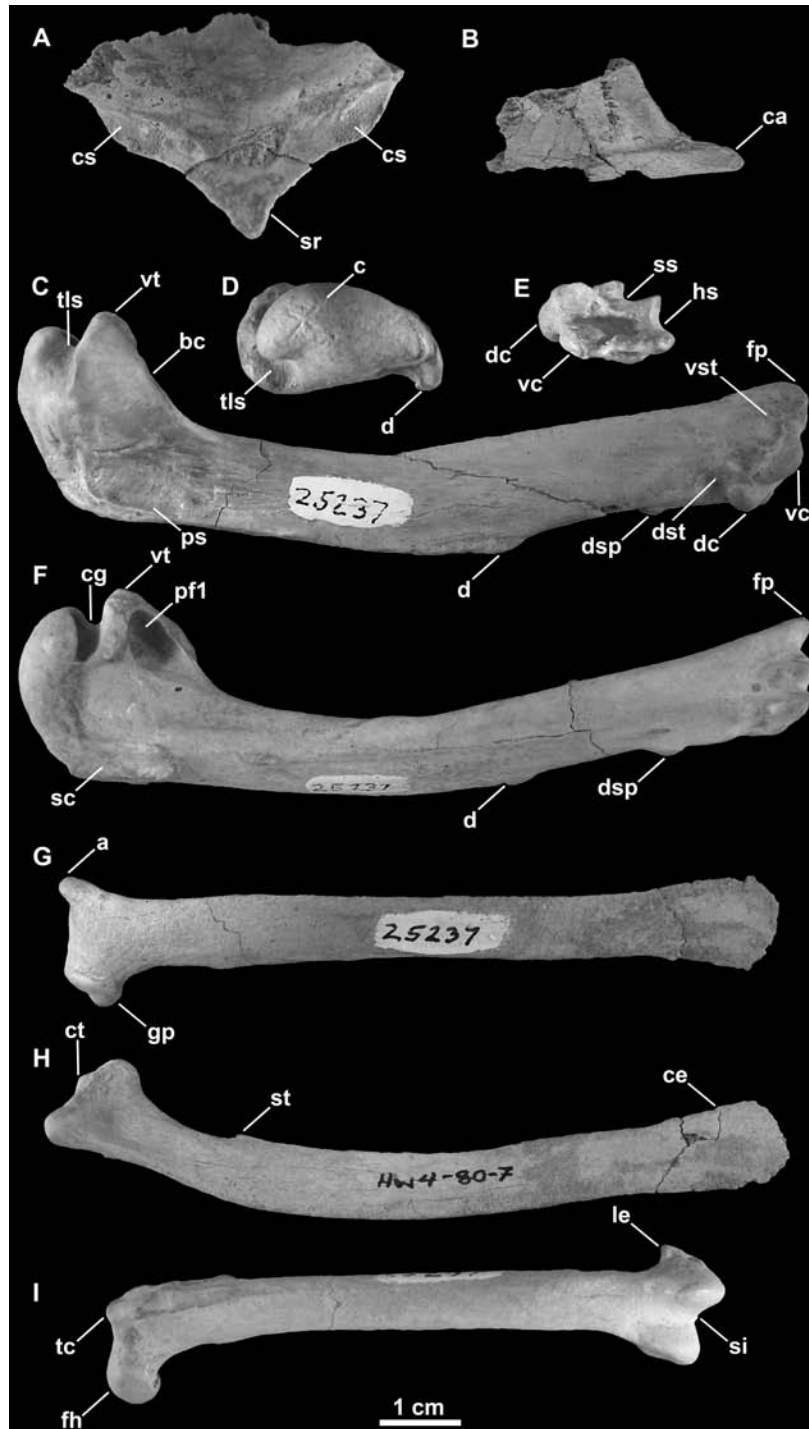


Figure 3.4- Holotype elements of *Mancalla lucasi* (SDSNH 25237). **A.** Fragment of anterior sternum in oblique anterior view; **B.** Carinal apex of sternum in right lateral view; **C.** Right humerus in anterior view; **D.** Left humerus in proximal view; **E.** Left



(caption continued from previous page) humerus in distal view; **F.** Left humerus in posterior view; **G.** Left scapula in lateral view; **H.** Right scapula in medial view; **I.** Left femur in anterior view. Anatomical abbreviations: (**a**) acromion process; (**bc**) bicipital crest; (**c**) caput; (**ca**) carinal apex; (**ce**) caudal extremity of scapula; (**cg**) capital groove; (**cs**) coracoidal sulcus; (**ct**) coracoidal tubercle; (**d**) deltopectoral crest; (**dc**) dorsal condyle; (**dsp**) dorsal supracondylar process; (**dst**) dorsal supracondylar tubercle; (**fh**) femoral head; (**fp**) flexor process; (**gp**) glenoid process; (**hs**) humerotricipital sulcus; (**le**) lateral epicondyle; (**pfl**) primary pneumotricipital fossa; (**ps**) pectoralis scar; (**sc**) m. supracoracoideus scar; (**si**) sulcus intercondylaris; (**sr**) sternal rostrum; (**ss**) scapulotricipital sulcus; (**st**) scapulotricipital tubercle; (**tc**) trochanteric crest; (**tls**) transverse ligament sulcus; (**vc**) ventral condyle; (**vst**) ventral supracondylar tubercle; (**vt**) ventral tubercle.



Figure 3.5- Referred humeri of *Mancalla* shown in anterior view. **A.** *Mancalla vegrandis* SDSNH 28152; **B.** *Mancalla vegrandis* SDSNH 42534; **C.** *Mancalla vegrandis* SDSNH 75051; **D.** *Mancalla vegrandis* SDSNH 42532; **E.** *Mancalla lucasi* SDSNH 59049.

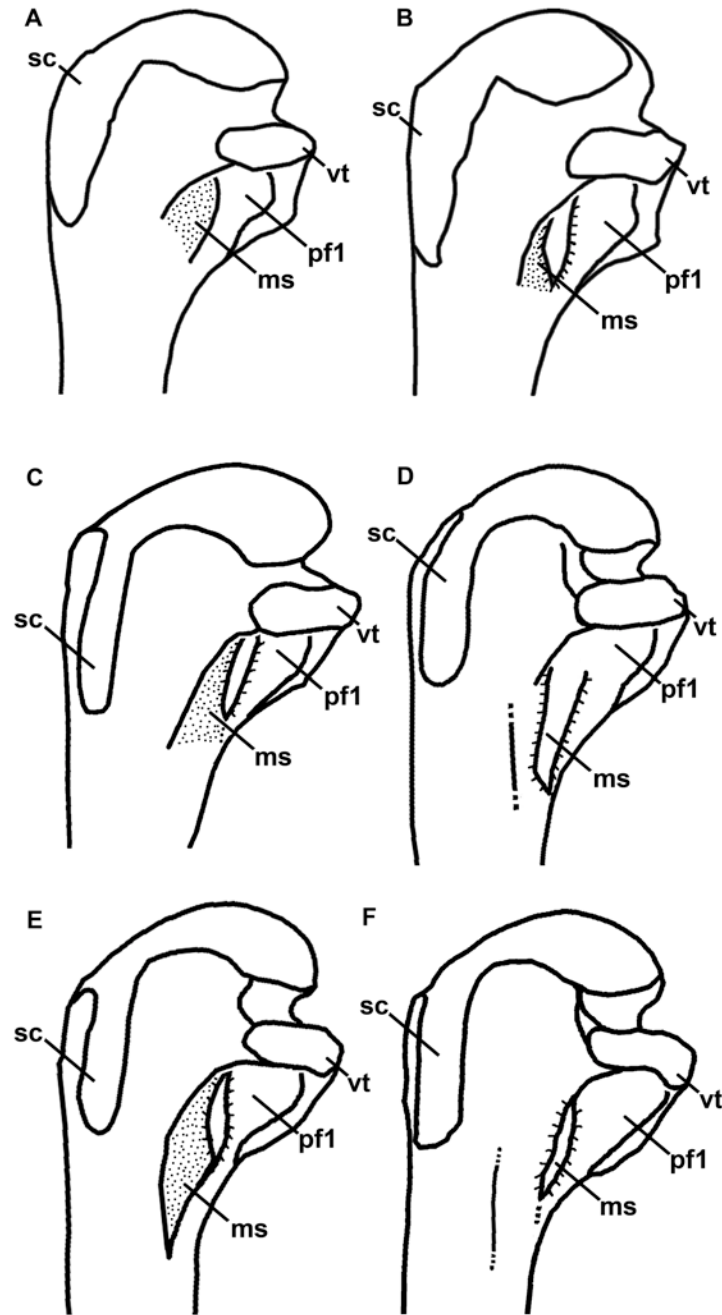


Figure 3.6- Line drawings comparing Mancallinae proximal ends of humeri in posterior view (not to scale). **A.** *Miomancalla wetmorei*; **B.** *Miomancalla howardi*; **C.** *Mancalla californiensis*; **D.** *Mancalla cedrosensis*; **E.** *Mancalla vegrandis*; **F.** *Mancalla lucasi*. Anatomical abbreviations: (**ms**) mancalline scar; (**pf1**) primary pneumotricipital fossa; (**sc**) m. supracoracoideus scar; (**vt**) ventral tubercle.

Table 3.2. Measurements of Mancallinae holotype humeri (mm). Abbreviations: (**Glh**) greatest length of humerus; (**Bph**) breadth of proximal humerus; (**Diph**) diagonal of proximal humerus; (**Whs**) width of humeral shaft; (**Bdh**) breadth of distal humerus; (**Ddh**) depth of distal humerus. Measurements following Von den Driesch (1976). ‘~’ signifies approximate measurement owing to damage. ‘—’ signifies missing data owing to damage.

Species	Specimen #	Glh	Bph	Diph	Whs	Bdh	Ddh
<i>Mancalla californiensis</i>	USNM 4976	~75.0	19.0	18.4	8.9	—	—
<i>Mancalla cedrosensis</i>	LACM 15373	73.3	17.8	17.1	9.1	13.0	7.1
<i>Mancalla lucasi</i>	SDSNH 25237	90.2	21.7	21.2	11.1	13.4	8.0
<i>Mancalla vegrandis</i>	SDSNH 77399	61.8	15.1	14.3	7.4	9.5	5.8
<i>Miomancalla wetmorei</i>	LACM 42653	~86.0	21.5	21.1	12.7	8.7	9.5
<i>Miomancalla howardi</i>	SDSNH 24584	103.2	22.9	22.2	11.1	12.2	8.7
<i>Miomancalla howardi</i>	SDSNH 68312	—	~25.0	~24.0	—	—	—

*vegrandis*, rather than remaining parallel as in *Mancalla californiensis* and *Mancalla cedrosensis* (126:1); humerus longer than *Mancalla cedrosensis*, *Mancalla californiensis*, and *Mancalla vegrandis* (Tables 3.2 & 3.3).

*Anatomical description*—Both scapulae are preserved (Fig. 3.4G&H). As in all Pan-Alcidae, the scapular shaft is mediolaterally compressed throughout its length. The proximal end of the scapular shaft is more rounded in other charadriiforms. As in *Mancalla vegrandis*, the acromion projects farther anteriorly than that of *Mancalla cedrosensis* and other alcids such as *Uria* and *Aethia*. As in *Mancalla cedrosensis*, the coracoidal tubercle is less pronounced than in *Mancalla vegrandis*. As in *Mancalla vegrandis* and *Mancalla cedrosensis*, a scapulotricipital tubercle is present just distal to

the glenoid process on the ventral margin of the scapular shaft. This feature is also present in other flightless wing-propelled divers such as Spheniscidae and *Pinguinus*, but is not known in any volant alcid. As in *Mancalla vegrandis*, the scapular shaft, including the caudal extremity, is slightly more robust than in other alcids (e.g., *Alca*, *Aethia*). The caudal extremity is less dorsoventrally expanded than in *Mancalla vegrandis*. The caudal extremity is not known for *Mancalla cedrosensis*.

Fragments of the sternum preserve the sternal rostrum, coracoidal sulci, and the carinal apex (Fig. 3.4A & B). These features are not preserved in *Miomancalla howardi* and comparisons are, therefore, limited to extant alcids and specimens of Mancallinae that are not currently referable to species. The morphology of the sternal rostrum is consistent with that of all other pan-alcids. Although no coracoid is preserved in the holotype specimen of *Mancalla lucasi*, the shape of the coracoidal sulci of the sternum is consistent with the  $\sim 150^\circ$  angle of the sternal articulation of the coracoid in *Mancalla cedrosensis* and *Mancalla vegrandis*. The sternal articulation of the coracoid, and the coracoidal sulci of the sternum in other alcids curves more acutely (e.g.,  $\sim 90^\circ$  in *Alca torda*; Fig. 3.7).

Complete right and left humeri are preserved (Fig. 3.4C, D, E&F). Based on humeral proportions *Mancalla lucasi* represents the largest known species of *Mancalla* (Table 3.2). As in other *Mancalla* species, the ventral margin of the ventral tubercle is convex and the capital groove is relatively narrower than that of other Alcidae. The ventral tubercle does not project as far ventrally as in *Mancalla californiensis* (Fig. 3.6).

Table 3.3. Measurements of newly described associated Mancallinae holotype specimens (in mm). ‘-’ = missing data owing to damage or lack of comparable element.

	<i>Miomancalla howardi</i> SDSNH 68312	<i>Mancalla lucasi</i> SDSNH 25237	<i>Mancalla vegrandis</i> SDSNH77399
<b>SKULL &amp; MANDIBLE</b>			
Greatest length of skull	122.9	-	-
Greatest breadth of frontal	11.4	-	-
Greatest length of rostrum	84.2	-	-
Greatest height of rostrum	21.1	-	-
Greatest length of mandible	127.8	-	-
<b>STERNUM</b>			
Smallest width between costal processes	-	-	5.9
<b>FURCULA</b>			
Dorsoventral height of apophysis	-	-	2.8
<b>CORACOID</b>			
Greatest length	-	-	45.8
<b>SCAPULA</b>			
Greatest proximal height	-	15.1	10.9
<b>CARPOMETACARPUS</b>			
Greatest length	46.8	-	-
Length of metacarpal one	23.2	-	-
Proximal breadth	11.9	-	-
<b>PELVIS</b>			
Greatest length	127.8	-	74.8
<b>FEMUR</b>			
Greatest length	79.9	67.8	-
Medial length	78.0	64.9	-
Proximal breadth	17.8	12.9	-
Proximal depth	10.9	9.2	-
Breadth of shaft	8.3	7.5	-
Distal breadth	18.0	12.5	-
<b>TIBIOTARSUS</b>			
Greatest length (preserved)	113.7	-	-
Breadth of shaft	7.8	-	-

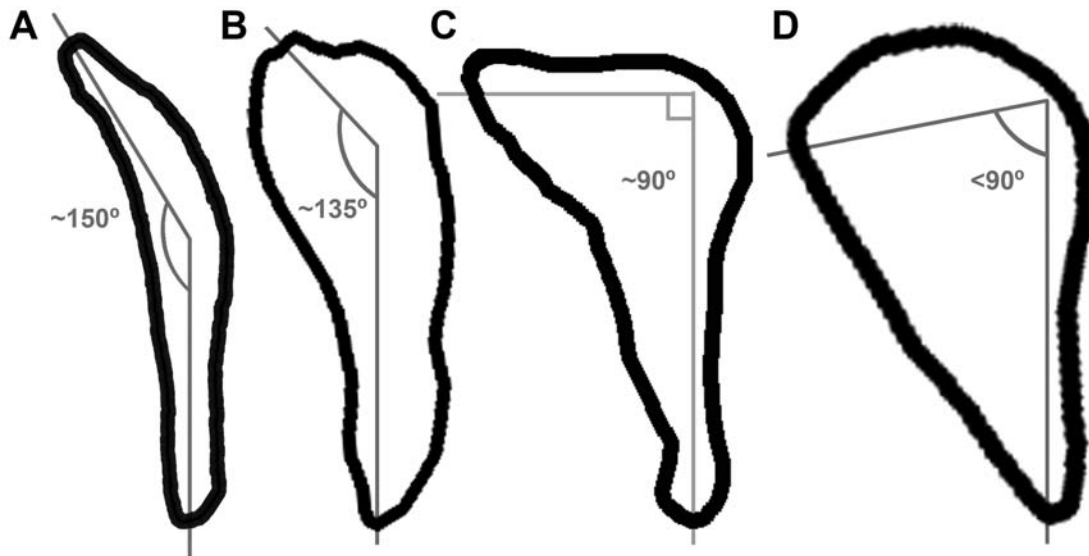


Figure 3.7- Comparison of the sternal facet curvature of selected charadriiform left coracoids (sternal view; not to scale). **A.** *Stercorarius*; **B.** *Mancalla*; **C.** *Alca*; **D.** *Aethia*.

The distal end of the deltopectoral crest transitions to the shaft more abruptly than in *Mancalla vegrandis*. As in other *Mancalla*, the humeral head is rotated anteriorly, and the m. supracoracoideus scar does not broaden proximally. Mancallinae is characterized by a scar of unknown function that is positioned adjacent to the primary pneumotricipital fossa (hereafter referred to as the ‘mancalline scar’; Fig. 3.6). The position of the ‘mancalline scar’ suggests an accessory insertion of m. humerotriceps (Howard, 1949), which can be divided into as many as four separate heads in some birds (Baumel and Witmer, 1993). However, the exact function of this feature is unknown because it is not present in any other charadriiform. The shape, position, and development of this scar is variable in Mancallinae. The ‘mancalline scar’ of *Mancalla lucasi* is raised in relief like that of *Mancalla cedrosensis*, rather than excavated as in *Mancalla californiensis* and *Mancalla*

*vegrandis* (Fig. 3.6). As in *Mancalla vegrandis*, the scar extends from a point just proximal to the junction of the bicipital crest with the humeral shaft, tapers to a point, and extends into the primary pneumotricipital fossa (Fig. 3. 6). The dorsal and ventral margins of the ‘mancalline scar’ remain approximately parallel in *Mancalla californiensis* and *Mancalla cedrosensis* (Fig. 3.6). As in all Mancallinae, the humeral shaft is arced rather than sigmoidal or straight. As in other *Mancalla*, the dorsal supracondylar tubercle is separated from the dorsal epicondyle it by a small notch. A tubercle or papilla is present on the posterior side of the distal end of the humerus adjacent to the dorsal condyle (Howard, 1976). As with all Mancallinae, the anterior surface of the ventral condyle is rounded, rather than flattened as in all other Pan-Alcidae. Rounded fossae are present at the proximal ends of the humerotricipital and scapulotricipital grooves. The flexor process extends distal to the ventral condyle as in all Mancallinae and *Pinguinus*.

The left femur is preserved (Fig. 3.4I). The femur is smaller (~15%; Table 3.2) than in *Miomancalla howardi* sp. nov. (Table 3.3), and larger (~19%) than that of *Mancalla cedrosensis* (Howard, 1971). As in *Alle*, *Cepphus*, *Synthliboramphus*, and *Brachyramphus*, the femoral trochanter projects anteriorly in lateral view. The femoral trochanter in *Uria*, *Aethia* Merrem, 1788, *Alca*, and *Pinguinus* is not projected anteriorly (i.e., straight), and the trochanter is concave in lateral view in *Fratercula* Brisson, 1760 and *Cerorhinca* Bonaparte, 1828. Femora of *Miocepheus* are not known. No diagnostic characteristics of the femur of *Mancalla lucasi* were identified.

*Remarks*—*Mancalla lucasi* corresponds in size and some humeral characteristics with material previously referred to *Mancalla diegensis*. However, *Mancalla diegensis* is a nomen dubium.

***MANCALLA VEGRANDIS*, sp. nov.**

*Holotype*—SDSNH 77399: a partial postcranial skeleton including the following elements: two cervical vertebrae, costal and vertebral ribs, partial furcula, scapulae, left coracoid, partial right coracoid, partial sternum, left humerus, and pelvis (Figs. 3.8 & 3.9; Tables 3.1, 3.2, & 3.3). The holotype specimen was collected by W. T. Stein in October, 1961.

*Etymology*—The species name *vegrandis* reflects the diminutive size of this species compared to other known species of *Mancalla* (*vegrandis*, from the Latin for small, diminutive or tiny).

*Locality and Horizon*—Middle Pliocene to Pleistocene (Zanclean-Calabrian) San Diego Formation of San Diego County, California. Latitude, longitude, and elevation data are on file at SDSNH (locality 4273). Details of the geologic setting are provided above.



*Referred specimens*—SDSNH 42532: a complete left humerus from the Middle Pliocene to Pleistocene San Diego Formation of San Diego County, California (SDSNH locality 3468); SDSNH 42534: a complete right humerus from the Middle Pliocene to Pleistocene San Diego Formation of San Diego County, California (SDSNH locality 3468); SDSNH 28152: a complete right humerus from the Early Pliocene upper member of the San Mateo Formation of San Diego County, California (SDSNH locality 3161); SDSNH 75051: a complete right humerus from the Early Pliocene upper member of the San Mateo Formation of San Diego County, California (SDSNH locality 2643; Fig. 3.5A-D).

*Differential Diagnosis*—Dorsal and ventral edges of the mancalline scar extending into primary pneumotricipital fossa of the proximal humerus taper to a point as in *Mancalla lucasi*, rather than remaining parallel as in *Mancalla californiensis* and *Mancalla cedrosensis* (126:1; Fig. 3.6); mancalline scar extending into primary pneumotricipital fossa is an excavated pit as in *Mancalla californiensis* rather than raised in relief to the floor of the primary pneumotricipital fossa and the humeral shaft as in *Mancalla cedrosensis* and *Mancalla lucasi* (124:0); humerus shorter than other known *Mancalla* (Tables 3.2 & 3.3).

*Anatomical description*—Two cervical vertebrae are preserved (Fig. 3.8A&B). Comparisons with *Miomancalla howardi* are limited to generalities regarding shape in dorsal view, for which the morphology of *Mancalla vegrandis* is consistent with that of

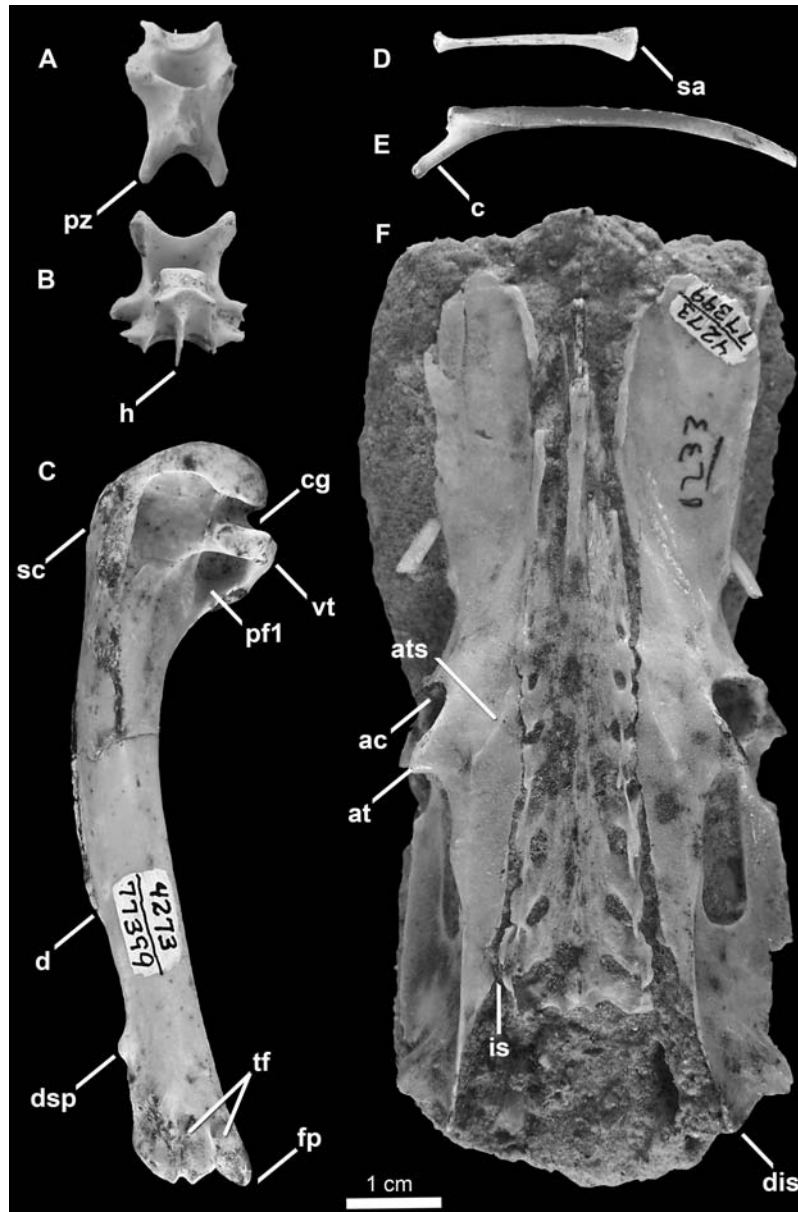


Figure 3.8- Holotype specimen of *Mancalla vegrandis* (SDSNH 77399; partial, see Fig. 3.9). **A.** Cervical vertebra (C3?) in dorsal view; **B.** Cervical vertebra (C4?) in ventral view; **C.** Left humerus in posterior view; **D.** Costal rib; **E.** vertebral rib; **F.** Pelvis in dorsal view. Anatomical abbreviations: (**ac**) acetabulum; (**at**) antitrochanter; (**ats**) antitrochanteral sulcus; (**c**) capitulum of vertebral rib; (**cg**) capital groove; (**d**) deltopectoral crest; (**dis**) dorsal iliac spine; (**dsp**) dorsal supracondylar process; (**fp**) flexor process; (**h**) hypapophysis; (**is**) iliosynsacral suture; (**pf1**) primary pneumotricipital fossa; (**pz**) postzygapophysis; (**sa**) sternal articulation of costal rib; (**sc**) m. supracoracoideus scar; (**tf**) tricipital fossae; (**vt**) ventral tubercle.

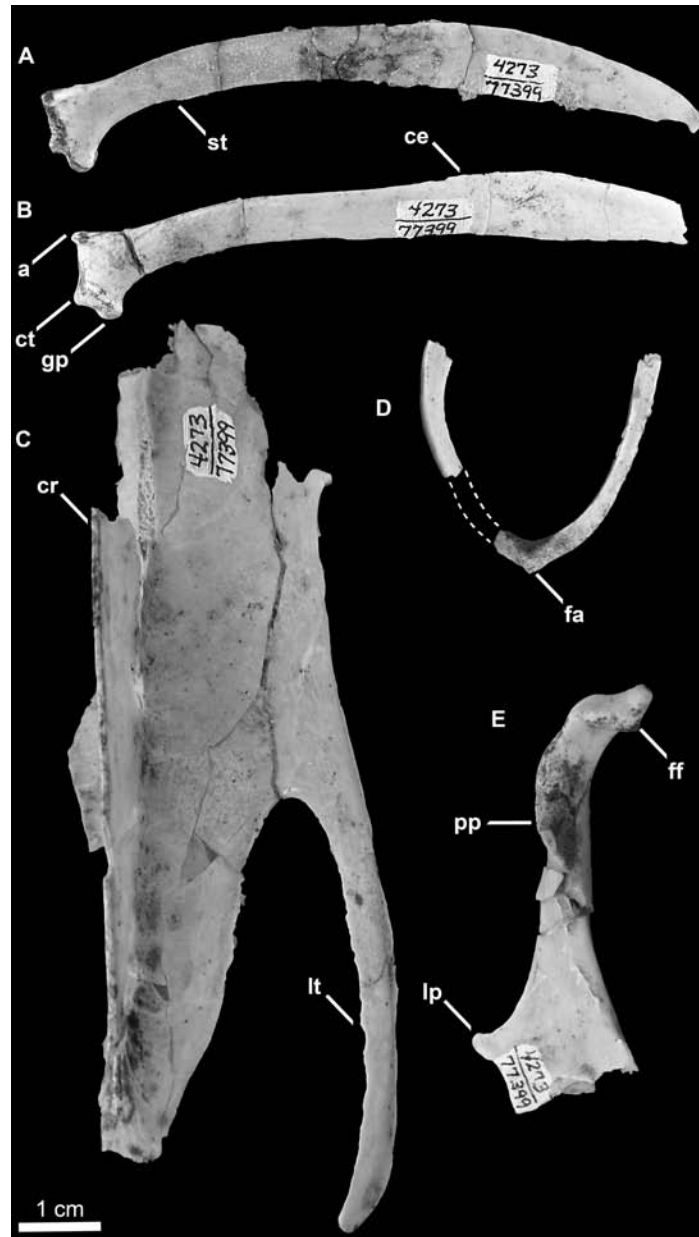


Figure 3.9- Holotype specimen of *Mancalla vegrandis* (SDSNH 77399; partial see Fig. 3.8). **A.** Right scapula in medial view; **B.** Left scapula in lateral view; **C.** Partial sternum in ventral view; **D.** Partial furcula in posterior view (dashed lines represent missing portion of left ramus); **E.** Left coracoid in posterior view. Anatomical abbreviations: (**a**) acromion process; (**ce**) caudal extremity of scapula; (**cr**) sternal carina; (**ct**) coracoidal tubercle; (**fa**) furcular apophysis; (**ff**) furcular facet of coracoid; (**gp**) glenoid process; (**lp**) lateral process of coracoid; (**lt**) lateral trabeculae of sternum; (**pp**) procoracoid process; (**st**) scapulotricipital tubercle.

*Miomancalla howardi*. Only thoracic vertebrae are known for *Mancalla cedrosensis*. One of the vertebrae (Fig. 3.8A) is mediolaterally narrower than the other (Fig. 3.8B).

Although the width of cervical vertebrae other than the axis and atlas do not vary markedly in extant alcids, the 3<sup>rd</sup> and 4<sup>th</sup> cervical vertebrae of some charadriiforms (e.g., *Larosterna inca* Lesson, 1827) are mediolaterally narrower than cervical vertebra posterior to the 4<sup>th</sup> (i.e., C5, C6, C7). The dorsal surface of the broader vertebra (Fig. 3.8B) is perforated by a small foramen (i.e., perforation of laminae arcocostales). In extant alcids, only the third and fourth cervical vertebrae are perforated. Typically in extant Alcidae, the third cervical vertebra is punctured by a small foramina, whereas the foramina in the fourth cervical vertebra is much larger, leaving only a thin strut of bone bordering it laterally. The morphology of the preserved vertebrae is suggestive of C3 and C4; however, definitive assignment cannot be made at this time.

One complete cervical rib and one complete costal rib (Fig. 3.8D&E) are preserved along with several other fragments of rib bones (not figured). No morphological differences were evident between the ribs of *Mancalla vegrandis*, Mancallinae specimen SDSNH 25236, and other pan-alcids for which the ribs are known.

All but the omal extremities of the furcula are preserved (Fig. 3.9D). The furcular rami are mediolaterally compressed as in all other Alcidae. The anterior surface of the furcular rami dorsal to the apophysis is rounded or convex as in *Uria*, rather than grooved like that of *Cepphus*. The furcular apophysis does not bear the ventrally expanded, bladelike interclavicular process characteristic of extant Alcidae. However, the possibility that this feature was lost to damage cannot be ruled out. No additional morphological

differences were evident between the preserved portions of the furcula of *Mancalla vegrandis* and other alcids for which the furcula is known.

The left coracoid is complete minus a small portion of the medial margin of the sternal facet (Fig. 3.9E). A fragment of the right coracoid preserves the medial margin of the sternal facet and the sternal portion of the coracoidal shaft (not figured). As in *Mancalla cedrosensis* the furcular facet is rounded rather than oval like that of *Aethia* and *Fratercula*. The head of the coracoid is apneumatic as in all Alcidae, but the brachial tuberosity is deeply undercut as in *Alca* and *Pinguinus*. The humeral articulation is more rounded than in extant Alcidae. As in *Cepphus*, the scar marking the position of m. supracoracoideus is less distinct than in other Alcidae. As in *Mancalla cedrosensis*, *Aethia*, and *Alle*, the procoracoidal process is not punctured by a foramen for passage of the m. supracoracoideus nerve. The procoracoid process points dorsomedially as in all Pan-Alcidae except *Aethia*, in which the procoracoid points more ventromedially. As in *Mancalla cedrosensis*, *Brachtyramphus*, *Uria*, *Aethia*, and *Ptychoramphus* Brandt, 1837, the sternal margin of the procoracoid process is concave, rather than convex as in *Cerorhinca*, *Fratercula*, and *Pinguinus*. As in many pan-alcids (e.g., *Alca*, *Brachyramphus*) a single, distinct, straight ridge, which extends from the lateral angle of the sternal facet towards the humeral facet is present. This ridge does not extend sternally in *Synthliboramphus*, *Cepphus*, *Fratercula*, *Aethia*, *Ptychoramphus*, and *Cerorhinca*. This ridge is less pronounced and positioned farther laterally in *Mancalla cedrosensis*. A well-developed lateral process is present. This feature is absent in *M. cedrosensis*. The dorsal margin of the medial sternal process is notched as in most pan-alcids (e.g., *Alca*

*torda*). As in *Mancalla cedrosensis*, the posterior surface of the sternal end of the coracoid is more excavated than in extant Alcidae, and the sternal facet is curved  $\sim 150^\circ$ .

Right and left scapulae are preserved (Fig. 3.9A&B). As in all Alcidae, the scapular shaft is mediolaterally compressed throughout its entire length. As in *Mancalla lucasi*, the acromion projects farther anteriorly than that of other alcids such as *Uria* and *Aethia*. The acromion of *Mancalla cedrosensis* does not project as far anteriorly as that of *Mancalla vegrandis*. The coracoidal tubercle is more pronounced than that of *Mancalla lucasi* and *Mancalla cedrosensis*. As in *Mancalla lucasi* and *Mancalla cedrosensis*, a scapulotricipital tubercle is present just distal to the glenoid process on the ventral margin of the scapular shaft. As in *Mancalla lucasi*, the scapular shaft, including the caudal extremity, is slightly more robust than in other pan-alcids (e.g., *Alca*, *Aethia*). The caudal extremity is more dorsoventrally expanded than in *Mancalla lucasi*. The caudal extremity is not known for *Mancalla cedrosensis*.

Parts of the left distal end of the sternum including the distal end of the carina, and the left lateral process are preserved (Fig. 3.9C). *Mancalla lucasi* and *Miomancalla howardi* do not preserve the same portions of the sternum so comparisons cannot currently be made between the sterni of Mancallinae. As a result of the deep incisure of the lateral notches, the lateral processes of *Mancalla vegrandis* are more elongate than that any other alcids for which the sternum is known. In other Charadriiformes this condition is present only in the Glareolidae and Scolopacidae, and resembles the sternum in Spheniscidae (Fig. 3.10).

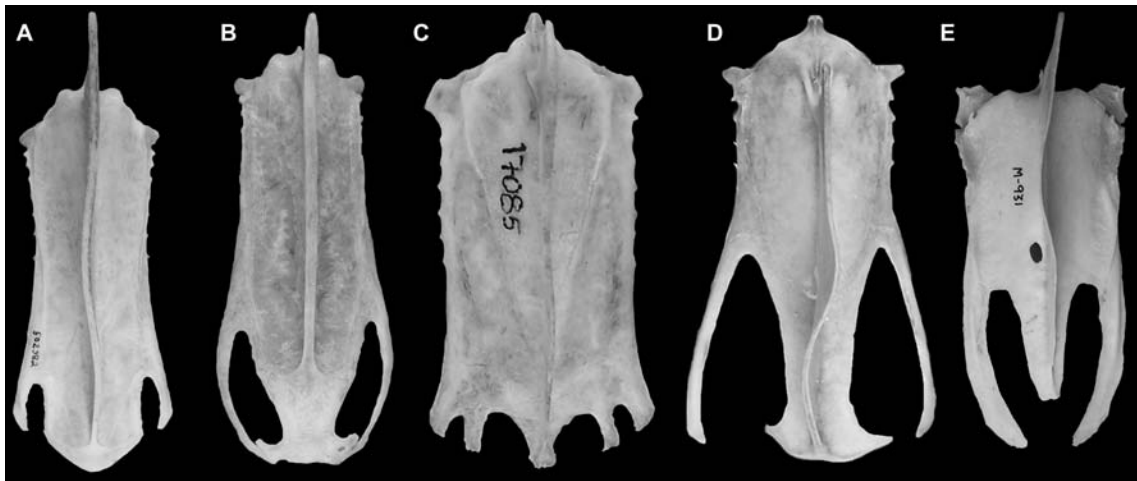


Figure 3.10- Comparison of charadriiform and spheisciiform sterni in ventral view. **A.** *Alca torda* (USNM 502382); **B.** *Aethia psittacula* (NCSM 18514); **C.** *Sterna anaethetus* (NCSM 17085); **D.** *Hydrophasianus chirurgus* (USNM 490566); **E.** *Eudyptula minor* (TMM M-391).

The left humerus is preserved (Fig. 3.8C). Based on humeral measurements (Table 3.2) *Mancalla vegrandis* is the smallest known species of *Mancalla*. As in other species of *Mancalla*, the ventral margin of the ventral tubercle is convex and the capital groove is relatively narrower than in other Pan-Alcidae. The ventral tubercle does not project as far ventrally as in *Mancalla californiensis*. The distal end of the deltopectoral crest transitions to the shaft less abruptly than in *Mancalla lucasi*. As in other Mancallinae, the humeral head is rotated anteriorly. As in other *Mancalla*, the m. supracoracoideus scar does not broaden proximally. The ‘mancalline scar’ is excavated as in *Mancalla californiensis*, rather than raised in relief like that of *Mancalla cedrosensis* and *Mancalla lucasi* (Fig. 3.6). As in *Mancalla lucasi*, the ‘mancalline scar’ extends from a point just proximal to the junction of the bicipital crest with the humeral shaft and tapers to a point, and extends into the primary pneumotricipital fossa. The

margins of this scar remain parallel in *Mancalla californiensis* and *Mancalla cedrosensis*. As in all Mancallinae, the humeral shaft is arced rather than sigmoidal or straight. As in other *Mancalla*, the dorsal supracondylar tubercle is separated from the dorsal epicondyle by a small notch. A tubercle or papilla is present on the posterior side of the distal end of the humerus adjacent to the dorsal condyle (Howard, 1966). As with all Mancallinae, the anterior surface of the ventral condyle is rounded, rather than flattened as in all other Alcidae. Rounded fossae are present at the proximal ends of the humerotricipital and scapulotricipital grooves. The flexor process extends distal to the ventral condyle as in all Mancallinae and *Pinguinus*.

The pelvis is preserved in dorsal view (Fig. 3.8F). Comparisons of pelves within Mancallinae are limited to *Miomancalla howardi*. As in all Pan-Alcidae the anteroposterior length of the pelvis is greater than two times the mediolateral width across the antitrochanters. The relative length of the pelves of other charadriiforms is anteroposteriorly shorter. The proximal end of the preacetabular ilium is wide as in *Miomancalla howardi* and most other pan-alcids (e.g., *Brachyramphus*). The distal end of the preacetabular ilium is broader than that of *Miomancalla howardi*. As in *Miomancalla howardi*, the antitrochanteral sulcus does not extend proximally to contact the antitrochanter. As in most Alcidae (e.g., *Brachyramphus*), the post-acetabular dorsal ilium narrows, rather than broadens as in *Uria*, *Cepphus*, and some Fraterculinae. The iliosynsacral suture is perforated as in *Uria*, *Alca*, *Pinguinus*, and *Synthliboramphus*, rather than fused along its entire length as in *Cepphus*, *Brachyramphus*, and



Fraterculinae. The dorsal iliac spine has a pointed tip as in all alcids other than *Aethia* and *Ptychoramphus*, in which the end of the spine is blunt.

*Remarks*—*Mancalla vegrandis* corresponds in size and some humeral characteristics with some material previously referred to *Mancalla milleri*. However, *Mancalla milleri* is a nomen dubium.

*MIOMANCALLA* taxon nov.

*Etymology*—*Mio* to reflect Miocene occurrences of known species within the taxon, and *mancalla* to reflect the sister group relationship with *Mancalla* Lucas, 1901.

*Differential Diagnosis*—*Miomancalla* is differentiated from *Mancalla* by the following characteristics of the humerus: capital groove wider (141:0); supracoracoidal crest (sensu Fürbringer, 1888; see Baumel and Witmer 1993:98) proximally broader (116:1); ventral margin of the ventral tubercle broader and deeply grooved rather than narrow and ventrally expanded (137:1); distal margin of the primary pneumotricipital fossa concave rather than convex (129:2).

*Remarks*—Based upon the phylogenetic results (see below) and apomorphies shared with *Miomancalla howardi* (see diagnosis above), *Praemancalla wetmorei*

Howard, 1966 is referred to *Miomancalla*, and becomes *Miomancalla wetmorei* (Howard, 1966).

***MIOMANCALLA HOWARDI*, sp. nov.**

*Holotype*—SDSNH 68312: a partial skeleton collected by B. O. Riney on May 31, 1990 and including the following elements: partial skull, mandible, cervical vertebrae, partial sternum, partial right humerus, left carpometacarpus, pelvis, femora, tibiotarsi, left tarsometatarsus (Figs. 3.11 & 3.12; Tables 3.1, 3.2 & 3.3).

*Etymology*—This new species is named in honor of Hildegard Howard and in recognition of her many contributions to the systematics of extinct alcids.

*Locality and Horizon*—Early Pliocene (Zanclean; Deméré and Berta, 2005) upper siltstone member of the Capistrano Formation, San Clemente, Orange County, California. Latitude, longitude and elevation data on file at SDSNH (locality 4160). Details of the geologic setting are provided above.

*Referred Specimen*—SDSNH 24584, a left humerus (Fig. 3.13) from the Late Miocene lower member (Messinian) of the San Mateo Formation of San Diego County, California (SDSNH locality 3177). This specimen was reported but not named or described by Chandler (1985) and Livezey (1988).

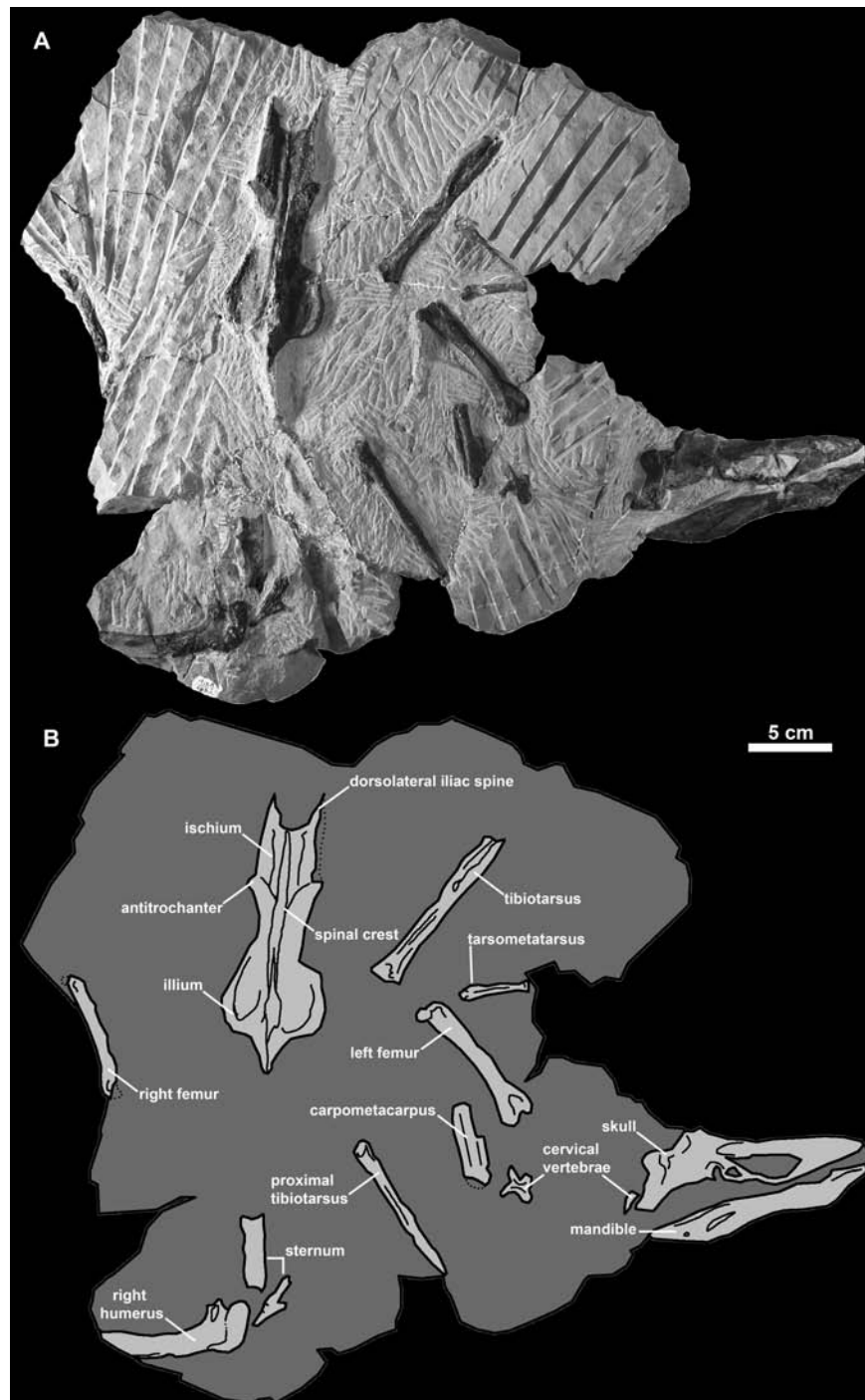


Figure 3.11- Holotype specimen of *Miomancalla howardi* (SDSNH 68312): **A.** Photograph with contrast digitally adjusted to better display bone against similarly colored matrix; **B.** Line drawing of holotype specimen showing position of preserved elements with fossil remains in light grey and matrix in dark grey.

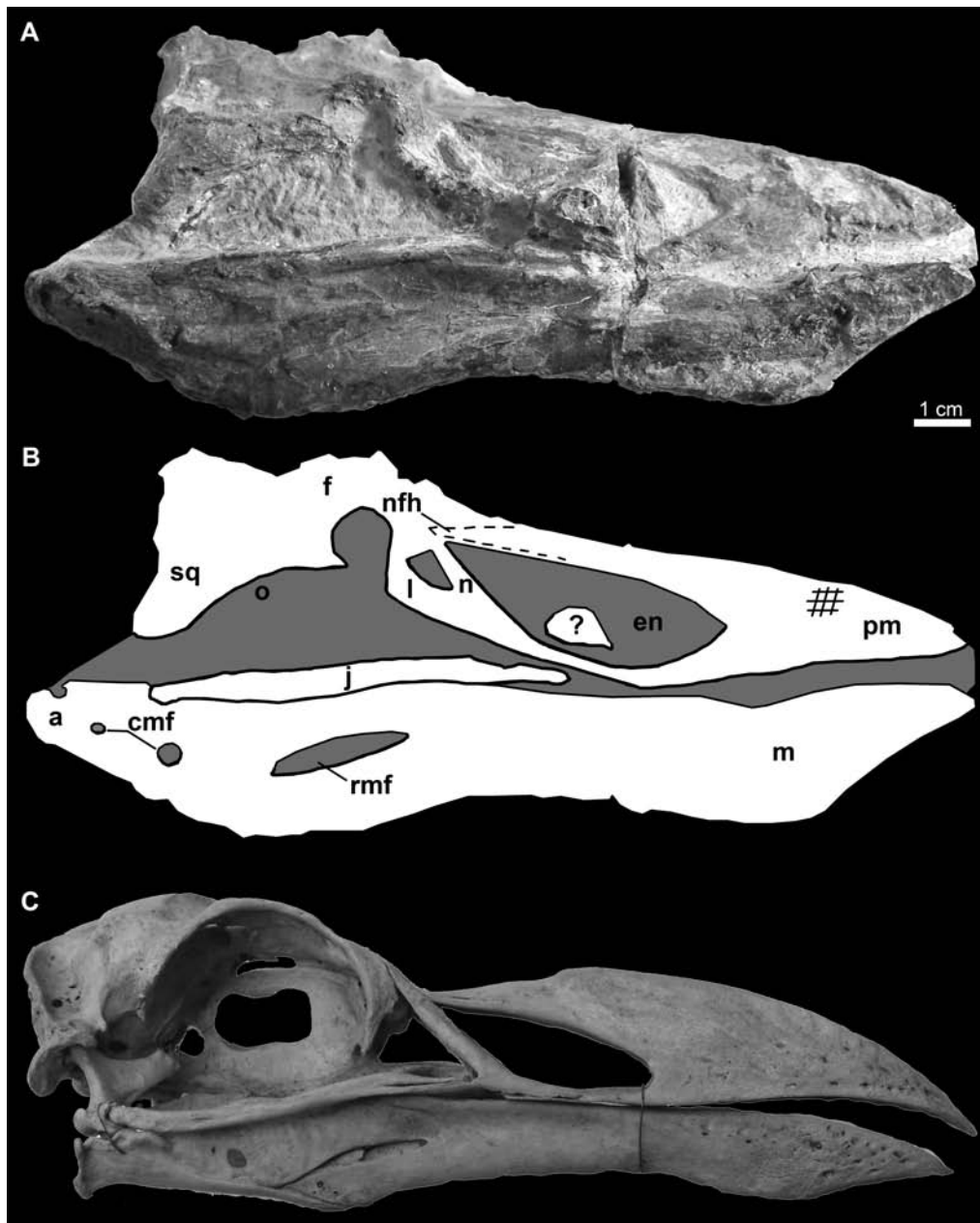


Figure 3.12- Photograph (A) and line drawing (B) of the skull of *Miomancalla howardi* compared with the skull of *Pinguinus impennis* (C; not to scale; USNM 346387). Cross-hatching on the premaxilla represents abrasion and dotted lines represent approximate reconstruction of elements. Anatomical abbreviations: (a) articular; (cmf) caudal mandibular fenestrae; (en) external nares; (f) frontal; (j) jugal; (l) lacrimal; (m) mandible; (n) nasal; (pm) premaxilla; (nfjh) nasofrontal hinge; (o) orbit; (rmf) rostral mandibular fenestra; (sq) squamosal; (?) unidentified fragment of bone.

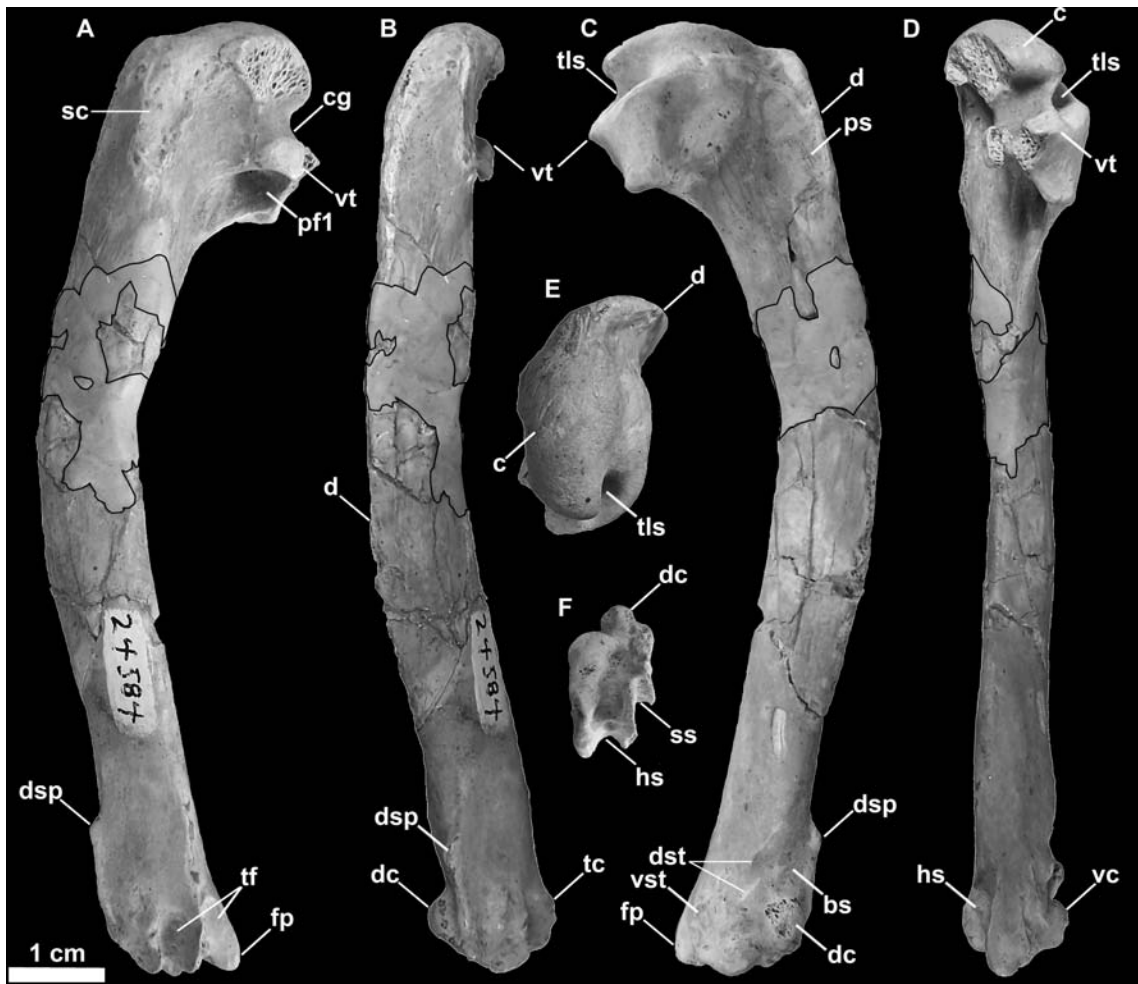


Figure 3.13- Left humerus referred to *Miomancalla howardi* (SDSNH 24584; dark outlined areas represent reconstructed areas obscured by repair). **A.** posterior view; **B.** dorsal view; **C.** anterior view; **D.** ventral view; **E.** proximal view; **F.** distal view. Anatomical abbreviations: (**bs**) brachialis scar; (**c**) caput; (**cg**) capital groove; (**d**) deltopectoral crest; (**dc**) dorsal condyle; (**dsp**) dorsal supracondylar process; (**dst**) dorsal supracondylar tubercles; (**fp**) flexor process; (**hs**) humerotricipital sulcus; (**pf1**) primary pneumotricipital fossa; (**ps**) pectoralis scar; (**sc**) m. supracoracoideus scar; (**ss**) scapulotricipital sulcus; (**tc**) tricipital crest; (**tf**) tricipital fossae; (**tls**) transverse ligament sulcus; (**vc**) ventral condyle; (**vc**) ventral condyle; (**vst**) ventral supracondylar tubercle; (**vt**) ventral tubercle.

*Differential Diagnosis*—Differs from *Miomancalla wetmorei* in the following characteristics of the humerus: ventral margin of ventral tubercle more deeply grooved; transverse ligament furrow deeper, with lateral lip extended farther medially; capital groove wider, and flatter; dorsal supracondylar process less dorsally projected; groove between dorsal supracondylar process and dorsal condyle wider; ventral supracondylar tubercle more prominent; tubercle present proximal to dorsal condyle as in *Mancalla cedrosensis* (159:1); humerus ~20% longer (Table 3.2; Livezey, 1988, Fig. 3A).

*Anatomical description*—The holotype specimen is preserved in a matrix of dark grey, highly indurated, siltstone (Fig. 3.11). Some elements have been slightly crushed, and many cortical bone surfaces are considerably abraded, obscuring fine morphological details in many portions of the specimen.

The cranium is exposed in oblique right lateral view (Figs. 3.11 & 3.12). The premaxilla, maxilla, nasal, lacrimal, jugal, frontal, and squamosal are present. Additional fragments of bone adjacent to the posterior frontal may represent a portion of the parietal. An unidentified fragment of bone protrudes from the external narial opening. The premaxilla is relatively shorter and mediolaterally compressed in comparison with the only other known premaxillae referable to Mancallinae (LACM 103940; SDSNH 25236; Fig. 3.3), which resemble the more terete bills of some other Alcidae (e.g., *Uria*). The maxilla, which broadens anteriorly before fusion with the premaxilla, is complete but broken at approximately its midpoint. As in many alcids (e.g., *Cepphus*, *Alca*) the nasal contacts the maxilla at ~45° angle. This angle is ~60° in the puffins and auklets (i.e.,

*Fratercula*, *Cerorhinca*, *Aethia*, and *Ptychoramphus*). As in *Pinguinus*, and in contrast to other alcids, the lacrimal appears to be directed ventrally rather than posteroventrally. However, crushing of the skull may have changed the relative orientation of elements and it is possible that distortion is responsible for this condition. The jugal is preserved in contact with the mandible. Fusion between the jugal and the jugal process of the premaxilla is visible. The frontal is distorted by crushing and most morphological details are obscured in this element. The outline of the right orbit is visible, but is deformed by ventrolateral displacement of the lateral margin of the frontal. The frontal bears a robust orbital rim as in *Uria*, *Miocepphus*, *Alle*, *Alca*, and *Pinguinus*.

The mandible is preserved in right lateral view (Figs. 3.11 & 3.12). The mandibular symphysis is elongate as in *Uria* and *Fratercula*. The mandibular rami are fused along a relatively shorter distance in some Alcidae (e.g., *Alle*). The proximal ends and distal ends of the mandible are dorsoventrally expanded, similar to the condition in *Alca* and *Pinguinus*. A pair of small posterior mandibular fenestrae is present as in other known Mancallinae mandibles (LACM 103940; SDSNH 25236; Fig. 3.3), Fraterculini, and some charadriiforms (e.g., *Stercorarius longicaudus* Vieillot, 1819).

Two cervical vertebrae are incompletely exposed on the surface of the slab (Fig. 3.11). Fine morphological details are obscured by matrix and the poor preservation of the vertebrae. One vertebra resembles the axis, but definitive identification is hindered by matrix and damage to the element. The other is a cervical vertebra exposed in dorsal view. Mancallinae vertebrae are known only from the holotype specimens of *Mancalla cedrosensis* and *Mancalla vegrandis*. Comparisons with *Mancalla cedrosensis* are not

possible because only a single thoracic vertebra is preserved in the holotype specimen of *Mancalla cedrosensis*. The shape of the dorsal surface of the cervical vertebrae of *Miomancalla howardi* is consistent with that of *Mancalla vegrans*. Further preparation of the holotype specimen of *Miomancalla howardi*, or discovery of additional material referable to this species are necessary before more details of vertebral anatomy can be described for this species.

Sternal fragments are preserved adjacent to the right humerus in what appears to be ventral view (Fig. 3.11). The craniolateral process appears to point dorsally, rather than anteriorly as in *Mancalla lucasi*. However, the possibility that crushing of this element altered the relative orientation of that feature cannot be ruled out. Other morphological details are obscured by matrix and the poor preservation of the sternum.

The holotype specimen preserves the proximal end of the right humerus in posterior view (Fig. 3.11). In addition to the head of the humerus, which is slightly crushed, the outline of the proximal half of the humeral shaft is visible as an impression in the siltstone matrix. A complete left humerus (SDSNH 24584; Fig. 3.13) is referable to *Miomancalla howardi* based upon its similar proportions (i.e., larger than any other known Mancallinae; Table 3.2), and the ventral surface of ventral tubercle being more deeply grooved than in any other pan-alcid. The ventral surface of the ventral tubercle is also grooved in *Pinguinus* and *Miomancalla wetmorei*, but the degree of excavation of this groove is more pronounced in *Miomancalla howardi* (Fig. 3.6). The ventral margin of the ventral tubercle of *Mancalla* is convex (Fig. 3.6). The capital groove is relatively wider than that of other species of Mancallinae, and it is incised more deeply into the



transverse ligament sulcus in anterior view than in *Miomancalla wetmorei*. The proximal end of the deltopectoral crest is less pronounced than in *Miomancalla wetmorei*. The distal end of the deltopectoral crest transitions to the shaft less abruptly than in *Mancalla*. The humeral head is rotated more anteriorly than in *Miomancalla wetmorei*, and is more similar to the condition in *Mancalla*. As in *Miomancalla wetmorei* and *Fratercula*, and in contrast to the condition in *Mancalla* species, the m. supracoracoideus scar broadens proximally. In *Miomancalla howardi* and *Miomancalla wetmorei* the ‘mancalline scar’ extends from a point just proximal to the junction of the bicipital crest with the humeral shaft and tapers to a point that meets the dorsal border of the primary pneumotricipital fossa (i.e., crus dorsale fossae of Baumel and Witmer, 1993:99). The scar is relatively smaller in *Miomancalla* and *Mancalla lucasi* than in comparison with other Mancallinae. The scar is an excavation in all Mancallinae except *Mancalla cedrosensis* and *Mancalla lucasi*, in which the scar is raised in relief to the floor of the primary pneumotricipital fossa and the humeral shaft. The shaft of the humerus is arced more so than in *Miomancalla wetmorei* or any other known alcid, and is less dorsoventrally compressed than in *Pinguinus*. As in all pan-alcids other than *Mancalla*, the dorsal supracondylar tubercle is continuous with the dorsal epicondyle, rather than separated from it by a small notch. The dorsal supracondylar tubercle is less pronounced than in *Miomancalla wetmorei*. A tubercle or papilla on the posterior side of the distal end of the humerus adjacent to the dorsal condyle was described by Howard (1966), who used that characteristic to differentiate between species of *Mancalla* that possessed the tubercle, and species of *Miomancalla* (*Praemancalla* sensu Howard 1966) that did not possess it.

The tubercle is present in *Miomancalla howardi*. As with all Mancallinae, the anterior surface of the ventral condyle is rounded, rather than flattened as in all crown Alcidae. Rounded fossae are present at the proximal ends of the humerotricipital and scapulotricipital grooves. That character cannot be evaluated in *Miomancalla wetmorei* or *Mancalla californiensis* owing to damage to the holotype specimens of those species and current lack of referable specimens. The flexor process extends distal to the ventral condyle as in all Mancallinae and *Pinguinus*.

The left carpometacarpus is preserved in dorsal view (Fig. 3.11). Although hundreds of Mancallinae carpometacarpi are known from Pliocene marine deposits in California, USA, the holotype specimens of *Miomancalla howardi* and *Mancalla cedrosensis* are the only associated specimens that allow for carpometacarpi to be referred to the species-level. The carpometacarpus of *Miomancalla howardi* is larger than that of *Mancalla cedrosensis* (~23%; Table 3.3; Howard, 1971), and displays the distal elongation of metacarpal I that is characteristic of Mancallinae. The abraded preservation of this element limits further comparisons.

The pelvis is complete and is exposed in dorsal view (Fig. 3.11). Comparisons within Mancallinae are limited to *Mancalla vegrandis*. As in all Pan-Alcidae the anteroposterior length of the pelvis is greater than two times the mediolateral width across the antitrochanters. The relative length of the pelvis of other charadriiforms is anteroposteriorly shorter. The proximal end of the preacetabular ilium is wide as in *Mancalla vegrandis* and most alcids (e.g., *Brachyramphus*). The distal end of the preacetabular ilium narrows more so than in *Mancalla vegrandis*. As with *Mancalla*

*vegrandis* the antitrochanteral sulcus does not extend proximally to contact the antitrochanter. The dorsal iliac spine has a pointed tip as in all alcids other than *Aethia* and *Ptychoramphus*, in which the end of the spine is blunt.

The distal ends of both tibiotarsi are missing or are obscured by matrix (Fig. 3.11). The poor preservation of these elements limits comparisons with the smaller holotype tibiotarsi of *Mancalla cedrosensis* to size (~26% larger; Table 3.3; Howard, 1971).

The right femur is exposed in posterolateral view along the edge of the block but is severely weathered. The left femur is well preserved and visible in anterior view (Fig. 3.11). The femur is robust and less sigmoidal in shape in comparison with the femora of extant alcids such as *Alca* or *Uria*, resembling the condition in *Mancalla lucasi* and *Mancalla cedrosensis*, the only other Mancallinae from which the femur is known. The intercondylar sulcus is relatively broader and more well defined proximally than that of *Mancalla lucasi* and *Mancalla cedrosensis*. As in *Cepphus*, *Brachyramphus*, and *Synthliboramphus*, the distally extending and anteriorly projected crest of the femoral trochanter is convex in shape. This feature is flattened (e.g., *Alca* and *Uria*) or concave (e.g., *Fratercula* and *Cerorhinca*) in other pan-alcids. The femoral head appears relatively smaller in comparison with this element in *Mancalla cedrosensis* and *Mancalla lucasi*. The length of the femur is greater than in *Mancalla cedrosensis* and *Mancalla lucasi* (Table 3.3; Howard, 1971).

The left tarsometatarsus is preserved in anterior view (Fig. 3.11). The anterior surface of the shaft is deeply grooved as in *Mancalla cedrosensis* and *Fratercula*.

Associated specimens with tarsometatarsi that might allow for referral of isolated tarsometatarsi to the species level are not presently known for other Mancallinae. The outlines of trochlea are visible but the distal end of the element is too badly abraded to discern fine morphological details.

## PHYLOGENETIC RESULTS

The primary combined phylogenetic analysis of the cladistic matrix including a Mancallinae SST resulted in two most parsimonious trees (MPTs; L: 15,974; CI: 0.38; RI: 0.50; RC: 0.19; Fig. 3.14). Additional analyses performed with all characters unordered did not result in topological differences, or an increase in the number of MPT's recovered. Pan-Alcidae is recovered as the sister to Stercorariidae, a result that is congruent with the results of previous molecular-based analyses (Ericson et al., 2003; Paton et al., 2003; Thomas et al., 2004; Paton and Baker, 2006; Baker et al., 2007), but conflicts with previous morphology-based analyses that placed Alcidae at or near the base of Charadriiformes (Strauch, 1978; Björklund, 1994; Chu, 1995, 1998; Chu et al., 2009). The combined analysis estimate of relationships among crown clade Alcidae is congruent with the results of recent analyses of molecular sequence data (Thomas et al., 2004; Paton et al., 2003; Baker et al., 2007; Pereira and Baker, 2008), except that *Synthliboramphus* is placed at the base of Alcinae, rather than as the sister to Alcini (Fig. 3.14). However, the parsimony analysis by Pereira and Baker (2008) also recovered

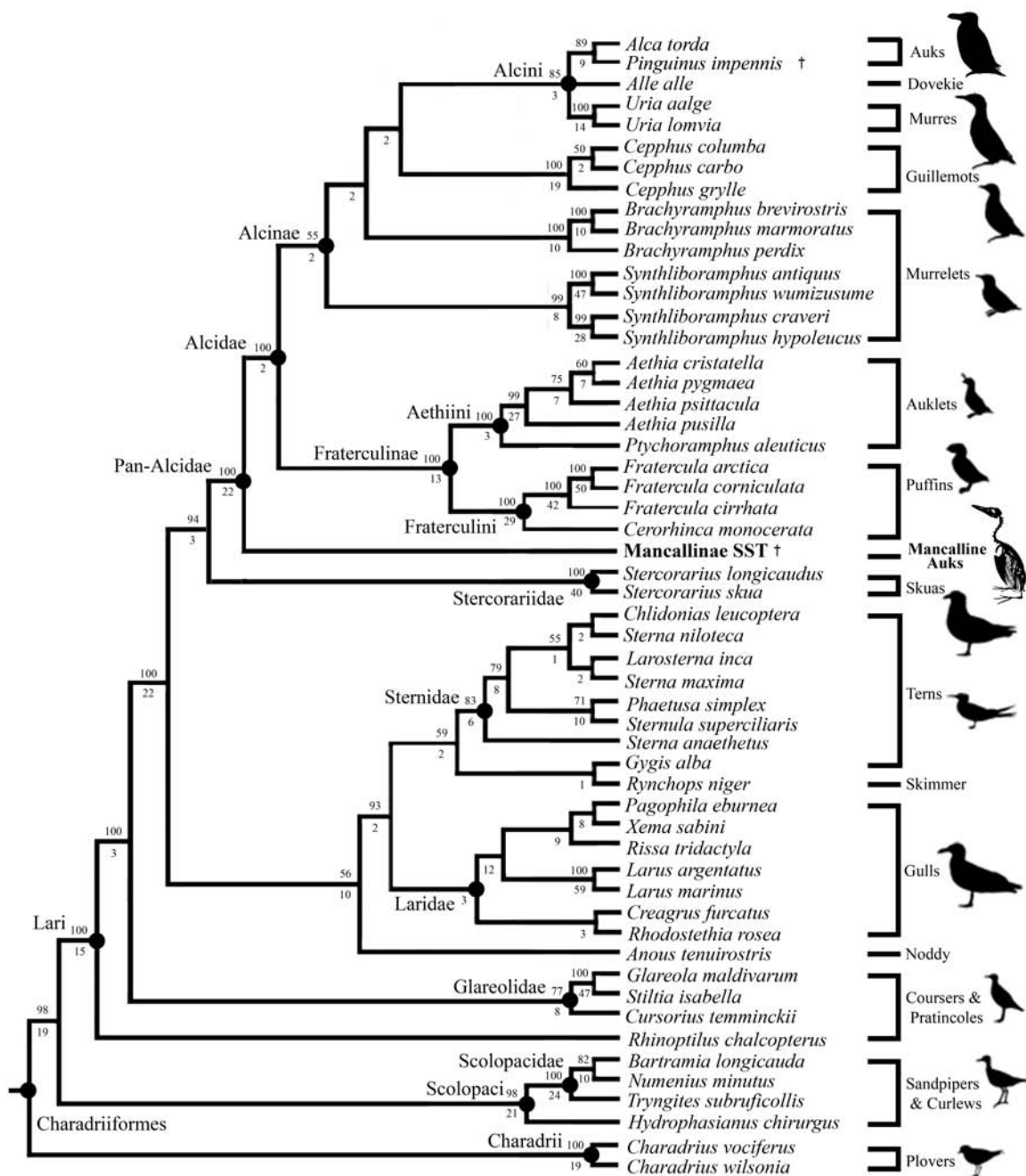


Figure 3.14- Results of primary phylogenetic analysis with 19 Mancallinae specimens combined into a supraspecific terminal (Mancallinae SST) to determine the systematic position of Mancallinae within Charadriiformes (2 MPT's; L:15,974; CI: 0.38; RI: 0.50; RC: 0.19). Bootstrap values > 50% are displayed above nodes, and Bremer support values are displayed below nodes.

*Synthliboramphus* at the base of Alcinae in one of two most-parsimonious topologies. The positions of other species (e.g., *Alca* + *Pinguinus*) and sub-clades in Alcidae (e.g., Fraterculinae + Alcinae) are consistent with the results of recent molecular-based analyses (Baker et al., 2007; Pereira and Baker, 2008) with dense taxonomic sampling for Alcidae. The only prior morphology-based analyses with sufficient taxonomic sampling for comparison to these results, those by Strauch (1985) and Chandler (1990a), resulted in topologies that strongly conflict with more recent hypotheses of alcid relationships in that they do not support a traditional Fraterculinae (i.e., monophyly of Fraterculini + Aethiini). The Aethiini (i.e., *Ptychoramphus* + *Aethia*) are placed basal to the Alcinae (*Alca* + *Pinguinus* + *Cephus* + *Brachyramphus* + *Synthliboramphus*), rather than as sister to the Fraterculini (i.e., *Cerorhinca* + *Fratercula*) in the topology of Strauch (1985). Although the work by Chandler (1990a) represented an increase in the number of characters scored for Alcidae, the results of that analysis placed *Alle alle* and *Cephus* in a clade with the Fraterculini, rather than in Alcinae. The combined analysis, as well as previous analyses (Watada et al., 1987; Moum et al., 1994; Friesen et al., 1996; Thomas et al., 2004; Baker et al., 2007; Pereira and Baker, 2008) strongly support monophyly of a Fraterculinae clade consisting of *Ptychoramphus*, *Aethia*, *Cerorhinca*, and *Fratercula*, and the sister-group relationship between Fraterculinae and Alcinae as defined here (Fig. 3.14).

Only the systematic position of *Alle alle* Link, 1806 remained unresolved within Alcini (Fig. 3.14). The systematic position of *Alle alle* is perhaps the most contentious issue in alcid systematics, as it has been recovered as the sister to *Alca* + *Pinguinus*

(Moum et al., 1994, 2002; Baker et al., 2007), sister to *Alca* + *Pinguinus* + *Uria* (Strauch, 1985), sister to *Uria* (Thomas et al., 2004; Pereira and Baker, 2008), sister to Fraterculinae (Chandler, 1990a), and sister to *Cephus* + *Aethia* + *Brachyramphus* (Chu, 1998). Resolution of this issue will likely require a comprehensive analysis of pan-alcid relationships including dense taxonomic sampling of extinct Pan-Alcidae.

Mancallinae is placed as the sister taxon to all other Alcidae (i.e., placed outside of the alcid crown clade; Fig. 3.14). This result is consistent with the only previous analysis that included Mancallinae (Chandler, 1990a). The clade composed of crown Alcidae + Mancallinae is, therefore, designated Pan-Alcidae. The monophyly of Pan-Alcidae is supported by five apomorphies with a CI = 1.0 (Table 3.4).

The relationships recovered among the 29 charadriiform outgroup taxa are largely congruent with prior molecular-based analyses of the clade, but do not support previous morphology-based results. *Larus* and *Hydrophasianus* (i.e., gulls and jacanas) are recovered as more closely related to one another than either are to *Charadrius* (i.e., plovers), as in the results obtained by Hackett et al. (2008). Also consistent with the results of prior molecular-based analyses (Ericson et al., 2003; Paton et al., 2003; Paton and Baker, 2006; Baker et al., 2007), Pan-Alcidae + Stercorariidae is placed as the sister to Laridae + Sternidae + Rynchopidae. The results of the combined analysis are congruent with recent molecular-based analyses that placed Lari (e.g., alcids, gulls, and pratincoles) as the sister to Scolopaci (e.g., sandpipers, jacanas, and curlews), and place Charadrii (e.g., plovers) at the base of Charadriiformes. This hypothesis contrasts with

Table 3.4. Unambiguously optimized morphological apomorphies with a CI = 1.0 supporting clades in the resultant phylogenetic hypothesis (Fig. 3.15). Character numbers from Appendix 2 are followed by character state symbols (e.g., 23:0 = character number 23, state 0).

Clade	Character numbers and states that support monophyly
Pan-Alcidae	36:0; 39:1; 78:1; 80:1; 166:1
Alcidae	69:1; 157:1; 176:1
Alcinae	50:1; :279:1; 290:1
Alcini	191:1; 246:1; 248:1; 283:1
Fraterculinae	73:1
Fraterculini	30:1; 36:1; 41:1; 64:1; 115:0; 284:1; 295:1; 296:1
Aethiini	11:1; 89:0; 96:1; 206:1
Mancallinae	107:2; 123:1; 143:1; 144:1; 152:1; 154:1; 189:0; 190:1
<i>Mancalla</i>	141:1

the morphology-based results of Björklund (1994) and Chu (1995), which were the result of parsimony-based re-analyses of the compatibility analysis of Strauch (1978). In the topology recovered by Björklund (1994) the Charadrii and Scolopaci are placed in an unresolved polytomy basal to the Lari, whereas the Lari and Charadrii are placed in an unresolved polytomy basal to the Scolopaci in the topology recovered by Chu (1995). The contents of Charadrii, Scolopaci, and Lari estimated by the combined analysis are consistent with the composition of those clades recovered in prior molecular-based phylogenetic analyses (Sibley and Ahlquist, 1990; Paton et al., 2003; Ericson et al., 2003;



Paton and Baker, 2006; Baker et al., 2007), supporting the monophyly of Charadrii, Lari, and Scolopaci.

Also of interest is the placement of *Rynchops* (i.e., skimmers). Recent molecular analyses have recovered *Rynchops* as the sister taxon to Laridae (Paton et al., 2003; Baker et al., 2007), and sister to Sternidae (Paton and Baker, 2006). The morphology-based analyses by Chu (1995, 1998) placed *Rynchops* as the sister to Sternidae + Laridae + Stercorariidae. The results of the combined analysis place the Black Skimmer *Rynchops niger* as the sister taxon to the White Tern *Gygis alba*. Considering the traditional placement of *Gygis alba* in Sternidae (Bridge et al., 2005), this result would suggest Sternidae paraphyly; although, this result is not entirely novel because an alternative hypothesis also placed *Gygis* outside Sternidae, as the sister to Laridae + Sternidae (Baker et al., 2007). However, denser taxonomic sampling of Rynchopidae, Sternidae, and other charadriiforms may resolve this issue in the future.

*Anous* (i.e., noddies) was recovered as the sister taxon to Sternidae + Laridae + Rynchopidae in the results of the combined analysis, a placement consistent with the molecular-based results reported by Baker et al. (2007), and in conflict with the morphology-based results obtained by Chu (1998) that placed *Anous* as the sister to Stercorariidae. The only study with dense taxonomic sampling of terns and noddies (Bridge et al., 2005) included only a single larid (*Larus delawarensis*) as an outgroup taxon, but placed *Anous* basally in Sternidae. Resolution of the systematic affinities of *Anous* will likely require dense taxonomic and character sampling across Laridae, Sternidae, Rynchopidae, *Anous*, and other non-Lari charadriiforms.

The secondary phylogenetic analysis that evaluated the interrelationships among Mancallinae resulted in two MPTs (Fig. 3.15; L: 15,971 steps; CI: 0.37; RI: 0.51; RCI: 0.19). The monophyly of Mancallinae is supported by eight apomorphies (Table 3.4). *Miomancalla wetmorei* and *Miomancalla howardi* are placed as sister taxa, and *Miomancalla* monophyly is supported by three locally optimized apomorphies; 108:0; 116:1; 141:1). *Miomancalla* is placed as the sister taxon to *Mancalla*. *Mancalla* monophyly is supported by one apomorphy (143:0) and an additional locally optimized apomorphy (133:1). The placement of *Mancalla californiensis* as the sister taxon of *Mancalla cedrosensis* is supported by one apomorphy (126:0), and an additional locally optimized apomorphy (112:1). *Mancalla vegrandis* and *Mancalla lucasi* are placed as successive outgroups to the clade composed of *Mancalla californiensis* and *Mancalla cedrosensis* (Fig. 3.15).

## DISCUSSION

The taxonomic revision and the new Mancallinae species described herein confirms previous estimates of high diversity in Mancallinae (Howard, 1970; Olson, 1981; Chandler, 1990a), and in combination with the phylogenetic results of the combined analysis, provide a new context for the interpretation of the evolutionary success of this lineage of flightless wing-propelled divers. The placement of Mancallinae as the sister taxon to crown Alcidae suggests that flightlessness evolved independently in the Mancallinae and *Pinguinus* lineages, making the many osteological characteristics



shared between these taxa an even more compelling example of morphological convergence. Phylogenetic support for the monophyly of *Miomancalla* and *Mancalla* also provides further contextualization for the interpretation of morphological differences between these sister taxa. Although known diversity is higher for *Mancalla*, there is an apparent trend towards decrease in size for more derived members of the clade, with the larger *Miomancalla* and *Mancalla lucasi* placed basally in the recovered topology. Although it is tempting to infer large body-mass as the ancestral state for Pan-Alcidae, the reconstruction of this character is ambiguous according to the phylogenetic results, and there is an ~25Ma gap in the fossil record between the oldest known fossil pan-alcid and the oldest Mancallinae fossils. The most important contributing factor regarding the ambiguity of ancestral states within Pan-Alcidae is the incompleteness of the early alcid fossil record. Although an abundance of taxa are known from the Miocene and Pliocene, only a single fragmentary alcid fossil is known from the Eocene (Chandler and Parmley 2002). The only Oligocene fossils that are currently referred to Pan-Alcidae are two fragmentary and isolated specimens from the Iwaki Formation in Japan (Ono and Hasegawa, 1991). Eocene and Oligocene localities and collections should be targeted to increase knowledge of early diversity and ancestral states within Pan-Alcidae.

Although impressive with regard to the quantity of taxa sampled ( $n = 242$ ) and the number of morphological characters scored for those taxa ( $n = 1107$ ), the results of a recent morphology-based analysis of Charadriiformes relationships (Livezey, 2009, 2010) are not considered herein because Alcidae was included only as a suprageneric terminal taxon. With respect to relationships among major charadriiform clades, some of

the results of Livezey (2010) are in conflict with a growing consensus of molecular results based upon a variety of methods and sampling schemes. For example, although the placement of Charadriidae in a derived position within Charadriiformes to the exclusion of other clades (Livezey, 2010) is in agreement with some previous hypotheses (Strauch, 1978; Sibley and Ahlquist, 1990; Christian et al., 1992; Björklund, 1994; Chu, 1995; Thomas et al., 2004; Livezey and Zusi, 2007), these hypotheses are in contrast with the results of more recent molecular-based hypotheses that recovered Charadriidae in a more basal position. (Ericson et al., 2003; Paton et al., 2003; Paton and Baker, 2006; Baker et al., 2007; Fain and Houde, 2007; Hackett et al., 2008). There exists no metric with which to choose between the contrasting results of those many analyses, and therefore, systematic relationships between major clades of Charadriiformes remain somewhat uncertain. However, the combined analysis reported herein represents the most inclusive analysis to date with respect to variety of phylogenetically informative data sampled.

***Referral of fossils to species level:*** Referral of specimens to named species, or recognition of new species based solely upon size, or provenience, or age, or any combination of those three criteria, take the risk of incorrectly assigning specimens to species or incorrectly assessing species richness (Norell, 1989; Nesbitt and Stocker, 2008; Bell et al., 2010). To avoid the possibility of recognizing two or more fossil species based upon different skeletal elements of the same species, recognition of new species must be predicated upon diagnoses or differentiation from previously named species within a taxon. Occurrence within the same deposit or deposits of similar age is not

considered strong evidence that fossils represent the same taxon. Similarly, a lack of recorded occurrences of a fossil taxon within a deposit or deposits of a particular age does not preclude the possibility that a taxon may be present in that deposit. For example, if the holotype specimen of a species is an isolated humerus, then only associated specimens with humeri consistent with that of the holotype specimen allow for initial referral of additional skeletal elements. When previously recognized holotype specimens consist of isolated elements, isolated material consisting of elements other than the holotype element cannot be referred to the species level until associated specimens are discovered that facilitate such referral. These criteria avoid incorrect estimation of diversity and incorrect assignment of specimens that results from less rigorous methods (i.e., size, provenience, or age-based methods) of specimen referral and species recognition. In the case of Mancallinae remains, there is little doubt that hundreds of isolated fossils are referable to that clade; however, to avoid future taxonomic confusion, referrals should only be made based upon the criteria outlined above. The morphological differences between Mancallinae holotype and referred specimens described and phylogenetically optimized herein provide a basis for the potential apomorphy-based referral of hundreds of additional isolated Mancallinae remains, which will facilitate future detailed study of morphologic and size variation in Mancallinae.

***Flightlessness and convergence:*** The etymology of *Mancalla* (*mancus*-from the Latin for crippled or lame, and *ala* from the Latin for wing; Brown, 1956) reflects an antiquated view of flightlessness. The flightless condition observed in ostriches and some rails for example, in which the pectoral elements are diminished in size, has been

attributed to lack of predatory pressures and energy conservation strategies (Livezey and Humphrey, 1986; McNab, 1994). The flightless condition of penguins and some alcids (i.e., Mancallinae and *Pinguinus*) reflects specialization for wing-propelled diving in the form of a functional ‘trade-off’ between aerial and sub-aqueous flight (Storer, 1960; Bengston, 1984; Livezey, 1988). This extreme specialization for wing-propelled diving results in characteristics that are shared not only among flightless pan-alcids, but also with penguins. It was the outward resemblance of Spheniscidae to the familiar Great Auk *Pinguinus impennis* of the northern Atlantic Ocean that prompted sailors who first encountered Spheniscidae in the southern hemisphere to call them penguins (Olson and Lund, 2007). Osteological characteristics shared between flightless alcids and penguins include decrease in range of motion and shortening of the distal wing elements in comparison with volant alcids (Raikow et al., 1988; Fig. 3.16), distal elongation of metacarpal one (Fig. 3.17), arced or curved wing elements (Fig. 3.2), an increase in the size of the tricipital crests of the distal humerus (Fig. 3.2), and a deeply grooved ventral margin of the ventral tubercle (Fig. 3.2). Mancallinae share additional convergent characteristics with Spheniscidae such as dorsoventral expansion of the omal extremity of the furcula, and deeply incised lateral sternal notches (Fig. 3.10). Although the functional significance of these modifications is not precisely known, the demands of wing-propelled pursuit diving for fish involving powered up-strokes and down-strokes likely played a role in the evolution of the convergent morphological characteristics shared by flightless pan-alcids and penguins.

One characteristic that is unique to Mancallinae among all known flightless birds

is the shorter length of the ulna compared with that of the carpometacarpus (180:1). In most birds these proportions are opposite of that observed in Mancallinae, with the carpometacarpus being shorter than the ulna. Three associated Mancallinae specimens (LACM 107028; SDSNH 77966), including the holotype specimen of *Mancalla cedrosensis* (LACM 15373) display this characteristic. Statistical analysis of osteological proportions of flightless alcids quantified the dorsoventral compression of wing elements and shortening of distal wing elements, but surprisingly, Livezey (1988) did not mention the unique relationship between the lengths of the ulna and carpometacarpus. A survey of the proportions of distal wing elements among extinct and extant birds was conducted to assess the distribution of this character state. The only other birds that are known to share this characteristic are several species of hummingbirds (e.g., *Phaethornis pretrei*; see Mayr, 2004, Table 1). The precise functional significance of having a longer carpometacarpus than ulna would require detailed functional morphological study, but given the extreme pectoral specialization of both Mancallinae and Trochilidae, and the need of both of these taxa to produce thrust on both up-strokes and down-strokes, it seems reasonable to postulate that the increased dependence on thrust generated from primary feathers attached to the carpometacarpus (Chai, 1997) may play a role in this osteological modification. Interestingly, this characteristic is not known in any extinct or extant penguin (J. Clarke, personal communication).

The relatively large size of *Pinguinus* and some Mancallinae (e.g., *Miomancalla howardi*) as compared to other alcids (Livezey, 1988) may be linked with flightlessness, because the decreased buoyancy of greater body mass confers an advantage to



piscivorous predators (Sparks and Soper, 1987). Additionally, because these diving birds likely spent the majority of their time in the water (i.e., flightless, and came ashore only to breed), the thermal constraints imposed on them are decreased by large body size (Furness and Burger, 1988). Estimates of body mass in Mancallinae (excluding *Miomancalla howardi*) range from 1 kg in the smallest species (i.e., *Mancalla californiensis*) to 4kg in larger species (i.e., *Mancalla lucasi*; Livezey 1988). Although smaller than the 5kg mass estimated for *Pinguinus*, the estimated body mass of Mancallinae is greater than volant extant alcids (Livezey, 1988). *Miomancalla howardi* is the largest known Mancallinae, and given the increased shortening and dorsoventral compression of wing elements of Mancallinae as compared to *Pinguinus*, it may have approached the mass of *Pinguinus*. Several Pliocene species of *Alca* are known to have exceeded the size of extant *Alca torda* (Olson and Rasmussen, 2001; Smith and Clarke, in press), and estimates based on fossils from Belgium indicate that at least one Pliocene Atlantic species, *Alca stewarti* Martin et al., 2001 was approaching the wing-loading threshold for flapping-flight (Martin et al., 2001; Dyke and Walker, 2005). This apparent trend towards increased size in two separate pan-alcid lineages, known from separate ocean basins during the Miocene and Pliocene is in stark contrast to the smaller body size of most extant alcids. The largest extant alcids are the Murres (*Uria aalge* and *Uria lomvia*), with an average body mass of 800-1000g, but the most speciose clade of extant alcids, the auklets *Aethia* and *Ptychoramphus*, are among the smallest of extant alcids with a body mass of 85-297g (del Hoyo et al., 1996). Additionally, the Mancallinae lineage and the *Alca* + *Pinguinus* lineage are considered the dominant seabirds in their

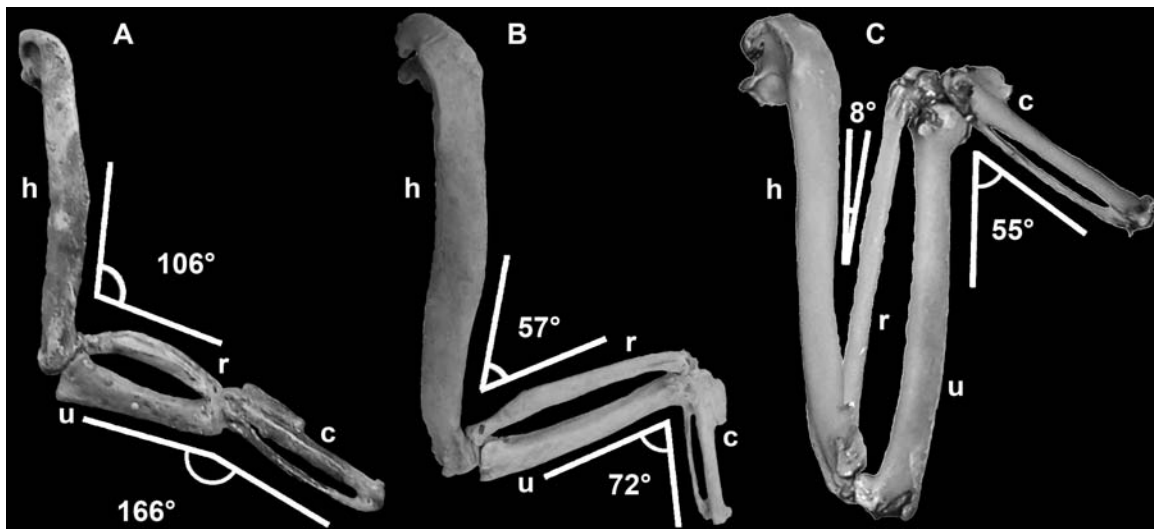


Figure 3.16- Wing elements of flightless and flighted alcids depicting decreased range of motion and shortening of distal wing elements (not to scale; degree of flexion estimated based on manual articulation of specimens). **A.** *Mancalla* (composite LACM 154560); **B.** *Pinguinus impennis* (composite USNM 346387); **C.** *Alca torda* (NCSM 20502). Anatomical abbreviations: (c) carpometacarpus; (h) humerus; (r) radius; (u) ulna.

respective oceans during the Pliocene (Olson, 1985; Olson and Rasmussen, 2001; Smith and Clarke, in press). This temporal disparity in size suggests that the conditions that led to radiations of large alcids in the Pacific and Atlantic Oceans are no longer in place, and that small to moderate size may have played a role in differential survival of pan-alcid species since the Pliocene. However, the largest known pan-alcid, the Great Auk *Pinguinus impennis*, was not driven to extinction by competition from smaller species or lack of ability to adapt to a changing environment, but rather was exterminated through human exploitation (Bengston, 1984; Fuller, 1999).

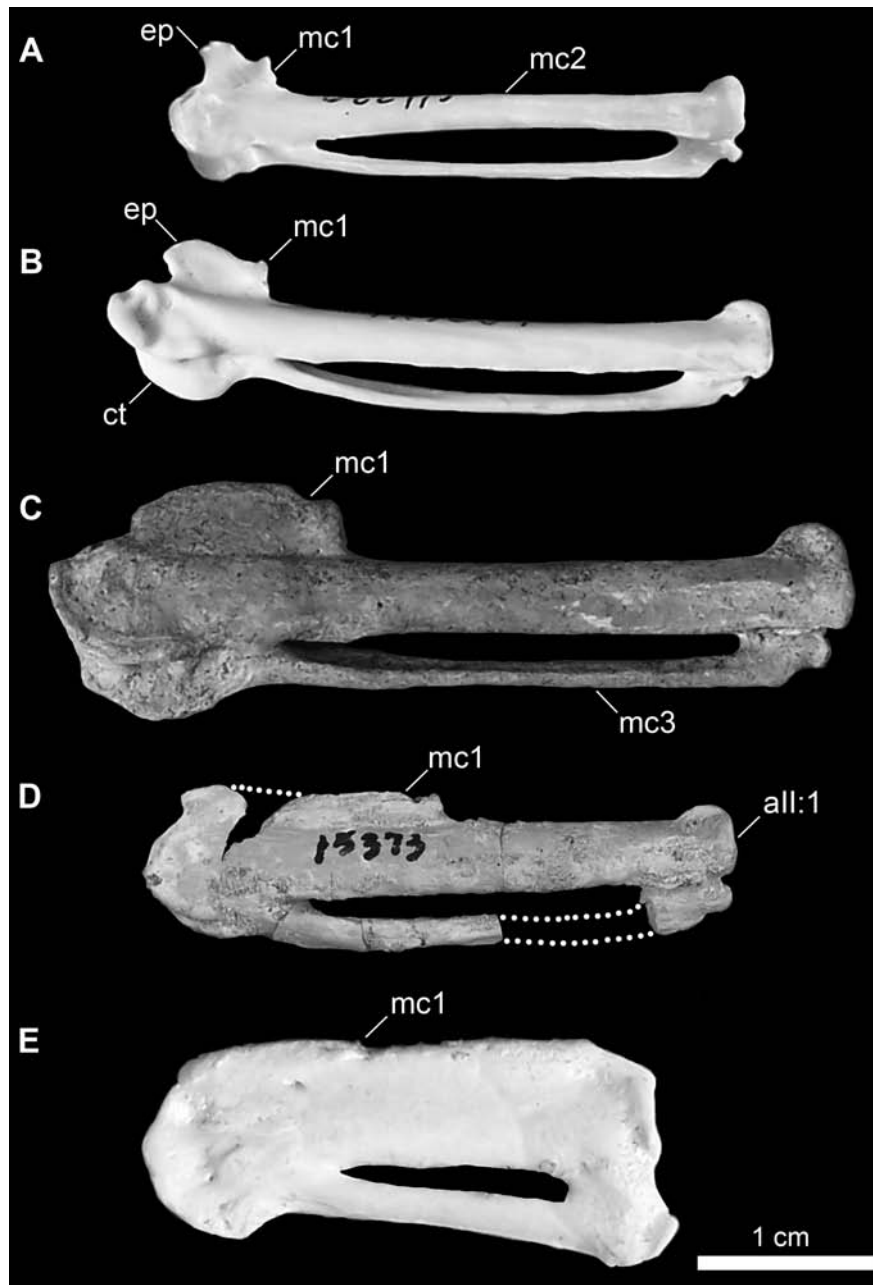


Figure 3.17- Comparison of charadriiform and sphenisciform carpometacarpal: **A.** *Anous minutus* (USNM 622415); **B.** *Cerorhinca monocerata* (USNM 620641); **C.** *Pinguinus impennis* (USNM 623465); **D.** *Mancalla cedrosensis* (LACM 15373); **E.** *Eudyptula minor* (TMM M-931). Anatomical abbreviations: (**all:1**) articulation of digit II phalanx 1; (**ct**) carpal trochlea; (**ep**) extensor process; (**mc1**) first metacarpal; (**mc2**) second metacarpal; (**mc3**) third metacarpal.

Body mass in living alcids has been correlated with dive depth and feeding ecology (Piat and Nettleship, 1985; Prince and Harris, 1988; Watanuki and Burger, 1999), and larger body size in extant alcids is associated with piscivory (Bradstreet and Brown, 1985). Foraging ranges, dive depths, and prey selection are similar in extant alcids and penguins (Prince and Harris, 1988). Little is known about the feeding strategies of *Pinguinus* (Olson, 1977), and there is no direct evidence of feeding strategies in Mancallinae; however, the large size of many Mancallinae and morphological comparisons with extant piscivorous alcids suggest that Mancallinae were specialized for piscivory. The terete bill of *Mancalla* (e.g., LACM 103940) may be additional evidence of piscivory, because this characteristic in alcids has been linked with that feeding strategy (Bédard, 1969).

***Geological and phylogenetic context for Pan-Alcidae:*** The oldest pan-alcid fossil (GCVP 5690) is from Late Eocene deposits of the Hardie Mine, Gordon, Georgia, USA (Chandler and Parmley, 2002). Likely because of the incompleteness of the specimen, phylogenetic results (not shown) place it at the base of Alcinae in an unresolved polytomy with other Alcinae clades. However, this placement is based upon a single shared character (equal width of the tricipital sulci; 151:1) and the possibility that characteristics shared with Alcinae are plesiomorphic for Alcidae cannot be ruled out. Accordingly, this fossil is considered Pan-Alcidae *incertae sedis*, rather than Alcinae *incertae sedis*. The presence of pan-alcids in Late Eocene (Chandler and Parmley, 2002) is congruent with divergence estimates placing the origin of Alcidae in the Paleocene (Baker et al., 2007; Pereira and Baker, 2008). Although, as pointed out by Wijnker and

Olson (2009) and Mayr (2011) those divergence estimates suffer from serious flaws, mainly with respect to the taxonomic status and ages assigned to fossils used as calibrations.

The taxonomic status of all but one earlier (i.e., Mesozoic, Paleocene, and Early-Middle Eocene) fossil referred to Charadriiformes (Olson and Paris, 1987; Harrison and Walker, 1977) consists of unassociated, undiagnosable fragments (Hope, 2002; Mayr, 2005, 2009). The earliest known definitive charadriiform fossil is a humerus that is tentatively referred to the Charadrii (Hou and Ericson, 2002). Although no radiometric-based date is known for this fossil, the age of *Jiliniornis huadianensis* Hou and Ericson, 2002 (IVPP V.8323) is estimated at ~40 Ma (i.e., Middle Eocene) based on biostratigraphic correlation (Hou and Ericson, 2002). A minimum age of divergence between Alcidae and other charadriiforms in the Eocene suggests that the Charadriiform fossil record is quite incomplete (i.e., extensive ghost lineages inferred based upon the fossil record).

The fossil record of Mancallinae ranges in age from Middle Miocene through Pleistocene (i.e., Turtonian-Calabrian; Becker, 1987). The oldest record of Mancallinae may be the holotype specimen of *Miomancalla wetmorei* (LACM 42653) from the Middle-Late Miocene Monterey Formation exposed in Laguna Niguel, California. However, the precise stratigraphic position of the holotype locality is unknown. Deposition of the Monterey Fm. spans ~10 Ma from 17.9-7.4 Ma (i.e., Turtonian; DePaolo and Finger, 1991). The holotype specimen is from the upper part of the formation (Domning and Deméré 1984), and would therefore be ~12-7.4 Ma..

*Miomancalla howardi* is known from the Late Miocene San Mateo Formation, which ranges in age from 8.7-4.9 Ma (Zanclean-Messinian; Deméré and Berta, 2005).

*Miomancalla* is replaced in Pliocene sediments by *Mancalla*, with four species known from the Capistrano, San Diego, San Mateo, Niguel, Almejas, and Purisima Formations. The San Mateo Fm. records the highest diversity of Mancallinae, with *Miomancalla howardi* found in the lower unit, and *Mancalla cedrosensis*, *Mancalla lucasi*, and *Mancalla vegrandis* from the upper unit. The Capistrano Fm., which may be correlative with the San Mateo Fm. (Deméré and Berta, 2005), has produced remains of *Miomancalla howardi* from the lower unit and *Mancalla californiensis* from the upper unit. The most geographically widespread and chronologically long-lived species (~5.0 Ma-470 ka) is *Mancalla lucasi*, known from the Pliocene San Mateo, San Diego, and Niguel formations, and also from the Pleistocene Hookton Formation (Howard, 1970; Kohl, 1974; Domning and Deméré, 1984).

Just as the upwelling of cold water is linked to bioproductivity and is depended on by extant seabird communities (Hyrenbach and Viet, 2003; Briggs et al., 1987), the Miocene appearance of *Miocepphus* in the Atlantic Ocean and *Miomancalla* in the Pacific Ocean coincides with the formation of permanent Arctic icecaps and shallowing of the Central American Seaway (CAS) that resulted in steeper latitudinal thermal gradients. This resulted in intensified gyral circulation of surface waters, and strengthened coastal and trade winds that promote upwelling (Ford and Golonka, 2003). The Early Pliocene (~5-3.5 Ma) was a time of relative climate stability and high sea level that coincides with the appearance of speciose alcid lineages in the Atlantic and Pacific

Oceans (Warheit, 1992b). High Mancallinae diversity in the Pacific Ocean, and high *Alca* diversity in the Atlantic Ocean (Smith and Clarke, in press) coincides with documented cooling during the Late Miocene and Early Pliocene (~14-3.6 Ma), and establishment of the California current system in the Pacific (Zachos et al., 2008; Lariviere et al., 2009). Although the geology of eastern Pacific marine units is more complex than that of coeval geologic formations from the passive Atlantic margin, sea-level fluctuation records indicate that the same Early Pliocene cycles of transgression and regression are recorded on western Atlantic and eastern Pacific coasts (Haq et al., 1988). The Middle Pliocene (~3.5-3.0 Ma) was characterized by continued global cooling, continued shallowing of the CAS, and the beginning of Northern Hemisphere glaciation cycles which led to increased cold-water upwelling in the Pacific Ocean (Bartoli et al., 2005; Lawrence et al., 2006). The emergence of the Panamanian Isthmus and the final closure of the CAS at ~2.7 Ma resulted in increased Northern Hemisphere glaciation, which is associated with a severe drop in sea-level (~45m) and the establishment of the modern profile of the California ocean-current system on which Pacific alcids rely today (Hyrenbach and Viet, 2003; Bartoli et al., 2005). The microfaunal record documents a southward shift in Atlantic and Pacific cold-adapted foraminiferal faunal regimes (Bartoli et al., 2005), and separation of Pacific and Caribbean coccolith assemblages at 2.74 Ma in response to final closure of the Isthmus, and an increase in thermohaline circulation as a result of separation of Atlantic and Pacific. By ~2.5Ma the modern climate regime was in place, involving small (i.e., meter scale) fluctuations in sea level associated with Late Pliocene and Pleistocene glacial cycles (Bartoli et al., 2005). The apparent response of seabirds to

those climate-related changes in the environment was a significant decrease in diversity (Warheit, 1992b; Olson and Rasmussen, 2001), because only a single species of *Alca* survives today in the Atlantic, and only a single specimen of *Mancalla* is known from the Pleistocene (Howard, 1970; Kohl, 1974; Smith and Clarke, in press). Confirmation of causal links between these climatic shifts and decreased seabird diversity will require more intense sampling of Late Pliocene and Pleistocene seabird fossils and evaluation of other proposed factors such as competition for nesting grounds with pinnipeds (Warheit and Lindberg, 1988) or competition for food with cetaceans (Dolphin and McSweeney, 1982).

Known diversity of extinct Atlantic pan-alcids now approaches that of extinct Pacific pan-alcids (~16-19 species ranging from Miocene-Pleistocene age; Smith and Clarke, in press). The differential extinction of Atlantic pan-alcids, compared with that of Pacific lineages, may be linked to climatic changes that effected the Atlantic and Pacific Ocean faunas in different ways. The Pacific Ocean origin hypothesis of pan-alcids is based primarily on higher extant diversity in the Pacific Ocean; however, higher extant diversity in the Pacific is not evidence of origination area, and the two oldest known pan-alcid fossils are both from Atlantic deposits (Wetmore, 1940; Chandler and Parmley, 2002; Wijnker and Olson, 2009). Although the lack of older fossils from the Pacific may simply reflect the vagaries of the fossil record, hypotheses concerning Pacific ancestral origination of pan-alcids based upon proposed greater extant Pacific species diversity should accordingly be re-evaluated. However, the basal position of Mancallinae and their restriction to the Pacific basin may be viewed as support for the Pacific origin hypothesis



for Pan-Alcidae (Storer, 1952; Kozlova, 1957; Olson, 1985; Konyukhov, 2002; Pereira and Baker, 2008; Smith, 2011).

Regardless of the ancestral area of the clade (i.e., Atlantic or Pacific), hypotheses regarding the spread of alcids from one ocean basin to another include dispersal through ice-free northern passage along the Bering Strait and Arctic Ocean, and southern dispersal through the CAS across the submerged Isthmus of Panama (Olson, 1985; Konyukhov, 2002; Pereira and Baker, 2008). These hypotheses are based upon the assumption of dispersal across water, and the first occurrence datum (FAD) for pan-alcid clades, which until the discovery of an auk from the Eocene of Georgia, USA (Chandler and Parmley, 2002), included Miocene examples of Mancallinae (Howard, 1976), *Cepphus* (Howard, 1982), and *Uria* (Howard, 1981) from Pacific Ocean basin deposits, and *Miocepphus* (Wetmore, 1940) and *Alca* (Wijnker and Olson, 2009) from Atlantic Ocean basin deposits. The ornithological literature is replete with records of occurrences of alcids hundreds or even thousands of miles from their normal ranges (see Konyukhov, 2002 for examples), and records of alcid ‘wrecks’, sometimes composed of thousands of individuals, that were blown many kilometers inland from the sea by storms (Fisher and Lockley, 1954; Stuart, 2002). Given the expanse of geologic time being considered (Eocene-Recent), the possibility that such events may have led to the dispersal of populations from one ocean basin to another ocean basin must be considered.

As suggested by Bédard (1985), the presence alcids in the Eocene (Chandler and Parmley, 2002) confirms that the cold adapted lifestyle of some alcids (e.g., *Uria*) evolved from ancestors that were tolerant of warmer (i.e., Eocene) sea temperatures. The

development of basically modern ocean circulation patterns was not achieved until ~24-20 Ma when opening of Drake Passage initiated dramatic cooling of Antarctica and formation of a strong Antarctic current that resulted in a switch from high productivity in equatorial regions, to more northern coastal regions (Lear et al., 2000; Ford and Golonka, 2003; Liu et al., 2009). Although the southern location of the earliest pan-alcid fossil locality (Georgia, USA) cannot necessarily be interpreted as support for a southern route of dispersal, warm-adapted pan-alcids in the Eocene likely were not restricted to a northern dispersal route.

## CONCLUSIONS

Rigorous taxonomic evaluation of pan-alcid fossil material resulted in a more refined picture of diversity within Mancallinae, and facilitated phylogenetic analysis of species-level relationships within the clade. The combined analysis and total evidence approach adopted herein resulted in a well-resolved and strongly supported hypothesis of the position of Mancallinae with respect to other Charadriiformes, and the inter-relationships of Mancallinae species. The phylogenetic position of Mancallinae as the sister taxon to all other Pan-Alcidae (i.e., crown clade Alcidae) suggests extensive ghost lineages in Pan-Alcidae, provides further evidence that the charadriiform fossil record is quite incomplete, and demonstrates that flightlessness evolved separately in at least two lineages of pan-alcids. The stem-lineage position of Mancallinae recovered in this

analysis is consistent with previous phylogenetic placement of this clade (Chandler, 1990a), but contrasts with previous hypotheses of close relationship between Mancallinae and Alcinae (Olson, 1985). Although extremely derived morphologically as a result of modifications related to flightlessness, Mancallinae do possess a unique suite of characters, some of which are otherwise found exclusively in Alcinae or Fraterculinae, and some of which are otherwise known only from non-alcid charadriiforms. Although it would not affect the number of inferred origins of flightlessness in Alcidae, the placement of Mancallinae at the base of Alcinae, or at the base of Fraterculinae, would only require an additional 2 steps of tree length (manually calculated in MacClade; Maddison and Maddison, 2005), and thus the position of Mancallinae recovered here may be sensitive to the inclusion of additional fossil taxa with morphologies representing ancestral states for Pan-Alcidae. The basal position of Mancallinae in Pan-Alcidae creates an ambiguous optimization at the base of the clade with respect to flightlessness. The hypothesized split between the lineages leading to Mancallinae and crown clade Alcidae raises questions about the evolution of flightlessness in charadriiforms, and the biological factors that may have lead to the split between Alcidae and their proposed sister taxon, Stercorariidae.

*Miomancalla howardi* is placed as the sister taxon of *Miomancalla wetmorei*, and is the largest known species of Mancallinae. The large size and resemblance of the bill of *Miomancalla howardi* to that of the Great Auk *Pinguinus impennis* provides another example of within-lineage convergence between two flightless clades separated by time and geography. The independent acquisition of morphological characteristics in both

lineages of flightless pan-alcids (i.e., Mancallinae and *Pinguinus*), and the similarity of these modifications to those of penguins, strongly suggests correlation between these morphologies and mode of locomotion. The study of convergence within Alcidae may provide insights about the evolution of flightlessness in penguins, in which there are no known volant species (Clarke et al., 2007).

Similarly diverse lineages of pan-alcids inhabited the eastern Pacific and western Atlantic coasts of North America during the Miocene and Pliocene. Approximately coeval Early Pliocene deposits in California and North Carolina record the replacement of *Miocepphus* by *Alca* in the Pliocene of the Atlantic, and the replacement of *Miomancalla* by *Mancalla* in the Pliocene of the Pacific. Global-scale environmental perturbations such as increased cooling following the MMCO, may have contributed to similar scenarios involving species turnover in Pan-Alcidae in both ocean basins.

## CHAPTER 4.

The fossil record and phylogeny of the puffins

(Pan-Alcidae, Fraterculini)

## INTRODUCTION

Among Charadriiformes (shorebirds and allies), members of the clade Alcidae such as auks, murres, and puffins are characterized by their pelagic ecology and pursuit of prey through wing-propelled diving. Puffins (Fratculini) are a clade including *Fratercula* and *Cerorhinca*, and are distinguished from other alcids by the brightly colored keratinous plates that cover their beaks during the breeding season and are subsequently molted (del Hoyo et al., 1996). These colorful rostral ornamentations and the gregarious nature of colonially nesting puffins have made them popular with ecotourists, and today puffins are the most widely recognized extant alcids. Extant puffins are monogamous and often return to the same nests each year (del Hoyo et al., 1996). Puffins excavate nesting cavities (i.e., burrows) where they incubate a single egg (del Hoyo et al., 1996). Extant puffins feed primarily on small fish, but also prey on crustaceans and cephalopods (del Hoyo et al., 1996). Extant diversity of puffins consists of three species native to the Pacific Ocean (Horned Puffin *Fratercula corniculata*, Tufted Puffin *Fratercula cirrhata*, and Rhinoceros Puffin *Cerorhinca monocerata*), and a single species endemic to the Atlantic Ocean (Atlantic Puffin *Fratercula arctica*).

The common English name Rhinoceros Auklet, which is currently applied to *Cerorhinca monocerata* by the American Ornithologists' Union (AOU; 1998) is a misnomer. Frequently encountered references to other common names applied to *Cerorhinca monocerata* including Rhinoceros Puffin, Horn-billed Puffin, and Unicorn Puffin (Coues, 1868; Storer, 1945a; Thoresen, 1985; De Santo and Nelson, 1995; del

Hoyo et al., 1996) are all more accurate characterizations of this taxon. *Cerorhinca monocerata* has been consistently recovered as the sister taxon to *Fratercula* in phylogenetic analyses of morphological (Strauch, 1985; Chandler, 1990a; Smith, 2011), and molecular sequence data (Friesen et al., 1996; Baker et al., 2007; Pereira and Baker, 2008). *Cerorhinca monocerata* was presumably allied with the auklets based upon its size, which is smaller than other Pacific endemic puffins. Size alone is not an appropriate criterion for classification, and furthermore, the size of *Cerorhinca monocerata* is larger than that of *Fratercula arctica* from the Atlantic Ocean (del Hoyo et al., 1996). A recent proposal to change the English name of *Cerorhinca monocerata* was rejected primarily on the basis of maintaining nomenclatural stability (AOU, 2008). *Cerorhinca monocerata* is not an auklet and emendation of the common name of this species to reflect its affinities with other puffins should be reconsidered by the AOU. To avoid confusion regarding the affinities of this taxon, only the scientific name *Cerorhinca monocerata* is used to refer to this species of puffin hereafter.

A Fraterculini (i.e., puffins) clade consisting of *Cerorhinca* and *Fratercula* has been supported in analyses of morphological (Strauch, 1985; Chandler 1990a; Smith, 2011) and molecular sequence data (Watada et al., 1987; Moum et al., 1994; Friesen et al., 1996; Thomas et al., 2004; Baker et al., 2007; Pereira and Baker, 2008). The morphology-based compatibility analysis of Strauch (1985) placed Fraterculini as the sister-group to all other alcids, whereas all subsequent phylogenetic analyses have recovered Fraterculini as the sister taxon to Aethiini (i.e., the auklets, *Aethia* and *Ptychoramphus*).

**Review of the Fraterculini fossil record:** Fossil remains of *Cerorhinca* and *Fratercula* have been reported from the western Atlantic and eastern Pacific Oceans (Table 4.1; Fig. 4.1; Olson, 1985) and are also present in Pleistocene deposits in Japan (Matsuoka and Smith, in preparation). The systematic position of fossils referred to Fraterculini has not been previously evaluated in a phylogenetic analysis. The inclusion of extinct Fraterculini in a combined phylogenetic analysis may help elucidate the poorly understood evolutionary history of this clade.

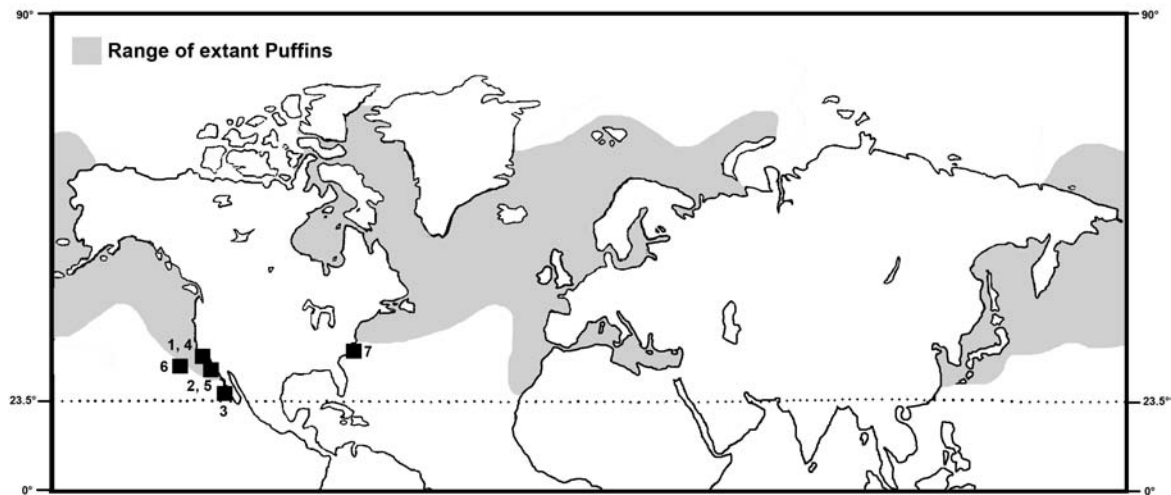


Figure 4.1- World map depicting published Fraterculini fossil localities and the extant distribution of Fraterculini (based on del Hoyo et al., 1996). **1.** Lompoc, California (Miller, 1925; **2.** Laguna Hills, California (Howard, 1968); **3.** Baja Peninsula, Mexico (Howard, 1971); **4.** Laguna Niguel, California (Howard, 1978); **5.** San Diego, California (Chandler, 1990b); **6.** Channel Islands, California (Guthrie et al., 1999); **7.** Aurora, North Carolina (Olson and Rasmussen, 2001; Smith et al., 2007).

*Cerorhinca monocerata* is the only extant representative of *Cerorhinca* and all but a single fossil record of *Cerorhinca* are from the Pacific Ocean basin (Miller, 1925; Howard, 1968; Howard, 1971; Howard, 1978; Chandler 1990b). However, *Cerorhinca*



remains were recently described from the Atlantic Ocean basin (Smith et al., 2007).

*Fratercula* remains are known from the Atlantic and Pacific Ocean basins (Guthrie et al., 1999; Olson and Rasmussen, 2001; Smith et al., 2007). With the exception of *Fratercula dowi* from the Pleistocene of California (Guthrie et al., 1999), Pleistocene and Holocene remains that presumably represent extant species (Lambrecht, 1933; Brodkorb, 1967; Hasegawa et al., 1988; Tyrberg, 1998) were not examined and are not treated further in this study. However, reexamination of Pleistocene and Holocene Fraterculini remains may provide refined estimates of species richness, and are deserving of further study.

Table 4.1- Previously published specimens referred to Fraterculini.

Taxa	Material	Provenience	Age	Reference
<i>Cerorhinca dubia</i>	associated pelvic limbs	California	Middle Miocene	Miller, 1925
<i>Cerorhinca</i> sp.	proximal ulna	California	Late Miocene	Howard, 1968
<i>Cerorhinca minor</i>	pectoral elements	Mexico	Middle Pliocene	Howard, 1971
Fraterculini indet.	humeri	California	Late Miocene	Howard, 1978
<i>Cerorhinca reai</i>	pectoral elements	California	Late Pliocene	Chandler, 1990b
<i>Cerorhinca</i> sp.	ulna	California	Late Pliocene	Chandler, 1990b
<i>Fratercula dowi</i>	partial skeleton	California	Pleistocene	Guthrie et al., 1999
<i>Fratercula</i> spp.	isolated elements	North Carolina	Early Pliocene	Olson and Rasmussen, 2001
<i>Fratercula</i> sp.	ulna	Belgium	Early Pliocene	Dyke and Walker, 2005
<i>Cerorhinca</i> sp.	humeri	North Carolina	Early Pliocene	Smith et al., 2007

*Cerorhinca* remains were reported from the Middle Miocene Monterey Formation diatomite deposits in Lompoc, California, USA by Miller (1925), who described a specimen consisting of associated pelvic limbs (UCMP 26546; Fig. 4.2). That specimen was tentatively described as a new taxon, *Cerorhinca dubia* Miller, 1925, based upon the relative proportions of the preserved elements as compared with *Cerorhinca monocerata*. *Cerorhinca dubia* could only be scored for 4 out of 353 morphological characters and is an operational equivalent of many charadriiforms including *Cerorhinca monocerata*, *Brachyramphus marmoratus*, *Mancalla cedrosensis*, and *Sterna maxima* (Appendix 3). Relative proportions are not strong evidence of affinity. The impression of the left tarsometatarsus preserves the deeply grooved anterior face of this element, a character consistent with Fraterculini but that is also present in other charadriiforms (e.g., *Sterna maxima*). The right tarsometatarsal impression appears to preserve the posterior face of this element, however, potentially phylogenetically informative characters of the hypotarsus cannot be clearly discerned. Relative lengths are the only characters that can be assessed for the tibiotarsi and femora owing to the lack of fine morphological detail preserved in the impressions of these elements. Apomorphies of charadriiform pedal phalanges that would allow referral of this specimen are not currently known. There are little data to support referral to Charadriiformes other than overall shape and relative proportions.

Late Miocene fossil remains from Laguna Hills, California, USA were referred to *Cerorhinca* by Howard in 1968. Those fragmentary remains included a proximal ulna (LACM 18274) and a humeral shaft fragment (LACM 18275). Those specimens were

referred to *Cerorhinca* based on their size and similarity to *Cerorhinca monocerata*.

In 1971 Howard described a new species of *Cerorhinca* from the Early Pliocene Almejas Formation of Cedros Island, Baja California, Mexico. The holotype specimen of *Cerorhinca minor* Howard 1971 is a proximal humerus (LACM 15408; Fig. 4.3) and was diagnosed relative to *Cerorhinca monocerata* based largely upon its smaller size and older age.

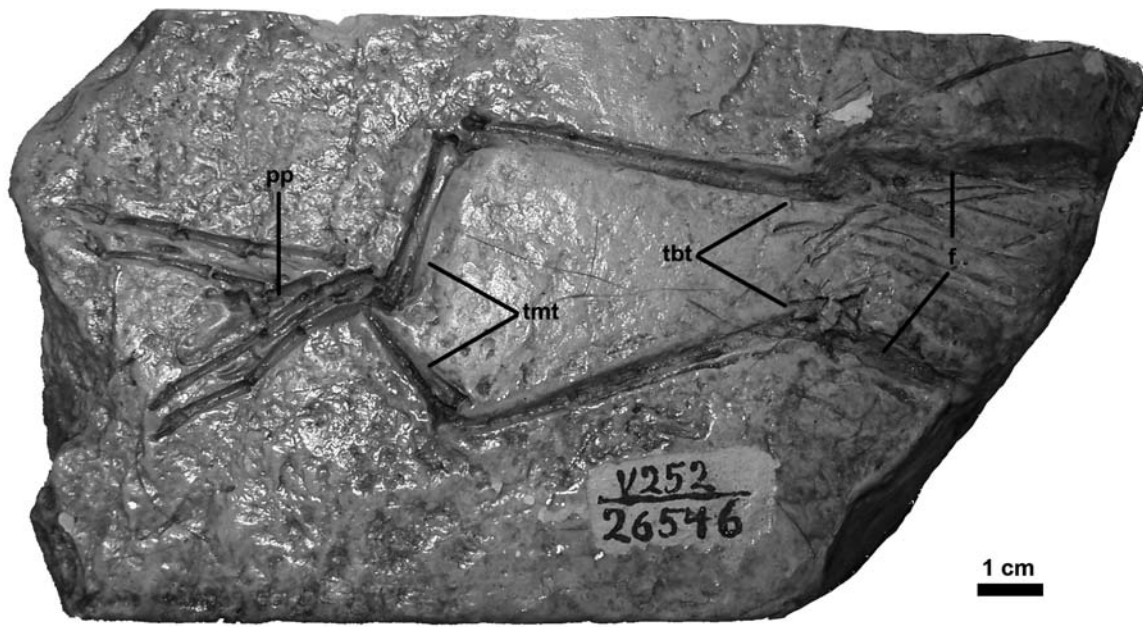


Figure 4.2- Holotype specimen of *Cerorhinca dubia* Miller 1925 (UCMP 26546). Anatomical abbreviations: (**f**) femora; (**pp**) pedal phalanges; (**tbt**) tibiotarsi; (**tmt**) tarsometatarsi.

In 1978 Howard referred two specimens consisting of a proximal humerus (LACM 42658) and a distal humerus (LACM 37638) from the Late Miocene Monterey Formation at Laguna Niguel, California, USA to Fraterculini. The location of those specimens is currently unknown (S. McLeod, personal communication). An empty

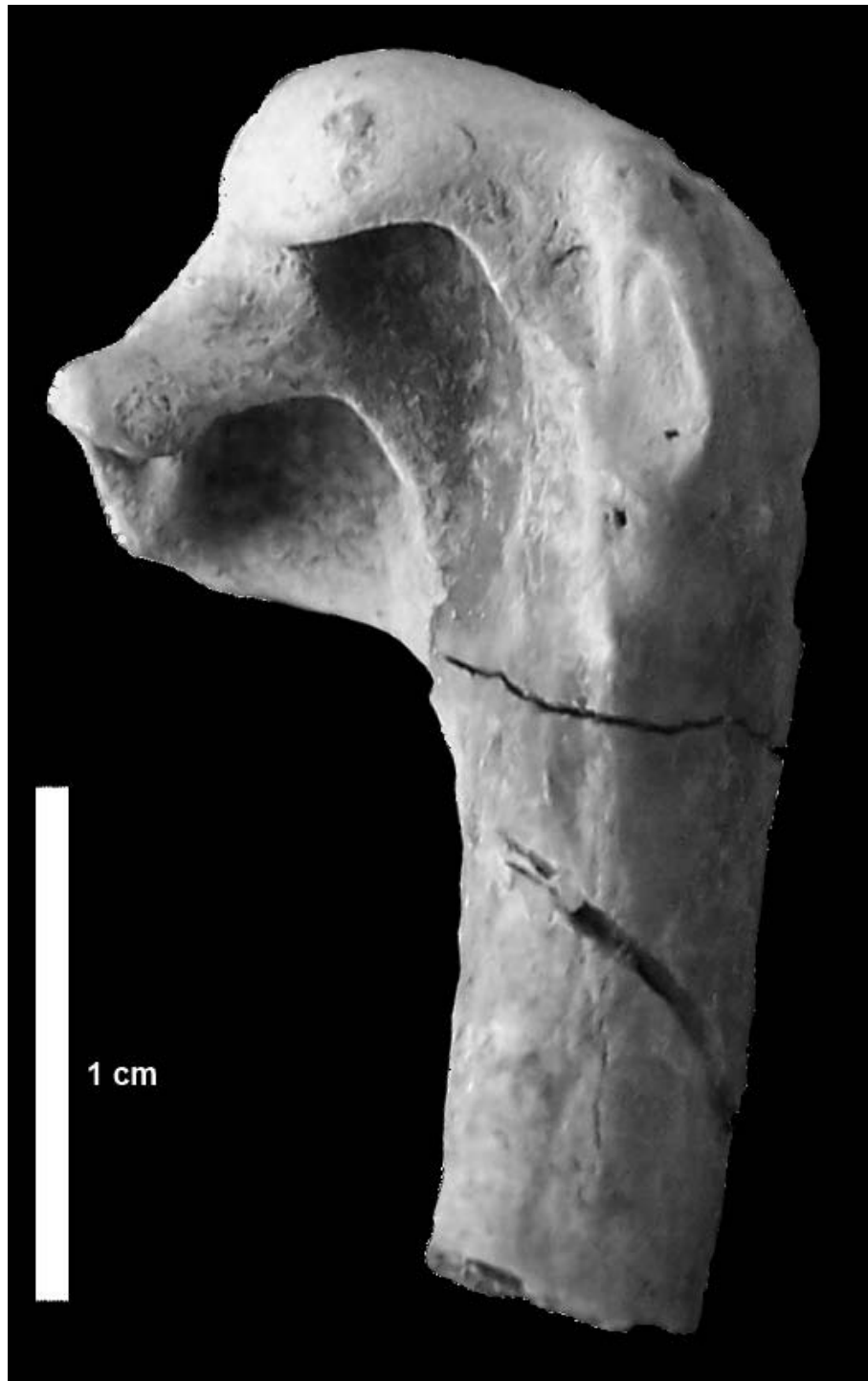


Figure 4.3- Holotype proximal right humerus of *Cerorhinca minor* Howard 1971 (LACM 15408) in posterior view.

specimen box with a temporary loan tag labeled ‘Hildegard Howard study cabinet’ was found during a thorough search of the LACM collections in 2007. Those specimens were not figured by Howard (1978). The short description provided by Howard (1978) did not allow for characters to be scored for the phylogenetic analysis. Therefore, the referral of those specimens to Fraterculini could not be verified and they are not treated further herein.

A new species of *Cerorhinca* was described from the Pliocene San Diego Formation of San Diego, California, USA by Chandler (1990b). The holotype specimen of *Cerorhinca reai* Chandler 1990 (SDSNH 25319) is a left humerus (Fig. 4.4). Additional elements referred to this species including a distal humerus (SDSNH 24572), an ulna (SDSNH 25175), a carpometacarpus (SDSNH 24925), and a premaxilla (LACM 117775) were referred to this taxon by Chandler (1990b) were not found in association with the holotype specimen. No associated specimens are known that would allow for referral of additional skeletal elements to *Cerorhinca reai*. Therefore, only the holotype specimen was scored for the phylogenetic analysis.

A right ulna (SDSNH 23079) was referred to *Cerorhinca* sp. by Chandler (1990b) and was differentiated from *Cerorhinca reai* by its smaller size and by the more pronounced posterior protrusion of the olecranon. However, no diagnostic characters for *Cerorhinca* ulnae were provided and ulnae of *Cerorhinca reai*, and *Cerorhinca minor* are not known. Therefore, referral of SDSNH 23079 to *Cerorhinca* remains uncertain.

A new species of puffin was described from the Pleistocene eolianite deposits of the Channel Islands, California, USA by Guthrie et al. (1999). The holotype specimen of

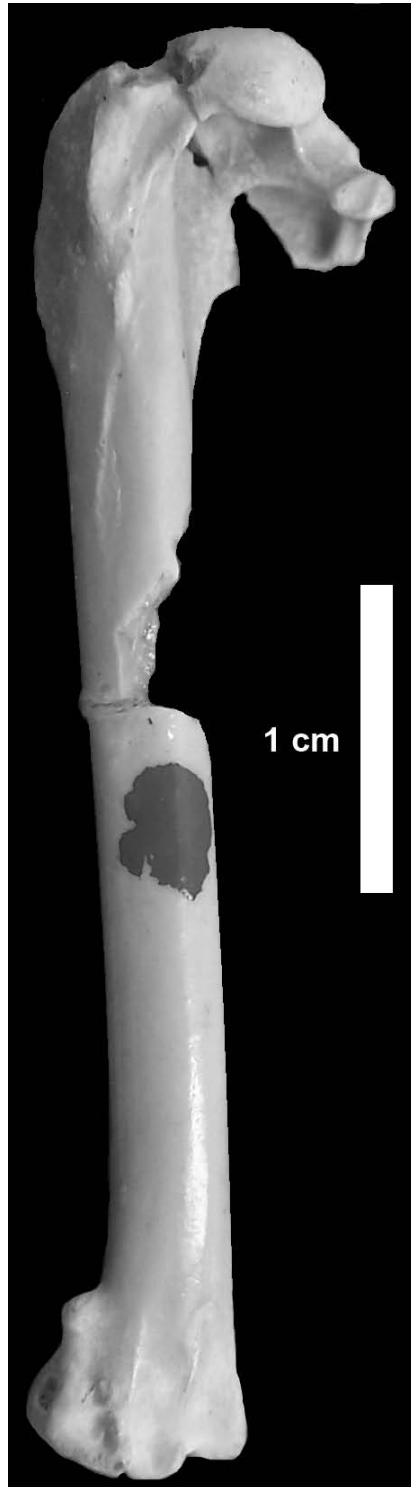


Figure 4.4- Holotype left humerus of *Cerorhinca reai* Chandler, 1990 (SDSNH 25319) in posterior view.

*Fratercula dowi* Guthrie et al., 1999 (LACM 127813; Fig. 4.5) consists of an associated partial skeleton including pectoral and pelvic limbs, sternum, vertebrae, and partial maxilla and mandible. This specimen represents the first verifiable record of *Fratercula* from the Pacific Ocean basin. Additionally, fossilized eggs (e.g., LACM 127814; Fig. 4.6) that were recovered from burrows associated with *Fratercula dowi* remains indicate that the Channel Islands were a breeding locality for this species (extant puffins also nest in burrows), and allowed oological characters to be scored for this extinct taxon (App. 3).

An ulna (NHMUK PV A 9034; previously numbered as BMNH A 9034; Fig. 4.7) from the Early Pliocene Kattendijk Sands Formation of Kallo, Belgium was referred to *Fratercula* by Dyke and Walker (2005). Although the size of that specimen was compared with extant species of *Fratercula*, no diagnostic characters were provided to support referral to *Fratercula*.

Among Pliocene material recovered from the PCS Phosphate Mine (formerly known as the Lee Creek Mine) in Aurora, North Carolina (Fig. 4.8), Olson and Rasmussen (2001) recognized remains that are indistinguishable from the two extant species *Fratercula arctica* and *Fratercula cirrhata*. Recent re-examination of the material assigned to *Fratercula* aff. *cirrhata* indicated that this material was a composite series of two distinct taxa (Smith et al., 2007). One complete and two proximal humeri are instead referable to *Cerorhinca*, thus, providing the first record of *Cerorhinca* from the Atlantic Ocean basin (Figs. 4.9 & 4.10; Smith et al., 2007). The remainder of the material was reconfirmed as *Fratercula* aff. *cirrhata* on the basis of morphological characteristics.



Figure 4.5- Holotype specimen of *Fratercula dowi* (LACM 127813).





Figure 4.6- Fossilized egg of *Fratercula dowi* (LACM 127814).



Figure 4.7- Left ulna (NHMUK PV A 9034) referred to *Fratercula* by Dyke and Walker (2005) in ventral view.

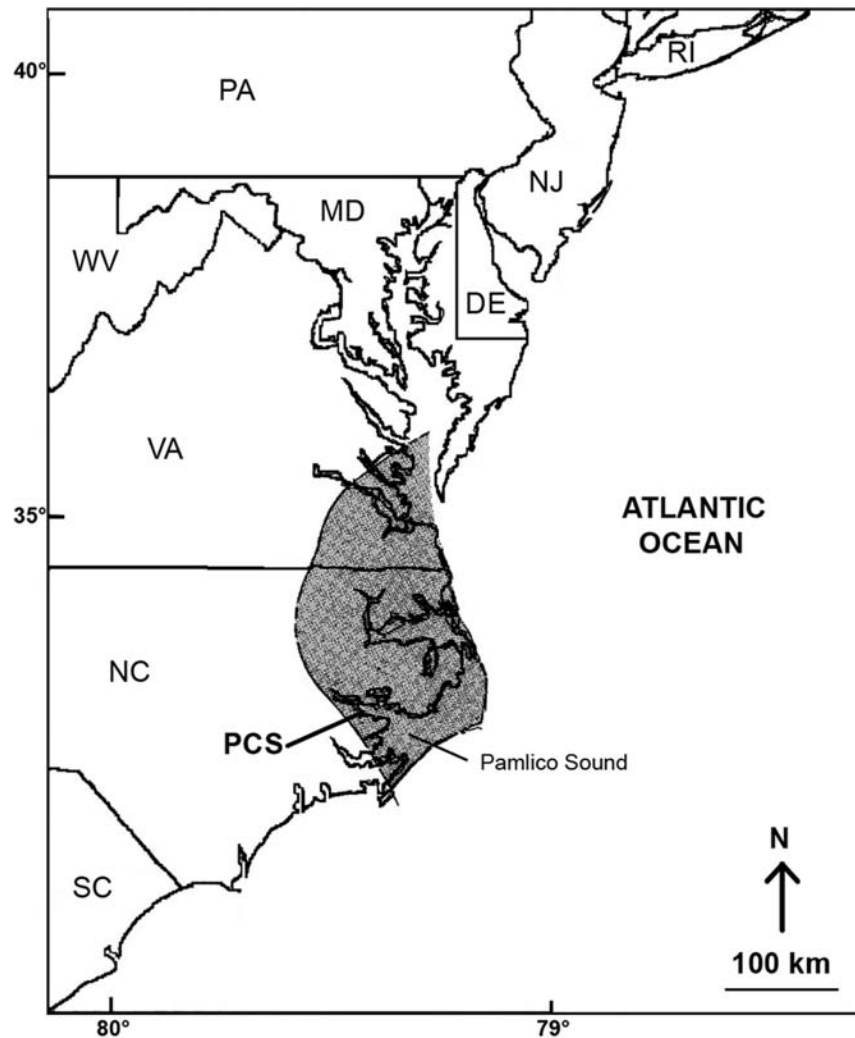


Figure 4.8- Map of the eastern USA indicating the locality of PCS Phosphate mine in Aurora, North Carolina where the first Atlantic Ocean basin *Cerorhinca* specimens were collected. Shaded area denotes the subsurface extent of Unit 1 of the Yorktown Formation (map altered from Gibson, 1983).

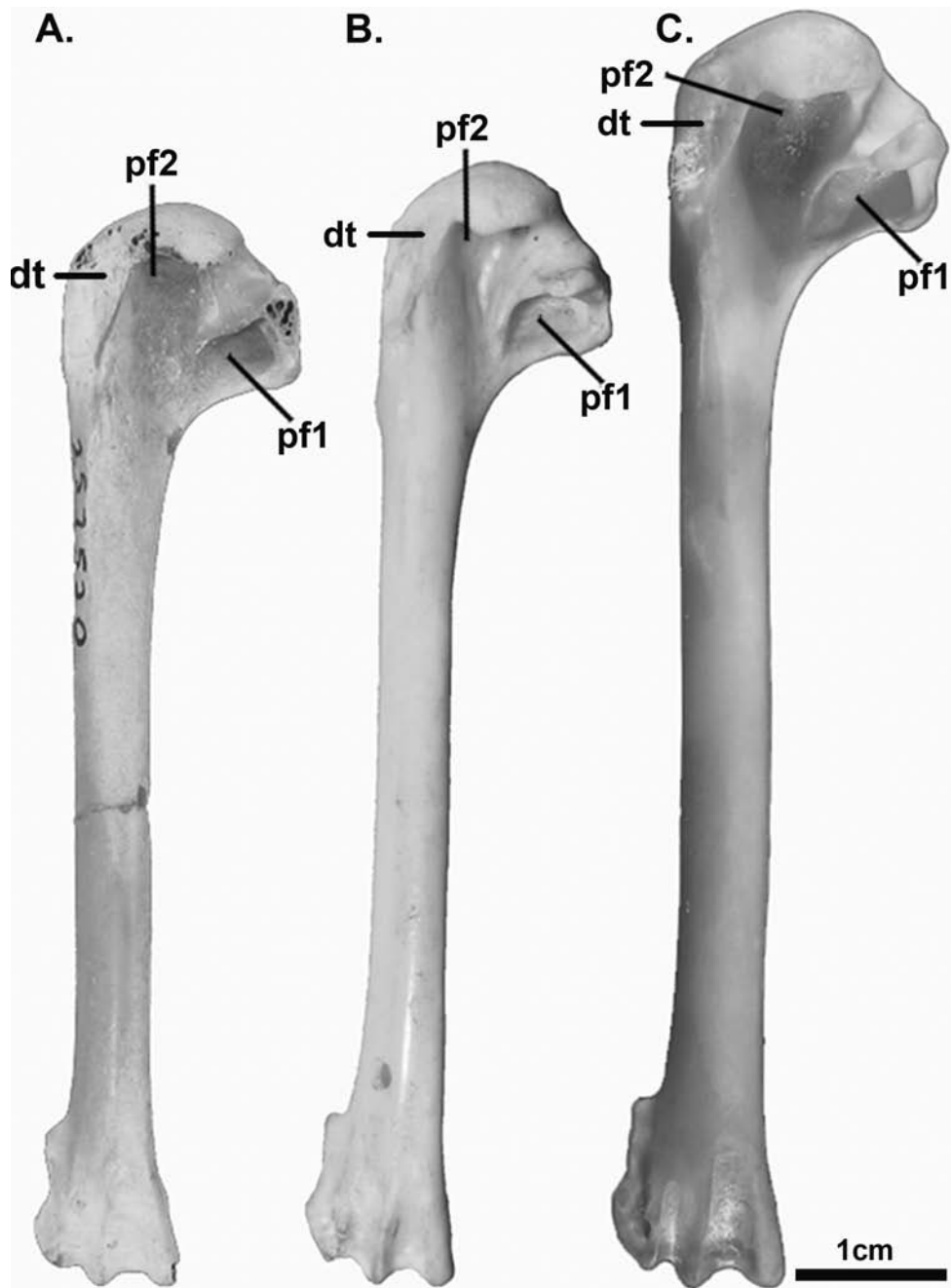


Figure 4.9- Comparison of three Fraterculini left humeri (posterior view). **A.** *Cerorhinca* sp. (USNM 257520); **B.** *Cerorhinca monocerata* (USNM 620643); **C.** *Fratercula cirrhata* (USNM 459395). Anatomical abbreviations: (**hs**) humerotricipital sulcus; (**pf1**) primary pneumotricipital fossa; (**pf2**) secondary pneumotricipital fossa; (**s**) shaft with flattened space ventral to dorsal tubercle.

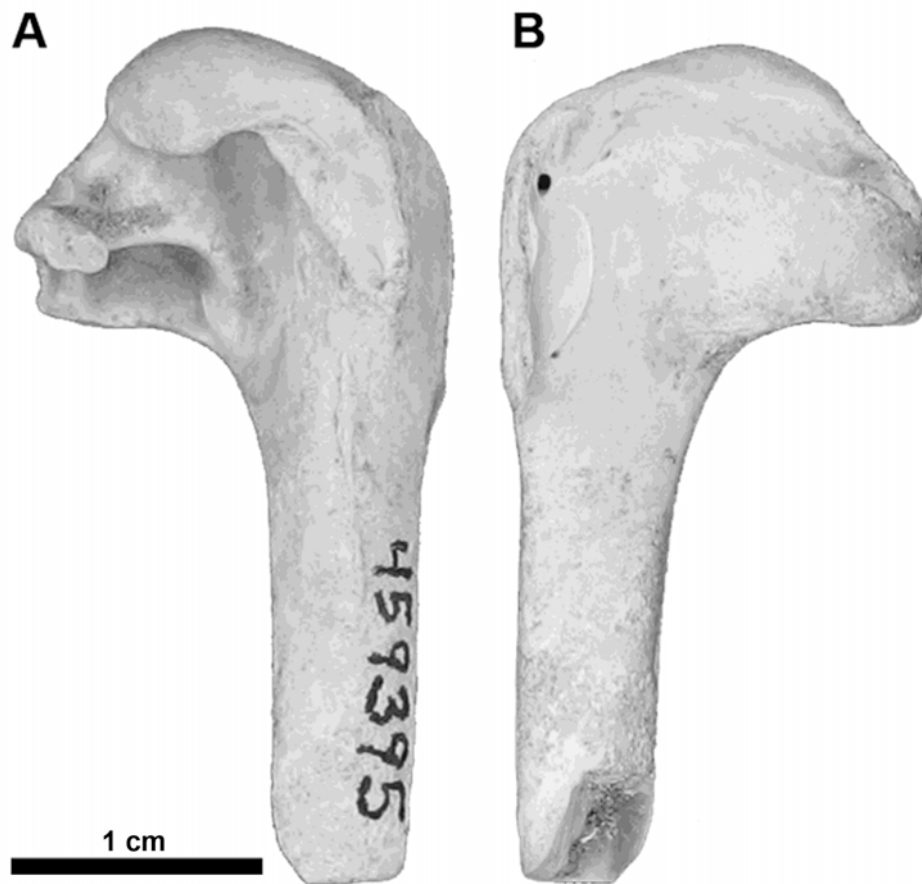


Figure 4.10- Proximal ends of *Cerorhinca* sp. right humeri in **A.** posterior view (USNM 459395); **B.** anterior view (USNM 193051).

Previously described puffin remains, extant species of puffins, other species of extant alcids, and charadriiform outgroup taxa are evaluated through phylogenetic analyses to assess the systematic positions of these taxa and referred remains. Taxonomic revisions are provided based on the results of the phylogenetic analyses. Implications for the evolution of Fraterculini are discussed in the context of revised estimates of Fraterculini species richness and the results of the phylogenetic analyses.

## MATERIALS AND METHODS

Anatomical descriptions primarily use the English equivalents of the Latin osteological nomenclature summarized by Baumel and Witmer (1993). The terminology of Howard (1929) is followed for features not treated by Baumel and Witmer (1993). With the exception of the terms anterior and posterior substituted for cranial and caudal, respectively, the terms used for the anatomical orientation of a bird are those used by Clark (1993). Measurements follow those of von den Driesch (1976). All measurements were taken using digital calipers and rounded to the nearest 0.1 millimeter. With the exception of species binomials, all taxonomic designations (e.g., Fraterculini) are clade names and are not intended to convey rank under the Linnaean system of nomenclature, regardless of use of italics or previous usage by other authors.

Morphological characters were scored for all 23 extant alcids, the recently extinct Great Auk *Pinguinus impennis*, five extinct Fraterculini taxa (*Cerorhinca dubia* Miller, 1925, *Cerorhinca minor* Howard, 1971, *Cerorhinca reai* Chandler, 1990, *Fratercula dowi* Guthrie et al., 1999, *Cerorhinca* sp. Smith et al., 2007), and four additional specimens previously referred to Fraterculini (LACM 18274, LACM 18275, SDSNH 23079, NHMUK PV A 9034). Specimens referred to *Fratercula* aff. *arctica* and *Fratercula* aff. *cirrhata* by Olson and Rasmussen (2001) are operational equivalents of the extant species *Fratercula arctica* and *Fratercula cirrhata* respectively (Appendix 3), and were not included as separate terminals in the phylogenetic analyses. A gull (*Larus marinus*) and a skua (*Stercorarius skua*) were included as charadriiform outgroup taxa.

See Appendix 2 for morphological character descriptions and Appendix 3 for morphological character scorings used in the phylogenetic analysis.

Morphological characters include osteological ( $n = 232$ ), integumentary ( $n = 32$ ), reproductive ( $n = 11$ ), dietary ( $n = 2$ ), myological ( $n = 24$ ) and micro-feather ( $n = 52$ ). One hundred and sixty-four characters were developed for this analysis. The other 189 characters were drawn from the work of Hudson et al. (1969;  $n = 24$ ), Strauch (1978, 1985;  $n = 39$ ), Chandler (1990a;  $n = 63$ ), Chu (1998;  $n = 11$ ), and Dove (2000;  $n = 34$ ). Only 34 of the 38 characters used by Dove (2000) varied in the taxa examined in this study. Of the 34 used in this analysis, eighteen were modified (i.e., split into 2 separate characters) according to the philosophy of character independence proposed by Hawkins et al. (1997), resulting in a total of 52 microfeather characters.

Whenever possible, five or more specimens of each extant species including both sexes were evaluated to account for intraspecific character variation and potential sexual dimorphism respectively (Appendix 1). Only adult specimens, assessed based upon degree of ossification (Chapman, 1965), were evaluated, and whenever possible specimens from multiple locations within the geographic range of extant species (i.e., sub-species) were examined to account for geographic variation. Characters for all extinct taxa were coded from direct observation of holotype and referred specimens.

Previously published molecular sequence data (mitochondrial: ND2, ND5, ND6, CO1, CYTB; ribosomal RNA: 12S, 16S; and nuclear: RAG1) were downloaded from GenBank (<http://www.ncbi.nlm.nih.gov/genbank>; see Appendix 4 for sequence authorship). Preliminary sequence alignments were obtained using ClustalX v2.0.6

(Thompson et al., 1997), and then adjusted manually using Se-AI v2.0A11 (Rambaut, 2002). Alignment and concatenation of sequence data resulted in a final molecular matrix of 11601 base pairs. Molecular sequence data were combined with morphological characters for a matrix of 11,954 characters.

Parsimony tree search criteria implemented in PAUP\* v4.0b10 (Swofford, 2002) are as follows: heuristic search strategy; 10,000 random taxon addition sequences; tree bisection-reconnection branch swapping; random starting trees; all characters equally weighted; minimum length branches = 0 collapsed; multistate (e.g., 0&1) scorings used only for polymorphism. Bootstrap values and descriptive tree statistics (e.g., CI, RI, RC) were calculated using PAUP\* v4.0b10 (Swofford, 2002). Bootstrap value calculation parameters included 1,000 heuristic replicates, 100 random addition sequences per replicate. All other settings were the same as the primary analysis. Bremer support values were calculated using a script generated in MacClade v4.08 (Maddison and Maddison, 2005) and analyzed with PAUP\* v4.0b10 (Swofford, 2002). Based on the results of previous phylogenetic analyses of charadriiform relationships that place the Laridae basal to Alcidae (Strauch, 1978; Sibley and Ahlquist, 1990; Chu, 1995; Ericson et al., 2003; Paton et al., 2003; Thomas et al., 2004; Baker et al., 2007) resultant trees were rooted with *Larus marinus*.

A Bayesian approach of phylogeny estimation was also explored, as Bayesian methods allow incorporation of complex models of nucleotide substitution not available with parsimony methods (Lewis, 2001a, 2001b; Huelsenbeck et al., 2001, 2002; Holder and Lewis, 2003; Nylander et al., 2004). Bayesian phylogenetic analyses of

morphological and molecular data were performed using the program Mr. Bayes v3.1.2 (Ronquist and Huelsenbeck, 2003). MrBayes parameters were as follows: two simultaneous independent runs with one cold and five heated chains each, starting trees random, Markov Chain Monte Carlo (MCMC) samples taken every 1000 generations, nine partitions in the combined analyses (1 morphological and 8 molecular sequence), parameters unlinked across partitions, all fully resolved topologies considered equally likely, branch lengths unconstrained (i.e., molecular clock not enforced): exponential (10.0), substitution rate flat Dirichlet (1, 1, 1, 1), state frequencies flat Dirichlet (1, 1, 1, 1), standard deviation of split frequencies < 0.01 considered evidence of convergence of MCMC chains, nodes with  $\geq 0.95$  posterior probability considered strongly supported. Log likelihoods were evaluated to determine burn-in with the software Tracer v1.4 (Rambaut and Drummond, 2009), and the resulting consensus of retained trees was plotted using FigTree v1.3.1 (Rambaut, 2009). Trees were rooted with *Larus marinus*. The combined data were run for 10 million MCMC generations and first 25% of retained trees were discarded as burn-in.

***Institutional abbreviations:*** LACM—Natural History Museum of Los Angeles County, Los Angeles, CA., USA; NHMUK PV A—The Natural History Museum, London, UK; NCSM—North Carolina Museum of Natural Sciences, Raleigh, NC, USA; SDSNH—San Diego Natural History Museum, San Diego, CA, USA; UCMP—University of California Museum of Paleontology, Berkeley, CA, USA; USNM—National Museum of Natural History, Smithsonian Institution, Washington, D.C., USA.



## PHYLOGENETIC RESULTS

A preliminary analysis including terminals for all nine extinct Fraterculini taxa and previously referred specimens of interest resulted in a tree with relationships unresolved at the base of Alcidae (results not shown). Additional analyses, which are described below, were performed to identify potential ‘wildcard taxa’ (Nixon and Wheeler, 1992; Kearney, 2002), which were removed from subsequent analyses to recover a reasonably resolved phylogenetic hypothesis that still maintained a reasonably high level of taxon sampling.

Inclusion of *Cerorhinca dubia* in a parsimony-based phylogenetic analysis with all 23 extant alcids, *Pinguinus impennis*, and two outgroup charadriiforms (*Stercorarius skua*, *Larus marinus*) resulted in 33 most parsimonious trees (MPTs; L: 7671; CI: 0.56; RI: 0.65; RC: 0.37). *Cerorhinca dubia* was placed in a polytomy at the base of a monophyletic Alcidae (Fig. 4.11). Because *Cerorhinca dubia* is an operational equivalent of multiple species, because it was not recovered as a part of Fraterculini, and because the inclusion of this taxon significantly reduced phylogenetic resolution, it was not included in subsequent analyses. *Cerorhinca dubia* is, therefore, a nomen dubium.

Because there is no evidence other than provenience to suggest that the fragmentary remains referred to *Cerorhinca* by Howard (1968) represent a single species, LACM 18274 and LACM 18275 were scored and analyzed separately. Parsimony-based phylogenetic analysis including extant species and LACM 18274 resulted in four MPTs (L: 7672; CI: 0.51; RI: 0.57; RC: 0.29). LACM 18274 was placed

in an unresolved position at the base of Alcinae (contents of Alcinae include Alcini + *Cepphus* + *Synthliboramphus* + *Brachyramphus*; Fig. 4.12). Parsimony-based phylogenetic analysis including extant species and LACM 18275 resulted in 15 MPTs (L: 7671; CI: 0.51; RI: 0.57; RC: 0.29). LACM 18275 was placed in a polytomy with other Fraterculini (Fig. 4.13). Because LACM 18274 was not recovered as a part of Fraterculini, and because the inclusion of LACM 18274 and 18275 significantly reduced phylogenetic resolution, these specimens were not included in subsequent analyses.

Inclusion of the ulna (SDSNH 23079) referred to *Cerorhinca* by Chandler (1990b) in a parsimony-based phylogenetic analysis with all 23 extant alcids, *Pinguinus impennis*, and two outgroup charadriiforms (*Stercorarius skua*, *Larus marinus*) resulted in 14 MPTs (L: 7674; CI: 0.55; RI: 0.63; RC: 0.34). SDSNH 23079 was placed in an unresolved position at the base of Alcinae (contents of Alcinae include Alcini + *Cepphus* + *Synthliboramphus* + *Brachyramphus*; Fig. 4.14). Because this specimen was not recovered as a part of Fraterculini, it was not included in subsequent analyses.

Inclusion of the ulna (NMHUK PV A 9034) referred to *Fratercula* by Dyke and Walker (2005) in a phylogenetic analysis with all 23 extant alcids, *Pinguinus impennis*, and two outgroup charadriiforms (*Stercorarius skua*, *Larus marinus*) resulted in 35 MPTs (L: 7672; CI: 0.68; RI: 0.79; RC: 0.53). NMHUK PV A 9034 was placed in a polytomy at the base of a monophyletic Alcidae (Fig. 4.15). Because NMHUK PV A 9034 was not recovered as a part of Fraterculini and because the inclusion of this specimen significantly reduced phylogenetic resolution, it was not included in subsequent analyses.

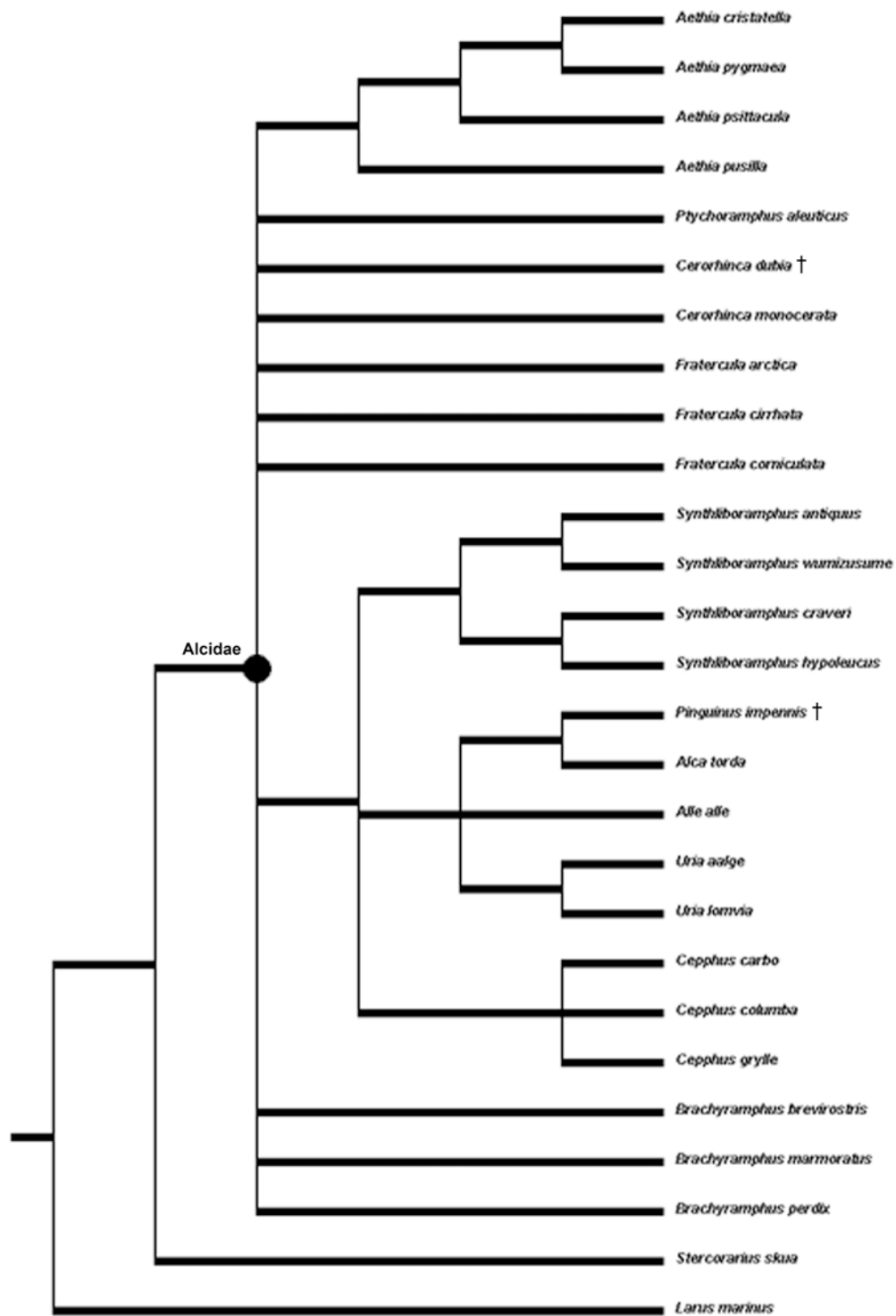


Figure 4.11- Strict consensus cladogram of 33 MPT's indicating the unresolved phylogenetic position of *Cerorhinca dubia* in Alcidae.

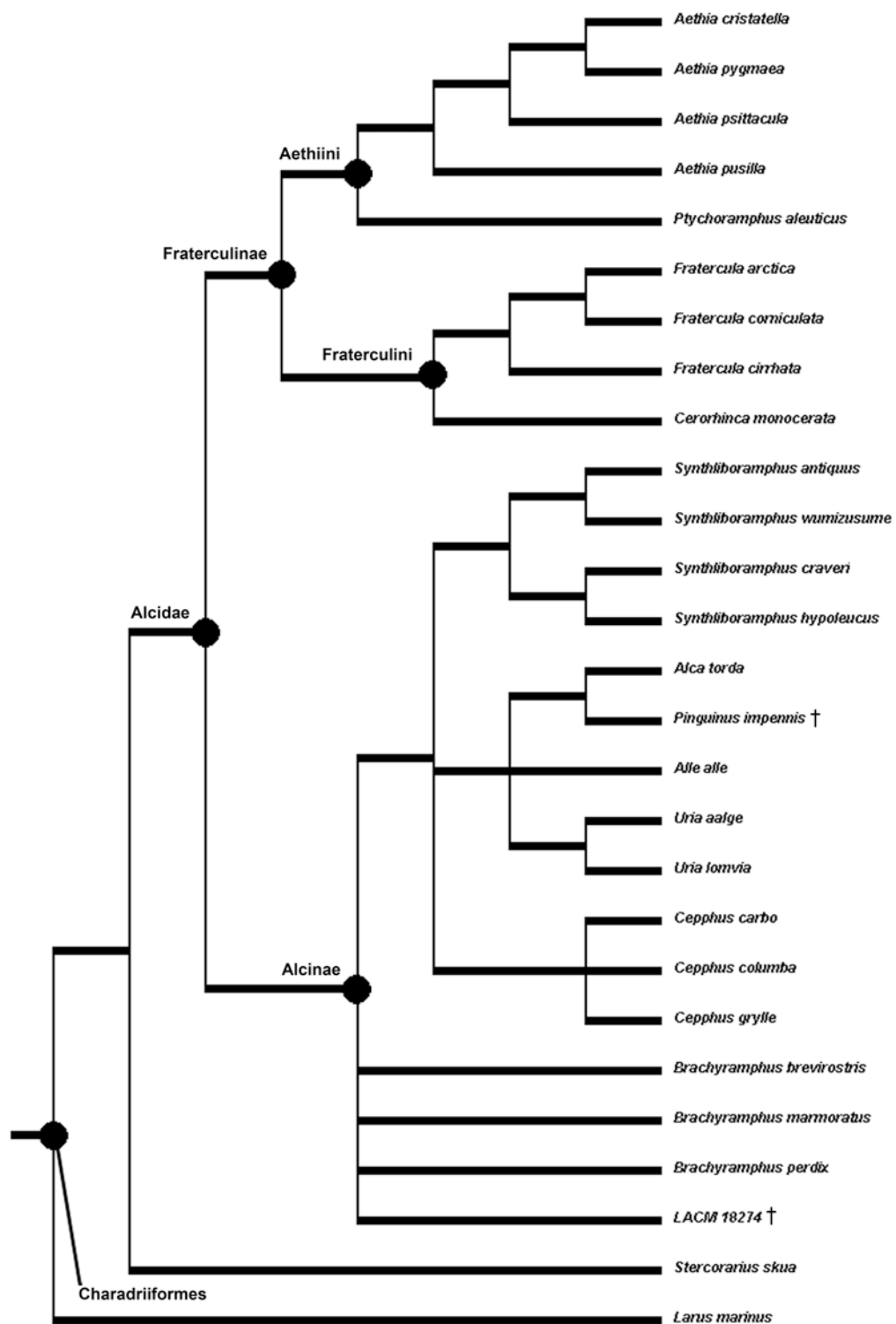


Figure 4.12- Strict consensus cladogram of four MPT's indicating the unresolved phylogenetic position of LACM 18274 in Alcinae.

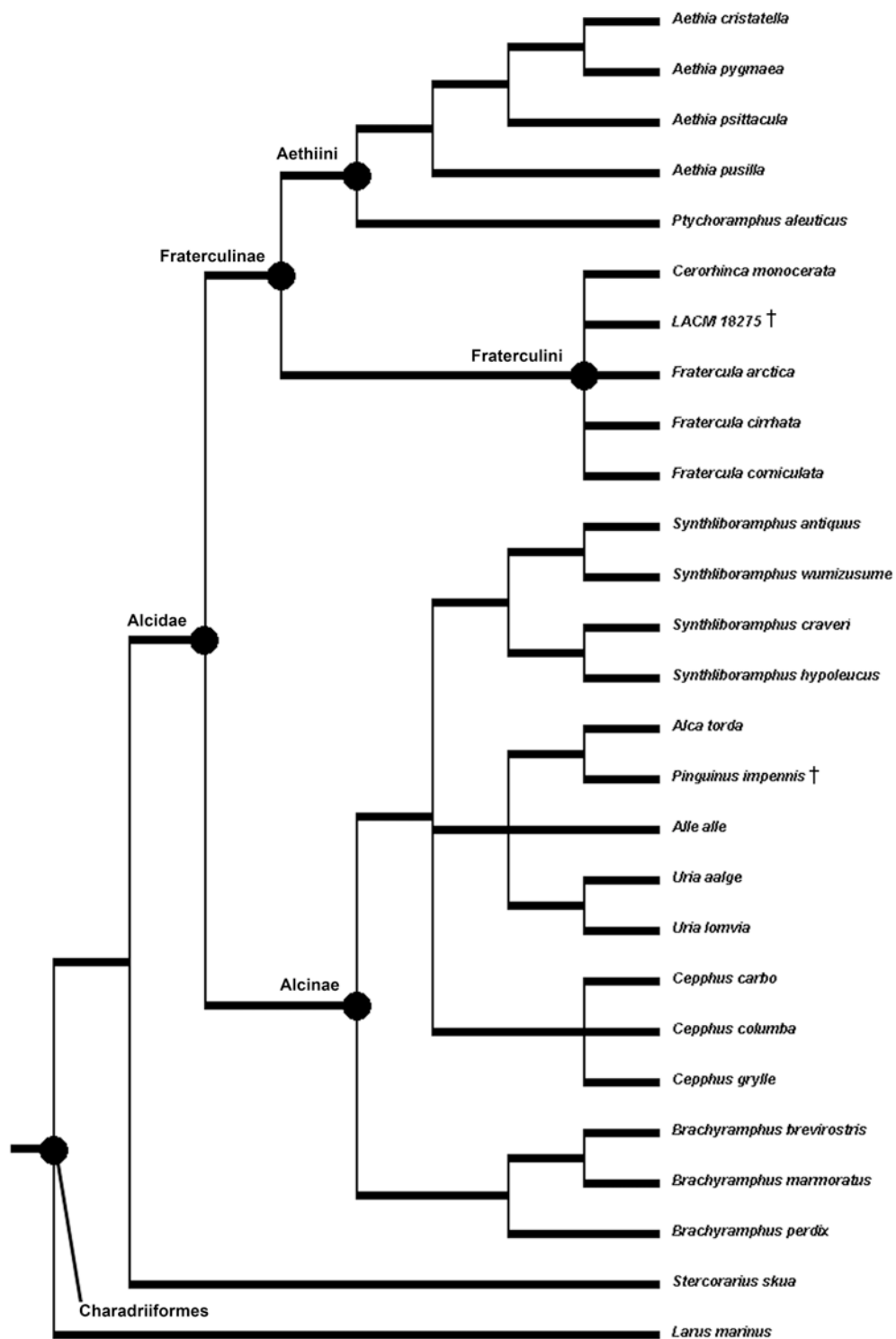


Figure 4.13- Strict consensus cladogram of 15 MPT's indicating the unresolved phylogenetic position of LACM 18275 in Fraterculini.

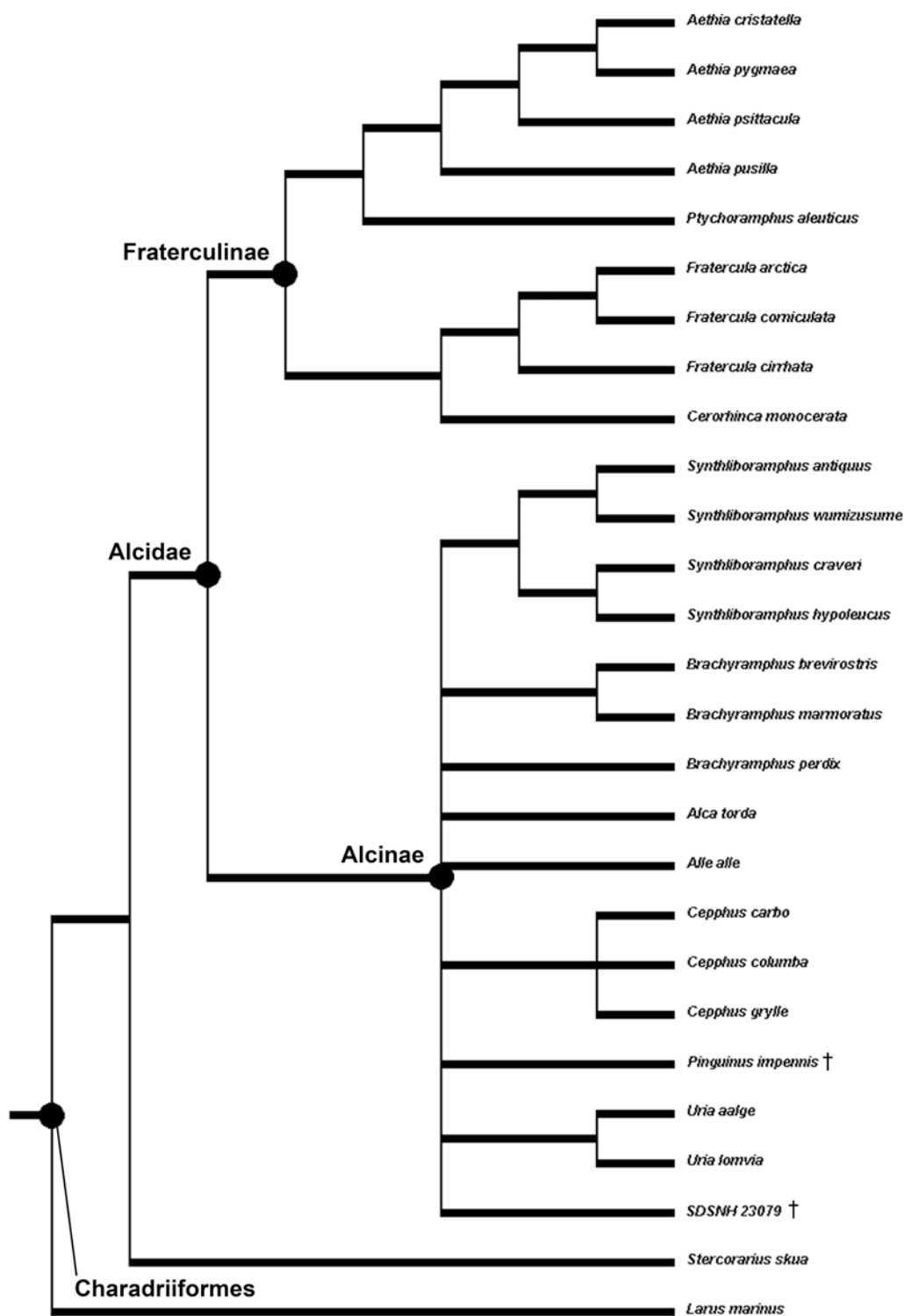


Figure 4.14- Strict consensus cladogram of 14 MPT's indicating the unresolved phylogenetic position of SDSNH 23079 in Alcinae.

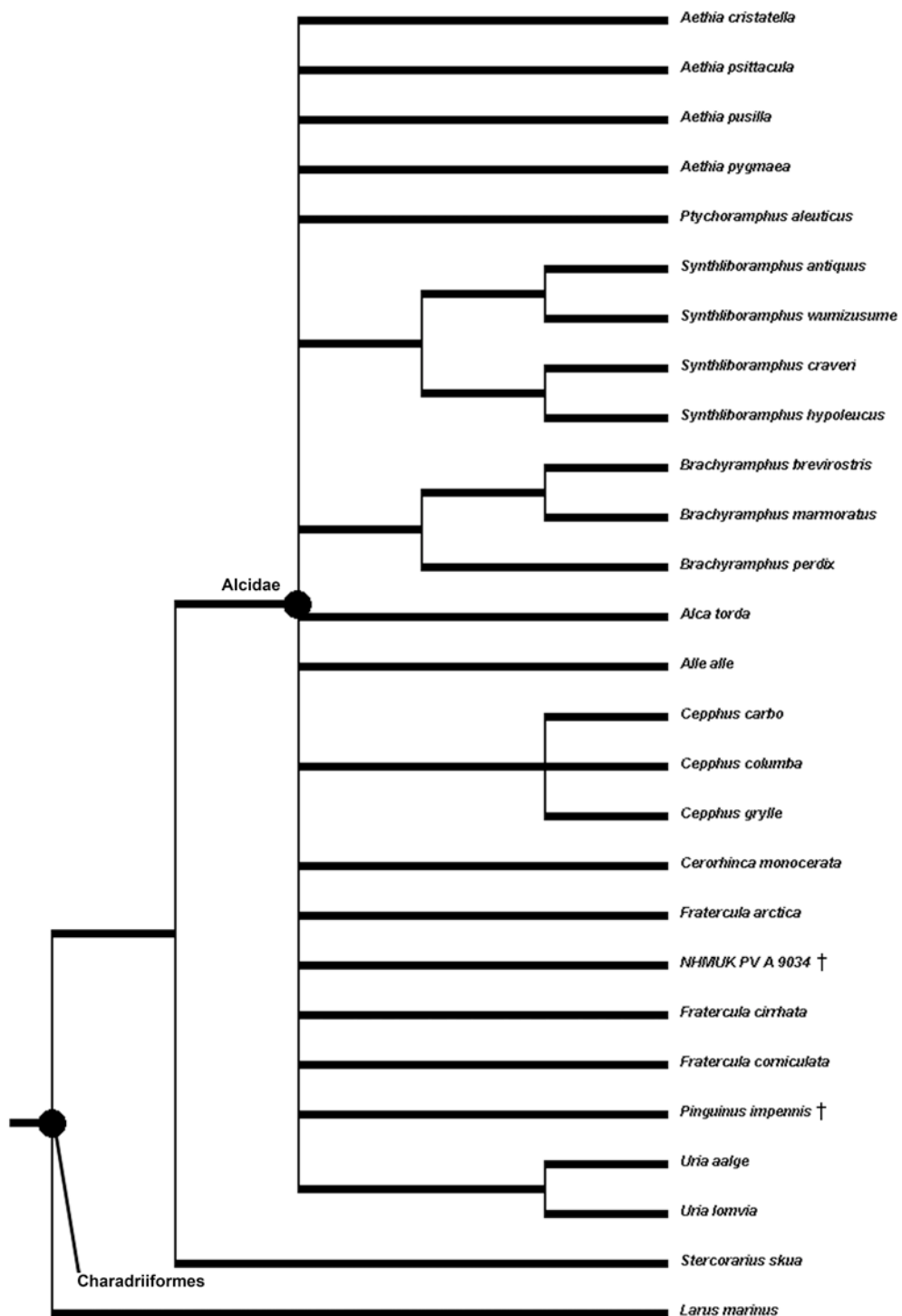


Figure 4.15- Strict consensus cladogram of 35 MPT's indicating the unresolved phylogenetic position of NHMUK PV A 9034 in Alcidae.

Subsequent to the exclusion of the taxa identified as potential wildcard taxa, the parsimony-based analysis of the combined data resulted in a single MPT (Fig. 4.16; L: 7691; CI: 0.49; RI: 0.54; RC: 0.27). Levels of bootstrap and Bremer support were highest for clades without extinct taxa included. The topology of the resultant tree is fully resolved and the monophyly of Fraterculini is supported by seven apomorphies with a CI = 1.0 (Table 4.2).

Fraterculini (i.e., puffins, *Fratercula* and *Cerorhinca*) is placed as the sister taxon to Aethiini (i.e., auklets, *Aethia* and *Ptychoramphus*). Together, Fraterculini and Aethiini form a monophyletic Fraterculinae, which is supported by two unambiguously optimized apomorphies (Table 4.2). Congruent with the results of previous analyses of alcid relationships, Fraterculinae was recovered as the sister taxon to all other extant Alcidae (i.e., Alcinae; Watada et al., 1987; Mouton et al., 1994; Friesen et al., 1996; Baker et al., 2007; Pereira and Baker, 2008; Smith 2011).

*Fratercula* monophyly is supported by a single locally optimized apomorphy with a CI < 1.0 (Table 4.2; 42:1; ventral margin of mandible ventrally expanded in lateral view). Congruent with previous phylogenetic results (Mouton et al., 1994; Friesen et al., 1996; Pereira and Baker, 2008; Smith, 2011), *Fratercula cirrhata* is recovered as the sister taxon to a clade including *Fratercula arctica* and *Fratercula corniculata*. *Fratercula dowi* is recovered as the sister taxon to all other *Fratercula* (Fig. 4.16).

*Cerorhinca* monophyly is supported by two locally optimized apomorphies (Table 4.2). The extant species *Cerorhinca monocerata* is placed as the sister taxon to *Cerorhinca* sp. Smith et al., 2007, and *Cerorhinca reai* is placed as the sister taxon to



*Cerorhinca minor* (Fig. 4.16). Based on these results, the remains referred to *Cerorhinca* sp. by Smith et al. (2007) are recognized as distinct and are named as a new species (see *Cerorhinca aurorensis* in the Systematic Paleontology section below).

The results of the Bayesian analysis (Fig. 4.17), although slightly less resolved with respect to relationships within Fraterculini, are largely congruent with the parsimony-based results. The monophyly of Fraterculinae, Fraterculini, and Aethiini are all supported with posterior probabilities of 1.0. Although *Cerorhinca* and *Fratercula* are not recovered as separate clades, the same sister taxon relationships between *Cerorhinca minor* and *Cerorhinca reai*, *Cerorhinca monocerata* and *Cerorhinca* sp. Smith et al., 2007, and *Fratercula arctica* and *Fratercula corniculata* were recovered (Fig. 4.17). Differences in the relationships among the outgroup in the Bayesian and parsimony-based topologies are limited to minor changes in position of species within clades, such as the position of *Aethia pygmaea* within *Aethia* and the position of *Alle alle* within Alcini (i.e., *Alle* as sister to *Uria* or sister to *Alca* + *Pinguinus*).

Table 4.2- Apomorphies supporting clades in the resultant parsimony-based phylogenetic tree (Fig. 4.15). Character numbers from Appendix 3 are followed by character state symbols (e.g., 23:0 = character number 23, state 0). Characters followed by ‘\*’ are locally optimized apomorphies with CI < 1.0. All other apomorphies have a CI = 1.0.

Clade	Character numbers and states that support monophyly
Fraterculinae	61:1; 73:1.
Fraterculini	30:1; 36:1; 41:1; 115:0; 284:1; 295:1; 296:1.
<i>Fratercula</i>	*42:1.
<i>Cerorhinca</i>	*117:1; *121:2.

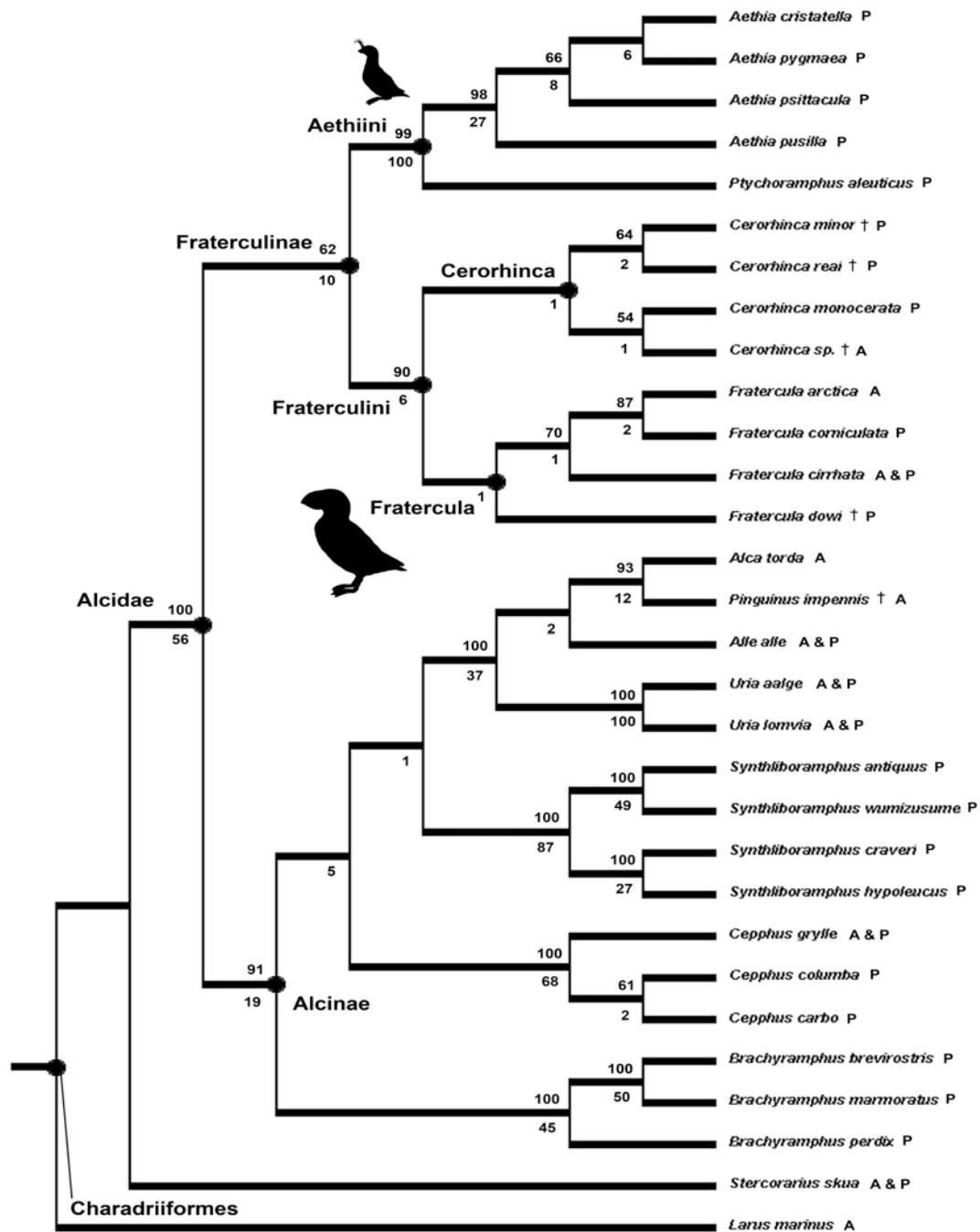


Figure 4.16- Parsimony-based topology depicting hypothesized Fraterculini relationships. Bootstrap values >50% and Bremer support values appear above and below nodes, respectively. Exclusively Atlantic Ocean endemic species are followed by an 'A' and exclusively Pacific endemic species are followed by a 'P'. Species that occur in both oceans (fossil evidence or extant distribution) are followed by 'A & P'.

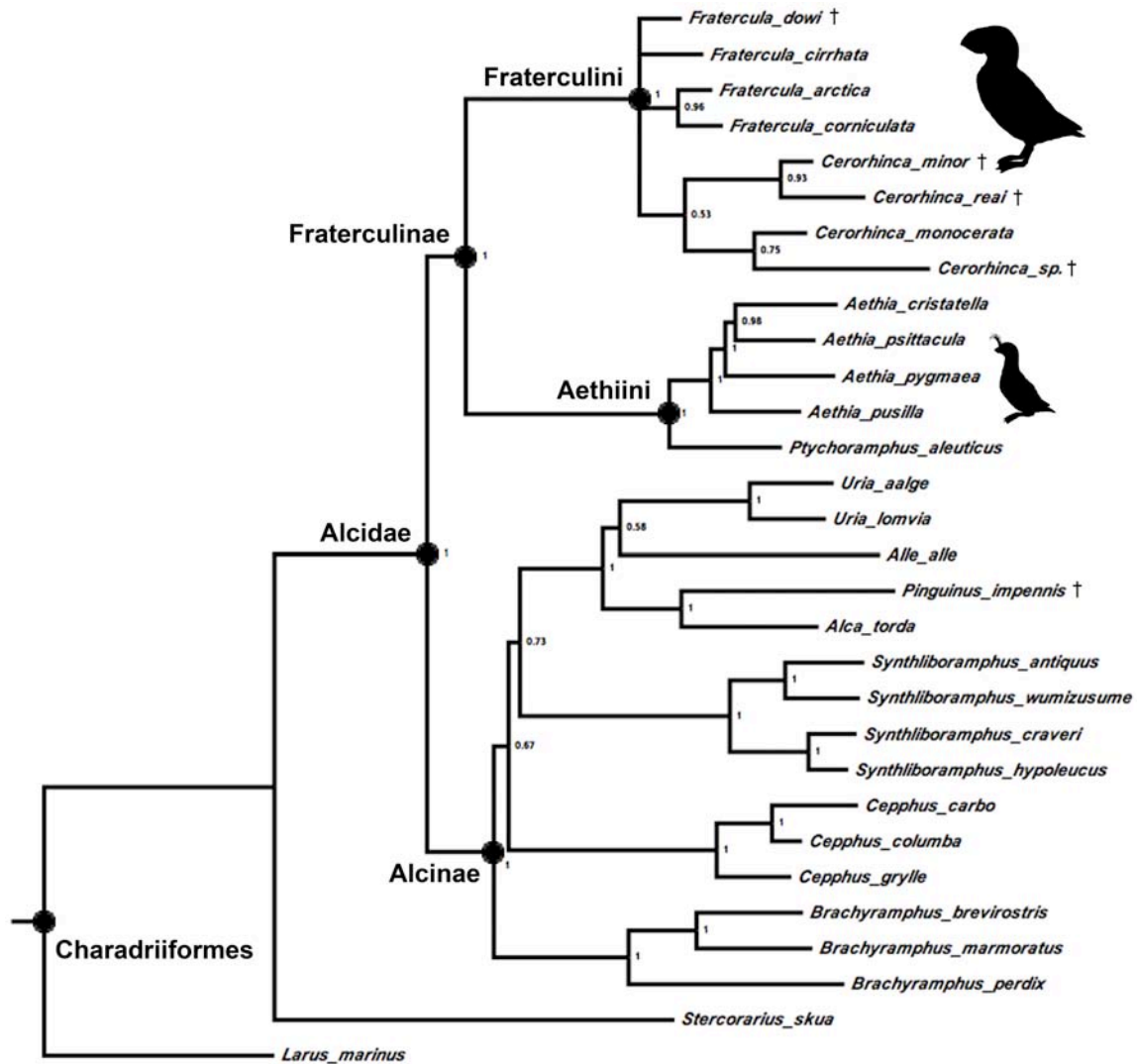


Figure 4.17- Bayesian hypothesis of Fraterculini relationships. Posterior probabilities are displayed beside recovered nodes.

## SYSTEMATIC PALEONTOLOGY

AVES Linnaeus, 1758

CHARADRIIFORMES Huxley, 1867

PAN-ALCIDAE Smith, 2011

ALCIDAE Leach, 1820

FRATERCULINAE nomen cladi novum

*Diagnosis*—The contents of Fraterculinae include Aethiini Storer, 1960 and Fraterculini Storer, 1960. The sister taxon relationship between these clades is supported by the results of the combined analysis and by the results of previous phylogenetic analyses (Watada et al., 1987; Chandler, 1990a; Moum et al., 1994; Friesen et al., 1996; Thomas et al., 2004; Baker et al., 2007; Pereira and Baker, 2008; Smith, 2011). Fraterculinae monophyly is supported by the following apomorphies: craniolateral process of sternum points anteriorly rather than dorsally as in Alcinae taxa (61:1); bladeliike extension of hypocleideum (apophysis furculae, Baumel and Witmer, 1993:163) smaller than other Alcidae (73:1).

FRATERCULINI Storer, 1960

*Diagnosis*—Fraterculini (contents include *Fratercula* and *Cerorhinca*) differ from other alcids in having a sclerotic ring that is wide and conical rather than thin and more

flattened as in other Alcidae (e.g., *Alca torda*; 30:1). Mancallinae scleral rings are not known. The cerebellar prominence protrudes posteriorly to as lesser degree than in other Alcidae (36:1). Unlike any other pan-alcid taxon, the mandibular rami of Fraterculini make contact posterior to mandibular symphysis (41:1). The m. supracoracoideus scar of the humerus is more deeply excavated than in other Pan-Alcidae (115:1), and the dorsal supracondylar (ectepicondylar) process of the humerus has a more pointed and more medially projected tip (Strauch, 1985; 147:2). The secondary (dorsal) pneumotricipital fossa of the humerus is well-excavated (130:1), a condition observed in the nearest outgroup taxa to Pan-Alcidae (e.g., Larinae, Sterninae, Stercorariidae; Strauch, 1978; Sibley and Ahlquist, 1990; Chu et al., 2009) and not present in any other pan-alcid taxa (Strauch, 1978, 1985; Chandler, 1990a, Smith, 2011). The ventral tubercle of the humerus is mediolaterally compressed (134:0), as opposed to the more robust condition seen in some other alcid taxa (e.g., *Alca*, *Cephus*). The triceps tendons not ossified (284:1; ossified in other sampled Alcidae), and an m. humerotriceps sesamoid is present (296:1; absent in other sampled Charadriiformes).

*FRATERCULA* Brisson, 1760

*Diagnosis*—*Fratercula* is differentiated from other Fraterculini (i.e., *Cerorhinca*) by a single unambiguously optimized apomorphy, the degree to which the mandibular rami are ventrally expanded (42:1). The mandibles are also ventrally expanded in *Aethia psittacula*, *Alca torda*, *Pinguinus impennis*, and *Miomancalla howardi*. An additional

locally optimized apomorphy differentiates *Fratercula* from *Cerorhinca*. The pneumotricipital fossa of *Cerorhinca* and *Fratercula* is divided into two separate fossae, the secondary or dorsal of which is the origin of the dorsal head of m. humerotriceps (Baumel and Witmer, 1993) and is considerably more excavated in *Fratercula* than in *Cerorhinca* (121:1). In *Fratercula*, the ventral margin of the m. supracoracoideus scar (i.e., distally elongated dorsal tubercle) transitions directly into the dorsal margin of the secondary pneumotricipital fossa (117:0), whereas *Cerorhinca* is characterized by a flat, proximal extension of the shaft just ventral to the dorsal tubercle and dorsal to the secondary pneumotricipital fossa (Fig. 4.9; Smith et al., 2007).

***FRATERCULA DOWI* Guthrie et al., 1999**

*Holotype*—LACM 127813, associated partial skeleton (Fig. 4.5).

*Original Diagnosis*—mandibular rami and premaxilla more dorsoventrally expanded, respectively, than in *Cerorhinca monocerata*, but less expanded than in *Fratercula*; smaller than *Fratercula cirrhata*; outside the geographic range of *Fratercula corniculata* and *Fratercula arctica* (Guthrie et al., 1999).

*Remarks*—Expansion of the mandibular rami and premaxilla intermediate to that of *Cerorhinca monocerata* and extant *Fratercula* is a potentially variable character (i.e., intraspecific variation). Although smaller than *Fratercula cirrhata*, the size of *Fratercula*

*dowi* is similar to *Fratercula arctica* (Table 4.2). Geographic range is not considered phylogenetically informative.

*Amended diagnosis*—The distal margin of humeral head in posterior view smoothly rounded (105:0) as in many other alcid species (e.g., *Cerorhinca reai*), rather than pointed as in other *Fratercula*. The m. coracobrachialis nerve passage of the humerus is a sulcus (113:0) as in *Alca*, rather than a closed duct as in other *Fratercula*. The olecranon projects anteriorly (171:1) as in *Synthliboramphus*, rather than posteriorly as in extant Fraterculini. As in *Cerorhinca aurorensis* and *Aethia pygmaea*, the absence of an anteriorly positioned crest extending distally from the anterior margin of the ventral cotyla of the ulna (173:0) differentiates *Fratercula dowi* from extant Fraterculini. Humeral characters (i.e., characters 105 and 113) were evaluated relative to all extant and extinct Fraterculini. Ulnae of *Cerorhinca minor*, *Cerorhinca reai*, and *Cerorhinca* sp. Smith et al., 2007 are not currently known.

#### *CERORHINCA* Bonaparte, 1831

*Diagnosis*—*Cerorhinca* is differentiated from *Fratercula* on the basis of two unambiguously optimized apomorphies. The secondary (dorsal) pneumotricipital fossa of the humerus is considerably less excavated in *Cerorhinca* than in *Fratercula* (121:2). *Cerorhinca* is also characterized by a flat, proximal extension of the shaft just ventral to the dorsal tubercle as opposed to the condition in *Fratercula* where the ventral margin of

the dorsal tubercle transitions directly into the dorsal margin of the secondary pneumotricipital fossa (117:1; Fig. 4.9).

***CERORHINCA MINOR* Howard, 1971**

*Holotype*—LACM 15408, proximal right humerus (Fig. 4.3; Table 4.3).

*Original diagnosis* (Howard, 1971)—Humeral head smoothly rounded on lower margin; deep channel undercutting head and proximomedial edge of m. pectoralis attachment; internal edge of channel limiting medial extent of capital groove and aligned with median crest; pneumotricipital fossa more round than oval; smaller than *Cerorhinca monocerata*.

*Amended diagnosis*—The following characters are added to those described by Howard (1971). *Cerorhinca minor* is differentiated from other *Cerorhinca* by the following suite of locally optimized apomorphies. A small scar distal to the primary pneumotricipital fossa (present in *Cerorhinca monocerata* and *Cerorhinca aurorensis* sp. nov.; can not be evaluated in *Cerorhinca reai* owing to damage) is absent (120:0). The primary pneumotricipital fossa is round (122:0) rather than oval as in other Fraterculini. As in *Cerorhinca reai* and *Brachyramphus*, there is a crest between the posterior side of the humeral head and the medial side of the ventral tubercle that separates the capital groove from the secondary pneumotricipital fossa (133:1; absent in all other *Cerorhinca*).



The posterior margin of the ventral tubercle is a single concavity as in *Cerorhinca reai* (135:0), rather than a double concavity as in *Cerorhinca monocerata* and *Cerorhinca aurorensis*. *Cerorhinca minor* is smaller (~35%) than all other *Cerorhinca* (Table 4.3). These humeral characters were evaluated in all extant and extinct Fraterculini species, with the exception of *Cerorhinca dubia*, which is known only from associated pelvis limbs and is not supported as a part of Fraterculini (Fig. 4.11).

### ***CERORHINCA REAI* Chandler, 1990**

*Holotype*—SDSNH 25319, complete left humerus (Fig. 4.4; Table 4.3).

*Original diagnosis* (Chandler 1990b)—m. subcoracoideus insertion scar of humerus more deeply excavated than in *Fratercula* and lacking in *Cerorhinca monocerata*; primary (ventral) pneumotricipital fossa oblong or oval, rather than rounded as in *Cerorhinca minor*; larger than *Cerorhinca minor*; smaller than *Cerorhinca monocerata* (Table 4.3).

*Amended diagnosis*—The following characters are added to or modified from those described by Chandler (1990b). *Cerorhinca reai* can be differentiated from other species of Fraterculini by the following suite of characters. The primary pneumotricipital fossa is oblong or oval as in other Fraterculini (122:1) rather than rounded as in *Cerorhinca minor*. The insertion scar for m. subcoracoideus is positioned more medially

along the border of the primary pneumotricipital fossa rather than ventrally positioned as in other Fraterculini (127:0). The m. latissimus dorsi scar curves dorsally (139:1) rather than straight as in other Fraterculini. *Cerorhinca reai* is larger than *Cerorhinca minor* and smaller than *Cerorhinca monocerata* and *Cerorhinca aurorensis* (Table 4.3). These humeral characters were evaluated in all extant and extinct Fraterculini species, with the exception of *Cerorhinca dubia*, which is known only from associated pelvis limbs and is not supported as a part of Fraterculini (Fig. 4.11).

***CERORHINCA AUORENSIS*, sp. nov.**

*Holotype*—USNM 257520, complete left humerus (Fig. 4.9; Table 4.3).

*Referred material*—USNM 459395, proximal end of right humerus (Fig. 4.10; Table 4.3); USNM 193051, proximal end of right humerus (Fig. 4.10; Table 4.3).

*Remarks*—These remains were referred to *Cerorhinca* by Smith et al. (2007) but not named as a new species at that time because this taxon had not yet been included in a phylogenetic analysis with other Fraterculini species. Based on the results of the phylogenetic analyses (Figs. 4.16, 4.17) these remains are recognized as a distinct species and named herein.

*Etymology*—The species epithet *aurorensis* reflects the geographic location where the holotype and referred specimens were recovered, the PCS Phosphate Mine (formerly known as the Lee Creek Mine; see Ray 1983, 1987) in Beaufort County, Aurora, North Carolina, USA.

*Locality and horizon*—The PCS Phosphate Mine is located along the south shore of the Pamlico River (35°23'N; 76°47'30"W) and exposes Middle Miocene through Pleistocene aged sediments (Fig. 4.8; Gibson, 1983). The Early Pliocene Yorktown Formation unconformably overlies the Middle Miocene Pungo River Formation (Gibson, 1983). An age of 4.4±0.2 Ma (Early Pliocene) has been assigned to the Yorktown Formation based on K/Ar dating of the *Orionina vughani* assemblage zone and correlated with planktonic foraminifera Zone N19 (Hazel, 1983; Berggren et al., 1995; Woodburne and Swisher, 1995).

There were no associated microfossils preserved with the remains, which could be used to precisely date the specimens. However, preservation of the *Cerorhinca aurorensis* fossils closely matches that of twelve other avian specimens (e.g., USNM 178084, 178150, 193334) referred to the Pliocene Yorktown Formation on the basis of the foraminiferal assemblage from matrix associated with those specimens (Gibson, 1975, unpublished data). A distinct patina often characterizes avian fossils from the Pungo River Formation, which is not present in the *Cerorhinca aurorensis* specimens reported here. The absence of *Fratercula* or *Cerorhinca* in coeval Miocene sediments of the Calvert Formation in Maryland, which also contain fossil alcids (Olson and Rasmussen, 2001), is also consistent with a Pliocene Yorktown Formation provenance.

However, because these remains were not collected in-situ, the possibility that they are from the older, Middle Miocene Pungo River Formation cannot be entirely ruled out.

*Diagnosis*—*Cerorhinca aurorensis* can be differentiated from other species of Fraterculini by the following combination of characters. In ventral view, the lateral margin of the ventral tubercle of *Cerorhinca monocerata* and *Cerorhinca aurorensis* are characterized by two distinct notches (135:0), whereas in other Fraterculini (e.g., *Cerorhinca minor*), this margin is a single concave curvature. In the holotype specimen (USNM 257520) the proximal end of the dorsal supracondylar process contacts the shaft at a  $\sim 120^\circ$  angle, whereas in *Cerorhinca monocerata* the angle is more acute at  $\sim 90^\circ$ . The dorsal condyle of *Cerorhinca aurorensis* is more rounded dorsally than that of *Cerorhinca monocerata*, and the ventral face of the ventral condyle of *Cerorhinca aurorensis* is more flattened than that of *Cerorhinca monocerata*. Within *Cerorhinca* only the holotype specimens of the two previously named extinct species *Cerorhinca reai* and *Cerorhinca minor* (Tables 4.2 & 4.3) are directly comparable to *Cerorhinca aurorensis*. *Cerorhinca dubia* is known only from associated pelvic limb elements and material identified as *Cerorhinca* sp. of Howard (1968) and Chandler (1990b) are ulnae (Table 4.1). *Cerorhinca aurorensis* is comparable in size to *Cerorhinca monocerata*, but is larger than *Cerorhinca reai* and *Cerorhinca minor* (Table 4.3).

*Anatomical description*—*Cerorhinca aurorensis* differs only slightly in morphology (Fig. 4.9) and size (Table 4.3) from specimens of extant *Cerorhinca*

*monocerata*. The size range observed among these remains (Table 4.3) is within the range of statistically determined size variation observed in modern alcids (Bédard, 1985; Burness and Montevicchi, 1992).

All three referred specimens display the anteroposteriorly flattened humeral shafts characteristic of many wing-propelled divers and of all Pan-Alcidae. In posterior view the proximal ends of *Cerorhinca aurorensis* humeri are characterized by a proximoventrally broad m. supracoracoideus scar (i.e., a distally expanded dorsal tubercle; Baumel and Witmer, 1993:98), although the proximal end of the m. supracoracoideus scar of *Cerorhinca* is less ventrally expanded than that of *Fratercula arctica*. In contrast to many other alcids (e.g., *Alca*, *Uria*) the secondary pneumotricipital fossa is more deeply excavated with a narrow dorsal margin and a broader ventral margin that merges with the base of the ventral tubercle. The brachial depression is a distinct proximally narrowing scar that extends proximally only slightly past the proximal extent of the dorsal supracondylar process.

## DISCUSSION

Owing to its state of preservation, *Cerorhinca dubia* could only be scored for four characters. Although the deep anterior groove and the robustness of the tarsometatarsus are suggestive of Fraterculini, there are no apomorphies preserved in the holotype specimen of *Cerorhinca dubia* that allow referral to *Cerorhinca* or Fraterculini. The phylogenetic position of this specimen is uncertain within Alcidae (Fig. 4.11) and

therefore, UCMP 26546 is best considered *Alcidae incertae sedis* (Table 4.4). *Cerorhinca dubia* could not be compared with *Cerorhinca reai*, *Cerorhinca minor*, or *Cerorhinca aurorensis*, which are known exclusively from humeri. The poor preservation of fine morphological detail in the holotype specimen of *Cerorhinca dubia* prevented

Table 4.3- Measurements of puffin humeri (in mm). ‘---’ denotes measurements not available due to damage. ‘\*’ denotes fossil specimens. Abbreviations (following von Den Driesch, 1976): (**glH**) greatest length of humerus; (**bpH**) breadth of proximal humerus; (**dipH**) diagonal of proximal humerus; (**scH**) smallest breadth of corpus (shaft); (**bdH**) breadth of distal humerus; (**ddH**) depth of distal humerus.

Taxa	Specimen #'s	glH	bpH	dipH	scH	bdH	ddH
<i>Cerorhinca aurorensis</i> *	USNM 257520	67.2	14.9	14.1	5.7	10.5	7.5
<i>Cerorhinca aurorensis</i> *	USNM 459395	---	15.8	15.3	---	---	---
<i>Cerorhinca aurorensis</i> *	USNM 193051	---	15.6	15.4	---	---	---
<i>Cerorhinca monocerata</i>	USNM 620643	70.0	14.4	14.3	5.7	10.7	7.4
<i>Fratercula cirrhata</i>	NCSM 177823	77.0	16.0	15.8	6.0	11.5	8.3
<i>Fratercula arctica</i>	USNM 292346	67.2	14.0	13.1	4.8	9.8	6.8
<i>Fratercula corniculata</i>	NCSM 18388	69.9	15.0	14.9	5.3	10.7	7.7
<i>Cerorhinca minor</i> *	LACM 15405	---	10.3	10.3	3.0	---	---
<i>Cerorhinca reai</i> *	SDSNH 25319	48.9	10.6	10.7	3.9	7.6	5.5
<i>Fratercula dowi</i> *	LACM 127813	67.0	15.0	14.8	6.1	10.5	7.4

comparisons other than size with the tibiotarsi and femora of *Fratercula dowi* and extant Fraterculini.

Phylogenetic analyses did not support Howard’s (1968) referral of LACM 18274 and LACM 18275 to *Cerorhinca*. The recovery of LACM 18274 outside of Fraterculinae

provides evidence that this specimen is not referable to *Cerorhinca*. LACM 18274 does not display the posteriorly flared olecranon (171:0) characteristic of all other Fraterculinae except *Fratercula dowi*. The placement of LACM 18274 in an unresolved position at the base of Alcinae (contents of Alcinae include Alcini + *Cepphus* + *Synthliboramphus* + *Brachyramphus*; Fig. 4.12) is not strongly supported, as only two additional steps would be required to position this specimen at the base of Alcidae or at the base of Fraterculini. Therefore, this fragmentary specimen is best considered Alcidae *incertae sedis* (Table 4.4).

The fragment of distal humerus (LACM 18275) referred to *Cerorhinca* by Howard (1968) could be scored for only two characters. However, the dorsoventrally compressed humeral shaft (145:2) supports referral to Alcidae and the square shape, position, and degree of dorsal projection of the dorsal supracondylar process (147:2) support referral to Fraterculini. The position of this specimen was unresolved with respect to other Fraterculini (Fig. 4.13), and this specimen is best considered Fraterculini *incertae sedis* owing to its incompleteness (Table 4.4).

With regard to the isolated ulna referred to *Cerorhinca* by Chandler (1990b), a survey of alcid ulnae failed to identify apomorphic character states that allow for the referral of isolated ulnae to *Cerorhinca*. However, ulnae are not known for extinct Fraterculini other than *Fratercula dowi*. Because the results of the phylogenetic analysis placed SDSNH 23079 in an unresolved position at the base of Alcinae (Fig. 4.14), SDSNH 23079 best considered Alcinae *incertae sedis* (Table 4.4).

Re-examination of the ulna (NHMUK PV A 9034) referred to *Fratercula* by

Dyke and Walker (2005) did not identify any apomorphies that would allow for referral of this specimen to Fraterculinae, and there are no unambiguously optimized apomorphies identified among known *Fratercula* species that would allow the identification of isolated *Fratercula* ulnae. Based on the unresolved position of NHMUK PV A 9034 in Alcidae (Fig. 4.15), this specimen is best considered Alcidae *incertae sedis* (Table 4.4).

Table 4.4- Summary of Fraterculini taxonomic revision. See Appendix 3 for *Fratercula* aff. *arctica* and *Fratercula* aff. *cirrhata* specimen numbers.

Original Taxonomic Assignment	Reference	Specimen #	Revised Taxonomic Assignment
<i>Cerorhinca dubia</i>	Miller, 1925	UCMP 26546	nomen dubium
<i>Cerorhinca</i> sp.	Howard, 1968	LACM 18274	Alcidae incertae sedis
<i>Cerorhinca</i> sp.	Howard, 1968	LACM 18275	Fraterculini indet.
<i>Cerorhinca minor</i>	Howard, 1971	LACM 15408	<i>Cerorhinca minor</i>
<i>Cerorhinca reai</i>	Chandler, 1990b	SDSNH 25319	<i>Cerorhinca reai</i>
<i>Cerorhinca</i> sp.	Chandler, 1990b	SDSNH 23079	Alcinae incertae sedis
<i>Fratercula dowi</i>	Guthrie et al., 1999	LACM 127813	<i>Fratercula dowi</i>
<i>Fratercula</i> aff. <i>arctica</i>	Olson and Rasmussen, 2001	USNM ( <i>n</i> = 17)	<i>Fratercula</i> aff. <i>arctica</i>
<i>Fratercula</i> aff. <i>cirrhata</i>	Olson and Rasmussen, 2001	USNM ( <i>n</i> = 16)	<i>Fratercula</i> aff. <i>cirrhata</i>
<i>Fratercula</i> sp.	Dyke and Walker, 2005	NHMUK PV A 9034	Alcidae incertae sedis
<i>Cerorhinca</i> sp.	Smith et al., 2007	USNM 25720, 45935, 193051	<i>Cerorhinca aurorensis</i>



The position of *Fratercula dowi* as the sister taxon to other *Fratercula* (Fig. 4.16) raises new questions about the historical biogeography of *Fratercula*. Given the systematic position of *Fratercula dowi*, its relatively young age (latest Pleistocene), and records of *Fratercula* aff. *arctica*, and *Fratercula* aff. *cirrhata* from the Early Pliocene of the Atlantic Ocean basin (Table 4.5), these data would suggest that *Fratercula dowi* or the lineage leading to it have been present since at least the Early Pliocene. Furthermore, the derived position of sister taxa *Fratercula arctica* and *Fratercula cirrhata*, with respect to successively more basal *Fratercula corniculata* and *Fratercula dowi* (Fig. 4.16), would likely push the origination of Fraterculini farther back into at least the Miocene, given the Early Pliocene (~4.4 Ma) records of these taxa from the Atlantic Ocean basin (Olson and Rasmussen, 2001; Table 4.5).

Although not considered reliable estimates by some authors because of the incorrect dating and incorrect taxonomic assignment of fossils used as calibrations (Wijnker and Olson, 2009; Mayr, 2011), the divergence estimates proposed by Pereira and Baker (2008) suggested that the basal divergence between *Fratercula* and *Cerorhinca* occurred ~30 Ma in the Early Oligocene. The only Oligocene fossils that are currently referred to Pan-Alcidae are two fragmentary, isolated, and taxonomically indeterminate specimens from the Iwaki Formation in Japan (Ono and Hasegawa, 1991). Eocene and Oligocene localities and collections should be targeted to increase knowledge of early diversity and ancestral states within Pan-Alcidae. If the currently unverifiable report of Fraterculini remains by Howard (1978) is valid (whereabouts of material currently unknown), then the oldest known puffin fossils would be from the Late

Miocene. Otherwise, the earliest records of the clade are the Early Pliocene (~4.4 Ma) *Cerorhinca* and *Fratercula* remains from the Pliocene of North Carolina, USA (Olson and Rasmussen, 2001; Smith et al., 2007). These data suggest that the Fraterculini fossil record may be quite incomplete and that previous hypotheses regarding a Pacific Ocean

Table 4.5- Geographic and temporal distribution of Fraterculini.

Epoch	Pacific Ocean	Atlantic Ocean
Miocene (23.0-5.0 Ma)	Fraterculini indet. (Howard, 1968) ? Fraterculini indet. (Howard, 1978)	No records
Pliocene (5.0-2.5 Ma)	<i>Cerorhinca minor</i> <i>Cerorhinca reai</i>	<i>Fratercula</i> aff. <i>arctica</i> <i>Fratercula</i> aff. <i>cirrhata</i> <i>Cerorhinca aurorensis</i>
Pleistocene (2.5 Ma-12.0 Ka)	<i>Fratercula dowi</i>	No records
Holocene (12.0 Ka-present)	<i>Fratercula cirrhata</i> <i>Fratercula corniculata</i> <i>Cerorhinca monocerata</i>	<i>Fratercula arctica</i>

origin of extant Fraterculini species should be re-evaluated in the context of the fossil record of the clade.

The phylogenetic analysis recovered relationships between species of *Cerorhinca* that are congruent with the hypothesis that *Cerorhinca aurorensis* from the Atlantic Ocean basin represents a taxon with close affinities to the extant *Cerorhinca monocerata* (Smith et al., 2007). The proposed sister relationship between *Cerorhinca reai* and *Cerorhinca minor* seems plausible given the age (i.e., younger than Atlantic *Cerorhinca aurorensis*) and Pacific distribution of known specimens referred to those taxa.

Fraterculini are thought to have originated in the Pacific primarily because of their greater diversity there (Storer, 1960; Olson, 1985). Fossil records of Pacific puffins

potentially extend at least as far back as the Late Miocene (Howard, 1978), whereas in the Atlantic there are no records of Fraterculini from the Miocene (Olson and Rasmussen, 2001; Table 4.5). The occurrence of *Cerorhinca* in the Atlantic documented by Smith et al. (2007) and the *Fratercula* species reported by Olson and Rasmussen (2001) indicates that the diversity of puffins was as great in the Atlantic in the Early Pliocene as it is in the Pacific Ocean basin today. Additionally, much like the radiation of *Alca* during the Pliocene (Olson and Rasmussen, 2001; Smith and Clarke, in press), the fossil record provides evidence that *Cerorhinca* was more diverse in the Pacific during the Late Miocene and Early Pliocene (Howard, 1971; Chandler, 1990b).

Atlantic Ocean basin puffin diversity was proposed to have been achieved rapidly during the Middle Miocene to Early Pliocene, presumably indicating an influx of three species of puffins (*Cerorhinca* plus two *Fratercula* species) from the Pacific through a northern passage between the oceans (Olson and Rasmussen, 2001). Although, a southern route of dispersal cannot be ruled out because the Central American Seaway (CAS) remained open until ~2.5 Ma (Warheit, 2002). Based on the results of a maximum likelihood-based ancestral area optimization, Pereira and Baker (2008) proposed a Pacific Ocean origin of puffins and colonization of the Atlantic Ocean basin by *Fratercula arctica* during an ice-free episode of the Pleistocene. The presence of *Fratercula* aff. *arctica* in Early Pliocene Atlantic Ocean first documented by Olson and Rasmussen (2001) clearly refutes a Pleistocene initial invasion of the Atlantic Ocean by *Fratercula*. When considered in combination, the occurrence of what appear to be extant taxa in the Early Pliocene of the Atlantic Ocean basin (e.g., *Fratercula* aff. *arctica*), the presence of

extinct species such as *Cerorhinca reai* that post-date the Atlantic occurrence of *Cerorhinca aurorensis* (Table 4.5), the absence of *Fratercula* remains from the Pliocene of the Pacific Ocean, and the phylogenetic hypothesis of puffin relationships presented herein, these data suggest a novel scenario in which extant puffin diversity in the Pacific Ocean basin could be a function of re-colonization of the Pacific Ocean by Atlantic endemic species after the faunal turnovers that characterized the Pliocene-Pleistocene climatic transition.

Just as climate changes in the Middle Miocene (~11-16 mya) are proposed to have influenced the initial diversification of alcids (Warheit, 2002), major oceanographic changes in the Late Pliocene (~2.9 Ma) due in part to closure of the CAS and the onset of severe glacial cycles in the North Atlantic (Bartoli et al., 2005), the smallest of the world's ocean basins (Briggs, 1970), also may have played a role in the evolutionary history of the Alcidae. Factors such as changing salinities, temperatures, current patterns, and the faunal turnover of pelagic invertebrates associated with these factors caused the Atlantic to become a much less hospitable place for many organisms (Bartoli et al., 2005). Additionally, the drop in sea level in southern parts of the North Atlantic Ocean, estimated at ~85m (Krantz, 1991), would have resulted in a regression of the shoreline many kilometers away from the once near-shore breeding grounds of puffins. Extant puffins display a high degree of nest-site fidelity, with pairs often returning to the same nest annually (Ainley et al., 1990a). The formation of ice on more northern shores associated with the onset of glaciation would have obstructed the traditional breeding grounds of puffins along the Atlantic and Pacific coasts (Olson and Rasmussen, 2001;

Warheit, 2002). Although extant Pacific *Fratercula* and *Cerorhinca monocerata* both forage for fish and small invertebrates at similar depths, the range of *Cerorhinca monocerata* does not extend as far north as that of *Fratercula corniculata* or *Fratercula cirrhata*, and extends further south (del Hoyo et al., 1996). Climate changes associated with the final emergence of the Panamanian Isthmus (i.e., closure of the CAS) including reorganization of ocean current patterns and decrease in sea surface temperatures led to dramatic faunal shifts to the south during the Middle Pliocene (Bartoli et al., 2005). By ~2.5 Ma climatic conditions were approaching a more modern range and the associated oceanic circulation regime including modern North Atlantic Gyre, Gulf-stream, and California current circulation patterns were in place. Changes in sea level involved relatively small, meter scale fluctuations associated with Late Pliocene and Pleistocene glacial cycles (Bartoli et al., 2005). If extinct species of *Cerorhinca* had environmental tolerances similar to those of extant *Cerorhinca*, climate changes linked with a tolerance for warmer waters (i.e., compared to other extant alcids) and associated prey species may have contributed to the extinction of *Cerorhinca* species in the Atlantic and Pacific Ocean basins. However, the role of these changes may have had on the pelagic avifauna of the eastern Pacific, which has remained relatively cold and productive since the Miocene is still poorly understood (Warheit, 2002).

Extinctions and retractions in range were also prevalent preceding the Pleistocene and overall diversity of seabirds in general and alcids in particular was greatly reduced (Emslie, 1998; Olson and Rasmussen, 2001; Smith and Clarke, in press). Albatross remains are not known from post-Pliocene deposits in the Atlantic (Olson and

Rasmussen, 2001) and Pelagornithidae are not known from post-Pliocene deposits in the Pacific or Atlantic Ocean basins (Mourer-Chaviré and Geraads, 2008, 2010; Boessenecker and Smith, 2011). Gannet species richness was reduced from at least three species in the Pliocene to a single Atlantic species today (Olson and Rasmussen, 2001). The growing list of North Atlantic disappearances recognized by ornithologists now includes *Cerorhinca*. Likewise, puffin diversity in the Pacific Ocean was augmented by at least one additional species, *Fratercula dowi*, as little as 10,000 years before the present (Guthrie et al., 1999). The inevitable conclusion that the extinction of *Fratercula dowi* is in some way related to climatic changes associated with the end of Pleistocene glaciation remains to be substantiated.

## CONCLUSIONS

The taxonomic reevaluation of Fraterculini fossil remains resulted in a more refined estimate of species richness in this clade. Referral of five previously reported specimens to Fraterculini was not supported (Table 4.4). However, the referral of *Fratercula dowi*, *Fratercula* aff. *arctica*, *Fratercula* aff. *cirrhata*, *Cerorhinca reai*, *Cerorhinca minor*, and *Cerorhinca aurorensis* to Fraterculini was confirmed (Table 4.4). Thus, fossil records comprise 3 species each from the Atlantic and Pacific Ocean basins (Fig. 4.16). Even though there are records of *Fratercula cirrhata* and *Cerorhinca* from both Atlantic and Pacific Ocean basins, the ancestral area of Fraterculini optimizes as the Pacific Ocean basin based on the recovered topology (Fig. 4.16). However, the older age

of Atlantic Fraterculini and the absence of *Fratercula* fossils from rich deposits such as the Pliocene San Diego Formation of southern California may be indicative of an Atlantic origin for the clade. Although, Fraterculini remains are comparatively rare compared to those of other Atlantic alcid taxa (e.g., *Alca*). Among the ~8,000 alcid fossils from the Early Pliocene Yorktown Formation along the western Atlantic coast, only 36 specimens of *Fraterculini* are known. The sample size of remains from the San Diego Formation is ~4,000 specimens. Thus, the possibility of un-sampled puffin diversity from that horizon cannot be excluded.

The placement of extinct species of Fraterculini in the phylogenetic results presented herein (Figs. 4.16 & 4.17) contribute importantly to our understanding of puffin evolution, which was previously limited by the absence of a phylogenetic hypothesis of relationships for all known species in this clade. *Cerorhinca* and *Fratercula* are supported as clades and united in a monophyletic Fraterculini that is the sister taxon to Aethiini within a monophyletic Fraterculinae (Fig. 4.16). Whereas *Cerorhinca* is represented only by *Cerorhinca monocerata* today, the clade was as diverse in the Pliocene as *Fratercula* is today (i.e., 3 species). Additionally, although *Cerorhinca* is restricted to the Pacific Ocean basin today, the fossil record shows that *Cerorhinca* had a Holarctic distribution during the Pliocene.

Considering the relatively sparse fossil record of Fraterculini in comparison with some other alcid clades (e.g., *Alca*), the biogeographical implications of the phylogenetic hypothesis presented here will only become clearer in the context of reliable divergence estimates for Alcidae. Estimation of molecular-based ghost ranges for this clade will

facilitate comparison to minimum cladogram fit to the fossil record. Furthermore, divergence dates based upon reliably dated and phylogenetically analyzed fossils will allow for detailed comparisons with the timing of geologic and associated paleoclimatic events that have been proposed as drivers of puffin dispersal and extinction.

The reasons for the demise of Atlantic Ocean populations of *Cerorhinca aurorensis* and *Fratercula cirrhata* warrant further investigation. The survival of *Fratercula arctica* and the differential extinction of *Fratercula cirrhata* and *Cerorhinca aurorensis* is reminiscent of the survival of *Alca torda* and the differential extinction of its six congeners (Smith and Clarke, in press). Given the co-occurrence of these ten species of auks and puffins (3 puffins and 7 auks) in the Early Pliocene Yorktown Formation and the lack of *Fratercula cirrhata*, *Cerorhinca aurorensis*, and auks other than *Alca torda* from the extant Atlantic Ocean basin avifauna, it seems plausible to conclude that the same factors may have affected populations of puffins and auks. The negative effects of the Pliocene-Pleistocene climatic transition have been well documented with respect to other marine organisms (Ray, 1983, 1987; Domning, 2001; Ray and Bohaska, 2001; Deméré et al., 2003; Fitzgerald, 2005; Ray et al., 2008) and there is no reason to suspect that alcids would not also have been negatively affected by these changes in climate and associated decreases in bioproductivity and prey-species richness. Pleistocene and Holocene collections and localities should be targeted to assess the timing and sequence of the extirpation of puffin species from the Atlantic Ocean avifauna and the timing of the arrival of *Fratercula* in the Pacific Ocean basin.



## CHAPTER 5.

The fossil record and phylogeny of the auklets

(Pan-Alcidae, Aethiini)

## INTRODUCTION

Alcidae Leach, 1820 are pelagic, wing-propelled pursuit-diving charadriiforms with an exclusively Holarctic range. Auklets are among the smallest of alcids, and ecologically, tend to be specialized for planktivory more so than many other alcids (Bédard, 1985; del Hoyo et al., 1996). Congruent with the distribution of extant auklets, all fossil records of *Aethia* Merrem, 1788 and *Ptychoramphus* Brandt, 1837 are restricted to the Pacific Ocean basin (Olson, 1985; Fig. 5.1).

There are five extant species of auklets: Cassin's Auklet *Ptychoramphus aleuticus*, Least Auklet *Aethia pusilla*, Parakeet Auklet *Aethia psittacula*, Whiskered Auklet *Aethia pygmaea*, and Crested Auklet *Aethia cristatella*. The Least Auklet is the smallest species of extant alcid, whereas other auklets are similar in size to the murrelets (i.e., *Brachyramphus* Brandt, 1837 and *Synthliboramphus* Brandt, 1837). As in their sister taxon the Fraterculini Storer, 1960 (i.e., puffins; *Cerorhinca* Bonaparte, 1831 and *Fratercula* Brisson, 1760), many Aethiini Storer, 1960 (i.e., auklets; *Ptychoramphus* and *Aethia*) are characterized by crests and tufts of feathers adorning their heads, and the bills of many auklets (e.g., *Aethia psittacula*) are broader than the more terete bills of primarily piscivorous alcids such as *Uria* Pontoppidan, 1763. Like all extant alcids, auklets are counter-shaded (colored dark dorsally and light ventrally).

No extinct species of *Ptychoramphus* or *Aethia* has been previously included in a phylogenetic analysis. Systematic positions for *Ptychoramphus tenuis* Miller and Bowman, 1958 and *Aethia rossmoori* Howard, 1968 were proposed in the form of a

cladogram by Chandler (1990a), but scorings for these taxa were not included in the cladistic matrix. The placement of extinct taxa in Chandler's (1990a) cladograms seems to stem from the optimization of selected characters (i.e., character mapping).

Two new species of *Aethia* and an additional potential new alcid taxon are described herein. These new fossils and previously described fossil auklet remains are included in combined phylogenetic analyses that may help elucidate the poorly understood relationships and evolutionary history of this clade.

The monophyly of Aethiini (i.e., the auklets, consisting of *Ptychoramphus* and *Aethia*) has been supported in analyses of morphological and molecular sequence data (Strauch, 1985; Watada et al., 1987; Chandler 1990a; Moum et al., 1994; Friesen et al., 1996; Thomas et al., 2004; Baker et al., 2007; Pereira and Baker, 2008). The morphology-based compatibility analysis of Strauch (1985) placed Fraterculini (i.e., the puffins, consisting of *Cerorhinca* and *Fratercula*) as the sister-group to all other alcids, with Aethiini in a more derived position as the sister taxon to the remainder of Alcidae. All subsequent phylogenetic analyses have recovered Aethiini as the sister taxon to Fraterculini (Watada et al., 1987; Chandler 1990a; Moum et al., 1994; Friesen et al., 1996; Thomas et al., 2004; Baker et al., 2007; Pereira and Baker, 2008). Although *Ptychoramphus* has been consistently recovered as the sister taxon to the other auklets (i.e., *Aethia*; Watada et al., 1987; Chandler 1990a; Moum et al., 1994; Friesen et al., 1996; Thomas et al., 2004; Baker et al., 2007; Pereira and Baker, 2008), relationships within *Aethia* are more contentious, with the relative positions of *Aethia* species variable or unresolved in previous analyses. It has been suggested that ancestral DNA

polymorphism or incomplete lineage sorting may be responsible for the variable placements recovered for *Aethia* species in previous phylogenetic analyses (Walsh and Friesen, 2003; Walsh et al., 2005).

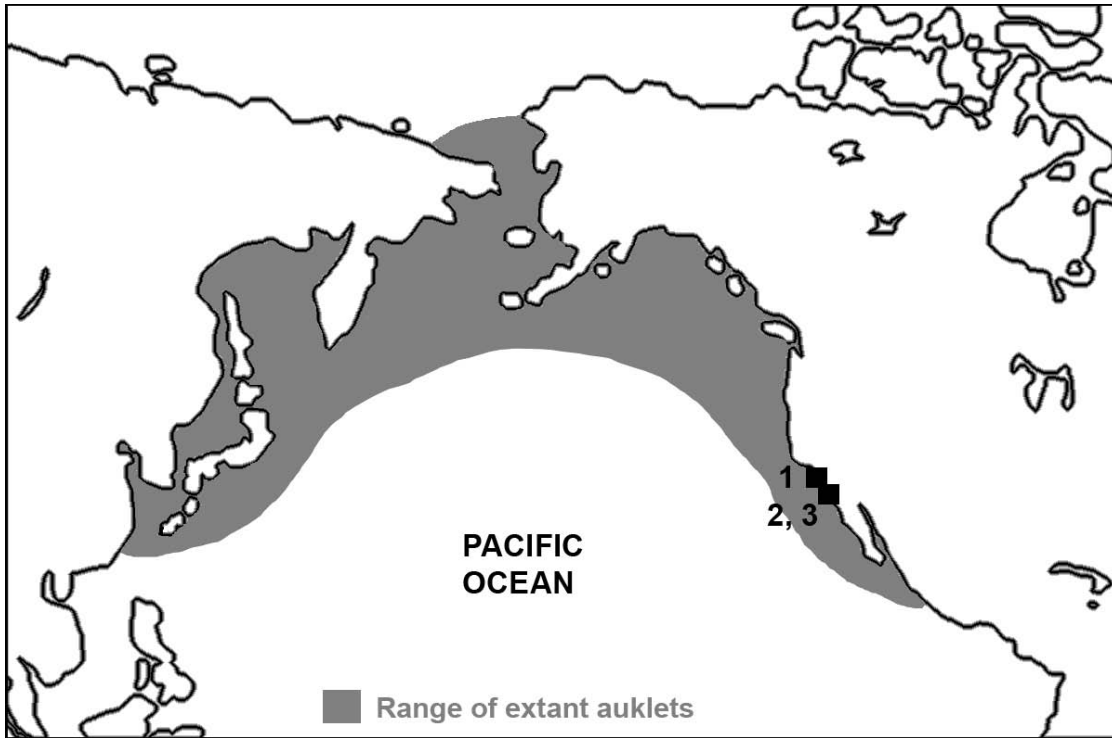


Figure 5.1- World map depicting published auklet fossil localities and the geographic distribution of extant auklets (based on del Hoyo et al., 1996). **1.** Laguna Niguel, California (Howard, 1978); **2.** Laguna Hills, California (Howard, 1968); **3.** San Diego, California (Howard, 1949; Miller and Bowman, 1958; Howard, 1982; Chandler, 1990b).

***The fossil record of auklets:*** A right tarsometatarsus (UCMP 45662; Fig. 5.2)

from the Pliocene San Diego Formation was initially referred, albeit tentatively, to *Brachyramphus pliocenium* Howard, 1949 by Miller (1956). However, the resemblance of that specimen to *Aethia* and *Ptychoramphus*, and notable differences from *Brachyramphus*, were noted by Miller (1956). UCMP 45662 was formally, yet tentatively

referred to *Ptychoramphus* and designated as the holotype specimen of *Ptychoramphus tenuis* by Miller and Bowman (1958; Table 5.1).



Figure 5.2- Holotype right tarsometatarsus of *Ptychoramphus tenuis* (UCMP 45562) in anterior view.

*Aethia rossmoori* was described by Howard in 1968 based upon a right ulna (LACM 18948; Fig. 5.3) from Late Miocene deposits in Laguna Hills, California, USA (Table 5.1). Based on its small size, *Aethia rossmoori* was originally diagnosed relative only to the extant species *Aethia pusilla*. Because the holotype specimen of *Aethia rossmoori* is an ulna, and because there are no known associated specimens of *Aethia rossmoori*, there was no basis for referral of additional material (humerus, radius, coracoids) by Howard (1968) from a locality that also contains other species of alcids (*Alcodes*, *Cerorhinca*, ‘*Praemancalla*’).

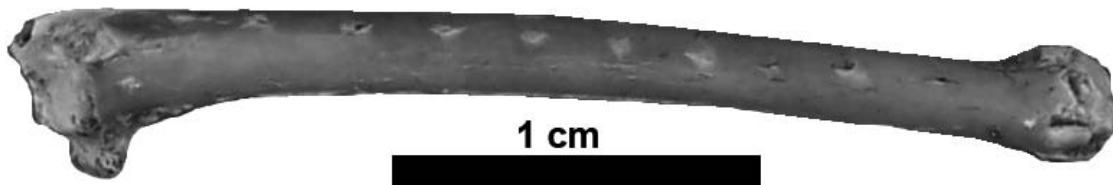


Figure 5.3- Holotype right ulna of *Aethia rossmoori* (LACM 18948) in anterodorsal view.

Table 5.1- Previously published auklet fossil remains.

Taxon	Material	Provenience	Age	Reference
<i>Ptychoramphus tenuis</i>	tarsometatarsus	California	Pliocene	Miller and Bowman, 1958
<i>Aethia rossmoori</i>	ulna	California	Late Miocene	Howard, 1968
<i>Aethia</i> sp.	distal humerus	California	Late Miocene	Howard, 1978
<i>Aethia</i> sp.	humerus	California	Late Miocene	Howard, 1982

A distal humerus (LACM 37686) from the Late Miocene Monterey Formation at Laguna Niguel, California, USA was referred to *Aethia* by Howard in 1978 (Table 5.1). LACM 37686 was not figured in publication (Howard, 1978) and its whereabouts are currently uncertain. An empty specimen box with a temporary loan tag labeled ‘Hildegard Howard study cabinet’ was found during a thorough search of the LACM collections in 2007. Because LACM 37686 could not be located it is not considered further herein.

A distal right humerus (LACM 107031; mistakenly identified as a left humerus by Howard, 1982) from the Late Miocene San Mateo Formation (San Luis Rey River Local Fauna) of San Diego, California was referred to *Aethia* by Howard in 1982 (Table 5.1; Fig. 5.4). Although there are no apomorphies that allow differentiation between *Ptychoramphus* and *Aethia* humeri, the ventral projection of the entepicondyle, lack of proximal extension of the dorsal supracondylar process, and the abrupt transition of the

deltopectoral crest to the humeral shaft support referral of this specimen to Aethiini (i.e., the clade composed of *Aethia* + *Ptychoramphus*).

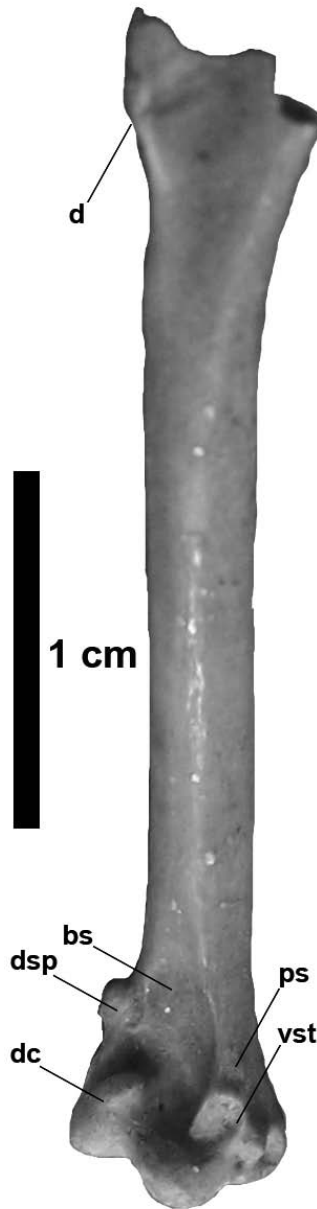


Figure 5.4- Aethiini sp. partial right humerus (LACM 107031) in anterior view.  
Anatomical abbreviations: (**bs**) m. brachialis scar; (**d**) deltopectoral crest; (**dc**) dorsal condyle; (**dsp**) dorsal supracondylar process; (**ps**) m. pronator sublimis scar; (**vst**) ventral supracondylar tubercle.

Previously described auklet remains, extant species of auklets, other species of extant alcids, and charadriiform outgroup taxa are evaluated through combined phylogenetic analyses to assess the systematic positions of these taxa. Taxonomic revisions are provided based on the results of the phylogenetic analyses and implications for the evolution of these taxa are discussed in the context of revised estimates of species richness and the results of the phylogenetic analyses.

## MATERIALS AND METHODS

In the anatomical descriptions, the English equivalents of the Latin osteological nomenclature summarized by Baumel and Witmer (1993) are primarily used. The terminology of Howard (1929) is followed for features not treated by Baumel and Witmer (1993). With the exception of the terms anterior and posterior substituted for cranial and caudal, respectively, the terms used for the anatomical orientation of a bird are those used by Clark (1993). Measurements follow those of Von den Driesch (1976). All measurements were taken using digital calipers and rounded to the nearest tenth of a millimeter. With the exception of species binomials, all taxonomic designations (e.g., Aethiini) are clade names and are not intended to convey rank under the Linnaean system of nomenclature, regardless of use of italics or previous usage by other authors.

Morphological characters were scored for all 23 extant alcids, the recently extinct Great Auk *Pinguinus impennis*, extinct auklet species, and fossils previously referred to Aethiini. A gull (*Larus marinus*) and a skua (*Stercorarius skua*) were included as



charadriiform outgroup taxa. See Appendix 2 for morphological character descriptions and Appendix 3 for morphological character scorings used in the phylogenetic analysis.

Morphological characters include osteological ( $n = 232$ ), integumentary ( $n = 32$ ), reproductive ( $n = 11$ ), dietary ( $n = 2$ ), myological ( $n = 24$ ) and micro-feather ( $n = 52$ ). One hundred and sixty-four characters were developed for this analysis. The other 189 characters were drawn from the work of Hudson et al. (1969;  $n = 24$ ), Strauch (1978, 1985;  $n = 39$ ), Chandler (1990a;  $n = 63$ ), Chu (1998;  $n = 11$ ), and Dove (2000;  $n = 34$ ). Only 34 of the 38 characters used by Dove (2000) varied in the taxa examined in this study. Of the 34 used in this analysis, eighteen were modified (i.e., split into 2 separate characters) according to the philosophy of character independence proposed by Hawkins et al. (1997), resulting in a total of 52 microfeather characters.

Whenever possible, five or more specimens of each extant species, and both sexes were evaluated to account for intraspecific character variation and potential sexual dimorphism respectively (Appendix 1). Only adult specimens, assessed based upon degree of ossification (Chapman, 1965), were evaluated, and whenever possible specimens from multiple locations within the geographic range of extant species (i.e., sub-species) were examined to account for geographic variation. Characters for all extinct taxa were coded from direct observation of holotype and referred specimens. Pleistocene and Holocene remains that presumably represent extant species (Lambrecht, 1933; Brodkorb, 1967; Tyrberg, 1998) were not examined, and are not treated further herein.

Previously published molecular sequence data (mitochondrial: ND2, ND5, ND6, CO1, CYTB; ribosomal RNA: 12S, 16S; and nuclear: RAG1) were downloaded from

GenBank (<http://www.ncbi.nlm.nih.gov/genbank>; see Appendix 4 for sequence authorship). Preliminary sequence alignments were obtained using ClustalX v2.0.6 (Thompson et al., 1997), and then manually adjusted using Se-Al v2.0A11 (Rambaut, 2002). Alignment and concatenation of sequence data resulted in a final molecular matrix of 11601 base pairs. Molecular sequence data were combined with morphological characters for a matrix of 11,954 characters.

A combined approach of phylogeny estimation was used to evaluate the systematic position of auklet species. Phylogenetic analyses employed the parsimony criterion of phylogenetic inference as implemented in PAUP\* v4.0b10 (Swofford, 2002). Parsimony tree search criteria were as follows: heuristic search strategy; 10,000 random taxon addition sequences; tree bisection-reconnection branch swapping; random starting trees; all characters equally weighted; minimum length branches = 0 collapsed; multistate (e.g., 0&1) scorings used only for polymorphism. Bootstrap values and descriptive tree statistics (e.g., CI, RI, RC) were calculated using PAUP\* v4.0b10 (Swofford, 2002). Bootstrap value calculation parameters included 1,000 heuristic replicates, 100 random addition sequences per replicate. All other settings were the same as the primary analysis. Bremer support values were calculated using a script generated in MacClade v4.08 (Maddison and Maddison, 2005) and analyzed with PAUP\* v4.0b10 (Swofford, 2002). Based on the results of previous phylogenetic analyses of charadriiform relationships (Strauch, 1978; Sibley and Ahlquist, 1990; Chu, 1995; Ericson et al., 2003; Paton et al., 2003; Thomas et al., 2004; Baker et al., 2007) resultant trees were rooted with *Larus marinus*.

***Institutional abbreviations:*** NCSM—North Carolina Museum of Natural Sciences, Raleigh, NC, USA; LACM—Natural History Museum of Los Angeles County, Los Angeles, CA., USA; SDSNH—San Diego Natural History Museum, San Diego, CA, USA; UCMP—University of California Museum of Paleontology, Berkeley, CA, USA; UMMZ—University of Michigan Museum of Zoology, Ann Arbor, MI, USA; USNM—National Museum of Natural History, Smithsonian Institution, Washington, D.C., USA.

## PHYLOGENETIC RESULTS

A preliminary analysis including all seven extinct taxa of interest *Pinguinus impennis*, and 25 extant taxa resulted in a tree with relationships completely unresolved at the base of Alcidae (results not shown). Additional analyses, which are described below, were performed to identify potential ‘wildcard taxa’ (Nixon and Wheeler, 1992; Kearney, 2002), which were removed from subsequent analyses to recover a reasonably resolved phylogenetic hypothesis that still maintained a reasonably high level of taxon sampling.

Inclusion of *Ptychoramphus tenuis* in a phylogenetic analysis with all 23 extant alcids, *Pinguinus impennis*, and two outgroup charadriiforms (*Stercorarius skua*, *Larus marinus*) resulted in a single most parsimonious tree (MPT; L: 7673; CI: 0.49; RI: 0.54; RC: 0.27; Fig. 5.5). Not surprisingly, *Ptychoramphus tenuis* is placed in as the sister taxon to the extant species *Ptychoramphus aleuticus*. *Ptychoramphus tenuis* could be scored for only 14 of 353 morphological characters. Because *Ptychoramphus tenuis* is an

operational equivalent of *Ptychoramphus aleuticus* (see Appendix 3) it was not included in subsequent analyses, and because *Ptychoramphus tenuis* is not morphologically distinct from *Ptychoramphus aleuticus*, it is considered a nomen dubium.

Inclusion of *Aethia rossmoori* in a phylogenetic analysis with all 23 extant alcids, *Pinguinus impennis*, and two outgroup charadriiforms resulted in two MPTs (L: 7674; CI: 0.51; RI: 0.56; RC: 0.29). *Aethia rossmoori* was placed in a polytomy at the base of a monophyletic Alcidae (Fig. 5.6). The two MPTs placed *Aethia rossmoori* as the sister taxon to all other Alcidae, or as the sister taxon to *Brachyramphus marmoratus*. Because *Aethia rossmoori* was not recovered in Aethiini, and because the inclusion of this taxon significantly reduced phylogenetic resolution, it was not included in subsequent analyses. *Aethia rossmoori* is, therefore, considered Alcidae *incertae sedis*.

All 23 extant alcids, *Pinguinus impennis*, two outgroup charadriiforms, and three additional fossils (SDSNH 63195, SDSNH 25358, LACM 107031) were included in a combined phylogenetic analysis that resulted in a well-resolved strict consensus tree (12 MPTs; L: 7678, CI: 0.52, RI: 0.59, RC: 0.31; Fig. 5.7). Aethiini (contents include *Aethia* + *Ptychoramphus*) is unresolved in the strict consensus topology and SDSNH 25358 is recovered as the sister taxon to Alcidae (Fig. 5.7). Removal of SDSNH 63195 (newly referred humerus; see below) in a subsequent analysis resulted in the placement of LACM 107031 (distal humerus; Fig. 5.5) in a polytomy with *Aethia cristatella* and *Aethia pygmaea*, with *Aethia psittacula*, *Aethia pusilla*, and *Ptychoramphus aleuticus* placed in successively more basal positions in Aethiini (Fig. 5.8A; 6 MPTs; L: 7677; CI: 0.52; RI: 0.59; RC: 0.31). Removal of LACM 107031 in a subsequent analysis resulted in

the placement of SDSNH 63195 in an unresolved position in Aethiini (Fig. 5.8B; 3 MPTs; L: 7674; CI: 0.50; RI: 0.56; RC: 0.28). Morphological apomorphies that support the monophyly of recovered clades are summarized below in Table 5.2.

Table 5.2- Apomorphies supporting clades in the resultant phylogenetic tree (Fig. 5.7). Character numbers from Appendix 3 are followed by character state symbols (e.g., 23:0 = character number 23, state 0). Characters followed by ‘\*’ are locally optimized apomorphies with a CI < 1.0. All other apomorphies have a CI = 1.0. Optimizations for *Aethia* based on the topology depicted in Fig. 5.8A. Optimizations for *Ptychoramphus* based on the topology depicted in Fig. 5.5.

Clade	Character numbers and states that support monophyly
Aethiini	8:1; 11:1; 89:0; 207:1.
SDSNH 25358 + Alcidae	145:1*; 147:1*; 153:1*; 155:1; 157:1.
<i>Aethia</i>	66:1*; 196:0*; 205:0*; 266:1*.
<i>Ptychoramphus</i>	224:0*.

## SYSTEMATIC PALEONTOLOGY

AVES Linnaeus, 1758

CHARADRIIFORMES Huxley, 1867

PAN-ALCIDAE Smith, 2011

ALCIDAE Leach, 1820

AETHIINI Storer, 1960

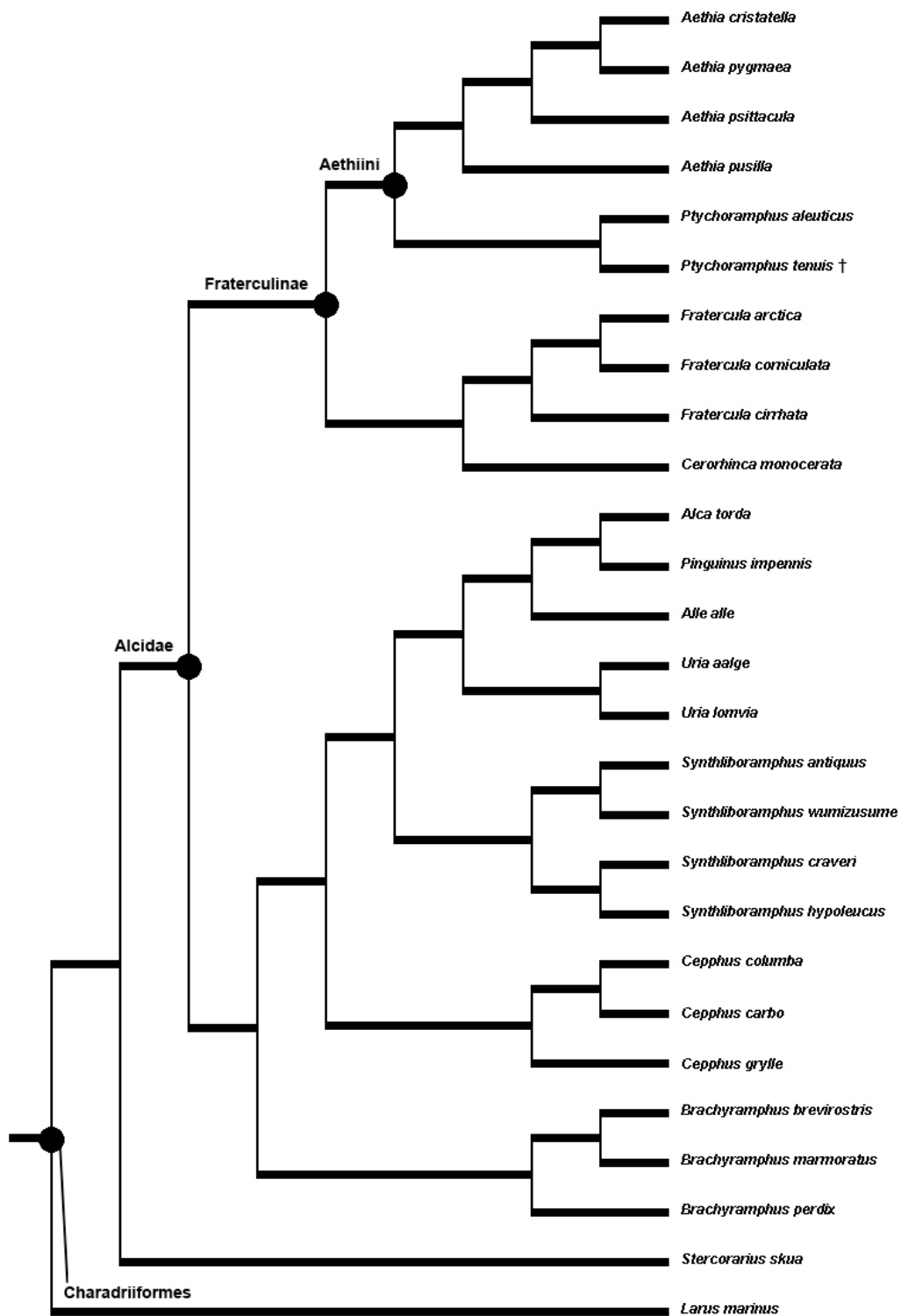


Figure 5.5- Single MPT indicating the sister taxon relationship between *Ptychoramphus tenuis* and *Ptychoramphus aleuticus*.

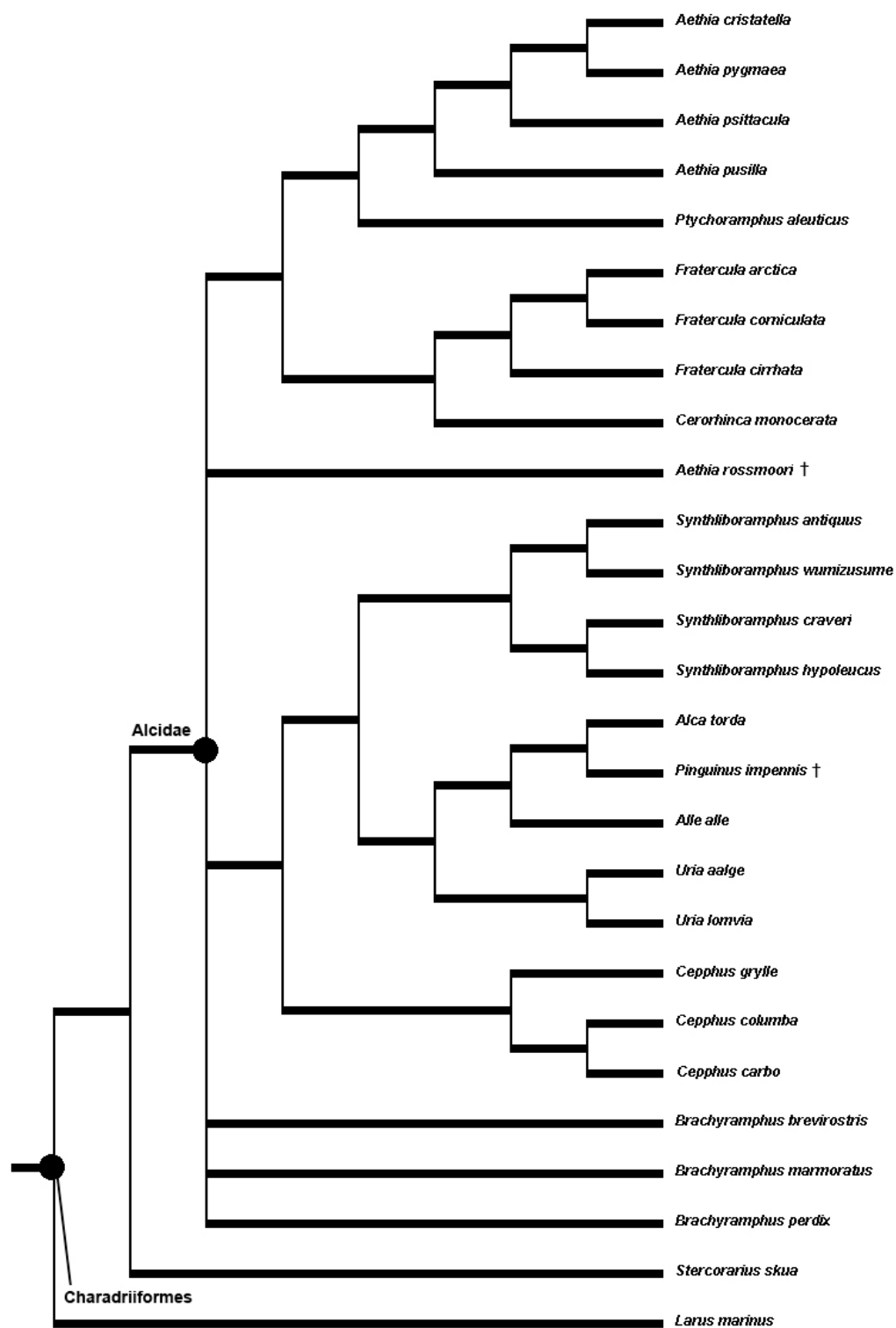


Figure 5.6- Strict consensus cladogram of two MPTs indicating the unresolved phylogenetic position of *Aethia rossmoori* in Alcidae.

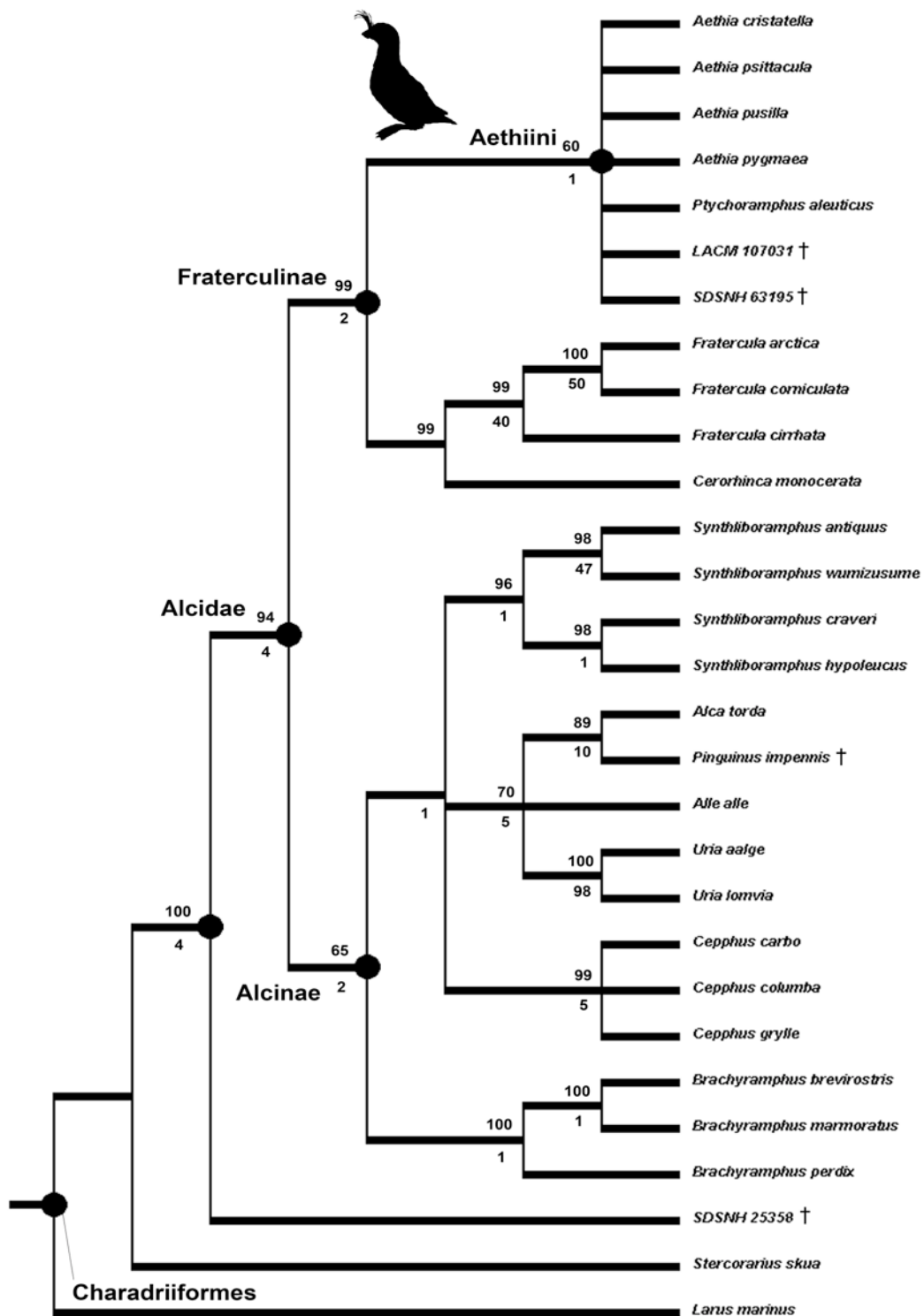


Figure 5.7- Strict consensus cladogram of 12 MPTs indicating the systematic positions of extinct auklets and the proposed sister taxon relationship between SDSNH 25358 and Alcidae.



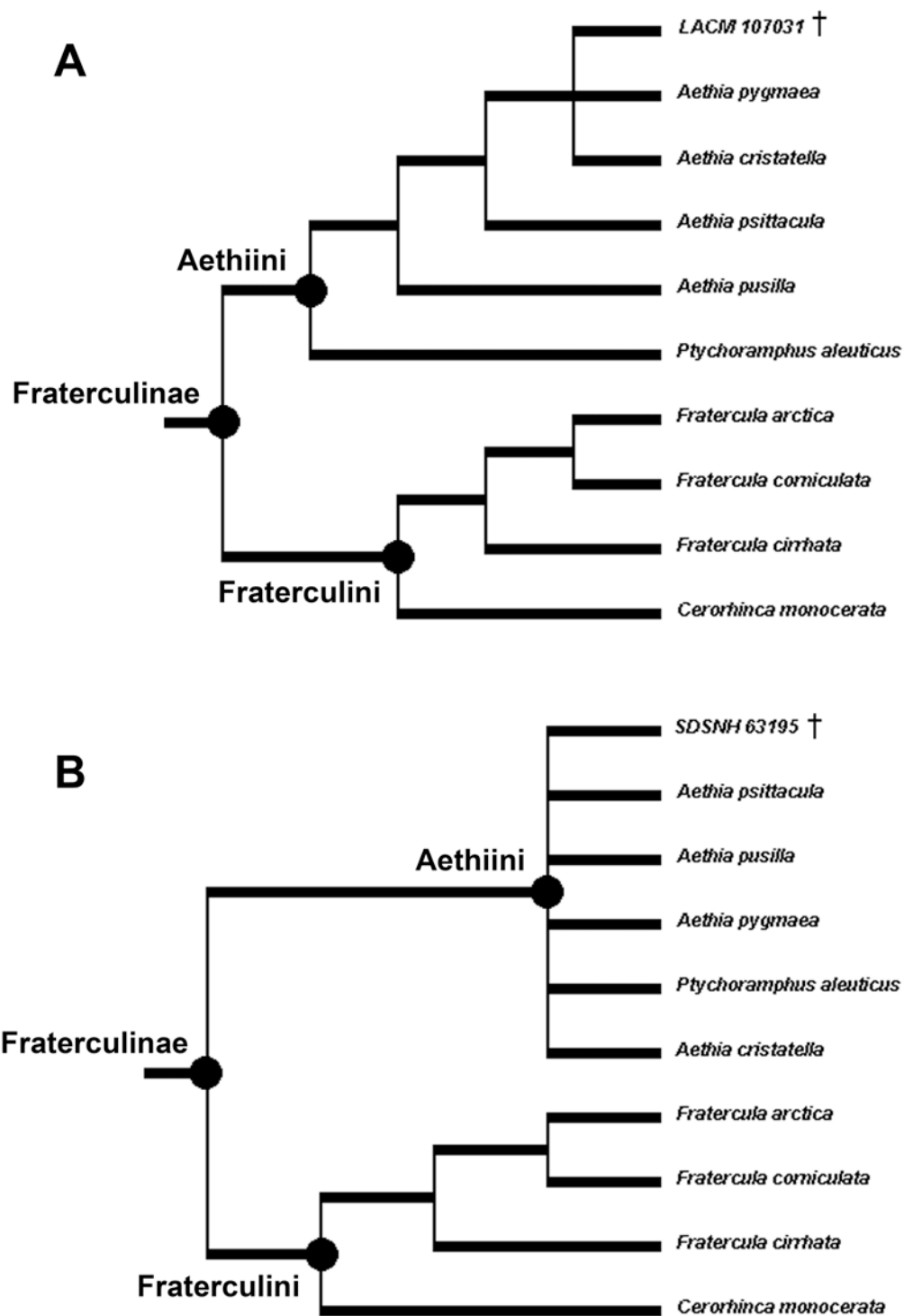


Figure 5.8- Strict consensus cladograms showing the phylogenetic positions recovered for LACM 107031 (A) and SDSNH 63195 (B).

*Diagnosis*—Aethiini, the clade composed of *Aethia* Merrem, 1788 and *Ptychoramphus* Brandt, 1837, is diagnosed based upon the four following apomorphies. The maxillopalatine process of the maxilla dorsoventrally flattened (8:1) rather than concave in ventral view as in other Alcidae. The ventral margin of the ventral palatine crest extends ventral to the lateral margin of the palatine (11:1). The ventral margin of this feature does not extend as far ventrally in all other Pan-Alcidae. The m. brachialis tuberosity of the coracoid is rounded (89:0) rather than elongated as in other Charadriiformes. As in *Rynchops niger*, the posterior end of the dorsal iliac spine is blunt rather than pointed (207:1) as in other Charadriiformes. These characters could not be evaluated in the extinct taxa described below, which are all known exclusively from humeri. However, the humeri of Aethiini can be differentiated from those of other alcids by the following combination of characters: the distal margin of the humeral head in posterior view is pointed (105:1) in all Aethiini except *Aethia storeri* rather than more rounded as in many other alcids (e.g., *Cerorhinca minor*); the deltopectoral crest transitions to the humeral shaft abruptly (108:1) rather than smoothly as in many other alcids (e.g., *Brachyramphus*); shallowly excavated m. supracoracoideus scar (115:1); m. supracoracoideus scar does not broaden proximally as in Fraterculini; secondary pneumotricipital fossa shallow (130:0) rather than moderately excavated as in Fraterculini; in anterior view the capital groove appears rounded as in *Cerorhinca monocerata* (140:0) rather than a notch or a deep groove as in all other alcids; dorsal supracondylar process a small dorsally pointing projection (147:1) as in *Brachyramphus*; ventral margin of ventral epicondyle flared ventrally as in all Fraterculinae.

*AETHIA* Merrem, 1788

*Diagnosis*—*Aethia* is differentiated from *Ptychoramphus* based upon the four following locally optimized apomorphies. As in the murrelets, a lateral sternal fenestra is present (66:1), rather than an unenclosed lateral sternal notch as in *Ptychoramphus aleuticus*. As in *Synthliboramphus*, the articulation facet for manual digit II:1 is level with articulation facet for manual digit III:1 in distal extent (196:0) rather than proximal to it as in *Ptychoramphus aleuticus*. The post-acetabular dorsal iliac crest broadens (205:0) as in *Cepphus*, *Uria*, and many other charadriiforms (e.g., *Rissa tridactyla*) rather than narrows as in the murrelets. The nest site is a natural crevice (266:1) as in *Synthliboramphus* rather than a bare rock as in *Ptychoramphus aleuticus*. As with the diagnostic characters of Aethiini, these characters could not be evaluated in the extinct taxa described below, which are all known only from humeri. There are no autapomorphies of the humerus of *Ptychoramphus aleuticus* that differentiate the humeri of that taxon from the humeri of *Aethia* species. *Ptychoramphus tenuis* is known only from an isolated tarsometatarsus.

***AETHIA BARNESI*, sp. nov.**

*Holotype*—LACM 107031, a partial right humerus missing the proximal end (Tables 5.1 & 5.3; Figs. 5.4 & 5.9) collected by L.G. Barnes on the 19<sup>th</sup> of March, 1975.

*Etymology*—Named after the collector of the holotype specimen and in recognition of the many contributions to the study of the vertebrate paleontology of California by Lawrence G. Barnes.

*Locality and horizon*—Late Miocene San Mateo Formation (San Luis Rey River Local Fauna) of Lawrence Canyon, Oceanside, San Diego County, California. The vertebrate assemblages of the San Mateo Formation were discussed by Barnes et al. (1981), who designated the lower assemblage the San Luis Rey River Local Fauna (SLRRLF), and the upper assemblage the Lawrence Canyon Local Fauna (LCLF). Alcid fossils, including the holotype humerus (LACM 107031) and those of the flightless alcid taxon *Mancalla*, have been recovered from the older SLRRLF. Age estimates for the SLRRLF based upon terrestrial mammal and marine bird fossils range from approximately 6.7-10.0 Ma (i.e., Late Miocene or Turtonian equivalent; Barnes et al., 1981; Domning and Deméré, 1984).

*Diagnosis*—Differentiated from all other species of Aethiini by the greater width of the scapulothoracic sulcus (151:2) as compared to the humerothoracic sulcus of the distal humerus (Howard, 1982). In all other species of Aethiini, the humerothoracic sulcus is wider than the scapulothoracic sulcus. *Aethia barnesi* differs from extant species of *Aethia* in the following characteristics noted by Howard (1982). The cross-section of the humerus at mid-shaft is slightly more rounded than that of other Aethiini. The m. brachialis impression has more distinct dorsal and ventral margins, and the

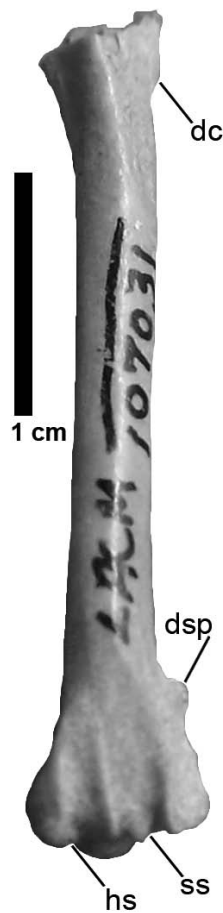


Figure 5.9- Holotype distal right humerus of *Aethia barnesi* (LACM 107031) in posterior view. Anatomical abbreviations: (**dc**) deltopectoral crest; (**dsp**) dorsal supracondylar process; (**hs**) humerotricipital sulcus; (**ss**) scapulotricipital sulcus.

ventral supracondylar tubercle is positioned more dorsally than that of extant species of auklets. *Aethia barnesi* is also smaller than all other species of Aethiini for which the humerus is known (Table 5.3).

*Anatomical description*—There are no apomorphies that allow differentiation between *Ptychoramphus* and *Aethia* humeri. However, the ventral projection of the ventral entepicondyle relative to the humeral shaft (150:0), dorsal supracondylar process

less proximally extended (148:0), and the abrupt transition of the deltopectoral crest to the humeral shaft (108:1) support the referral of this specimen to Aethiini (i.e., the clade composed of *Aethia* + *Ptychoramphus*; Fig. 5.8A). Like *Ptychoramphus aleuticus*, *Aethia psittacula*, and *Aethia pygmaea*, there is a small scar that contacts the ventral supracondylar tubercle (163:1). This scar marks the attachment point of m. pronator sublimis and in *Aethia barnesi* this scar is located at the proximal point of the ventral supracondylar tubercle as in *Aethia pygmaea* (164:0).

*Remarks*—This specimen was previously referred to *Aethia* by Howard (1982). (Table 5.1; Figs. 5.4 and 5.9). The placement of LACM 107031 in a polytomy with *Aethia cristatella* and *Aethia pygmaea* (Fig. 5.8A) is supported by the proximal position of the m. pronator sublimis scar adjacent to the ventral supracondylar tubercle of the distal humerus. However, the possibility that this specimen is referable to *Aethia rossmoori* cannot be ruled out because the humerus of that taxon is not known. Although, as stated above, my survey of Alcidae ulnae, including the holotype specimen of *Aethia rossmoori*, did not identify any apomorphies that allow isolated ulnae of *Aethia*, *Ptychoramphus*, *Synthliboramphus*, *Brachyramphus*, or *Alle* to be differentiated from one another. It is, therefore, unlikely that the true affinities of *Aethia rossmoori* in Alcidae will ever be known unless a specimen with multiple associated elements including an ulna that is comparable to the holotype ulna of *Aethia rossmoori* is discovered.

***AETHIA STORERI*, sp. nov.**

*Holotype*—a complete left humerus (SDSNH 63195; Table 5.3, Fig. 5.10) collected by R. A. Cerutti on the 11<sup>th</sup> of December, 1994.

*Referred specimens*—distal left humerus (SDSNH 24937; previously referred to *Ptychoramphus tenuis* by Chandler, 1990b; Table 5.3); proximal right humerus (SDSNH 59027; Table 5.3); proximal left humerus (SDSNH 59028; Table 5.3). All referred specimens were collected from the Pliocene San Diego Formation in San Diego County, California, USA. There was no basis for referral of SDSNH 24937 to *Ptychoramphus tenuis* by Chandler (1990b) because the holotype specimen of *Ptychoramphus tenuis* (UCMP 45562) is a tarsometatarsus and there are no known associated specimens of *Ptychoramphus tenuis* that would allow for referral of humeri to that species.

*Etymology*—This species epithet *storeri* is in recognition of the many contributions to ornithology by the late Robert W. Storer (1914-2008).

*Locality and horizon*—Member 4 (sensu Wagner et al., 2001) of the Pliocene San Diego Formation, San Diego County, California, USA. Latitude, longitude, and elevation data are on file at SDSNH (locality 3982). The San Diego Formation predominantly consists of Pliocene and Pleistocene marine sandstones with minor amounts of conglomerates and claystones, which are interpreted as shore-face and shallow depth

shelf facies deposits (Deméré, 1982, 1983; Wagner et al., 2001). Based upon microfaunal analysis and correlation with mammalian and molluscan assemblages of known age, the age of San Diego Formation sediments are estimated to range from 3.6-1.5 Ma (i.e., Middle Pliocene to Pleistocene; Piacenzian-Early Calabrian; Wagner et al., 2001).

*Diagnosis*—*Aethia storeri* is differentiated from all other Aethiini by the convexly rounded margin of the posteriorly overturned head of the humerus (105:0; pointed in *Uria*, *Alle*, and some species of *Alca*). The secondary (i.e., dorsal) pneumotricipital fossa is not divided by a crest beneath posteriorly overturned head of humerus (132:0) as in other Aethiini and extant *Cerorhinca* and Fraterculini. The ventral supracondylar tubercle is triangularly shaped (162:0) as in *Synthliboramphus* rather than rounded as in other Aethiini.

*Anatomical description*—The holotype specimen of *Aethia storeri* (SDSNH 63195) is complete except for a small chip of bone missing at the junction of the bicipital crest and the humeral shaft (Fig. 5.10). Like the recent species *Aethia pusilla*, *Aethia pygmaea* and *Ptychoramphus aleuticus*, the distal edge of the bicipital crest is nearly perpendicular to the humeral shaft (111:1; Fig. 5.11). As in *Aethia pygmaea* the dorsal margin of the primary pneumotricipital fossa (i.e., crus dorsale fossae, Baumel and Witmer, 1993) ends proximal to the junction of the bicipital crest and the humeral shaft (118:0). The m. subcoracoideus scar is positioned more ventrally along the posteroventral margin of the primary pneumotricipital fossa than in other Aethiini (127:1). Character



numbers 132 and 105 (see diagnosis above) could not be evaluated in *Aethia barnesi* because the holotype specimen is missing the proximal end. Within Aethiini only *Aethia pusilla* and *Aethia barnesi* are smaller in size (Table 5.3).

Table 5.3- Measurements of auklet humeri and SDSNH 25358 (in mm). Abbreviations (following Von den Driesch, 1976): **Bd**, breadth of the distal end; **Bp**, breadth of proximal end; **Dd**, distal diagonal; **Dip**, diagonal of proximal end; **Gl**, greatest length; **Sc**, smallest dorsoventral breadth of corpus (shaft). Extant specimen numbers listed in Appendix 1. ‘-’ = data not available due to damage.

Taxa	Specimen #	Bd	Bp	Dd	Dip	Gl	Sc
<i>Ptych. aleuticus</i>	average (n=5)	7.0	9.4	5.0	9.3	45.1	3.4
<i>Aethia cristatella</i>	average (n=5)	8.4	11.5	5.9	11.4	52.3	4.1
<i>Aethia psittacula</i>	average (n=7)	8.7	11.9	6.3	11.3	54.3	4.3
<i>Aethia pusilla</i>	average (n=6)	5.5	7.7	4.0	7.3	34.9	2.5
<i>Aethia pygmaea</i>	average (n=4)	5.9	8.1	4.3	7.8	37.9	2.8
<i>Aethia barnesi</i>	LACM 107031	5.0	-	3.4	-	-	2.7
<i>Aethia storeri</i>	SDSNH 63195	6.2	9.0	5.3	8.1	41.0	2.7
<i>Aethia storeri</i>	SDSNH 24937	6.2	-	5.0	-	-	2.8
<i>Aethia storeri</i>	SDSNH 59027	-	9.0	-	8.4	-	3.1
<i>Aethia storeri</i>	SDSNH 59028	-	9.2	-	8.4	-	-
<i>Alcidae</i> <u>indet.</u>	SDSNH 25358	5.3	-	4.1	-	-	2.3

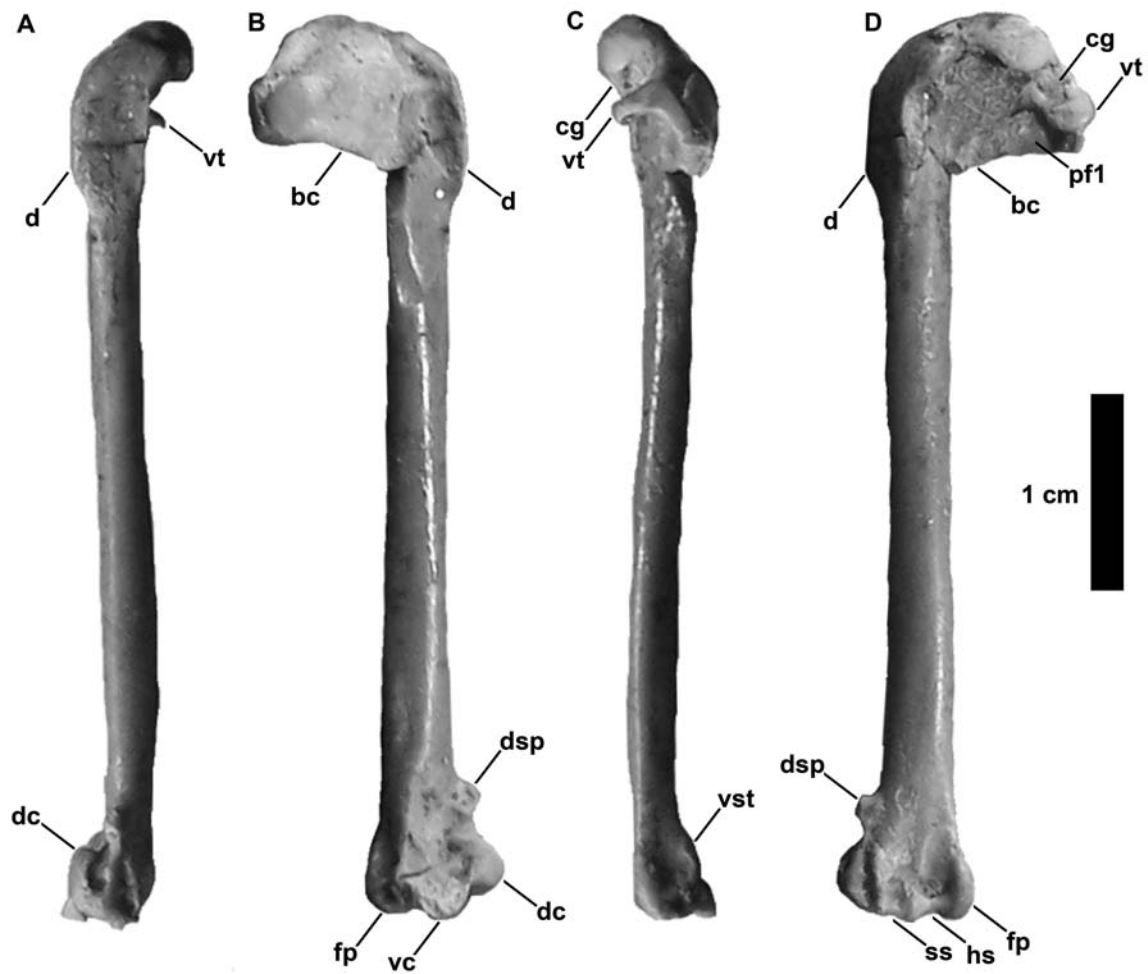


Figure 5.10- Holotype left humerus of *Aethia storeri* (SDSNH 63195) in **A.** dorsal view, **B.** anterior view, **C.** ventral view, and **D.** posterior view. Anatomical abbreviations: (**bc**) bicipital crest; (**cg**) capital groove; (**d**) deltopectoral crest; (**dc**) dorsal condyle; (**dsp**) dorsal supracondylar process; (**fp**) flexor process; (**hs**) humerotricipital sulcus; (**pf1**) primary pneumotricipital fossa; (**ss**) scapulotricipital sulcus; (**vc**) ventral condyle; (**vst**) ventral supracondylar tubercle; (**vt**) ventral tubercle.

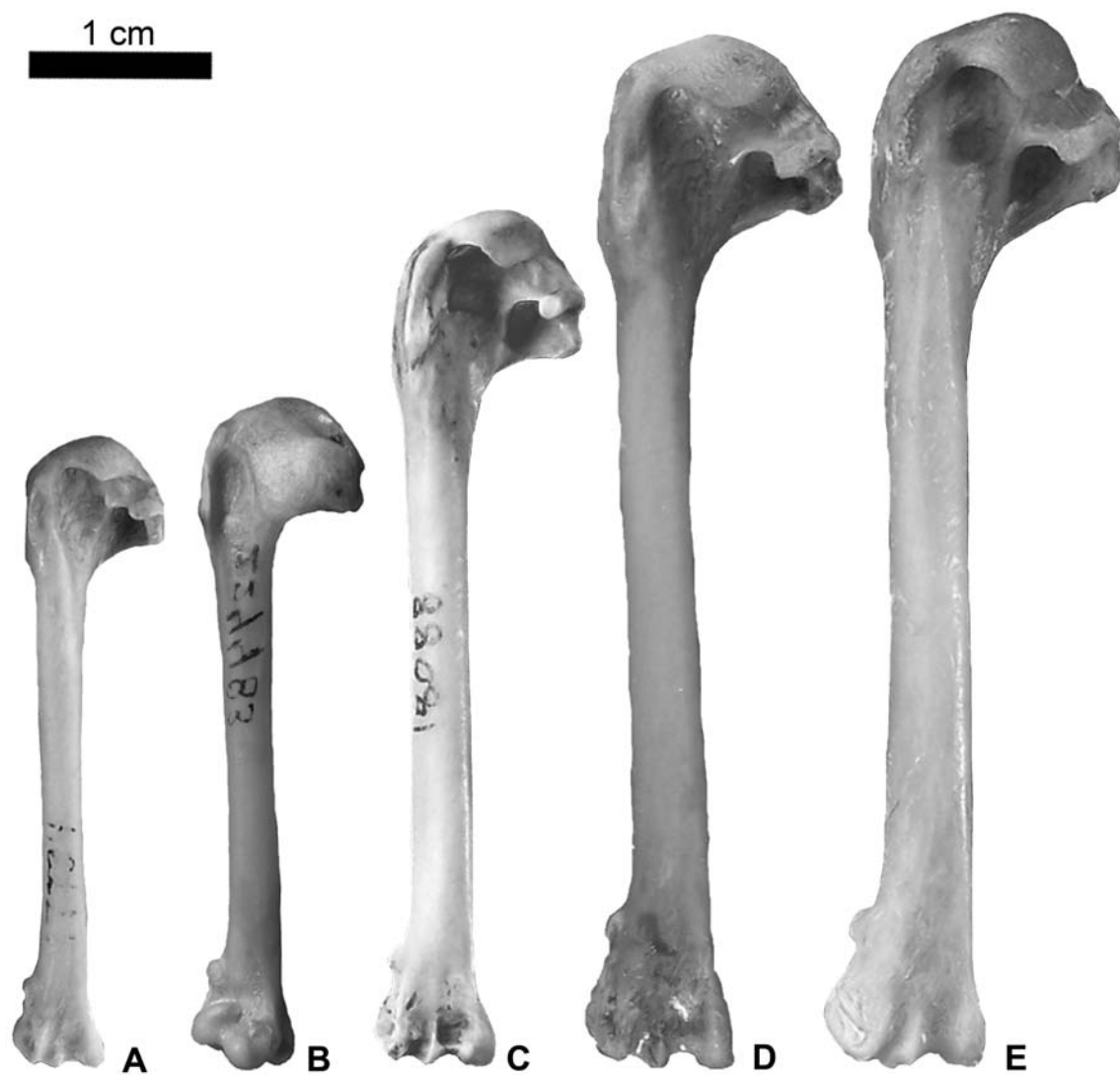


Figure 5.11- Comparison of extant auklet left humeri in posterior (**A, C, D, E**) and anterior (**B**) views. **A.** *Aethia pusilla* (NCSM 17734); **B.** *Aethia pygmaea* (UMMZ 224883, specimen mislabeled 224483 in photo; specimen image flipped for comparison); **C.** *Ptychoramphus aleuticus* (NCSM 18088); **D.** *Aethia cristatella* (NCSM 17746); **E.** *Aethia psittacula* (NCSM 14804).

### PAN-ALCIDAE indet.

*Referred specimen*—a distal right humerus (SDSNH 25358; Table 5.3; Fig. 5.12) collected by D. Baer and J. A. Lillegraven on the 2<sup>nd</sup> of May, 1970.

*Locality and horizon*—Middle Miocene (14-16 Ma) La Misión Local Fauna of the Los Indios Member of the Rosarito Beach Formation of Baja California, Mexico (Deméré et al., 1984). Latitude, longitude, and elevation data are on file at SDSNH (locality 3459).

*Anatomical description*—Although the proximal end of SDSNH 25358 is missing (Fig. 5.12), the specimen is otherwise well preserved with respect to fine morphological details. The ventral margin of the distal humeral shaft (i.e., ventral epicondyle) is ventrally projected as in the Fraterculinae (150:0) and many non-alcid charadriiforms (e.g., *Sterna niloteca*), rather than straight as in most Alcinae (e.g., *Uria lomvia*). The ventral supracondylar tubercle (i.e., anterior articular ligament scar; *sensu* Howard, 1929) is rounded (162:1) like that of all Fraterculinae except *Aethia storeri*. As in *Alle alle*, *Aethia barnesi*, and *Synthliboramphus rineyi*, the scapulotricipital sulcus is broader than the humerotricipital sulcus (151:2). The anterior face of the ventral humeral condyle is flattened (157:1) as in all Pan-Alcidae except Mancallinae. As in all Alcidae the dorsal supracondylar process is proximally extended along the shaft of the humerus and projects dorsally to a degree that is less (147:1) than that of most other charadriiforms (e.g., *Larus*

*marinus*. SDSNH 25358 is differentiated from all other Pan-Alcidae by having the scapulothoracic sulcus of the distal humerus bifurcated lengthwise (i.e., proximodistally) by a crest (152:2; Fig. 5.12). Additionally, the humeral shaft is less dorsoventrally compressed than in all pan-alcids (145:0) including *Cepphus* Moehring, 1758 and *Pseudocepphus teres* Wijnker and Olson, 2009.

*Remarks*—SDSNH 25358 was previously described by Deméré et al. (1984) as part of a report on the paleontology of the Rosarito Beach Formation. The diagnostic characteristic of this specimen, the bifurcated scapulothoracic sulcus, was noted by Deméré et al. (1984). However, they refrained from designating the specimen as the holotype of a new taxon at that time because of a lack of comparative material. SDSNH 25358 possesses a combination of characters found in Fraterculinae (e.g., ventrally flared ventral epicondyle, 150:0; triangular ventral supracondylar tubercle, 162:0); hence its inclusion here along with the treatment of fossil auklets.

## DISCUSSION

The relatively slender proportions of the shaft and the trochlea of the holotype tarsometatarsus of *Ptychoramphus tenuis* (UCMP 45662), and all morphological characters scored for UCMP 45662 are consistent with that of the extant species *Ptychoramphus aleuticus*. Based upon the phylogenetic results, which place UCMP

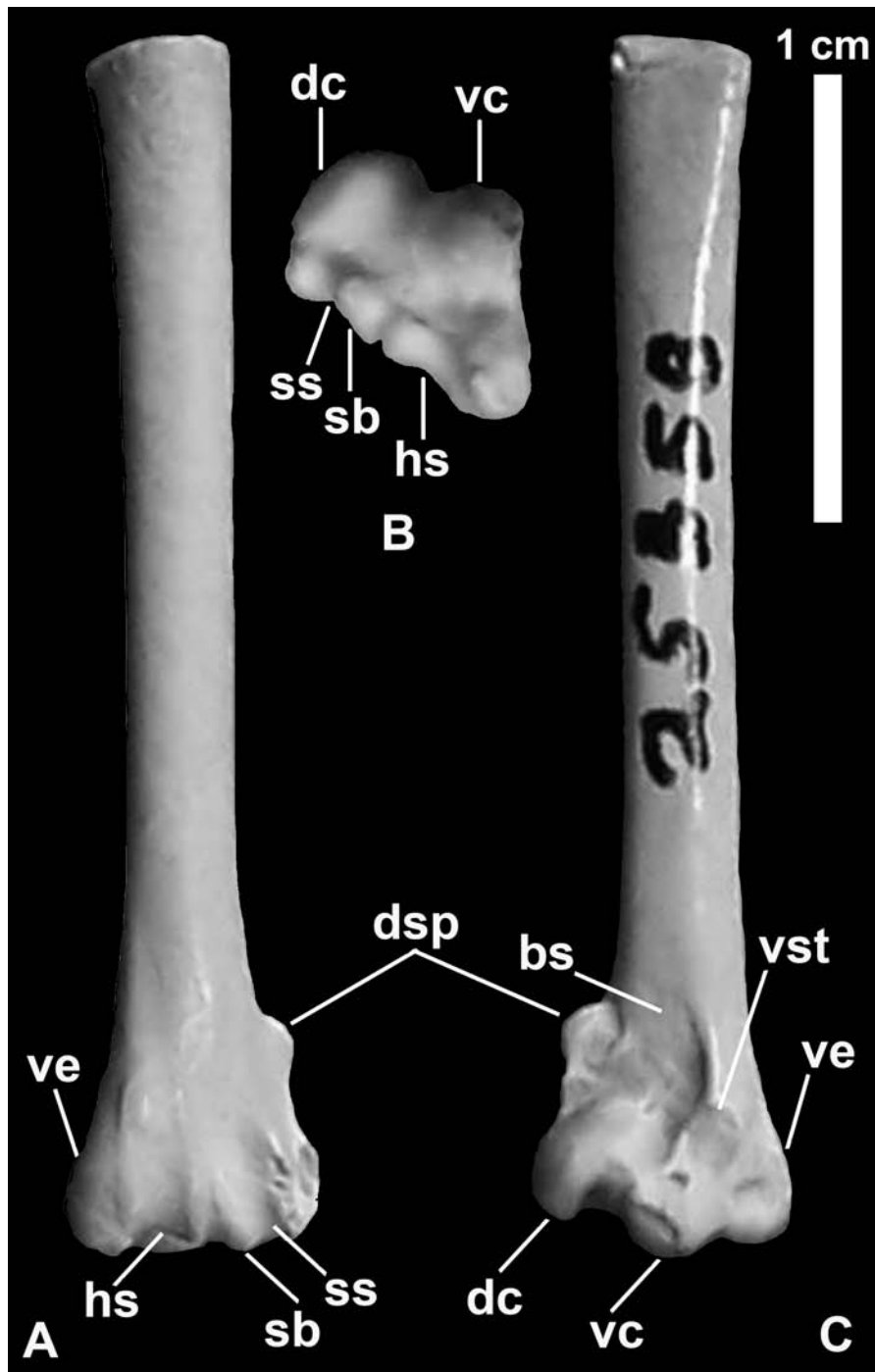


Figure 5.12- SDSNH 25358 in posterior (A), distal (B), and anterior (C) views. Anatomical abbreviations: bicipital crest (**bc**); dorsal condyle (**dc**); dorsal supracondylar process (**dsp**); humerotricipital sulcus (**hs**); scapulotricipital bifurcation (**sb**); scapulotricipital sulcus (**ss**); ventral condyle (**vc**); ventral epicondyle (**ve**); ventral supracondylar tubercle (**vst**).

45662 as the sister taxon to *Ptychoramphus aleuticus* (Fig. 5.5), *Ptychoramphus tenuis* is best considered a nomen dubium.

A survey of alcid ulnae did not identify any apomorphies that allow isolated ulnae of *Aethia*, *Ptychoramphus*, *Synthliboramphus*, or *Brachyramphus* to be differentiated from one another. Because the phylogenetic results place *Aethia rossmoori* in an unresolved position at the base of Alcidae (Fig. 5.6), *Aethia rossmoori* is best considered *Alcidae incertae sedis*.

Although the systematic positions of *Aethia barnesi* and *Aethia storeri* are unresolved in the strict consensus topology (Fig. 5.7), their inclusion in a monophyletic Aethiini does provide definitive evidence that auklets were a part of the Miocene and Pliocene avifauna of the eastern Pacific Ocean basin. Additionally, *Aethia barnesi* is the earliest fossil record of Fraterculinae (6.7-10.0 Ma; Late Miocene or Turtonian equivalent; Barnes et al., 1981; Domning and Deméré, 1984) and provides a calibration point (i.e., minimum age of 6.7 Ma) for the divergence between Aethiini and Fraterculini.

The systematic position recovered for SDSNH 25358 as the sister taxon to Alcidae is intriguing because, including the Mancallinae, this would potentially be the second record of stem alcids in the Miocene of the Pacific Ocean basin. However, given the inclusion of only two non-alcid charadriiforms in the phylogenetic analysis (i.e., *Larus marinus* and *Stercorarius skua*), the inclusion of SDSNH 25358 in Pan-Alcidae is not strongly supported. Referral of SDSNH 25358 to Pan-Alcidae will require its inclusion in a morphology-based phylogenetic analysis including a broad sample of non-alcid charadriiforms (i.e., dense taxonomic sampling of Charadrii, Lari, and Scolopaci),

and morphological comparison with other seabirds and shorebirds. The total current taxonomic sample (i.e., in this dissertation) of extant non-alcid charadriiforms consists primarily of *Lari* species and is limited to 2 species of Charadrii and 4 species of Scolopaci (see Fig. 1.26). SDSNH 25358 is not designated as the holotype of a new specimen at this time because morphological comparisons between SDSNH 25358 and all of Charadriiformes will be necessary to determine if this specimen represents a new taxon.

With respect to the morphology of SDSNH 25358, the ventrally flared ventral margin of the distal humeral shaft (150:0) is an apomorphy of Fraterculinae within Alcidae, but is also characteristic of many other outgroup charadriiforms (e.g., *Larus marinus*). Dorsoventral compression of the humeral shaft is an apomorphy of Pan-Alcidae. The degree of compression in SDSNH 25358 is reminiscent, albeit less than that seen in *Cepphus*. However, the combination of character states otherwise known exclusively in Fraterculinae or Alcinae (e.g., *Cepphus*) may be responsible for the placement of SDSNH 25358 as the sister taxon to all other Alcidae in the results of the phylogenetic analysis. More complete specimens of this potentially new taxon are needed to facilitate further evaluation of its systematic position.

Detailed examination of alcid fossils continues to reveal previously undocumented diversity among Miocene and Pliocene remains, with eleven new species recognized since 2007 (Smith et al., 2007; Wijnker and Olson, 2009; Smith and Clarke, in press; also see Chapters 2 3, and 4). Only a single auklet species from the Miocene and one from the Pliocene are currently known (i.e., *Aethia barnesi* and *Aethia storeri*).



Table 5.4- Summary of taxonomic revisions.

Original Taxonomic Assignment	Reference	Specimen #	Revised Taxonomic Assignment
<i>Ptychoramphus tenuis</i>	Miller and Bowman, 1958	UCMP 45562	<i>nomen dubium</i>
<i>Aethia rossmoori</i>	Howard, 1968	LACM 18948	Alcidae incertae sedis
<i>Aethia</i> sp.	Howard, 1978	LACM 37686	Specimen lost ?
<i>Aethia</i> sp.	Howard, 1982	LACM 107031	<i>Aethia barnesi</i>
Alcidae indet.	Deméré et al. 1984	SDSNH 25358	Alcidae indet.

However, sparse and often fragmentary remains of auklets reported in the last century (Table 5.1) and auklet fossils described herein, suggest that independent lineages of small alcids have been a part of the Pacific Ocean avifauna since at least the Late Miocene. The small size of early alcids such as SDSNH 25358 and extant auklets in combination with the basal position hypothesized for small Alcinae taxa *Brachyramphus* and *Synthliboramphus* (Thomas et al., 2004; Pereira and Baker, 2008) suggests that small body size may be a plesiomorphy of Alcidae. However, the earliest known pan-alcid fossil is comparable in size to extant specimens of *Alca torda*, one of the largest extant alcids (Chandler and Parmley, 2002; del Hoyo et al, 1996) and the stem alcid lineage Mancallinae displays a range of sizes from quite small (e.g., *Mancalla vegrandis*) to quite large (e.g., *Miomancalla howardi*; Smith, 2011).

Body size in extant alcids has been correlated with dive depth and feeding ecology (Piat and Nettleship, 1985; Prince and Harris, 1988; Watanuki and Burger, 1999), and smaller body size in extant alcids is associated with planktivory (Bradstreet

and Brown, 1985). Although planktivory is optimized as pleisiomorphic for Aethiini based upon extant auklets, it would be premature to ascribe ecological attributes such as planktivory to these extinct species of auklets in the absence of associated skeletal remains that preserve characteristics associated with particular feeding strategies (i.e., bill shape; Bédard, 1969). However, the co-occurrence of multiple species of small alcids with multiple species of larger alcids such as the flightless Mancallinae auks suggests that niche partitioning by size among alcids may have been in place since the Miocene.

Although the Early to Middle Miocene was a time of relative warmth, little or no glacial activity, and relatively unstratified oceans, this time period was immediately followed by a cooling trend that has led to the cooler temperatures, prevalent Northern Hemisphere glaciation, and temperature stratified oceans of today (Schoell et al., 1994; You et al., 2009; Westerhold et al., 2005). The Middle Miocene Climatic Optimum (MMCO) and the cooling trend that followed have been documented using a variety of methods including oxygen and carbon isotope stratigraphy, palynology, and magnetostratigraphy (Schoell et al., 1994; Krijgsman et al., 1994; You et al., 2009; Westerhold et al., 2005). The age range of fossils described herein (~16-3 Ma) bracket the transition from a warmer climate in the Middle Miocene to a colder climate at the end of the Pliocene. This cooling trend was punctuated by several episodes of potentially intense Northern Hemisphere glaciation that would have dramatically decreased sea level. One such episode between 13.8-10.4 Ma would have resulted in an ~40m drop in global sea level (Westerhold et al., 2005). The severity of such an event with respect to the reproductive success and ultimately the survival of pelagic birds such as auklets may

have been significant given the tendency of extant auklets for nest site fidelity (Ainley, 1990).

The age of SDSNH 25358 corresponds with the timing of the Middle Miocene Climatic Optima (~15 Ma). Sea surface temperatures for the MMCO are estimated at ~3°C higher than today, near the levels predicted to result from global warming in the next century (You, et al., 2009). Because sea surface temperature has been correlated with reproductive success in alcids, with warmer temperatures leading to decreased reproduction in planktivorous alcids (Kitaysky and Golubova, 2000), the post-MMCO cooling trend may offer an explanation for the faunal turnover among Miocene and Pliocene alcids. The fossil record provides evidence that alcids were successful, potentially dominant seabirds throughout the Middle Miocene and Early Pliocene (Wijnker and Olson, 2009; Smith, 2011; Smith and Clarke, in press). However, there are very few examples of alcids species that span this time period. Thus, it would appear that the Miocene-Pliocene boundary represents a faunal turnover for alcids similar to the one documented for the Pliocene-Pleistocene climatic transition.

## CONCLUSIONS

The two new species of *Aethia* described herein add to our knowledge of Miocene and Pliocene auklet diversity, and the potential new taxon represented by SDSNH 25358 demonstrates that Miocene diversity may have included at least one pan-alcid taxon that

was previously unknown. These new discoveries, along with the phylogenetic evaluation of previously referred potential fossil auklets provide a more detailed picture of the evolution of these clades and also provide phylogenetically analyzed calibration points for molecular-based divergence estimation.

Given the basal placement of *Aethia storeri* in Aethiini in the results of the combined phylogenetic analysis, the small quantity of morphological characters that separate *Aethia* and *Ptychoramphus*, and the dubious status of the only fossil referred to *Ptychoramphus* (i.e., *Ptychoramphus tenuis*), the monotypic taxon *Ptychoramphus* should be considered for synonymy with *Aethia* by the American Ornithologists' Union.

There are few differences in range of size (Table 5.3) or morphological characteristics (Appendix 3) between the newly described extinct auklets *Aethia barnesi* and *Aethia storeri* and extant auklets, and known auklet fossil localities are within the range of extant auklets (Fig. 5.1). These data suggest that the ecology of auklets may have changed little since the Late Miocene and that the auklet avifauna of the past 5-10 Ma may have resembled their extant congeners. One unanswered question is why this clade has not colonized the Atlantic Ocean basin, where only a single small planktivorous alcid, *Alle alle*, is endemic today. The feeding ecology of other small extinct Atlantic Ocean Alcini (e.g., *Miocepphus mergulellus* and *Alca minor*) are not known. Regardless of the feeding ecology of these other small Atlantic Ocean alcids, current data suggest that the small, primarily planktivorous, Atlantic Ocean alcid niche has been occupied solely by *Alle alle* since at least the late Pliocene.

The restriction of auklets to the Pacific Ocean basin and the relatively low degree of morphological and size changes in auklets through time might be viewed as evidence of ecological stability and may be a reflection of a relatively limited set of environmental tolerances in this clade. Although not considered endangered by the International Union for Conservation of Nature (IUCN) because of the relatively large size of their geographic range and relatively large numbers of mature individuals, population sizes of extant auklets are decreasing (IUCN, 2010). Links between large-scale-climatic factors that affect auklet prey species (i.e., primary marine productivity) and adult auklet survival and reproductive rates have been demonstrated (Springer et al., 1993; Jones et al., 2002). Although most records involve short-term trends (e.g., responses to decadal cycles of the California Current System; Yen et al., 2004), population-level changes associated with large-scale and more long-lasting environmental events have been documented. For example, the colonization of the Farallon Islands by *Ptychoramphus aleuticus* between 1870 -1900 was proposed to be directly related to the end of a prolonged episode of tropical warm water intrusion into the North Pacific (Springer et al., 1993), and today *Ptychoramphus aleuticus* is one of the most abundant species on the Farallon Islands (Ainley, 1990). It is unknown if the scale of population decline experienced by other alcids in response to climatic change is similar to that of auklets. However, given the ability of *Ptychoramphus* to track suitable prey and environmental conditions, it is even more surprising that fossil records of Aethiini are relatively rare and restricted to the Pacific Ocean basin.

Although Miocene alcid diversity was once considered insignificant (Brodkorb, 1967; Olson, 1985) in comparison with much more well-known Pliocene alcid faunas (Olson and Rasmussen, 2001; Chandler, 1990b), a more complete picture of Miocene alcid diversity is emerging from recent re-examination of alcid fossil remains (Wijnker and Olson, 2009; Smith, 2011). Even though the alcid fossil record is by far the most complete among Charadriiformes, previous divergence estimates suggest that the early fossil record of alcids is still significantly incomplete (Baker et al., 2007; Pereira and Baker, 2008). Therefore, Eocene and Oligocene localities with marine sediments that have produced other vertebrates often found in association with alcid remains (e.g., sharks and whales) should be targeted for collection of fossils that may elucidate the early history of Pan-Alcidae.

## CHAPTER 6.

The fossil record and phylogeny of the guillemots  
(Pan-Alcidae, Cepphini)

## INTRODUCTION

Alcidae (Aves, Charadriiformes) are pelagic seabirds with a geographic range extending across the Northern Hemisphere. Extant alcid diversity includes auks, murres, auklets, murrelets, puffins, and guillemots. Extant guillemots have a Holarctic range (Fig. 6.1), are moderately sized in comparison with smaller auklets and murrelets and larger murres and auks, and are placed together in the taxon *Cepphus* Moehring, 1758.

Guillemots are generalist feeders, with a diet consisting of a variety of vertebrate and invertebrate prey, generally captured in relatively shallow water compared to more deep diving alcids such as murres (del Hoyo et al., 1996). Characteristics of extant guillemots that differentiate them from other alcids include red mouth lining and foot scales, and darkly colored, rather than lightly colored belly plumage during the breeding season.

Guillemots have terete bills like those of murres and murrelets, rather than the mediolaterally compressed bills of puffins and true auks (i.e., *Alca* and *Pinguinus*).

Extant Atlantic Ocean guillemot diversity includes only the Black Guillemot *Cepphus grylle* Linnaeus, 1758, whereas Pacific Ocean guillemot diversity also includes the Pigeon Guillemot *Cepphus columba* Pallas, 1811, and the Spectacled Guillemot *Cepphus carbo* Pallas, 1811. Guillemots were considered by Storer (1952) to be more representative of the ancestral alcid stock than other extant alcids, although the classification of Storer (1960) did not place them at the base of the alcid tree.

Monophyly of extant *Cepphus* species is supported by analyses of morphological and molecular sequence data (Strauch, 1985; Chandler 1990a; Moum et al., 1994; Friesen



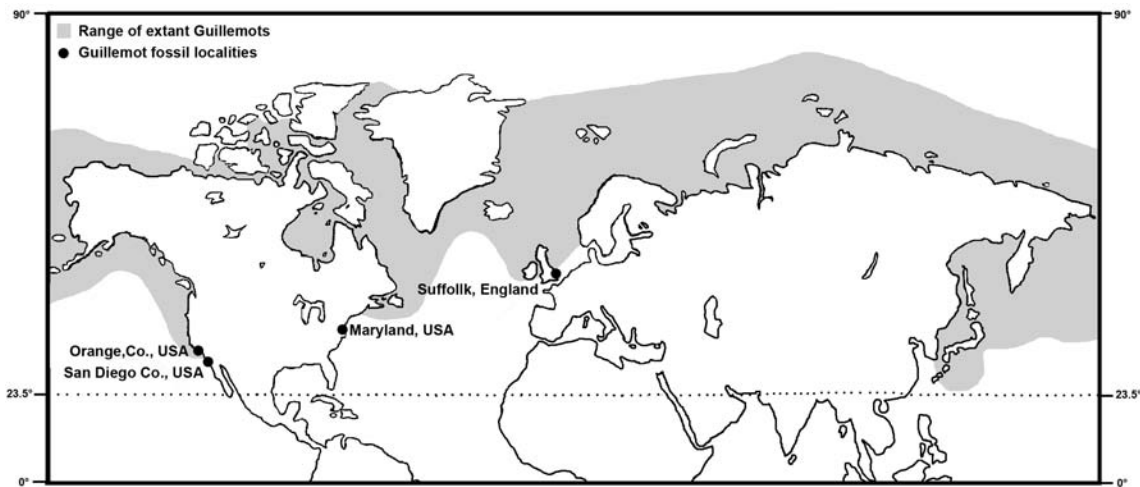


Figure 6.1- World map depicting guillemot fossil localities and the range of extant guillemot species (based on del Hoyo et al., 1996).

et al., 1996; Thomas et al., 2004; Pereira and Baker, 2008; Smith, 2011). The guillemot clade has been recovered in a variety of systematic positions within Alcidae. The morphology-based compatibility analysis of Strauch (1985) placed *Cepphus* as the sister taxon to *Synthliboramphus* a result that has not been supported in the results of subsequent analyses (Watada et al., 1987; Chandler, 1990a; Moum et al., 1994; Friesen et al., 1996; Thomas et al., 2004; Baker et al., 2007; Pereira and Baker, 2008; Smith, 2011). *Cepphus carbo* was placed as the sister taxon to *Uria lomvia* in the genetic distance analysis of Watada et al. (1987), whereas *Cepphus* was placed in at the base of an *Alle* + *Fraterculinae* (i.e., the auklets and puffins) clade in the morphology-based results of Chandler (1990a; i.e., not recovered in Alcinae). More recent analyses of mitochondrial DNA sequence data have all placed *Cepphus* in various positions in Alcinae (i.e., not closely allied with the auklets and puffins). *Cepphus* was recovered as the sister taxon to *Synthliboramphus* + *Brachyramphus* in the results of Moum et al. (1994), and was

recovered in an unresolved position at the base of Alcinae (contents of Alcinae include *Alca*, *Pinguinus*, *Uria*, *Alle*, *Miocepphus*, *Cepphus*, *Synthliboramphus*, *Brachyramphus*) by Friesen et al. (1996). *Cepphus* was placed in an unresolved position at the base of a clade composed of all Alcidae except *Brachyramphus* (i.e., *Brachyramphus* was recovered as the sister taxon to all other Alcidae) in the phylogenetic results of Thomas et al. (2004). *Cepphus columba* was recovered as the sister taxon to *Synthliboramphus antiquus* + Alcini Storer, 1960 (contents of Alcini include *Alca*, *Pinguinus*, *Uria*, *Alle*, *Miocepphus*) in the results of Baker et al. (2007). The analysis of Pereira and Baker (2008) was the first to include nuclear DNA sequence data sampled from all three extant species of *Cepphus*, and placed the guillemots as the sister taxon to *Synthliboramphus* + Alcini. *Cepphus* was recovered as the sister taxon to Alcini in the combined phylogenetic analysis by Smith (2011). In summary, although there is some congruence among the results of recent molecular-based phylogenetic analyses with respect to the inclusion of *Cepphus* in Alcinae, the position of *Cepphus* within Alcinae remains uncertain.

With regard to relationships within *Cepphus*, the Pacific endemic species (Spectacled Guillemot and Pigeon Guillemot) have been consistently recovered as sister taxa to the exclusion of the primarily Atlantic endemic Black Guillemot in analyses of molecular sequence data (Friesen et al., 1996; Kidd and Friesen, 1998; Thomas et al., 2004; Pereira and Baker, 2008) and in the combined analysis of Smith (2011). In contrast to molecular sequence-based and combined data hypotheses, the only morphology-based analysis to include all three extant species of *Cepphus* placed the Spectacled Guillemot as the sister taxon to the other guillemots (Chandler, 1990a). In a

study of *Cepphus* mitochondrial control sequence variation Kidd and Friesen (1998) found evidence that extant species of guillemots are recently diverged from one another (i.e., Pleistocene or later). Although a recent divergence between extant *Cepphus* species offers a potential explanation for incongruence between the placements of *Cepphus* species in different analyses, it does not explain the incongruence between hypotheses for the systematic placement of *Cepphus* in Alcidae. The fossil record of *Cepphus* extends back at least into the Late Miocene (Howard, 1982), allowing ample time for divergence from other clades of alcids. If as Kidd and Friesen (1998) suggest, extant species of *Cepphus* are quite recently diverged, then the inclusion of *Cepphus* fossil taxa in a phylogenetic analysis may help to resolve the systematic position of *Cepphus*. *Cepphus* fossils may preserve phylogenetically informative character states that are ancestral for the clade, and that are not retained in extant *Cepphus* species. Extinct species of guillemots have not been previously included in a phylogenetic analysis.

***A Review of the fossil record of guillemots:*** Guillemot fossil remains are relatively rare in comparison with other alcids, with only three individual specimens referred to Cepphini Storer, 1960 (i.e., the clade including extant and extinct guillemots; Harrison, 1977; Howard, 1978, 1982), and an additional six specimens referred to the taxon *Pseudoceppus* (Wijnker and Olson, 2009; Table 6.1). Despite its name, the taxon *Miocepphus* Wetmore, 1940 is not included in Cepphini (Olson, 1985; Olson and Rasmussen, 2001; Wijnker and Olson, 2009; Smith and Clarke, in press).

Table 6.1- Previously published guillemot fossil remains.

Taxon	Material	Provenience	Age	Reference
<i>Cepphus storeri</i>	carpometacarpus	England	Pleistocene	Harrison, 1977
<i>Cepphus</i> sp.	proximal ulna	California	Late Miocene	Howard, 1978
<i>Cepphus olsoni</i>	humerus	California	Late Miocene	Howard, 1982
<i>Pseudoceppus teres</i>	humeri	Maryland	Middle Miocene	Wijnker and Olson, 2009

The first report of guillemot fossil remains was that of Harrison (1977), who described *Cepphus storeri* based upon a partial left carpometacarpus (NHMUK PV A 4986; formerly numbered as BMNH A 4986) from the Pleistocene Red Crag of Suffolk, England (Figure 6.2). *Cepphus storeri* was diagnosed primarily based upon overall differences in size and relative proportions with extant species of *Cepphus* (Harrison, 1977).

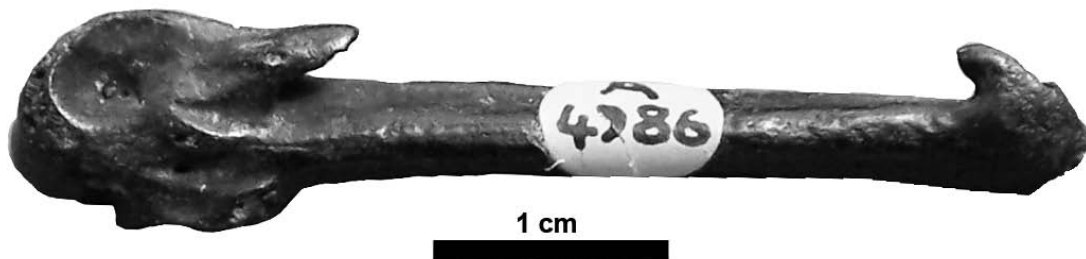


Figure 6.2- Holotype left carpometacarpus of *Cepphus storeri* (BMNH A 4986) in ventral view.

A proximal ulna (LACM 47045) from the Late Miocene Monterey Formation of Orange County, California, USA (LACM locality 6906) was tentatively referred to *Cepphus* by Howard (1978). LACM 47045 was not figured in publication (Howard,

1978) and its whereabouts are currently uncertain. An empty specimen box with a temporary loan tag labeled 'Hildegard Howard study cabinet' was found during a thorough search of the LACM collections in 2007. Because it could not be located, LACM 47045 is not considered further herein.

*Cepphus olsoni* was described by Howard (1982) based upon a right humerus (LACM 107032) from the San Luis Rey River Local Fauna of the Late Miocene San Mateo Formation (Fig. 6.3). This study represents the first time that scorings for this species have been included in a phylogenetic analysis.

Six partial humeri were referred to the monotypic taxon *Pseudoceppus* by Wijnker and Olson (2009). As noted by Wijnker and Olson (2009), and implied by the name of this taxon, the rounded shaft of *Pseudoceppus teres* is like that of *Cepphus* (i.e., less dorsoventrally compressed than that of other Pan-Alcidae). The rounded shape (in cross-section) of the humeral shaft was considered plesiomorphic by Wijnker and Olson (2009), and those authors hypothesized affinity between *Pseudoceppus* and Alcini (contents of Alcini include *Alca*, *Pinguinus*, *Alle*, *Miocepphus*, and *Uria*). Although there is some morphological support for placement of *Pseudoceppus* in Alcini, preliminary phylogenetic results supported a close systematic relationship between *Pseudoceppus* and *Cepphus*, hence its inclusion here.

Previously described guillemot remains, extant species of guillemots, other species of extant alcids, and charadriiform outgroup taxa are evaluated through phylogenetic analyses to assess the systematic positions of these taxa. Taxonomic revisions are provided based on the results of the phylogenetic analyses. Implications for

the evolution of Cepphini are discussed in the context of revised estimates of Cepphini species richness and the results of the phylogenetic analyses.

## MATERIALS AND METHODS

In the anatomical descriptions, the English equivalents of the Latin osteological nomenclature summarized by Baumel and Witmer (1993) are used. The terminology of Howard (1929) is followed for features not treated by Baumel and Witmer (1993). With the exception of the terms anterior and posterior substituted for cranial and caudal, respectively, the terms used for the anatomical orientation of a bird are those of Clark (1993). Measurements follow those of Von den Driesch (1976). All measurements were taken using digital calipers and rounded to the nearest tenth of a millimeter. With the exception of species binomials, all taxonomic designations (e.g., Fraterculini) are clade names and are not intended to convey rank under the Linnaean system of nomenclature, regardless of use of italics or previous usage by other authors.

Morphological characters were scored for all 23 extant alcids, the recently extinct Great Auk *Pinguinus impennis*, and extinct guillemot taxa. A gull, *Larus marinus*, and a skua, *Stercorarius skua*, were included as charadriiform outgroup taxa. See Appendix 2 for morphological character descriptions and Appendix 3 for morphological character scorings used in the phylogenetic analysis.

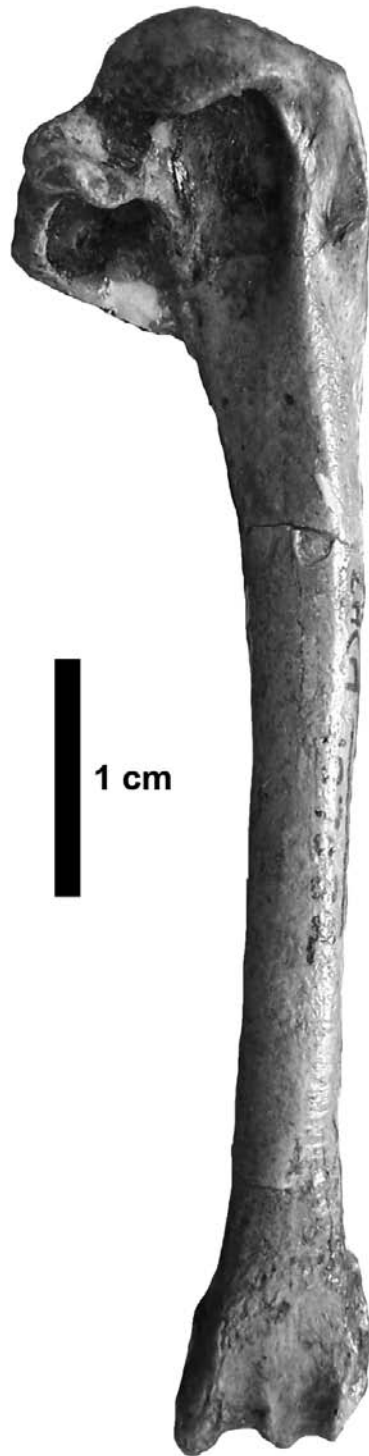


Figure 6.3- Holotype right humerus of *Cepphus olsoni* (LACM 107032) in posterior view.

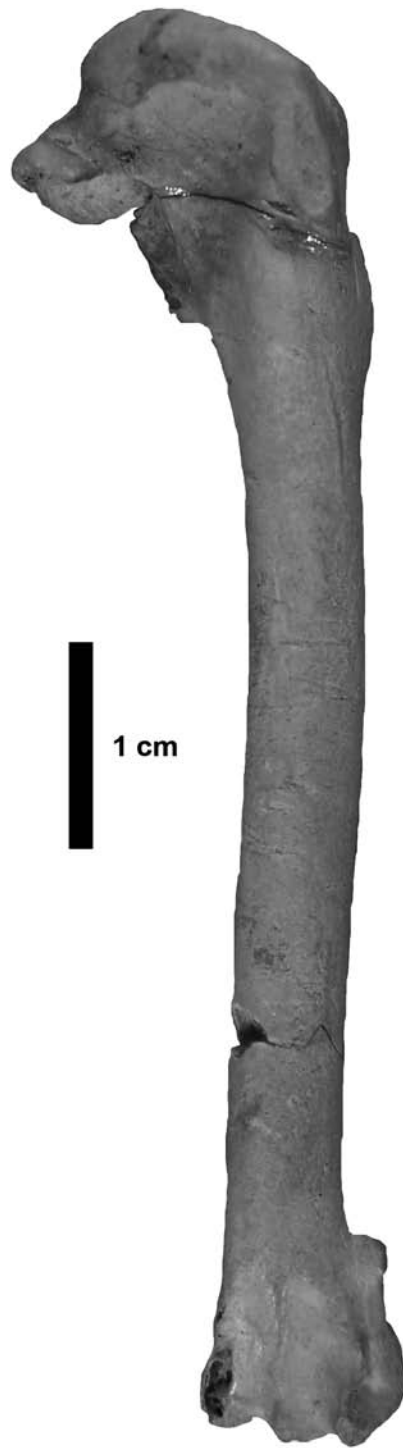


Figure 6.4- Holotype right humerus of *Pseudocephalus teres* (USNM 214537) in posterior view.



Morphological characters include osteological ( $n = 232$ ), integumentary ( $n = 32$ ), reproductive ( $n = 11$ ), dietary ( $n = 2$ ), myological ( $n = 24$ ) and micro-feather ( $n = 52$ ). One hundred and sixty-four characters were developed for this analysis. The other 189 characters were drawn from the work of Hudson et al. (1969;  $n = 24$ ), Strauch (1978, 1985;  $n = 39$ ), Chandler (1990a;  $n = 63$ ), Chu (1998;  $n = 11$ ), and Dove (2000;  $n = 34$ ). Only 34 of the 38 characters used by Dove (2000) varied in the taxa examined in this study. Of the 34 used in this analysis, eighteen were modified (i.e., split into 2 separate characters) according to the philosophy of character independence proposed by Hawkins et al. (1997), resulting in a total of 52 microfeather characters.

Whenever possible, five or more specimens of each extant species, and both sexes were evaluated to account for intraspecific character variation and potential sexual dimorphism respectively (Appendix 1). Only adult specimens, assessed based upon degree of ossification (Chapman, 1965), were evaluated, and whenever possible specimens from multiple locations within the geographic range of extant species (i.e., sub-species) were examined to account for geographic variation. Characters for all extinct taxa were coded from direct observation of holotype and referred specimens. Pleistocene and Holocene remains that have been referred to extant species (Lambrect, 1933; Brodkorb, 1967; Tyrberg, 1998) were not examined and are not treated further in this study.

Previously published molecular sequence data (mitochondrial: ND2, ND5, ND6, CO1, CYTB; ribosomal RNA: 12S, 16S; and nuclear: RAG1) were downloaded from GenBank (<http://www.ncbi.nlm.nih.gov/genbank>; see Appendix 4 for sequence

authorship). Preliminary sequence alignments were obtained using the program ClustalX v2.0.6 (Thompson et al., 1997), and then manually adjusted using the program Se-Al v2.0A11 (Rambaut, 2002). Alignment and concatenation of sequence data resulted in a final molecular matrix of 11601 base pairs. Molecular sequence data were combined with morphological characters for a matrix of 11,954 characters.

A combined approach of phylogeny estimation was used to evaluate the systematic position of guillemot species. Parsimony-based phylogenetic analyses implemented in PAUP\* v4.0b10 (Swofford, 2002) used the following tree-search parameters: heuristic search strategy; 10,000 random taxon addition sequences; tree bisection-reconnection branch swapping; random starting trees; all characters equally weighted; minimum length branches = 0 collapsed; multistate (e.g., 0&1) scorings used only for polymorphism. Bootstrap values and descriptive tree statistics (e.g., CI, RI, RC) were calculated using PAUP\* v4.0b10 (Swofford, 2002). Bootstrap value calculation parameters included 1,000 heuristic replicates, 100 random addition sequences per replicate. All other settings were the same as the primary analysis. Bremer support values were calculated using a script generated in MacClade v4.08 (Maddison and Maddison, 2005) and analyzed with PAUP\* v4.0b10 (Swofford, 2002). Based on the results of previous phylogenetic analyses of charadriiform relationships (Strauch, 1978; Sibley and Ahlquist, 1990; Chu, 1995; Ericson et al., 2003; Paton et al., 2003; Thomas et al., 2004; Baker et al., 2007) resultant trees were rooted with *Larus marinus*. Because the characters reported by Wijnker and Olson (2009) were not phylogenetically analyzed, these

characters were subjected to phylogenetic analyses herein to facilitate comparison between their hypothesis of relationships and that recovered in this study.

Note that Wijnker and Olson (2009) apply the Linnaean subfamily rank of Alcinae Leach, 1820 to the clade referred to herein as Alcini Storer, 1960 (contents of Alcini include *Alca*, *Pinguinus*, *Uria*, *Alle*, *Miocepphus*), and that herein, the clade name Alcinae is applied to a more inclusive clade composed of Alcini + *Synthliboramphus* + *Brachyramphus* + Cepphini. Wijnker and Olson cited Leach, 1820 as taxonomic authority for Alcinae; however, Leach (1820:70) makes no mention of subfamily ranks within his Family ‘Alcadae’, which includes “puffin, awk, rasorbill, and seadove”. Although early versions of the American Ornithologists’ Union classification (AOU, 1895) include only *Alca*, *Pinguinus*, *Uria*, and *Alle* in subfamily Alcinae, that classification also included *Cepphus*, *Brachyramphus*, and *Synthliboramphus* in subfamily Fraterculinae (i.e., a paraphyletic grouping). The use of Alcinae herein is phylogenetically-based (Fig. 6.7; Appendix 8) and is also more consistent with respect to inclusiveness with the Linnaean rank of subfamily.

***Institutional abbreviations:*** LACM—Natural History Museum of Los Angeles County, Los Angeles, CA., USA; NCSM—North Carolina Museum of Natural Sciences, Raleigh, North Carolina, USA; SDSNH—San Diego Natural History Museum, San Diego, CA, USA; UCMP—University of California Museum of Paleontology, Berkeley, CA, USA; USNM—National Museum of Natural History, Smithsonian Institution, Washington, D.C., USA.

## PHYLOGENETIC RESULTS

A phylogenetic analysis including extant taxa and *Cepphus storeri* resulted in 65 most parsimonious trees (MPTs; L: 7671; CI: 0.64; RI: 0.74; RC: 0.47). *Cepphus storeri* was placed in a polytomy with other Alcinae (contents of Alcinae include *Alca*, *Pinguinus*, *Uria*, *Alle*, *Miocepphus*, *Cepphus*, *Synthliboramphus*, *Brachyramphus*; Fig. 6.5).

The only previous treatment of the systematic positions of *Pseudocepphus teres* and *Miocepphus* species was that by Wijnker and Olson (2009). The systematic position of *Pseudocepphus teres* was represented on a cladogram; however, character data was presented in a tabular format but not phylogenetically analyzed by Wijnker and Olson (2009). Furthermore, several of the taxa scored by Olson and Wijnker are known from associated specimens including elements other than humeri (e.g., *Alca stewarti*, *Miocepphus blowi*) and these additional character data, which may have influenced recovered relationships, were not considered by Wijnker and Olson (2009). All of the characters and taxa treated by Olson and Wijnker are included in the phylogenetic matrix presented herein. Phylogenetic analyses were performed to evaluate support for the systematic positions proposed for *Pseudocepphus teres* and *Miocepphus* species based on both the restricted sample of character data cited by Wijnker and Olson (2009) and the complete character matrix developed herein.

The strict consensus cladogram of the 11 MPTs resulting from the phylogenetic analysis of the humeral character data cited by Wijnker and Olson (2009) recovered

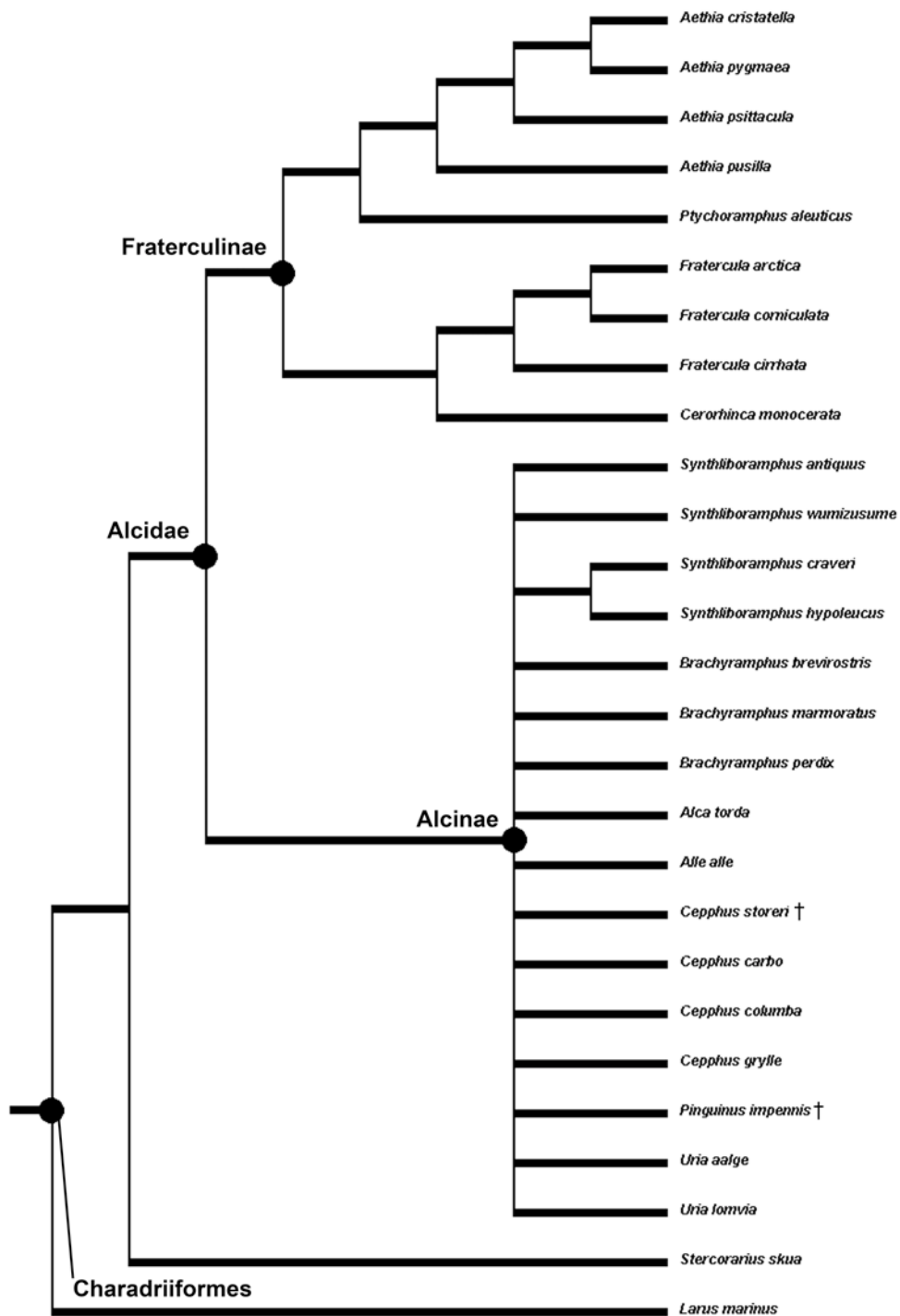


Figure 6.5- Strict consensus cladogram of 65 MPTs resulting from the inclusion of *Cepphus storeri* in phylogenetic analysis along with extant alcid species and *Pinguinus impennis*.

unresolved relationships among the four species of *Miocepphus*, *Alle alle*, and *Pseudocepphus teres* (Fig. 6.6). The lack of resolution is not unexpected given only 12 morphological characters for 9 taxa. The topology of the tree was somewhat sensitive to rooting. However, no clear choice of outgroup is present among the taxa scored by Olson and Wijnker (2009) because all of the taxa sampled were considered potentially part of Alcini by Olson and Wijnker (2009).

An additional analysis was performed after modification of three of the characters of Olson and Wijnker (2009). Characters eight and nine of Wijnker and Olson (2009) describe three character states of a single feature, the degree to which the humeral shaft is dorsoventrally compressed. These two characters were combined according to the philosophy of character independence described by Hawkins et al. (1997). Character number two, which deals with the relative width of the tricipital sulci was modified to include three character states that reflect the full range of morphological variation present in the taxa included by Olson and Wijnker (2009): (0) scapulotricipital sulcus wider than humerotricipital sulcus; (1) sulci of approximately equal width; (2) scapulotricipital sulcus narrower than humerotricipital sulcus. Interpretation of character states was maintained (i.e., Wijnker and Olson's scorings applied to the modified characters when applicable). Analysis of these modified data did not increase phylogenetic resolution (results not shown). In summary, the close affinity between *Miocepphus* spp. and *Pseudocepphus teres* proposed by Olson and Wijnker (2009) is not supported by phylogenetic analysis of their data and the referral of *Pseudocepphus* to the clade containing *Alca*, *Pinguinus*, *Alle*, *Uria*, and *Miocepphus* (i.e., Alcini) was not warranted

in the absence of comparison with other alcid taxa.

The combined phylogenetic analysis including all 23 extant alcids, the recently extinct Great Auk *Pinguinus impennis*, two outgroup charadriiforms, *Cephus olsoni*, and *Pseudocepphus teres* resulted in a fairly well resolved strict consensus tree (Fig. 6.7; 7 MPTs; L: 7680; CI: 0.52; RI: 0.58; RC: 0.30). Relationships in Alcinae were partially unresolved with *Brachyramphus* placed basally to a polytomy composed of Alcini, Cepphini, and *Synthliboramphus*. *Pseudocepphus teres* is placed as the sister taxon to all other Cepphini. Placement of *Pseudocepphus teres* in Alcini, as hypothesized by Wijnker and Olson (2009), would require an additional six steps of tree length, and is, therefore, a less parsimonious placement for this taxon. Furthermore, an additional analysis was performed in which the humeral shaft compression character that was considered a potential pleisiomorphy by Wijnker and Olson (see character # 145 in Appendix 2) was excluded. That analysis did not result in the placement of *Pseudocepphus* with Alcini or any other topological differences from the previously recovered hypothesis (Fig. 6.7) of Cepphini relationships (results not shown). Characters supporting the resulting combined analysis topology (Fig. 6.7) are summarized below (Table 6.2).

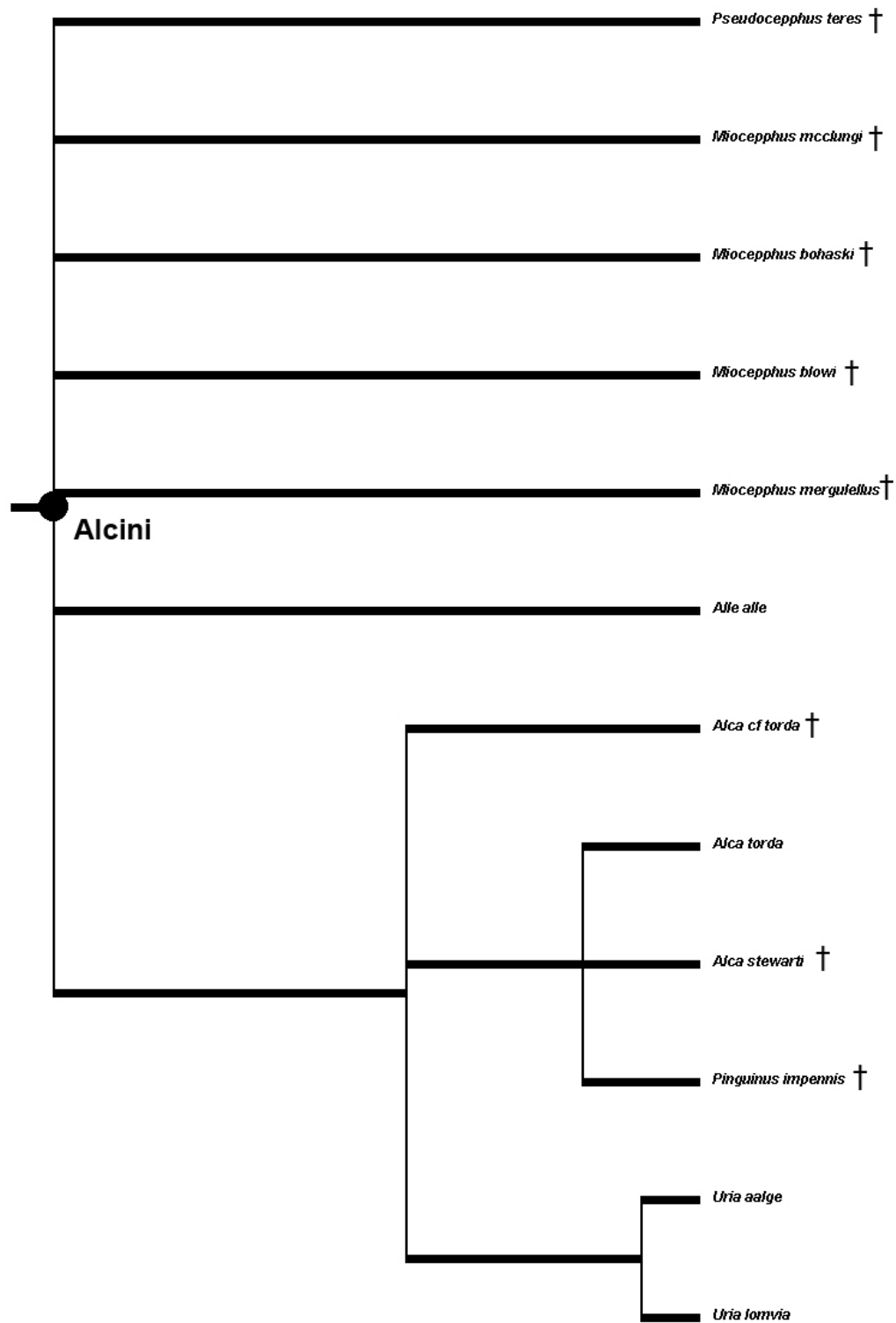


Figure 6.6- Strict consensus cladogram of 11 MPTs resulting from the phylogenetic analysis of the character data of Wijnker and Olson (2009; CI: 0.90, RI: 0.95, RC: 0.86).



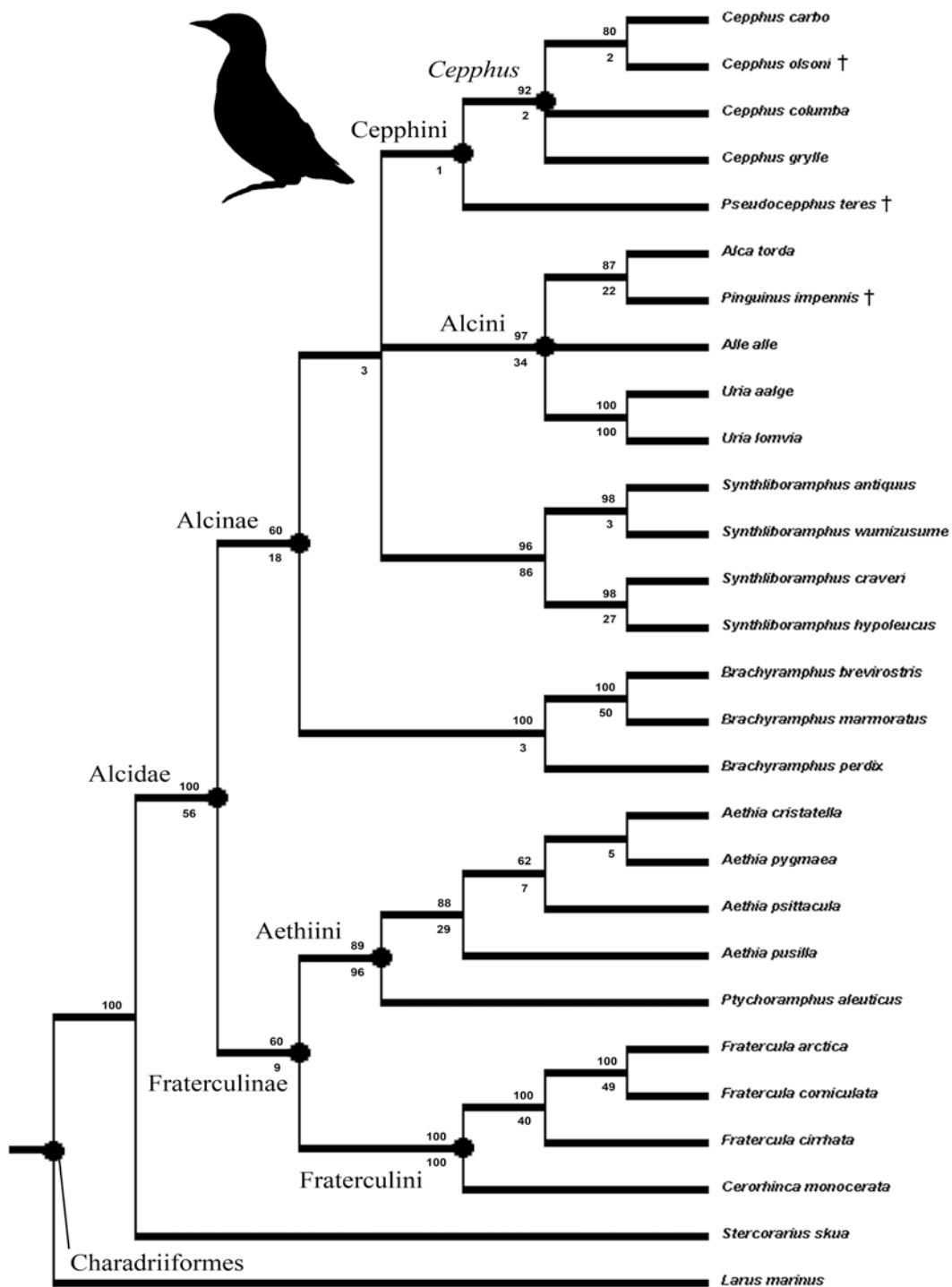


Figure 6.7- Strict consensus cladogram of 3 MPTs showing the placement of *Pseudocepphus teres* as the sister taxon to all other Cepphini. Bootstrap values > 50% and Bremer support values are displayed above and below nodes respectively.

Table 6.2- Apomorphies supporting clades. All optimizations are based on the topology depicted in Figure 6.7. Character numbers from Appendix 3 are followed by character state symbols (e.g., 23:0 = character number 23, state 0). Characters preceded by an ‘\*’ are locally optimized apomorphies with a CI < 1.0. All other apomorphies have a CI = 1.0.

Clade	Character numbers and states that support monophyly
Cepphini + Alcini	*33:1; *51:1; *70:1; *258:0; *299:0.
Cepphini	*13:1; 17:1; 92:1; 94:1; *106:0; *110:1; *112:1; *117:1; *127:0; 145:1; 182:1.
<i>Cepphus</i>	*116:1; *118:1; *134:1; *147:3; *151:0.
<i>C. carbo</i> + <i>C. olsoni</i> + <i>C. columba</i>	*88:2; *203:1; *251:1.
<i>C. carbo</i> + <i>C. olsoni</i>	*136:0; *160:1; *163:0.

## SYSTEMATIC PALEONTOLOGY

AVES Linnaeus, 1758

CHARADRIIFORMES Huxley, 1867

PAN-ALCIDAE Smith, 2011

ALCIDAE Leach, 1820

CEPPHINI Storer, 1960

*Diagnosis*—Relative to other Alcidae, Cepphini (contents include *Cepphus* Moehring 1758 + *Pseudocepphus* Wijnker and Olson 2009) is differentiated by possession of the following combination of osteological characters. The posterolateral

margin of the ventral palatine crest is rounded (13:1) as in *Alle alle*, *Synthliboramphus antiquus* and *Synthliboramphus hypoleucus* rather than angled as in Fraterculinae. The anterior tip of the vomer is bifurcated (17:1) as in *Stiltia isabella* rather than a single point as in other sampled charadriiforms. The m. supracoracoideus scar of the coracoid is reduced (92:1) as in many non-alcid charadriiforms and Mancallinae rather than a distinct raised scar as in other Alcidae. The m. supracoracoideus nerve foramen of the procoracoid process is positioned sternally (94:1) leaving only a thin strut of bone rather than positioned more omally as in other alcids (e.g., *Uria aalge*). The posterior margin of the humeral head in proximal view is rounded (106:0) as in Fraterculini and Mancallinae rather than notched as in the murrelets. The m. coracobrachialis impression of the humerus is deep (110:1) as in Fraterculinae rather than shallow as in other Alcinae. The bicipital crest of the humerus is notched at junction with the humeral shaft (112:1) as in *Alle alle* and *Miocepheus* rather than smoothly transitioning as in Fraterculinae and other Alcinae. The m. supracoracoideus scar of the humerus is separated from the secondary pneumotricipital fossa by a flat space (117:1) as in *Cerorhinca*. As in many species of *Synthliboramphus* and *Aethia* (e.g., *Aethia cristatella*), the m. subcoracoideus scar is positioned more medially (rather than ventrally) on border of primary pneumotricipital fossa of humerus (127:0). The humeral and ulnar shafts are less dorsoventrally compressed than that of other Alcidae (145:1; 182:1). Only the humeral characters noted above could be evaluated in fossil Cepphini, which are all known exclusively from humeri.

*CEPPHUS* Moehring, 1758

*Diagnosis*—*Cepphus* is differentiated from other Cepphini (i.e., *Pseudocepphus teres*) by the following locally optimized humeral apomorphies. The m. supracoracoideus scar of the humerus is long and proximally broad (116:1) as in Fraterculini rather than long and proximally narrow as in *Pseudocepphus teres*. The medial pneumotricipital crest (i.e., crus dorsale fossae, Baumel and Witmer, 1993) extends distally to a point level with the junction of the bicipital crest and the humeral shaft (118:1), whereas this crest terminates more proximally in *Pseudocepphus teres*. The ventral tubercle of the humerus is robust (134:1) as in *Alca* rather than gracile as in Fraterculinae. The dorsal supracondylar process transitions smoothly to the humeral shaft (147:3) as in *Synthliboramphus*, *Pinguinus*, and *Uria* rather than projecting dorsally at its proximal termination as in *Pseudocepphus teres*. As in many other Alcidae (e.g., *Aethia*), the scapulotricipital sulcus is narrower than the humerotricipital sulcus (151:0), whereas in *Pseudocepphus teres* the humerotricipital sulcus is narrower than the scapulotricipital sulcus.

***CEPPHUS OLSONI* Howard, 1982**

*Holotype*—right humerus (LACM 107032; Fig. 6.3).

*Original diagnosis* (Howard, 1982)—Differentiated from extant species of *Cepphus* (Table 6.3; Fig. 6.8) by: deltopectoral crest extended further distally and terminated more abruptly; m. pectoralis scar less distally extended and more distinct; humeral shaft relatively stouter; humeral shaft more dorsoventrally compressed; bicipital surface distinctly bordered medially and raised from level of shaft; dorsal supracondylar process more rounded; tricipital grooves shallower. Larger (based upon greatest length of humerus) than *Cepphus grylle* and smaller than *Cepphus columba*.

*Amended diagnosis*—The following characters are added to or modified from those described by Howard (1982). *Cepphus olsoni* is differentiated from other Cepphini by the deltopectoral crest being less abruptly terminated (*contra* Howard, 1982; 108:0) than in other Cepphini. The posterior tip of the ventral tubercle is rounded as in *Cepphus carbo* (136:0) rather than elongated as in *Cepphus columba* and *Cepphus grylle* (not assessed in *Pseudocepphus teres* owing to damage). The tubercle dorsal to scapulotricipital sulcus is reduced as in *Cepphus carbo* (160:1) rather than prominent as in *Cepphus columba* and *Cepphus grylle* (not assessed in *Pseudocepphus teres* owing to damage).

***PSEUDOCEPPHUS TERES* Wijnker and Olson, 2009**

*Holotype*—right humerus (USNM 214537; Fig. 6.4).

*Original diagnosis*—Shaft of humerus terete like *Cepphus*; differentiated from *Cepphus* by having the scapulotricipital sulcus broader than humerotricipital sulcus; dorsal supracondylar process contacts the humeral shaft at a more acute angle than in *Cepphus*; m. coracobrachialis nerve sulcus a closed duct as in *Alca*.

*Amended diagnosis*—The following characters are added to or modified from those described by Wijnker and Olson (2009). *Pseudocepphus teres* is differentiated from other Cepphini (i.e., extant *Cepphus* spp. and *Cepphus olsoni*) by the posterior margin of humeral head being notched in proximal view as in *Alcini* (106:1) rather than rounded as in other Cepphini. The m. coracobrachialis nerve sulcus a closed duct as in *Alca torda* and *Pinguinus* (113:1) rather than an open sulcus as in *Uria*. As in *Alcini*, the m. supracoracoideus scar does not broaden proximally (116:2), but remains fairly constant in width throughout its length. The medial pneumotricipital crest of humerus does not extend distally to the bicipital crest (118:0). The ventral tubercle is more gracile in ventral view (134:0) than that of other Cepphini. The dorsal supracondylar process is more dorsally projected (147:1) than that of other Cepphini. As in *Alle alle*, the scapulotricipital sulcus is broader than the humerotricipital sulcus (151:2).

Placement of *Pseudocepphus teres* in Cepphini is supported by the following characters: m. coracobrachialis impression of humerus deep rather than shallow (110:1); bicipital crest of humerus notched at junction with humeral shaft (112:1); m. supracoracoideus scar of humerus separated from secondary pneumotricipital fossa by a flat space (117:1); m. subcoracoideus scar positioned more ventrally (rather than

medially) on border of primary pneumotricipital fossa of humerus (127:1); humeral shaft less dorsoventrally compressed than other alcids (145:1).

*Remarks*—Given the placement of this taxon as the sister taxon to all other Cepphini, the name *Pseudocepphus* Wijnker and Olson, 2009 may not be appropriate, and *Pseudocepphus* should be considered for synonymization with *Cepphus* Moerhing, 1758. However, the placement of *Pseudocepphus teres* as the sister taxon to *Cepphus* is not strongly supported (only 4 additional steps required to place *Pseudocepphus teres* in Alcini along with *Miocepphus*. Although the intermediate degree of humeral shaft compression (compared to other Alcidae and other Charadriiformes) is like that of *Cepphus*, the other characters that differentiate *Pseudocepphus* from other *Cepphus* are characters that are shared with Alcini. Therefore, the name *Pseudocepphus* is retained until additional material can be brought to bear on the systematic relationships of this taxon to other Alcidae.

Table 6.3- Measurements of Cepphini humeri (in mm). Abbreviations (following von den Driesch, 1976): **Bd**, breadth of the distal end; **Bp**, breadth of proximal end; **Dd**, distal diagonal; **Dip**, diagonal of proximal end; **Gl**, greatest length; **Sc**, smallest dorsoventral breadth of corpus (shaft). Extant specimen numbers listed in Appendix 1.

Taxa	Specimen #	Bd	Bp	Dd	Dip	Gl	Sc
<i>Cepphus columba</i>	average (n=5)	9.7	15.3	7.6	13.9	66.6	5.1
<i>Cepphus grylle</i>	average (n=5)	8.9	14.1	6.8	12.9	60.0	4.4
<i>Cepphus olsoni</i>	LACM 107032	9.5	15.5	4.3	7.8	61.5	4.9
<i>Pseudocepphus teres</i>	USNM 214537	10.1	15.0	6.9	13.8	67.4	5.6



Figure 6.8- Comparison of extant *Cepphus* left humeri in posterior view. **A.** *Cepphus columba* (NCSM 18096); **B.** *Cepphus carbo* (USNM 347757); **C.** *Cepphus grylle* (USNM 612214).



## DISCUSSION

Recent re-examination of the severely weathered holotype carpometacarpus (BMNH A 4986) of *Cepphus storeri* revealed that this specimen is indistinguishable from carpometacarpi of the extant species *Alca torda*. Features of BMNH A 4986 that agree more with *Alca torda* than with *Cepphus* include: its size, the position of the pisiform process, and depth and size of the infratrochlear fossa (larger and deeper than in *Cepphus*). The only character that would allow definitive referral of this specimen to *Cepphus* (rounded shape of the extensor process; 191:0) rather than *Alca*, is not preserved. The preponderance of evidence suggests that this specimen may be referable to *Alca*. However, the phylogenetic results are inconclusive with respect to the systematic position of *Cepphus storeri*. Therefore, *Cepphus storeri* is a nomen dubium (Table 6.4).

The phylogenetic results place *Cepphus olsoni* as the sister taxon to *Cepphus carbo*. These two species share three characters to the exclusion of *Cepphus columba* and *Cepphus grylle*: posterior tip of ventral tubercle rounded rather than elongated (136:0); presence of a tubercle dorsal to the scapulotricipital sulcus (160:1); absence of an m. pronator sublimis scar associated with the ventral supracondylar tubercle (163:0). This systematic hypothesis would place the divergence between extant Pacific congeners *Cepphus columba* and *Cepphus carbo* in the at least the Late Miocene, and the hypothesized split between those taxa and *Cepphus grylle* earlier. Although this hypothesis of more ancient origins for *Cepphus* is not congruent with molecular evidence, which suggests that extant species of *Cepphus* are recently diverged (i.e.,

Pleistocene or younger; Kidd and Friesen, 1998), this hypothesis is congruent with an older age for the basal divergence in Cepphini, if *Pseudocepphus* is a stem representative of Cepphini. However, placement of *Cepphus olsoni* as the sister taxon to extant *Cepphus* species requires only one additional step in tree length.

Although the holotype specimen of *Pseudocepphus teres* (USNM 214537) shares some characteristics with Alcini taxa to the exclusion of other Cepphini (e.g., a more dorsally projected dorsal supracondylar process), the phylogenetic results (Fig. 6.7)

Table 6.4- Summary of Cepphini taxonomic revision.

Original Taxonomic Assignment	Reference	Specimen #	Revised Taxonomic Assignment
<i>Cepphus storeri</i>	Harrison, 1977	NHMUK PV A 4986	nomen dubium
<i>Cepphus</i> sp.	Howard, 1978	LACM 47045	Presumed lost ?
<i>Cepphus olsoni</i>	Howard, 1982	LACM 107032	<i>Cepphus olsoni</i>
<i>Pseudocepphus teres</i> (included in Alcini)	Wijnker and Olson, 2009	USNM 214537	<i>Pseudocepphus teres</i> (included in Cepphini)

reflect a sister taxon relationship between *Pseudocepphus teres* and other Cepphini. As pointed out by Wijnker and Olson (2009), the terete (i.e., less dorsoventrally compressed) humeral shaft of Cepphini may be the ancestral condition in Pan-Alcidae. A progression from the rounded humeral shafts of non-alcid charadriiforms, to the semi-compressed shafts of Cepphini, to the extremely dorsoventrally compressed humeral shafts of all other Pan-Alcidae represents a potential morphocline. The intermediate degree of

dorsoventral compression may represent a pleisiomorphic character state retained by Cepphini. The Miocene age of *Pseudocepphus teres* supports this hypothesis. However, *Cepphus* has never been recovered in a basal position in Alcidae in the results of any previous phylogenetic analysis, suggesting that the semi-compressed shafts of Cepphini may, alternatively, represent a homoplastic character in Pan-Alcidae. Furthermore, the oldest known alcid fossil from the Late Eocene of Georgia, USA (Chandler and Parmley, 2002) displays the derived (with respect to other charadriiforms) dorsoventral compression of the humeral shaft common to all extant Pan-Alcidae except Cepphini. Thus, the semi-rounded shaft of *Pseudocepphus teres* supports, albeit weakly, the inclusion of this specimen in Cepphini. The independent evolution of this feature in *Cepphus* and *Pseudocepphus* is a less parsimonious, but not unreasonable hypothesis. Only discovery of additional fossils referable to *Pseudocepphus teres* will likely resolve this issue.

Placement of *Pseudocepphus teres* at the base of Alcini (i.e., the systematic position hypothesized by Wijnker and Olson, 2009) would require 6 additional steps of tree length and is therefore a less parsimonious hypothesis for the placement of this taxon. If the phylogenetic hypothesis that places *Pseudocepphus teres* in Cepphini is correct, this would provide the first record of Cepphini from the Atlantic Ocean basin, would represent the oldest record of the clade, and would provide a calibration point for the divergence of Cepphini from other Alcidae.

## CONCLUSIONS

The taxonomic revisions based on the phylogenetic analyses presented herein revealed that *Cepphus storeri*, the only previously named species of guillemot from the Atlantic Ocean basin, is not referable to Cepphini based on apomorphies. However, phylogenetic results place *Pseudocepphus teres* as the sister taxon to *Cepphus*. Thus, the fossil record of Cepphini is limited to *Cepphus olsoni* in the Pacific Ocean basin and *Pseudocepphus teres* in the Atlantic Ocean basin. Although the inclusion of extinct species did not contribute to the resolution of the systematic position of Cepphini (Fig. 6.7), it does confirm the monophyly of Cepphini, including extinct taxa. The currently hypothesized systematic position of Cepphini (Fig. 6.7) suggests that the intermediate degree of dorsoventral shaft compression that characterizes this taxon is an independently derived character state.

The inclusion of *Pseudocepphus teres* in Cepphini extends the known temporal range of Cepphini from ~8 Ma (based on the inclusion of *Cepphus olsoni* in the crown) to ~14 Ma (based on the maximum age of *Pseudocepphus teres* and its status as a stem Cepphini taxon) and raises novel biogeographical questions about the dispersal of Cepphini between the Pacific and Atlantic Ocean basins. If, as the phylogenetic results suggest, *Pseudocepphus teres* represents the earliest record of Cepphini, biogeographical hypotheses of clade origin may need to be re-evaluated. The hypothesized basal position and Pacific Ocean basin range of Pan-Alcidae clades including *Brachyramphus* and *Synthliboramphus* are evidence in favor of a Pacific Ocean origin of Pan-Alcidae.

However, the oldest fossils of Cepphini (*Pseudocepphus teres*, ~14 Ma; Wijnker and Olson, 2009), *Miocepphus* (*Miocepphus bohaski*, ~20 Ma; Wijnker and Olson, 2009), Fraterculini (~4.4 Ma; Olson and Rasmussen, Smith et al., 2007), and the oldest record of Pan-Alcidae (~35.1 Ma; Chandler and Parmley, 2002) are all from the Atlantic Ocean basin. Pacific fossil records of *Synthliboramphus*, *Brachyramphus*, *Cepphus*, *Aethia*, and *Cerorhinca* are all younger (Howard, 1949; Howard, 1982; Chandler, 1990b; Chapters 4, 5, 7). In the absence of additional fossil discoveries (i.e., more complete associated specimens) that might elucidate the relationships and biogeography of early alcids, the inclusion of phylogenetically analyzed and rigorously dated fossils such as the examples described herein provide calibration points for molecular-based divergence estimation that may facilitate further assessment of hypotheses regarding the origins of Pan-Alcidae and Cepphini.

The fossil record of Cepphini currently consists of a handful of specimens ( $n = <20$ ; Smith, personal observation) referred to 2 species, and is, therefore, the poorest among Pan-Alcidae. Mancallinae is represented by ~4,000 specimens representing at least six species (Smith, 2011). *Alca* is represented by ~8,000 specimens representing at least seven species (Smith and Clarke, in press). Puffins, auklets, murrelets, and dovekeys are all represented by at least as many taxa and greater quantities of material than Cepphini (see Chapters 2, 4, 5, and 7). However, at ~8 Ma and ~14 Ma respectively, fossils of *Cepphus olsoni* and *Pseudocepphus teres* represent two of the oldest records of Pan-Alcidae. Earlier records of Pan-Alcidae are limited to the auk remains reported from the Late Eocene (~35 Ma) of Georgia by Chandler and Parmley (2002), Miocene (~10-20

Ma) examples of *Alca* and *Miocepphus* from the Atlantic Ocean basin, and Miocene (~8.7-10 Ma) examples including *Uria brodkorbi* and Mancallinae from the Pacific Ocean basin. Given the expanse of time that Cepphini are known to have been a part of both the Atlantic and Pacific Ocean basin avifaunas, it is surprising that fossils of this taxon are so rare.

Fossils of Fraterculini (i.e., puffins) are also comparatively rare to those of other alcids with only ~30 puffin fossils recorded from the ~8,000 alcid fossils recovered from the Yorktown Formation (Olson and Rasmussen, 2001; Smith et al., 2007). Likewise, fossils of puffins are rare in comparison to the abundant remains of Mancallinae recovered from the San Diego Formation (Chandler, 1990b). It is possible that relative abundance of Miocene and Pliocene guillemots and puffins was simply lower than that of other pan-alcids and that the rarity of these taxa in the fossil record is a direct reflection of community structure. Although relative abundance of different alcid clades has likely fluctuated throughout their history, guillemots compose a large percentage of many extant colonies of breeding alcids (e.g., Ainley, 1990). However, extant guillemots tend to nest in lower densities than other alcids and their numbers are historically harder to assess than that of some other alcid species (e.g., *Uria aalge*; del Hoyo et al., 1996).

The rarity of puffin and guillemot fossils might also be a function of the different ecology of these taxa in comparison with other pan-alcids. Because the puffin and guillemot fossil record is so poor, there is little if anything that can be inferred regarding the ecology of Miocene and Pliocene species. However, extant puffins and guillemots share a similar moderate body size in comparison with smaller alcids such as auklets and

larger alcids such as murres, and also share a more generalist feeding strategy than dedicated planktivores such as *Aethia pusilla* and dedicated piscivores such as *Alca torda*. Body mass in extant alcids has been correlated with dive depth and feeding ecology (Prince and Harris, 1988; Watanuki and Burger, 1999), and moderate body size in extant alcids has been associated with more generalist feeding strategies (e.g., moderately sized *Cepphus* commonly prey on both vertebrates and invertebrates; Bradstreet and Brown, 1985). Furthermore, the maximum recorded dive depth of puffins and guillemots are shallower than larger bodied murres and auks (Piatt and Nettleship, 1985; del Hoyo et al., 1996; Croll et al., 1992; Hedd et al., 2009). Perhaps guillemot and puffin fossils are more rare than other alcids because they are foraging in different areas where the potential for preservation is lower. The potential for increased subaqueous weathering at shallower depths may have created a taxonomic bias in the fossil record towards piscivores that forage at greater depths and, therefore, may have a higher potential for preservation in less turbulent, deeper-water deposits.

*Cepphus* is one of the few extant alcid taxa that have a Holarctic distribution. Extant species of *Fratercula*, *Uria*, and *Alle* are also present in both the Atlantic and Pacific Oceans. However, *Aethia*, *Brachyramphus*, *Synthliboramphus*, and *Cerorhinca* are restricted to the Pacific Ocean basin, and *Alca* is restricted to the Atlantic Ocean basin (del Hoyo et al., 1996). In the absence of Pliocene and Pleistocene records of Cepphini it would be speculative to propose that Cepphini have maintained a Holarctic distribution since the Miocene. Additional fossil remains of Cepphini representing un-sampled time

periods (i.e., Pliocene and Pleistocene) are needed to resolve the lingering questions regarding the evolution and biogeography of this clade.



## CHAPTER 7.

The fossil record and phylogeny of the murrelets

(Pan-Alcidae, Alcinae)

## INTRODUCTION

The Alcidae are pelagic, wing-propelled diving charadriiforms that range in size from diminutive murrelets such as *Brachyramphus marmoratus*, to larger seabirds that approach the hypothesized limit of body mass that would allow for both aerial and underwater flight (e.g., *Uria lomvia*; Simpson, 1946). There are seven extant species of murrelets systematically placed in two clades, *Synthliboramphus* Brandt, 1837 and *Brachyramphus* Brandt, 1837. The synthliboramphine murrelets include the Ancient Murrelet *Synthliboramphus antiquus*, Xantus's Murrelet *Synthliboramphus hypoleucus*, Craveri's Murrelet *Synthliboramphus craveri*, and the Japanese Murrelet *Synthliboramphus wumizusume*. The brachyramphine murrelets include the Marbled Murrelet *Brachyramphus marmoratus*, Kittlitz's Murrelet *Brachyramphus brevirostris*, and the Long-billed Murrelet *Brachyramphus perdix*.

The murrelets are among the smallest of alcids (del Hoyo et al., 1996), and ecologically, display a range of prey preferences that include primarily planktivorous (e.g. *Brachyramphus marmoratus*), primarily piscivorous (e.g., *Synthliboramphus craveri*), and more generalist feeders that regularly include both fish and invertebrates in their diet (e.g., *Synthliboramphus antiquus*). Whereas the *Synthliboramphus* murrelets essentially appear as miniature versions of murres (i.e., colored black dorsally, with white bellies and terete bills), the *Brachyramphus* murrelets are characterized by a cryptic, mottled brown Summer plumage that has been proposed as evidence of close relationship with guillemots who also display this type of Summer plumage (Storer, 1952; Strauch,

1985). *Endomychura* (contents included '*Endomychura hypoleucus* and *Endomychura craveri*'), which was later synonymized with *Synthliboramphus* by the American Ornithologists' Union (1983), was considered by Storer (1945b) to represent the most 'primitive' clade of alcids (i.e., most similar to non-alcid charadriiforms). Phylogenetic studies have not consistently supported that viewpoint as *Synthliboramphus* has never been recovered as the sister taxon to all other Alcidae. However, *Synthliboramphus* has been recovered as the base of Alcinae in the results of several previous analyses (Strauch, 1985; Watada et al., 1987; Chandler, 1990a; Smith, 2011).

The extant murrelets are treated together herein to allow comparisons between these independent radiations of small, Pacific Ocean endemic alcids with overlapping geographic ranges, feeding strategies, and fossil records. With the exception of *Alle* Link 1806, which has been recovered in a variety of systematic positions within Alcidae (see Chapter 2), the systematic positions of *Synthliboramphus* and *Brachyramphus* are potentially the most intractable issues in alcid systematics.

The monophyly of *Synthliboramphus* and the monophyly of *Brachyramphus* are supported by analyses of morphological (Strauch, 1985; Chandler 1990a), molecular sequence data (Friesen et al., 1996; Thomas et al., 2004; Baker et al., 2007; Pereira and Baker, 2008), and combined analysis (Smith, 2011). The murrelets *Synthliboramphus* and *Brachyramphus* have only been recovered as sister taxa in the results of one previous analysis (Moum et al., 1994). Other previous analyses have placed *Synthliboramphus* as the sister taxon to *Cepphus* (Strauch, 1985), at the base of Alcinae (contents of Alcinae include *Alca*, *Pinguinus*, *Uria*, *Alle*, *Miocepphus*, *Cepphus*, *Synthliboramphus*,

*Brachyramphus*; Watada et al., 1987; Chandler, 1990a; Smith, 2011), or as the sister taxon to Alcini (contents of Alcini include *Alca*, *Pinguinus*, *Uria*, *Alle*, *Miocepphus*; Friesen et al., 1996; Thomas et al., 2004; Baker et al., 2007; Pereira and Baker, 2008).

In previous phylogenetic analyses *Brachyramphus* has been recovered in an unresolved position at the base of Alcinae (contents of Alcinae include *Alca*, *Pinguinus*, *Uria*, *Alle*, *Miocepphus*, *Cepphus*, *Synthliboramphus*, *Brachyramphus*; Strauch, 1985; Friesen et al., 1996), as the sister taxon to all other Alcinae (Baker et al., 2007; Pereira and Baker, 2008), as the sister taxon to Alcini (contents of Alcini include *Alca*, *Pinguinus*, *Uria*, *Alle*, *Miocepphus*; Watada et al., 1987; Chandler, 1990a), as the sister taxon to *Aethia* (Chu, 1998), and as the sister taxon to all other Alcidae (Thomas et al., 2004). Clearly there is little congruence regarding the systematic position of murrelets.

Congruent with the extant distribution of murrelets, all fossil records of *Synthliboramphus* and *Brachyramphus* are restricted to the Pacific Ocean basin (Olson, 1985; Chandler, 1990b; Fig. 7.1). No extinct species of *Synthliboramphus* or *Brachyramphus* has been previously included in a phylogenetic analysis. Systematic positions for *Synthliboramphus rineyi*, *Brachyramphus pliocenium*, and *Brachyramphus dunkeli* were proposed in the form of a cladogram by Chandler (1990a), but scorings for these taxa were not included in the phylogenetic matrix. The placement of extinct taxa in Chandler's (1990a) cladograms seems to stem from the optimization of particular characters (i.e., character mapping).

***The fossil record of murrelets:*** In 1949 Howard described *Brachyramphus pliocenium* based upon a right humerus (LACM 2119) from the Pliocene San Diego

Formation of San Diego, California, USA (Table 7.1; Fig. 7.2). This species was the first fossil record of *Brachyramphus* and was diagnosed relative to extant taxon

*Brachyramphus marmoratus* owing to the geographic distribution of that species.

Because geographic distribution of extant species is an inappropriate criterion to exclude other potentially comparable taxa (Bell et al., 2010), the diagnosis of *Brachyramphus pliocen* is amended below. The species name *Brachyramphus pliocen* was amended to *Brachyramphus pliocen* by Brodkorb (1967) to reflect proper latinization of the Pliocene epoch for which the taxon is named. Additional material including a partial cranium, a partial mandible, ulnae, a coracoid, and scapulae were referred by Howard (1949) and Chandler (1990b). Because there are no known associated specimens of *Brachyramphus pliocen*, there is no basis for referral of remains other than humeri.

In 1971 Howard referred a partial cranium (LACM 15426) and proximal humerus (LACM 26571) from the Early Pliocene Almejas Formation of Cedros Island, Baja California, Mexico to *Endomychura* (Table 7.1; Fig. 7.3). In response to the American Ornithologists' Union (AOU) decision to synonymize *Endomychura* with *Brachyramphus* (AOU, 1944), Storer (1945b) provided osteological, oological, integumentary, and behavioral support for the affinity between *Endomychura* and *Synthliboramphus*. Based upon the comparative work of Storer (1945b) *Endomychura*, which previously included the species *Endomychura hypoleucus* and *Endomychura craveri*, was later synonymized with *Synthliboramphus* by the AOU (1983). Those species are known today as *Synthliboramphus hypoleucus* and *Synthliboramphus craveri*, and fossils described by Howard (1971) are referred to here as *Synthliboramphus*.

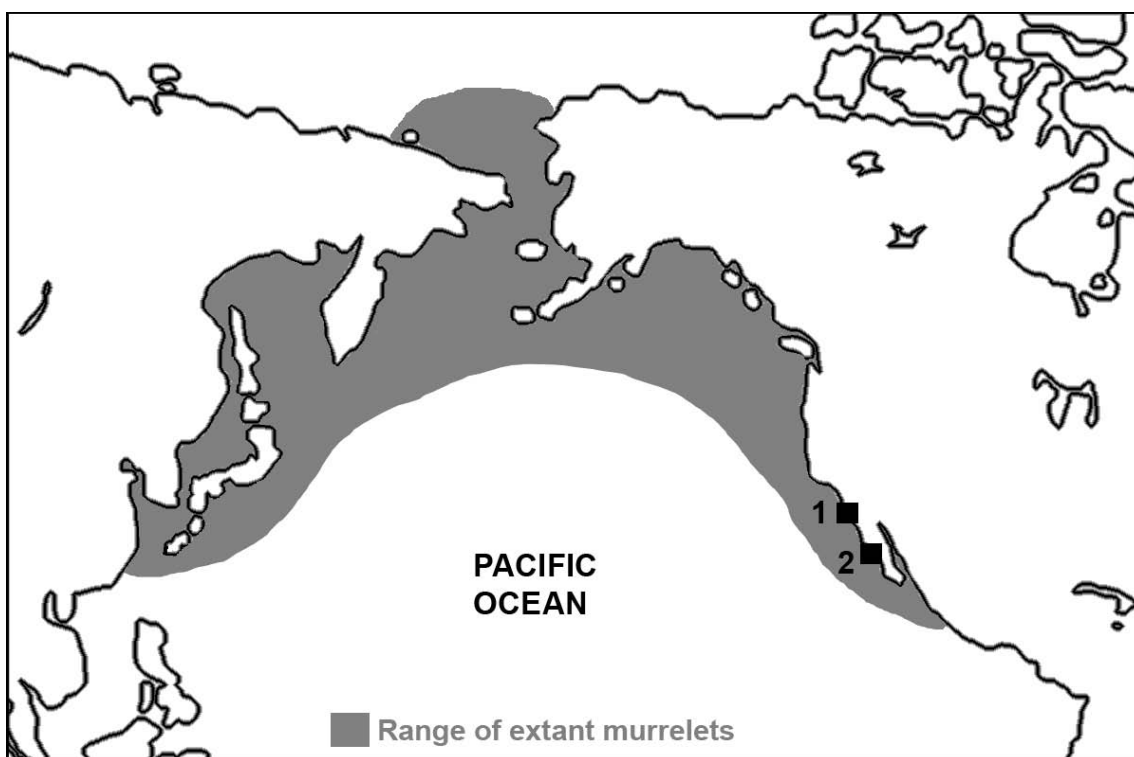


Figure 7.1- World map depicting previously published murrelet fossil localities (numbered) and extant murrelet distribution (based on del Hoyo et al.,1996). **1.** San Diego, California (Howard, 1949; Chandler, 1990b); **2.** Baja Peninsula, Mexico (Howard, 1971).

Table 7.1- Previously published murrelet fossil remains.

Taxon	Material	Provenience	Age	Reference
<i>Brachyramphus pliocenium</i>	humerus	California	Pliocene	Howard, 1949
<i>Synthliboramphus indeterminate</i>	partial skull and proximal humerus	Mexico	Pliocene	Howard, 1971
<i>Brachyramphus dunkeli</i>	humerus	California	Pliocene	Chandler 1990b
<i>Synthliboramphus rineyi</i>	humerus	California	Pliocene	Chandler 1990b



Figure 7.2- Holotype specimen (partial left humerus) of *Brachyramphus pliocenium* (LACM 2119) in posterior view.

*Brachyramphus dunkeli* was described by Chandler (1990b) based upon a left humerus (SDSNH 24573; Fig. 7.4) from the Pliocene San Diego Formation of San Diego California, USA. Because the holotype specimen of *Brachyramphus dunkeli* is a humerus, because there are no known associated specimens of this taxon, and because there are other alcid taxa known from the San Diego Fm. (*Synthliboramphus*, *Mancalla*, *Cerorhinca*, *Aethia*), there was no basis for referral of additional material (ulna, radius) to this species by Chandler (1990b).

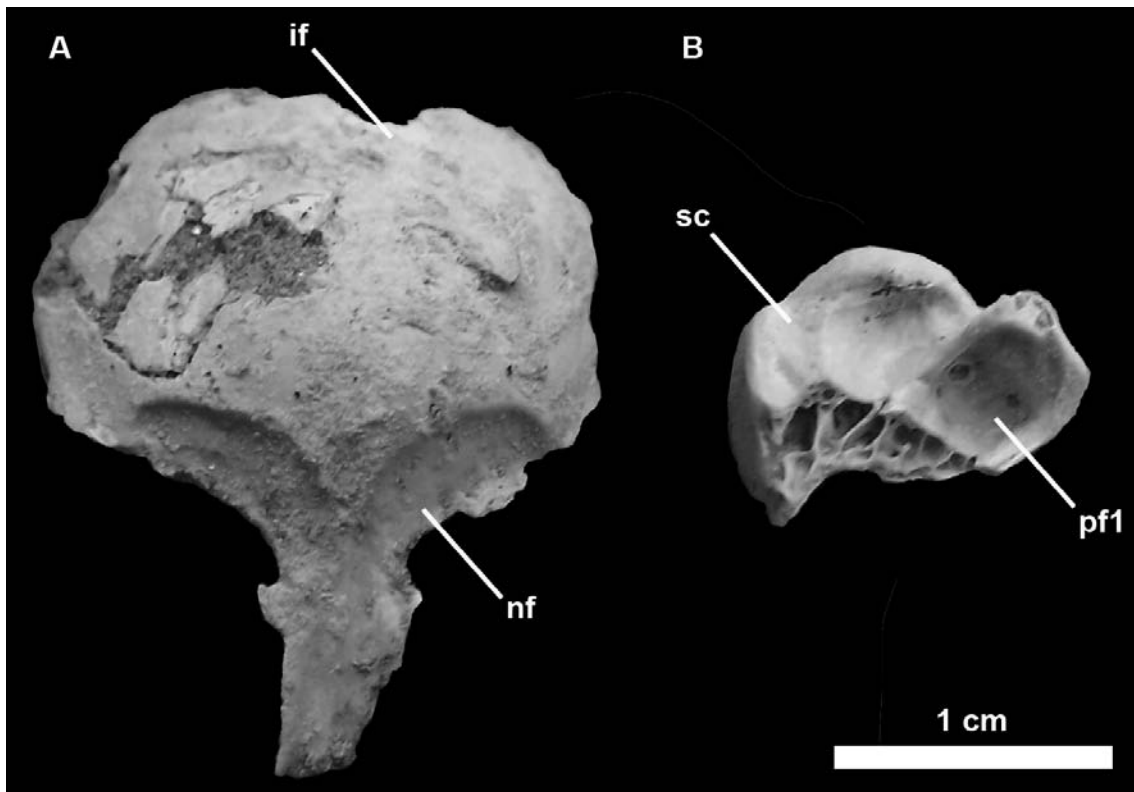


Figure 7.3- Specimens referred to *Synthliboramphus* by Howard (1971). **A.** partial cranium in dorsal view (LACM 15426); **B.** left proximal humerus in posterior view (LACM 26571). Anatomical abbreviations: (**if**) interhemispherical furrow; (**pf1**) primary pneumotricipital fossa; (**nf**) nasal fossa; (**sc**) m. supracoracoideus scar.

*Synthliboramphus rineyi* was described by Chandler (1990b) based upon a right humerus (UCMP 61590; Fig. 7.5) from the Pliocene San Diego Formation of San Diego, California, USA. Because the holotype specimen of *Synthliboramphus rineyi* is a humerus, because there are no known associated specimens of this taxon, and because there are other alcid taxa known from the San Diego Fm. (*Brachyramphus*, *Mancalla*, *Cerorhinca*, *Aethia*), there was no basis for referral of additional material (coracoids, ulna, tarsometatarsus) to this species by Chandler (1990b).



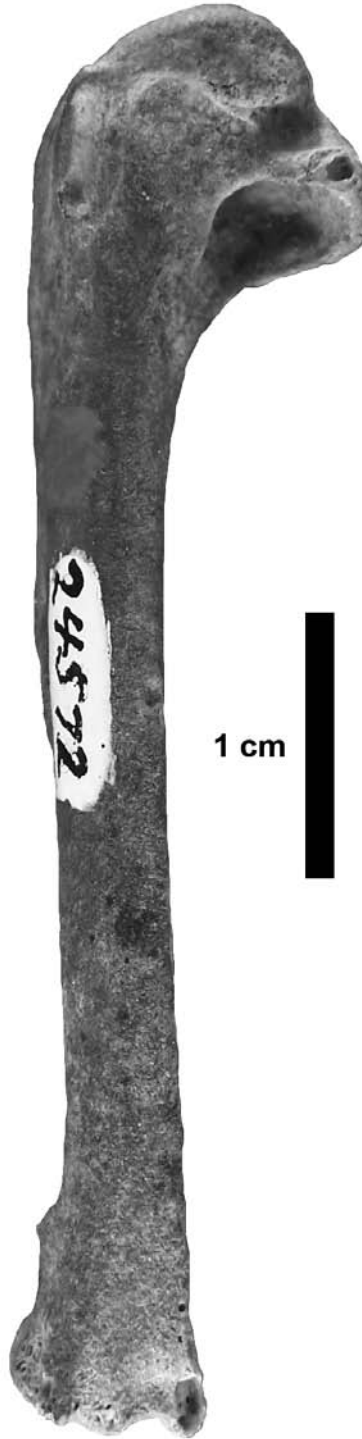


Figure 7.4- Holotype left humerus of *Brachyramphus dunkeli* (SDSNH 24573) in posterior view.

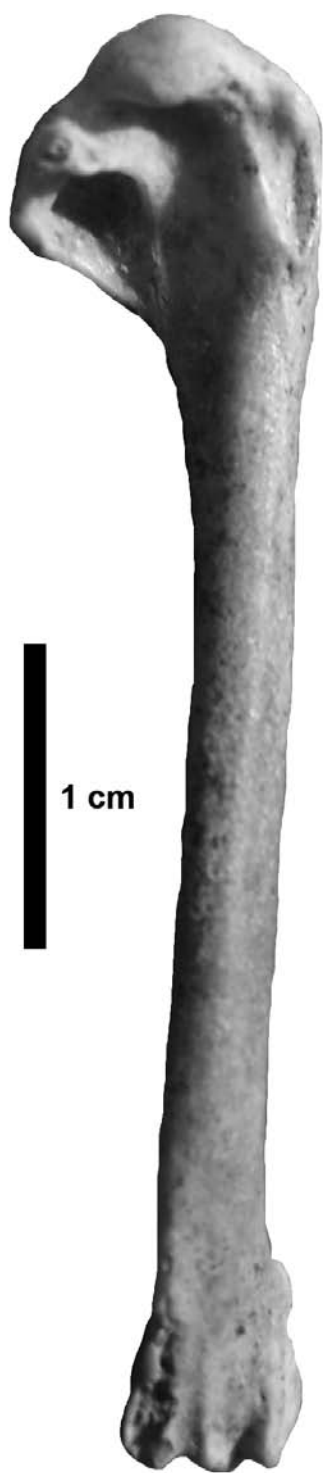


Figure 7.5- Holotype right humerus of *Synthliboramphus rineyi* (UCMP 61590) in posterior view.

Previously described murrelet fossil remains, newly described murrelet fossil remains, extant species of murrelets, other species of extant alcids, and charadriiform outgroup taxa are evaluated through phylogenetic analyses to assess the systematic positions of these taxa. Taxonomic revisions are provided based on the results of the phylogenetic analyses. Implications for the evolution of these taxa are discussed in the context of revised estimates of species richness and the results of the phylogenetic analyses.

## MATERIALS AND METHODS

In the anatomical descriptions, the English equivalents of the Latin osteological nomenclature summarized by Baumel and Witmer (1993) are used. The terminology of Howard (1929) is followed for features not treated by Baumel and Witmer (1993). With the exception of the terms anterior and posterior substituted for cranial and caudal, respectively, the terms used for the anatomical orientation of a bird are those used by Clark (1993). Measurements follow those of Von den Driesch (1976). All measurements were taken using digital calipers and rounded to the nearest tenth of a millimeter. With the exception of species binomials, all taxonomic designations (e.g., Alcinae) are clade names and are not intended to convey rank under the Linnaean system of nomenclature, regardless of use of italics or previous usage by other authors.

Morphological characters were scored for all 23 extant alcids, the recently extinct Great Auk *Pinguinus impennis*, and extinct murrelet taxa. A gull *Larus marinus*, and a

skua, *Stercorarius skua* were included as charadriiform outgroup taxa. See Appendix 2 for morphological character descriptions and Appendix 3 for morphological character scorings used in the phylogenetic analysis. Pleistocene and Holocene remains that presumably represent extant species (Lambrect, 1933; Brodkorb, 1967; Hasegawa et al., 1988; Tyrberg, 1998) were not examined and are not treated further in this study.

Because there is no evidence other than provenience that the specimens referred to *Synthliboramphus* by Howard (1971; LACM 15426, LACM 26571; Fig. 7.3) represent the same species, they were scored as separate terminals in the phylogenetic analysis.

Morphological characters include osteological ( $n = 232$ ), integumentary ( $n = 32$ ), reproductive ( $n = 11$ ), dietary ( $n = 2$ ), myological ( $n = 24$ ) and micro-feather ( $n = 52$ ). One hundred and sixty-four characters were developed for this analysis. The other 189 characters were drawn from the work of Hudson et al. (1969;  $n = 24$ ), Strauch (1978, 1985;  $n = 39$ ), Chandler (1990a;  $n = 63$ ), Chu (1998;  $n = 11$ ), and Dove (2000;  $n = 34$ ). Only 34 of the 38 characters used by Dove (2000) varied in the taxa examined in this study. Of the 34 used in this analysis, eighteen were modified (i.e., split into 2 separate characters) according to the philosophy of character independence proposed by Hawkins et al. (1997), resulting in a total of 52 microfeather characters.

Whenever possible, five or more specimens of each extant species, and both sexes were evaluated to account for intraspecific character variation and potential sexual dimorphism respectively (Appendix 1). Only adult specimens, assessed based upon degree of ossification (Chapman, 1965), were evaluated, and whenever possible specimens from multiple locations within the geographic range of extant species (i.e.,

sub-species) were examined to account for geographic variation. Characters for all extinct taxa were coded from direct observation of holotype and referred specimens (Appendix 3). Pleistocene and Holocene remains that presumably represent extant species (Lambrect, 1933; Brodkorb, 1967; Tyrberg, 1998) were not examined, and are not treated further herein.

Previously published molecular sequence data (mitochondrial: ND2, ND5, ND6, CO1, CYTB; ribosomal RNA: 12S, 16S; and nuclear: RAG1) were downloaded from GenBank (<http://www.ncbi.nlm.nih.gov/genbank>; see Appendix 4 for sequence authorship and inclusion). Preliminary sequence alignments were obtained using the program ClustalX v2.0.6 (Thompson et al., 1997), and then manually adjusted using the program Se-Al v2.0A11 (Rambaut, 2002). Alignment and concatenation of sequence data resulted in a final molecular matrix of 11601 base pairs. Molecular sequence data were combined with morphological characters for a matrix of 11,954 characters.

A parsimony tree search was performed in PAUP\* v4.0b10 (Swofford, 2002) with the following parameters: heuristic search strategy; 10,000 random taxon addition sequences; tree bisection-reconnection branch swapping; random starting trees; all characters equally weighted; minimum length branches = 0 collapsed; multistate (e.g., 0&1) scorings used only for polymorphism. Bootstrap values and descriptive tree statistics (e.g., CI, RI, RC) were calculated using PAUP\* v4.0b10 (Swofford, 2002). Bootstrap value calculation parameters included 1,000 heuristic replicates, 100 random addition sequences per replicate. All other settings were the same as the primary analysis. Bremer support values were calculated using a script generated in MacClade v4.08

(Maddison and Maddison, 2005) and analyzed with PAUP\* v4.0b10 (Swofford, 2002). Based on the results of previous phylogenetic analyses of charadriiform relationships (Strauch, 1978; Sibley and Ahlquist, 1990; Chu, 1995; Ericson et al., 2003; Paton et al., 2003; Thomas et al., 2004; Baker et al., 2007) resultant trees were rooted with *Larus marinus*.

***Institutional abbreviations:*** NCSM—North Carolina Museum of Natural Sciences, Raleigh, NC, USA; LACM—Natural History Museum of Los Angeles County, Los Angeles, CA., USA; SDSNH—San Diego Natural History Museum, San Diego, CA, USA; UCMP—University of California Museum of Paleontology, Berkeley, CA, USA; UMMZ—University of Michigan Museum of Zoology, Ann Arbor, MI, USA; USNM—National Museum of Natural History, Smithsonian Institution, Washington, D.C., USA.

## PHYLOGENETIC RESULTS

A preliminary analysis including all three extinct murrelet species (*Brachyramphus pliocenum*, *Brachyramphus dunkeli*, *Synthliboramphus rineyi*), two additional specimens that were previously referred to *Synthliboramphus* (LACM 15426, LACM 26571), two newly described specimens (SDSNH 24865, SDSNH 24866) and 25 extant taxa and *Pinguinus impennis* resulted in a tree with murrelet relationships largely unresolved at the base of Alcidae (Fig. 7.6). Although a *Brachyramphus* clade including SDSNH 24865 and SDSNH 24866 was recovered, relationships among *Synthliboramphus* and the relationships between other Alcinae (contents of Alcinae

include *Alca*, *Pinguinus*, *Uria*, *Alle*, *Miocepphus*, *Cepphus*, *Synthliboramphus*, *Brachyramphus*) were unresolved. Additional analyses, which are described below, were performed to identify potential ‘wildcard taxa’ (Nixon and Wheeler, 1992; Kearney, 2002). These problematic taxa were removed from subsequent analyses in order to recover a mostly resolved phylogenetic hypothesis that still maintained a reasonably high level of taxon sampling for extinct murrelets.

Removal of LACM 15426 and LACM 26571 in a subsequent combined phylogenetic analysis resulted in a well-resolved strict consensus of the 3 most parsimonious trees (MPTs; L: 7675; CI: 0.49; RI: 0.54; RC: 0.27; Fig. 7.7) in which *Brachyramphus* and *Synthliboramphus* were recovered as clades. Relationships among other alcid clades are congruent with previous analyses of alcid relationships (see Chapter 1).

*Brachyramphus* is placed as the sister taxon to all other Alcinae. *Brachyramphus pliocenum*, and coracoid specimens SDSNH 24865 and SDSNH 24866 are placed in a polytomy at the base of *Brachyramphus*. Alternative placements for SDSNH 24865 and SDSNH 24866 included the placement of SDSNH 24865 in a polytomy with *Brachyramphus pliocenum* and SDSNH 24866 placed as the sister taxon to all other *Brachyramphus*. The second alternative placement of the terminals representing SDSNH 24865 and SDSNH 24866 recovered SDSNH 24866 and *Brachyramphus pliocenum* in a polytomy at the base of *Brachyramphus* with SDSNH 24865 and other *Brachyramphus* in successively more derived positions.

*Brachyramphus dunkeli* is placed as the sister taxon to *Brachyramphus*

*marmoratus*, with *Brachyramphus brevirostris* placed as an outgroup to these taxa.

*Synthliboramphus* is placed as the sister taxon to an Alcini + *Cepphus* clade (contents of Alcini include *Alca*, *Pinguinus*, *Uria*, *Alle*, *Miocepphus*). *Synthliboramphus rineyi* is placed as the sister taxon to *Synthliboramphus hypoleucus*, in a clade with *Synthliboramphus craveri* at its base. This clade is placed as the sister to extant sister taxa *Synthliboramphus antiquus* and *Synthliboramphus wumizusume*.

An additional analysis including extant taxa and LACM 15426 resulted in a strict consensus tree (56 MPTs; L: 7671; CI: 0.65; RI: 0.76; RC: 0.49) with LACM 15426 placed in a polytomy with other Alcinae taxa unresolved at the base of Alcidae (Fig. 7.8). An additional analysis including extant taxa and LACM 26571 resulted in a strict consensus cladogram (6 MPTs; L: 7671; CI: 0.51; RI: 0.57; RC: 0.29) with LACM 26571 in a polytomy with other *Synthliboramphus* species (Fig. 7.9), supporting the referral of this specimen by Howard (1971) to *Synthliboramphus*.

Table 7.2- Apomorphies supporting clades in the resultant phylogenetic tree (Fig. 7.10). Character numbers from Appendix 3 are followed by character state symbols (e.g., 23:0 = character number 23, state 0). Characters preceded by an asterisk ‘\*’ are locally optimized apomorphies with a CI < 1.0. All other apomorphies have a CI = 1.0.

Clade	Character numbers and states that support monophyly
<i>Brachyramphus</i>	*93:0; 98:1; *100:0.
<i>Synthliboramphus</i>	*15:1; *218:0; 230:1; *231:0; *232:0; *273:1.
<i>S. rineyi</i> + <i>S. hypoleucus</i>	*116:1; *127:1.
<i>B. dunkeli</i> + <i>B. marmoratus</i>	*105:1; *118:0.



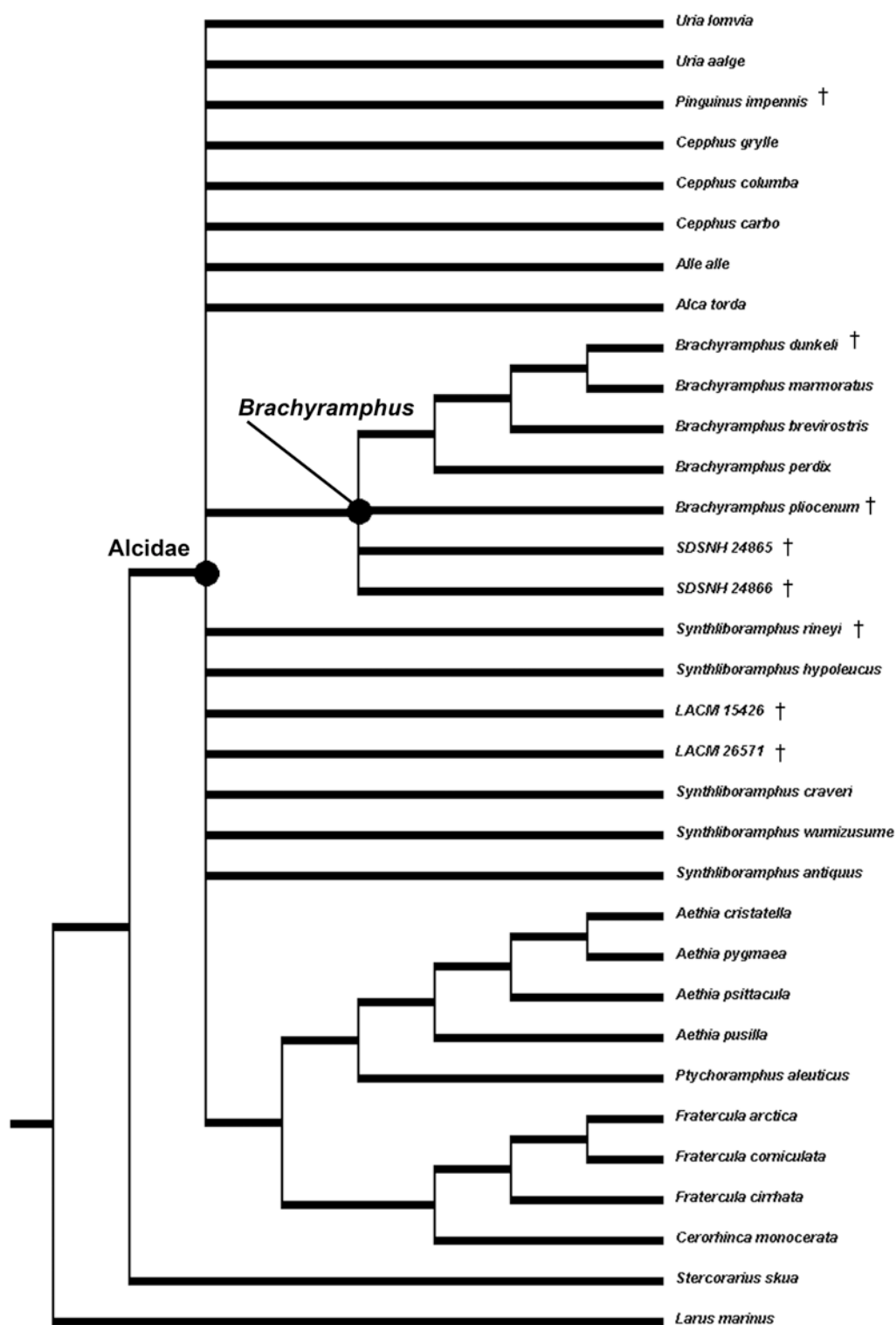


Figure 7.6- Strict consensus cladogram indicating the unresolved systematic positions of murrelet species and previously referred specimens.

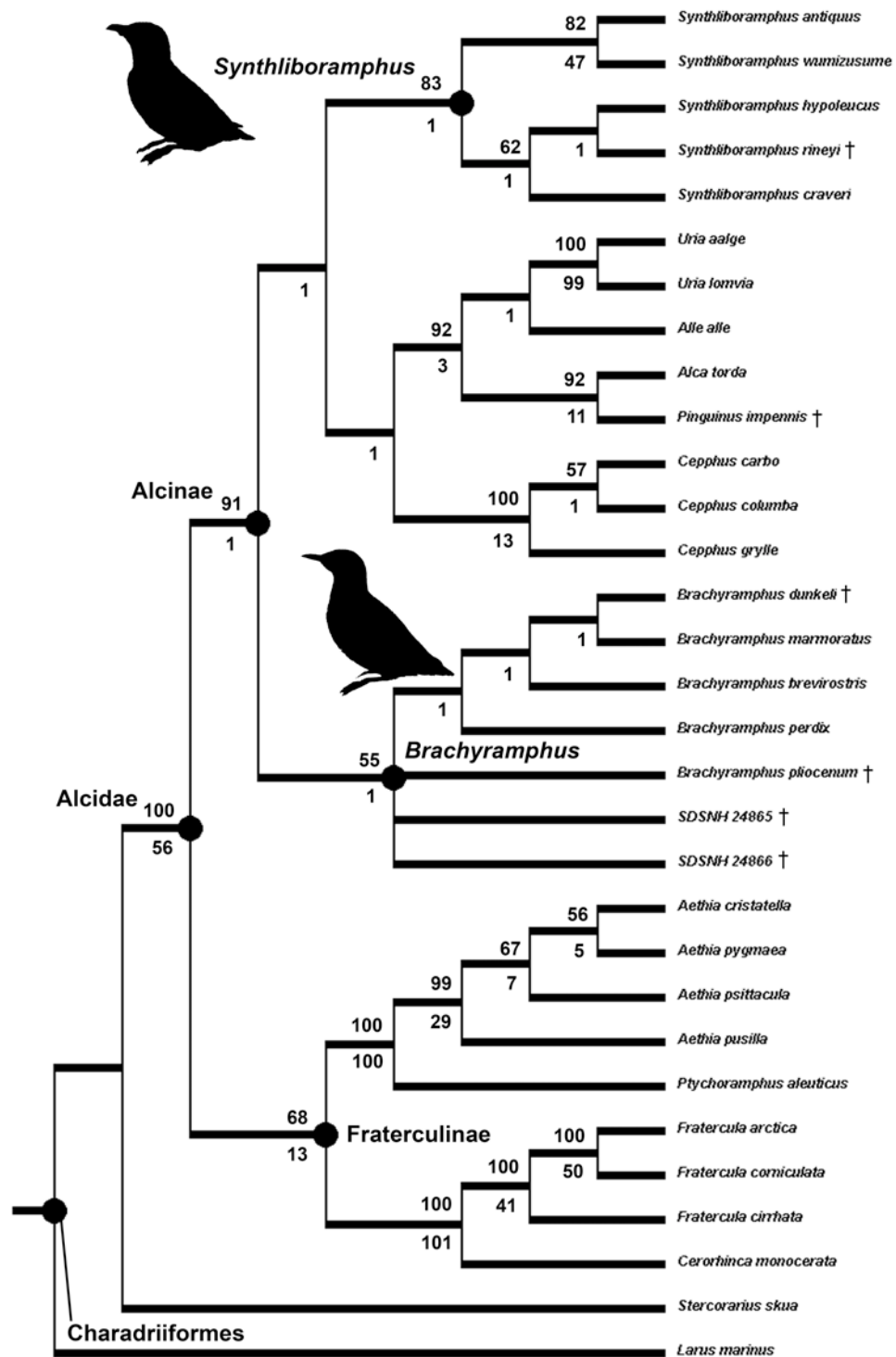


Figure 7.7- Strict consensus topology of the resultant phylogenetic tree for *Synthliboramphus* and *Brachyramphus* murrelets. Bootstrap values > 50% and Bremer support values are placed above and below nodes, respectively.

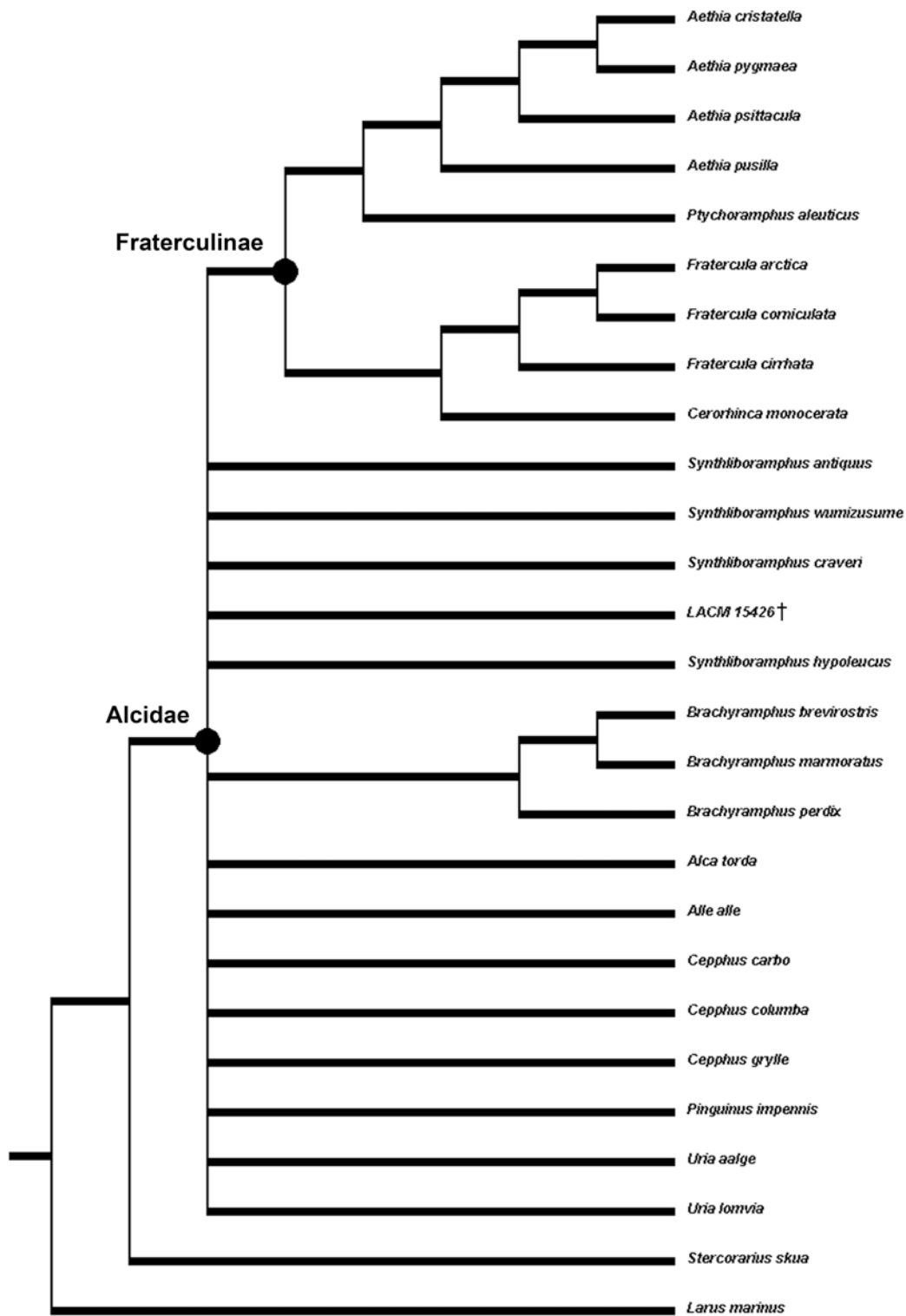


Figure 7.8- Strict consensus cladogram indicating the unresolved systematic position of LACM 15426 in Alcidae.

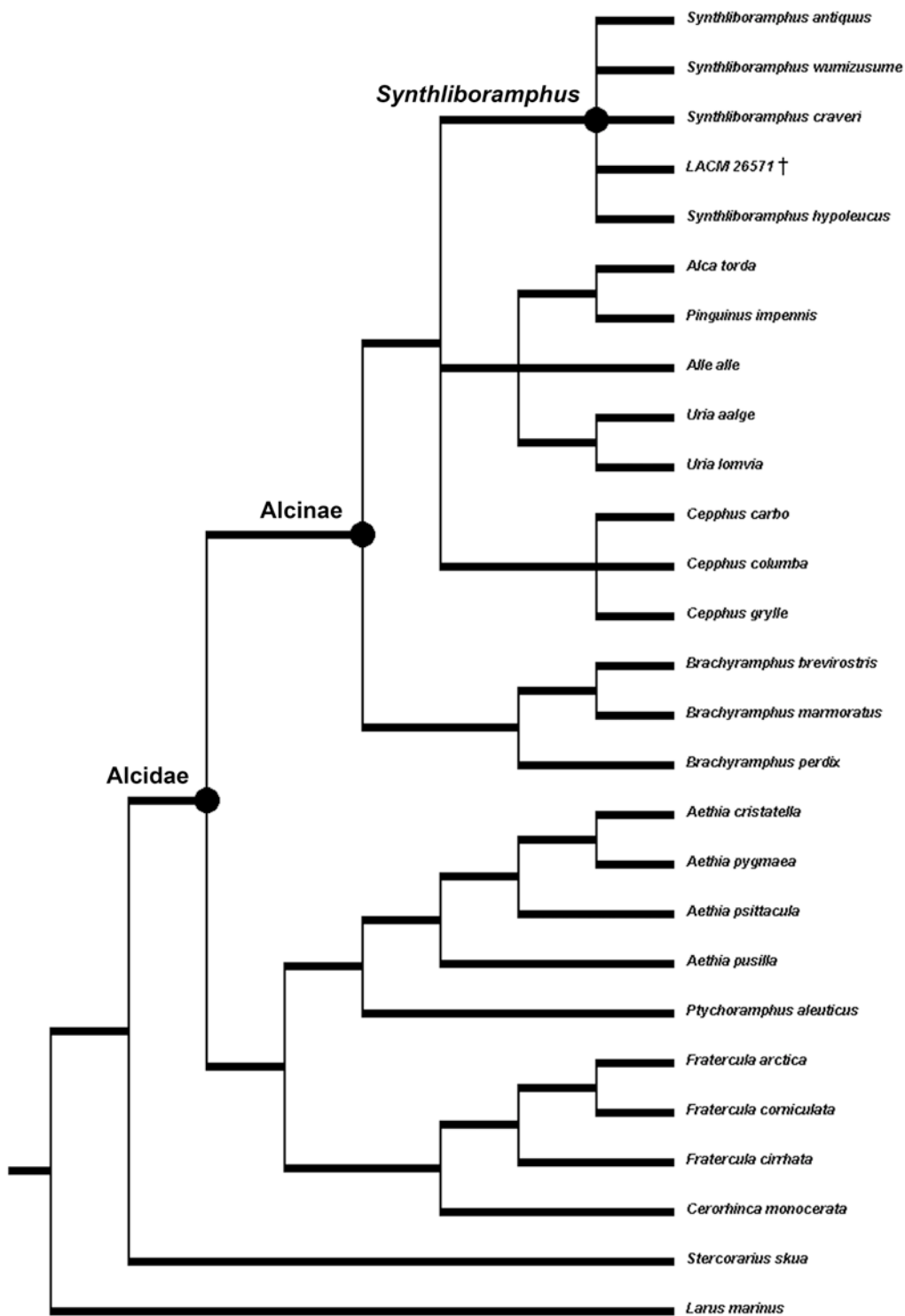


Figure 7.9- Strict consensus cladogram indicating showing the unresolved systematic position of LACM 26571 in *Synthliboramphus*.

## SYSTEMATIC PALEONTOLOGY

AVES Linnaeus, 1758

CHARADRIIFORMES Huxley, 1867

PAN-ALCIDAE Smith, 2011

ALCIDAE Leach, 1820

*BRACHYRAMPHUS* Brandt, 1837

*Diagnosis*—*Brachyramphus* is differentiated from all other Alcidae by a single unambiguously optimized apomorphy with a CI = 1.0. *Brachyramphus* species have a distinct medially deflected hook on the tip of the procoracoid process of the coracoid (98:1). The combination of three additional locally optimized morphological apomorphies separate *Brachyramphus* from other Alcidae. As in *Alle alle*, Aethiini, Mancallinae, and many other charadriiforms (e.g., *Rhinoptilus chalcopterus*) the procoracoid process of the coracoid is not punctured by the m. supracoracoideus nerve foramen (93:0). The lateral margin of the anterior face of the coracoid is excavated sternally (100:0) as in *Uria* rather than bordered ventrally by a ridge as in *Synthliboramphus*. As in *Cerorhinca monocerata*, a ridge extends from the humeral head to the ventral tubercle and divides the capital groove (133:1). Only the humeral characters listed above could be evaluated in *Brachyramphus pliocenium* and *Brachyramphus dunkeli* because the holotype specimens representing those extinct species are humeri and

no associated specimens are currently known that would allow of referral of additional skeletal elements to those species.

***BRACHYRAMPHUS PLIOCENUM* Howard, 1949**

*Original diagnosis*—*Brachyramphus pliocenum* was originally differentiated from *Brachyramphus marmoratus* by Howard (1949) by having the proximal end of the humerus broader and more robust, the m. pectoralis scar longer, the m. latissimus dorsi scar more prominent and slanting more posteriorly, and the humeral shaft slightly convex between the m. latissimus dorsi scar and the dorsal border of the humeral shaft.

*Remarks*—Presumably, Howard (1949) compared *Brachyramphus pliocenum* only with the extant species *Brachyramphus marmoratus* owing to the extant range of that species (eastern Pacific). Because geographical ranges of birds are known to change, comparison with all extant species of *Brachyramphus* is warranted. However, the character differences between *Brachyramphus pliocenum* and *Brachyramphus marmoratus* noted by Howard (1949) also differentiate *Brachyramphus pliocenum* from the extant species *Brachyramphus brevirostris* and *Brachyramphus perdix*.

*Amended diagnosis*—The following locally optimized apomorphy is added to the differentia provided by Howard (1949). The ventral tubercle is robust (134:1) as in *Alcatorda* rather than gracile as in other *Brachyramphus* species (Fig. 7.2).

***BRACHYRAMPHUS DUNKELI* Chandler, 1990**

*Original diagnosis (sensu* Chandler, 1990b)—Differentiated from other species of *Brachyramphus* by: its relatively larger size; the presence of a ridge extending from the humeral head to the ventral tubercle; bicipital crest broader; lateral contour of secondary pneumotricipital fossa stepped from attachment of m. dorsalis scapulae to the dorsal tubercle; primary pneumotricipital fossa large, oblong, and dorsal border thinner than other species in the clade.

*Amended diagnosis*—The following diagnostic characters are added to or modified from those described by Chandler (1990b). *Brachyramphus dunkeli* is differentiated from other species of *Brachyramphus* (Fig. 7.10) by its larger size (see Chandler, 1990b, Table 29). The ventral supracondylar tubercle of the humerus is rounded (162:1) as in *Fratercula*, rather than triangularly shaped as in *Synthliboramphus*. *Brachyramphus dunkeli* is differentiated from *Brachyramphus pliocenium* by the pointed, rather than rounded distal margin of the humeral head (105:1) and the restriction of the dorsal border of the primary pneumotricipital fossa (i.e., medial pneumotricipital crest *sensu* Chandler, 1990b) proximal to the junction of the bicipital crest with the humeral shaft (118:0). As in extant species of *Brachyramphus*, the ventral tubercle is relatively more gracile than that of *Brachyramphus pliocenium* (134:0; Fig. 7.4). Although this taxon can be differentiated from other species of Alcidae based on the combination of

characters listed above, all of those characters are locally optimized (i.e., those characters display a rather high degree of homoplasy among Alcidae).



Figure 7.10- Left humeri of extant brachyramphine murrelets in posterior view: (A) *Brachyramphus perdix* (USNM 599498); (B) *Brachyramphus marmoratus* (NCSM 18143); (C) *Brachyramphus brevirostris* (USNM 288086).



***BRACHYRAMPHUS* sp.**

*Referred specimen*—a left coracoid (SDSNH 24865; Fig. 7.11) collected by R. A. Cerutti on the 6<sup>th</sup> of March 1983.

*Locality and horizon*—Pliocene San Diego Formation, San Diego County, California, USA. Latitude, longitude, and elevation data are on file at SDSNH (locality 3179).

*Diagnosis*—This specimen is referred to *Brachyramphus* based upon the medially hooked tip of the procoracoid process (98:1; a proposed autapomorphy of *Brachyramphus*) and the absence of an m. supracoracoideus nerve foramen in the procoracoid process (93:0; also absent in Aethiini, *Alle*, and Mancallinae). The lateral margin of the anterior face of the coracoid has a sternally extended excavation medial to the lateral process (100:0) as in *Alca*, rather than a ventrally bordered excavation demarcated by a distinct ridge proximal to the sternal articulation facet as in Fraterculinae. This specimen is differentiated from all extant species of *Brachyramphus* by the less deeply undercut acrocoracoid process of the coracoid (88:2) and the relatively shorter length of the acrocoracoid process of the coracoid (91:0).

*Remarks*—Although this specimen is distinct from living species of *Brachyramphus*, because the coracoidal characters that diagnose this specimen cannot be

evaluated in *Brachyramphus pliocenium* and *Brachyramphus dunkeli*, which are known only from humeri, this specimen is not named as a new taxon.

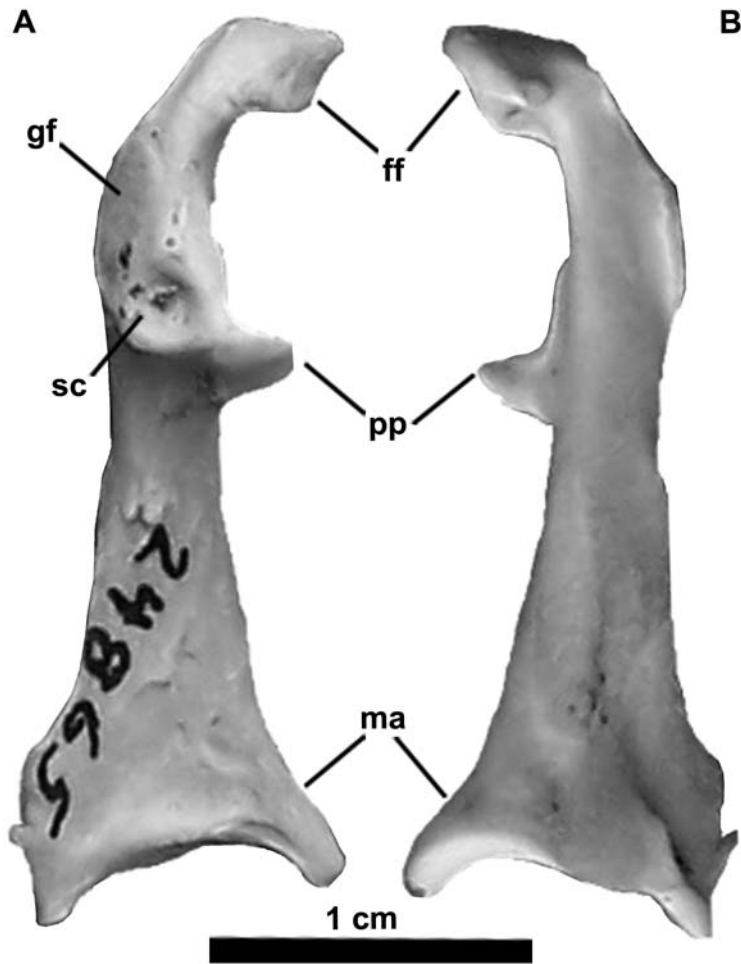


Figure 7.11- *Brachyramphus* sp. referred left coracoid (SDSNH 24865) in posterodorsal (A), and anteroventral (B) views. Anatomical abbreviations: furcular facet (**ff**); glenoid facet (**gf**); medial angle (**ma**); procoracoid process (**pp**); scapular cotyla (**sc**).

***BRACHYRAMPHUS* sp.**

*Referred specimen*—a right coracoid (SDSNH 24866; Fig. 7.12) collected by R. A. Cerutti on the 18<sup>th</sup> of November 1982.

*Locality and horizon*—Pliocene San Diego Formation, San Diego County, California, USA. Latitude, longitude, and elevation data are on file at SDSNH (locality 3006).

*Diagnosis*—This specimen is referred to *Brachyramphus* based upon the medially hooked tip of the procoracoid process (98:1; a proposed autapomorphy of *Brachyramphus*) and the absence of an m. supracoracoideus nerve foramen in the procoracoid process (93:0; also absent in Aethiini, *Alle*, and Mancallinae). The lateral margin of the anterior face of the coracoid has a sternally extended excavation medial to the lateral process (100:0) as in *Alca*, rather than a ventrally bordered excavation demarcated by a distinct ridge proximal to the sternal articulation facet as in Fraterculinae. This specimen is differentiated from all extant species of *Brachyramphus*, SDSNH 24865, and all other Pan-Alcidae by the ‘wing-shaped’ procoracoid process of the coracoid (95:2; i.e., flanges projecting from the sternal and omal margins of the procoracoid process; Fig. 7.12). This specimen is differentiated from all extant species of *Brachyramphus* by the less deeply undercut acrocoracoid process of the coracoid (88:2) and the relatively shorter length of the acrocoracoid process of the coracoid (91:0).

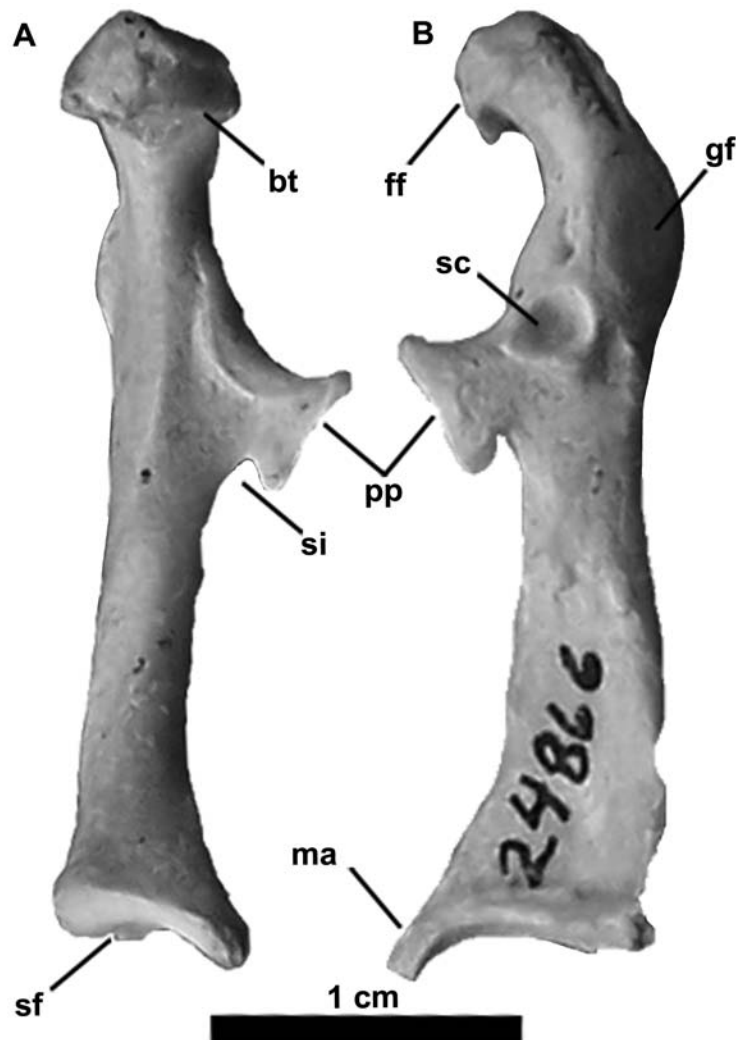


Figure 7.12- *Brachyramphus* sp. referred right coracoid (SDSNH 24866) in medial (A) and lateral (B) views. Anatomical abbreviations: brachial tubercle (**bt**); furcular facet (**ff**); glenoid facet (**gf**); medial angle (**ma**); procoracoid process (**pp**); scapular cotyla (**sc**); m. supracoracoideus nerve incisure; sternal facet (**sf**).

*Remarks*—Because these coracoidal characters cannot be evaluated in *Brachyramphus pliocenium* and *Brachyramphus dunkeli*, which are known only from humeri, this specimen is not named as a new taxon. The presence of two species of *Brachyramphus* in the San Diego Formation known from humeri, and the presence of two

distinct types of *Brachyramphus* coracoids suggests that all these remains represent *Brachyramphus pliocenum* and *Brachyramphus dunkeli*. However, in the absence of associated remains that would allow for the referral of elements other than humeri to *Brachyramphus pliocenum* and *Brachyramphus dunkeli*, these new remains (SDSNH 24865 and SDSNH 24866) are best considered *Brachyramphus incertae sedis*.

*SYNTHLIBORAMPHUS* Brandt, 1837

*Diagnosis*—*Synthliboramphus* is differentiated from all other Pan-Alcidae by a single unambiguously optimized apomorphy with a CI = 1.0. The trochlear proportions of the tarsometatarsus are more gracile (i.e., mediolaterally and anteroposteriorly narrower) than those of other Pan-Alcidae; 230:1). Five additional locally optimized apomorphies separate *Synthliboramphus* from other Pan-Alcidae. The palatines narrow before articulation with the pterygoid (15:1) as in *Brachyramphus perdix* rather than maintain width throughout their length as in Fraterculinae. As in many non-alcid charadriiforms, the tibiotarsus is less than two times length of tarsometatarsus (218:0). The tarsometatarsus is relatively shorter in all other Pan-Alcidae. As in Mancallinae and many non-alcid charadriiforms, the trochlea of metatarsal II of the tarsometatarsus does not overlap trochlea of metatarsal III in medial view (i.e., in medial view the trochlea of metatarsal II is posteriorly positioned so that the anterior margin of the trochlea of metatarsal II does not extend anterior to the posterior margin of the trochlea of metatarsal II; 231:0). The tarsometatarsus is longer than femur (232:0). As in the sister taxon of Pan-

Alcidae, the Stercorariidae, the eggs of *Synthliboramphus* have a glossy luster (273:1). These characters could not be evaluated in the only known extinct species of *Synthliboramphus*, because the holotype specimen of *Synthliboramphus rineyi* is a humerus and no associated specimens that would allow for referral of additional elements to this taxon are currently known. However, isolated *Synthliboramphus* humeri can be differentiated from those of other alcids on the basis of the following combination of characters. As in *Brachyramphus*, the posterior face of the humeral head is notched in proximal view (106:1). *Synthliboramphus* is differentiated from Fraterculinae (contents of Fraterculinae include *Fratercula*, *Cerorhinca*, *Aethia*, *Ptychoramphus*) by the more shallowly excavated m. coracobrachialis impression on the anterior surface of the proximal humerus (110:2), and the concave distal edge of the primary (ventral) pneumotricipital fossa (129:2). This margin is straight (e.g., *Brachyramphus*, *Alle*, *Uria*, *Cepphus*) or convex (e.g., *Cerorhinca aurorensis*) in many other alcids. As in *Pinguinus* and *Uria*, the dorsal supracondylar process transitions smoothly to the humeral shaft in the humeri of *Synthliboramphus* rather than the more angled and dorsally projecting dorsal supracondylar process of *Alca*, *Alle*, and *Brachyramphus*.

***SYNTHLIBORAMPHUS RINEYI* Chandler, 1990**

*Original diagnosis*—Differentiated from other *Synthliboramphus* only by its smaller size.

*Amended diagnosis*—*Synthliboramphus rineyi* is differentiated from all other species of *Synthliboramphus* by having the scapulotricipital sulcus broader than the humerotricipital sulcus (151:2). It is further differentiated from *Synthliboramphus wumizusume* and *Synthliboramphus craveri* by the shape of the m. supracoracoideus crest (i.e., the distally elongated dorsal tubercle; see Baumel and Witmer, 1993:98; Fürbringer, 1888), which, as in *Fratercula*, is long and broadens proximally (116:1; Fig. 7.13). As in *Synthliboramphus antiquus* and *Synthliboramphus hypoleucus*, the dorsal border of the primary pneumotricipital fossa (crus dorsale fossae, Baumel and Witmer, 1993) extends to the junction of the bicipital crest with the humeral shaft (118:1), as opposed to the condition in some alcids (e.g., *Fratercula arctica*) in which this crest is more proximally restricted. The m. subcoracoideus is positioned medially (127:0) as in *Synthliboramphus antiquus* and *Synthliboramphus hypoleucus* rather than ventrally as in *Synthliboramphus wumizusume* and *Synthliboramphus craveri*. The ventral tubercle is robust (i.e., mediolaterally broad) as in *Synthliboramphus antiquus* and *Synthliboramphus hypoleucus* (134:1). *Synthliboramphus rineyi* is differentiated from *Synthliboramphus antiquus* and *Synthliboramphus hypoleucus* by the rounded posterior margin of humeral head (105:0) and the smooth transition from the deltopectoral crest to the humeral shaft (108:0). *Synthliboramphus rineyi* is further differentiated from *Synthliboramphus antiquus* and *Synthliboramphus hypoleucus* by the lack of a bony division of the secondary pneumotricipital fossa (132:0) and the presence of an m. pronator sublimis scar along the proximodorsal margin of the ventral supracondylar tubercle (163:1; Fig. 7.5; absent in *Alle alle* and some species of auklets including *Aethia cristatella*).



Figure 7.13- Left humeri of extant synthliboramphine murrelets in posterior view: (A) *Synthliboramphus antiquus* (NCSM 18090); (B) *Synthliboramphus hypoleucus* (USNM 500652); (C) *Synthliboramphus wumizusume* (UMMZ 152356); (D) *Synthliboramphus craveri* (SDSNH 36390).

## DISCUSSION

The re-examination of the partial cranium (LACM 15426) referred to *Synthliboramphus* by Howard (1970) did not identify any apomorphies preserved in this



fragmentary specimen that would facilitate referral to *Synthliboramphus*; however, this specimen could be scored for only 2 characters (20:1, deep rather than shallow salt gland fossa; 22:0, shallow rather than deep interhemispherical furrow). Deep salt gland fossae are characteristic of many Alcinae (e.g., *Synthliboramphus*, *Uria*, and *Alle*) and are also observed in many other charadriiforms (e.g., *Xema sabini*). Deep interhemispherical furrows are present only in Mancallinae among Charadriiformes. Based on the unresolved placement of this specimen at the base of Alcidae in the phylogenetic analysis (Fig. 7.8), this specimen is best considered Alcidae *incertae sedis* (Table 7.3).

Re-examination of the proximal humerus (LACM 26571) referred to *Synthliboramphus* by Howard (1970) did not identify any discrete character or size-based differences between that specimen and *Synthliboramphus craveri* or *Synthliboramphus wumizusume*. Based upon the unresolved position of LACM 26571 in *Synthliboramphus* in the results of the phylogenetic analysis (Fig. 7.9), this specimen is best considered *Synthliboramphus incertae sedis* (Table 7.3).

The derived position of *Synthliboramphus rineyi* as the sister of *Synthliboramphus hypoleucus* suggests at least one divergence among *Synthliboramphus* occurred prior to the Middle to Late Pliocene occurrence of *Synthliboramphus rineyi*. Although the charadriiform divergence estimates of Pereira and Baker (2008) are not considered a reliable estimate by some authors (Wijnker and Olson, 2009; Mayr, 2011) because of the incorrect dating and incorrect taxonomic assignment of many of the fossils used as calibrations, those results suggest that the basal divergence between extant *Synthliboramphus* species occurred ~20 Ma in the Early Miocene. Early Miocene

divergence of *Synthliboramphus* would indicate that the fossil record of this clade is significantly incomplete. *Synthliboramphus rineyi* is the oldest record of *Synthliboramphus*, and based on the position recovered for *Synthliboramphus rineyi* in the phylogenetic results, the age of this taxon could be used to date the age of the minimum divergence between the extant species *Synthliboramphus craveri* and *Synthliboramphus hypoleucus*.

Although SDSNH 24865 and SDSNH 24866 can be differentiated from extant species of *Brachyramphus*, the coracoids of *Brachyramphus pliocenium* and *Brachyramphus dunkeli* are not known. Based upon the unresolved placement of these specimens in *Brachyramphus* in the results of the phylogenetic analysis (Fig. 7.7), SDSNH 24865 and SDSNH 24866 are considered *Brachyramphus incertae sedis*. These results do, however, support the placement of *Brachyramphus pliocenium* and *Brachyramphus dunkeli* as part of a monophyletic *Brachyramphus*.

Unresolved placement of the newly referred *Brachyramphus* coracoids (SDSNH 24865 and 24866) in *Brachyramphus* is not unexpected given the lack of overlapping scorings with *Brachyramphus pliocenium* and *Brachyramphus dunkeli*, which are known only from humeri. The newly referred *Brachyramphus* coracoids, *Brachyramphus pliocenium*, and *Brachyramphus dunkeli* are all present in the San Diego Formation. SDSNH 24865 and 24866 represent two distinct species of *Brachyramphus*. The possibility that these coracoids are representative of *Brachyramphus pliocenium* and *Brachyramphus dunkeli* cannot be confirmed in the absence of specimens that preserve associated humeri and coracoids, but should be considered. *Brachyramphus pliocenium*

does, however, provide a potential calibration point for the divergence of *Brachyramphus* from other Alcidae.

*Brachyramphus perdix* was considered a sub-species of *Brachyramphus marmoratus* by the American Ornithologist's Union (AOU, 1983; i.e., *Brachyramphus marmoratus perdix*) until Friesen et al. (1996b) showed that there is greater mitochondrial sequence divergence between *Brachyramphus marmoratus* and *Brachyramphus perdix* than between *Brachyramphus brevirostris* and *Brachyramphus marmoratus*. Congruent with the results of previous phylogenetic analyses that sampled all three species of brachyramphine murrelets (Friesen et al., 1996b; Pereira and Baker, 2008), *Brachyramphus marmoratus* and *Brachyramphus brevirostris* were recovered as sister taxa to the exclusion of more basally positioned *Brachyramphus perdix*.

Table 7.3- Summary of taxonomic revision of previously published murrelet fossil remains.

Original Taxonomic Assignment	Reference	Specimen #	Revised Taxonomic Assignment
<i>Brachyramphus pliocenium</i>	Howard, 1949	LACM 2119	<i>Brachyramphus pliocenium</i>
<i>Synthliboramphus indeterminate</i>	Howard, 1971	LACM 26571	<i>Synthliboramphus incertae sedis</i>
		LACM 15426	Alcidae incertae sedis
<i>Brachyramphus dunkeli</i>	Chandler 1990b	SDSNH 24573	<i>Brachyramphus dunkeli</i>
<i>Synthliboramphus rineyi</i>	Chandler 1990b	UCMP 61590	<i>Synthliboramphus rineyi</i>

## CONCLUSIONS

The results presented herein confirm previous estimates of extinct murrelet diversity and describe previously undocumented morphological variation in these clades. The phylogenetic hypothesis supports *Brachyramphus* and *Synthliboramphus* monophyly including fossil taxa, places *Brachyramphus* basally within Alcinae (contents of Alcinae include *Alca*, *Pinguinus*, *Uria*, *Alle*, *Miocepphus*, *Cepphus*, *Synthliboramphus*, and *Brachyramphus*), and places *Synthliboramphus* as the sister taxon to an Alcini + *Cepphus* clade. Although *Brachyramphus* and *Synthliboramphus* have been previously recovered in a variety of systematic positions with Alcinae, both clades have been recovered at or near the base of Alcinae in the results of nearly every phylogenetic analysis that has included these taxa, including the results presented herein (Fig. 7.7; Strauch, 1985; Watada et al., 1987; Chandler, 1990a; Friesen et al., 1996; Thomas et al., 2004; Baker et al., 2007; Pereira and Baker, 2008; Smith, 2011).

The oldest fossil representatives of *Brachyramphus* and *Synthliboramphus* are from the Pliocene (Howard, 1949; Howard, 1971; Chandler, 1990b; Table 7.1). Given the hypothesis that these clades represent basal divergences within Alcidae, it is surprising that the fossil record of other more derived clades of alcids (e.g., *Alca*, *Uria*, *Aethia*) have much richer fossil records in terms of quantity and temporal range of known specimens. The hypothesized basal position of murrelets in Alcidae suggests that the fossil record of these clades is quite incomplete, with the longest ghost ranges known for Alcidae.

Perhaps the small size of murrelets has not favored preservation of their remains and has

produced a size-based bias in the fossil record, or perhaps the geographic range of early murrelets does not coincide with older (i.e., Miocene and earlier) geologic units that have been sampled to date. Another possibility is that alcid fossil-bearing deposits represent deep-water environments that are not frequented by smaller, shallowly diving murrelets.

Although alcid remains older than Miocene are rare (Olson, 1985), consisting of a single specimen from the Eocene of Georgia (Chandler and Parmley, 2002), the apparent absence of murrelet fossils from previously sampled Miocene deposits suggests that the geographic range of these birds may have been restricted preceding the Pliocene. The modern range of *Synthliboramphus* extends farther south of the Tropic of Cancer than any other clade of extant alcids. It has been suggested that the ancestral alcid stock was more adapted to warmer climates than their modern counterparts (Bédard, 1985) and it is possible that the cold-water upwelling that characterizes the depositional environments of many alcid fossil-bearing deposits such as the San Diego Fm. (Wagner et al., 2001), may not have been the habitat occupied by pre-Pliocene *Synthliboramphus*. The possibility that *Synthliboramphus* was species depauperate until post-Pliocene times should also be considered.

Based on the basal position of *Synthliboramphus* and *Brachyramphus* in Alcinae, the sister taxon relationship recovered between Fraterculini and Aethiini (Fig. 7.7), and the relatively small body mass of Aethiini, *Synthliboramphus*, and *Brachyramphus* in comparison with other alcids (del Hoyo et al., 1996), small body mass is optimized as the ancestral condition in Alcidae (Fig. 7.14). Body mass estimates are not known for the extinct flightless Mancallinae that are placed as the sister taxon to Alcidae. However,

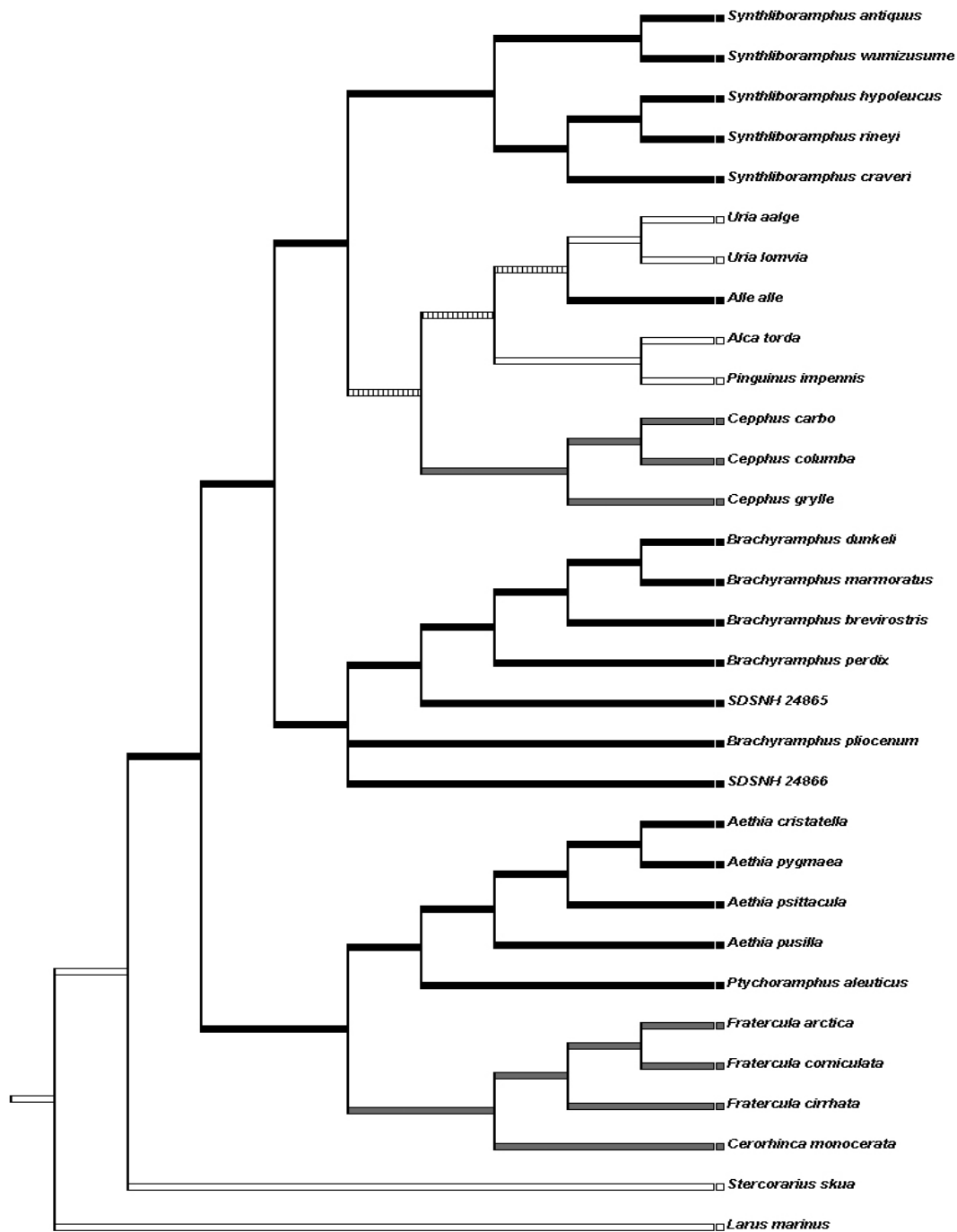


Figure 7.14- Small body mass of extant alcids is optimized as ancestral on the topology recovered in the combined phylogenetic analysis (Fig. 7.7). Character states for species are indicated by the colored squares between the taxon names and the cladogram: small (white); moderate (grey); large (black). Dashed lines represent ambiguous reconstruction of hypothesized ancestral character states.

given the hypothesized reduction in size of the pectoral elements of flightless alcids in comparison with other body regions (Livezey, 1988, 1989), the smaller size of *Mancalla vegrandis* Smith, 2011 in comparison with other Mancallinae may not be indicative of overall smaller body mass. Thus, body mass reconstruction for Pan-Alcidae would likely be ambiguous.

The fossil record of *Synthliboramphus* and *Brachyramphus* murrelets indicates that these small alcids have been a part of the Pacific Ocean avifauna since at least the Pliocene. Older records of more derived alcid taxa (e.g., *Uria brodkorbi* from the Late Miocene) provide evidence that the early fossil record of murrelets is quite incomplete given their basal position in Alcinae (Fig. 7.7). The almost complete lack of Oligocene fossil records of Alcidae and the basal position of murrelets in Alcinae should serve as motivation in the search for additional fossil remains of murrelets.

## CHAPTER 8.

The systematics and evolution of the Pan-Alcidae  
(Aves, Charadriiformes) inferred through  
combined phylogenetic analysis and  
divergence estimation



## INTRODUCTION

Collectively known as the Alcidae, auks, auklets, murres, murrelets, guillemots, and puffins are pelagic charadriiform seabirds characterized by wing-propelled diving and anatomical modifications associated with this derived method of prey pursuit. Extant diversity within Alcidae includes twenty-three species of exclusively Holarctic distribution (del Hoyo et al., 1996). Alcids are small to medium sized seabirds with plumage in the 23 extant species that is generally countershaded darkly above (dorsally) and lightly below (ventrally). Sexes are similar in both size and plumage (del Hoyo et al., 1996). The bills of many alcids are relatively broader or deeper (i.e., mediolaterally or dorsoventrally expanded) than many other seabirds (e.g., loons), which prompted early naturalists to refer to them as ‘sea-parrots’ (Swainson, 1837). Like parrots, alcids display a high degree of mate fidelity (Harris and Birkhead, 1985; del Hoyo et al., 1996). Alcids spend ~10 months of the year at sea and generally come ashore only to reproduce. Most alcids nest in large colonies on rocky beaches or sea cliffs that are relatively inaccessible to predation by mammals, although two non-colonial species, Kittlitz’s Murrelet *Brachyramphus brevirostris* and the Marbled Murrelet *Brachyramphus marmoratus*, nest farther inland on the ground or in trees respectively (del Hoyo et al., 1996). Extant alcids are not strong or acrobatic aerial flyers and have relatively short wings (i.e., low aspect ratio) and tails (Pennycuik, 1975, 1987). However, alcids more than compensate for any loss of aerial prowess with underwater maneuverability approaching that seen in penguins. Diet varies between species, with larger alcids such as murres feeding

primarily on vertebrates (mainly fish) and smaller alcids such as auklets feeding primarily on invertebrates (mainly crustaceans; Bradstreet and Brown, 1985; Ainley et al., 1990b).

Archaeological evidence and historical accounts show that alcids have long been a source of eggs, meat, feathers, fat, and oil for humans (Friedmann, 1934, 1937, 1941; Fuller, 1999; Dingus and Rowe, 1998). Predation by humans and human-introduced predators, ocean pollution, nesting habitat destruction, and overfishing by humans has dramatically decreased numbers of alcids since the early 1900's (Gaston, 1990; Wiese et al., 2004). Although many seabirds are protected, alcid populations rebound slowly and are sensitive to disturbance owing to low reproductive rates and late attainment of sexual maturity (Harris and Birkhead, 1985; Ainley, 1990). The changing temperatures and associated changes in ocean currents and ocean bioproductivity related to the current global warming trend also poses a threat to alcids (Ainley, 1990; Gaston et al., 2005; Hyrenbach and Veit, 2003; Gaston and Woo, 2008). Support for seabird conservation has been bolstered by ecotourism focused on brightly colored and gregarious alcids such as the Atlantic Puffin. Hopefully, lessons learned from the extinction of the Great Auk at the hand of humans will be heeded and other seabirds will be spared a similar fate.

Although the ecological interactions, ethology, and systematics of extant alcids have been intensively studied, more than half of known alcid diversity is extinct and only two extinct alcids have been previously included in a phylogenetic analysis. DNA was extracted from the recently extinct Great Auk *Pinguinus impennis* and utilized in a molecular-based phylogeny of Atlantic alcids (Moum et al., 2002), and *Mancalla* was included as a supraspecific-terminal taxon in the morphology-based analysis of Chandler

(1990a). Ancestral ethology and ecology of alcids can be estimated only through study of extinct species in a phylogenetic context.

The alcid fossil record is the richest among Charadriiformes, with approximately 17,000 known specimens representing at least 28 species known from approximately 12 localities worldwide (Smith, personal observation; Fig. 8.1). These localities have an age distribution spanning more than 35 million years from the Late Eocene through the Holocene (Olson, 1985; Tyrberg, 1998; Chandler and Parmley, 2002). Fossil records of alcids from the Late Miocene, Pliocene, and Pleistocene are quite numerous (Brodkorb, 1967), though plagued by an abundance of dubiously identified taxa (e.g., Miller, 1931; Howard, 1968) and large quantities of undescribed or systematically un-assessed material (Olson and Rasmussen, 2001). All extant alcid clades have records that stretch back into the Miocene or Pliocene, and two clades (Mancallinae, *Pinguinus*) have no extant representatives. The first records of at least 34 species occur in the Miocene or Pliocene and 17 of 23 extant alcids are known from Pleistocene or younger deposits (Table 8.1). The oldest known stem clade alcid remains are from the Late Eocene (~35 Ma; Chandler and Parmley, 2002). By the Early Pliocene there was a diverse group of pan-alcids inhabiting the northern zones of both the Pacific and Atlantic Oceans. Refined estimates of species richness among extinct pan-alcids, divergence estimation, and assessment of the systematic position of extinct species in a phylogenetic context holds potential to elucidate the evolution of the clade in ways that have not been possible with other methods (i.e., non-apomorphy-based/non-phylogenetic methods) applied previously.

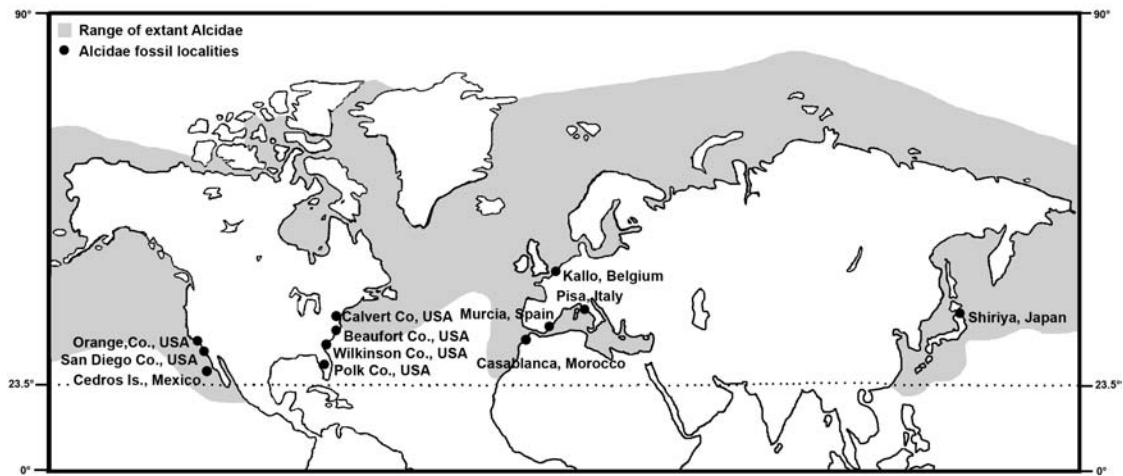


Figure 8.1- Map of extant alcid geographical range and pan-alcid fossil localities (altered from del Hoyo et al., 1996).

Biogeographically, pan-alcids are hypothesized to have originated in the Pacific Ocean basin and dispersed to the Atlantic Ocean basin by the Late Eocene (Olson, 1985; Konyukhov, 2002; Pereira and Baker, 2008). The modern distribution of alcids (18 Pacific, 4 Atlantic, 3 spanning both Northern Hemisphere ocean basins) has been used to support that hypothesis (Olson, 1985). Given the taxonomic revisions outlined in previous chapters, the fossil record of pan-alcids is not as clear-cut, with ~18 currently recognized species from the Pacific and ~18 species from the Atlantic (Table 8.2). Although a Pacific origin for the Pan-Alcidae is widely accepted (Storer, 1960; Olson, 1985; Pereira and Baker, 2008, Konyukhov, 2002), molecular evidence (Kidd and Friesen, 1998; Friesen et al., 1996) suggests the biogeography of some clades (e.g., *Fratercula* and *Cepphus*) may be more complex than a simple Miocene migration of species from the Pacific to the Atlantic. The questions of whether pan-alcids originated in the Pacific or Atlantic, and whether there were multiple periods of exchange remain

Table 8.1- Age range of pan-alcid species based on published fossil material. Extant species appear in bold font.

<b>Taxon</b>	<b>Age Range</b>	<b>Reference</b>
<i>Aethia cristatella</i>	~2.5 ka - present	Friedmann, 1934
<i>Aethia pygmaea</i>	no fossil record	
<i>Aethia psittacula</i>	~1.5 ka - present	Friedmann, 1941
<i>Aethia pusilla</i>	~2.0 ka - present	Friedmann, 1941
<i>Aethia storeri</i>	~3.6 Ma	Chapter 5
<i>Aethia barnesi</i>	6.7-10.0 Ma	Chapter 5
<b><i>Ptychoramphus aleuticus</i></b>	~25.0 ka - present	Howard, 1949; Guthrie, 1992
<i>Cerorhinca minor</i>	~5.0 Ma	Howard, 1971; Addicot, 1972
<b><i>Cerorhinca monocerata</i></b>	~2.0 ka - present	Friedmann, 1937
<i>Cerorhinca aurorensis</i>	4.4 Ma	Smith et al., 2007, Chapter 4
<i>Cerorhinca reai</i>	~3.6 Ma	Chandler, 1990b; Wagner et al., 2001
<b><i>Fratercula arctica</i></b>	4.4 Ma - present	Olson and Rasmussen, 2001
<b><i>Fratercula corniculata</i></b>	~15.0 ka - present	Friedmann, 1941
<b><i>Fratercula cirrhata</i></b>	4.4 Ma - present	Olson and Rasmussen, 2001
<i>Fratercula dowi</i>	46.0 - 31.0 ka	Guthrie et al., 1999
<i>Alca ausonia</i>	4.4 Ma	Olson and Rasmussen, 2001
<i>Alca carolinensis</i>	4.4 Ma	Smith and Clarke, in press
<i>Alca stewarti</i>	7.0 - 4.4 Ma	Wijnker and Olson, 2009
<i>Alca minor</i>	4.4 Ma	Smith and Clarke, in press
<b><i>Alca torda</i></b>	10.0 Ma - present	Wijnker and Olson, 2009
<i>Alca olsoni</i>	4.4 Ma	Smith and Clarke, in press
<i>Alca grandis</i>	4.4 Ma	Olson and Rasmussen, 2001
<i>Pinguinus alfrednewtoni</i>	4.4 Ma	Olson and Rasmussen, 2001
<i>Pinguinus impennis</i>	500.0 ka - 1844	Harrison and Stewart, 1999
<b><i>Alle alle</i></b>	34.0 ka - present	Stewart, 2002
<i>Miocepphus mergulellus</i>	14.0 Ma	Wijnker and Olson, 2009
<i>Miocepphus blowi</i>	~6.5 Ma	Wijnker and Olson, 2009
<i>Miocepphus bohaski</i>	20.0 - 12.0 Ma	Wijnker and Olson, 2009
<i>Miocepphus mcclungi</i>	16.0 - 12.0 Ma	Wijnker and Olson, 2009
<b><i>Uria aalge</i></b>	~25.0 ka - present	Guthrie, 1992
<b><i>Uria lomvia</i></b>	~12.0 ka - present	Marsh, 1870
<i>Uria brodkorbi</i>	~10.0 Ma	Howard, 1981
<b><i>Cepphus carbo</i></b>	no fossil record	
<i>Cepphus olsoni</i>	~8.0 Ma	Howard, 1982
<b><i>Cepphus columba</i></b>	~25.0 ka - present	Guthrie, 1992; Friedmann, 1934
<b><i>Cepphus grylle</i></b>	Pleisto. - present	Lambrecht, 1933
<i>Pseudocepphus teres</i>	14.0 - 8.0 Ma	Wijnker and Olson, 2009
<b><i>Brachyramphus brevirostris</i></b>	~2.5 ka - present	Friedmann, 1934

Table 8.1- (continued from previous page) Age range of pan-alcid species based on known fossil material.

<b>Taxon</b>	<b>Age Range</b>	<b>Reference</b>
<i>Brachyramphus marmoratus</i>	~2.0 ka - present	Friedmann, 1937
<i>Brachyramphus perdix</i>	no fossil record	
<i>Brachyramphus dunkeli</i>	~3.6 Ma	Chandler, 1990b
<i>Brachyramphus pliocenium</i>	~3.6 Ma	Howard, 1949; Wagner et al., 2001
<i>Synthliboramphus antiquus</i>	~130.0 ka - present	Brodkorb, 1967; Hasegawa et al., 1988
<i>Synthliboramphus wumizusume</i>	no fossil record	
<i>Synthliboramphus craveri</i>	no fossil record	
<i>Synthliboramphus hypoleucus</i>	~25.0 ka- present	Guthrie, 1992
<i>Synthliboramphus rineyi</i>	~3.6 Ma	Chandler, 1990b
<i>Mancalla californiensis</i>	10.0 - 3.6 Ma	Howard, 1982; Becker, 1987
<i>Mancalla cedrosensis</i>	5.0 - 3.6 Ma	Howard, 1970; Becker, 1987
<i>Mancalla lucasi</i>	3.6 Ma - 470 ka	Kohl, 1974; Smith, 2011
<i>Mancalla vegrandis</i>	3.6 - 1.8 Ma	Smith, 2011
<i>Miomancalla howardi</i>	8.7 - 4.9 Ma	Smith, 2011
<i>Miomancalla wetmorei</i>	6.7 - 10.0 Ma	Howard, 1976; Smith, 2011

unanswered. Evaluations of conflicting biogeographical hypotheses based upon different ancestral area optimizations of alcid evolution have been hindered by the lack of a phylogeny including extinct species and divergence estimates that used inaccurate fossil calibrations (Baker et al., 2007; Pereira and Baker, 2008).

Because pelagic seabirds such as alcids depend on the ocean for sustenance but must return to shore to reproduce, they provide a proxy for the study of changes in the marine and terrestrial environments. Changes in climate that effect sea level have potential to impact the availability of suitable breeding sites, and changes in ocean temperatures have potential to impact the distribution and availability of food. Previous

researchers (Warheit, 1992b; Emslie, 1998; Olson and Rasmussen, 2001; Smith et al., 2007; Pereira and Baker, 2008) have correlated radiation and extinction of alcids with paleoclimatic events that effected sea level and oceanic circulation patterns such as the Mid-Miocene Climatic Optimum (MMCO; ~16-11 Ma; Zachos et al., 2001), the closure of the Central American Seaway (CAS; ~2.5-3.5 Ma; Bartoli et al., 2005), and Pleistocene glaciations (2.5 Ma-present; Versteegh, 1997; Warheit, 2002; Moum et al., 1994). Hypothesized increases in alcid diversity during the Miocene have been attributed to the onset of increased cold-water upwelling in the Atlantic and Pacific Ocean basins (Warheit, 1992b; Emslie, 1998). Similarly, hypothesized decreases in alcid diversity during the Pliocene have been attributed to changes in the location of cold-water upwelling centers associated with the emergence of the Panamanian Isthmus (Olson and Rasmussen, 2001; Smith et al., 2007). Evaluation of climate-driven hypotheses of alcid evolution requires the estimation of the timing of major cladogenetic events for Pan-Alcidae. The comparison of estimates of pan-alcid diversification based on fossil age, cladogram topology, and divergence times estimated utilizing published molecular sequence data and employing programs such as BEAST (Drummond et al., 2010) will allow different hypotheses resulting from these different methods to be compared. Multiple approaches may also allow a more robust estimate of the pattern of pan-alcid diversification and will allow assessment of possible error associated with those estimates. Only then will it be possible to more fully evaluate hypotheses of the effect of climate on pan-alcid evolution and to potentially answer long-standing questions such as why did a diverse Pliocene Atlantic taxon like *Alca*, not disperse to the Pacific, and why

did the diverse Pliocene Pacific flightless taxon *Mancalla* go extinct in the Pacific whereas *Pinguinus* (a presumably species depauperate taxon based on its fossil record) continue to flourish in the Atlantic until it was driven into extinction by humans.

Table 8.2- Extinct Cenozoic Pan-Alcidae based on taxonomic revisions and new species description from Chapters 2-7 organized by Atlantic and Pacific Ocean basin occurrence. Pleistocene occurrences of extant taxa are not included. The 10 species newly described by the author are denoted with an asterisk '\*'. Note that *Mancalla lucasi* remains are also known from the Pleistocene and that *Miomancalla* remains are also known from the Pliocene.

Atlantic Fossil Taxa	Epoch	Pacific Fossil Taxa	Epoch
<i>Alca ausonia</i>	Pliocene	<i>Aethia barnesi</i> *	Miocene
<i>Alca carolinensis</i> *	Pliocene	<i>Aethia rossmoori</i>	Miocene
<i>Alca grandis</i>	Pliocene	<i>Aethia storeri</i> *	Pliocene
<i>Alca minor</i> *	Pliocene	SDSNH 25358*	Miocene
<i>Alca olsoni</i> *	Pliocene	<i>Brachyramphus dunkeli</i>	Pliocene
<i>Alca</i> aff. <i>torda</i>	Miocene	<i>Brachyramphus pliocenum</i>	Pliocene
<i>Alca stewarti</i>	Miocene	<i>Cepphus olsoni</i>	Miocene
<i>Cerorhinca aurorensis</i> *	Pliocene	<i>Cerorhinca minor</i>	Pliocene
<i>Fratercula</i> aff. <i>arctica</i>	Pliocene	<i>Cerorhinca reai</i>	Pliocene
<i>Fratercula</i> aff. <i>cirhata</i>	Pliocene	<i>Fratercula dowi</i>	Pleistocene
<i>Miocepheus blowi</i>	Miocene	<i>Mancalla californiensis</i>	Pliocene
<i>Miocepheus bohaski</i>	Miocene	<i>Mancalla cedrosensis</i>	Pliocene
<i>Miocepheus mergelellus</i>	Miocene	<i>Mancalla lucasi</i> *	Pliocene
<i>Miocepheus mcclungi</i>	Miocene	<i>Mancalla vegrandis</i> *	Pliocene
<i>Pinguinus alfrednewtoni</i>	Pliocene	<i>Miomancalla howardi</i> *	Miocene
<i>Pinguinus impennis</i>	Pliocene	<i>Miomancalla wetmorei</i>	Miocene
<i>Pseudocepheus teres</i>	Miocene	<i>Synthliboramphus rineyi</i>	Pliocene
Eocene Alcidae indet.	Eocene	<i>Uria brodkorbi</i>	Miocene

***Previous phylogenetic hypotheses of charadriiform relationships:*** The Charadriiformes (shorebirds and allies) comprise a morphologically and ecologically diverse clade (Sibley and Ahlquist, 1990; Paton et al., 2002; Ericson et al., 2006; Livezey and Zusi 2006, 2007; Hackett et al., 2008), with a fossil record that stretches back to the



late Eocene (35-40 Ma; Chandler & Parmley, 2002; Hou and Ericson, 2002). Previous analyses of charadriiform phylogeny have been based on several types of character data including morphology (Strauch, 1978; Chu, 1995; Livezey and Zusi 2006, 2007; Livezey, 2010; Mayr, 2011), DNA hybridization (Sibley and Ahlquist, 1990), mitochondrial DNA sequence data (Thomas et al., 2004; Paton and Baker, 2006), nuclear DNA sequence data (Ericson et al., 2003; Paton et al., 2003), and combined mitochondrial (12S, ND2, cyt-b) and nuclear (RAG-1) DNA sequence data (Baker et al., 2007). Previous studies of charadriiform relationships have all supported Alcidae monophyly (Strauch, 1978; Sibley & Ahlquist 1990; Chu, 1995 Thomas et al., 2004). Interestingly, molecular studies have placed Alcidae nested in a derived position within Charadriiformes (Sibley & Ahlquist 1990; Thomas et al., 2004), commonly as the sister taxon to the Laridae + Sternidae, while some morphology-based studies have placed Alcidae as the sister taxon to all other charadriiforms (Strauch, 1978; Chu, 1995). The differing results of those many analyses are discussed in detail in Chapter 1.

***Previous estimates of charadriiform divergence times:*** Prior to the development of molecular-based methods of divergence estimation the charadriiform lineage was hypothesized to have originated in the Late Cretaceous or Early Paleocene (Olson, 1985; Feduccia, 1995). Termed ‘transitional shorebirds’ by Olson (1985) because of morphological features shared with extant Charadriiformes such as a dorsally projected dorsal supracondylar process of the humerus, fossils referred to the taxon Graculavidae Fürbringer, 1888 have been considered to have affinities with a variety of avian clades including geese, flamingos, cranes, and gulls (Hope, 2002). In part because of their

fragmentary preservation and in part because of the mosaic of morphological features preserved by those remains (i.e., lack of apomorphies), the systematic positions of fossils referred to Graculavidae remain uncertain (Hope, 2002). Hypotheses of charadriiform cladogenesis based on those fossils are not considered reliable (Hope, 2002; Clarke and Norell, 2002).

Hypotheses regarding the timing of early radiation in Alcidae prior to the advent of molecular dating techniques were based on the first appearance data for extant lineages in the fossil record. Although these hypotheses did not include details of the timing of branching events between major subclades (e.g., timing of split between Aethiini and Fraterculini), Miocene records of auks, auklets, puffins, murre, and guillemots (Wetmore, 1940; Howard, 1978, 1981, 1982) suggested that splits among major extant subclades of Alcidae likely predated the Miocene (Olson, 1985; Feduccia, 1996; Warheit, 2002). However, with the exception of a single fossil record of an auk from the western Atlantic (Chandler and Parmley, 2002), previously reported records of Eocene and Oligocene Alcidae have been taxonomically re-assigned to other clades (i.e., no longer considered alcids). Species of *Nautilornis* Wetmore, 1926 from the Early Eocene of Utah were referred to Presbyornithidae (Feduccia and McGrew, 1974) and *Hydrotherikornis* Miller, 1931 from the Late Eocene of Oregon was referred to Procellariiformes (Chandler 1990a; Chandler and Parmley, 2002). *Petalca austriaca* from the Late Oligocene of Austria was referred to Gaviidae (Wijnker and Olson, 2009). The occurrence of the earliest alcid fossils in the Atlantic Ocean and the lack of earlier Pacific Ocean records have biogeographical implications. The presence of alcids in the Eocene and the diversity

alcid clades recorded in the Miocene fossil record supports previously proposed non-molecular-based scenarios of alcid divergence times (Olson, 1985; Feduccia, 1996; Warheit, 2002).

Estimates ranging from 57-93 Ma have been proposed for the basal divergence among crown Charadriiformes based on the results of previous molecular sequence-based divergence analyses (Table 8.3; Paton et al., 2002; Paton et al., 2003; Pereira and Baker, 2006; Ericson et al. 2006; Brown et al., 2007; Baker et al., 2007). Previous analyses have employed different methods of divergence estimation (Table 8.3; r8s, Sanderson, 2002; Multidistribute, Thorne and Kishino, 2002; PATHd8, Britton et al., 2007), each with different methods of estimating divergence times (see Rutschmann, 2006). All previous analyses of charadriiform divergence times have utilized inaccurate dates assigned to fossil taxa, taxa of uncertain phylogenetic affinity, and/or external calibrations that are considered problematic.

Table 8.3- Previous estimates of the basal divergence among crown Charadriiformes. Mean divergence estimates are followed by the 95% confidence intervals (in parentheses; \* = 95% CI not reported).

Reference	Divergence Estimate (Ma)	Method
Paton et al., 2002	77-78 (71.0 - 94.0)	r8s
Paton et al., 2003	~78*	r8s
Pereira & Baker, 2006	76.7 (67.9-86.3)	Multidistribute
Ericson et al., 2006	~57*	PATHd8
Brown et al., 2007	~85 (~69 – 106)	Multidistribute
Baker et al., 2007	93.1 (84.7 - 102.1)	Multidistribute

Three external calibrations, the accuracy of which have been subsequently criticized by some authors (Reisz and Müller 2004; Müller and Reisz, 2005), were used by Paton et al. (2002) to estimate the origins of modern clades of birds including Charadriiformes. Calibrations included the hypothesized splits of bird-alligator at 245 Ma, Galliformes-Anseriformes at 85 Ma, and emu-cassowary at 35 Ma. The use of unsubstantiated dates within Aves to estimate dates of divergence within Aves is a questionable methodology.

The taxon *Petralca austriaca*, a taxon considered *Aves incertae sedis* by Chandler (1990b), was used to date the divergence between Alcidae and Stercorariidae by Paton et al., (2003). Although originally described as an Oligocene representative of Alcidae (Mlikovsky and Kovar, 1987), this specimen (NMW 1980/25) is now considered to be a loon (Gaviidae; Wijnker and Olson, 2009). I examined digital photographs of the holotype specimen and I agree with the removal of this taxon from Alcidae based on the shape and curvature of the deltopectoral crest of the humerus, the curvature of the humeral shaft, and the relative length of the carpometacarpus as compared with the radius and ulna, characters which are shared with Gaviidae and are not seen in Alcidae (also see Mayr, 2009). An incorrect age of 40 Ma was also assigned to *Nupharanassa tolutaria* Rasmussen et al., 1987 by Paton et al. (2003), a fossil that has been dated to ~31-33 Ma (Fleagle et al., 1986; Rasmussen et al., 1987). Additionally, a secondary external calibration based on the age of the split between *Arenaria interpes* and *Haematopus ater* recovered by Paton et al. (2002) was used by Paton et al. (2003).

The divergence analysis of Pereira and Baker (2006) utilized 12 external

calibrations and a single internal calibration. The calibration for the split between Galliformes and Anseriformes was based on *Vegavis iaai* Clarke et al., 2005. Although the difference is slight, this calibration was incorrectly dated to 65 Ma, as the age of *Vegavis iaai* was cited as 66-68 Ma by Clarke et al. (2005).

Although the divergence analysis of Ericson et al. (2006) utilized 23 internal fossil calibrations, the results of that analysis hypothesize extensive post-Cretaceous divergences in Neoaves. These results have been questioned owing to issues with choice of fossil calibrations and the use of the divergence estimation software r8s (Sanderson, 2002), a program that had not been thoroughly tested (see Brown et al., 2007). In a re-analysis of Ericson et al.'s (2006) data using a modified set of fossil calibrations implemented in the program Multidistribute (Thorne and Kishino, 2002), Brown et al. (2007) recovered considerably older dates than Ericson et al. (2006). However, both r8s (Sanderson, 2002) and Multidistribute (Thorne and Kishino, 2002) require the specification of at least one fixed date or rate, a parameterization that has been categorized as a limitation of these programs (Drummond et al., 2006).

In a study of shorebird relationships and divergence times, mitochondrial and nuclear DNA sequence data were used by Baker et al. (2007) to recover a tree for Charadriiformes that agrees well with the results of previous analyses of relationships within the clade. Fourteen fossil calibrations (internal calibrations) and two previously derived dates (external calibrations) were used to date divergences between Charadriiformes and other birds, and also within Charadriiformes (Table 8.4). The novel result of the aforementioned study is that it claims 14 pre-Cretaceous divergences in

Charadriiformes, with the basal divergence of crown Charadriiformes dated at ~93 Ma. That hypothesis conflicts with previous estimates of younger divergence times for this clade (Table 8.3) and suggests the most extensive ghost lineages ever proposed for this clade based on the charadriiform fossil record. For example, Baker et al. (2007) date the divergence between Alcidae and its sister taxon the Stercorariidae at ~61.0 Ma, thus inferring a ~26.0 Ma ghost lineage for this clade based on its fossil record. Previous estimates of charadriiform divergence times have all placed fewer divergences in the Cretaceous, and have also obtained younger (57-86 Ma; Table 8.3) estimates of the basal-most divergence within the clade (Paton et al., 2002; Paton et al., 2003; Pereira and Baker, 2006; Ericson et al., 2006; Brown et al., 2007).

Two previously calculated molecular-based estimates (i.e., secondary external calibrations) were used by Baker et al. (2007) to calibrate the age of nodes representing divergences between charadriiform outgroup taxa (see Table 8.4). The dates used for those external calibrations by Baker et al. (2007) were derived in a previous analysis by Pereira and Baker (2006). Additionally, the analysis of Pereira and Baker (2006) from which the node age estimates used by Baker et al. (2007) were drawn, also contains several inaccurate dates assigned to fossil calibrations (Benton and Donoghue, 2007). Therefore the results of both analyses might be questioned.

There are several inaccuracies associated with the internal fossil calibration points used by Baker et al. (2007). These inaccuracies include incorrect dates assigned to fossil specimens, inclusion of taxa of uncertain age, inclusion of taxa of ambiguous systematic position, and inclusion of taxa that are not representatives of the nodes they were used to

calibrate (i.e., incorrect taxonomic assignment). Given the issues mentioned above, 12 of the 14 internal fossil calibrations utilized by Baker et al. (2007) are either inappropriate for use as charadriiform calibration points or were incorrectly dated (Table 8.4). All but one internal calibration used by Baker et al. (2007) was drawn from Brodkorb (1967; incorrectly referenced in Baker et al. 2007 as ‘Brodkorb, 1964’). The ages and taxonomic assignments of many fossil species have been revised since the publication of Brodkorb (1967). Furthermore, chronological ages of fossils and associated geologic intervals are not provided in millions of years (e.g., 22.0 Ma) in Brodkorb (1967) and Baker et al. (2007) make no mention of how dates were assigned to the taxa they chose as calibration points. Dates assigned to fossils appear to be minimum age boundaries for associated geologic epochs referenced by Brodkorb (1967). Additional details regarding rejected and revised charadriiform calibrations used by Baker et al., (2007) are provided in Appendix 7.

The divergence time analysis by Pereira and Baker (2008) proposed a Paleocene (~61 Ma) origin for Alcidae. That analysis was an extension of the previous analysis by Baker et al. (2007), and suffered from the same issues with regard to choice of fossil calibrations (Table 8.5; also see Appendix 7). The most puzzling example being the use of *Halcyornis toliapicus* Koenig, 1825 to date the split between Lari (e.g., alcids, gulls, and allies) and Scolopaci (e.g., sandpipers, jacanas, and curlews). Although *Halcyornis toliapicus* was originally considered a larid (Koenig, 1825), it was subsequently removed from Charadriiformes and referred to Coraciiformes (Harrison and Walker, 1972). *Halcyornis toliapicus* was recently identified as a stem parrot (Mayr, 2007). Inferences

regarding the timing and sequence of alcid evolution reported by Pereira and Baker (2008) are based on flawed estimates of divergence times and are not considered further herein.

The only other divergence estimate with a focus on Alcidae was that of Moum et al. (1994) who calibrated mitochondrial DNA sequence divergence with a molecular clock estimate based on the DNA-DNA hybridization study of Sibley and Ahlquist (1990). The results of that analysis suggested that initial radiation of alcids took place during the Early to Middle Miocene (~18 Ma). The presence of multiple lineages of alcids in the Miocene (e.g., *Miomancalla*, *Miocepheus*, *Alca*, *Uria*) and an Eocene fossil record of Pan-Alcidae (Chandler and Parmley, 2002) do not support that hypothesis.

## MATERIALS AND METHODS

***Anatomical terminology, measurements, and taxonomy:*** Anatomical descriptions use the English equivalents of the Latin osteological nomenclature summarized by Baumel and Witmer (1993). The terminology of Howard (1929) is followed for features not treated by Baumel and Witmer (1993). With the exception of the terms anterior and posterior substituted for cranial and caudal, respectively, the terms used for the anatomical orientation of a bird are those used by Clark (1993). Measurements follow those of von den Driesch (1976). All measurements were taken using digital calipers and rounded to the nearest tenth of a millimeter. Ages of geologic time intervals are based on the International Geologic Timescale (Gradstein et al., 2004;



Table 8.4- Critique of calibrations used by Baker et al. (2007). Abbreviations: incorrect age assigned to taxon (**IA**); incorrect taxonomic assignment (**IT**); questionable taxonomic status (**QT**); questionable secondary or tertiary external calibration date (**QD**). Additional details provided in Appendix 7.

<b>Taxon</b>	<b>Split Calibrated</b>	<b>Reason Rejected</b>	<b>References</b>
<i>Larus</i> spp.	<i>Larus</i> x <i>Rissa</i>	IA	Olson, 1985; Gradstein et al., 2004
<i>Uria antiqua</i>	<i>Uria</i> x <i>Alca</i> + <i>Alle</i>	IA, IT	Olson and Rasmussen, 2001
<i>Brachyramphus pliocenens</i>	<i>Brachyramphus</i> x <i>Cepphus</i> + <i>Synthliboramphus</i> + <i>Uria</i> + <i>Alca</i> + <i>Alle</i>	IA	Wagner et al., 2001
<i>Ptychoramphus tenuis</i>	<i>Ptychoramphus</i> x <i>Aethia</i>	QT	See Chapter 5
<i>Cerorhinca dubia</i>	<i>Cerorhinca</i> x <i>Fratercula</i>	QT	See Chapter 4
<i>Calidris pacis</i>	<i>Caladris</i> x <i>Aphriza</i>	IA	Dodd and Morgan, 1992
<i>Limosa gypsorum</i>	<i>Limosa</i> x <i>Prosobonia</i>	QT	Olson, 1985
<i>Numenius antiquus</i>	<i>Numenius</i> x <i>Bartramia</i>	IA	Sen & Ginsburg, 2000
<i>Charadrius sheppardianus</i>	<i>Charadrius</i> x <i>Elseyornis</i> + <i>Thinornis</i>	QT	Olson, 1985
<i>Vanellus selysii</i>	<i>Vanellus</i> x <i>Anarhynchus</i> + <i>Peltohyas</i> + <i>Erythrogonys</i>	QT	Olson, 1985
<i>Paleotringa</i> spp.	<i>Scolopaci</i> x <i>Lari</i>	QT	Olson, 1985
<i>Cimilopteryx</i> spp.	Charadriiformes x outgroup	QT	Hope, 2002
<i>Ceramornis major</i>	Charadriiformes x outgroup	QT	Hope, 2002
<i>Vegavis iaai</i>	<i>Anas</i> x <i>Anhima</i> + <i>Chauna</i>	IA	Clarke et al., 2005
External molecular calibration	Anseriformes / Galliformes	QD	Graur and Martin, 2004; Reisz and Müller, 2004
External molecular calibration	Galloanserae / Neoaves	QD	Graur and Martin, 2004; Reisz and Müller, 2004

Table 8.5- Critique of calibrations used by Pereira and Baker (2008). Abbreviations: incorrect age assigned to taxon (**IA**); incorrect taxonomic assignment (**IT**); questionable taxonomic status (**QT**); questionable secondary or tertiary external calibration date (**QD**).

Taxon	Split Calibrated	Reason Rejected	References
<i>Uria antiqua</i>	<i>Uria</i> x <i>Alle</i>	IA, IT	Olson and Rasmussen, 2001
<i>Ptychoramphus tenuis</i>	<i>Ptychoramphus</i> x <i>Aethia</i>	QT	See Chapter 5
<i>Cerorhinca dubia</i>	<i>Cerorhinca</i> x <i>Fratercula</i>	QT	See Chapter 4
<i>Miocepphus</i> , <i>Alcodes</i>	Alcidae x Stercorariidae	IA	Wijnker and Olson, 2009
<i>Paleotringa</i> spp.	Scolopaci x Lari	QT	Olson, 1985
<i>Cimilopteryx</i> spp.	Charadriiformes x outgroup	QT	Hope, 2002
<i>Halcyornis toliapicus</i>	Lari x Scolopaci	IT	Mayr, 2007
External molecular calibration	Alcidae x Stercorariidae	QD	Graur and Martin, 2004; Reisz and Müller, 2004
External molecular calibration	Galloanserae x Neoaves	QD	Graur and Martin, 2004; Reisz and Müller, 2004

Ogg et al., 2008). As such, the boundary between the Pliocene and Pleistocene Epochs is recognized as 2.58 Ma in accordance with the International Commission on Stratigraphy (Gibbard et al., 2010). Taxonomy of extant North American charadriiform species follows the 7th edition of the Checklist of North American Birds (American Ornithologists' Union, 1998). With the exception of species binomials, all taxonomic designations (e.g., Alcidae) are clade names as defined by the PhyloCode v 4c (Dayrat et al., 2008; Cantino and de Queiroz, 2010) and are not intended to convey rank under the Linnaean system of nomenclature, regardless of use of italics or previous usage by other authors.

***Taxon and character sampling:*** The phylogenetic data matrix comprises 143 terminals, scored for a maximum of 353 morphological characters (293 binary; 45 unordered multistate; 15 ordered multistate). Morphological character scorings are reported for all twenty-three extant alcids, 43 other extinct alcid species, and 36 additional alcid fossil specimens (Appendix 3). Twenty-nine extant charadriiforms and 5 extinct charadriiforms complete the remainder of the taxa scored for analysis, and provide a dense outgroup taxon sample to test the monophyly of Pan-Alcidae with respect to other charadriiforms. Seven terminals representing scorings that were combined for multiple specimens referred to a taxon (supraterminal or supraspecific combinations) are also provided. Character variation was scored as polymorphism in supraspecific terminals. Morphological characters include osteological ( $n = 232$ ), integumentary ( $n = 32$ ), reproductive ( $n = 11$ ), dietary ( $n = 2$ ), myological ( $n = 24$ ) and micro-feather ( $n = 52$ ). One hundred and sixty-four characters were developed for this analysis. The other 189 characters were drawn from the work of Hudson et al. (1969;  $n = 24$ ), Strauch (1978, 1985;  $n = 39$ ), Chandler (1990a;  $n = 63$ ), Chu (1998;  $n = 11$ ), and Dove (2000;  $n = 34$ ). Only 34 of the 38 characters used by Dove (2000) varied in the taxa examined in this study. Of the 34 used in this analysis, 18 were modified (i.e., split into 2 separate characters) according to the philosophy of character independence proposed by Hawkins et al. (1997), resulting in a total of 52 microfeather characters.

Whenever possible, five or more specimens of each extant species including both sexes were evaluated to account for intraspecific character variation and potential sexual dimorphism respectively (Appendix 1). Only adult specimens, assessed based upon

degree of ossification (Chapman, 1965), were evaluated and whenever possible specimens from multiple locations within the geographic range of extant species (i.e., sub-species) were examined to account for intraspecies geographic variation. Reproductive, chick integument, dietary, and some myological characters were scored from published sources (Appendix 2). Characters for all extinct alcid taxa were coded from direct observation of holotype and referred specimens. Characters for extinct non-alcid charadriiforms were scored from published sources and photos that were kindly provided by colleagues. Many Pleistocene and Holocene remains that presumably represent extant species (Lambrect, 1933; Brodkorb, 1967; Tyrberg, 1998) were not examined, and are not treated further herein.

The cladistic matrix also includes aligned molecular sequences of 11,601 base pairs in length for sampled taxa (including gaps, 3.7-84.1 % incomplete; average sequence completeness for sampled taxa = 38.6%). See Appendix 4 for full details of sequence availability and sequence authorship and see Table 1.3 for details of sequence completeness for each species sampled. Molecular sequence data (mitochondrial: ND2, ND5, ND6, COI, *cyt-b*; ribosomal RNA: 12S, 16S; and nuclear: RAG1) were downloaded from GenBank. Preliminary sequence alignments for each gene were obtained using ClustalX v2.0.6 (Thompson et al., 1997), and then manually adjusted using Se-AI v2.0A11 (Rambaut, 2002). The general time reversible model with invariant sites and gamma distribution (GTR + I + G) was estimated as the best nucleotide substitution model for each gene partition and for the concatenated molecular data including all eight genes by MrModeltest v.2.3 (Nylander, 2008).

**Phylogeny estimation:** A combined approach of phylogeny estimation was used to evaluate the systematic position of pan-alcid species. Parsimony and Bayesian phylogeny estimation approaches were explored because Bayesian methods allow incorporation of complex models of nucleotide substitution not available with parsimony methods (Lewis, 2001a, 2001b; Huelsenbeck et al., 2001, 2002; Holder and Lewis, 2003; Nylander et al., 2004).

Phylogenetic analyses employing a maximum parsimony criterion of phylogenetic estimation were implemented in PAUP\* v4.0b10 (Swofford, 2002). Parsimony tree search criteria are as follows: heuristic search strategy; 10,000 random taxon addition sequences; tree bisection-reconnection branch swapping; random starting trees; all characters equally weighted; minimum length branches = 0 collapsed; multistate (e.g., 0&1) scorings used only for polymorphism. Bootstrap values and descriptive tree statistics (i.e., CI, RI, RC) were calculated using PAUP\* v4.0b10 (Swofford, 2002). Bootstrap value calculation parameters included 1,000 heuristic search replicates with 100 random addition sequences per replicate. All other settings were the same as the phylogenetic analysis. Bremer support values were calculated using a script generated in MacClade v4.08 (Maddison and Maddison, 2005) and analyzed with PAUP\* v4.0b10 (Swofford, 2002). Based on the results of previous phylogenetic analyses of charadriiform relationships (Strauch, 1978; Sibley and Ahlquist, 1990; Chu, 1995; Ericson et al., 2003; Paton et al., 2003; Thomas et al., 2004; Baker et al., 2007), resultant trees were rooted with the clade including *Charadrius vociferous* and *Charadrius*

*wilsonia*. Tree graphics were produced in MacClade v4.08 (Maddison and Maddison, 2005) and FigTree v1.3.1 (Rambaut, 2009).

Bayesian phylogenetic analyses of the combined data were performed using MrBayes v3.1.2 (Ronquist and Huelsenbeck, 2003). MrBayes parameters were as follows: two simultaneous independent runs with one cold and five heated chains each, starting trees random, Markov chain monte carlo (MCMC) samples taken every 1000 generations, nine partitions in the combined analyses (1 morphological and 8 gene partitions), parameters unlinked across partitions, all fully resolved topologies considered equally likely, branch lengths unconstrained (i.e., molecular clock not enforced): exponential (10.0), substitution rate flat Dirichlet (1, 1, 1, 1), state frequencies flat Dirichlet (1, 1, 1, 1), standard deviation of split frequencies < 0.01 considered evidence of convergence of MCMC chains, nodes with  $\geq 0.95$  posterior probability considered strongly supported. Log likelihoods and effective sample size (ESS) were evaluated to determine burn-in with the software Tracer v1.5 (Rambaut and Drummond, 2009), and the resulting consensus of retained trees was plotted using FigTree v1.3.1 (Rambaut, 2009). All trees were *a priori* rooted with *Charadrius vociferus*. In the Bayesian analyses the Mk model (standard model; Lewis, 2001a) was applied to morphological data.

Because many of the extinct taxa sampled are known from isolated and often fragmentary specimens, and because missing data can decrease phylogenetic resolution of resultant consensus trees (i.e., many equally parsimonious trees; Nixon and Wheeler, 1992; Wilkinson, 1995), taxa were iteratively excluded from subsequent analyses based on their level of completeness (i.e., percent of missing data entries; see Rowe, 1988;

Fraser and Benton, 1989; Gao and Norell, 1998). Dozens of iterations (i.e., multiple phylogenetic analyses) using the maximum parsimony estimator of phylogeny implemented in PAUP\* v4.0b10 (Swofford, 2002) were performed to identify potential ‘wildcard taxa’ (Nixon and Wheeler, 1992; Kearney, 2002), which were removed from subsequent analyses to recover a reasonably resolved phylogenetic hypothesis that still maintained a reasonably high level of taxon sampling. So-called ‘wildcard’ taxa contribute to the recovery of multiple most-parsimonious trees, which in turn can lead to poor resolution in the strict consensus of those trees. The effect of wildcard taxa can be attributed to missing data, character conflict, or a combination of these issues (Kearney, 2002). Because of the incomplete preservation of many of the fossils included in the phylogenetic analyses, several fossils are taxonomic equivalents of closely related taxa (e.g., *Larus elegans*). Therefore, in many analyses reported herein, the poor resolution of strict consensus trees including wildcard taxa can be attributed to missing data.

***Divergence time estimation:*** The age of cladogenetic events for Charadriiformes was estimated using a relaxed Bayesian molecular clock with uncorrelated lognormal rates model as implemented in BEAST v1.6.1 (Drummond et al., 2010). Recent studies (e.g., Drummond et al., 2006; Ho, 2009) have shown that this method may provide a more realistic way to model rate evolution than methods such as Multidivtime (Thorne et al., 1998; Thorne and Kishino, 2002) that autocorrelate rates. The general time reversible model with invariant sites and gamma distribution (GTR + I + G) was applied as the nucleotide substitution model. The Yule model of speciation was applied as a prior on the branching rates. Unlike other divergence estimation programs (e.g., r8s, Sanderson, 2002;

Multidistribute, Thorne and Kishino, 2002; PATHd8, Britton et al., 2007) which allow only point estimates or intervals to model calibration age uncertainty, BEAST (Drummond et al., 2010) allows the user to choose from several models of age distribution for priors on a given node (e.g., normal, log-normal; reviewed by Ho and Phillips, 2009). Twelve internal fossil calibrations were used to date the minimum divergence of charadriiform cladogenetic events and assigned a lognormal prior distribution. Because fossil evidence directly dates the minimum age of divergences, the lognormal distribution was configured with a relatively steep pre-peak slope that signifies that the peak probability of fossil calibration age is soon after the age assigned to the calibrated node. The analysis was run for 25 million MCMC generations and the MCMC chain was sampled every 1000 generations. Effective sample size was assessed in Tracer v1.5 (Rambaut and Drummond, 2009) to determine if the MCMC chain was of sufficient length (effective sample size >200 considered evidence of a sufficiently long run). Burn-in was assessed using Tracer v1.5 (Rambaut and Drummond, 2009) and the retained sample of trees was summarized using TreeAnnotator v1.6.1 (Rambaut and Drummond, 2010). The resulting phylogenetic tree including node age estimates and associated error bars (95% highest posterior density interval) was plotted using FigTree v1.3.1 (Rambaut, 2009).

***Charadriiformes fossil calibrations:*** The fossil record of Alcidae is the richest among Charadriiformes (Table 8.1), providing several fossil calibrations for use in molecular divergence estimation. Although five extant alcid species have no known fossil record, every major clade of alcids (e.g., Alcini) is represented by at least one fossil taxon



(Table 8.1). Twelve internal fossil calibrations were used to constrain the ages of nodes in the divergence estimation analysis (Table 8.6). The ages of all calibrations were verified through a rigorous search of recent paleontological and geological literature. The taxonomic status of potential fossil calibrations that had not been previously included in a phylogenetic analysis were evaluated through phylogenetic analyses prior to their use in the divergence analysis. Details regarding the age and systematic position of calibrations are provided in Table 8.6. Apomorphies supporting the referral of fossil taxa to the clades that they were used to calibrate are provided in Table 8.7.

Because *Brachyramphus pliocenium* Howard, 1949 was placed at the base of *Brachyramphus* in a previous phylogenetic analysis (see Chapter 7), and because the oldest remains of this taxon are younger than the age of fossils used as calibrations for relatively more derived nodes in the tree (e.g., *Uria-Alle* split at 20 Ma), *Brachyramphus pliocenium* was not used to date the split between *Brachyramphus* and the remainder of Alcinae. Instead, *Brachyramphus dunkeli* Chandler, 1990, which is placed as the sister taxon to *Brachyramphus marmoratus*, was used to date the minimum age of divergence between *Brachyramphus marmoratus* and *Brachyramphus brevirostris*. Remains of this taxon are known from middle Pliocene sediments of the San Diego Formation of southern California (Howard, 1949; Chandler, 1990b). The fossil-bearing units of that formation from which remains of this taxon were recovered have been assigned an age of ~3.6 Ma (Wagner et al., 2001).

Table 8.6- Fossil calibrations used in the divergence time analysis. Note that the calibration for the split between *Alca* and *Pinguinus* is based on material described by Wijnker and Olson (2009), and whereas the extension of the range of an extant species into the Miocene prompts questions about the longevity of species, no size-based or morphological differences exist between Miocene remains referred to *Alca* aff. *torda* and extant specimens of *Alca torda* (see Chapter 2 for further discussion of this issue).

Fossil Taxon	Split Calibrated	Age (Ma)	Dating Method	Material	Reference
<i>Brachyramphus pliocenum</i> (LACM 2119)	<i>Brachyramphus</i> spp.	3.6	Magnetostratigraphic	Humeri	Howard, 1949
<i>Synthliboramphus rineyi</i> (UCMP 61590)	<i>S. craveri</i> x <i>S. hypoleucus</i>	3.6	Magnetostratigraphic	Humerus	Chandler, 1990a
<i>Fratercula</i> aff. <i>arctica</i>	<i>F. corniculata</i> x <i>F. arctica</i>	4.4	Radiometric	Humeri	Olson and Rasmussen, 2001
<i>Cerorhinca auroreensis</i>	<i>Cerorhinca</i> x <i>Fratercula</i>	4.4	Radiometric	Humeri	Smith et al., 2007
<i>Aethia barnesi</i> (LACM 107031)	<i>Aethiini</i> x <i>Fraterculini</i>	6.7	Biostratigraphic	Humerus	Smith, 2011
<i>Cephus olsoni</i> (LACM 107032)	<i>Cephus carbo</i> x <i>C. grylle</i> + <i>C. columba</i> (stem)	8.0	Biostratigraphic	Humerus	Olson and Wijnker, 2009
<i>Alca</i> aff. <i>torda</i> (e.g., USNM 446656)	<i>Alca</i> x <i>Pinguinus</i>	10.0	Biostratigraphic	Humeri	Wijnker and Olson, 2009
<i>Miocepheus bohaski</i> (USNM 237270)	<i>Alle</i> x <i>Uria</i>	20.0	Biostratigraphic	Partial skeleton	Wijnker and Olson, 2009
<i>Larus elegans</i> (Milne-Edwards 1869-71)	<i>Larus</i> x <i>Rissa</i>	24.1	Biostratigraphic	Hypodigm: partial skull, scapula, coracoid, humeri, ulnae, carpometacarpi, femur, furcula, sacrum, tarsometatarsus	Milne Edwards, 1867-71; Huguency et al., 2003; Mourer-Chauvire et al., 2004
<i>Nupharanassa bulorum</i> (DPC 3848) & <i>Boutersemia belgica</i> (IRSvNB Av 41)	<i>Hydrophasianus</i> x <i>Batramia</i> + <i>Numenius</i> + <i>Tryngites</i>	33.0	Biostratigraphic and Radiometric	Distal tarsometatarsi	Rasmussen et al., 1987; mayr and Smith, 2001
Alcidae incertae sedis (GCVF 5690)	Alcidae x <i>Stercorarius</i>	35.1	Biostratigraphic	Distal humerus	Chandler & Parmley, 2002
<i>Jiliniornis huadianensis</i> (IVPP V.8323)	Charadrius x Scolopacidae	40.4	Biostratigraphic	Humerus	Hou and Ericson, 2002

*Synthliboramphus rineyi* Chandler, 1990 is the oldest known representative of *Synthliboramphus*. Remains of this taxon are known from the Pliocene (~3.6 Ma) San Diego Formation of southern California. Based on the position recovered for *Synthliboramphus rineyi* in the results of a previous phylogenetic analysis (Chapter 7), the age of this taxon was used to date the age of the minimum divergence between the extant species *Synthliboramphus craveri* and *Synthliboramphus hypoleucus*.

Based on apomorphies, the oldest currently known fossils referable to the Fraterculini (*Fratercula* and *Cerorhinca*) occur in the Early Pliocene (~4.4 Ma) sediments of the Yorktown Formation in Beaufort County, North Carolina (Olson and Rasmussen, 2001). Fossil material referred to *Fratercula* aff. *arctica* by Olson and Rasmussen (2001) and Smith et al. (2007) was used to constrain the age of the split between extant sister taxa *Fratercula arctica* and *Fratercula corniculata*. *Fratercula* aff. *arctica* is a taxonomic equivalent of extant *Fratercula arctica* with respect to scorings in the phylogenetic data set. Material referable to *Cerorhinca* sp. by Smith et al. (2007) was used to date the minimum time of divergence between *Cerorhinca* and its sister taxon *Fratercula* (also see *Cerorhinca auroreensis*, Chapter 4).

*Aethia barnesi* from the Late Miocene San Mateo Formation (at least 6.7 Ma; Domning and Deméré, 1984) is the oldest known fossil referable to the Aethiini (contents of Aethiini include *Aethia* and *Ptychoramphus*; see Chapter 5). This taxon was used to date the minimum age of divergence between Aethiini (auklets) and its sister taxon the Fraterculini (puffins).

Because *Pseudocepphus teres* Wijnker and Olson, 2009 is dated to ~14 Ma, remains of this species likely represent the oldest records of Cepphini. However, the systematic position of this taxon is not strongly supported (see Chapter 6). *Cepphus olsoni* Howard, 1982 from the San Luis Rey River Local Fauna of the late Miocene (~8.0 Ma) San Mateo Formation is the oldest record of crown Cepphini and was used to calibrate the split between *Cepphus carbo* and *Cepphus columba* + *Cepphus grille* based on the phylogenetic analysis of Cepphini detailed in Chapter 6.

Fossils from the Late Miocene (~10.0 Ma) of Maryland, USA were referred to *Alca* cf. *torda* by Wijnker and Olson (2009) and represent the oldest records of the taxon *Alca*. Accordingly, a date of 10.0 Ma was used as a minimum constraint on the age of the node representing the common ancestor of *Alca torda* and *Pinguinus impennis*.

*Miocepphus bohaski* Wijnker and Olson, 2009 from the early Miocene (~20.0 Ma) of Maryland, USA is the oldest known representative of *Miocepphus* Wetmore, 1940. Based on the position of *Miocepphus bohaski* in the results of a previous phylogenetic analysis (Chapter 2), this taxon was used to constrain the age of the split between *Uria lomvia* + *Uria aalge* and *Alle alle*.

The oldest larids are *Larus elegans* Milne-Edwards, 1868 and *Larus totanoides* Milne-Edwards, 1868 from the Late Oligocene and early Miocene of France (Milne-Edwards, 1867-1871; Hugueney et al., 2003; Mourer-Chaviré et al., 2004). The vertebrate fauna from Créchy, France corresponds with Paleogene mammalian zones MP29 and MP30, and are considered to bracket the Miocene-Oligocene boundary with an age estimated between 24.1-23.6 Ma (Hugueney et al., 2003). *Larus elegans* was

included in the combined phylogenetic analysis and based on its recovered position (see results) was used to calibrate the split between *Larus marinus* + *Larus argentatus* and *Rissa tridactyla*.

The oldest known fossils referable to the Jacanidae are from the Early Oligocene (~33.0 Ma) Jebel Qatrani Formation of Egypt (Rasmussen et al., 1987). Although this material consists entirely of distal tarsometatarsi, all three jacanid species described from this deposit are characterized by the “huge distal foramen, broad tendinal groove, and flattened shaft unique to this family” (Rasmussen et al., 1987:7). The relatively enlarged distal vascular foramen (227:1) is optimized as an apomorphy of Jacanidae (i.e., *Hydrophasianus chirurgis*, *Nupharanassa bulotorum*, and *Boutersemia belgica*) among sampled charadriiforms. The possession of a broad anterior groove (229:1) that extends proximally from the distal vascular foramen is optimized as an apomorphy of Jacanidae, Glareolidae, and Scolopacidae among sampled charadriiforms. *Nupharanassa bulotorum* was used to calibrate the split between the Jacanidae, represented in this analysis by *Hydrophasianus chirurgis*, and sampled Scolopacidae (*Bartramia longicauda*, *Tryngites subruficollis*, *Numenius minutus*).

The oldest fossil pan-alcid is from Late Eocene deposits of the Hardie Mine, Gordon, Georgia USA (Chandler and Parmley, 2002). Fossils of sharks, rays, bony fishes, snakes, and the auk specimen have been recovered from an approximately one meter thick, in-situ bed of the Late Eocene Clinchfield Formation, a basal unit of the Barnwell Group (Huddelstun and Hetrick, 1986; Westgate, 2001). The Hardie Mine exposures of the Clinchfield Formation are a discrete fossiliferous unit with no evidence

of mixing with older or younger bounding units (Parmley and Holman, 2003). Evidence from shark, mammalian, mollusk, and dinocysts assemblages support a Late Eocene age for the Clinchfield Formation sediments exposed at Hardie Mine (Parmley and Holman, 2003). The dinocyst assemblage is correlated with assemblages from other localities in Georgia and South Carolina that are placed in calcareous nannofossil zone NP 19/20, and have been assigned an age of 36.0–34.2 Ma according to the timescale of Berggren et al., (1995). GCVP 5690 displays the characteristic flattened shaft and proximally extended dorsal supracondylar process that distinguishes the humeri of alcids from all other charadriiforms (Fig. 8.2). Additionally, the specimen has an anteriorly flattened ventral

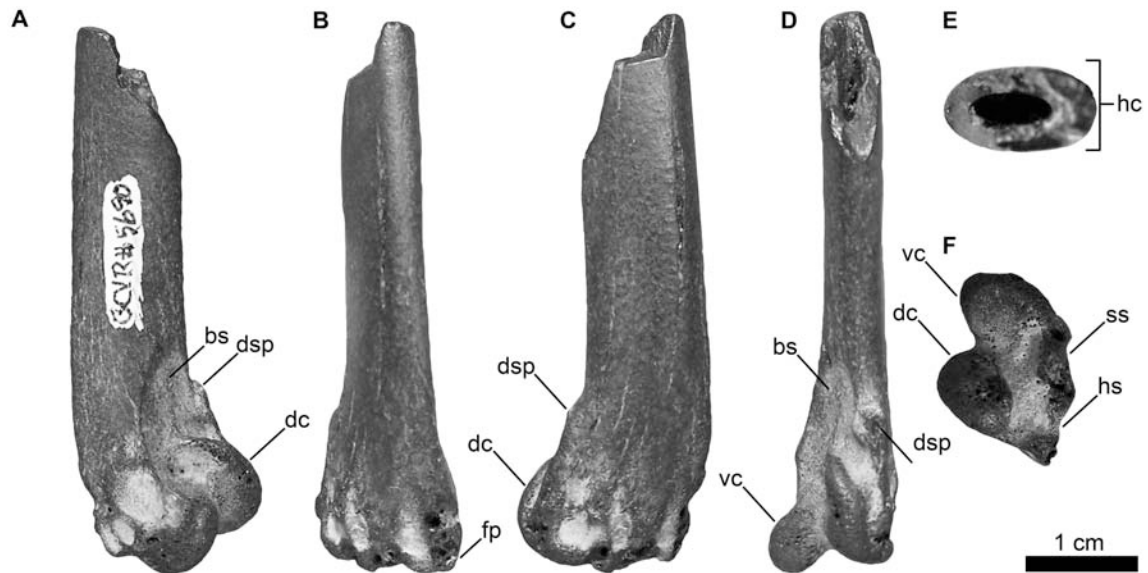


Fig. 8.2- Earliest known pan-alcid fossil (GCVP 5690) from the Hardie Mine in Gordon Georgia, USA. **A.** anterior view; **B.** ventral view; **C.** posterior view; **D.** dorsal view; **E.** proximal view; **F.** distal view. Anatomical abbreviations: (**bs**) brachialis scar; (**dc**) dorsal condyle; (**dsp**) dorsal supracondylar process; (**fp**) flexor process; (**hc**) humeral shaft compression; (**hs**) humerotricipital sulcus; (**ss**) scapulotricipital sulcus; (**vc**) ventral condyle.

condyle, a characteristic common to all Alcidae except Mancallinae. This fossil was used to date the minimum time of divergence (~35 Ma) between Alcidae and its sister taxon Stercorariidae (Table 8.6).

All Mesozoic and Paleocene fossils referred to Charadriiformes (Harrison and Walker, 1977; Olson and Paris, 1987) consist of unassociated and undiagnostic fragments (Hope, 2002; Clarke and Norell, 2002; Mayr, 2005). Therefore, the Late Eocene (~35 Ma) fossil alcid specimen (GCVP 5690; Chandler and Parmley, 2002) is one of the oldest currently known fossils to be identified as a part of crown Charadriiformes based on unambiguously optimized apomorphies.

Three additional taxa from the Eocene of western North America were originally described as alcids. *Hydrotherikornis oregonus* Miller, 1931 from the Late Eocene (~35.0 Ma) of Oregon, USA was originally described as an auklet (i.e., Aethiini) but has subsequently been referred to Procellariiformes (Chandler, 1990a; Chandler and Parmley, 2002). *Nautilornis proavitus* Wetmore, 1926 and *Nautilornis avus* Wetmore, 1926 from the Early Eocene (~52.0 Ma) of Utah were originally described as auks, but were referred to Phoenicopteridae (flamingos) by Feduccia and McGrew (1974). *Nautilornis* is now considered part of Presbyornithidae (Mayr, 2008). These fossils are, therefore, not used as calibrations in the divergence analysis.

Potential records of non-alcid charadriiforms from the Eocene include a single report from Germany (Mayr, 2000), one from China (Hou and Ericson, 2002), and another from eastern North America (Olson, 1999). Although a putative crown charadriiform from the Middle Eocene (~47.0 Ma) Messel Shale of Germany potentially

provides an earlier record of Charadriiformes (Mayr, 2000), the affinities of that specimen (SMF-ME 2458A+B) are uncertain because it has not been included in a phylogenetic analysis. To establish the charadriiform affinities of that specimen will require its inclusion in a phylogenetic analysis with sampling of charadriiform outgroups, and is therefore, outside the scope of this study. However, an additional divergence time analysis was conducted to ascertain the effect of the use of that specimen as a calibration for the basal split among the charadriiform crown clade. Early Eocene (~53 Ma) material referred to Charadriiformes by Olson (1999) is too fragmentary for referral to Charadriiformes (Mayr, 2005).

With the exception of the putative crown charadriiform from the Middle Eocene (~47.0 Ma) Messel Shale of Germany (discussed above), the earliest known crown charadriiform fossil is a humerus (IVPP V.8323) from the Middle Eocene Huadian Formation of Jilin Province, China. The holotype specimen of *Jiliniornis huadianensis* (IVPP V.8323) was tentatively referred to Charadrii (Hou and Ericson, 2002). Because the age of the Middle Eocene Huadian Formation is not precisely known a conservative approach was taken regarding the choice of the age prior on the node representing the split between Charadrii and the rest of the charadriiform crown clade. Although the holotype of *Jiliniornis huadianensis* may be older than latest Middle Eocene, an age of 40.4 Ma, corresponding to the uppermost Middle Eocene boundary (Lutetian-Bartonian boundary; Ogg et al., 2008) was used as a qualitative prior on the split between Charadrii (represented in the analysis by *Charadrius wilsonia* and *Charadrius vociferus*) and the rest of crown Charadriiformes. Additionally, the log mean of the distribution associated



with the prior for the node calibrated by *Jiliniornis huadianensis* was extended to 1.0 to allow the possibility of recovering a pre-Cretaceous-Tertiary boundary origin of the charadriiform crown clade in the divergence analysis.

The systematic positions of four other fossils referred to Charadriiformes were assessed through phylogenetic analyses to gauge their suitability for use as fossil calibrations. Those taxa included a purported curlew, *Numenius antiquus* Milne-Edwards, 1867-1871 from the early Miocene of France, and two potential glareolids. *Mioglareola gregaria* Ballmann, 1979 was described from the middle Miocene Nordlinger Ries of Germany. According to Olson (1985) the holotype specimen (BSM1970 XVIII 851) is a partial skeleton containing the skull, mandible, and other elements. However, the association of these fossils is not certain. The material described by Ballmann (1979) is from a site called Steinberg (a.k.a., Spitzberg) and was acetic acid-prepared from several loose blocks of fossiliferous calcareous tufa found in 1969 on the southwest slope of the Steinberg (U. Göhlich, personal communication). There are no known articulated skeletons from this locality and thus the referral of material attributed to *Mioglareola gregaria* is uncertain. Although much of this material was figured by Ballmann (1979), the figures are of relatively low resolution and no re-description of this material has been published. Therefore, *Mioglareola gregaria* was not used to date the minimum time of divergence between *Glareola* and *Stiltia*.

The oldest potential glareolid is *Boutersemia belgica* Mayr and Smith, 2001 from the early Oligocene (~33.0 Ma) of Belgium. The referral of tarsometatarsi representing *Boutersemia belgica* to Glareolidae was not based on a phylogenetic analysis (Mayr and

Smith, 2001), and therefore, the systematic position of *Boutersemia belgica* was evaluated to assess its utility as a calibration point for Charadriiformes.

***Institutional Abbreviations:*** AMNH—American Museum of Natural History, New York, NY, USA; BSM—Bayerische Staatssammlung für Palaeontologie, Munich, Germany; DPC—Duke University Primate Center, Durham, North Carolina, USA; GCVP—Georgia College and State University Vertebrate Paleontology Collection, Milledgeville, GA, USA; IVPP—Institute of Vertebrate Paleontology and Paleoanthropology, Beijing, China; IRScNB—Institut Royal des Sciences Naturelles de Bruxelles, Belgium; LACM—Natural History Museum of Los Angeles County, Los Angeles, CA., USA; NHMUK—The Natural History Museum, London, UK; NMW—Naturhistorisches Museum Wien, Wien Austria; NSM PO—National Museum of Nature and Science Paleontology Osteological Collection, Tokyo, Japan; NCSM—North Carolina Museum of Natural Sciences, Raleigh, NC, USA; SDSNH—San Diego Natural History Museum, San Diego, CA, USA; TMM—Texas Natural Science Center Vertebrate Paleontology Laboratory, Austin, TX, USA; UCMP—University of California Museum of Paleontology, Berkeley, CA, USA; USNM—National Museum of Natural History, Smithsonian Institution, Washington, D.C., USA.

## RESULTS

***Phylogenetic results:*** Although supraspecific terminals (e.g., Mancallinae SST), specimen-level terminals (e.g., SDSNH 25236) and previously identified wildcard taxa

(see Chapters 4, 5, 6, & 7) were excluded, a preliminary analysis including 88 species-level terminals resulted in a strict consensus cladogram with relationships largely unresolved (results not shown). This lack of resolution was addressed by identifying incompletely preserved taxa that negatively affected the resolution of resulting strict consensus cladograms through iterative analyses and then removing those taxa from subsequent analyses. Because many of these problematic taxa were fragmentary charadriiform fossils targeted for use as calibrations for the divergence time analysis, separate analyses were performed to assess the systematic positions of those taxa. Specimens that were used as fossil calibrations (or that were rejected as fossil calibrations) but that were not included in the final phylogenetic analysis were evaluated in phylogenetic analyses that otherwise included only extant taxa. This method allowed for phylogenetic assessment of taxa used as fossil calibrations independent of the influence of other highly incomplete taxa (i.e., fossils with large percentages of missing data).

*Boutersemia belgica* was tentatively referred to the Glareolidae in the original description of this taxon (Mayr and Smith, 2001). The results of the phylogenetic analysis including *Boutersemia belgica* and extant charadriiforms place it as the sister taxon to *Hydrophasianus chirurgus* (Fig. 8.3). Referral of *Boutersemia belgica* to Jacanidae (lily trotters) is supported by a unique suite of tarsometatarsal characters (Table 8.7). However, owing to its incomplete preservation, *Boutersemia belgica* could be scored for only 6 osteological characters (character #'s 225, 227-231) and is a taxonomic equivalent of the extant species *Hydrophasianus chirurgus*.

The results of the phylogenetic analysis including *Nupharanassa bulotorum* and extant charadriiforms place it as the sister taxon to *Hydrophasianus chirurgus* (Fig. 8.4), providing further support that Jacanidae were present in the early Oligocene. Referral of *Nupharanassa bulotorum* to Jacanidae is supported by a unique suite of tarsometatarsal characters (Table 8.7). *Nupharanassa bulotorum* and *Boutersemia belgica* were used as calibrations to date the minimum age of divergence of Jacanidae from other charadriiforms (Table 8.6) and were both included in the final combined phylogenetic analysis. However, owing to its incomplete preservation, *Boutersemia belgica* could be scored for only 7 osteological characters (character #'s 225-231) and is a taxonomic equivalent of the extant species *Hydrophasianus chirurgus*.

The results of the phylogenetic analysis including *Larus elegans* and extant charadriiforms place it in a polytomy with *Larus marinus* and *Larus argentatus* (Fig. 8.5), confirming the referral of this taxon by Milne-Edwards (1867-1871) and subsequent authors (e.g., Mourer-Chauviré, 2004) to *Larus*. Referral of *Larus elegans* to Laridae is supported by two larid synapomorphies of the coracoid and tarsometatarsus (Table 8.7). *Larus elegans* is a taxonomic equivalent of *Larus marinus*.

*Numenius antiquus* was placed in an unresolved position with other Scolopaci (e.g., sandpipers, jacanas, and curlews) and Charadrii (e.g., plovers) species in the strict consensus topology resulting from the analysis of *Numenius antiquus* and extant charadriiform species (Fig. 8.6). *Numenius antiquus* was placed as the sister to *Numenius minutus* in two of the four most parsimonious topologies, and was placed as the sister to *Stiltia isabella* or sister to *Bartramia longicauda* in the other two most parsimonious

topologies. Owing to its incomplete preservation, *Numenius antiquus* could be scored for only 11 osteological characters (character #'s 219-223, 225-231) and is a taxonomic equivalent of the extant species *Numenius minutus*. Because the inclusion of this taxon decreased phylogenetic resolution and because the systematic position of *Numenius antiquus* is uncertain, it was not included in additional phylogenetic analyses or used as a calibration in the divergence analysis.

*Jiliniornis huadianensis* is placed in a polytomy at the base of Charadriiformes along with other Scolopaci and Charadrii species in the strict consensus cladogram resulting from the analysis of this taxon and extant charadriiform species (Fig. 8.7). *Jiliniornis huadianensis* could be scored for only 28 osteological characters. With the exception of a single character (111:1), scorings for *Jiliniornis huadianensis* are identical to those of the extant species *Charadrius wilsonia* and *Charadrius vociferus*. Because the inclusion of *Jiliniornis huadianensis* decreased phylogenetic resolution it was not included in additional phylogenetic analyses. Alternative placements for *Jiliniornis huadianensis* among the 24 MPT's recovered included a variety of positions at or near the base of Charadriiformes (i.e., alternatively recovered as part of *Charadrius*, Scolopacidae, and Glareolidae). The possibility that *Jiliniornis huadianensis* represents a stem charadriiform should be considered, but is outside the taxonomic scope of the present analysis. However, because *Jiliniornis huadianensis* is potentially the oldest referred charadriiform fossil, it was used as calibration prior on the minimum divergence among the charadriiform crown clade in the divergence time analysis.

The final combined phylogenetic analysis of charadriiform relationships included all 23 extant alcids, 25 extinct acid species, 29 extant charadriiforms, 3 extinct charadriiforms, and 1 supraspecific terminal representing the extinct flightless alcid lineage Mancallinae for a total of 81 terminals. The parsimony-based analysis resulted in 32 MPT's (L:16,901; CI:0.37; RI:0.51; RC:0.19). An additional analysis performed with all characters unordered did not result in topological differences, or an increase in the number of MPTs recovered. The strict consensus topology is well resolved with polytomies restricted to three clades, Jacanidae, *Larus*, and the *Alca* + *Pinguinus* clade. Bootstrap and Bremer support values are highest for clades with low proportions of fossil taxa included (e.g., *Uria*; Fig. 8.8). Apomorphies of recovered clades are provided in Table 8.8.

Charadrii is recovered in a basal position in Charadriiformes as the sister taxon to a Scolopaci + Lari clade (Fig. 8.8). Among Scolopaci a monophyletic Jacanidae is placed as the sister taxon to Scolopacidae. *Rhinoptilus chalcopterus* is placed basally in Lari, with Glareolidae, and a Sternidae + Laridae + Rynchops clade in successively more derived positions in the strict consensus tree (Fig. 8.8). Pan-Alcidae is nested in Lari as the sister-taxon to Stercorariidae.

Congruent with the results of previous analyses (Chandler, 1990a; Smith, 2011; Chapter 3), Mancallinae is placed as the sister taxon to Alcidae (Fig. 8.8). However, the placement of Mancallinae is sensitive to the inclusion of SDSNH 25358 which like Mancallinae, was recovered as the sister taxon to all other Alcidae in a previous analysis (see Chapter 5). An additional analysis (results not shown) including SDSNH 25358

Table 8.7- Apomorphies supporting taxonomic referrals of fossil used as calibrations for divergence estimation.

<b><i>Brachyramphus dunkeli</i>:</b> <i>Brachyramphus</i> apomorphies (relative to other Alcinae): presence of a ridge between the head and the ventral tubercle on the posterior face of humerus (133:1), posteriorly facing tip of the ventral tubercle elongate/oval in shape (136:1); humeral condyles separated more than other Alcidae (158:1).
<b><i>Synthliboramphus rineyi</i>:</b> <i>Synthliboramphus</i> apomorphies (relative to other Alcinae): distal edge of primary pneumotricipital fossa concave (129:2); dorsal supracondylar process smoothly transitions to humeral shaft (147:3).
<b><i>Fratercula cirrhata</i>:</b> “football-shaped” pit for insertion of m. humerotriceps along distal margin of primary pneumotricipital fossa (an autapomorphy of <i>Fratercula cirrhata</i> ; 119:1).
<b><i>Cerorhinca aurorensis</i>:</b> Doubly concave posterior margin of the ventral tubercle (135:1).
<b><i>Cephus olsoni</i>:</b> <i>Cephus</i> apomorphies: shaft of humerus more rounded (i.e., less dorsoventrally compressed) than all other Alcidae (145:1); secondary pneumotricipital fossa more excavated than other Alcinae.
<b><i>Alca</i> aff. <i>torda</i>:</b> <i>Alca</i> + <i>Pinguinus</i> apomorphies (relative to other Alcini): equal width of the tricipital sulci of distal humerus (151:1); m. coracobrachialis sulcus a closed duct (113:1); differentiated from <i>Pinguinus</i> by the restriction of the deltopectoral crest to the proximal half of the humeral shaft (107:0).
<b><i>Aethia barnesi</i>:</b> Aethiini apomorphies relative to Fraterculini: ventral projection of the entepicondyle (150:0), lack of proximal extension of the dorsal supracondylar process (148:0), and the abrupt transition of the deltopectoral crest to the humeral shaft (108:1).
<b><i>Miocepphus bohaski</i>:</b> <i>Miocepphus</i> apomorphies (relative to <i>Uria</i> ): distal edge of bicipital crest nearly perpendicular with humeral shaft (111:1); notch between bicipital crest and humeral shaft (112:1); dorsal supracondylar process a small dorsally pointing projection (147:1); sulcus tendinosus of distal radius absent (168:0); posterior notch on distal radius absent (169:0).
<b><i>Larus elegans</i>:</b> canal two of hypotarsus posteromedial to canal 1 and bordered medially by hypotarsal crest (220:2); presence of a distinct scar along anterior surface of the lateral edge of coracoid (99:1).
<b><i>Nupharanassa bulotorum</i>:</b> distal vascular foramen larger than other charadriiforms (227:1); with deeply incised tendinal groove on anterior surface proximal to trochlea II (229:1); shaft compressed (226:1).
<b><i>Boutersemia belgica</i>:</b> distal vascular foramen larger than other charadriiforms (227:1); with deeply incised tendinal groove on anterior surface proximal to trochlea II (229:1); shaft compressed (226:1).
<b><i>Alcidae incertae sedis</i>:</b> Alcidae apomorphies (relative to all other Charadriiformes): humeral shaft dorsoventrally compressed (145:2); anterior surface of ventral condyle flattened as in all Alcidae except Mancallinae (157:1); dorsal supracondylar process proximally elongated along shaft (148:1); dorsal projection of the dorsal supracondylar process reduced relative to many other charadriiforms (e.g., <i>Larus</i> ; 147:1).
<b><i>Jiliniornis huadianensis</i>:</b> large, dorsally projecting dorsal supracondylar tubercle (147:0); rounded humeral shaft (145:0), deeply pneumatized primary pneumotricipital fossa (121:0), secondary pneumotricipital fossa apneumatic (130:0).

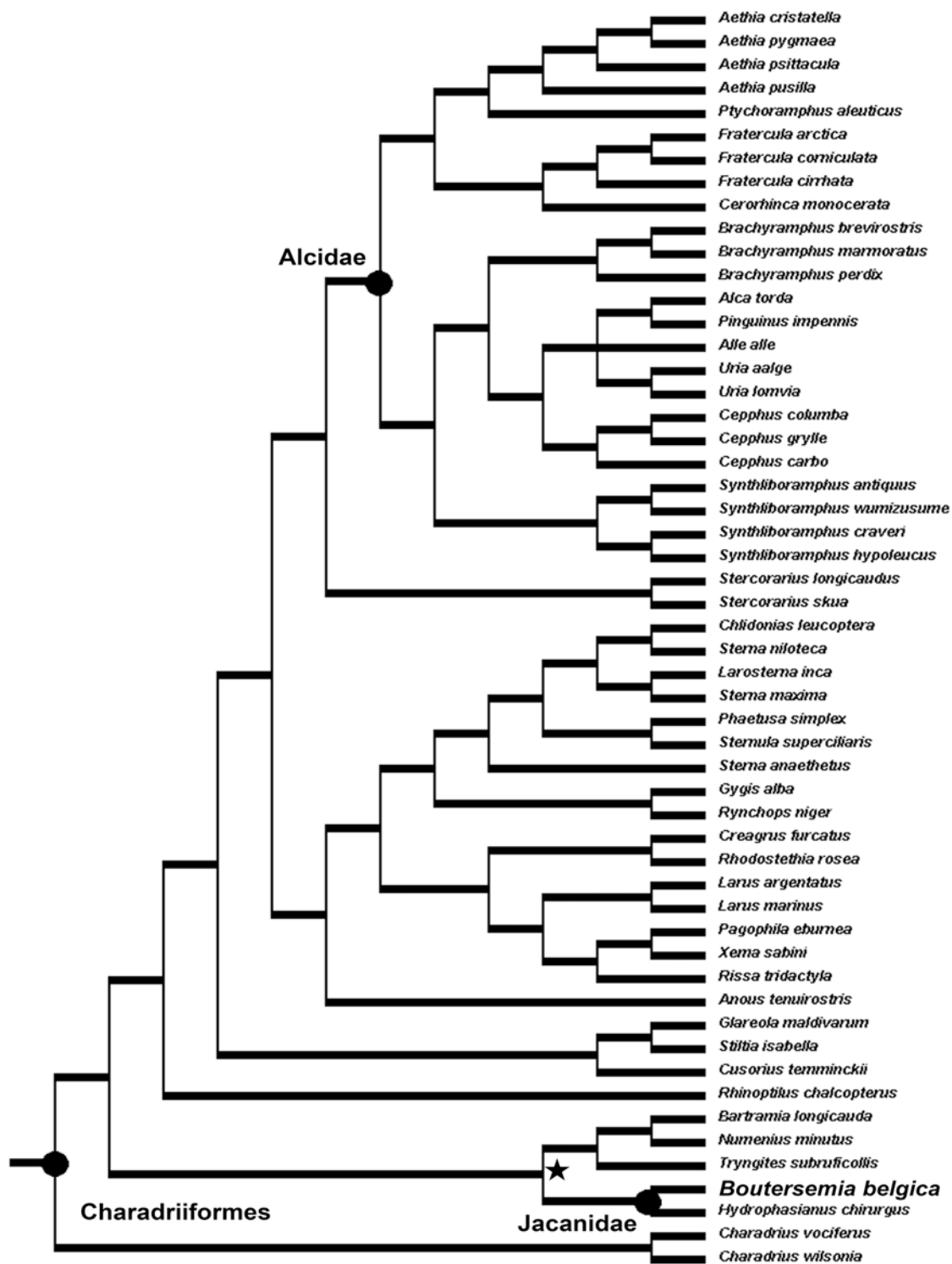


Figure 8.3- Strict consensus cladogram of 2 MPT's (L:15,911; CI:0.38; RI:0.50; RC:0.19) indicating the placement of *Boutersemia belgica* in Jacanidae. The node calibrated by this fossil in the divergence analysis is marked with a star.



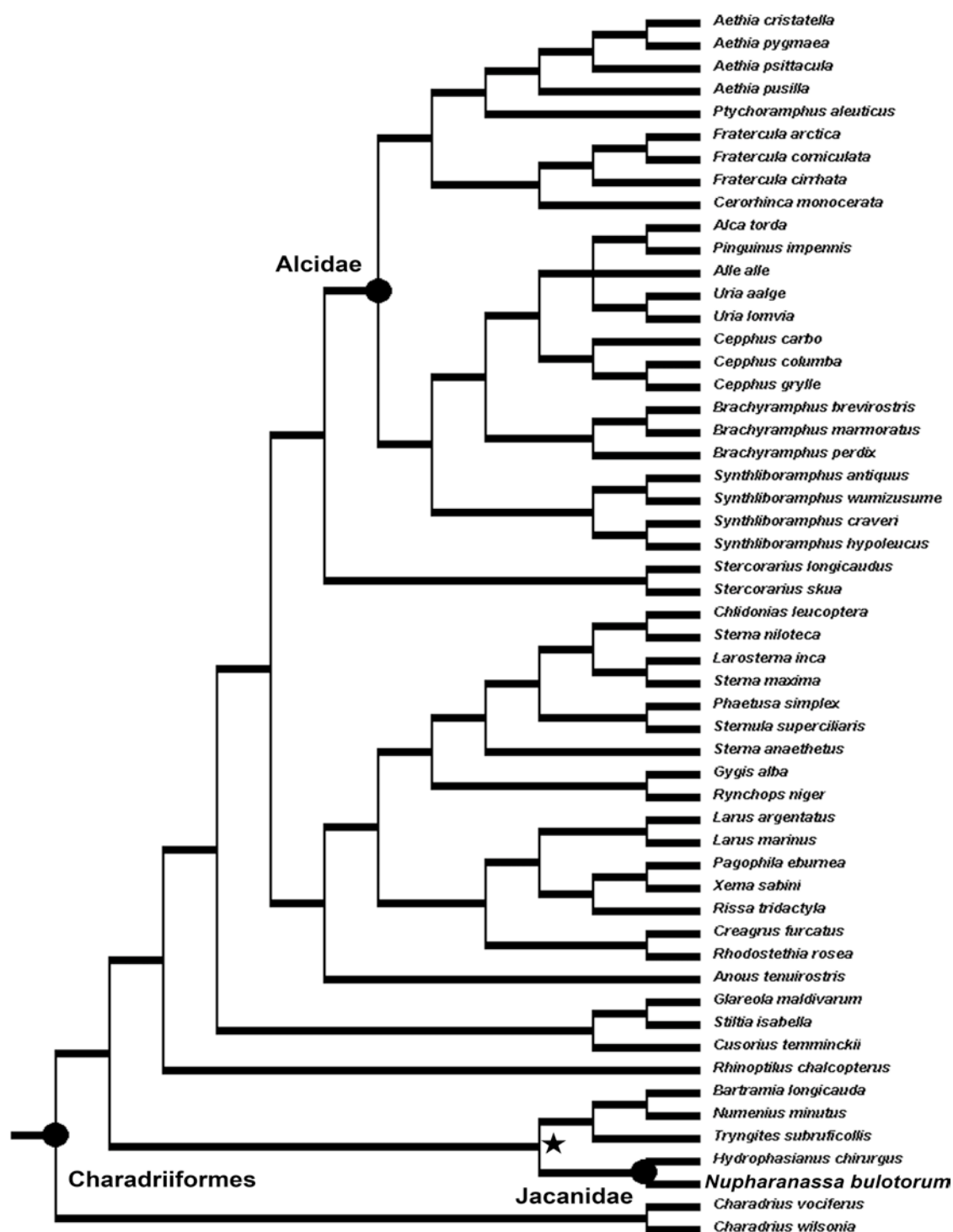


Figure 8.4- Strict consensus cladogram of 2 MPT's (L:15,911; CI:0.38; RI:0.50; RC:0.19) indicating the placement of *Nupharanassa bulotorum* in Jacanidae. The node calibrated by this fossil in the divergence analysis is marked with a star.

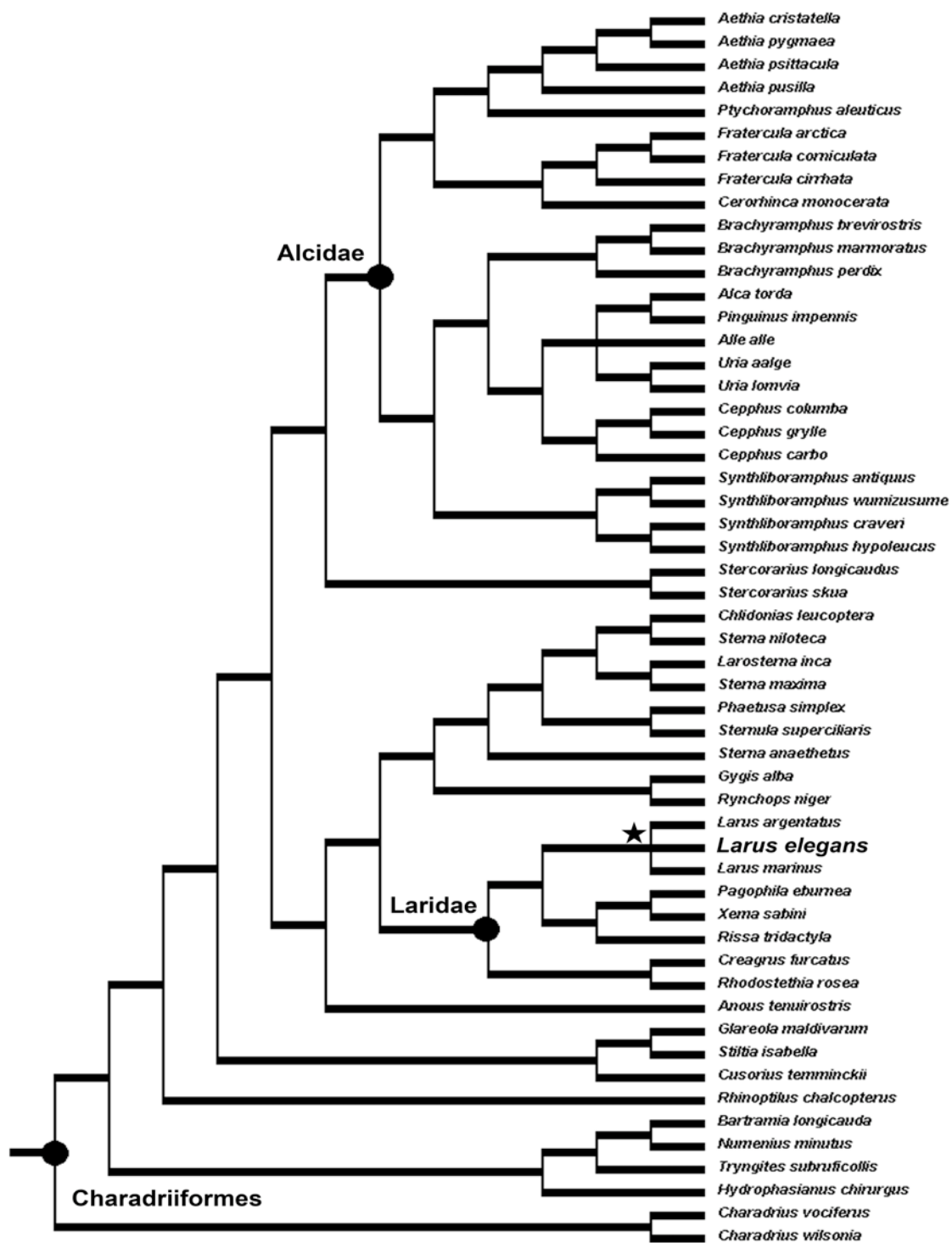


Figure 8.5- Strict consensus cladogram of 2 MPT's (L:15,911; CI:0.38; RI:0.50; RC:0.19) indicating the placement of *Larus elegans* in Laridae. The node calibrated by this fossil in the divergence analysis is marked with a star.

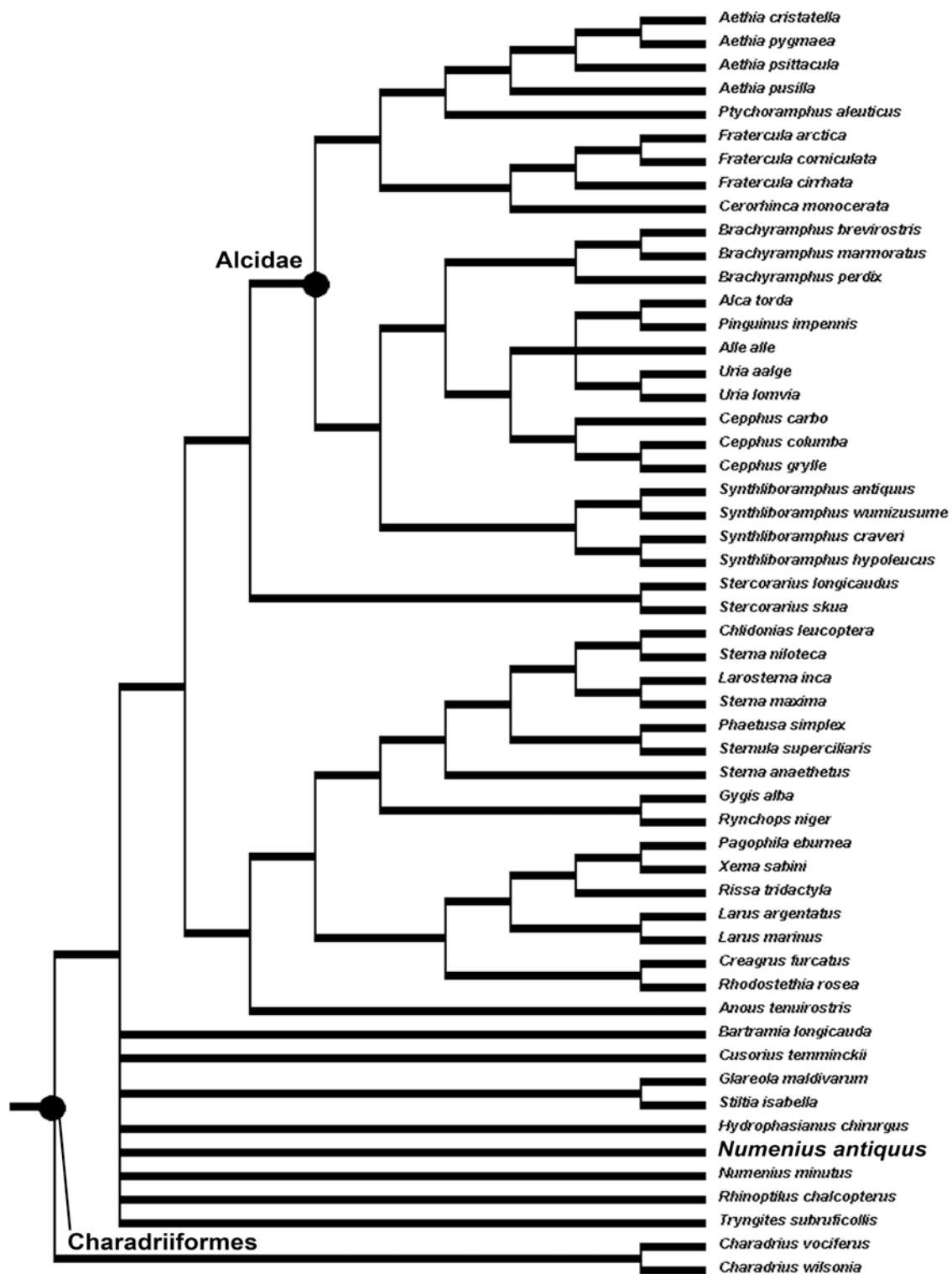


Figure 8.6- Strict consensus cladogram of 4 MPT's (L:15,911; CI:0.40; RI:0.54; RC:0.22) indicating the unresolved placement of *Numenius antiquus* in Charadriiformes.

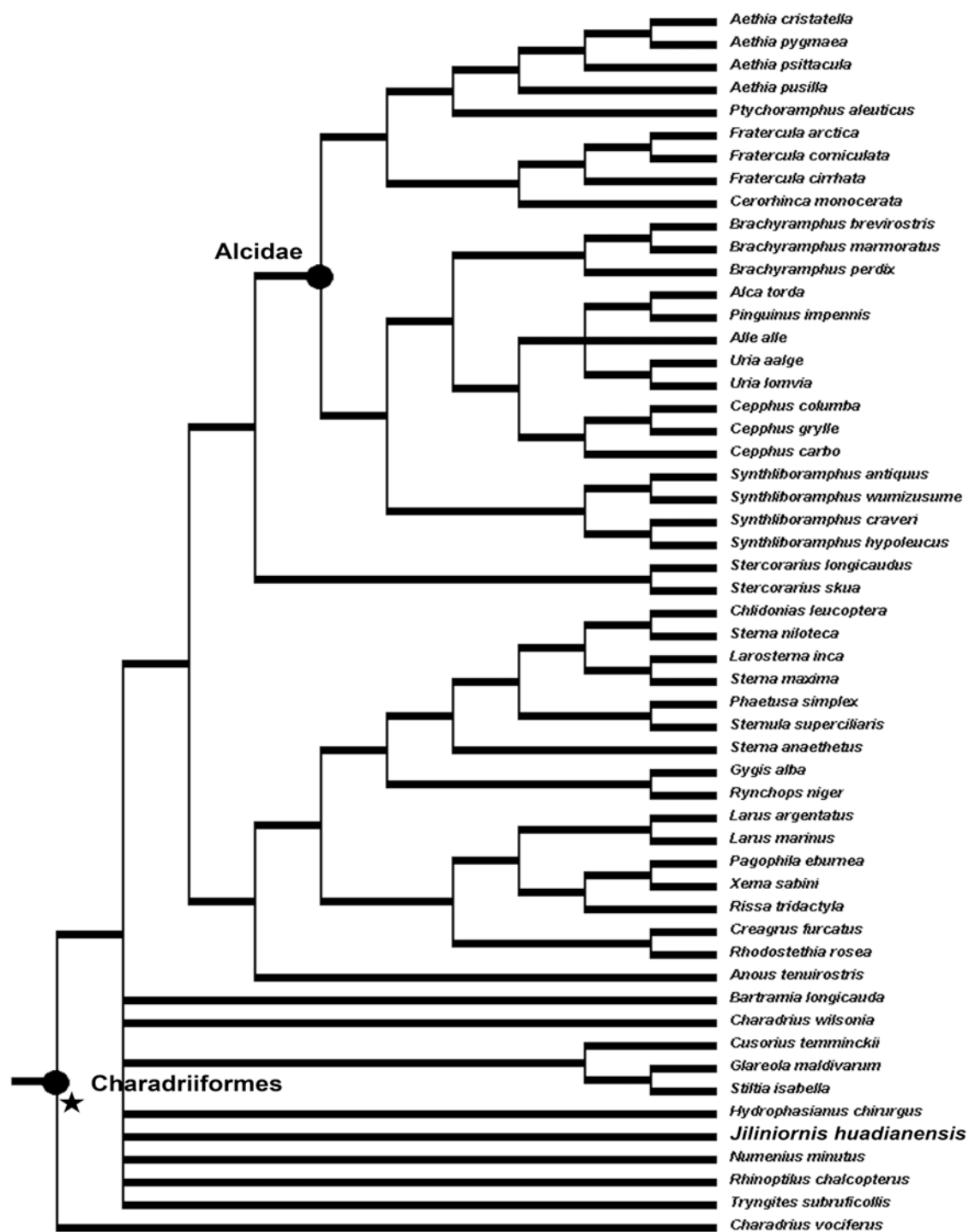


Figure 8.7- Strict consensus cladogram of 24 MPT's (L:15912; CI:0.39; RI:0.54; RC:0.21) indicating the unresolved placement of *Jiliniornis huadianensis* in Charadriiformes. The node calibrated by this fossil in the divergence analysis is marked with a star.

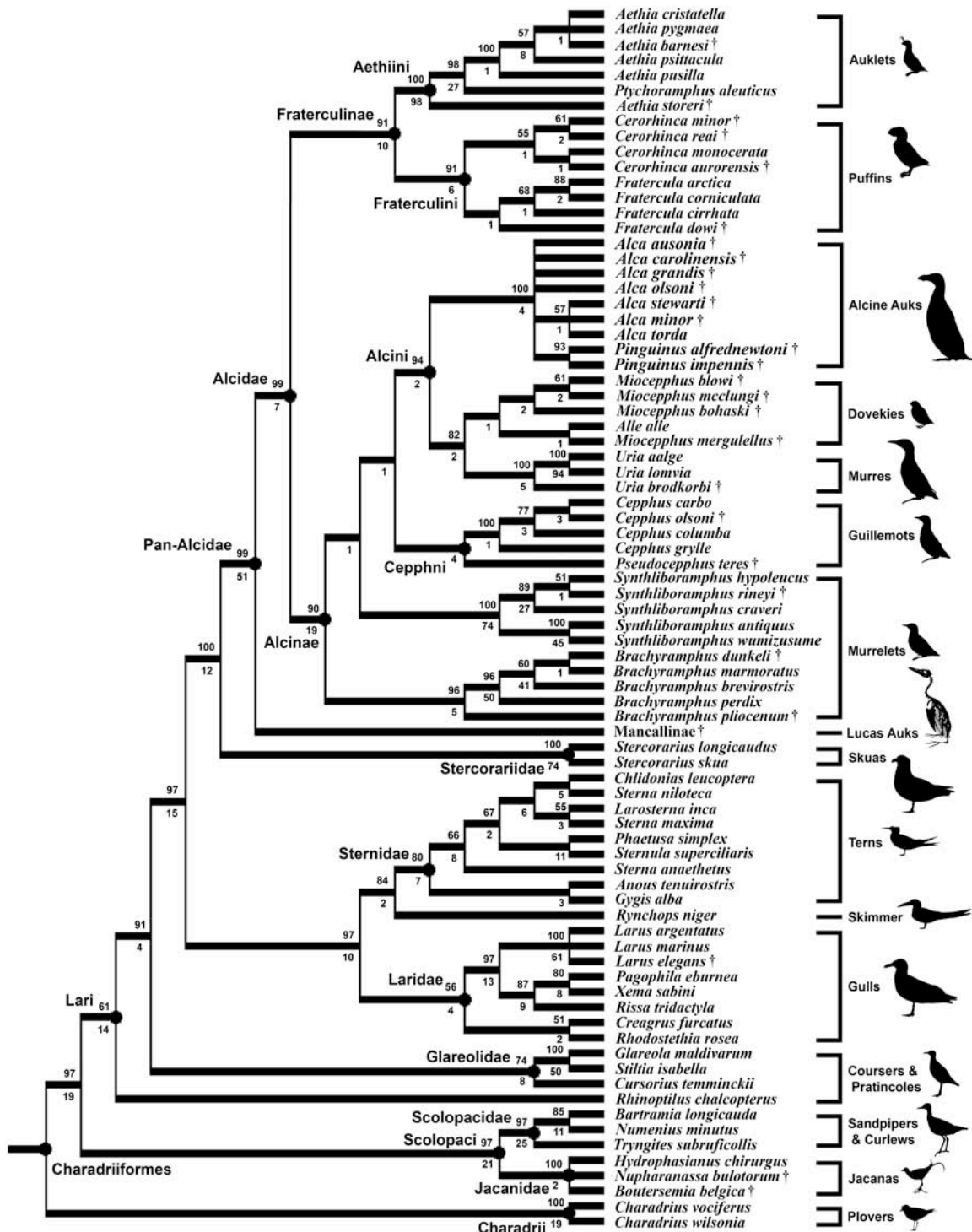


Figure 8.8- Parsimony-based results of the combined phylogenetic analysis (32 MPT's; L:16,901; CI:0.37; RI:0.51; RC:0.19). Bootstrap values >50% and Bremer support values appear above and below nodes respectively.

Table 8.8- Apomorphies supporting clades in the resultant phylogenetic tree from the parsimony-based combined analysis (Fig. 8.8). Character numbers from Appendix 2 are followed by character state symbols (e.g., 23:0 = character 23, state 0). ‘\*’ represents locally optimized apomorphies with CI < 1.0. All other apomorphies have a CI = 1.0.

Clade	Character numbers and states that support monophyly
Pan-Alcidae + Stercorariidae	*36:0; *64:0; *127:1; *205:1; 324:1; 352:1.
Pan-Alcidae	*5:1; *40:1; *60:0; *62:2; 78:1; *79:1; 80:1; *84:1; *96:0; *99:1; *109:1; *116:1/2; *117:0/1; *121:1/2; 128:0; *145:1; 147:1/2/3/4; *153:1; *155:1; 166:1; *170:1/2; *177:0; 181:1; *182:2; *206:1; *209:1; *214:0; *218:1; *223:0; *232:1.
Alcidae	*69:1 *85:1; 157:1; 176:1.
Mancallinae	22:1; 123:1; 143:1; 144:1; 152:1; 154:1; 186:1; 187:1; 188:0; 189:0; 190:1; 194:1.
Alcinae	50:1; *57:0/1/2/3; *66:1; *108:0; *110:2; *150:1; *198:1; *213:1; 279:1; *290:1.
Fraterculinae	*4:1; *10:1; *16:1; *53:1; *54:1; *68:1; *70:1; *71:1; *73:1; *81:1; *108:1; *111:1; *134:0; *150:0; *164:1; *173:1; *175:1; 179:0; *192:0; *195:1; *200:0; *202:0; *274:1.
Fraterculini	30:1; 41:1; 115:0; 295:1; 296:1.
Aethiini	*139:1; *140:0; *146:1; *160:0.
Alcini	*16:2; *21:1; *24: 1; *74:0; *100:0; 191:1; 246:1; *248:1; *270:1; 283:1.
Cepphini	*108:1; *110:1; *112:1; *114:1; *117:1; *127:0; *128:1; *139:1; *145:1.
Lari	336:0; 338:1.
Laridae	*14:1; *82:0; 310:1; *344:0.
Sternidae + <i>Rynchops</i>	*18:0; *40:1; *43:1; *199:1; *232:1; 301:0; *345:1.

recovered this specimen as the sister taxon to all other pan-alcids and recovered Mancallinae as the sister taxon to Fraterculinae.

The alcid crown clade, Alcidae, comprises Fraterculinae and Alcinae (Fig. 8.8). The sister taxon relationship recovered between Fraterculinae (contents include Fraterculini and Aethiini) and Alcinae (contents include *Brachyramphus*, *Synthliboramphus*, *Cepphus*, and Alcini) is congruent with the results of previous analyses of alcid relationships (Watada et al., 1987; Moum et al., 1994; Friesen et al., 1996; Baker et al., 2007; Pereira and Baker, 2008; Smith, 2011).

Fraterculini (contents include *Fratercula* and *Cerorhinca*) is recovered as the sister taxon to Aethiini (contents include *Aethia* and *Ptychoramphus*; Fig. 8.8). The sister taxon relationship between Fraterculini and Aethiini was recovered in the results of previous phylogenetic analyses (Watada et al., 1987; Chandler, 1990a; Moum et al., 1994; Friesen et al., 1996; Thomas et al., 2004; Baker et al., 2007; Pereira and Baker, 2008; Smith, 2011).

*Fratercula arctica* and *Fratercula corniculata* are sister taxa, with *Fratercula cirrhata* and *Fratercula dowi* in successively more basal positions. *Fratercula* is the sister taxon to *Cerorhinca*. *Cerorhinca minor* and *Cerorhinca reai* are recovered as sister taxa to a clade composed of *Cerorhinca monocerata* and *Cerorhinca aurorensis* (Fig. 8.8). The sister taxon relationship between *Fratercula* and *Cerorhinca* has been recovered in every previous analysis of Fraterculini relationships (Strauch, 1985; Watada et al., 1987; Chandler, 1990a; Moum et al., 1994; Friesen et al., 1996; Thomas et al., 2004; Baker et al., 2007; Pereira and Baker, 2008; Smith, 2011).

*Aethia storeri* is the sister taxon to the remainder of Aethiini, with *Ptychoramphus aleuticus*, *Aethia pusilla*, *Aethia psittacula*, and polytomy consisting of *Aethia barnesi*, *Aethia pygmaea*, and *Aethia cristatella* in successively more derived positions (Fig. 8.8). These results are largely congruent with previous analyses of Aethiini interrelationships (Watada et al., 1987; Chandler, 1990a; Moum et al., 1994; Friesen et al., 1996; Thomas et al., 2004; Baker et al., 2007; Pereira and Baker, 2008; Smith, 2011).

*Brachyramphus* is recovered as the sister taxon to all other Alcinae (i.e., *Synthliboramphus* + Cepphini + Alcini; Fig. 8.8). This position for *Brachyramphus* is congruent with the position of this taxon recovered in recent molecular-based phylogenetic analyses of alcid relationships (Thomas et al., 2004; Baker et al., 2007; Pereira and Baker, 2008) but conflicts with the position of *Brachyramphus* in the results of the parsimony-based analysis of extant taxa (Fig. 1.25), and the results of Watada et al., (1987) and Chandler (1990a), in which *Synthliboramphus* is placed as the sister taxon to all other Alcinae and *Brachyramphus* is placed in a successively more derived position as the sister taxon to the remainder of Alcinae.

*Brachyramphus pliocenum* is placed as the sister to all other *Brachyramphus* species, with *Brachyramphus perdix* and *Brachyramphus brevirostris* in successively more derived positions (Fig. 8.8). *Brachyramphus marmoratus*, and *Brachyramphus dunkeli* are sister taxa, and together are placed as the sister to *Brachyramphus brevirostris*.

*Synthliboramphus* is placed as the sister taxon to Cepphini (contents include *Cepphus* + *Pseudocepphus*) + Alcini (contents include *Alca*, *Pinguinus*, *Alle*,



*Miocepphus*, *Uria*; Fig. 8.8). This systematic position for *Synthliboramphus* has not been recovered in previous phylogenetic analysis of alcid relationships. *Synthliboramphus* has been placed as the sister to *Cepphus* (Strauch, 1985; Moum et al., 1994), sister to other Alcinae (Watada et al., 1987; Chandler 1990a), and sister to Alcini (Friesen et al., 1996; Thomas et al., 2004; Baker et al., 2007; Pereira and Baker, 2008). This position for *Synthliboramphus* also conflicts with the position of this taxon in the results of the parsimony-based analysis of extant taxa (Fig. 1.25) in which *Synthliboramphus* is placed as the sister taxon to all other Alcinae.

Congruent with the results of all previous analyses of *Synthliboramphus* interrelationships (Friesen et al., 1996; Thomas et al., 2004; Baker et al., 2007; Pereira and Baker, 2008; Smith 2011), *Synthliboramphus antiquus* and *Synthliboramphus wumizusume* are recovered as sister taxa (Fig. 8.8). *Synthliboramphus craveri*, *Synthliboramphus hypoleucus*, and *Synthliboramphus rineyi* are recovered in a clade that is the sister to *Synthliboramphus antiquus* and *Synthliboramphus wumizusume*.

Cepphini is placed as the sister taxon to Alcini (Fig. 8.8). This systematic position for Cepphini has not been recovered in previous analysis of alcid relationships. Cepphini has been previously hypothesized as the sister to *Synthliboramphus* (Strauch, 1985; Moum et al., 1994), sister to *Uria* (Watada et al., 1987), sister to *Alle* + Fraterculinae (Chandler, 1990a), sister to *Aethia* + *Brachyramphus* (Chu, 1998), and sister to *Synthliboramphus* + Alcini (Baker et al., 2007; Pereira and Baker, 2008; see Figs. 1.2 & 1.3).

As in the previous analysis of Cepphini relationships (Chapter 6), *Pseudocepphus teres* is placed as the sister to the other Cepphini (Fig. 8.8). *Cepphus grylle* and *Cepphus columba* are placed in successively more derived positions with sister taxa *Cepphus carbo* and *Cepphus olsoni* sister to *Cepphus columba*. These results are congruent with the parsimony-based results of extant taxa from Chapter 1 (Fig. 1.25), and with previous molecular-based analyses of *Cepphus* interrelationships that place Pacific Ocean endemic congeners *Cepphus carbo* and *Cepphus columba* as sister taxa to the exclusion of Atlantic Ocean endemic *Cepphus grylle* (Friesen et al., 1996; Thomas et al., 2004; Pereira and Baker, 2008).

Alcini is placed in a derived position near the crown of Alcinae (Fig. 8.8). This result is congruent with the position of Alcini in previous phylogenetic analyses (Strauch, 1985; Chandler, 1990a; Moum et al., 1994; Friesen et al., 1996; Thomas et al., 2004; Baker et al., 2007; Pereira and Baker, 2008). Although *Pinguinus impennis* and *Pinguinus alfrednewtoni* are recovered as sister taxa, the relationship between *Pinguinus* and *Alca* species is unresolved. *Alca stewarti*, *Alca minor*, and *Alca torda* are placed in a polytomy to the exclusion of other *Alca* species and *Pinguinus*.

*Uria* is recovered as the sister taxon to a clade including *Alle alle* and *Miocepphus* species (Fig. 8.8). *Uria brodkorbi* is placed as the sister taxon to extant congeners *Uria aalge* and *Uria lomvia*. *Alle alle* is placed as the sister taxon to *Miocepphus mergulellus*. *Miocepphus bohaski* is placed as the sister taxon to *Miocepphus blowi* and *Miocepphus mcclungi*. Alcini relationships are less resolved but congruent with those previously recovered (Chapter 2).

Differences in relationships among the outgroup to Pan-Alcidae between the parsimony-based topology resulting from the analysis of extant taxa (Fig. 1.25) and the results of the combined analysis of extant and extinct taxa (Fig. 8.8) are limited to the placement of three species, *Anous tenuirostris*, *Gygis alba*, and *Rynchops niger*. A detailed discussion of the varying systematic positions previously recovered for these taxa is provided in Chapter 1. *Anous tenuirostris* is placed as the sister taxon to *Gygis alba* as part of a monophyletic Sternidae in these results (Fig. 8.8), rather than as the sister taxon to Laridae + Sternidae as in the results of previous analyses that were limited to extant taxa (Fig. 1.25; Baker et al., 2007). This placement for *Anous* is largely consistent with the results of the only previous analysis with dense taxon sampling for Sternidae (Bridge et al., 2005) in which *Anous* and *Gygis* were recovered in successively more basal positions at the base of Sternidae.

*Rynchops niger* is placed as the sister taxon to Sternidae in the results of the combined analysis of extant and extinct charadriiforms (Fig. 8.8), rather than as the sister taxon to *Gygis alba* (Fig. 1.25) in a position that is basal to an otherwise monophyletic Sternidae (Fig. 1.25). Other outgroup relationships are consistent with those recovered in the analysis of extant taxa and are largely congruent with other recent analyses of charadriiform relationships (Ericson et al., 2003; Paton and Baker, 2006; Baker et al., 2007; Livezey, 2009, 2010; Mayr, 2011). However, Jacanidae and *Larus* relationships are unresolved, likely owing to the inclusion of incomplete fossil taxa (i.e., *Boutersemia belgica*, *Nupharanassa bulorum*, *Larus elegans*).

The MCMC chains in the Bayesian analysis of the combined charadriiform data were run for 50 million generations. The standard deviation of split frequencies never stayed below 0.01. However, convergence of the MCMC chains was assessed through evaluation of log likelihoods in MrBayes v3.1.2 (Ronquist and Huelsenbeck, 2003) and Tracer (Rambaut and Drummond, 2009), and both programs determined that stationarity had been reached. The complexity of the combined data matrix or the large amount of missing data may be responsible for the disparity between the standard deviation of split frequencies. Burn-in was assessed using Tracer (Rambaut and Drummond, 2009) and the first 35,000 of the 50,001 retained trees were discarded as burn-in. Because relationships in Alcinae were largely unresolved in the 50% consensus tree (i.e., contype=halfcompat; Fig. 8.9), an additional tree summarizing all compatible results (i.e., contype=allcompat) was constructed using MrBayes v3.1.2 (Ronquist and Huelsenbeck, 2003; Fig. 8.10).

Pan-Alcidae relationships recovered in the Bayesian results (Fig. 8.10) are largely congruent with the parsimony-based results (Fig. 8.8). Notable differences include the recovery of *Cerorhinca* paraphyly. *Cerorhinca aurorensis* and *Cerorhinca monocerata* were recovered at the base of Fraterculini, with other *Cerorhinca* and *Fratercula* in more derived positions. Also, *Alle alle* was recovered as the sister taxon to a monophyletic *Uria*, with *Miocepphus* species forming a paraphyletic grouping in Alcini. The only major topological difference was that *Brachyramphus* was recovered as the sister taxon to

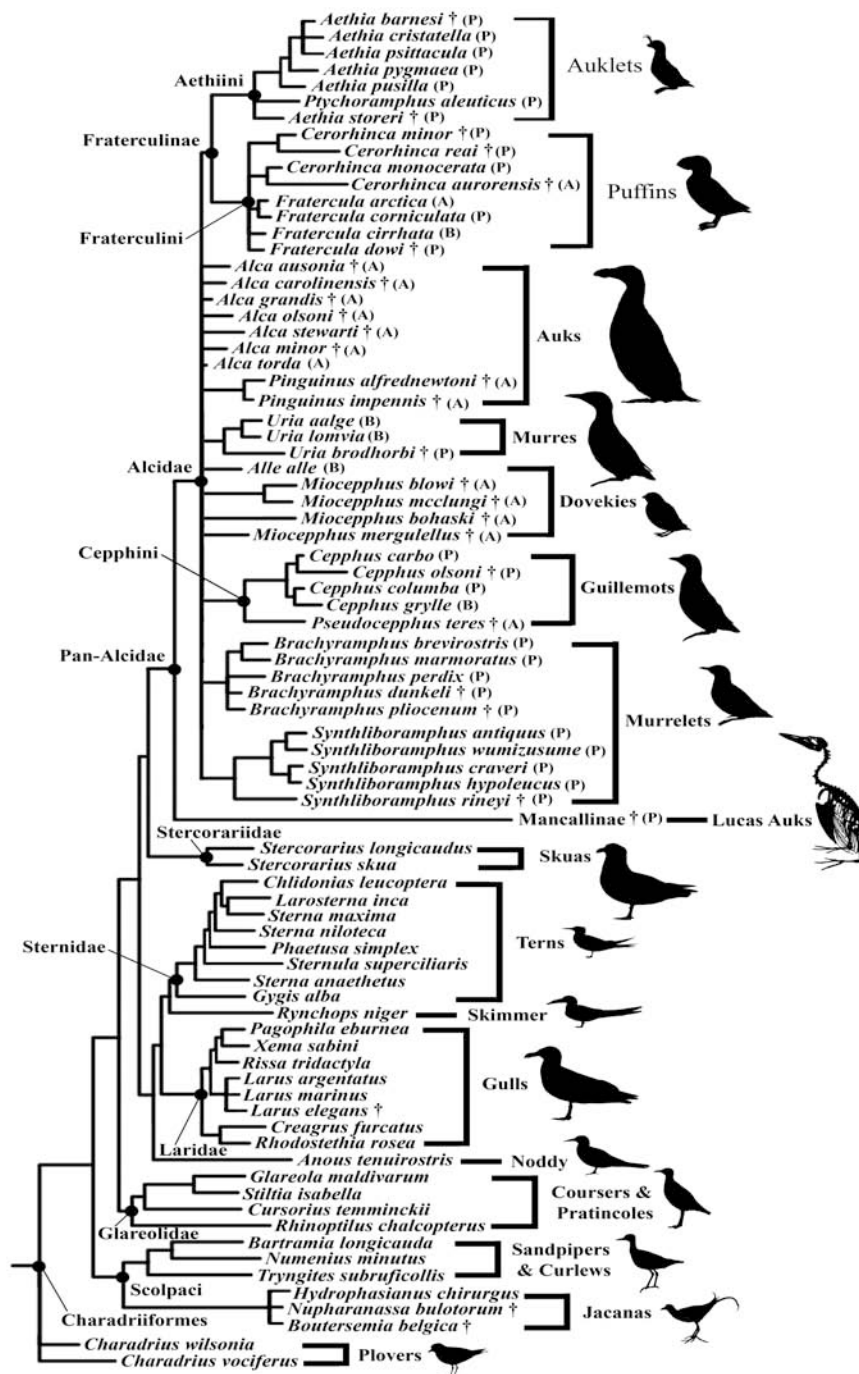


Figure 8.9- Charadriiform relationships recovered in the Bayesian analysis. Nodes with posterior probabilities less than 0.5 have been collapsed. Posterior probabilities for all nodes are displayed in Fig. 8.10. Letters in parentheses following pan-alcid species names indicate geographic distribution: Atlantic Ocean (A); Pacific Ocean (P); present in both Atlantic and Pacific Ocean basins (B).

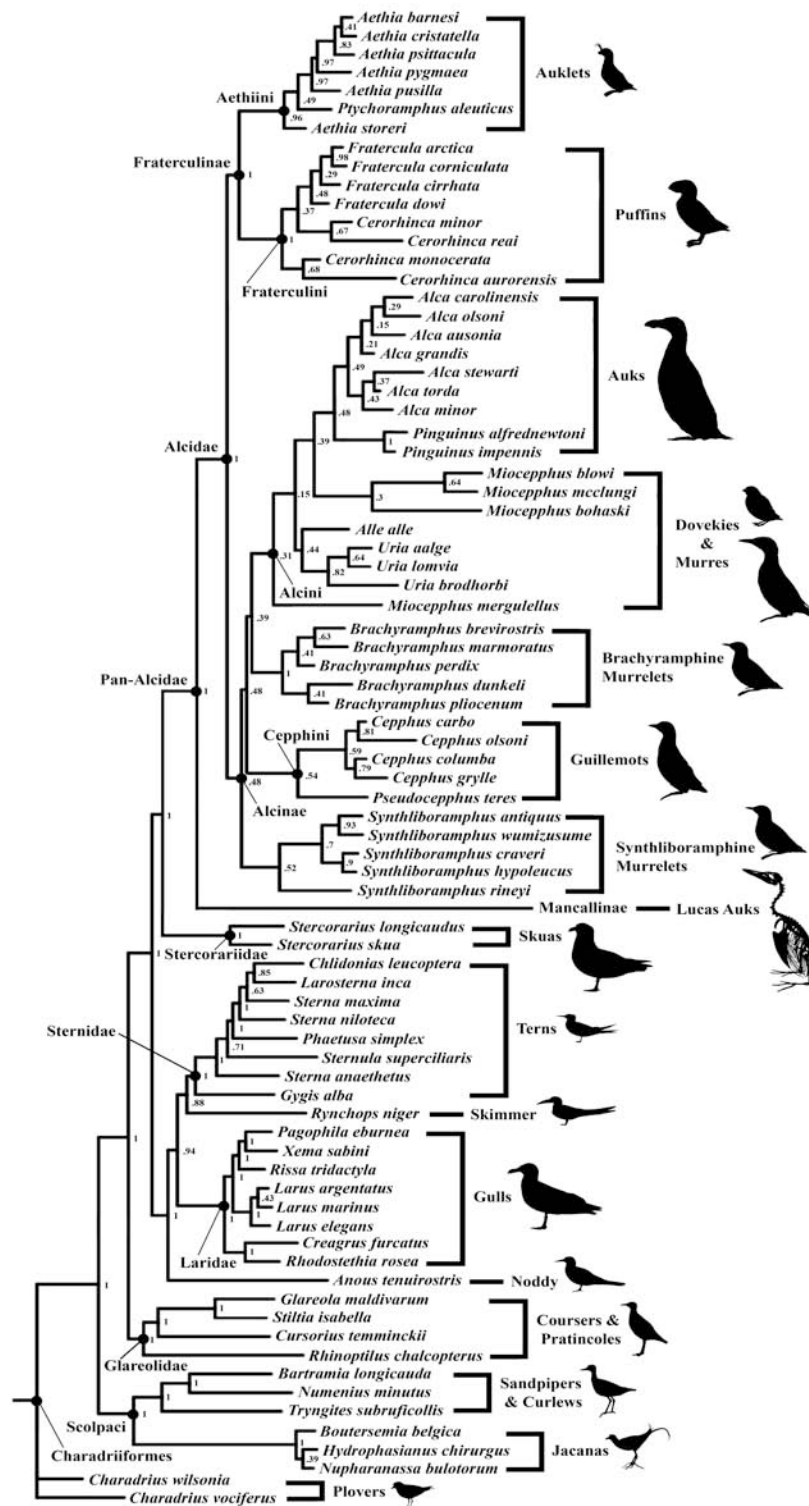


Figure 8.10- Charadriiform relationships recovered in the Bayesian analysis. Nodes with posterior probabilities less than 0.5 have not been collapsed (i.e., contype=allcompat).

Alcini rather than as the sister taxon to all other Alcinae as in the parsimony based results.

Relationships among the outgroup taxa and Pan-Alcidae recovered in the Bayesian results (Fig. 8.10) are also largely congruent with the parsimony-based results (Fig. 8.8). Exceptions include the placement of *Anous tenuirostris* as the sister to Laridae + Sternidae + *Rynchops*. This result was also recovered in the Bayesian analysis results presented by Baker et al. (2007). *Anous* was placed as the sister to *Gygis alba* within Sternidae in the parsimony-based results (Fig. 8.8). *Rhinoptilus chalcopterus* was recovered as the sister taxon to other Glareolidae in the Bayesian results (Fig. 8.10). This result also agrees with the placement of this taxon recovered in the Bayesian results of Baker et al. (2007). *Rhinoptilus chalcopterus* was recovered as the sister to Glareolidae plus the rest of Charadriiformes in the parsimony-based results (Fig. 8.8).

A phylogenetic classification of Pan-Alcidae is proposed based on the results of the phylogenetic analyses (Figs. 8.8, 8.10; Appendix 8).

***Morphological character optimization:*** The sister taxon relationship recovered between Pan-Alcidae and Stercorariidae (Fig. 8.8) is supported by 2 morphological (microfeather) apomorphies with a CI = 1.0: nodal prongs present (324:1), and distal prongs present (352:1; Dove, 2000; Table 8.8). The expanded nodes along the barbules of alcids, skuas, and loons bear proximally projecting, pointed structures referred to as prongs (see Dove, 2000; figure 143). These microfeather characteristics cannot be evaluated in extinct alcids because no fossilized pan-alcid feathers are known. A Pan-Alcidae + Stercorariidae clade is also supported by four locally optimized osteological

apomorphies. The cerebellar prominence of Stercorariidae, all extant alcids (except Fraterculini), and all extinct alcids in which the skull is known (e.g. *Miocepphus blowi*, *Pinguinus impennis*) protrudes farther posteriorly (36:0) than in other charadriiforms (e.g., *Chardarius vociferus*) in which the posterior margin of the skull is more spherical. Stercorariidae, all extant alcids except Fraterculini, and all extinct alcids in which the sternum is known (e.g. *Mancalla vegrandis*) lack medial sternal notches (64:0) as found in other charadriiforms (e.g., *Anous tenuirostris*). The m. subcoracoideus scar on the posterior surface of the ventral tubercle of the humerus is positioned more ventrally (127:1; rather than medially along the margin of the primary pneumotricipital fossa) in Stercorariidae, all extant alcids except Fraterculini, and all extinct alcids in which this feature is known (e.g. *Alca carolinensis*), than in other charadriiforms (e.g., *Gygis alba*). The post-acetabular dorsal iliac crest of most alcids (e.g., *Cepphus columba*) and Stercorariidae narrows posteriorly (205:1), whereas in many other charadriiforms (e.g., *Sterna maxima*) this crest maintains its width or is mediolaterally broader towards its posterior end.

The monophyly of Pan-Alcidae (contents include Mancallinae + Alcidae; Fig. 8.8) is supported by six apomorphies with a CI = 1.0 and 24 additional locally optimized apomorphies with a CI < 1.0 (Table 8.8). The pneumatic foramen of the anterodorsal surface of the sternum is reduced in pan-alcids (60:1) compared to other charadriiforms. The angle of the distal extremity of the furcula with respect to the furcular rami of pan-alcids is more acute than that of other charadriiforms (78:1).



Many of the characters that are diagnostic for Pan-Alcidae are humeral characters because of the modification of this skeletal element for wing-propelled diving. Although variable in depth among pan-alcids, the primary pneumotricipital fossa of pan-alcids is relatively less excavated than that of other charadriiforms (121:1/2). The scar for insertion of m. subcoracoideus is not as deeply excavated in pan-alcids as in other charadriiforms (128:0). Although variable within Pan-Alcidae, the humeral and ulnar shafts of all pan-alcids are more dorsoventrally compressed than those of other charadriiforms (145:1/2; 182:1/2).

The dorsal supracondylar process of all alcids and the Jacanidae (e.g., *Hydrophasianus chirurgis*) does not project as far dorsally (147:1/2/3/4) as in other charadriiforms (e.g., *Larus marinus*). The dorsal supracondylar process is the attachment point of m. extensor metacarpi radialis, a muscle that controls flexion of the carpometacarpus. The reduction of the dorsal supracondylar process in alcids relative to non-wing-propelled diving charadriiforms may be related to the decrease in length of the distal wing elements and the reduced flexion of the distal wing in alcids while diving (Pennycuik, 1975).

In distal view, the humerotricipital sulcus of the distal humerus of nearly all alcids is strongly concave or 'V shaped' (153:1). Only *Alle alle* and *Cerorhinca auroreensis* display the more flattened (i.e., less posteriorly depressed) condition representative of many other charadriiforms (e.g., *Xema sabini*). The significance, if any exists, to wing-propelled diving is uncertain. The dorsal humeral condyle of all known alcids is proximally rotated in relation to the ventral condyle (155:1) as compared to other

charadriiforms (e.g., *Larosterna inca*). This feature, along with the elongated sternum and pelvis of alcids (in comparison with most other charadriiforms; 72:1; 209:1) has been associated with wing-propelled diving (Storer, 1952). Furthermore, the sternal facet of the coracoid of all alcids other than Mancallinae is more curved than in other charadriiforms (104:1&2&3; i.e., angled 135°, ~90°, or > 90°). In other charadriiforms the sternal facet of the coracoid is nearly straight (104:0). Finally, the humerotricipital sulcus of the distal humerus of all sampled outgroup charadriiforms is wider than the scapulotricipital sulcus (151:0; Fig. 8.11). In many Alcinae the tricipital sulci are of relatively equal width (e.g., *Alca torda*; 151:1), whereas in some Alcinae (e.g., *Alle alle*) the scapulotricipital sulcus is wider than the humerotricipital sulcus (151:2). Among Fraterculinae and Mancallinae, only *Aethia barnesi* has a wider scapulotricipital sulcus than humerotricipital sulcus. The relevance of this modification in some alcids from the ancestral charadriiform condition is uncertain. Presumably variation in this character is related to wing-propelled diving because this modification is not seen in non-diving charadriiforms (Fig. 8.11). However, this character is variable even within clades such as *Miocepphus*, in which *Miocepphus blowi*, *Miocepphus bohaski*, and *Miocepphus mcclungi* have sulci of relatively equal width, *Miocepphus mergulellus* has a broader humerotricipital sulcus, and its sister taxon *Alle alle* has a broader scapulotricipital sulcus.

Five characters associated with m. supracoracoideus are optimized as local apomorphies of Pan-Alcidae. The m. supracoracoideus scar along the ventral sternum and carina of alcids extends distally in a relatively straight line in all Pan-Alcidae, except

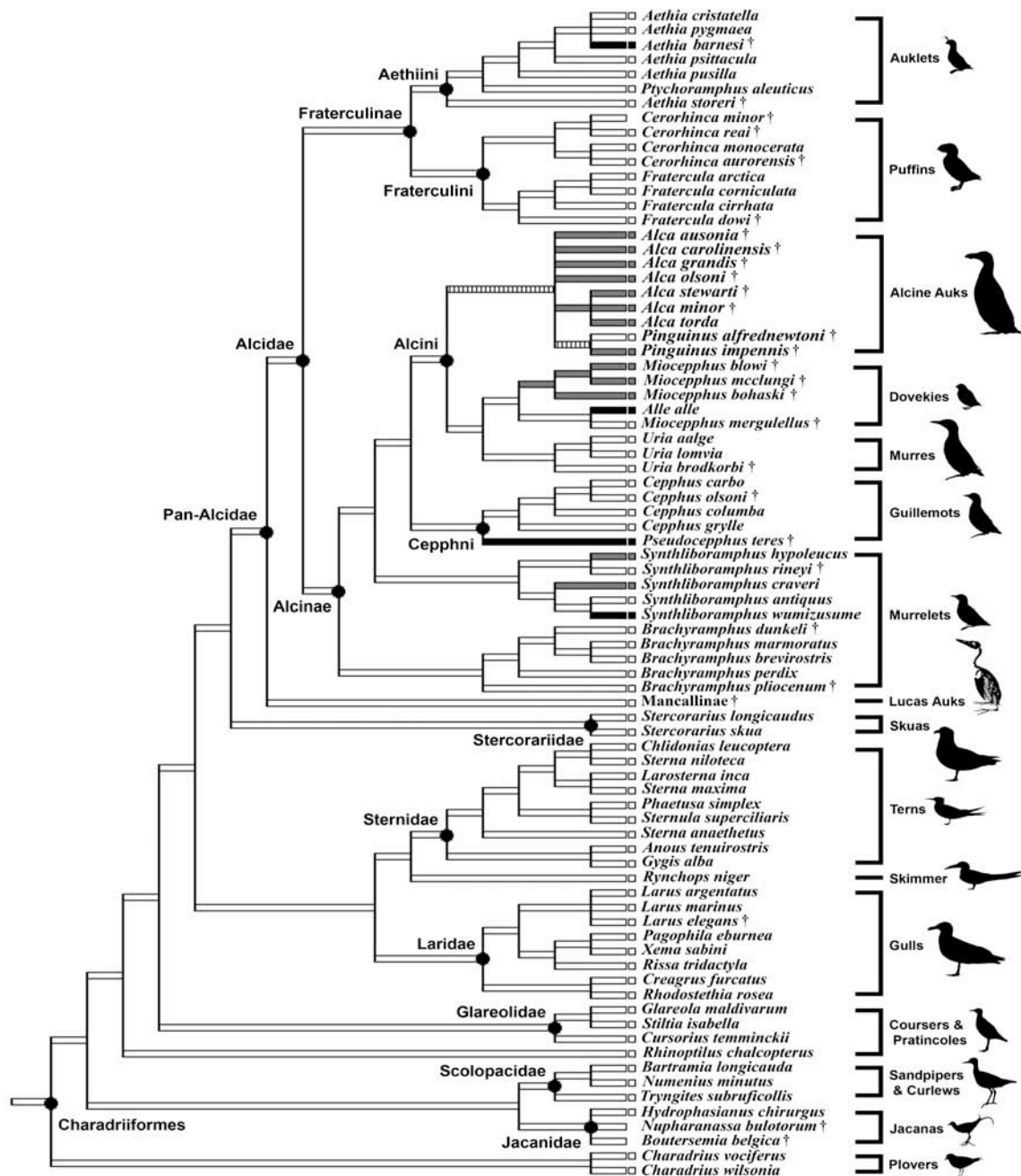


Figure 8.11- Charadriiform cladogram (topology based on Fig. 8.8) indicating the distribution of variation of the width of the tricipital sulci of the distal humerus (character 151). Character states for species are indicated by the colored squares between the taxon names and the cladogram: humerotricipital sulcus wider than scapulotricipital sulcus (white); sulci of equal width (grey); humerotricipital sulcus narrower than scapulotricipital sulcus (black). Species without colored squares (e.g., *Nupharanassa bulotorum*) do not preserve this character. Dashed lines represent ambiguous reconstruction of hypothesized ancestral character states.

Mancallinae, for which the sternum is known (69:1). Among sampled outgroup charadriiforms, only *Bartramia longicauda* and *Numenius minutus* displayed this character state. The anteromedial surface of the coracoid of all Pan-Alcidae except *Cepphus* and some species of Mancallinae is characterized by a distinctly raised m. supracoracoideus scar (92:0). This scar is reduced or absent in all other sampled charadriiforms except *Stercorarius skua*, *Rhinoptilus chalcopterus*, and *Anous tenuirostris*. An m. supracoracoideus nerve foramen of the procoracoid process of the coracoid (93:1) is present in Fraterculini, *Synthliboramphus*, *Cepphus*, and Alcini (except *Alle*) but is absent in smaller alcids including *Brachyramphus*, Aethiini, and the flightless Mancallinae lineage (Fig. 8.12). An m. supracoracoideus nerve foramen is also present in Laridae, Sternidae, and *Charadrius*. The attachment of m. supracoracoideus on the proximal humerus of all sampled charadriiforms (e.g., *Larus marinus*) is a rounded protuberance termed the dorsal tubercle, whereas in alcids this scar is distally elongated into what Fürbringer termed the supracoracoidal crest (116:1/2; crista m. supracoracoidei; Baumel and Witmer, 1993).

Although the relative contribution of the m. supracoracoideus and m. pectoralis to forward thrust at varying depths and during various diving behaviors is still debated, consensus has emerged regarding the contribution of m. supracoracoideus to a powered upstroke in wing-propelled diving birds including alcids and penguins (Lovvorn, 2001; Johansson and Aldrin, 2002; Watanuki et al., 2006; Hamilton, 2006). Although the mass of m. supracoracoideus relative to the m. pectoralis major is not as great in alcids as in penguins (Kovacs and Meyers, 2000), the greater exertion required for underwater flight

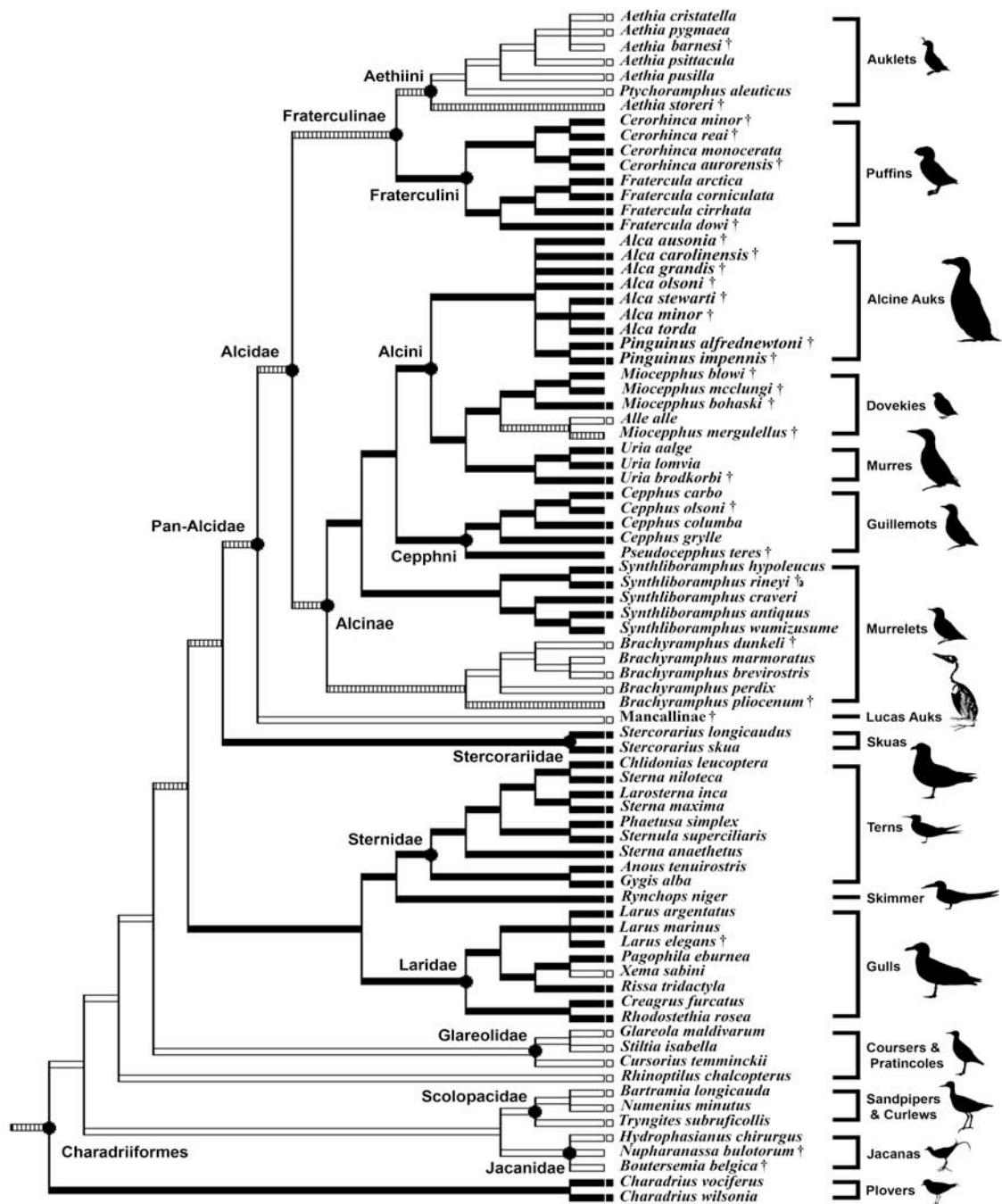


Figure 8.12- Charadriiform cladogram (topology based on Fig. 8.8) indicating the distribution of the presence of an m. supracoracoideus nerve foramen of the procoracoid process of the coracoid (character 93). Character states for species are indicated by the color of nodes adjacent to species terminals: absent (white); present (black). Species without nodes (e.g., *Nupharanassa bulotorum*) were not scored for this character. Dashed lines represent ambiguous reconstruction of hypothesized ancestral character states.

(i.e., relative to aerial flight) is proposed to have led to other structural changes including increased cortical bone thickness of forelimb elements (Habib and Ruff, 2008; Habib, 2010). The increased dependence on a powered upstroke is likely responsible for the concentration of myological and associated osteological changes in the forelimb and pectoral girdle of extant and extinct Pan-Alcidae documented herein.

Other diagnostic characters of note for Pan-Alcidae include the shorter length of the olecranon process of the ulna (170:1/2) in comparison with other charadriiforms, and the distal extension of the bicipital tubercle of the radius in to a crest (166:1). The tarsometatarsus of alcids is relatively shorter (i.e., tarsometatarsus length less than half the length of the tibiotarsus) than those of most other charadriiforms (218:1). Although this character is variable among non-alcid charadriiforms, *Synthliboramphus* is the only pan-alcid that has long and relatively gracile tarsometatarsi. The medial hypotarsal crest of pan-alcids is not as posteriorly projected as those of other charadriiforms.

Monophyly of the alcid crown clade (i.e., Alcidae) is supported by two apomorphies with a CI = 1.0 and two additional locally optimized apomorphies with a CI < 1.0 (Table 8.8). All Alcidae are characterized by a flattened anterior surface of the ventral condyle of the distal humerus (157:1). This character may be linked with wing propelled diving because it is not seen in other charadriiforms or in foot-propelled divers such as Gaviidae (Smith, personal observation). Alcidae are also characterized by an anteriorly projected dorsal cotylar process of the ulna (176:1). The dorsal cotylar process (sensu Baumel and Witmer, 1993:100) all other Charadriiformes (including Mancallinae) is relatively smaller and does not project as far anteriorly over the radial incisure. The

distal extremity of the scapulae of alcids are more acutely angled than the more gently curving scapulae of most other charadriiforms (e.g., *Larus marinus*).

Alcinae (contents include *Brachyramphus*, *Synthliboramphus*, Cepphini, and Alcini; see Fig. 8.8) monophyly is supported by two morphological apomorphies with a CI = 1.0 (Table 8.8): m. subcoracoideus long (279:1); medial articular process of the mandible points posteromedially (50:1). The distribution of these characters is uncertain among extinct Alcinae because musculature characters could not be scored for extinct taxa. Further characters of the mandible could be scored only for *Pinguinus impennis*, and *Miocepphus blowi*. Alcinae monophyly is also supported by 8 additional locally optimized apomorphies with a CI < 1.0. The lateral sternal notches of Alcinae are posteriorly enclosed, making them lateral sternal fenestrae (66:1). The lateral sternal notches of Mancallinae, Fraterculini, and *Ptychoramphus aleuticus* are not enclosed. Among other sampled charadriiforms, extant species of *Aethia* and *Bartramia longicauda* also possessed lateral sternal fenestrae. The ventral margin of the ventral epicondyle of the distal humerus of most Alcinae does not project ventral to the humeral shaft (150:1) as in Fraterculinae and many other charadriiforms (e.g., *Anous tenuirostris*). Among Alcinae, ventral projection of the ventral epicondyle (in anterior view) is observed only some species of *Miocepphus* (e.g., *Miocepphus blowi*).

The sister taxon relationship recovered between Fraterculinae + Mancallinae in an alternative analysis including SDSNH 25358 was supported by a single osteological apomorphy, an anteriorly pointing craniolateral process (i.e., sternocoracoidal process sensu Howard, 1929) of the sternum (61:1). This condition is unique to Mancallinae and

Fraterculinae among sampled charadriiforms. Among fossil taxa, the anteriorly pointing craniolateral process of the sternum was evaluated in *Miomancalla howardi*, *Mancalla lucasi*, 2 additional specimens referred to Mancallinae (SDSNH 24262, SDSNH 21295) and *Fratercula dowi* (see Appendix 3). The sterni of other Mancallinae and extinct *Cerorhinca* are not known.

Fraterculinae (contents include *Fratercula*, *Cerorhinca*, *Aethia*, *Ptychoramphus*) monophyly is supported by a single apomorphy with a CI = 1.0 and 22 additional locally optimized apomorphies with a CI < 1.0 (Table 8.8). The intramuscular line of the ulna of Fraterculinae is less distinct than in many other charadriiforms (e.g., *Alca torda*). Three locally optimized characters were evaluated in all extinct Fraterculinae. The deltopectoral crest of Fraterculinae transitions to the shaft of the humerus more abruptly (108:1) than the more smoothly transitioning deltopectoral crest of many Alcinae (e.g., *Alca torda*). The bicipital crest meets the shaft at an angle approaching 90° (111:1) in all Fraterculinae except *Aethia cristatella* and *Aethia psittacula*, in which the bicipital crest contacts the humeral shaft at a more obtuse angle as in most Alcinae (e.g., *Synthliboramphus antiquus*; see Fig. 7.13). A small scar corresponding to the attachment point of m. pronator sublimis is located ventrally to the most proximal extension of the ventral supracondylar tubercle on the distal humerus of all Fraterculinae except *Aethia pygmaea* and *Aethia barnesi*, in which the m. pronator sublimis scar is located just proximal to the ventral supracondylar tubercle as in many Alcinae (e.g., *Brachyramphus perdix*; 164:0). The proximal margin of the intermetacarpal spatium is distal to the distal margin of metacarpal I in Fraterculinae (192:0). The renal depression of Fraterculinae is



relatively broader than in many other charadriiforms (i.e., *Synthliboramphus antiquus*; 202:0).

Fraterculini (contents include *Fratercula* and *Cerorhinca*) monophyly is supported by five apomorphies with a CI = 1.0 (Table 8.8). Two of those apomorphies (295:1; 296:1) are myological characters that could not be evaluated in extinct Fraterculini species. Although the sclerotic ring is not known for any extinct Fraterculini, its shape in all extant species of the clade varies from that of all other Charadriiformes. The sclerotic ring of Fraterculini is mediolaterally broader and has a relatively smaller corneal aperture (i.e., anteroposteriorly broader) than the more narrow sclerotic rings of other charadriiforms (30:1). This feature was first described and figured by Shufeldt (1889, Figure 15) and was subsequently scored for phylogenetic analysis and figured by Strauch (1985, Figure 4, character 7). Broader sclerotic rings were hypothesized to be associated with diving by Curtis and Miller (1938). Those authors proposed that this characteristic is an adaptation to deal with the greater pressures exerted on the eyes of diving species while underwater. However, positive correlation between this feature and dive depth is not supported by current data which indicate that the dive depth of puffins (20-50m) is on average more shallow than murrelets (50-210m) and razorbills (1-180m) that display the sclerotic rings typical of other charadriiforms (Piatt and Nettleship, 1985; Croll et al., 1992; Table 8.9; Fig. 8.13). Among Aethiini, the sister taxon to Fraterculini, *Ptychoramphus aleuticus* has been recorded to dive to depths of up to 80m (del Hoyo et al., 1996), but also does not display the broader sclerotic rings of puffins.

Table 8.9- Mass, dive depth, and feeding ecology of extant charadriiforms. Body mass and dive depths from Piatt and Nettleship (1985), del Hoyo et al., (1996), Croll et al., (1992), and Hedd et al., 2009. Estimated mass for *Pinguinus impennis* from Livezey (1988).

Taxa	Avg. mass (g)	Est. dive depth (m)	Feeding Ecology
<i>Aethia cristatella</i>	260	30	Wing-propelled diver
<i>Aethia psittacula</i>	297	30	Wing-propelled diver
<i>Aethia pusilla</i>	85	15-25	Wing-propelled diver
<i>Aethia pygmaea</i>	99-136	?	Wing-propelled diver
<i>Ptychoramphus aleuticus</i>	150-200	20-80	Wing-propelled diver
<i>Fratercula arctica</i>	460	20	Wing-propelled diver
<i>Fratercula cirrhata</i>	773	40-50	Wing-propelled diver
<i>Fratercula corniculata</i>	612	40	Wing-propelled diver
<i>Cerorhinca monocerata</i>	533	30-40	Wing-propelled diver
<i>Pinguinus impennis</i>	~5000	?	Wing-propelled diver
<i>Alca torda</i>	524-890	10-180	Wing-propelled diver
<i>Alle alle</i>	140-192	30	Wing-propelled diver
<i>Uria aalge</i>	~940	60-150	Wing-propelled diver
<i>Uria lomvia</i>	810-1080	50-210	Wing-propelled diver
<i>Cepphus carbo</i>	490	15-20	Wing-propelled diver
<i>Cepphus columba</i>	450-550	10-20	Wing-propelled diver
<i>Cepphus grylle</i>	450-550	~20	Wing-propelled diver
<i>Synthliboramphus antiquus</i>	177-249	10-20	Wing-propelled diver
<i>Synthliboramphus craveri</i>	128-149	?	Wing-propelled diver
<i>Synthliboramphus hypoleucus</i>	148-167	?	Wing-propelled diver
<i>Synthliboramphus wumizusume</i>	183	10-20	Wing-propelled diver
<i>Brachyramphus brevirostris</i>	224	?	Wing-propelled diver
<i>Brachyramphus marmoratus</i>	196-269	30	Wing-propelled diver
<i>Brachyramphus perdix</i>	?	?	Wing-propelled diver
<i>Stercorarius longicaudus</i>	250350	n/a	Generalist
<i>Stercorarius skua</i>	1100-1700	n/a	Generalist
<i>Anous tenuirostris</i>	97-120	n/a	Surface skimming
<i>Chidonias leucoptera</i>	42-79	n/a	Surface sk. / Terrestrial
<i>Gygis alba</i>	92-139	<1	Plunge diver
<i>Sterna anaethetus</i>	95-150	< 1	Plunge diver / surface sk.
<i>Sterna maxima</i>	320-500	?	Plunge diver / surface sk.
<i>Sterna nilotica</i>	130-300	n/a	Terrestrial
<i>Sternula supercilialis</i>	40-57	<1	Plunge diver
<i>Phaetusa simplex</i>	208-247	<1	Plunge diver / surface sk.
<i>Larosterna inca</i>	180-210	<1	Plunge diver / surface sk.
<i>Pagophila eburnea</i>	520-700	n/a	Surface skimmer
<i>Rynchops niger</i>	232-374	n/a	Surface skimmer
<i>Creagrus furcatus</i>	610-780	n/a	Surface skimmer
<i>Larus argentatus</i>	720-1500	n/a	Generalist
<i>Larus marinus</i>	1435-2272	n/a	Generalist
<i>Rhodostethia rosea</i>	120-250	n/a	Surface skimmer
<i>Rissa tridactyla</i>	305-512	<1	Plunge diver / surface sk.
<i>Xema sabini</i>	135-225	n/a	Surface sk. / Terrestrial
<i>Rhinoptilus chalcopterus</i>	117-172	n/a	Terrestrial

Table 8.9- (continued from previous page) Mass, dive depth, and feeding ecology for extant charadriiforms. Body masses and dive depths from Piatt and Nettleship (1985), del Hoyo et al., (1996), and Croll et al., (1992).

Taxa	Avg. mass (g)	Est. dive depth (m)	Feeding Ecology
<i>Tryngites subruficollis</i>	48-117	n/a	Terrestrial
<i>Stiltia isabella</i>	65	n/a	Terrestrial
<i>Cursorius temminckii</i>	64-80	n/a	Terrestrial
<i>Glareola maldivarum</i>	87	n/a	Terrestrial
<i>Bartramia longicauda</i>	98-226	n/a	Terrestrial
<i>Hydrophasianus chirurgis</i>	126-231	n/a	~Terrestrial
<i>Numenius minutus</i>	118-121	n/a	Terrestrial
<i>Charadrius wilsonia</i>	55	n/a	Terrestrial
<i>Charadrius vociferous</i>	72-93	n/a	Terrestrial

Other apomorphies of Fraterculini also included the contact of the mandibular rami posterior to the mandibular symphysis (41:1). The distinctive beak of puffins is rather broad near its suture with the nasals but dorsoventrally compressed rostrally. The relative length of the mandibular symphysis is longer in puffins (40:1) than in some alcids (e.g., *Aethia pygmaea*). Although not fused, the mandibular rami of puffins do remain in contact posterior to the mandibular symphysis.

The m. supracoracoideus of puffins is relatively larger than that of non-diving charadriiforms (Kovacs and Meyers, 2000). However, comparisons between the relative size of the m. supracoracoideus in puffins and other alcids are not known. The m. supracoracoideus scar on the proximal humerus of puffins is relatively deeper than in all other sampled charadriiforms (115:0). This may be indicative of a relatively larger m. supracoracoideus muscle body and stronger dependence on a powered upstroke. Although puffins do not dive as deeply as some other alcids (Table 8.9; Fig. 8.13), puffins have been noted to traverse longer underwater distances than some other

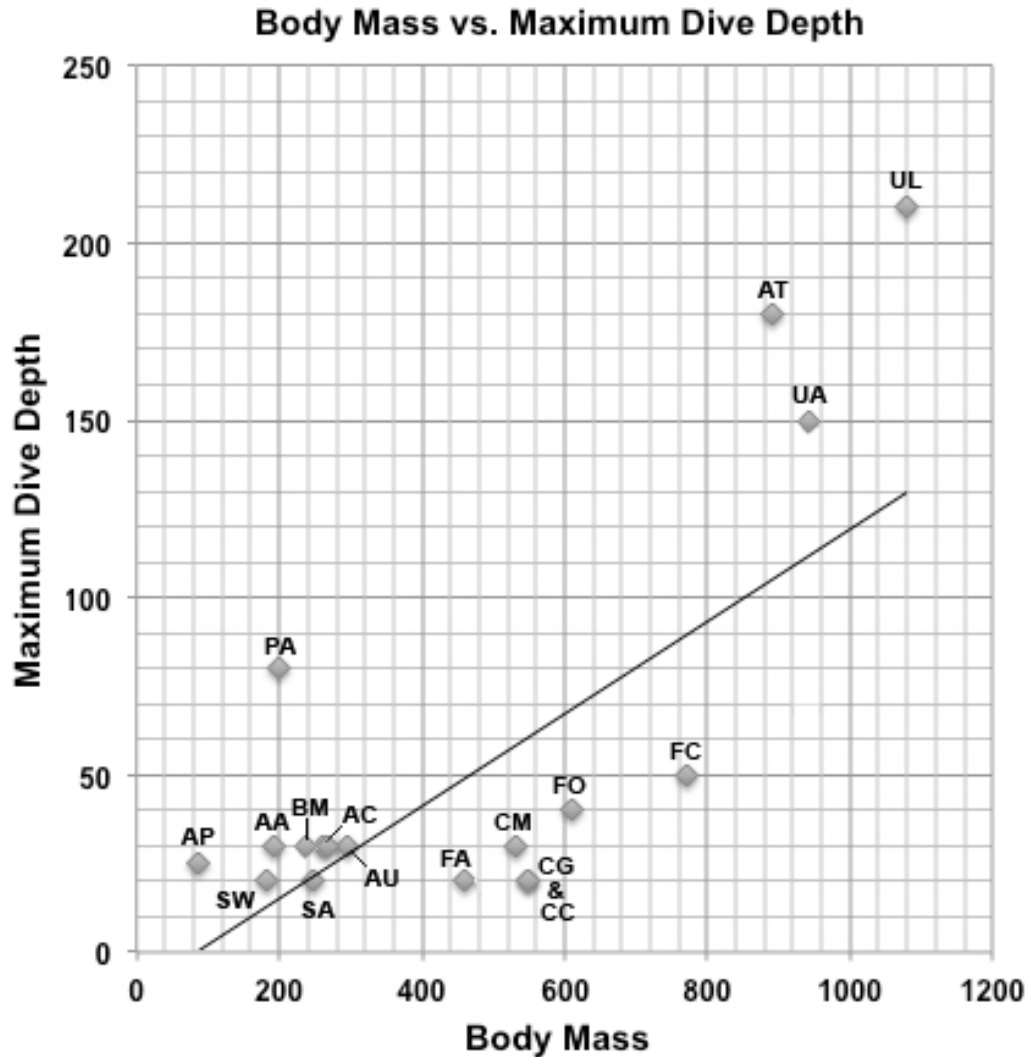


Figure 8.13- Positive relationship between maximum body mass and estimated maximum dive depth for extant alcids (data from Table 8.9). Taxon abbreviations: *Aethia cristatella* (AC), *Aethia psittacula* (AP), *Aethia pusilla* (AU), *Ptychoramphus aleuticus* (PA), *Fratercula arctica* (FA), *Fratercula cirrhata* (FC), *Fratercula corniculata* (FO), *Cerorhinca monocerata* (CM), *Alca torda* (AT), *Alle alle* (AA), *Uria aalge* (UA), *Uria lomvia* (UL), *Cepphus carbo* (CC), *Cepphus columba* (CO), *Cepphus grylle* (CG), *Synthliboramphus antiquus* (SA), *Synthliboramphus wumizusume* (SW), *Brachyramphus marmoratus* (BM). *Aethia pygmaea*, *Pinguinus impennis*, *Synthliboramphus craveri*, *Synthliboramphus hypoleucus*, *Brachyramphus brevirostris*, and *Brachyramphus perdix* were not included owing to missing data. Note that the moderately sized, shallow diving guillemots and puffins group together below the best-fit line and that *Cepphus columba* (CO) and *Cepphus grylle* (CG) are represented by a single data point because values for these two species are identical.

alcids (Duffy et al., 1987; Watanuki et al., 2006).

Another locally optimized apomorphy of Fraterculini is the presence of an m. supracoracoideus nerve foramen of the procoracoid process of the coracoid (93:1). This foramen is also present in most Alcinae, but is absent in *Alle alle*, and in species of *Brachyramphus*, Mancallinae, and Aethiini for which the coracoid is known (Fig. 8.12). The coracoids of Mancallinae (sister taxon to Alcidae) lack an m. supracoracoideus nerve foramen of the procoracoid process of the coracoid, whereas this foramen is present in the coracoids of Stercorariidae (sister taxon to Pan-Alcidae). Therefore, optimization of the ancestral state of this character for Pan-Alcidae is ambiguous (Fig. 8.12). Because this foramen is absent in all of the smaller sized alcids except *Synthliboramphus* (i.e., Aethiini, *Brachyramphus*, and *Alle alle*), it is possible that there is some link between small size (i.e., body mass) and the potential loss of this foramen. The only relatively large alcids that lack this feature are the Mancallinae. In comparison with other alcids in which the m. supracoracoideus nerve foramen is positioned more distally/omally near center of the procoracoid process, in the intermediately sized *Cepphus* (Table 8.9) this foramen is positioned so proximally/sternally that only a thin strut of bone borders the foramen (94:1). Perhaps the condition in *Cepphus* represents an intermediate stage in the loss of this foramen. Fossil coracoids of *Cepphus* that might provide insight regarding this hypothesis are not currently known. The maximum dive depth of guillemots is shallower than other similarly sized alcids such as *Cerorhinca monocerata* (Table 8.9; Figure 8.13). Perhaps a decreased dependence on an underwater powered upstroke or a difference in feeding strategy (i.e., feeding in the water column versus feeding along the

ocean floor) is affecting a change in the m. supracoracoideus that is reflected by the osteological changes documented in the m. supracoracoideus nerve foramen of the procoracoid process of the coracoid.

Alcini (contents include *Alca*, *Pinguinus*, *Alle*, *Miocepphus*, *Uria*) monophyly is supported by four apomorphies (i.e., unambiguously optimized morphological characters with a CI = 1.0; Table 8.8). Two of those apomorphies and an additional locally optimized apomorphy (248:1), were integumentary (246:1) or myological (283:1) and could not be evaluated in extinct Alcini species. The anterior faces of the furcular rami are smooth rather than grooved (74:0) in Alcini. However, this character could not be assessed in *Alca ausonia*, *Alca stewarti*, *Alca grandis*, *Alca minor*, *Miocepphus mcclungi*, *Miocepphus blowi*, *Miocepphus mergulellus*, or *Pinguinus alfrednewtoni* because furculae are not known for those taxa and the anterior face of the furcular rami is not exposed in *Uria brodkorbi* (see Fig. 2.17). The first metacarpal of Alcini is anteriorly flattened (i.e., extensor process absent; 191:1; see Fig. 3.17) in Alcini. However, this character could not be assessed in *Alca ausonia*, *Alca stewarti*, *Alca grandis*, *Alca minor*, *Alca olsoni*, *Miocepphus mcclungi*, *Miocepphus bohaski*, *Miocepphus mergulellus*, or *Pinguinus alfrednewtoni* because carpometacarpi are not known for those taxa. Alcini monophyly is also supported by six additional locally optimized apomorphies including a dorsally deflected anterior tip of the vomer (16:2; straight or indented in other Alcidae), the presence of heavily ossified orbital rims lateral to the nasal salt gland fossae (21:1), and lack of a fenestra in the portion of the mesethmoid that extends into the nasal capsule (24:1). These cranial characters could only be assessed in *Miocepphus blowi* and

*Pinguinus impennis* because skulls are largely unknown for other extinct Alcini. The incomplete preservation of partial skulls referred to *Alca* (see Fig. 2.7) prevented assessment of these cranial characters in those specimens. The excavation of the anterolateral face of the sternal end of the coracoid is extended sternally (100:0) in Alcini, rather than restricted by a bony ridge that forms the sternal margin of the anterior face of the sternal end of the coracoid, This character could not be evaluated in *Uria brodkorbi* because that surface of the coracoid is not exposed in the only known specimen. The coracoids of *Miocepphus mcclungi*, *Miocepphus blowi*, *Miocepphus mergulellus*, *Alca ausonia*, and *Alca minor* are not known.

The monophyly of Cepphini is supported by nine locally optimized humeral apomorphies (Table 8.8). All of these characters could be evaluated for extinct taxa because all known extinct Cepphini are known from humeri. Cepphini are characterized by an abrupt rather than gradual transition of the deltopectoral crest to the humeral shaft (108:1); m. coracobrachialis impression that is deeper (110:1) than in some alcids (e.g., *Alca torda*); a notch rather than a smooth or curved transition at the junction of the bicipital crest and the humeral shaft (112:1); m. coracobrachialis nerve sulcus curved ventrally rather than dorsally (114:1); m. supracoracoideus scar separated from the secondary pneumotricipital fossa by a flat space as in *Cerorhinca monocerata* (117:1); m. subcoracoideus scar located medially rather than ventrally as in *Pinguinus impennis* (127:0); m. subcoracoideus scar deeper than in many alcids (128:1; e.g., *Alle alle*); in anterodorsal view the scar of m. latissimus dorsi curves dorsally across the shaft of the humerus rather than extending distally in a relatively straight line as in *Uria aalge*

(139:1); the shaft of the humerus is less dorsoventrally compressed than in all other alcids (145:1; see Chapter 6 for further discussion of this character).

**Divergence estimation results:** Based on the resulting data from the divergence time analysis (evaluated in Tracer v1.5) the first 5000 of the 25000 retained trees were discarded as burn-in. The topology of the resultant maximum clade credibility tree (Fig. 8.14) is largely congruent with previous analyses of extant charadriiform relationships (see Chapter 1). Node support was high with 37 of 51 nodes receiving a Bayesian posterior probability of 1.0 (Fig. 8.14). The basal divergence of the charadriiform crown clade was estimated to have occurred in the Early Eocene (53.6 Ma; Figure 8.15; Table 8.10). An additional analysis in which an age of 47.0 Ma was used as the minimum age constraint on the basal divergence among crown Charadriiformes (see Mayr, 2000) rather than the 40.4 Ma date based on *Jiliniornis huadianensis* did not result in a significantly older age for this node (54.44 Ma). Contrary to previous divergence estimates for Charadriiformes (Table 8.3), no divergence dates or associated confidence intervals extended into the Cretaceous. The divergence between Alcidae and its sister taxon the Stercorariidae was estimated to have occurred in the Late Eocene (38.3 Ma; Figure 8.15; Table 8.10) and does not support a Paleocene origin of Alcidae as inferred by Pereira and Baker (2008). The basal divergence among crown Alcidae (i.e., the split between Alcinae and Fraterculinae) is estimated at 33.83 Ma (Early Oligocene). Estimated ages for all recovered nodes and the error associated with each estimate are provided in Table 8.10. The estimated potential range of error in the age estimates (i.e., the 95% Highest Posterior Density) is generally higher (i.e., a broader range of inferred dates) for more



basal nodes (Fig. 8.15). For example, the HPD for the basal split among crown Charadriiformes (i.e., the split between Charadrii and the Scolopaci + Lari clade) spans 15.71 Ma from 45.86 - 61.57 Ma, whereas the HPD of sister taxa *Fratercula arctica* and *Fratercula corniculata* spans only 1.87 Ma from 4.45 - 6.32 Ma (Table 8.10).

Figure 8.14- Bayesian topology estimated for extant taxa by BEAST (Drummond et al., 2010) with posterior probabilities for clades displayed to the right of nodes. The twelve nodes that were assigned a lognormal age distribution using fossil data are marked with a star and the priors (i.e., ages in Ma) assigned to nodes are displayed to the left of the stars.

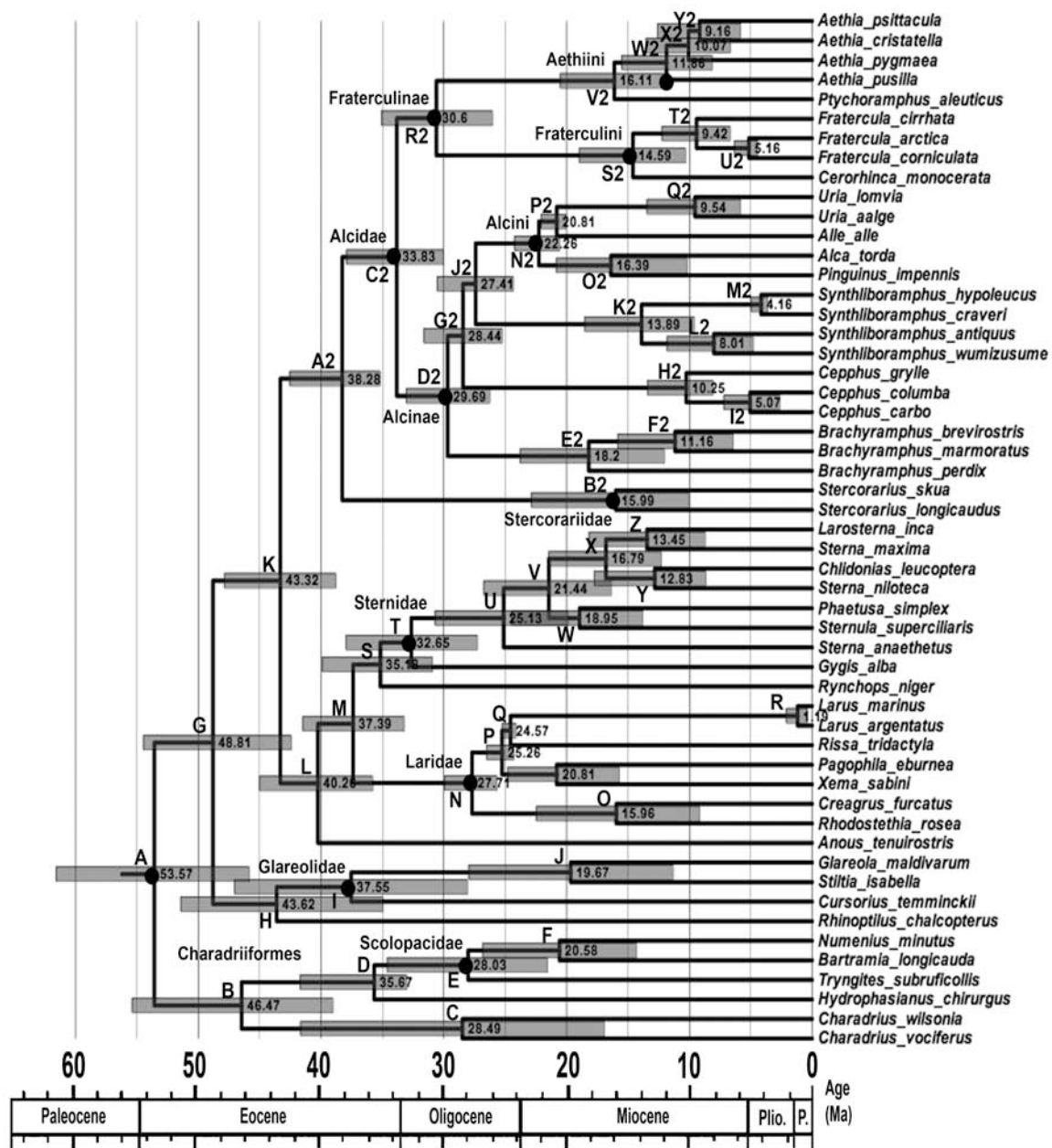


Figure 8.15- Chronogram of charadriiform relationships with estimated divergence times and associated error bars (95% Highest Posterior Density). Letters next to nodes correspond to nodes listed in Table 8.10.

Table 8.10- Estimated divergence times, 95% posterior density (HPD; error bars), prior ages based on fossil data (i.e., minimum age constraints), and posterior probabilities for each node recovered.

Node	Mean Age (Ma)	95% HPD (Ma)	Prior (Ma)	Posterior Probability
A	53.57	45.86 - 61.57	40.4	1.0
B	46.47	39.04 - 55.37	—	0.91
C	28.49	16.91 - 41.67	—	1.0
D	35.67	33.02 - 41.7	33.0	1.0
E	28.03	21.56 - 34.60	—	1.0
F	20.58	14.33 - 26.83	—	1.0
G	48.81	42.43 - 54.45	—	0.79
H	43.62	34.99 - 51.42	—	0.98
I	37.55	28.07 - 47.04	—	1.0
J	19.67	11.34 - 27.96	—	1.0
K	43.32	38.79 - 47.89	—	1.0
L	40.26	35.80 - 45.81	—	0.99
M	37.39	33.23 - 41.48	—	0.96
N	27.71	25.68 - 29.94	—	1.0
O	15.96	9.16 - 22.46	—	1.0
P	25.26	24.30 - 26.52	—	1.0
Q	24.57	24.12 - 25.23	24.1	1.0
R	1.19	0.38 - 2.10	—	1.0
S	35.18	30.93 - 40.89	—	0.62
T	32.65	27.28 - 37.96	—	1.0
U	25.13	19.89 - 30.74	—	1.0
V	21.44	16.37 - 26.74	—	1.0
W	18.95	13.78 - 24.48	—	0.81
X	16.79	12.28 - 21.45	—	1.0
Y	12.83	8.67 - 17.75	—	0.62
Z	13.45	8.71 - 18.18	—	0.78
A2	38.28	35.18 - 42.55	35.1	1.0
B2	15.99	10.05 - 22.86	—	1.0
C2	33.83	30.0 - 37.93	—	1.0
D2	29.69	26.25 - 33.06	—	1.0
E2	18.20	12.04 - 23.78	—	1.0
F2	11.16	6.45 - 15.84	3.6	1.0
G2	28.44	25.24 - 31.62	—	0.89
H2	10.25	8.08 - 13.42	8.0	1.0
I2	5.07	2.65 - 7.19	—	1.0
J2	27.41	24.34 - 30.54	—	0.93
K2	13.89	9.62 - 18.51	—	1.0
L2	8.01	4.80 - 1.82	—	1.0

Table 8.10- (continued from previous page) Estimated divergence times, 95% posterior density (HPD; error bars), prior ages based on fossil data, and posterior probabilities for each node recovered.

Node	Mean Age (Ma)	95% HPD (Ma)	Prior (Ma)	Posterior Probability
M2	4.16	3.63 - 4.97	3.6	1.0
N2	22.26	20.58 - 24.23	—	1.0
O2	16.39	10.18 - 20.83	10.0	1.0
P2	20.81	20.04 - 22.07	20.0	1.0
Q2	9.54	5.82 - 13.46	—	1.0
R2	30.6	26.04 - 35.08	6.7	1.0
S2	14.59	10.31 - 18.97	4.4	1.0
T2	9.42	6.68 - 12.23	—	1.0
U2	5.16	4.45 - 6.32	4.4	1.0
V2	16.11	11.64 - 20.52	—	1.0
W2	11.86	8.13 - 15.51	—	1.0
X2	10.07	6.66 - 13.53	—	0.99
Y2	9.16	5.84 - 12.58	—	0.91

## DISCUSSION

***Phylogeny of Pan-Alcidae:*** The phylogenetic hypothesis resulting from the final combined analyses (Figs. 8.8, 8.10) represents the most inclusive hypothesis of alcid relationships to date and provides an example of how taxon sampling and phylogenetic estimation methods can affect resulting systematic hypotheses. The placement recovered for several alcid taxa in the final combined analysis topology contrasts with the placement of those taxa in previous analyses that were limited to extant taxa (e.g., Chapter 1; Pereira and Baker, 2008), analyses that were limited to closely related extant and extinct taxa (Chapters 2-7), or analyses that included a limited sampling of outgroup taxa (see Chapters 2-7; Chandler, 1990a; Pereira and Baker, 2008). Additionally, as

shown in Chapter 1 and also evident in the results of the divergence estimation analysis, Bayesian (i.e., MrBayes and BEAST) and parsimony-based estimation methods frequently recover different topologies in analyses of the same data. For example, despite dense taxon sampling (i.e., the inclusion of fossils) and a wide range of character sampling (i.e., multiple types of morphological data and 8 genes), the relative positions of *Cepphus*, *Synthliboramphus*, and *Brachyramphus* within Alcinae are not strongly supported. However, Fraterculinae, Aethiini, Fraterculini, Alcinae and Alcini have nearly always been recovered as monophyletic and the positions of these taxa are consistent between analyses presented herein.

The inclusion of SDSNH 25358 and its effect on the placement of Mancallinae is a good example of how taxon inclusion can affect the results of phylogenetic analyses. Exclusion of SDSNH 25358 results in the previously recovered position for Mancallinae as the sister taxon to all other Pan-Alcidae (Fig. 8.8; Chandler, 1990a; Smith 2011). The possibility that Mancallinae might be either the sister to Alcinae or the sister to Fraterculinae was raised in Chapter 3 owing to the relatively small number ( $n = 2$ ) of additional steps that would be required to achieve these alternative placements. It is, however, somewhat surprising that the inclusion of a single taxon known only from a distal humerus scored for only 20 characters would have this result. However, as stated in Chapter 5, the systematic position of SDSNH 25358 remains uncertain until it can be compared to a broader taxonomic sample of non-alcid charadriiforms.

Other topological results of note include the placement of *Alle alle* as the sister taxon to *Miocepphus mergulellus* and nested within a clade otherwise composed of

*Miocepphus* species. Although this placement for *Alle alle* is congruent with the previous placement of this taxon as the sister to *Uria* (Thomas et al., 2004; Baker et al., 2007; Pereira and Baker, 2008), the hypothesis that *Alle* is the sole survivor of a Miocene Alcini lineage that was once more diverse has some explanatory power with regards to the many alternative placements of *Alle alle* in other previous phylogenetic analyses (Strauch, 1985; Chandler, 1990a; Moum et al., 1994, 2002; Chu, 1998; also see Chapters 1 & 2). *Alle alle* was placed as the sister to *Uria* in the results of the Bayesian combined analysis of extant taxa (Fig. 1.26) and was placed in an unresolved position at the base of Alcini in the results of the parsimony-based analysis of extant taxa (Fig. 1.25). The phylogenetic results from the analysis of Alcini relationships (Fig. 2.6) and the results of the final combined analysis (Fig. 8.8) both place *Alle alle* as the sister taxon to *Miocepphus mergulellus*. Therefore, a strong case can be made for the inclusion of incomplete fossils in phylogenetic analyses and their potential effect on the interpretation of the placement of extant taxa such as *Alle alle*. Although the inclusion of extinct taxa such as *Miocepphus mergulellus* did not have a marked effect on the systematic position recovered for *Alle alle* (i.e., *Alle alle* is still recovered in a clade that is the sister to *Uria*), the implications of *Alle alle* being placed as part of an otherwise extinct lineage are key to developing a more nuanced understanding of the differences between *Alle alle* and other extant alcids.

Although the position of Cepphini (contents include *Cepphus* and *Pseudocepphus*) was unresolved (i.e., in a polytomy with Alcini and *Synthliboramphus*) in the results of the phylogenetic analysis of Cepphini relationships outlined in Chapter 6,

and in the phylogenetic results of Chapter 5 (auklets), *Cepphini* was recovered as the sister taxon to *Alcini* in the results of the final combined analysis (Fig. 8.8). Additionally the three extant species of *Cepphus* were recovered as the sister taxon to *Alcini* in the results the phylogenetic hypotheses presented in Chapter 3 (Mancallinae), Chapter 7 (murrelets), and in the parsimony-based combined analysis of extant alcids presented in Chapter 1 (Fig. 1.25). Alternatively, the three extant species of *Cepphus* were recovered as the sister taxon to *Synthliboramphus* + *Alcini* in the Bayesian analysis of combined data for extant alcids in Chapter 1 (Fig. 1.26), and in both the Bayesian and parsimony-based topologies recovered in Chapter 4 (puffins).

The lack strong nodal support in the final combined Bayesian analysis and the variable results recovered elsewhere (Chapters 1-7) make it difficult to tease apart the relative contributions of taxon sampling and phylogenetic estimation method with respect to the ambiguity regarding the systematic position of *Cepphini*. However, the congruent results recovered in the parsimony and Bayesian analyses reported in Chapter 4 suggest that taxon sampling, and not phylogenetic estimator, may be responsible for the incongruence between hypotheses of the relationship of *Cepphini* and *Synthliboramphus* to other alcids. Therefore, the inclusion of extinct *Cepphini* species may be responsible for the unresolved placement of *Cepphini* in the results of the phylogenetic analysis discussed in Chapter 6 and the alternative placement of *Cepphini* as the sister taxon to *Alcini* in the results of the final combined analysis.

The final combined parsimony-based phylogenetic analysis recovered *Brachyramphus* as the sister taxon to all other Alcinae (Fig. 8.8) with *Synthliboramphus*

in a more derived position relative to *Brachyramphus* as the sister taxon to Cepphini + Alcini. This combination of relationships is a novel result. Although *Brachyramphus* or *Synthliboramphus* were alternatively recovered as the sister taxon to all other Alcinae (contents of Alcinae include *Alca*, *Pinguinus*, *Alle*, *Miocepheus*, *Uria*, *Cepphus*, *Pseudocepheus*, *Synthliboramphus*, *Brachyramphus*) in the results of Pereira and Baker (2008), *Synthliboramphus* has also been recovered as the sister taxon to Alcini in four previously published analyses (Friesen et al., 1996; Thomas et al., 2004; Baker et al., 2007; Pereira and Baker 2008). All four of those previous phylogenetic analyses included only molecular sequence data for extant species. *Synthliboramphus* was also recovered as the sister taxon to Alcini in the Bayesian analysis of combined data for extant alcids in Chapter 1 (Fig. 1.26) and in both the Bayesian and parsimony-based topologies recovered in Chapter 4 (puffins). However, as mentioned above, *Cepphus* was recovered as the sister taxon to Alcini more frequently (Chapter 1 parsimony and Chapters 3 & 7).

The hypothesis of extant charadriiform relationships estimated with MrBayes v3.1.2 (Ronquist and Huelsenbeck, 2003; Fig. 1.22) differed from that recovered for extant taxa using BEAST V1.6.1 (Drummond et al., 2010; Fig. 8.14). Although these two phylogenetic estimators both utilize a Bayesian MCMC approach to estimating phylogeny, there are differences in the way these programs are parameterized (e.g., branch lengths, inclusion of rate priors from fossils, shape parameters on rates; Drummond et al., 2006). The relaxed-clock models implemented in BEAST are arguably “both more accurate and more precise at estimating phylogenetic relationships than the unrooted methods implemented in MrBayes” (Drummond et al., 2006:706).



Although relationships in Alcidae were completely congruent between results of MrBayes (Fig. 1.22) and BEAST (Fig. 8.14), outgroup charadriiform relationships differed in the relative positions of eight species. Six of the eight topological differences include relative positions of species in Sternidae. Additional topological differences include the placement of *Rynchops niger* as the sister taxon to Laridae in the results from BEAST (Fig. 8.14) rather than the sister taxon to Sternidae as in the results from MrBayes (Fig. 1.22), and the position of *Rissa tridactyla* with respect to other Laridae. Sternidae interrelationships and the systematic position of skimmers (e.g., *Rynchops niger*) remain contentious issues in charadriiform systematics (Bridge et al., 2005; Baker et al., 2007; Smith, 2011; also see Chapter 3).

The topology recovered using BEAST is largely congruent with the most recent and most inclusive (with respect to taxon and DNA sampling) molecular-based analyses of charadriiform relationships by Baker et al. (2007). Both analyses recover Charadrii as the sister taxon to a Scolopaci + Lari clade. In contrast, a recent morphology-based phylogenetic analysis of Charadriiformes by Mayr (2011) recovered Scolopaci as the sister taxon to a Lari + Charadrii clade. Although the phylogenetic analysis of Livezey (2009, 2010) included 1024 morphological characters scored for 242 charadriiform species, that analysis did not recover monophyly of Charadrii, Scolopaci, or Lari as defined in the results of other previous analyses (Chu, 1995; Paton et al., 2003; Baker et al., 2007; Mayr, 2011; Smith, 2011).

The role of increased taxon sampling through inclusion of extinct taxa and the impact of increased character sampling through the inclusion of morphological characters

with respect to the topology recovered in the final combined analysis is difficult to assess. However, in comparison with previous analyses that were limited to molecular sequence data for extant taxa (Friesen et al., 1996; Thomas et al., 2004; Baker et al., 2007; Pereira and Baker 2008), the results of the final combined analysis are based upon a larger molecular set of data (11601 bp's including gaps versus largest previous molecular matrix 7,403 bp's, Pereira and Baker, 2008) and a larger total set of data (11954 characters including morphological data) scored for more taxa (81 taxa versus 30 charadriiform taxa sampled by Pereira and Baker, 2008). Previous morphology-based phylogenetic analyses of Alcidae, those of Strauch (1985) and Chandler (1990a) were limited to 33 and 106 characters respectively. Alcidae was included as a single, taxon-level terminal in the analysis of Livezey (2009, 2010) and Mayr (2011). Furthermore, simulations show that the combination of molecular and morphological data often provides a more accurate estimate of phylogeny (Wiens, 2009) and studies have shown that increased taxon and character sampling increases phylogenetic accuracy (Wheeler, 1992; Huelsenbeck et al., 1996; Zwickl and Hillis, 2002). Thus, the results of the combined analysis are arguably the most robust hypothesis of charadriiform relationships to date.

***Divergence time estimates and inferred relationships between paleoclimatic events and charadriiform evolution:*** Previous estimates of divergence times for Charadriiformes have recovered older dates for the basal split among crown Charadriiformes than the results presented here (Tables 8.3, 8.10). Only the results of Ericson et al. (2006), which used a different approach (Table 8.3) are similar to the dates

recovered herein. Baker et al. (2007) reported support for 14 charadriiform divergences prior to the Cretaceous-Tertiary boundary at ~65 Ma. Although Baker et al. (2007) calculated 95% confidence intervals (CI) for the age of divergences they did not represent those intervals of uncertainty on their chronogram, and the 95% CI of only six divergences are placed entirely within the Cretaceous (see Baker et al., 2007, supplemental material). The hypothesis that basal charadriiform lineages diverged between 79-102 Ma during the Late Cretaceous (i.e., Cenomanian-Turonian Stages) requires the inference of a ghost lineage (Norell, 1992) for Charadriiformes of at least 40 Ma based on the fossil record. Such an early origin for Charadriiformes would indicate that the clade was not recorded in the fossil record during approximately the first half of its existence. With the exception of the anseriform *Vegavis iaai* Clarke et al., 2005, Cretaceous records of neognathous birds consist primarily of isolated and fragmentary specimens that are of uncertain taxonomic affinity (Clarke et al., 2005; Mayr, 2009). Cretaceous records of birds are largely dominated by basal stem taxa and non-crown clade Ornithurines (Chiappe and Witmer, 2002; Clarke and Norell, 2002; Clarke, 2004). The lack of neoavian fossils from the Cretaceous and the derived position of Charadriiformes within Neoaves (Mayr and Clarke, 2003; Hackett et al., 2008) do not support an Early Cretaceous origin for Charadriiformes.

The ~54 Ma estimate of basal divergence among crown Charadriiformes resulting from the analysis reported herein is considerably more congruent with the fossil record of the clade (Fig. 8.15; Table 8.10) than previous estimates that placed this divergence in the Cretaceous (Table 8.3). The earliest supported crown charadriiform fossil is ~40 Ma

(Hou and Ericson, 2002). Thus, a ghost lineage of only ~14 Ma is inferred based upon the hypothesis presented herein. However, the caveat that a divergence analysis including outgroups to Charadriiformes might be more accurate should be considered.

The timing of the basal divergence of crown Charadriiformes is concurrent with the timing (~55 Ma, Ypresian) of the Early Eocene Climatic Optimum (EECO), during which sea surface temperatures have been estimated to be ~8-10°C warmer than today and sea levels may have been as high as 50 m above present levels (Zachos et al., 2001, 2003; Fig. 8.16). Reconstructions of continental positions during the Ypresian suggest that the northern Atlantic Ocean, northern Pacific Ocean, and Arctic Ocean basins would have been ice free with unrestricted circulation between the Atlantic and Pacific Oceans via the CAS (Scotese, 2004; Smith et al., 1994). However, circulation between the Arctic and Atlantic Oceans may have been restricted by the close proximity of Greenland and Europe to North America (Scotese, 2004; Smith et al., 1994). The EECO was characterized by an intense global, greenhouse-style warming event that has been proposed to be related to an increase in carbon that has been attributed to dissolution of oceanic methane hydrates (Zachos et al., 2001, 2003). This warm period in Earth history is hypothesized to have affected the distribution and diversity of marine (e.g., ostracods, foraminifera, diatoms, dinoflagellates) and terrestrial organisms (e.g., mammals, plants; Kelley et al., 1998; Thomas, 1998; Clyde and Gingerich, 1998; Wing et al., 2005). Although the exact effects of the EECO on early charadriiforms are unknown, warming and resulting ocean de-stratification resulted in a decrease in poleward circulation of bottom waters and an associated decrease in cold-water-related bioproductivity (Kennett

and Scott, 1991; Nunes and Norris, 2006) that might have negatively impacted seabird populations. What effect this change in climate may have had is unknown because the climatic conditions that were tolerated by Early Eocene charadriiforms are also unknown. Based on the divergence estimates, the initial radiation of early charadriiforms occurred despite a hypothesized decrease in ocean bioproductivity (Kennett and Scott, 1991; Nunes and Norris, 2006). However, whether early charadriiforms inhabited an oceanic niche is also unknown (see discussion below).

The divergence time analysis results dated the split between Alcidae and Stercorariidae at ~38 Ma during the Late Eocene (Figs. 8.15, 8.16; Table 8.10). This estimate is more congruent with the earliest fossil record of Pan-Alcidae at ~35 Ma. The divergence estimate by Pereira and Baker (2008) dated the basal divergence between Alcidae and Stercorariidae during the Paleocene at ~61 Ma. Because the oldest known pan-alcid fossil has been dated to ~35 Ma (Chandler and Parmley, 2002), Pereira and Baker's (2008) hypothesis requires the inference of a ~26 Ma ghost lineage for the clade.

In contrast to Eocene global ocean circulation patterns that were driven by formation of deep-water exclusively in the southern oceans, the Early Oligocene marked the onset of northern ocean deep-water production and a more modern bi-polar deep-water circulation regime, albeit in the absence of a true Gulf Stream (Via and Thomas, 2006). That the timing of this major reorganization of oceanic circulation patterns coincides with the hypothesized basal radiation in Alcidae is likely not coincidence. The cooling trend that began after the EECO continued into the Early Oligocene and was

associated with a drop in sea temperature of  $\sim 7^{\circ}\text{C}$  and a  $\sim 55$  m lowering of sea level compared to the earlier EECO (Zachos et al., 2001; Miller et al., 2005).

Well stratified oceans and the more complex ocean circulation patterns that characterized the pre-EECO oceans had returned by the Middle Eocene (Kennett and Scott, 1991; Zachos et al., 2001). By the Late Eocene ( $\sim 36$  Ma) the growing development of Antarctic ice sheets had changed coastlines worldwide by lowering sea level and would have resulted in ongoing geographic shifts in coastally nesting seabird communities. Hypotheses regarding the Eocene-Oligocene climate transition (EOCT) suggest a  $\sim 4^{\circ}\text{C}$  drop in average sea-surface temperatures, increased latitudinal thermal gradients, increased thermohaline circulation, and associated changes in sea chemistry (Miller et al., 2009). The EOCT was characterized by relatively rapid cooling that is proposed to have initiated biotic changes such as the decline of warm-adapted mammals and broad leaf forests in the terrestrial realm, and the appearance of baleen whales in the marine realm (Prothero and Berggren, 1992; Prothero, 1994). That early alcids were tolerant of a warmer climate than today is suggested by the presence of alcids in the Late Eocene of Georgia, USA (Chandler and Parmley, 2002). That alcids were able to tolerate the colder climatic conditions that followed is suggested by their survival through the Eocene-Oligocene climatic transition and to the present. Thus, the presence of alcids during these periods of different climatic regimes demonstrates that early alcids either had a broader range of environmental tolerance than that of extant alcids or that the tolerances of pan-alcids to differing climatic conditions have evolved along with the lineage.

The latitudinal range of extant alcids may be limited by their dependence on nutrient-rich, cold-water upwelling systems or the prey that are associated with those systems. Only four of the 23 extant alcid species have ranges that extend below the Tropic of Cancer (i.e., below 23.5° N latitude; Fig. 2.18). The ranges of *Cepphus carbo* and *Synthliboramphus antiquus* in the Western Pacific Ocean extend south to the Ryuku Islands, while the ranges of *Synthliboramphus hypoleucus* and *Synthliboramphus craveri* in the Eastern Pacific Ocean extend just south of the southern tip of Baja California (del Hoyo et al., 1996).

As a clade, extant alcids do not conform to Bergman's Rule (Bédard, 1985). However, examples of species (e.g., *Alle alle*, *Uria aalge*) with more northern populations that are statistically larger have been documented (Hipfner and Greenwood, 2008; Wojczulanis-Jakubas et al., 2010). More prevalent than a latitudinal trend of increasing north-south body mass in alcids is a longitudinal increase from west to east (Barret et al., 1997; Wojczulanis-Jakubas et al., 2010). There is no correlation between latitude and the distribution of small (<300g; e.g., *Aethia cristatella*), medium (300-800g; e.g., *Cepphus grylle*) and larger sized alcids (>800g; e.g., *Uria lomvia*; Table 8.9). Within these size-based categories, species are distributed throughout the latitudinal range of Alcidae. Even among clades such as *Aethia* that are distributed throughout the majority of the geographic range of Pacific Ocean endemic alcids, there is no positive relationship between body mass and latitude. *Aethia psittacula* is the largest auklet and is also the most widely distributed (del Hoyo et al., 1996; Table 8.9) and *Aethia pusilla* is the smallest auklet species but also has a range that extends further northward than any other

species of auklet. Other alcid clades with differently sized species have distributions that overlap one another (e.g., *Synthliboramphus*) or that are geographically separated along longitudinal oriented boundaries (e.g., *Cepphus*). Body mass in alcids appears to be correlated with other factors such as competition for nest sites and partitioning of prey resources at varying depths (Ainley et al., 1990a, 1990; Hipfner and Greenwood, 2008). Additional support for the lack of a link between body mass and latitude comes from a recent study that found no evidence of correlations between body mass and sea surface temperature or air temperature in populations of *Alle alle* (Wojczulanis-Jakubas et al., 2010).

The divergence estimation results suggest that the split between the two major alcid clades, Alcinae (auks, murre, murrelets, and guillemots) and Fraterculinae (auklets and puffins), took place close to the EOCT at ~34 Ma (Figs. 8.15, 8.16; Table 8.10). The hypothesized timing of this divergence is approximately concurrent with the documented drop in temperatures and initial formation of Antarctic ice sheets (Zachos et al., 2001; Liu et al., 2009). If Oligocene alcids were intolerant of warmer climates and dependent on cold-water upwelling systems as extant alcids are (Kitaysky and Golubova, 2000), then the cooling climate of the Oligocene may have played a role in the radiation and dispersal of pan-alcids.

Basal divergences in Fraterculinae (i.e., the split between Aethiini and Fraterculini) and in Alcinae (i.e., the split between *Brachyramphus* and other Alcinae) are estimated at ~30 Ma (Figs. 8.15, 8.16; Table 8.10), suggesting an approximately 4 Ma interval between the basal divergence among crown Alcidae and subsequent divergences



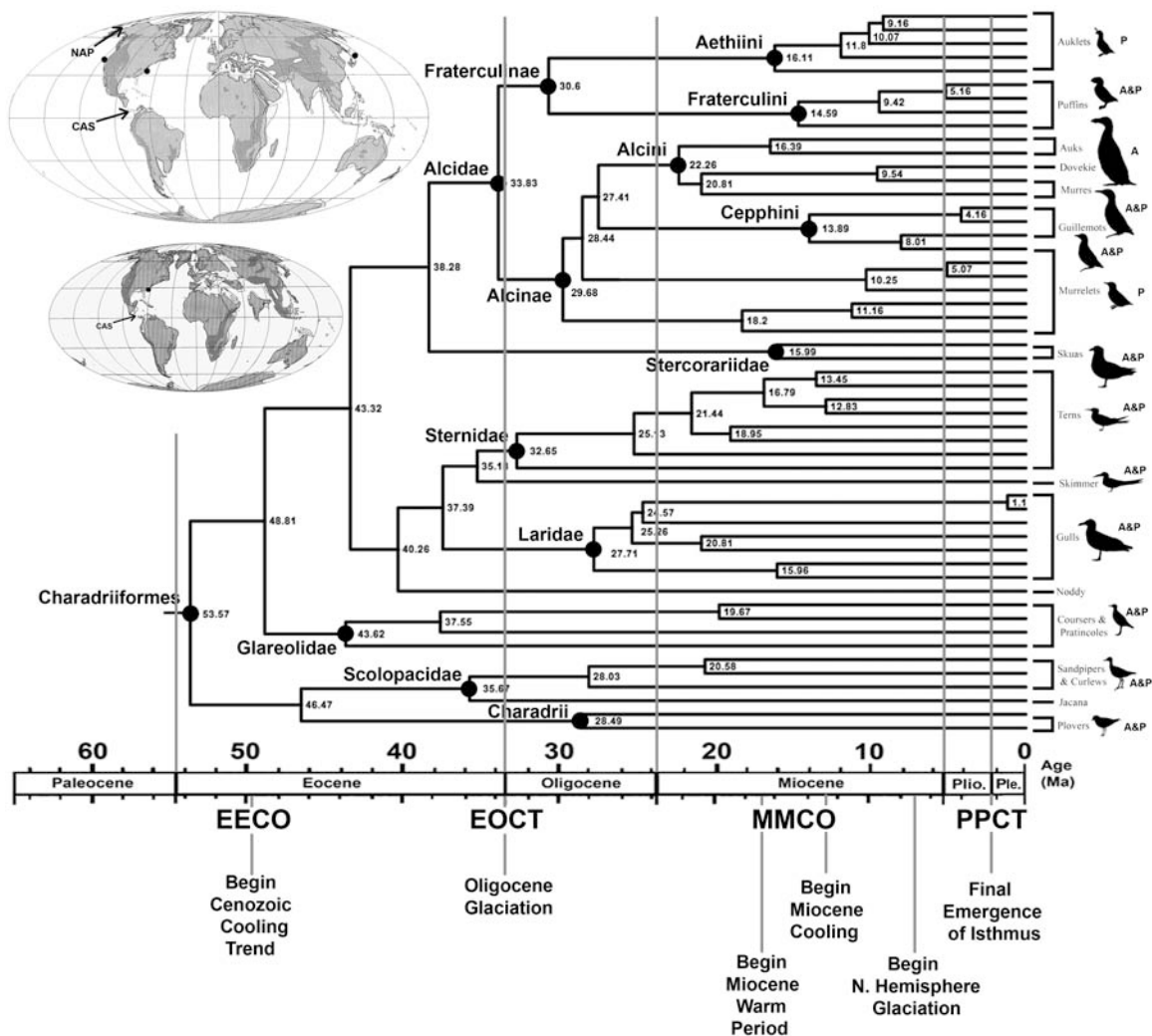


Figure 8.16- Comparison of divergence estimates for Charadriiformes with geologic epochs and major paleoclimatic events. Abbreviations: (**EECO**) Early Eocene Climatic Optimum; (**EOCT**) Eocene-Oligocene Climatic Transition; (**MMCO**) Middle Miocene Climatic Optimum; (**PPCT**) Pliocene-Pleistocene Climate Transition. Silhouettes representing charadriiform clades are labeled according to extant geographic distribution: (**A**) Atlantic; (**P**) Pacific. Upper map shows Middle Miocene (~10 Ma) continental reconstruction with Northern Atlantic Passage (**NAP**) and Central American Seaway (**CAS**) both open. Miocene alcid fossils have been found on the eastern and western coasts of North America and Japan (black dots). Lower map shows Late Eocene continental reconstruction with Northern Atlantic Passage (**NAP**) closed and the sole Eocene alcid fossil locality (maps modified from Smith et al., 1994).

among these sister clades. The drastic cooling that characterized the Eocene-Oligocene boundary was followed by partial recovery towards warmer temperatures, and subsequently, temperatures from ~32-26 Ma were relatively stable (Zachos et al., 2001). Continental positions were similar to those of today (Scotese, 2004; Smith et al., 1994) and the Northern Atlantic Passage (NAP) between the Atlantic Ocean, Pacific Ocean, and the CAS would likely have been open to dispersal for alcids and other seabirds. The results of the divergence analysis suggest that Oligocene climate stability coincided with further radiation of alcids. The long branches between basal divergence in Fraterculinae and estimated divergences among extant species of auklets and puffins is suggestive of an incomplete fossil record for this clade.

Three divergences in Alcinae and the 95% HPD of these divergences are estimated during the Oligocene (Figs. 8.15, 8.16; Table 8.10). These splits represent the basal divergences of *Brachyramphus*, *Synthliboramphus*, *Cepphus*, and Alcini, and are hypothesized to have taken place within ~3 Ma of one another (Fig. 8.15; not considering error bars). As discussed above, the systematic relationships recovered for these three clades in previous phylogenetic analyses have been quite variable. The relatively short time span between these divergences of alcid clades is less than the estimated divergences between extant taxa in some cases (see Fraterculini or Aethiini). If the *Brachyramphus*, *Synthliboramphus*, *Cepphus*, and Alcini lineages diverged relatively quickly and if extant species in these clades are recently diverged from one another, this might explain the difficulty in recovering strongly supported positions for the relationships between these clades in previous phylogenetic analyses. With the exception

of *Alle alle*, systematic relationships within these clades (e.g., among *Synthliboramphus* species) are relatively congruent between previous analyses and relatively strongly supported in the results of the final combined analysis (Fig. 8.8).

A comparison of cladogram fit to the age ranges of known fossil taxa indicates a minimum of eight divergences in Pan-Alcidae by ~20 Ma (Fig. 8.17). The pre-Miocene fossil record of Pan-Alcidae currently includes a single isolated distal humerus from the Late Eocene (Chandler and Parmley, 2002) and an unsubstantiated report of fragmentary alcid remains from the Early Oligocene (Ono and Hasegawa, 1991). However, the Miocene fossil record of Pan-Alcidae includes examples of every major lineage within the clade (Table 8.1). Although Oligocene fossil localities need to be targeted for collection of fossil pan-alcids, the presence of every major lineage of pan-alcid in the Middle to Late Miocene demonstrates that divergences between these lineages must have occurred earlier, and thus an initial diversification of Pan-Alcidae in the Oligocene is somewhat congruent with the fossil record. However, the possibility that alcid lineages diverged relatively quickly in the Early Miocene and that the results of the molecular-based analysis are an overestimation of divergence times cannot be ruled out.

With the exception of the basal divergences in the Eocene and Oligocene discussed above, all but four remaining charadriiform divergences and the associated 95% HPD are estimated to have occurred during the Miocene (~23-5 Ma; Figs. 8.15, 8.16; Table 8.10). Only divergences between extant sister taxa *Cepphus columba* and *Cepphus carbo* (~5 Ma), *Fratercula arctica* and *Fratercula corniculata* (~5 Ma), and *Larus marinus* and *Larus argentatus* (~1 Ma) were estimated to have occurred during the

Pliocene or Pleistocene. Therefore, hypotheses of recent divergences among alcids owing to orbitally-forced Pleistocene glaciation events (Moum et al., 1994; Pereira and Baker, 2008) are not supported by these results. Rather, the results of the divergence analysis suggest that extant alcid diversity is a function of a profound radiation during the Miocene and differential survivorship across the Pliocene-Pleistocene boundary. The hypothesis presented here, that extant alcid sister-species (e.g., *Uria aalge* and *Uria lomvia*) likely diverged from one another prior to the Pleistocene, is also congruent with the results of other studies of avian mitochondrial sequence divergence (Klicka and Zink, 1997, 1998; Avise and Walker, 1998; Zink et al., 2004). Although the use of a molecular clock to calculate divergence times in those previous studies has been questioned (Arbogast and Slowinsky, 1998), there is little support for an increased rate of divergence across Aves during the Pleistocene as compared to other time periods (Zink et al., 2004). Pliocene speciation among extant sister-species of alcids is supported by the results of the divergence estimation. Furthermore, in some instances the fossil record of Pan-Alcidae records divergences between sister-species in the Pliocene (e.g., *Fratercula arctica* and *Fratercula corniculata*; Olson and Rasmussen, 2001; Smith et al., 2007).

Whether number of divergences for a given period of time is calculated based on epochal boundaries (i.e., divergences estimated during the Paleocene) or using slices of time of equal length (i.e., 5 Ma periods), a Miocene radiation of Charadriiformes is evident. By adhering to epochal boundaries, numbers of estimated divergences (based on means from Fig. 8.16 and Table 8.10) are as follows: Paleocene = 0; Eocene = 12; Oligocene = 11; Miocene = 27; Pliocene = 1; Pleistocene = 1. More divergences are

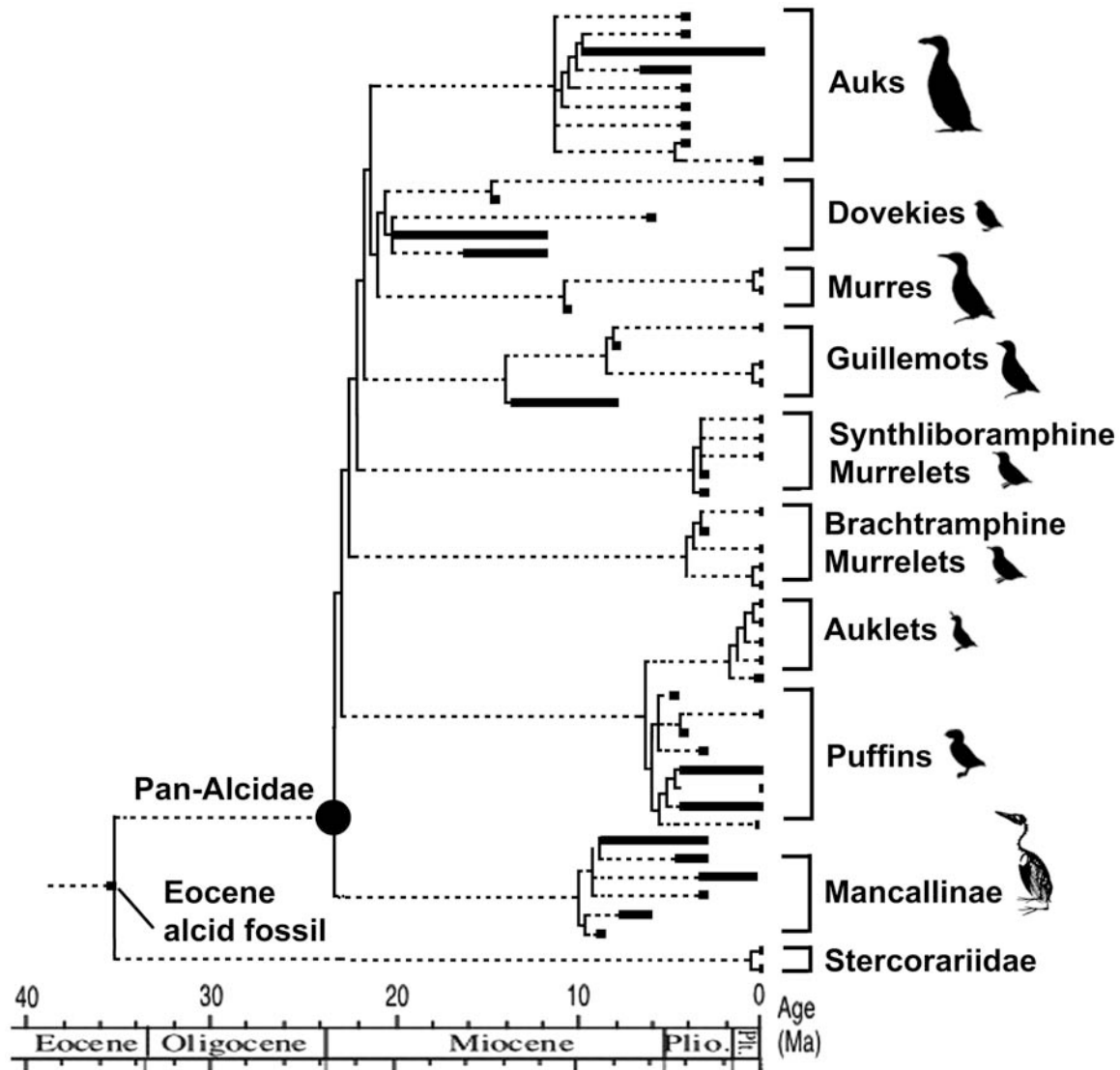


Figure 8.17- Minimum cladogram fit to the fossil record. Topology based on Figure 8.8 and age ranges taken from Table 8.1. Pleistocene occurrences of extant species represented by points at terminals.

estimated during the 17.7 Ma span of the Miocene than during the remaining 47.8 Ma of the Cenozoic (i.e., during the Paleocene, Eocene, Oligocene, Pliocene, and Pleistocene). Likewise, the density of divergences calculated using 5 Ma long slices of time (i.e., slightly longer duration than the MMCO;  $3 \pm 1$  Ma) reveals that the means of the posterior distribution of estimated node ages (Table 8.10) of more divergences correspond with the MMCO than any other period. Ten divergences are estimated between 18-13 Ma, a 20% increase over the preceding and following 5 Ma periods.

The Miocene fossil record of Pan-Alcidae (Table 8.1) and the results of the divergence estimation analysis (Figs. 8.15, 8.16) are congruent with an increase in alcid diversity during the Miocene. The MMCO lasted from ~17~14 Ma (Zachos et al., 2001). Fifteen divergences are estimated within the alcid crown clade during the Miocene and the 95% HPD of 8 of those divergences falls within the timespan of the MMCO (Fig. 8.16; Table 8.10). Among non-alcid charadriiforms half of the 26 divergences (considering the associated 95% HPD) occur in the Miocene, with 9 of those 13 divergences hypothesized among the close relatives of Alcidae, the Stercorariidae, Laridae, and Sternidae. Furthermore, the first marine records of Laridae also occur in the Miocene (~15 Ma; Warheit, 1992b). Many extant larids prey on alcids (Ainley et al., 1990b; Stempniewicz, 1994) and although there is currently no evidence to suggest that this ecological interaction dates back to the Miocene, the colonization of the marine realm by Laridae may have played some role in potential coevolution of these lineages.

The Middle Miocene Climatic Optimum (MMCO) was the warmest period in Earth history since the EECO and has been previously proposed as a factor in the

diversification of extant alcid lineages (Warheit, 1992b; Emslie, 1998; Smith et al., 2007; Smith, 2011). However, the contribution of factors other than those related to sea-surface temperature (e.g., biotic interactions or other geological processes) to alcid radiation during this time period may also be uncertain. As in extant alcids, fossils of Miocene pan-alcids are associated with deposits from cold water upwelling systems (Vedder, 1960; Kern and Wicander, 1974; Vedder, 1972; Ingle, 1979; Wagner et al., 2001; Ford and Golonka, 2003), suggesting that Miocene pan-alcids inhabited a similar ecospace as they do today. Just as cold-water upwelling is linked to productivity in modern seabird communities (Hyrenbach and Viet, 2003; Briggs et al., 1987) the Miocene radiations of alcids such as *Miocepphus* in the Atlantic Ocean and the appearance of *Miomancalla* in the Pacific Ocean coincides with the initial formation of the modern Arctic icecaps and initial shallowing of the CAS that resulted in steeper latitudinal thermal gradients in the Atlantic and Pacific Oceans (Butzin et al., 2011). This resulted in intensified gyral circulation of surface waters, and strengthened coastal and trade winds that promote upwelling (Ford and Golonka, 2003). The overall increase in upwelling strength that is associated with the Miocene development of basically modern ocean circulation patterns would presumably have been conducive to radiation of alcids and other seabirds that are ecologically linked with cold-water upwelling systems (Warheit, 1992b; Flowers and Kennett, 1994). Documented cooling during the Late Miocene and Early Pliocene (~14-3.6 Ma) has been correlated with the establishment of the California current system in the Pacific on which extant Pacific Ocean endemic alcids rely today (Zachos et al., 2008; Lariviere et al., 2009).

Although hypothesized temperatures during the MMCO (~17-14 Ma) were the highest since the EECO, temperatures rose during the late Oligocene and remained relatively stable throughout the Early and Middle Miocene (Zachos et al., 2001). The Early to Middle Miocene was a time of relative warmth, little or no glacial activity, and relatively unstratified oceans that was immediately followed by a cooling trend that has led to the lower temperatures, prevalent northern hemisphere glaciation, and temperature stratified oceans of today (Schoell et al., 1994; You et al., 2009; Westerhold et al., 2005).

The MMCO and the cooling trend that followed have been documented using a variety of methods including oxygen and carbon isotope stratigraphy, palynology, and magnetostratigraphy (Schoell et al., 1994; Krijgsman et al., 1994; You et al., 2009; Westerhold et al., 2005). Early and Middle Miocene sea temperatures were ~6 °C warmer than cooler Late Miocene and Pliocene temperatures that followed, and sea level during this period was relatively stable, characterized by 10-20 m scale fluctuation that have been linked with 41,000 year Milankovitch obliquity cycles (Miller et al., 2005). However, this slow cooling trend was punctuated by several episodes of potentially intense Northern Hemisphere glaciation that would have dramatically decreased sea level. One such episode dated to between 13.8-10.4 Ma would have resulted in an ~40m drop in global sea level (Westerhold et al., 2005). Additionally, the cooling that followed the MMCO was accompanied by a shift in ocean productivity from more equatorial regions to more northern regions (Warheit, 1992d; Butzin et al., 2011). How these changes in the environment might have affected Miocene pan-alcids is not clear. However, it is clear that Miocene alcids were tolerant of environmental conditions that



are different from those of today and that the pan-alcid lineage has been able to adapt to those changes through time.

Of the approximately 17,000 fossils referred to Pan-Alcidae, more than 16,000 are from the Pliocene (Smith, personal observation). However, this disparity may be primarily due to the vagaries of the fossil record and/or potential undersampling of earlier (i.e., pre-Pliocene) fossil localities. Regardless of earlier alcid diversity, the number of species present in the Pliocene that are absent from the Pleistocene according to published accounts (Lambrecht, 1933; Brodkorb, 1967; Tyrberg, 1998) strongly suggests that the Pliocene-Pleistocene boundary marks a real change in the seabird communities of the Northern Hemisphere. For example, albatross remains are not known from post-Pliocene deposits in the Atlantic (Olson and Rasmussen, 2001) and Pelagornithidae are not known from post-Pliocene deposits in the Pacific or Atlantic Ocean basins (Mourer-Chaviré and Geraads, 2008, 2010; Boessenecker and Smith, 2011).

The Pliocene, and especially the transition from the Pliocene to the Pleistocene, was a time period marked by continued abiotic changes (e.g., climatic and related oceanic changes) and notable biotic changes. Early Pliocene North Atlantic Ocean sea surface temperatures have been estimated at ~6°C warmer than current temperatures (Naafs et al., 2010). As temperatures fell and the CAS continued to shallow throughout the Pliocene, North Atlantic Ocean bioproductivity increased along with the strength of the North Atlantic current (Naafs et al., 2010). Subsequently, the Pliocene-Pleistocene boundary at ~2.6 Ma was characterized by reorganization of ocean currents owing to the final closure of the CAS that was associated with the onset of Northern Hemisphere glaciation (Bartoli

et al., 2005; Naafs et al., 2010). Late Pliocene glaciation in the Northern Hemisphere resulted in a drop in sea level of ~45m, an associated initial drop in sea temperatures of ~3 C°, and the establishment of the modern profile of the California ocean-current system on which Pacific Ocean endemic alcids rely today (Hyrenbach and Viet, 2003; Ravelo et al., 2004; Bartoli et al., 2005; Sarnthein et al., 2009). Subsequently, the separation of the Atlantic and Pacific Oceans resulted in an increase in Atlantic Ocean temperatures, an associated decrease in bioproductivity in that ocean basin, and the establishment of a more modern profile of the Gulf Stream current (Versteegh, 1997; Bartoli et al., 2005; Kameo and Sato, 2000; Sarnthein et al., 2009). The relative contributions and interactions of the shallowing CAS, the onset Northern Hemisphere glaciation, and the reorganization of ocean circulation currents with respect to the Pliocene-Pleistocene climatic transition (PPCT) are still debated (Haug and Tiedemann, 1998; Lunt et al., 2008; Molnar, 2008). Overall, what is clear from a biological standpoint is that the timing of the Pliocene-Pleistocene climatic transition was congruent with dramatic faunal turnovers involving exchange of terrestrial faunas between North America and South America and decline of numerous marine taxa (Repenning and Tedford, 1977; Vermeij, 1991; Warheit, 1992b; Versteegh, 1997; Kameo and Sato, 2000; Ray and Bohaska, 2001; Bartoli et al., 2005; Ray et al., 2008; Boessenecker, 2011; Boessenecker and Smith, 2011).

In contrast to changes in the Atlantic Ocean, the Pacific Ocean would have maintained flow of cold, nutrient-rich water from high latitudes after the closure of the CAS (Lawrence et al., 2006) and the reasons for the decline of Pacific pan-alcid lineages such as the Mancallinae (Smith, 2011) and other seabirds such as the Pelagornithidae

(Boessenecker and Smith, 2011) are unclear. The microfaunal record documents a southward shift in Atlantic and Pacific cold-adapted foraminiferal faunal regimes (Bartoli et al., 2005), and separation of Pacific and Caribbean coccolith assemblages at 2.74 Ma in response to final closure of the CAS, and an increase in Pacific thermohaline circulation as a result of separation of Atlantic and Pacific. By ~2.5 Ma the modern climate regime including modern North Atlantic Gyre, Gulf Stream, and California current circulation patterns were in place, and changes involved small (i.e., meter scale) fluctuations in sea level associated with Late Pliocene and Pleistocene glacial cycles (Bartoli et al., 2005). The apparent response of alcids to the Pliocene-Pleistocene climate transition was a significant decrease in diversity. Only a single species of *Alca* (rather than 7 Pliocene species) survives today in the Atlantic and only a single species of Mancallinae (rather than 5 Pliocene species) is known from the Pleistocene (Howard, 1970; Kohl, 1974; Smith, 2011; Smith and Clarke, in press). Higher extant diversity of Pacific Ocean endemic alcids may be a function of differential recovery linked to the relatively less severe changes in that ocean basin following the final closure of the CAS.

The tight correlation between major charadriiform diversification events and notable “climatic aberrations” (Zachos et al., 2001:690) is striking (Fig. 8.16). These climatic aberrations represent brief ( $\sim 10^3$  to  $10^5$  years) yet intense climatic changes that Zachos et al. (2001) dated to ~55 Ma, ~34 Ma, and ~23 Ma. These dates correspond to the EECO, the EOCT, and the epochal boundary between the Oligocene and Miocene, which in turn correspond to the hypothesized origination of Charadriiformes, the

hypothesized origination of Pan-Alcidae, and the beginning of the hypothesized Miocene radiation of Pan-Alcidae respectively.

The close association of seabird evolution and large-scale paleoclimatic change is not surprising given the documented response of extant seabirds to much smaller scale environmental changes such as El Niño Southern Oscillations (ENSO; Hatch, 1987; Duffy et al., 1988; Warheit, 1992b; Ainley 1990; Hyrenbach and Veit, 2003). Recent research indicates that ENSO-like conditions may have existed in the Pliocene also (Ravelo et al., 2006). However, evidence of short-term oceanic disturbances is rare in the fossil record (Emslie and Morgan, 1994; Emslie et al., 1996) and other currently known pan-alcid deposits do not appear to be death assemblages (Smith, personal observation).

The ranges of extant alcid are being displaced northward in response to the current global warming trend (Hyrenbach and Veit, 2003; Gaston et al., 2005; Gaston and Woo, 2008) and adult alcid survival and reproductive success rates have been negatively impacted by yearly warming trends that decreased food availability (Ainley et al., 1990b; Sandvik et al., 2005). Additionally, phenological studies of alcid have discovered advances in the timing of breeding in Atlantic and Pacific Ocean species (Hipfner, 2008; Moe et al., 2009; Watanuki, 2010) in response to ocean warming and prey abundances. The potential for mismatched timing between alcid breeding and high prey densities is a conservation concern for alcid and other seabirds (Hipfner, 2008; Schroeder et al., 2009). Compared with birds that have limited geographic ranges (e.g., island endemics), extinction of most extant alcid species owing to human-induced global warming is somewhat unlikely given the advantage of the very large geographic ranges of most

alcids (e.g., circumpolar range of *Uria aalge*). However, given the nest site fidelity of many alcid species (Ainley, 1990), individual populations of alcids may be differentially affected by global warming based on variable climatic and associated biotic effects at different geographic locations.

Given the documented effects of climate change on extant seabird communities it is reasonable to conclude that inherently linked past changes in sea temperature, ocean circulation patterns, and sea level would have also impacted seabird populations, either negatively or positively. What remains unclear is how exactly these changes affected seabird community structure. Although it is clear that alcid ecology has been linked with cold-water upwelling systems since the Late Miocene, it is not well understood how the widespread cooling that resulted in formation of ice sheets and lower sea levels, such as that during Eocene-Oligocene transition, would have impacted pan-alcid populations.

Although fossil records of terrestrial charadriiforms (e.g., buttonquail and jacanas) are known from the Oligocene (Rasmussen et al, 1987; Mayr, 2000; Mayr and Smith, 2001; Mayr and Knopf, 2007), Oligocene fossil records of alcids that might elucidate the effect of the EECO and EOCT on alcids are limited to two very fragmentary specimens from the western Pacific Ocean basin (Ono and Hasegawa, 1991; see chapter 3). That the earliest records of Charadriiformes are from lineages that are primarily non-marine/terrestrial today (e.g., Jacanidae, Turnipacidae, Charadriidae; Rasmussen et al., 1987; Hou and Ericson, 2002; Mayr and Smith, 2001; Mayr, 2002; Mayr and Knopf, 2007) might be interpreted as evidence that basal charadriiforms occupied a terrestrial niche. However, given that the Eocene fossil record of charadriiforms comprises a single

fossil from the Middle Eocene (~40 Ma) of China (Hou and Ericson, 2002) and a single fossil from the Middle Eocene (~47 Ma) of Germany (Mayr, 2000), there is little evidence to support this hypothesis at this time.

The notion that extinct pan-alcids benefitted from cooler climates (Emslie, 1998; Konyukhov, 2002; Warheit, 2002) because extant alcids are cold-adapted pelagic predators is an assumption that is not supported by the results of the divergence estimate or the early fossil record of the clade. For example, the cooling trend associated with Northern Hemisphere glaciation at the end of the Pliocene is linked with the emergence of the Panamanian Isthmus which interrupted Atlantic cold-water upwelling and lowered Atlantic Ocean bioproductivity (Bartoli et al, 2005). So, even though extant alcids generally prefer cooler temperatures, extremes of cold climate can potentially be harmful in to alcid populations in ways that may not be directly related to sea temperature. Furthermore, the lack of abundant pre-Pliocene remains of basally positioned Alcinae *Brachyramphus* and *Synthliboramphus* in deposits linked with cold-water upwelling (e.g., San Diego Fm.) may be an indication that these lineages did not occupy that habitat before the Pliocene. The interaction between large-scale and small-scale tectonics, ocean circulation, weather patterns, and marine productivity is a complex system with a myriad of potential effects on seabird populations (Ainley, 1990; Kitaysky and Golubova, 2000; Hyrenbach and Veit, 2003). Finally, the severity of these effects on any population of seabirds is a function of the tolerance of those birds to change. These tolerances are not well known for extinct lineages and whether these tolerances have changed throughout time is also not known.

***Pan-Alcidae paleodiversity:*** Although it is a crude metric, the overall diversity of alcids through time recorded by the fossil record agrees with the hypothesis of Eocene origins for Pan-Alcidae, a limited number of divergences in the Oligocene, extensive Miocene radiation, and a decrease in diversity at the Pliocene-Pleistocene boundary (Fig. 8.17). As stated previously, only a single fossil record of the clade exists from the Eocene (Chandler and Parmley, 2002) and the only Oligocene record of Pan-Alcidae is based on very fragmentary material (Ono and Hasegawa, 1991). However, if the Oligocene record from the eastern Pacific is valid, it would suggest that pan-alcids had colonized both the Atlantic and Pacific Oceans by the Early Oligocene. The extensive Miocene radiation hypothesized by the divergence estimation analysis is supported by an increase from 1 to 12 recorded species between the Oligocene and Miocene. A caveat to this comparison of diversity through time is that the Eocene and Oligocene marine sedimentary record has not been as extensively sampled as that of the Pliocene, and the possibility that the notable increase to 21 Pliocene species is an artifact of sampling cannot be ruled out. Twelve of the 15 Pleistocene records are of extant species. *Mancalla lucasi* is known from Pliocene and Pleistocene sediments (Kohl, 1974; Smith, 2011) and records of *Pinguinus impennis* and *Fratercula dowi* are restricted to the Pleistocene (Guthrie et al., 1999; Stewart, 2007). Twenty of the 23 extant species of alcids are known from Holocene deposits, suggesting that extant alcid diversity has been relatively stable since the end of the Wisconsin glacial episode ~12,000 years ago.

In contrast to the general increase in diversity through time based on raw estimates of species diversity (i.e., counting the number of species that have fossil records

for a given time period), species diversity inferred based on phylogeny and implied ghost lineages (Norell, 1992) indicates that a general decrease in species diversity is apparent from the Miocene onward (Fig. 8.18). This provides a good example of how estimates of diversity can be misled in the absence of a phylogenetic hypothesis. The presence of numerous alcid species from the Miocene and Pliocene that are not known from Pleistocene and younger deposits agrees with the trends in faunal turnover that have been documented for other marine faunas (Versteegh, 1997; Bartoli et al., 2005; Kameo and Sato, 2000). Seals, walrus, squalodon, albatross, and Pelagornithidae are all present in Atlantic Ocean during the Miocene and Pliocene (Ray et al., 1987; Ray and Bohaska, 2001; Ray et al., 2008) but are absent there today. Furthermore, Pacific Ocean diversity of other seabirds and marine mammals is also noted to decline from the Miocene to today (Repenning and Tedford, 1977; Warheit, 1992b; Boessenecker, 2011; Boessenecker and Smith, 2011). However, these statements regarding chronological trends in diversity must necessarily be considered along with the caveat that Pleistocene alcid diversity was assessed based only on published records (Lambrecht, 1933; Brodkorb, 1967; Tyrberg, 1998). Whether additional diversity exists among Pleistocene alcid remains deserves further scrutiny and the morphological characters (Appendix 2) and morphometric methods (Chapter 2) described herein provide a basis for that evaluation.

Just as areas of highest extant alcid diversity correspond with areas of intense cold-water upwelling today, fossil pan-alcid localities also correspond with known areas of past cold-water upwelling (Fig. 8.19). Pan-Alcidae fossil bearing deposits have been interpreted as the result of deposition in cold-water upwelling systems based on



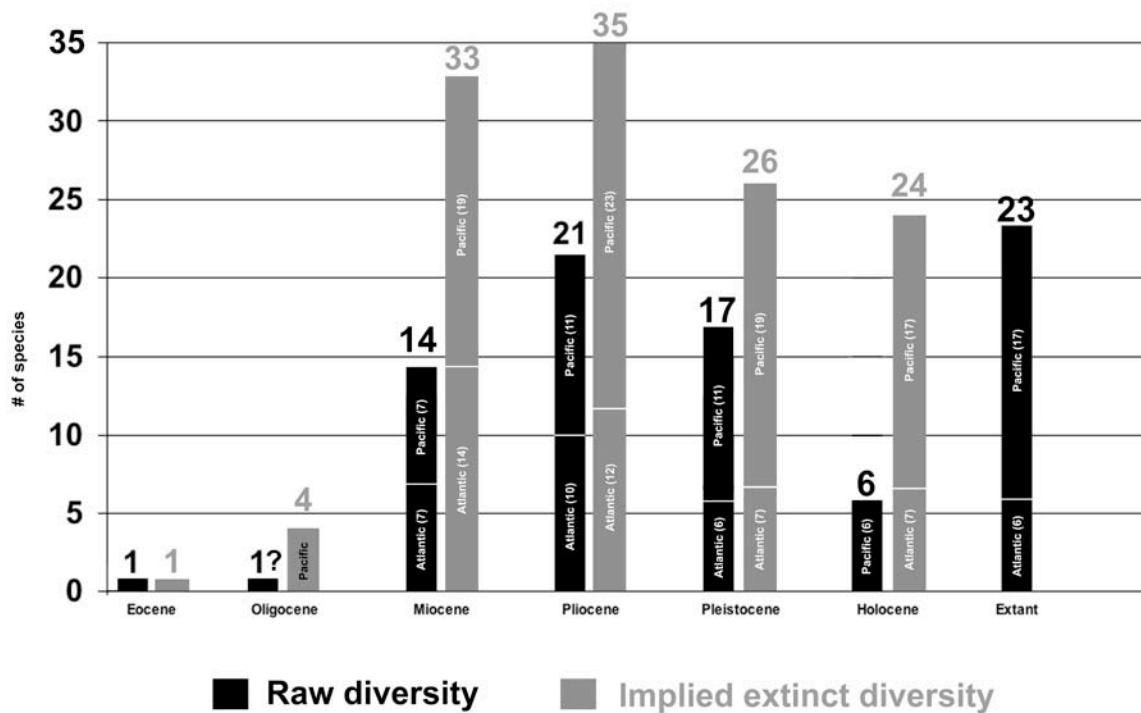


Figure 8.18- Graphical representation of alcid diversity through time based on the age ranges from Table 8.1 (black) and numbers of species inferred based on stratigraphic occurrence of alcid fossils based on Fig. 8.17 (grey). For raw diversity counts, species present in more than one epoch (e.g., *Mancalla lucasi* remains known from Pliocene and Pleistocene deposits) are counted in each age bin. Note that diversity counts and estimates are categorized by Atlantic and Pacific Ocean basin occurrences, and that raw numbers of Pliocene and Miocene occurrences are equal. Also note that the ranges of four of the six extant Atlantic Ocean endemic alcids extend into the Pacific Ocean basin also. Only a single pan-alcid fossil is known from the Eocene (Atlantic), and only a single occurrence of Pan-Alcidae is known from the Oligocene (Pacific).

stratigraphic and paleontological evidence (Gibson, 1967; Ingle, 1979; Snyder, 2001; Wagner et al., 2001). Although cold-water upwelling has likely been constant along the west coast of North America since at least the Early Miocene (Flower and Kennett, 1994), along the eastern coast of North America, upwelling shifted northward at the end of the Pliocene (Dowsett et al., 1992; Marlow et al., 2000; Naafs et al., 2010). Whereas

all Pacific pan-alcid fossil localities are within the range of extant Alcidae, Western Atlantic alcid fossil localities are south of the normal range of extant alcids (Fig. 8.19).

***Pan-Alcidae origination area and dispersal:*** The pan-alcid Pacific Ocean origin hypothesis is based primarily on higher extant diversity in the Pacific Ocean; however, higher extant diversity in the Pacific is not evidence of origination area, and the two oldest known pan-alcid fossils are both from Atlantic deposits (Wetmore, 1940; Chandler and Parmley, 2002; Wijnker and Olson, 2009). Although the lack of older fossils from the Pacific may simply reflect a gap in the fossil record, hypotheses concerning Pacific ancestral origination of pan-alcids based upon proposed greater extant Pacific species diversity should be re-evaluated. Known diversity of extinct Atlantic pan-alcids is now equal to that of extinct Pacific pan-alcids (Table 8.2), and the differential extinction of Atlantic pan-alcids, compared with that of Pacific lineages, may be linked to climatic changes that affected the Atlantic and Pacific Oceans in different ways.

Based on fossil records, seven species each are known from the Miocene of the Atlantic and Pacific Ocean basins (Table 8.2). Numbers of species from the Pliocene are also equal with 10 species each known from the Atlantic and Pacific Ocean basins (Table 8.2). However, numbers of species estimated in each ocean basin based on inferred ghost lineages (Figs. 8.17, 8.18) are quite different from raw diversity counts, with 17 species from the Miocene of the Atlantic, 19 species from the Miocene of the Pacific, 15 species from the Pliocene of the Atlantic, and 26 species from the Pliocene of the Pacific.

The basal position of *Brachyramphus* and *Synthliboramphus* in Alcinae and their restriction to the Pacific basin might be viewed as support for the Pacific origin

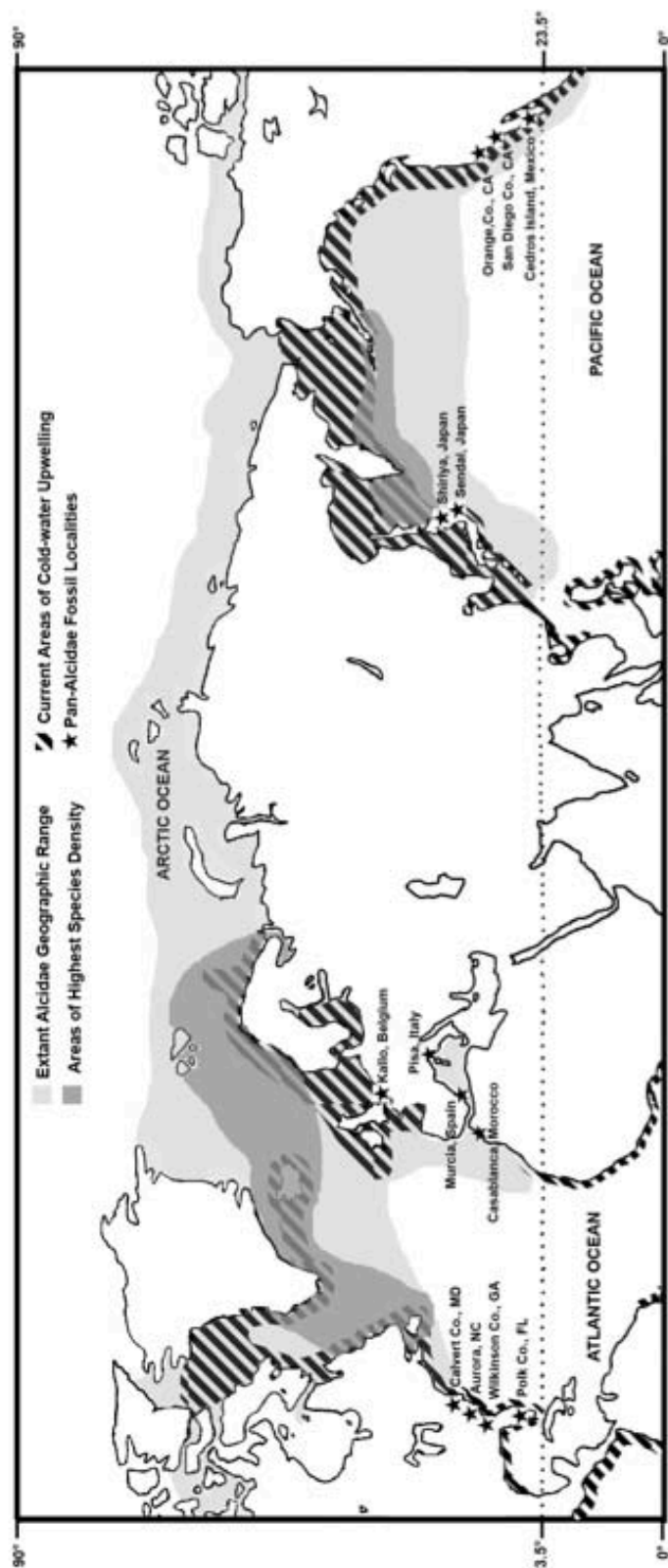


Figure 8.19- Distribution of Extant Alcidae compared with distribution of modern cold-water upwelling locations and Pan-Alcidae fossil localities. Atlantic Ocean area of highest extant species density represents area in which all 6 Atlantic endemic species ranges overlap. Pacific Ocean area of highest extant species density represents the area in which 14 of the 21 Pacific Ocean endemic species ranges overlap. The ranges of 5 additional Pacific endemic species partially overlap the shaded area of highest Pacific species density. The ranges of *Synthliboramphus hypoleucus* and *Synthliboramphus craveri* are outside the range of highest species density (i.e., southern California, USA and Baja California, Mexico). Ranges of extant alcids based on del Hoyo et al. (1996). Upwelling intensities based on NOAA (2011). Map altered from del Hoyo et al. (1996).

hypothesis for Pan-Alcidae (Storer, 1952; Kozlova, 1957; Olson, 1985; Konyukhov, 2002; Pereira and Baker, 2008). Likewise the placement of Mancallinae as the sister taxon to Alcidae and the restriction of Mancallinae to the Pacific Ocean also could be viewed as support for a Pacific Ocean basin origin for the clade. Despite all of the evidence in favor of the Pacific Ocean origin hypothesis for Pan-Alcidae, the oldest fossils of the clade are from the Atlantic Ocean basin (Chandler and Parmley, 2002; Wijnker and Olson, 2009). Given the ~15 Ma gap in the alcid fossil record (Late Eocene-Early Miocene; Fig. 8.17) and the mobility of birds in general, there is currently not enough information to conclude whether alcids originated in the Atlantic or Pacific Ocean basin. Although present in the Eocene of Georgia, USA (Chandler and Parmley, 2002), and the Pliocene of North Carolina, USA (Olson and Rasmussen, 2001), curiously, there is no record of pan-alcids from the Oligocene of the Atlantic coast (Olson, 1985). Additional Oligocene marine sediments from the Atlantic and Pacific Ocean basins should be explored in the hopes of discovering fossils that will elucidate the early evolutionary history of pan-alcids.

Whether the ancestral area of Pan-Alcidae is in the Atlantic or Pacific Ocean basin, periods of exchange between oceans have no doubt taken place. Proposed hypotheses regarding the spread of pan-alcids from one ocean basin to another include dispersal through the ice-free NAP (i.e., through the Bering Strait and Arctic Ocean) and southern dispersal across the submerged Isthmus of Panama prior to ~2.5 Ma (Olson, 1985; Konyukhov, 2002; Pereira and Baker, 2008). These hypotheses are based upon the assumption of dispersal across water, and the first occurrence datum (FAD) for alcid

clades, which until the discovery of an auk from the Eocene of Georgia, USA (Chandler and Parmley, 2002), included Miocene examples of *Mancallinae* (Howard, 1976), *Cepphus* (Howard, 1982), and *Uria* (Howard, 1981) from Pacific deposits, and *Miocepphus* (Wetmore, 1940) and *Alca* (Wijnker and Olson, 2009) from Atlantic deposits. Alcids have been reported hundreds or even thousands of miles from their normal ranges (see Konyukhov, 2002 for examples). Additional records of alcid ‘wrecks’, sometimes composed of thousands of individuals blown many kilometers inland from the sea by storms are also common (Fisher and Lockley, 1954; Stewart, 2002). Given the expanse of geologic time being considered (Eocene-Recent), the possibility that such events may have led to the dispersal of populations from one ocean basin to another ocean basin must be considered.

Although the southern location of the earliest alcid fossil locality (Georgia, USA) cannot be interpreted as support for a southern route of dispersal, warm-adapted alcids in the Eocene likely were not restricted to a northern dispersal route. As suggested by Bédard (1985), the presence of Atlantic alcids in the Eocene (Chandler and Parmley, 2002) confirms that the cold-tolerant lifestyle of some alcids (e.g., *Uria*) evolved from ancestors that were likely tolerant of warmer (i.e., Eocene) climates. Even today, murre ( *Uria aalge* ) have been recorded off the coast of South Carolina, USA, far south of their reported geographic range, and dovekies (*Alle alle*) are considered residents of the Bahamas (Post and Bogart, 2007; Lee, 2009).

***Potentially biasing factors in divergence time analyses:*** Potential error is inherent in every step of the divergence estimation process, including sequence

alignment, phylogeny estimation, rate estimation, and the effect of fossil or other calibrations on resulting node age estimates (Roger and Hug, 2006). A review of the evolutionary-based models behind the many different algorithms applied to sequence alignment, phylogeny estimation and divergence estimation in general is beyond the scope of this study. However, choice of fossil calibrations is a topic of particular interest herein because fossil calibrations can have significant effects on the resulting estimation of divergence ages (Smith and Peterson, 2002; Shaul and Graur, 2002; Graur and Martin, 2004; Near and Sanderson, 2004; Reisz and Müller, 2004; Drummond et al., 2006; Roger and Hug, 2006; Hug and Roger, 2007; Yang and Rannala, 2006). Issues with regards to the choice of calibration points include: (1) incorrect dates assigned to fossil specimens; (2) inclusion of taxa of uncertain age; (3) inclusion of taxa of ambiguous systematic position; (4) the use of problematic external calibrations (5) the temporal distribution of fossil calibrations.

The bias created by the first two age-related issues mentioned above is clear. Obviously fossils used to constrain the age of nodes in a divergence time analysis should be correctly, and as precisely dated as possible. The ages assigned to fossil-bearing strata in the paleontological and geological literature of the previous two centuries (i.e., the 1800's and 1900's) may have been revised since the original publication describing fossil species. An informed reading of recent paleontological and geological literature is critical for establishing accurate and precise estimates for the age of previously described fossils.

The taxonomic status of fossils used as calibration points in a divergence analysis should be rigorously assessed prior their use. Once again, reliance on older

paleontological literature to choose fossil calibrations ignores the possibility that previously described taxa have been taxonomically revised since their original description. Ideally fossils used as calibration points will have been previously included in a phylogenetic analysis to unambiguously establish their systematic position and therefore the divergence that any particular fossil should be used to calibrate.

The potential error associated with any phylogenetic analysis and divergence estimation has resulted in criticism of the use of secondarily derived calibration points for divergence estimation (Shaul and Graur, 2002; Graur and Martin, 2004; Reisz and Müller, 2004). The literature on this issue is largely concerned with the accuracy of the 310 Ma molecular time estimate (MTE) for the split between birds and mammals, and subsequent dates (i.e., secondary and tertiary calibrations) for other divergences derived from the 310 Ma date. The obvious potential for propagation of error inherent in the use of MTE's and secondary or tertiary calibrations argues against their use in divergence estimation analyses.

Ideally, nodes in the ingroup and outgroup of the clade of interest and both deep and shallow nodes (i.e., nodes of several different ages) are available for the estimation of divergence times for any clade. Although potential sources of bias related to choice of fossil calibrations have been the focus of previous study (e.g., Reisz and Müller, 2004), and although the use of multiple calibrated nodes has become commonplace, the potential effect of the temporal distribution of fossil calibrations has not been evaluated in detail. Given that divergence estimation methods rely on dated fossils and sequence divergence between taxa, the results of evaluating the effect of the temporal distribution of fossil

calibrations may provide profound insights related to model selection and design, and ability to account for rate heterogeneity. The fossil records of many taxa are dominated by specimens from a single geologic deposit of a particular age, which can be very informative with respect to ‘snapshots’ of paleodiversity, but less informative with respect to the timing of cladogenetic events that led to that diversity. As is the case with alcid, the majority of extinct diversity comes from two deposits with an age range of only 3.6-4.4 Ma.

These examples highlight the need for interdisciplinary cooperation between molecular biologists and paleontologists with respect to divergence time estimation. Collaboration between paleontologists who possess current knowledge of paleontological and geological literature and a nuanced understanding of the systematic position of extinct species, with molecular biologists who possess extensive knowledge of molecular evolutionary processes and analytical skills, will hopefully lead to more reliable estimates of divergence times in future analyses. The past two decades have seen a revolution in our ability to identify, sequence, and analyze molecular data. Likewise, our knowledge of extinct birds is also experiencing a renaissance due to increasing numbers of new fossil discoveries, and the increasing knowledge of the systematics of extinct avians made possible by the advent of increasingly sophisticated phylogenetic methodologies. Molecular and morphological systematists both have a wealth of information to bring to the table. The sentiments of Reisz and Müller (2004) are echoed here with respect to the hope that the future will see an increase in the number of collaborations between molecular systematists and paleontologists, resulting in increased confidence in estimates



of divergence times.

***Limitations of current phylogenetic and divergence estimation software:***

Although BEAST (Drummond et al., 2010) simultaneously estimates divergence times and phylogeny, currently the software does not allow for the analysis of combined morphological and molecular sequence data. This limitation needs to be addressed because the inclusion of fossil taxa can affect the topology of resultant trees (Donoghue et al., 1989; Huelsenbeck, 1991; Wiens et al., 2010). Phylogenetic analyses in the absence of fossils (when they are available for a clade) have the potential to produce inherently ‘extant biased’ results. This is demonstrated well by the variation between phylogenetic results recovered in analyses that were limited to extant taxa (e.g., Chapter 1, Baker et al., 2007) and analyses including fossil taxa (Chapters 2-8). If the topology recovered by divergence estimation programs such as BEAST (Drummond et al., 2010) is incongruent with the topology recovered when fossils are included, then the validity of age estimates for nodes that differ from the combined analysis topology may be unreliable. Divergence estimation software that allows combined analysis of molecular and discrete morphological character data is needed to address this issue.

A related issue is Bayesian phylogenetic analysis of combined data including a large proportion of missing data such as that for incomplete fossil taxa. As has been shown elsewhere (Kearney and Clark, 2003; Wiens, 2003, 2005), large proportions of missing data can sometimes interfere with the efficient estimation of phylogeny. Because of the large proportion of molecular data included in the combined analysis (11,601 bp’s including gaps), every fossil analyzed was effectively > 98% incomplete. The large

percentage of missing data were presumably why the standard deviation of split frequencies of the MCMC chains in the Bayesian combined analyses including 81 taxa (29 fossil taxa) did not remain below 0.01 and why nodal support was low for many clades (Fig. 8.10). Whether this complication is a function of these particular data or is a broader methodological issue with the Bayesian framework deserves further research.

## CONCLUSIONS

The taxonomic revision of previously published fossil pan-alcid remains and the evaluation of the great quantities of undescribed pan-alcid fossils resulted in the recognition of 10 new species of extinct pan-alcids and the realization that eight previously named species of extinct pan-alcids were not morphologically distinct from previously named taxa. This new assessment of extinct pan-alcid diversity has erased the perceived greater diversity of Pacific pan-alcids, as 18 species each are now recognized from the Atlantic and Pacific Ocean basins respectively (Table 8.2).

The species-level phylogenetic evaluation of extant and extinct charadriiforms provides an evolutionary hypothesis of charadriiform relationships that expands our knowledge of the systematics of this clade in ways would not have been possible without the inclusion of fossils that record millions of years of morphological evolution (Fig. 8.8). That pan-alcids are so morphologically derived with respect to other charadriiforms makes the story of character changes associated with the transformation to wing-propelled diving even more compelling. For example, the results of the combined

phylogenetic analyses (Figs. 8.8, 8.10) indicate that flightlessness evolved independently in two separate lineages of pan-alcids, Mancallinae and *Pinguinus*. The degree of morphological convergence between both lineages of flightless pan-alcids and other flightless wing-propelled diving seabirds (i.e., penguins and plotopterids) can now be examined further in the context of a phylogenetic hypothesis of pan-alcid relationships including extinct species.

The phylogenetic evaluation of fossil charadriiforms also facilitated identification of fossil calibrations for use in divergence time estimation of Charadriiformes and for the first time, previous hypotheses regarding the link between paleoclimatic events such as the MMCO and Pleistocene glacial periods could be evaluated in the context of detailed knowledge of the pan-alcid fossil record. The newly gained understanding of pan-alcid systematics and extinct diversity resulted in an age estimate of divergences for Charadriiformes and for Pan-Alcidae that are congruent with the fossil records of those clades and that potentially demonstrate an association between seabird evolution and major paleoclimatic events such as the MMCO, and the Pliocene-Pleistocene climatic transition (Fig. 8.17). The results of the divergence analysis suggest that extant alcid diversity may be function of radiation of modern lineages during the Miocene and differential survival among those lineages across the Pliocene-Pleistocene boundary. Pleistocene glaciation is not supported as a major influence on extant alcid diversity.

The results of this study are ambiguous with respect to the origination area of Pan-Alcidae. The oldest fossils are from Atlantic deposits but phylogenetic and extant diversity-based hypotheses support a Pacific Ocean basin origin for the clade. Additional

discoveries of Eocene and Oligocene pan-alcid remains will likely be required to further address this question. In the absence of additional fossils from the Eocene and Oligocene, what can be gleaned from the results of the fossil record, the results of the phylogenetic analyses and the divergence estimates is that there were diverse lineages of pan-alcids inhabiting the Atlantic Ocean and Pacific Ocean basins by the Miocene. Furthermore, estimates of diversity based on the fossil record suggest that the PPCT affected Pliocene pan-alcid diversity in different ways. Only a single species, *Alca torda*, representing the dominant pan-alcid lineages of the Pacific and Atlantic (i.e., Mancallinae and *Alca*) survives today and extant Atlantic Ocean basin alcid species richness pales in comparison to that of the Pacific Ocean basin.

The results of the combined phylogenetic analyses of morphological and molecular sequence data and the results of the divergence time analysis, which was calibrated with charadriiform fossils, clearly demonstrate the value of fossils in resolving systematic relationships and assessing evolutionary patterns among extant and extinct organisms. The reduction in species diversity in Atlantic auks (*Alca* and *Pinguinus*) and dovekies (*Alle* and *Miocepphus*) has left only a single extant representative of each of those clades, and the Pacific Ocean endemic Mancallinae are extinct. The magnitude of these compelling examples of potentially climate-change driven extinction was not realized previous to this study. The implications of this study regarding the sensitivity of seabird communities to environmental change have direct bearing on the plight of seabirds in the face of current global warming and pressures from over-fishing and ocean pollution. If, as proposed, alcids are good candidates for environmental indicator species

(Furness and Nettleship, 1991; Montevecchi, 1993), the increased understanding of extinct pan-alcid responses to environmental change may have unexplored conservation value. Extant seabird distributions, ecological interactions, and population dynamics that are changing rapidly in response to the current global warming trend (Kitaysky and Golubova, 2000; Hyrenbach and Veit, 2003; Gaston and Woo, 2008) are best contextualized with insights derived from knowledge of how past climate changes may have affected the mode and tempo of seabird evolution. This study provides the estimates of diversity, phylogenetic context, and estimates of charadriiform divergence that will facilitate future comparisons between changes in extant seabird populations and factors that have influenced the diversity and distribution of extant seabirds such as the Pan-Alcidae.

## APPENDIX 1.

### EXTANT COMPARATIVE MATERIAL

*Aethia cristatella* Crested Auklet:

Skins: NCSM 6564, 6565, 6567, 16419, 17749.

Skeletons: NCSM 17749; USNM 223707, 488675, 498282, 561934, 61094.

Eggs: USNM 32126, 32128, 32131, 33167.

*Aethia psittacula* Parakeet Auklet:

Skins: NCSM 16423, 16424, 18387; USNM 89143, 493708.

Skeletons: NCSM 14147, 14804, 18387, 18514, 20177; NSM PO 355; USNM 12640, 226451, 610513, 610514, 610937.

Eggs: USNM 42123, 42124, 42125, 42126.

Dissection: NCSM 20881.

*Aethia pusilla* Least Auklet:

Skins: NCSM 17735, 17736, 17751, 17797.

Skeletons: NCSM 17734, 17736, 17737; USNM 224009, 224010, 498285; NSM PO 356, 357.

Eggs: USNM 16725, 18052, 25103, 33886.

*Aethia pygmaea* Whiskered Auklet:

Skins: NCSM 13159; USNM 4163, 67399, 85617, 92971, 110194.

Skeletons: USNM 344544; UMMZ 204592, 224279, 224882, 224883.

Eggs: Scored from Baicich and Harrison (1997).

*Alca torda* Razorbill Auk:

Skins: NCSM 298, 299, 2236, 4455, 18760, 20015.

Skeletons: NCSM 20058, 20502; USNM 18062, 347946, 501644, 502378, 502382, 502387, 502388, 502389, 502549, 555666, 555668.

Eggs: NCSM 13447, 13448; USNM 18476, 21571, 23259.

*Alle alle* Dovekie:

Skins: NCSM 301, 302, 303, 304, 20111, 20630, 40060,.

Skeletons: NCSM 18374; USNM 344740, 344748, 499471, 560929.

Eggs: USNM 2634, 18490, 18491, 19053.

Dissection: NCSM 21042.

*Anous tenuirostris* Lesser Noddy:

Skins: USNM 486718, 486723, 486725, 486728.

Skeletons: USNM 488400, 622578.

*Bartramia longicauda* Upland Sandpiper:

Skins: NCSM 825, 826, 827, 828, 3093.

Skeletons: USNM 227823, 347894, 610844, 610845, 501160.

*Brachyramphus brevirostris* Kittlitz's Murrelet:

Skins: NCSM 35213; USNM 286494, 333257, 589672.

Skeletons: USNM 288086, 288087.

Eggs: USNM 47733.

*Brachyramphus marmoratus* Marbled Murrelet:

Skins: NCSM 5669, 5670, 18144, 18145, 18146, 18148.

Skeletons: NCSM 18143, 18144, 18145, 18146, 18147, 18148, 18149; NSM PO 354, 358, 551.

Eggs: USNM 21545, 28473, 40125, 417778.

*Brachyramphus perdix* Long-billed Murrelet:

Skins: USNM 108952, 109985, 120704, 200411, 200412.

Skeletons: USNM 582506, 599498.

*Charadrius vociferus* Killdeer:

Skins: NCSM 791, 792, 17610, 18671, 19284.

Skeletons: NCSM 18305, 21905; USNM 61432, 492870, 553817, 622526.

Eggs: NCSM 13382, 13383, 13384, 13385, 13386, 13387.

*Charadrius wilsonia* Wilson's Plover:

Skins: USNM 220535, 338822, 338823, 524172.

Skeletons: NCSM 5818; USNM 1250, 556652, 610801.

Eggs: NCSM 13388, 13389; USNM 43430, 43431, 43432.

*Cepphus carbo* Spectacled Guillemot:

Skins: USNM 40637, 102199, 406348, 424970.

Skeletons: USNM 347755, 347756, 347757.

*Cepphus columba* Pigeon Guillemot:

Skins: NCSM 16153, 16155, 16414, 16438, 16439.

Skeletons: NCSM 18094, 18095, 18096, 18097.

Eggs: NCSM 13449; USNM 19063, 21546, 27059.

Dissection: NCSM 21075.

*Cepphus grylle* Black Guillemot:

Skins: NCSM 6830; USNM 331585, 393556, 394525.

Skeletons: USNM 344759, 344760, 347265, 612213, 612214.

Eggs: NCSM 7435, 13450, 13451; USNM 2578, 18494.

*Cerorhinca monocerata* Rhinoceros Puffin:

Skins: NCSM 8064, 10628, 16420, 16421, 16430.

Skeletons: NSM PO 189; USNM 557613, 557614, 561468, 620641, 620643.

Eggs: USNM 12866, 24634, 27632, 27633.

*Chlidonias leucopterus* White-winged Black Tern:

Skins: NCSM 11351, 11352, 11358, 11470, 11471.

Skeletons: USNM 43173, 290154, 430844, 431172, 488879.

*Creagrus furcatus* Swallow-tailed Gull:

Skins: NCSM 183825. USNM 115967, 115968, 131674, 543878, 543879.

Skeletons: USNM 18492, 19029, 498301.

*Cursorius temminckii* Temminck's Courser:

Skins: USNM 448378, 520019, 545851, 545853, 545854.

Skeletons: USNM 429182, 431709.

*Fratercula arctica* Atlantic Puffin:

Skins: NCSM 17824, 17825; USNM 589716, 627638.

Skeletons: USNM 18055, 18057, 18058, 224189, 621331.

Eggs: NCSM 13452; USNM 2637, 14977, 31034.

*Fratercula cirrhata* Tufted Puffin:

Skins: NCSM 16147, 16148, 16150, 16433, 18098.

Skeletons: NCSM 17823, 18099, 18100; USNM 19449, 488748.

Eggs: NCSM 13453, 13454; USNM 16335, 12861.

*Fratercula corniculata* Horned Puffin:

Skins: NCSM 7761, 10629, 18102; USNM 610504, 612200, 499957.

Skeletons: NCSM 17835, 18083, 18388; USNM 499961, 499964.

Eggs: USNM 16329, 19706, 22052, 25095, 29216.

Dissection: NCSM 21095.

*Glareola maldivarum* Oriental Pratincole:

Skins: NCSM 9756, 11059, 11060, 11061, 11062.

Skeletons: USNM 19580.

*Gygis alba* White Tern:

Skins: NCSM 7859, 7860, 8021, 18890, 18932.

Skeletons: NCSM 16895; USNM 498081, 498415, 559583, 621328.

*Hydrophasianus chirurgis* Pheasant-tailed Jacana:

Skins: NCSM 10609, 11018, 11019, 11473.

Skeletons: USNM 226034, 431604, 431609, 490560, 490566.



*Larosterna inca* Inca Tern:

Skins: USNM 15503, 15516, 212050, 212051, 371303.

Skeletons: USNM 292869, 430271, 430375, 430580, 430625, 631761.

*Larus argentatus* Herring Gull:

Skins: NCSM 17738, 21188, 21444, 21462, 21791.

Skeletons: NCSM 8624, 10116, 10211, 10251, 22218.

Eggs: NCSM 5934, 13395.

*Larus marinus* Great Black-backed Gull:

Skins: NCSM 7376, 7861, 7863, 7941, 7992.

Skeletons: NCSM 6590, 16190, 102451; USNM 491592, 502396.

Eggs: NCSM 5968; USNM 42295, 42296, 42297.

*Numenius minutus* Little Curlew:

Skins: NCSM 1907, 22227, 22228, 22229, 22230.

Skeletons: USNM 347648.

*Pagophila eburnea* Ivory Gull:

Skins: USNM 17766, 22217, 22221.

Skeletons: NCSM 17766; USNM 344734, 491595, 491596, 491597.

*Phaetusa simplex* Large-billed Tern:

Skins: NCSM 22224. USNM 316370, 326609, 349836, 512940.

Skeletons: USNM 345827, 345828.

*Pinguinus impennis* Great Auk:

Skins: USNM 57388 (eye and mouth color scored based on Smith, 1879).

Skeletons: USNM 346387 (composite), 557975 (composite), 623465 (composite)  
additional series of disarticulated USNM material from the expedition to  
Funk Island (Lucas, 1890).

Eggs: USNM 15141, 15144.

*Ptychoramphus aleuticus* Cassin's Auklet:

Skins: NCSM 5666, 7222, 10624, 19137, 19140.

Skeletons: NCSM 18088; USNM 491305, 491845, 491846, 557607, 557609,  
557611.

Eggs: NCSM 7901; USNM 2353, 16635, 16636.

*Rhinoptilus chalcopterus* Bronze-winged Courser:

Skins: USNM 117798, 216168, 437251, 448203, 460101.

Skeletons: USNM 321515.

*Rhodostethia rosea* Ross's Gull:

Skins: NCSM 22222, 22223. USNM 93346, 93356, 93357, 332306, 495943.

Skeletons: USNM 491606, 491607, 491608, 491609, 491611.

*Rissa tridactyla* Black-legged Kittiwake:

Skins: NCSM 18072, 18073, 18074, 18075, 18076.

Skeletons: NCSM 18123, 18124, 18125, 18126.

Eggs: NCSM 13403.

*Rynchops niger* Black Skimmer:

Skins: NCSM 281, 282, 287, 289, 20262.

Skeletons: NCSM 4228, 6280, 6281, 7790, 7791, 9725, 19048, 19063

Eggs: NCSM 13441, 13442, 13443, 13444, 13445.

*Stercorarius longicaudus* Long-tailed Skua:

Skins: NCSM 8385, 10269, 11725, 17144, 17801.

Skeletons: NCSM 10269, 17801; USNM 491643, 491951, 501243.

Eggs: USNM 7789, 11692, 11694, 11681, 11699.

*Stercorarius skua* Great skua:

Skins: NCSM 13193, 14891, 22191, 22192.

Skeletons: NCSM 11747; USNM 488294, 488295, 560938, 576076, 623300.

Eggs: USNM 14918, 24541, 34243, 42219, 42221, 46504.

*Sterna anaethetus* Bridled Tern:

Skins: NCSM 4066, 6037, 6039, 6042, 6086.

Skeletons: NCSM 10268, 17085, 19073; USNM 488397, 554970, 554972,  
558277.

*Sterna maxima* Royal Tern:

Skins: NCSM 7213, 7294, 7614, 20050, 20668.

Skeletons: NCSM 1640, 10248, 16010, 17514.

Eggs: NCSM 2603, 2604, 5317, 13245, 13424, 13426.

*Sterna nilotica* Gull-billed Tern:

Skins: NCSM 242, 10461, 11469, 15044, 15046.

Skeletons: 10228, 15046, 17188, 289676, 501253, 610912.

Eggs: NCSM 8397, 8398, 8399, 9943, 9944.

*Sternula superciliaris* Yellow-billed Tern:

Skins: USNM 283, 682, 401268, 512943, 512944.

Skeletons: USNM 227482, 345825, 345826.

*Stiltia isabella* Australian Pratincole:

Skins: USNM 279023, 405699, 405698, 405700, 405701.

Skeletons: AMNH 9599.

*Synthliboramphus antiquus* Ancient Murrelet:

Skins: NCSM 16146, 17742, 18089, 19143.

Skeletons: NCSM 17742, 18089, 18090; NSM PO 351, 352, 427, 428, 564;  
USNM 488688, 561926.

Eggs: USNM 16618, 27130, 27131, 28369.

Dissection: NCSM 21074.

*Synthliboramphus craveri* Craveri's Murrelet:

Skins: USNM 544024, 544034, 597160, 597163.

Skeletons: SDSNH 36390, 36391, 37767.

Eggs: USNM 42144, 46625, 46627, 46628.

*Synthliboramphus hypoleucus* Xantus' Murrelet:

Skins: USNM 544886, 544887, 544889, 544893.

Skeletons: USNM 19387, 291879, 345427, 345428, 500652.

Eggs: USNM 28131, 31480, 46623, 46624.

*Synthliboramphus wumizusume* Japanese Murrelet:

Skins: USNM 15803, 85796, 111653, 114529, 466256.

Skeletons: NSM PO 10, 353, 359; UMMZ 152355, 152356, 152357, 152358,  
152359, 152360.

*Tryngites subruficollis* Buff-breasted Sandpiper:

Skins: NCSM 7621, 21581, 22225, 22226.

Skeletons: USNM 7995, 227481, 227771, 492110.

*Uria aalge* Common Murre:

Skins: NCSM 8074, 11188, 18115, 18992, 20551.

Skeletons: NCSM 17822, 18116, 18117, 18118, 18234.

Eggs: NCSM 5935, 5936, 13455, 13456, 13457, 13773.

Dissection: NCSM 21070.

*Uria lomvia* Thick-billed Murre:

Skins: NCSM 6347, 16144, 16145, 17754, 17779.

Skeletons: NCSM 18114, 19414; USNM 344435, 561265.

Eggs: USNM 18502, 18504, 18505, 19049, 24420.

*Xema sabini* Sabine's Gull:

Skins: NCSM 3678, 16393, 16394, 17777, 17778.

Skeletons: NCSM 17778; USNM 499111, 533882, 533905, 557605, 557606.

## APPENDIX 2.

### MORPHOLOGICAL CHARACTER LIST

OSTEOLOGY: CHARACTERS 1-232

INTEGUMENT: CHARACTERS 233-275

REPRODUCTION & DIET: CHARACTERS 276-277

MYOLOGY: CHARACTERS 278-301

FEATHER MICROSTRUCTURE: CHARACTERS 302-353

### SKULL

**1. Premaxilla, anterior tip:** (0) decurved; (1) hooked. The anterior tip of the premaxilla is hooked ventrally in a raptorial fashion in some alcids (e.g., *Alca torda*). The anterior tip of the premaxilla in other alcids (e.g., *Brachyramphus marmoratus*) is decurved slightly ventrally but does not possess a hooked tip.

**2. Premaxilla, dorsal margin** (modified from Chandler, 1990b, character 17): (0) not anteriorly enlarged; (1) anteriorly enlarged. While the premaxilla of most alcids is acute (e.g., *Uria aalge*) the premaxilla of some species (e.g., *Alca torda*) is mediolaterally compressed, and enlarged anteriorly and dorsally.

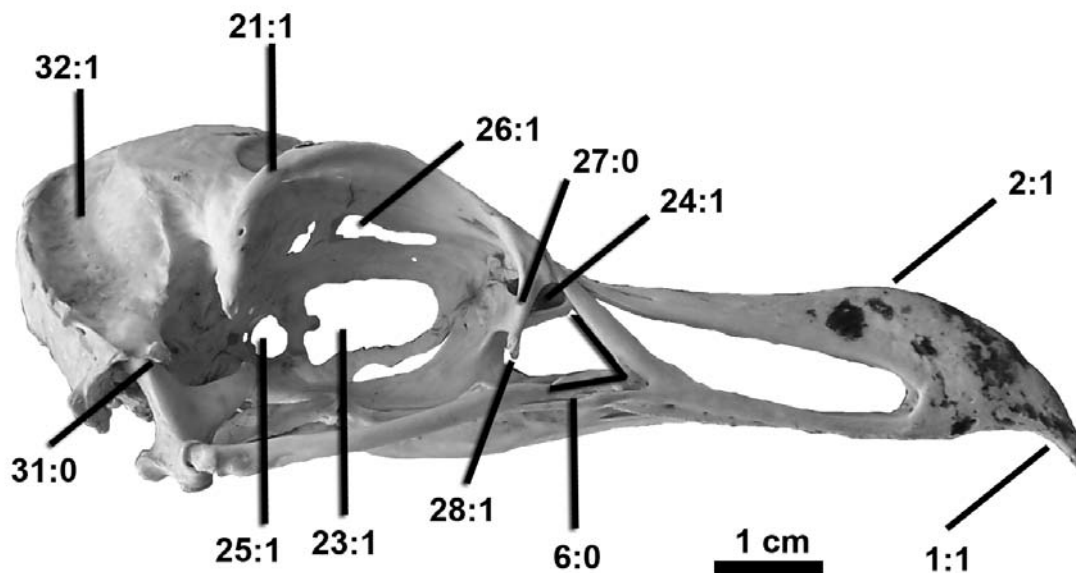


Figure A2.1- Skull of *Alca torda* (NCSM 20058) in right lateral view.

**3. Maxilla, fenestra adjacent to junction of premaxilla and palatine:** (0) absent; (1) present. The ventral surface of the distal end of the maxilla is fenestrated in some alcids

(e.g., *Cerorhinca monocerata*). This opening (fenestra ventrolateralis, Livezey and Zusi, 2006:516) is absent in many other alcids (e.g., *Cephus grylle*). In life the fenestra is covered by a thin membrane and because the fenestra does not serve as a passageway for muscle, tendon, or nerves, its purpose may be related to flexion or weight reduction.

**4. Nasal, extent of anterior projection along the ventral surface of the frontal process of the premaxilla** (Chandler, 1990b, character 9): (0) contacting; (1) separated. The nasals converge beneath the premaxilla in some species (e.g., *Uria aalge*), while in other species (e.g., *Fratercula cirrhata*) the lateral nasal bars merge with the ventral premaxilla but do not contact one another.

**5. Nasal, maxillary spine on narial bar** (Chandler, 1990b, character 13): (0) short (i.e.,  $\leq 1/2$  the length of the narial bar); (1) long (i.e.,  $> 1/2$  nasal bar). A maxillary process extends dorsally from the posterior maxilla and incompletely fuses with the nasal along the posterior margin of the external nares. In most alcids and other charadriiform species (e.g., *Uria lomvia*) the process is only a short protuberance. In other species (e.g., *Brachyramphus brevirostris*) this process extends more than halfway up the lateral nasal bar towards the nasofrontal hinge.

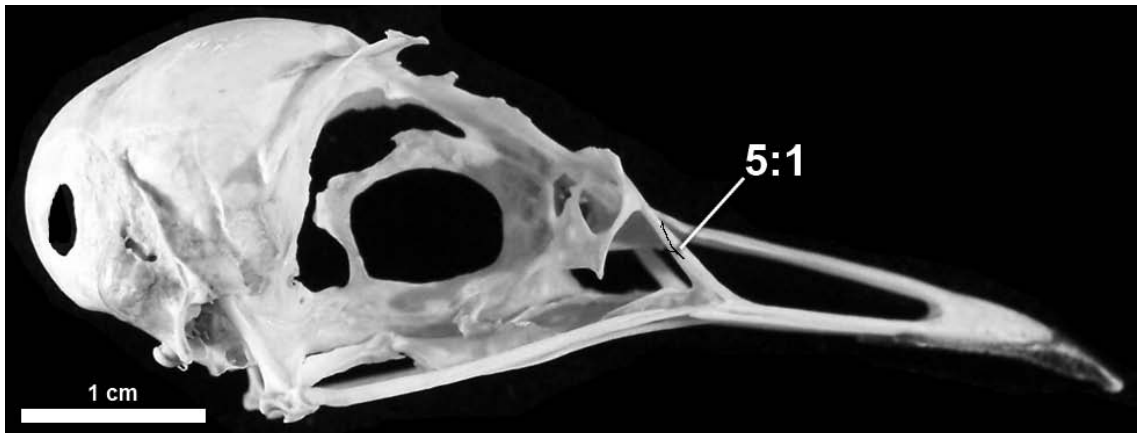


Figure A2.2- Skull of *Brachyramphus marmoratus* (NCSM 18149) in right lateral view. Suture line between maxillary spine and nasal bar marked by black line.

**6. Nasal, narial bar, angle with respect to jugal:** (0) ~45 degrees; (1) ~60 degrees. The angle formed where the anterior margin of the nasal meets the jugal of most alcids (e.g., *Uria aalge*) is ~45 degrees, while in the auklets and puffins (e.g., *Fratercula cirrhata*) this angle is around ~60 degrees.

**7. Maxilla, maxillopalatine strut** (Strauch, 1985, character 1; Chandler, 1990b, character 16): (0) absent; (1) present. The maxillopalatine strut is a small projection connecting the maxillopalatine process to the nasal bar. The maxillopalatine strut, which is found only in *Fratercula* among the Alcidae, does not appear to be homologous with

those found in other charadriiforms (Lowe, 1931; Bock, 1958; Zusi and Jehl, 1970; Strauch, 1978). Its presence is considered derived (Strauch, 1985).



Figure A2.3- Skull of *Fratercula arctica* (USNM 621331) in right lateral view.

**8. Maxilla, maxillopalatine process, shape** (Strauch, 1985, character 2; Chandler, 1990b, character 3): (0) ventrolaterally concave; (1) flat. In most alcids (e.g., *Alca torda*) the maxillopalatine process is a rounded, medially inflated structure, while in *Aethia*, the maxillopalatine process is flat.

**9. Maxilla, maxillopalatine process, orientation in ventral view** (Chu, 1998, character 45): (0) dorsally tilted; (1) ventral, flat lying. The maxillopalatine process of some alcids (e.g., *Aethia pygmaea*) are dorsoventrally oriented (i.e., horizontally lying), whereas the maxillopalatine process of other alcids (e.g., *Alca torda*) are tilted such that their medial edges are dorsally elevated in relation to their lateral edges.

**10. Maxilla, maxillopalatine process, anteriomedial margin in ventral view** (Chandler, 1990b, character 6): (0) rounded; (1) angled. In some species (e.g., *Alca torda*) the medial margin of the maxillopalatine process forms a gentle curve. This feature is anteriorly angled in other species of alcids (e.g., *Aethia pusilla*).

**11. Palatine, relative ventral extension of the ventral crest and the lateral margin of the palatine in distal view** (Strauch, 1985, character 3): (0) ventral crest does not extend ventral to lateral margin; (1) ventral crest extends ventral to lateral margin of palatine. The ventral extent of the ventral crest of the palatine (crista ventralis medialis, Baumel and Witmer, 1993) does not extend as far ventrally as the lateral margin of the palatine in most charadriiforms (e.g., *Alca torda*). In the auklets (e.g., *Aethia psittacula*) however, it extends ventral to the lateral margin of the palatine (Strauch, 1985).

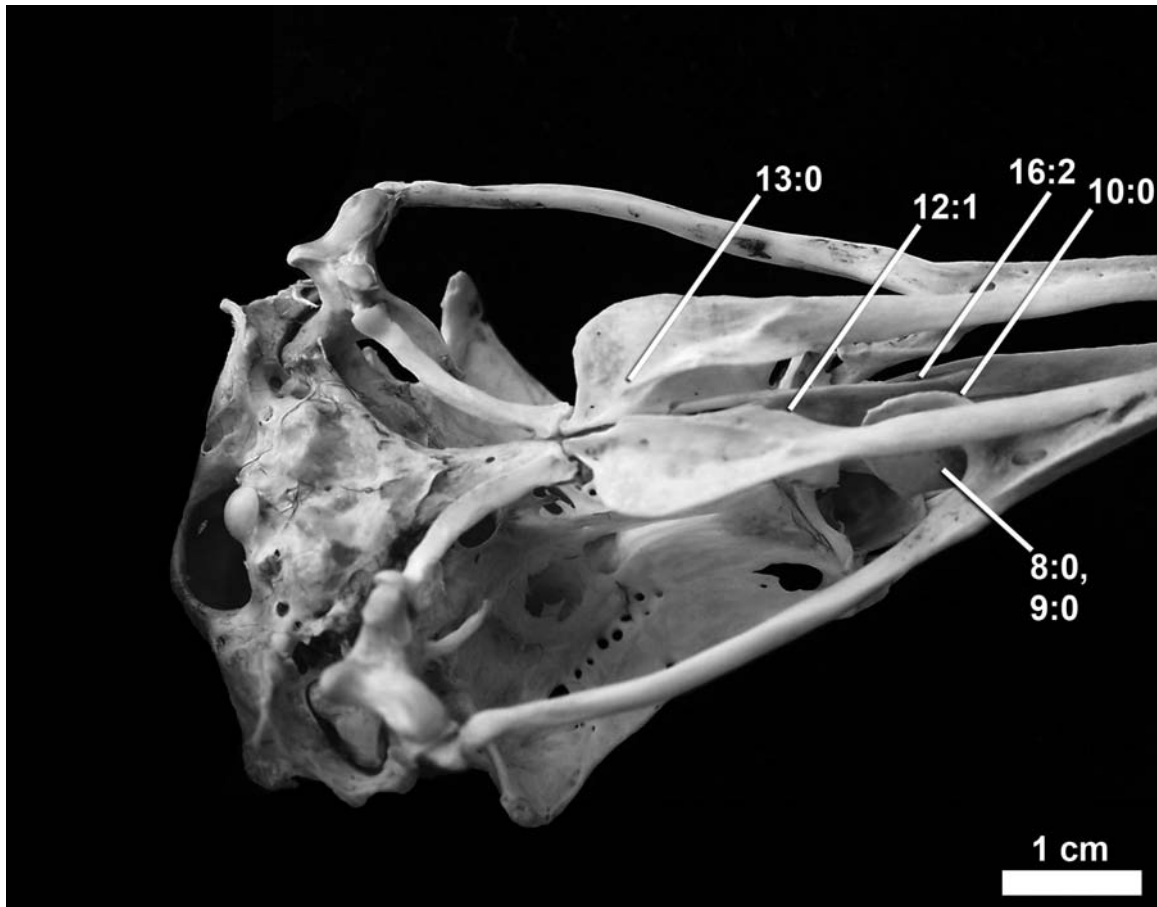


Figure A2.4- Skull of *Alca torda* (NCSM 20058) in oblique ventral view.

**12. Palatine, anterior margin of the ventral crest in ventral view** (crista ventralis medialis; Baumel and Witmer, 1993; modified from Chandler, 1990b, character 3): (0) notched; (1) rounded. The anterior end of the medial palatal crest can be either rounded in shape (e.g., *Alca torda*) or angular (e.g., *Cephus carbo*).

**13. Palatine, posterior margin of the medial palatal crest** (crista ventralis medialis; Baumel and Witmer, 1993; modified from Chandler, 1990b, character 3): (0) notched (1) rounded. The posterior end of the medial palatal crest can be either rounded (e.g., *Cephus carbo*) or angular (i.e., notched; e.g., *Brachyramphus brevirostris*).

**14. Palatine, corpus shape in ventral view** (angulus caudolateralis; Baumel and Witmer, 1993; Chandler, 1990b, character 2): (0) broadens posteriorly; (1) narrows posteriorly. The posterior end of the palatine broadens before angling medially to articulate with the pterygoid in some species of alcids (e.g., *Alca torda*), while in others (e.g., *Synthliboramphus antiquus*) the palatines remain the same width or narrow.

**15. Palatine, posterior end in ventral view** (Chandler, 1990b, character 4): (0) broad at pterygoid articulation; (1) narrow and relatively straight anterior to pterygoid articulation. The lateral margins of the palatines are mediolaterally narrower before the pterygoid articulation in some species of alcids (e.g., *Synthliboramphus antiquus*).

**16. Vomer, anterior end, shape** (Chandler, 1990b, character 1): (0) straight; (1) indented; (2) dorsally deflected. The ventral edge of the anterior vomer is straight in some alcids (e.g., *Brachyramphus marmoratus*), while in some species (e.g., *Alca torda*), the anterior end of the vomer curves dorsally (i.e., is dorsally concave).

**17. Vomer, anterior tip shape:** (0) pointed; (1) bifurcated. The anterior tip of the vomer is pointed in most alcids (e.g., *Alca torda*), while in some species (i.e., *Cephus grylle*) the anterior tip of the vomer is bifurcated.

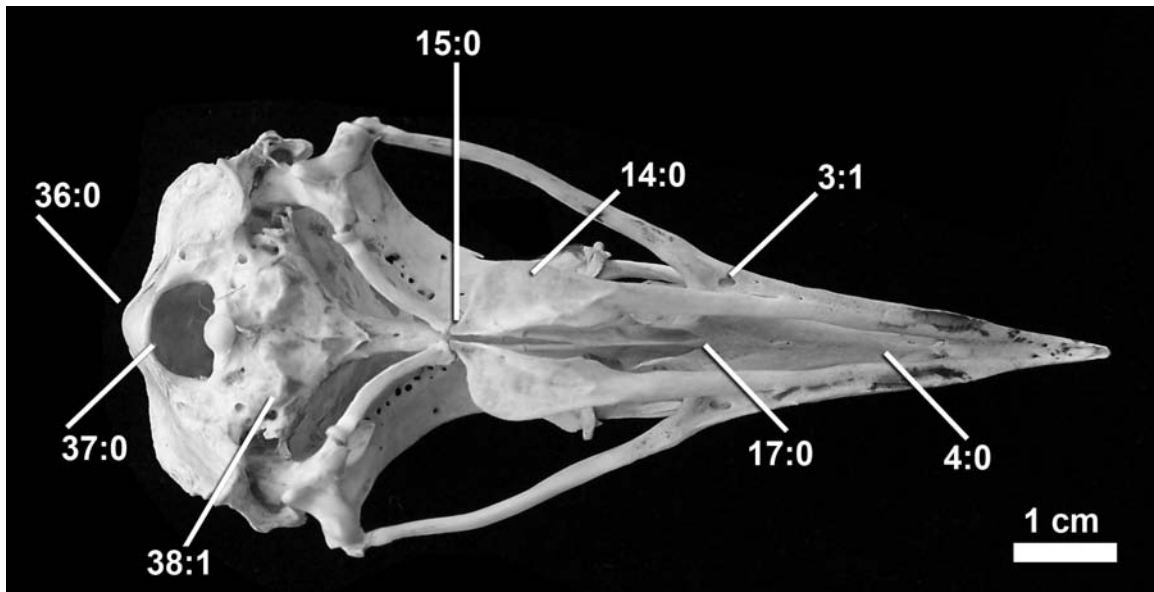


Figure A2.5- Skull of *Alca torda* (NCSM 20058) in ventral view.

**18. Lamina dorsalis, segmentation:** (0) not segmented; (1) segmented. The lamina dorsalis is an extension of the mesethmoid that lies against the ventral side of the frontal (Baumel and Witmer, 1993). This osseous feature is segmented and may play some part in bill kinesis in alcids (e.g., *Uria lomvia*). The lamina dorsalis is fused to the rest of the mesethmoid in many charadriiform species (e.g., *Rynchops niger*).

**19. Lamina dorsalis, size:** (0) large; (1) small. The lamina dorsalis of most alcids (e.g., *Alca torda*) is a large (mesethmoid margin interrupted only by suture between it and the lamina dorsalis), triangular, anteriorly pointing structure with a medial crest, while in



some species (e.g., *Alle alle*) it is reduced to a small (lamina dorsalis not continuous with margin of mesethmoid, appears to be a separate accessory structure), elongate point.

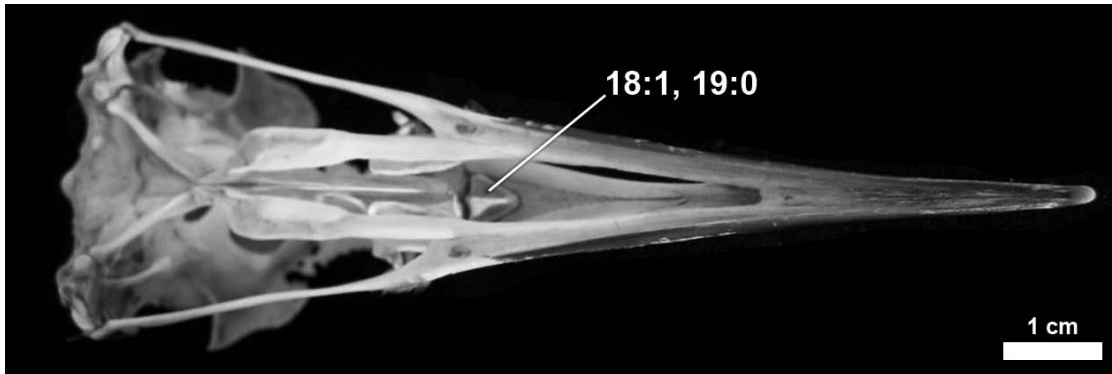


Figure A2.6- Skull of *Uria aalge* (NCSM 18118) in oblique ventral view.

**20. Frontal, salt gland fossa, depth** (modified from Strauch, 1985, character 5; Chandler, 1990b, character 11): (0) shallow; (1) deep. In some species of alcids (e.g., *Alca torda*) deep (i.e., fossa concave) excavations of the frontals are separated by a medial cranial crest, while in some alcids (e.g., *Aethia psittacula*) the nasal fossae are shallower (i.e., semi-flattened or convex).

**21. Frontal, supraorbital rims** (lateral to fossa glandulae nasalis; Baumel and Witmer, 1993; modified from Strauch, 1985, character 5; Chandler, 1990b, character 11): (0) absent; (1) present. This structure associated with the salt glands is completely absent in some alcid species (e.g., *Brachyramphus brevirostris*) while in other alcid species (e.g., *Alca torda*) it is a robust, fully ossified lip that follows along the entire dorsal outline of the orbits.

**22. Interhemispherical furrow, depth:** (0) shallow; (1) deep. The interhemispherical furrow is noticeably deeper in Mancallinae compared to all other charadriiforms (e.g., *Larus marinus*).

**23. Mesethmoid, fenestra in interorbital septum posterior to nasofrontal hinge:** (0) small fenestra; (1) large fenestra. In contrast with many closely related charadriiforms (e.g., *Larus marinus*) that have only a small (i.e., fenestra height  $\leq 1/3$  height of septum) interorbital fenestra, alcids possess a large (i.e., fenestra height  $> 1/3$  height of septum) interorbital fenestra.

**24. Mesethmoid, fenestra in nasal capsule anterior to nasofrontal hinge** (0) fenestrated; (1) not fenestrated. Between the lamina dorsalis and the ectethmoid, the mesethmoid of some alcids (e.g., *Fratercula arctica*) is fenestrated. The mesethmoid of other alcids (e.g., *Alca torda*) is not fenestrated.

**25. Foramen opticum internum** (Chu, 1998, character 15): (0) absent; (1) present. This foramen, which punctures the interorbital septum near the junction of the mesethmoid and the orbit, is present in all alcids (e.g., *Aethia psittacula*), but is absent in some charadriiforms not closely related to Alcidae (e.g., *Charadrius wilsonia*).

**26. Fonticulus orbitocranialis** (Chu, 1998, character 33): (0) not enclosed; (1) enclosed. In most alcids (e.g., *Aethia psittacula*) the mesethmoid does not extend dorsally to fuse with the ventral frontals, thus the fonticulus orbitocranialis is not entirely enclosed by bone. In alcids that have a dorsally ossified mesethmoid (e.g., *Alca torda*), the fonticulus orbitocranialis is a clearly defined foramina near the dorsal margin of the posterior mesethmoid.

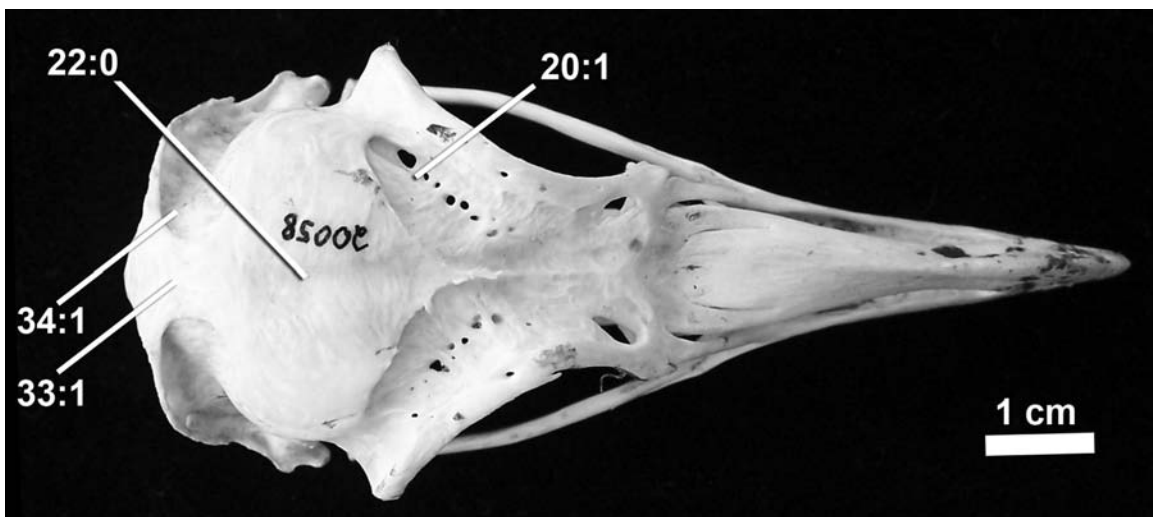


Figure A2.7- Skull of *Alca torda* (NCSM 20058) in dorsal view.

**27. Lacrimal, articulation with ectethmoid** (Chu, 1998, character 26): (0) occupies entire lateral margin of ectethmoid; (1) occupies only the ventral half of the lateral margin of the ectethmoid. In the Alcidae (e.g., *Alca torda*), the lateral margin of the ectethmoid is dorsoventrally expanded and anteroposteriorly flattened, giving this element a square shape when viewed anteriorly. The lacrimal articulates with the ectethmoid along its entire lateral margin. In many other charadriiforms (e.g., *Sterna maxima*) the ectethmoid tapers laterally to a point. In these taxa the lacrimal extends dorsally from the medially extending ectethmoid.

**28. Lacrimal, position in lateral view:** (0) posteroventrally directed; (1) ventrally directed.. With the exception of *Pinguinus impennis* and *Rynchops niger*, the lacrimal of all taxa examined in this study are directed posteroventrally. In contrast, the lacrimal of *P. impennis* extends ventrally. The condition shared by *P. impennis* and *R. niger* is not considered homologous here, as the cranium of *R. niger* is extremely derived (with respect to other charadriiforms).

**29. Lacrimal, supraorbital process** (Chu, 1998, character 30): (0) absent; (1) present. The supraorbital process of the lacrimal (sensu Cracraft, 1968), while present in all alcids (e.g., *Cepphus grylle*), is absent in many other charadriiforms (e.g., *Rissa tridactyla*).

**30. Sclerotic ring, shape** (from Strauch, 1985, character 7; Chandler, 1990b, character 18): (0) narrow, flat ring; (1) wide conical ring with serrated inner edge. The sclerotic ring of most charadriiforms (e.g., *Rynchops niger*) is a flat and narrow. That of puffins (e.g., *Fratercula arctica*), however, is distinctly conical and has a serrated inner edge. Shufeldt (1889) was the first to describe this condition in puffins (Strauch, 1985).

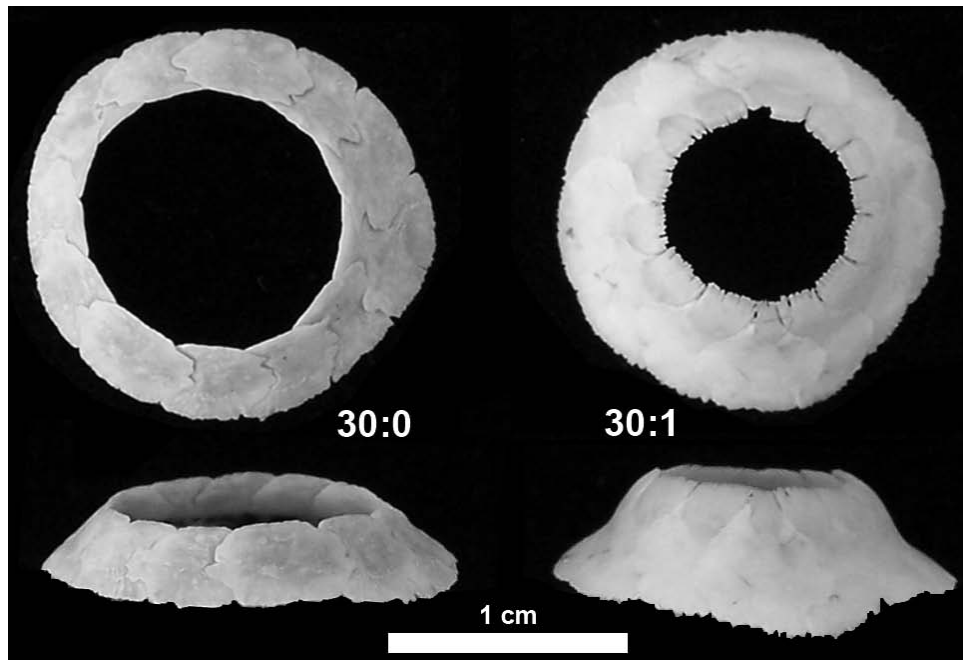


Figure A2.8- Sclerotic rings of *Alca torda* (NCSM 20058; left) and *Fratercula corniculata* (NCSM 17835; right) in lateral (top) and dorsal (bottom) views.

**31. Squamosal, zygomatic process, shape** (Chandler, 1990b, character 12): (0) short; (1) elongate. The zygomatic process, which extends ventrolaterally over the articulation of the quadrate with the skull, is a short (i.e.,  $<3\times$  long than wide), relatively rounded structure in many alcids (e.g., *Cepphus grylle*). In some alcids (e.g., *Fratercula arctica*), this process is a long (i.e.,  $\geq 3\times$  long than wide) pointed projection.

**32. Squamosal, temporal fossa depth** (Chandler, 1990b, character 19): (0) shallow; (1) deep. The temporal fossa is a shallow (not bordered anteriorly and posteriorly by a distinct lip/crest) depression in most alcids (e.g., *Aethia psittacula*), although, in the a few species (e.g., *Alca torda*) it is a deep (bordered anteriorly and posteriorly by a distinct lip or crest) excavation bordered anteriorly by the temporal crest (Baumel and Witmer, 1993).

**33. Squamosal, temporal fossa, medial extent:** (0) not medially extended; (1) separated by a thin flat space; (2) separated only by a thin crest. In many alcids (e.g., *Aethia psittacula*) the temporal fossa is not expressed on the dorsal surface of the skull, although, in some species (e.g., *Alca torda*) the temporal fossa nearly converge on the dorsal surface of the skull. In *Pinguinus impennis* the temporal fossa are very deep and separated only by a thin crest. **Ordered**

**34. Squamosal, temporal fossa, shape of medial margin:** (0) narrow; (1) broad. In species that possess medially expanded temporal fossa (see character 32) the medial-most extent of the temporal fossa varies in alcids from a broad, relatively ‘U-shaped’ curve (e.g., *Alca torda*) to a more pointed, medially narrowing groove (e.g., *Uria aalge*).

**35. Supraoccipital foramina** (foramen venae occipitalis externae; Baumel and Witmer, 1993; Strauch, 1985, character 6; Chandler, 1990b, character 14): (0) absent; (1) present. Supraoccipital foramina are absent in the skulls of adult Lari and most other groups of charadriiforms (e.g., *Uria aalge*); they are present in some species of alcids (e.g., *Aethia pygmaea*; Strauch, 1985).

**36. Cerebellar prominence** (Chu, 1998, character 3): (0) strongly protruding; (1) weakly to moderately protruding. In contrast to charadriiforms with rounded (i.e., posteriorly convex) occipitals (e.g., *Xema sabini*) in which the cerebellar prominence does not protrude a great distance relative to the occipitals, the Alcidae (e.g., *Cephus grylle*) have anteroposteriorly-flattened occipitals, such that the cerebellar prominence noticeably protrudes posteriorly.

**37. Foramen magnum, dorsal margin shape** (modified from Strauch, 1978, character 19: (0) rounded; (1) pointed. The dorsal margin of the foramen magnum of most alcids (e.g., *Alca torda*) is rounded, while this feature in some alcids (e.g., *Alle alle*) is more pointed.

**38. Secondary articulation of mandible** (ala parasphenoidalis; Baumel and Witmer, 1993; Strauch, 1985, character 4; Chandler, 1990b, character 8): (0) well developed; (1) absent. The Laridae and Fraterculinae have a well-developed secondary articulation of the mandible (a.k.a., lateral process of the basisphenoid). The articulation is absent in the murrelets, *Cephus*, *Alle*, and the auks. Kozlova (1957) reported the presence of the basisphenoid processes associated with this articulation in alcids. Bock (1960) reported the articulation absent in alcids, but did not report which taxa he examined (Strauch, 1985).

**39. Quadrate** (Chandler, 1990b, character 10): (0) pneumatic; (1) apneumatic. While the medial surface of the quadrate of many charadriiforms (e.g., *Rynchops niger*) is perforated by a foramina, which leads to the pneumatic interior of the quadrate, the quadrate of all alcids in which this element is known (e.g., *Fratercula corniculata*) is apneumatic.

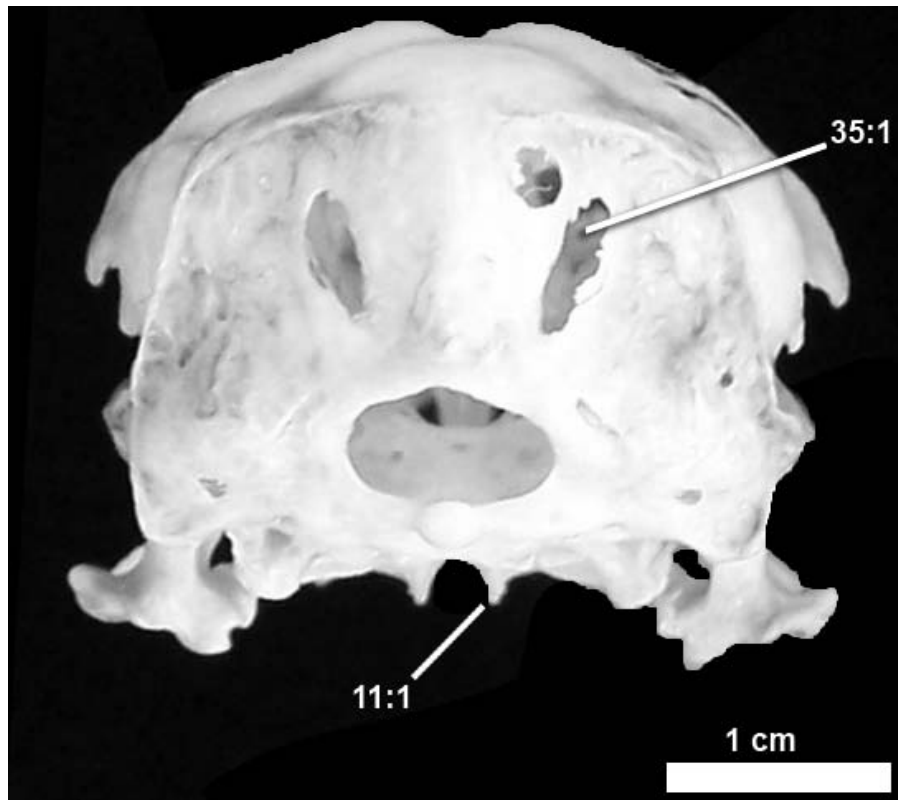


Figure A2.9- Skull of *Aethia cristatella* (NCSM 17749) in posterior view.

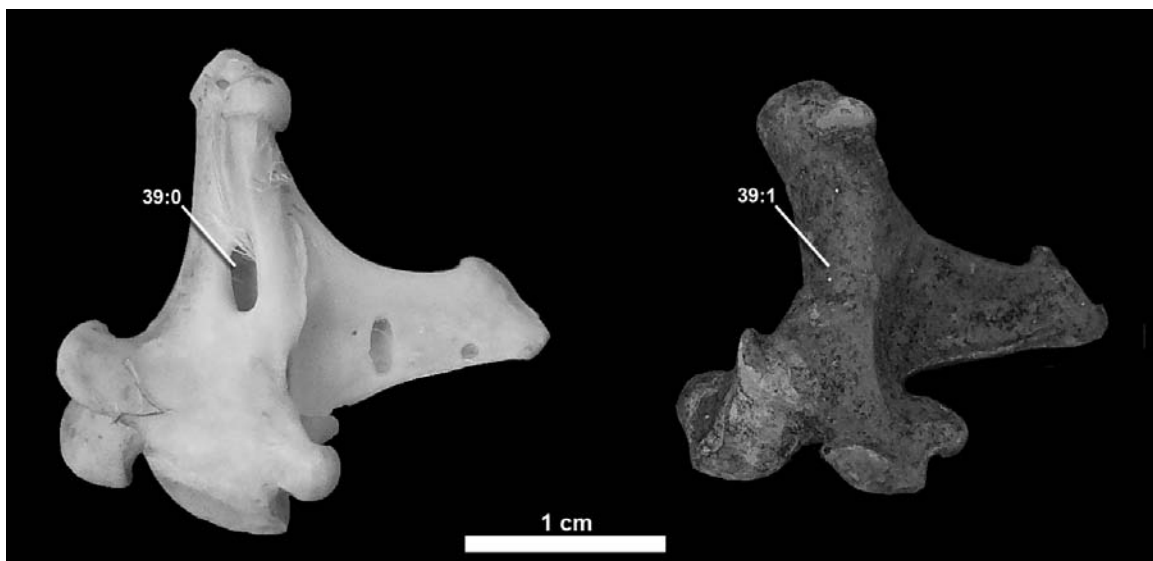


Figure A2.10- Left quadrates of *Larus marinus* (NCSM 10245) and *Pinguinus impennis* (USNM 623465) in medial view.

## MANDIBLE

**40. Mandible, length of symphysis** (modified from Chandler, 1990b, character 22): (0) short; (1) long. The left and right rami of the mandible fuse at the anterior end of the mandible. The length of area fused can be either short (i.e., <15% of the total length of the mandible; e.g., *Alca torda*) or long (i.e., >15% of the total length of the mandible; e.g., *Uria aalge*).

**41. Mandible, contact posterior to symphysis:** (0) non-contacting; (1) contacting. In most alcids (e.g., *Alca torda*) the mandibular rami are in contact only where fused at the symphysis. In Fraterculini (e.g., *Fratercula arctica*) the mandibular rami, although not fused, remain in contact posterior to the mandibular symphysis.

**42. Mandible, ventral expansion:** (0) absent; (1) present. The mandibles of most alcids (e.g., *Cephus columba*) are not ventrally expanded. The mandibles of some species (e.g., *Fratercula arctica*) have a pronounced ventral expansion at the anterior end of the mandible (i.e., beak tip).

**43. Mandible, thickening of junction between pars dorsalis and dorsal splenial** (Chu, 1998, character 56): (0) flat to moderate; (1) gross, forming massive longitudinal crista. The dorsomedial surface of the mandible is noticeably thickened in terns (e.g., *Sterna maxima*). In the Alcidae (e.g., *Cephus columba*) and most other charadriiforms, the medial surface of the mandible is flat (i.e., lateromedially compressed).

**44. Mandible, mediolateral curvature:** (0) laterally concave; (1) laterally convex. The mandibular rami of many alcids (e.g., *Fratercula arctica*) are laterally concave distal to the tip of the bill, while in other alcids (e.g., *Alle alle*) the rami are curved outward or laterally convex.

**45. Prearticular, anterior end** (modified from Chandler, 1990b, character 21): (0) forked; (1) not forked. The anterior-most end of the prearticular is forked (i.e., bifurcates around the distal edge of the rostral mandibular fenestra) in some alcids (e.g., *Alca torda*), while in other alcids (e.g., *Alle alle*) the prearticular is present only ventral to the rostral mandibular fenestra.

**46. Surangular, fenestration:** (0) absent; (1) present. The posterior mandible in many charadriiforms (e.g., *Larus marinus*) is perforated (fenestra caudalis mandibulae; Baumel and Witmer, 1993) just anterior to the lateral mandibular cotyla. Some charadriiforms (e.g., *Charadrius wilsonia*) lack this feature. This fenestra provides passage for a nerve, which originates inside the adductor mandibulae pars ventralis muscle, and passes medially through the caudal mandibular foramen and then continues along the medial surface of the angular.

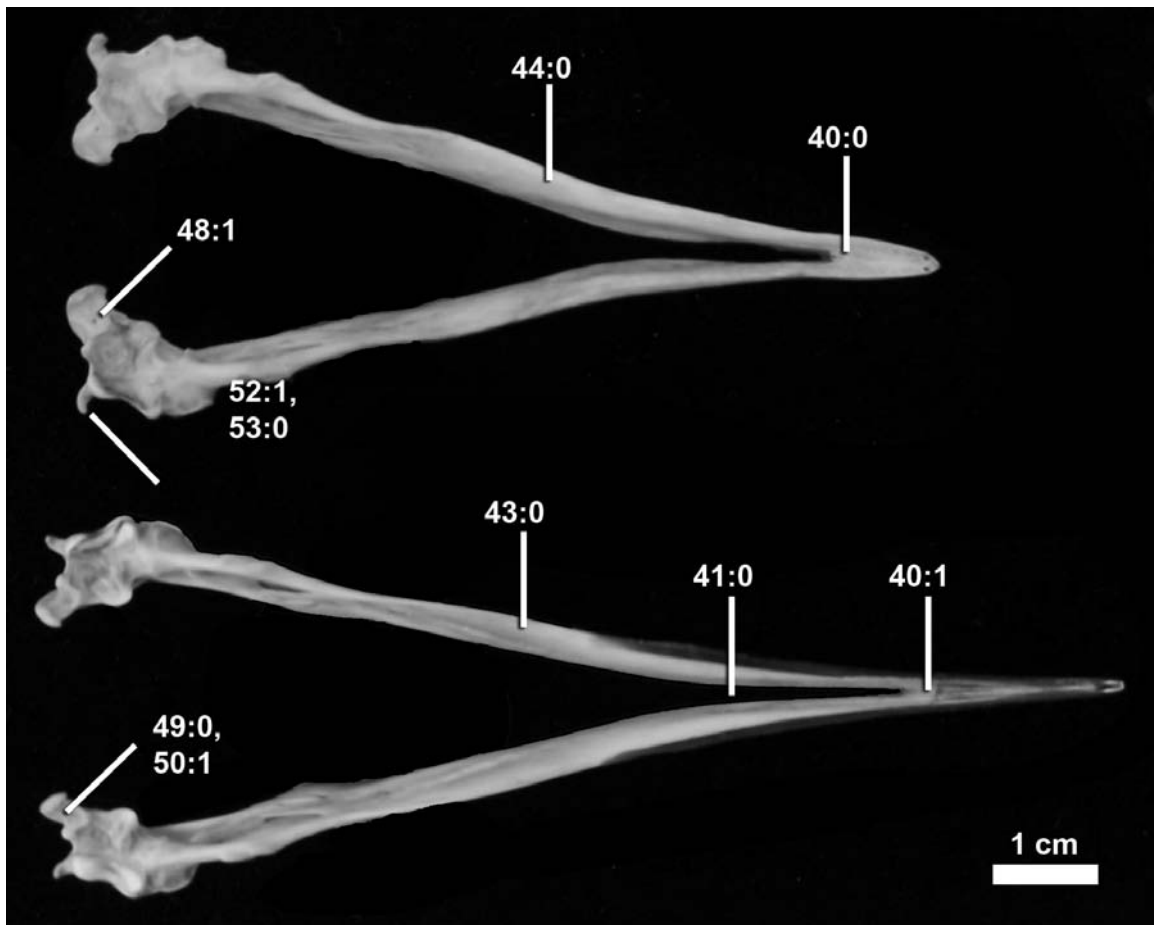


Figure A2.11- Mandibles of *Alca torda* (NCSM 20058; top) and *Uria aalge* (NCSM 18118; bottom) in dorsal view.

**47. Surangular, fenestration, quantity:** (0) one; (1) two. Most alcids (e.g., *Cepphus grylle*) have a single caudal mandibular fenestra, while the Fraterculini (puffins; e.g., *Fratercula arctica*) and Mancallinae (e.g., *Miomancalla howardi*) are characterized by the presence of two small caudal mandibular fenestrae perforating the dorsal surangular.

**48. Articular, medial articular process foramen** (foramen pneumaticum articulare; Baumel and Witmer, 1993; Chandler, 1990b, character 20): (0) absent; (1) present. An opening in the upper surface of the processus medialis mandibulae that leads to pneumatic spaces in the posterior segment of the mandibular ramus is present in some alcids (e.g., *Cepphus grylle*).

**49. Articular, medial articular process, shape:** (0) anteroposteriorly compressed; (1) dorsoventrally compressed; (2) rounded point. In posterior view the medial articular process of the mandible, which articulates with the parasphenoid process (Baumel and Witmer, 1993, p. 80) in many charadriiforms, varies in shape from an anteroposteriorly-

compressed projection (e.g., *Cepphus carbo*) to a dorsoventrally-compressed projection (e.g., *Alca torda*).

**50. Articular, medial articular process, orientation:** (0) projects medially; (1) projects posteromedially. The medial articular process of the mandible points medially in some alcids (e.g., *Fratercula cirrhata*), while in other alcids (e.g., *Cepphus grylle*) this same process points more posteriorly.

**51. Articular facet in ventral view, shape:** (0) rounded knob; (1) anteromedial projection. In ventral view, the articular facet of the mandible is visible as a small, often rounded knob in some alcids (e.g., *Alca torda*). In some alcids (e.g., *Cepphus grylle*) this facet is more pointed and projects anteromedially.

**52. Articular, retroarticular process** (modified from Chandler, 1990b, character 23): (0) absent; (1) present. This characteristic, although present in all alcids, is absent in many other Lari (e.g., *Stercorarius longicaudus*).

**53. Articular, retroarticular process length** (modified from Chandler, 1990b, character 23): (0) short; (1) long. In some species (e.g., *Aethia pygmaea*) the dorsoposteriorly projecting process of the cotyla lateralis is long (i.e., as long or longer than the dorsoventral height from the articular facet to the ventral margin of the mandible in lateral view), while in other species (e.g., *Alca torda*) this process is shorter.

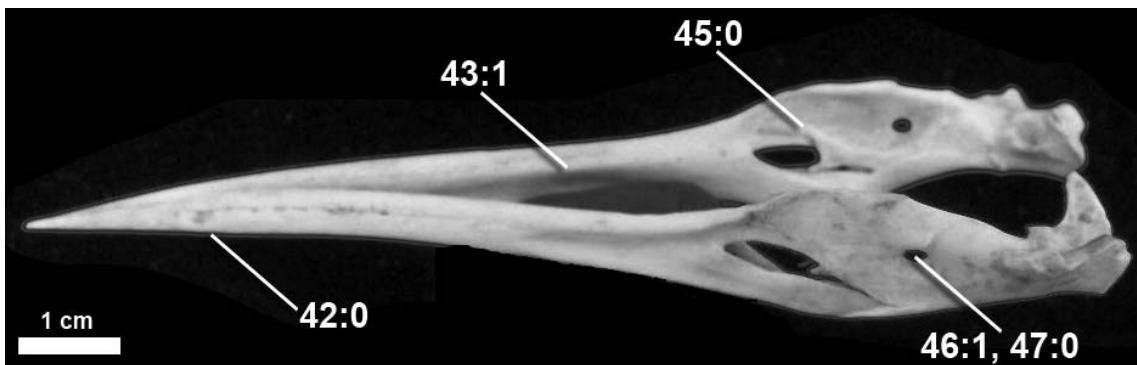


Figure A2.12- Mandible of *Sterna maxima* (NCSM 10248) in oblique dorsolateral view.

## VERTEBRAE

**54. Atlas, flange on the lateral margins of the arcus atlanticus in dorsal view::** (0) straight; (1) laterally angled. The posteriorly-projecting processes for articulation with the axis project posteriorly in most species of alcids (e.g., *Uria aalge*). In some species of alcids (e.g., *Fratercula arctica*) the zygapophyses angle laterally.



**55. Axis, dorsal extension of neural spine:** (0) short; (1) long. In posterior view, the neural spine of the axis in most alcids (e.g., *Uria aalge*) is short (i.e., less than half of the length of the neural spine extends above the level of the anapophyses), although in some alcids (e.g., *Alca torda*) this projection of the axis is lengthened and extends to a point well above the anapophyses (i.e., more than half of the length of the neural spine extends above the level of the anapophyses).

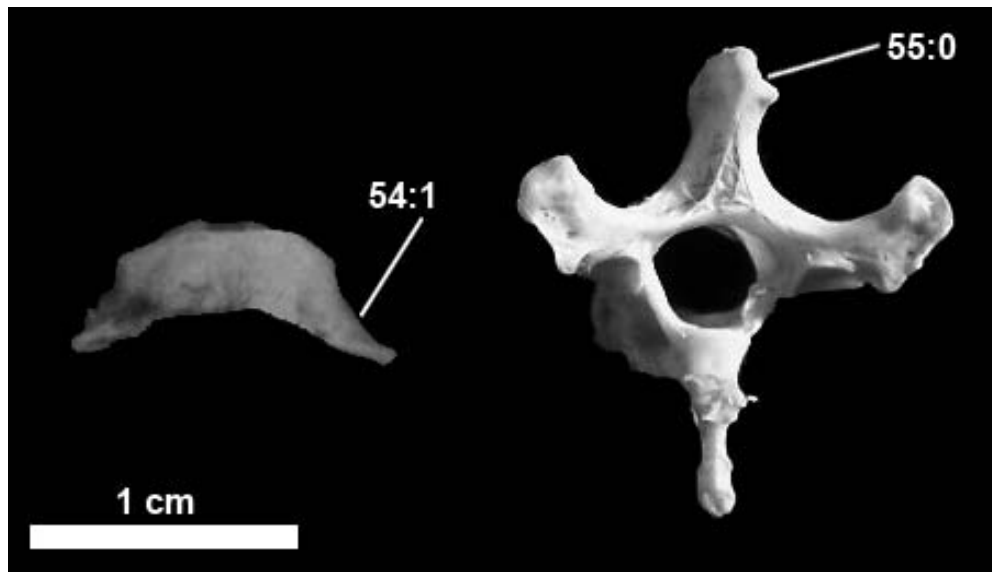


Figure A2.13- Atlas (left; dorsal view) and axis (right; posterior view) vertebrae of *Alca torda* (NCSM 20058).

**56. Thoracic vertebrae, hypapophyses:** (alae cristae ventralis; Baumel and Witmer, 1993; modified from Strauch, 1985, character 14): (0) not present on any thoracic vertebrae; (1) present on some thoracic vertebrae. The Lari and other non-alcid charadriiforms (e.g., *Larus marinus*) have poorly developed hypapophyses on their thoracic vertebrae. Well-developed hypapophyses, most with bilateral flanged wings, are found in all alcids, but the number of vertebrae on which they occur varies among the species. These structures serve as increased area for attachment of m. longus colli ventralis, are functionally correlated with the strength needed by diving birds (Kuroda, 1954). It is hypothesized that a greater number of vertebrae with well-developed hypapophyses is a more derived condition. Similar structures are found in other diving birds such as loons, grebes, penguins, and some anseriforms (Beddard, 1898 in Strauch, 1985).

**57. Thoracic vertebrae, number of hypapophyses** (crista [processus] ventralis corporis; Baumel and Witmer, 1993; modified from Strauch, 1985, character 14): (0) well developed on all thoracic vertebrae; (1) well developed on all but last vertebrae; (2) well developed on all but last two vertebrae; (3) well developed on all but last three vertebrae;

(4) well developed on all but last four vertebrae; (5) well developed on all but last five vertebrae. **Ordered**

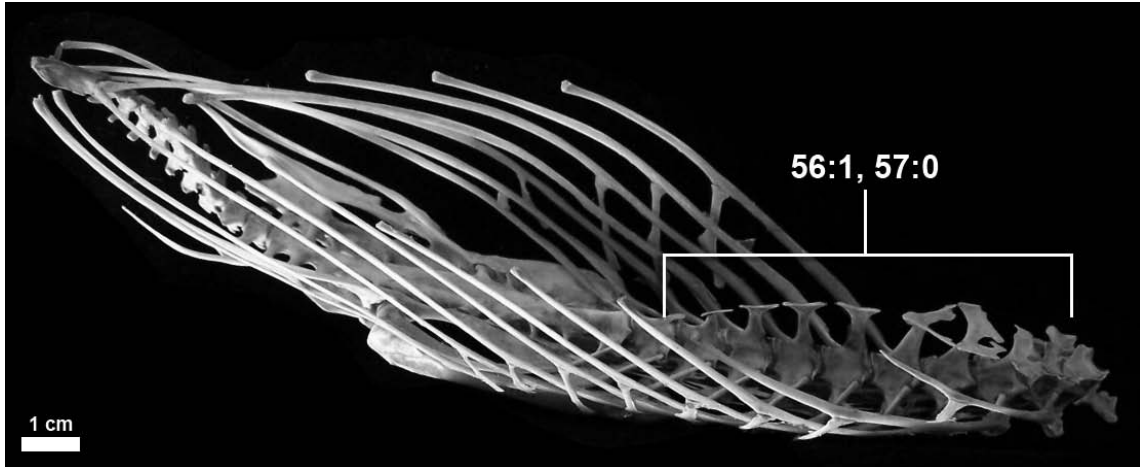


Figure A2.14- Vertebrae and pelvis of *Uria aalge* (NCSM 18117) in oblique ventral view.

**58. Pygostyle, dorsal margin** (Chu, 1998, character 67): (0) dorsally restricted; (1) dorsally expanded. In contrast to the dorsally expanded pygostyle observed in all other charadriiforms examined during this study (e.g., *Larus argentatus*), the Alcidae are characterized by a pygostyle lacking dorsal expansion.

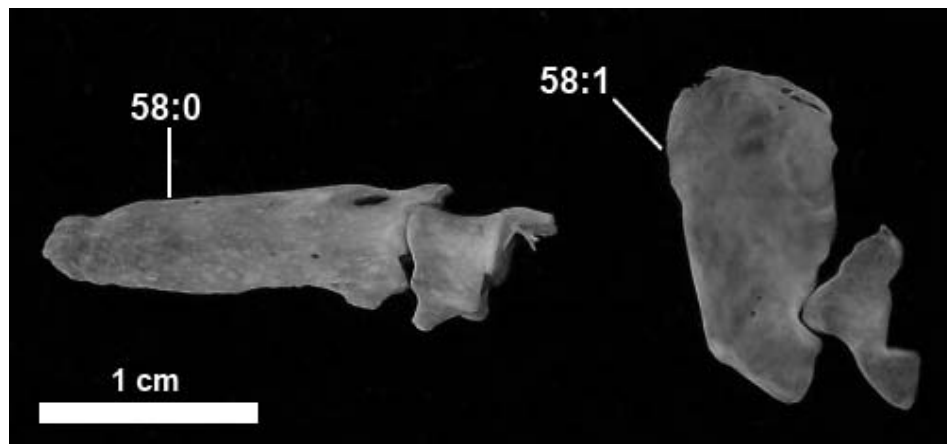


Figure A2.15- Pygostyle and caudal vertebrae of *Alca torda* (NCSM 20058; left) and *Larus argentatus* (NCSM 8624; right) in lateral view.

## STERNUM

**59. Sternum, coracoidal sulci, separation** (modified from Chandler, 1990b, character 35): (0) continuous above dorsal manubrium; (1) sulci separated by manubrium. The sternal articular surface of the coracoid is a continuous, smooth, depression in many charadriiforms (e.g., *Larus marinus*), while in Alcidae (e.g., *Alca torda*) the sulci are separated by the manubrium (i.e., rostrum sterni; Baumel and Witmer, 1993).

**60. Sternum, anterior pneumatic foramen:** (0) reduced; (1) pneumatic. The pneumatic foramen located at the anterior end of the sternal basin is reduced to a tiny ‘pin-sized’ hole in alcids (e.g., *Alca torda*). In most other charadriiforms examined (e.g., *Larus marinus*) this feature is a deep pneumatic foramen.

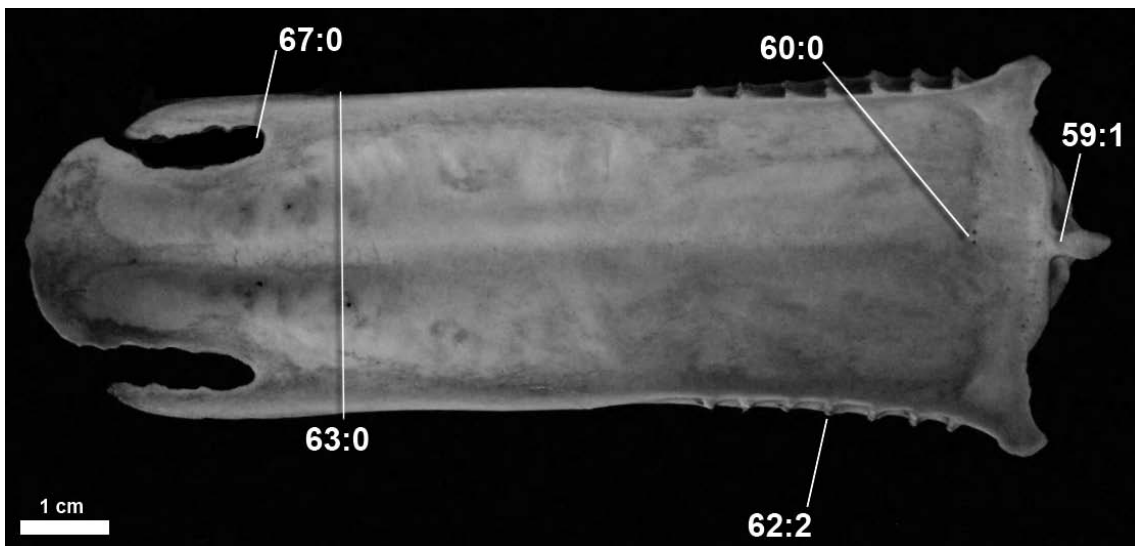


Figure A2.16- Sternum of *Uria aalge* (NCSM 18118) in dorsal view.

**61. Sternum, craniolateral process, orientation** (Strauch, 1985, character 10; Chandler, 1990b, character 36): (0) points dorsally; (1) points anteriorly. In the Lari and most other charadriiforms the sternocoracoidal process (processus craniolateralis, Baumel and Witmer, 1993) of the sternum points dorsally; in the puffins (e.g., *Fratercula arctica*), auklets (e.g., *Aethia psittacula*) and Mancallinae (e.g., SDSNH 26242) it points anteriorly.

**62. Sternum, costal processes, quantity** (Strauch, 1985, character 12; Chandler, 1990b, character 41): (0) five; (1) six; (2) seven. Although some charadriiforms (e.g., *Glareola maldivarum*) not closely related to Alcidae have five costal processes of the sternum, the Lari and most other charadriiforms (e.g., *Larus marinus*) have six. Some alcids (e.g., *Alca torda*) have seven. **Ordered**

**63. Sternum, width** (modified from Chandler, 1990b, character 39): (0) narrow posteriorly; (1) broad posteriorly. In dorsal view the posterior sternum of most alcids (e.g., *Aethia pygmaea*) is lateromedially broader than the anterior sternum (i.e., the area of the sternum proximal to the distal-most costal process), while in other species (e.g., *Alca torda*) the sternum is roughly the same width throughout its length.



Figure A2.17- Sterni of *Uria aalge* (NCSM 18118; top) and *Cerorhinca monocerata* (USNM 557614; bottom) in lateral view.

**64. Sternum, medial notch** (Strauch, 1985, character 8): (0) absent; (1) present. Most charadriiforms (e.g., *Larus marinus*) have a medial sternal notch, but several, including members of the Lari and Alcidae (e.g., *Aethia pusilla*), do not. Distribution of the states among other charadriiforms thus does not indicate which state is primitive in the alcids. Only the puffins (Fratrunculini) retain the remnant of the medial sternal notch as a medial sternal fenestra.

**65. Sternum, medial notch, shape:** (0) a notch; (1) a fenestra. Among alcids, only the puffins (Fratrunculini) retain the remnant of the medial sternal notch as a medial sternal fenestra.

**66. Sternum, lateral notch, shape** (Strauch, 1985, character 9; Chandler, 1990b, character 38): (0) a notch; (1) a fenestra. Almost all charadriiforms (including all Lari) have a lateral sternal notch. In the auklets it is reduced to a fenestra, a condition assumed to be a derived state in the Alcidae. Shufeldt (1888, 1889) and Lucas (1890) reported that in the auks the lateral sternal notch tends to become ossified with age. This condition clearly differs from that in the auklets; it is hypothesized to represent merely a variant of the state with the notch present. Kuroda (1954, 1955) illustrated the variation with age of the sternal notching of some alcids (Strauch, 1985).

**67. Sternum, lateral notch, anterior extent of incisure:** (0) shallow; (1) deeply incised. In most charadriiforms, the extent to which the lateral sternal notches incise proximally is limited (e.g., *Larus marinus*), while in some charadriiforms (e.g., *Mancalla vegrandis*), these incisures are extensive.

**68. Sternum, posterior extension of carina relative to lateral sternal notches/fenestrae** (modified from Chandler, 1990b, character 40): (0) carina extends to distal ends of notches/fenestrae; (1) lateral sternal notches/fenestrae extend posteriorly beyond posterior extent of carina. The length of the carina relative to the posterior extent of the lateral sternal notches/fenestrae of alcids varies from extending to a point about equally posterior to the posterior margins of the lateral sternal notches/fenestrae in some alcids (e.g., *Alca torda*), to a condition in which the lateral sternal notches/fenestrae extend posterior to the carina (e.g., *Aethia cristatella*).

**69. Sternum, m. supracoracoideus scar, position:** (0) angled medially; (1) straight. In contrast to the condition observed many charadriiforms (e.g., *Sterna maxima*) in which the scar for the supracoracoideus muscle on the ventral surface of the sternum angles medially from the coracoidal sulcus towards the carina, in Alcidae this scar extends posteriorly for almost the entire length of the carina. This feature is correlated with the increased resistance during the upstroke experienced by alcids while flying underwater (Kozlova, 1957).

**70. Sternum, posterior margin ossification** (margo caudalis sterni; Baumel and Witmer, 1993; modified from Chandler, 1990b, character 43): (0) not ossified; (1) ossified. The posterior-most portion of the sternum is an ossified posteriorly projecting structure in many species (e.g., *Uria lomvia*), while in other species (e.g., *Brachyramphus marmoratus*) it is completely unossified and not preserved in dry skeletal specimens.

**71. Sternum, length of area between distal extent of medial fenestra and posterior margin** (modified from Chandler, 1990b, character 43): (0) short; (1) long. The ossified area of sternum posterior to the termination of the carina (i.e., the xiphial area sensu Howard, 1929) is short (i.e., wider than long) in some alcids (*Alle alle*), while in others (e.g., *Cephus grylle*) this feature is much longer (i.e., nearly as long or longer than it is wide).

**72. Sternum, length:** (0) short; (1) long. When compared to their immediate outgroup, the Stercorariidae, alcids have an elongated sternum (i.e., sternum  $>2\times$  long than wide), a character which has been associated with diving (Storer, 1960). The greatest length of the sternum (i.e., from the anterior manubrium to the distal xiphoid) is more than two times the width of the sternum across the sternocoracoidal processes in all alcids (e.g. *Alca torda*).

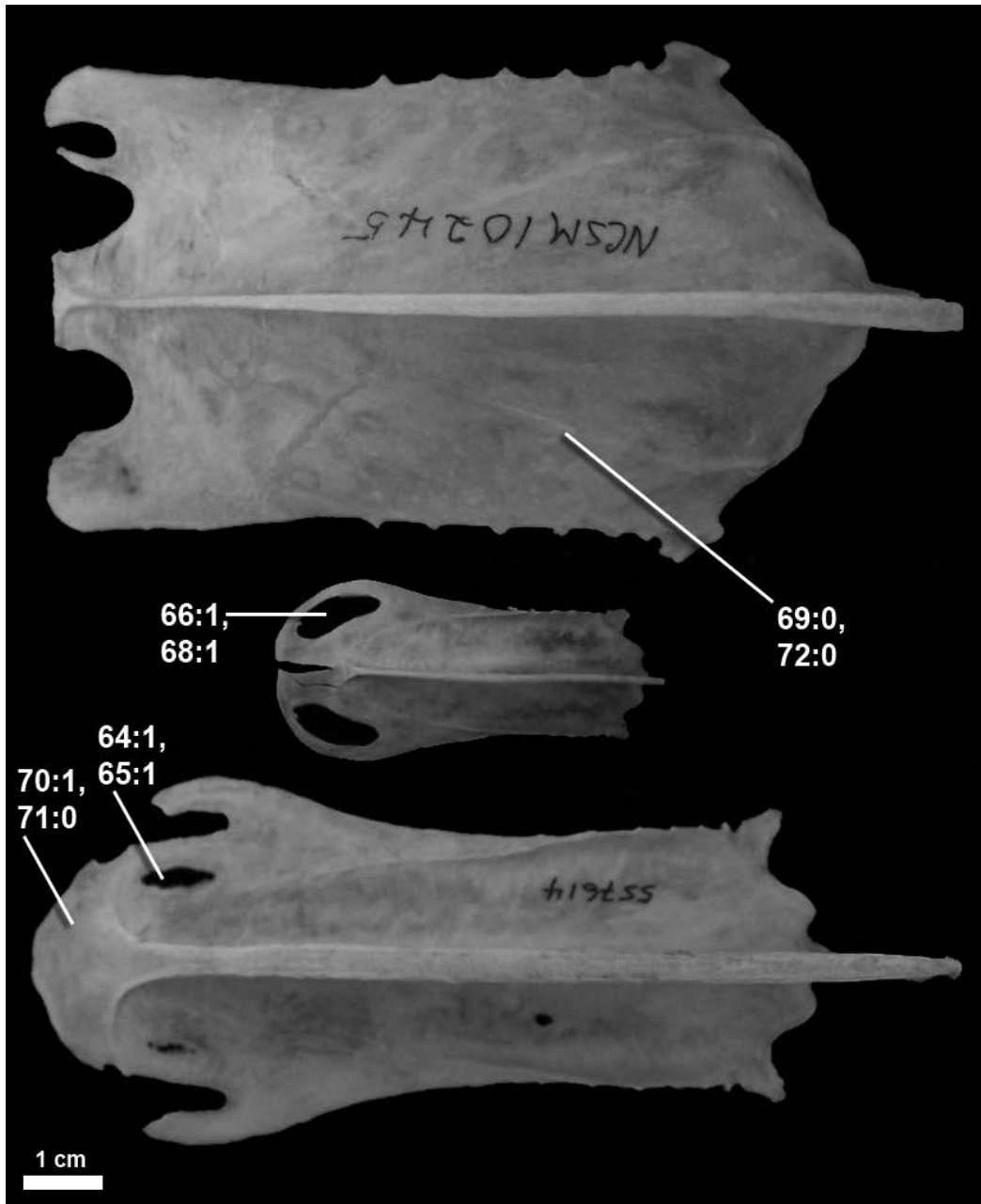


Figure A2.18- Sterni of *Larus marinus* (NCSM 10245; top), *Aethia pusilla* (NCSM 17734; middle), and *Cerorhinca monocerata* (USNM 557614; bottom) in ventral view.

## FURCULA

**73. Furcular, symphysis (apophysis), size** (modified from Chandler, 1990b, character 30): (0) large; (1) small. A medially oriented crest-like projection characterizes the furcular symphysis of alcids. This crest can be either small (i.e., projects less than the width of individual clavicles at symphysis; *Aethia psittacula*) or large (i.e., projection as wide or wider than that of individual clavicles at symphysis; (e.g., *Brachyramphus marmoratus*).

**74. Furcula, anterior surface of rami** (Strauch, 1978, character 41): (0) smooth; (1) grooved. The anterior surface of the furcula dorsal to the apophysis is characterized by a distinct mediolaterally oriented groove or concavity in some alcids (e.g., *Cepphus grylle*; see Strauch, 1978, Fig.22, pg.310). The furculae of other alcids (e.g., *Alca torda*) are rounded or convex on the anterior surface of the furcula dorsal to the furcular symphysis.

**75. Furcula, symphysis, anterior tubercle:** (0) absent; (1) present. A dorsally pointing tubercle on the anterior edge of the apophysis is present in *Alca torda* and *Alca carolinensis*, but is absent in all other alcids in which the furcula is known.

**76. Furcula, symphysis, posterior tubercle:** (0) absent; (1) present. A dorsally pointing tubercle on the posterior edge of the apophysis is a proposed autapomorphy of *Alca carolinensis*.

**77. Furcula, cristae on anterior surface of rami:** (0) absent; (1) present. The anterior surface of the furcular rami dorsal to the apophysis is characterized by the presence of small cristae/tubercles in some alcids (e.g., *Alca torda*).

**78. Furcula, curvature of omal extremity** (Chu, 1998, character 76): (0) smoothly curving; (1) sharply curved or angled at posterior extremity. The transition from the dorsally extending shaft of the clavicles to the omal extremity of the clavicles in Alcidae (e.g., *Brachyramphus perdix*) is characterized by a distinctly angular bend. The furculae of all other charadriiforms (e.g., *Larus marinus*) examined during the course of this study exhibited a more gently sloping furcular curvature.

**79. Furcula, dorsoventral expansion of omal extremity:** (0) absent; (1) present. Ventral to the coracoidal facet, the clavicles of most alcids (e.g., *Pinguinus impennis*) are dorsoventrally expanded and lateromedially compressed (i.e., bladelike; scapular tuberosity much thinner than clavicular shaft ventral to the coracoidal facet). The clavicles of many other charadriiforms (e.g., *Tryngites subruficollis*) are more circular in cross section and much less dorsoventrally expanded (i.e., scapular tuberosity same width or thicker than clavicular shaft ventral to the coracoidal facet).

**80. Furcula, coracoidal tuberosity, position relative to coracoidal facet** (Chandler, 1990b, character 33): (0) medially adjacent to coracoidal facet; (1) separate and anterior

to facet. The coracoidal tuberosity contacts the medial margin of the coracoidal facet in many charadriiforms (e.g., *Gygis alba*), whereas in alcids (e.g., *Brachyramphus perdix*), this tuberosity is more robust, separate from, and anterior to the coracoidal facet.

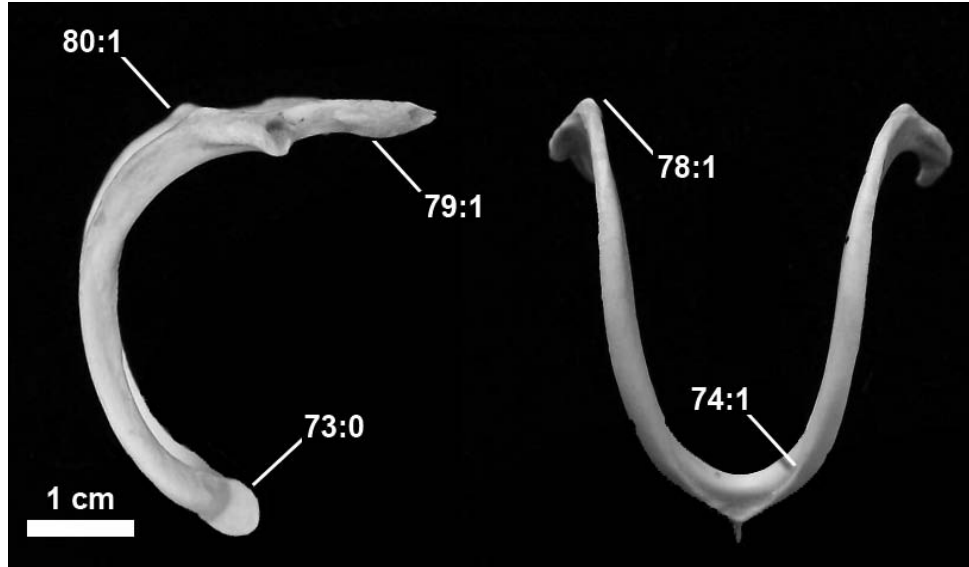


Figure A2.19- Furcula of *Cephus columba* (NCSM 18096) in left lateral (left) and anterior (right) views.



Figure A2.20- Furcula of *Alca torda* (USNM 502388; left) in ventral view and *Alca carolinensis* (NCSM 13474; right) in anterior view.



## SCAPULA

**81. Scapula, acromium, attachment of acrocoracoacromiale ligament in proximal view:** (0) anteriorly oriented pit; (1) laterally oriented scar. In some alcids (e.g., *Uria aalge*), the attachment of the acrocoracoacromiale ligament is an anteriorly oriented excavation of the ventral surface of the acromium process bordered medially by a crest. This same attachment point in other alcids (e.g., *Aethia cristatella*) is rotated laterally and is characterized by a relatively smooth attachment surface.

**82. Scapula, acromium, shape in lateral view:** (0) blunt, rounded; (1) angular, pointed. The acromium process of all extant alcids (e.g., *Uria aalge*) has a pointed proximal tip, while the tip of the acromium in some larids (e.g., *Larus marinus*) is rounded/truncated and does not project anteriorly.

**83. Scapula, scapulothoracic tubercle:** (0) absent; (1) present. A raised process for attachment of m. scapulothoracicus on the ventral surface of the scapula (tuberculum m. scapulothoracicus, Baumel and Witmer, 1993) just distal to the glenoid facet is present in flightless alcids (e.g., *Pinguinus impennis*) but absent in all extant alcids (e.g., *Alca torda*). The presence of this structure in penguins (Schreiweis, 1982), argues in favor of it being correlated with flightlessness.

**84. Scapula, width of distal extremity:** (0) tapering; (1) dorsoventrally expanded. The dorsal margin of the scapula (margo dorsalis; Baumel and Witmer, 1993) is expanded dorsally in some species of alcids (e.g., *Cerorhinca monocerata*). The distal ends of the scapulae of other alcids (e.g., *Aethia pygmaea*) are tapered to a point.

**85. Scapula, shape of distal extremity:** (0) curved; (1) angled. In contrast to the gently ventrally curving distal extremity of many charadriiforms (e.g., *Larus argentatus*), the scapulae of all known alcids are characterized by a ventrally directed angular bend proximal to the distal most extremity.

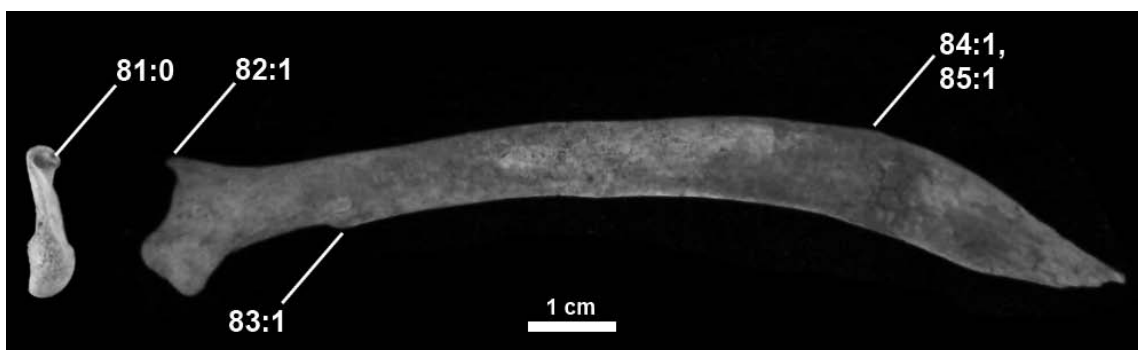


Figure A2.21- Left scapula of *Pinguinus impennis* (USNM 623465) in proximal (left) and lateral (right) views.

## CORACOID

**86. Coracoid, furcular facet shape** (modified from Chandler, 1990b, character 28): (0) oval; (1) rounded. The furcular facet of the coracoid is rounded in the puffins and auklets (e.g., *Fratercula arctica*) but is more oval with a vertical long axis in the auks and murrees (e.g., *Uria lomvia*).

**87. Coracoid, furcular facet, notch posterior to bicipital tubercle:** (0) absent; (1) present. The ventral margin of the furcular facet is curves dorsally just posterior to the process for the attachment of the bicipital muscle in some species of alcids (e.g., *Uria aalge*). The ventral margin of this feature in other alcids (e.g., *Alca torda*) is gently curved but not notched.

**88. Coracoid, m. supracoracoideus sulcus:** (0) pneumatic; (1) apneumatic, but deeply undercut; (2) not deeply undercut. The medial side of the distal end or head of the coracoid of some charadriiforms (e.g., *Anous tenuirostris*) are characterized by a pneumatic excavation. The coracoids of all alcids are apneumatic, although the brachial crest is deeply undercut for the passage of the supracoracoideus muscle in some species of alcids (e.g. *Cephus grille*), while in some alcids (e.g., *Cerorhinca monocerata*) the brachial crest is not deeply undercut (i.e., ventrally concave). **Ordered**

**89. Coracoid, brachial tuberosity, shape:** (0) a tubercle; (1) a crest. The brachial tuberosity is developed as an anteroposteriorly oriented crest in some alcids (e.g., *Cephus grille*), while in other alcids (e.g., *Aethia psittacula*) the brachial tuberosity is developed simply as a small rounded tubercle positioned roughly at the midpoint on the neck of the coracoid. The term brachial crest is used here to describe the latter condition.

**90. Coracoid, brachial tuberosity, shape in medial view:** (0) approximately straight; (1) distinctly curved. In species that possess a brachial crest rather than a brachial tubercle (see character 88), the crest varies from an approximately straight crest (e.g., *Alle alle*) to a distinctly concave curve (e.g., *Alca torda*).

**91. Coracoid, neck in dorsal view** (Chandler, 1990b, character 29): (0) short; (1) long. The neck of alcid coracoids (defined here as the head of the coracoid distal to the distal-most extent of the glenoid facet), which extends medially to articulate with the furcula, is elongate (i.e., considerably longer than wide) in some species (e.g., *Uria aalge*) and gives the neck of the coracoid a rectangular appearance in dorsal view. In other species (e.g., *Fratercula cirrhata*) this neck is shorter (i.e., roughly as wide as it is long) and results in a rather square coracoidal neck.

**92. Coracoid, m. supracoracoideus scar development:** (0) a distinct ridge; (1) ridge reduced or absent. Contact with m. supracoracoideus creates a distinct, medially oriented ridge/scar in most alcids (e.g., *Alca torda*) that gives the shaft of the coracoid a distinctly

angular cross-section, while in *Cepphus* this structure is greatly reduced or absent and the cross-section of the coracoid element is more rounded.

**93. Coracoid, n. supracoracoideus foramen** (Strauch, 1985, character 13; Chandler, 1990b, character 25): (0) absent; (1) present. The Lari and most other charadriiforms have a coracoidal foramen (e.g., *Pinguinus impennis*); it is absent in some species of alcids (e.g., *Aethia pusilla*; Strauch, 1985).

**94. Coracoid, position of n. supracoracoideus foramen** (0) distal; (1) proximal. In alcids that possess a procoracoidal foramen, the position of this feature is typically near the midpoint of the of the procoracoid process near the shaft of the coracoid (e.g., *Pinguinus impennis*), although in *Cepphus* this foramen is positioned on the extreme anteroproximal edge of the procoracoid process leaving only a very thin strut of bone which forms the dorsal margin of the procoracoid process.

**95. Coracoid, procoracoid process, shape:** (0) rectangular; (1) triangular; (2) wing-shaped. The procoracoid process of some alcids (e.g., *Aethia psittacula*) is ‘strap-like’ and has a roughly rectangular shape, resembling the condition in the outgroup to Alcidae. The shape of the procoracoid process in most alcids (e.g., *Fratercula cirrhata*) is triangular.

**96. Coracoid, procoracoid process, orientation:** (0) points dorsomedially; (1) points ventromedially; (2) points anteriorly. The tip of the procoracoid process in the auklets (e.g., *Aethia pygmaea*) is hooked, and points ventromedially, while in all other alcids (e.g., *Uria aalge*) the tip of the procoracoid process points dorsomedially. In many other charadriiforms (e.g., *Larus marinus*) the procoracoid process is noticeably hooked to provide passage for the m. supracoracoideus tendon, and as a result the tip of the procoracoid process points anteriorly.

**97. Procoracoid process, shape of proximal edge:** (0) concave; (1) convex. In posterior view the proximal edge of the procoracoid process (lower or sternal side) in some alcids (e.g., *Cerorhinca monocerata*) curves convexly. The procoracoid process of other alcids (e.g., *Uria aalge*) is concave in curvature.

**98. Coracoid, tip of procoracoid:** (0) straight; (1) hooked. In *Brachyramphus*, the tip of the procoracoid is hooked anteriorly. This feature is absent in all other Alcidae for which the coracoid is known.

**99. Coracoid, excavation along anterior face of lateral edge of coracoid:** (0) absent; (1) present. Alcids (e.g., *Cepphus grylle*) possess a distinct scar along the anterior surface of the lateral process that is lacking in other charadriiforms (e.g., *Bartramia longicauda*). The exact origin of this scar is unclear, although Fürbringer (1888) discusses several accessory ligaments that attach in this area.

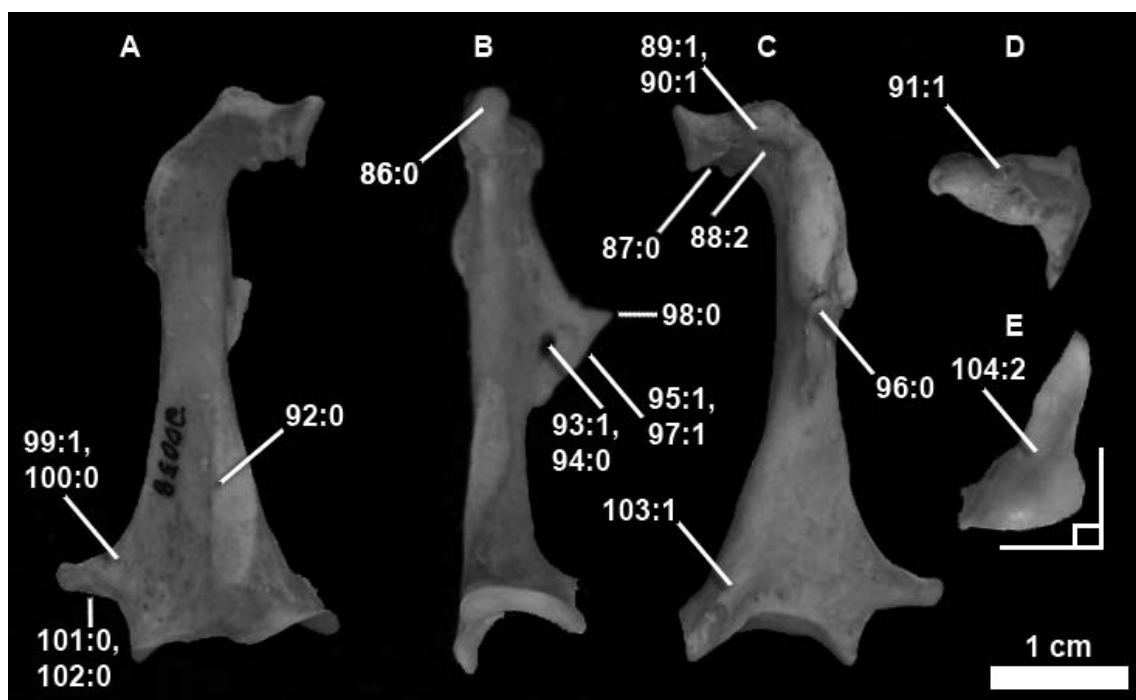


Figure A2.22- Right coracoid of *Alca torda* (NCSM 20058) in (A) anterior; (B) medial; (C) posterior; (D) omal; and (E) sternal views.

**100. Coracoid, extension of excavation along anterior surface of lateral process:** (0) extends to sternal articulation; (1) bordered sternally by crest. This scar is less medially and sternally extended and more excavated in the auklets and puffins (e.g., *Fratercula cirrhata*) than in other alcids (e.g., *Alca torda*) in which this scar is less excavated and extends to the sternal margin of the coracoid (i.e., not bordered sternally by a crest).

**101. Coracoid, crest along sternal edge of lateral process:** (0) absent; (1) present. In anterior view the sternal edge of the lateral process of some alcids (e.g., *Uria aalge*) is characterized by a crest or thickening of the sternal margin. This characteristic is absent in some alcids (e.g., *Alca torda*).

**102. Coracoid, lateral (sternocoracoidal) process length** (modified from Strauch, 1985, character 11): (0) elongate, with anteriorly pointing tip; (1) short, with laterally pointing tip. The lateral process of the coracoid is a well developed, elongate projecting process with an anteriorly projecting tip in most alcids (e.g., *Alca torda*) the Laridae and most other charadriiforms; it is absent or poorly developed in some of the auklets (e.g., *Aethia pusilla*). These differences are illustrated by Kuroda (1954: Fig. 7) and are mentioned by Shufeldt, 1889 in Strauch, 1985).

**103. Coracoid, medial sternal process, notch in dorsal margin:** (0) absent; (1) present. The posteromedial margin of the proximal coracoidal shaft just distal to the medial sternal articulation (angulus medialis; Baumel and Witmer, 1993) is characterized by a

small dorsoanterior oriented projection, giving the shaft a notched appearance in medial view at this point in most alcids (e.g., *Aethia cristatella*). The medial angle is more pointed in other alcids (e.g., *Alca torda*).

**104. Coracoid, sternal facet curvature** (Chandler, 1990b, character 26): (0) angled  $\sim 135^\circ$ ; (1) angled  $\sim 90^\circ$ ; (2) angled  $>90^\circ$ . Among the alcids the sternal articulation facet of the coracoid varies, the anterior margin curving roughly  $135^\circ$  in some (e.g., *Cepphus grylle*), roughly  $90^\circ$  in others (e.g., *Alca torda*), and greater than  $90^\circ$  in the auklets (e.g., *Aethia pusilla*). **Ordered**

## HUMERUS

**105. Humerus, head, distal extent of posterior margin (caput):** (0) rounded, convex curve; (1) pointed. The distally overturned posterior margin of the humeral head of some alcids (e.g., *Cepphus grylle*) is characterized by a distinct, distally extending semi-triangular point. The margin of this feature is rounded in most other alcids (e.g., *Alca torda*).

**106. Humerus, dorsal caput, posterior side** (modified from Chandler, 1990b; character 49): (0) not notched; (1) notched. The posterior surface of the dorsal caput in proximal view is notched ventral to the dorsal tubercle in some species of alcids (e.g., *Pinguinus impennis*) owing to the posterior projection of the m. supracoracoideus scar, whereas in some alcids (e.g., *Fratercula cirrhata*) this transition curves gently anteriorly (i.e., is not notched).

**107. Humerus, deltopectoral crest, distal extension** (modified from Chandler, 1990b, character 53): (0) does not extend to midpoint of shaft; (1) extends distally to the midway point of shaft; (2) extends beyond the midpoint of the humeral shaft. The deltopectoral crest extends distally along the anterodorsal margin of the humeral shaft to a point roughly  $\frac{1}{3}$  to one half of the distance towards the distal end of the shaft in most species of alcids (e.g., *Fratercula arctica*), while in *Pinguinus* the deltopectoral crest extends to the halfway point along the shaft. In *Mancalla* this crest extends distally beyond the midpoint of the shaft.

**108. Humerus, deltopectoral crest, transition to shaft:** (0) smooth; (1) abrupt. As noted by Howard (1982) the deltoid crest merges smoothly with the shaft of the humerus in most alcids (e.g., *Pinguinus impennis*) while in some alcids (e.g., *Fratercula arctica*) this transition is more abrupt or angled.

**109. Humerus, deltopectoral crest, dorsal curvature:** (0) concave; (1) flat. In dorsal view, the area between the dorsal surface of the deltopectoral crest and the dorsal tubercle (i.e., the dorsal shaft distal to the head) is concave in many charadriiforms (e.g., *Creagrus furcatus*). In all alcids except *Alca stewarti* this space is flat or slightly convex in some cases (e.g., *Brachyramphus marmoratus*).

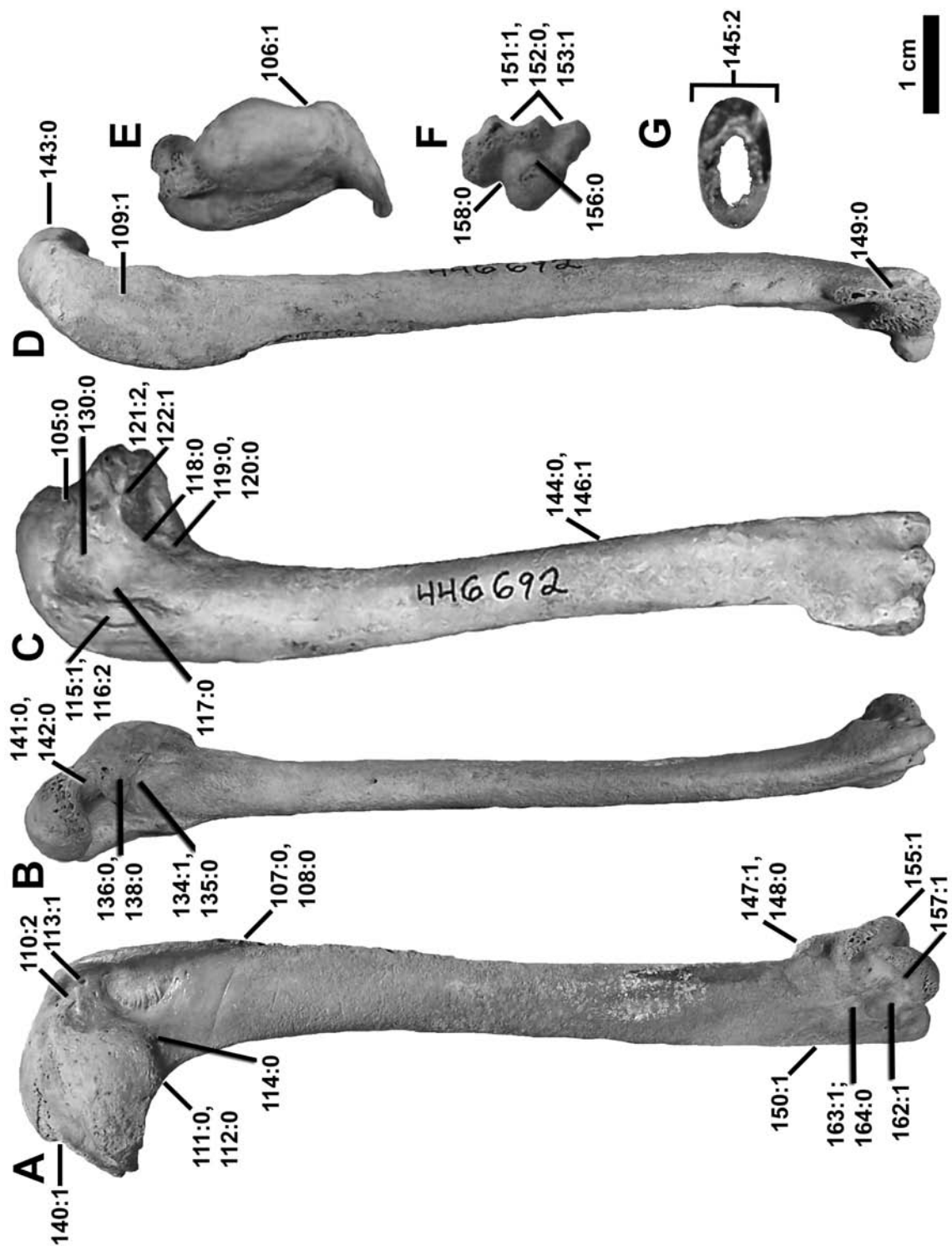


Figure A2.23- Left humerus of *Alca ausonia* (USNM 446692) in anterior (A); ventral (B); posterior (C); dorsal (D); proximal (E); and distal (F) views, and cross-sectional view of Pan-Alcidae humerus (GCV 5690; G).

**110. Humerus, coracobrachial impression, depth** (Chandler, 1990b, character 60): (0) very deep; (1) deep; (2) shallow. The scar for attachment of the impressio coracobrachialis muscle in alcids (e.g., *Aethia psittacula*) is a shallow (i.e., smoothly transitions to anterior surface of humeral head), usually rounded impression (e.g., *Alca torda*). This is in contrast to the condition in most other charadriiforms, in which this muscle scar is a very deeply excavated, usually triangular pit. **Ordered**

**111. Distal edge of bicipital crest, angle with respect to long axis of shaft:** (0) not perpendicular; (1) nearly perpendicular. The ventral edge of the bicipital crest forms a nearly perpendicular angle to the shaft in some species (e.g., *Pinguinus impennis*) while in other species (e.g., *Alca torda*) the bicipital crest is positioned at an obtuse angle with respect to the long axis of the humeral shaft.

**112. Humerus, bicipital crest, transition to shaft:** (0) smooth; (1) notched. This character, noted by Olson and Winker, (2009), varies from a condition where (in anterior view) the bicipital crest transitions smoothly onto the humeral shaft (e.g., *Aethia pusilla*) to a condition in which there is a distinct notch or separation between these structures (e.g., *Alle alle*).

**113. Humerus, n. coracobrachialis sulcus, conformation:** (0) open sulcus; (1) closed duct. As noted by Olson and Winker, (2009), the coracobrachial sulcus is an open sulcus in most species of alcids (e.g., *Aethia pusilla*), although in some species of alcids (e.g., *Alca torda*) the sulcus is enclosed to form a duct.

**114. Humerus, n. coracobrachial sulcus, curvature: (0) dorsal; (1) ventral.** The distal most point of the bicipital surface, as defined by the curvature of the coracobrachial sulcus, which curves or angles dorsal to the bicipital crest on the anterior surface of the humerus in some alcids (e.g., *Pinguinus impennis*), while in other alcids (e.g., *Alle alle*) the coracobrachial sulcus and the distal edge of the bicipital surface extend ventrally to terminate where the bicipital crest contacts the ventral surface of the humeral shaft.

**115. Humerus, m. supracoracoideus scar, depth:** (0) deep; (1) shallow. The attachment of m. supracoracoideus on the posterior humerus is a deep (i.e., excavated) scar in puffins (e.g., *Fratercula arctica*) and a shallow (i.e., basically flat) impression in others (e.g., *Cepphus grylle*).

**116. Humerus, m. supracoracoideus scar, shape:** (0) round; (1) long, proximally broadening; (2) long, does not broaden proximally. The attachment of m. supracoracoideus on the proximal humerus of most charadriiforms (e.g., *Larus marinus*) is a rounded scar, while in alcids this scar is distally elongated (crista m. supracoracoidei; Baumel and Witmer, 1993). In some alcids (e.g., *Fratercula arctica*) the proximal end of the scar is much broader than the distal end, whereas in other alcids (e.g., *Alca torda*) the scar is relatively the same width throughout its length.

**117. Humerus, m. supracoracoideus scar, transition into the secondary pneumotricipital fossa (pf2):** (0) pf2 borders scar; (1) scar separated from pf2; (2) margo caudalis widely separates pf2 and scar. In most alcids (e.g., *Alca torda*) the dorsal extent of the excavation of the secondary pneumotricipital fossa parallels the ventral margin of the m. supracoracoideus scar. In some species (e.g., *Cerorhinca monocerata*) the excavation of the secondary pneumotricipital fossa is separated from the supracoracoideus scar by a thin, flat, mediolaterally oriented projection of the humeral shaft (which is most like the very reduced remains of the margo caudalis). The m. supracoracoideus attachment point in many other charadriiforms (e.g., *Larus marinus*) is widely separated from the medial portion of the humeral shaft by the margo caudalis and does not extend as far distally as the condition seen in alcids. **Ordered**

**118. Humerus, medial crest between pneumotricipital fossae, extension relative to the bicipital crest** (modified from Chandler, 1990b, character 51; crus dorsale fossae, Baumel and Witmer, 1993:126): (0) ends proximal to distal-most extension of bicipital crest; (1) crest extends to distal extent bicipital crest; The crest which divides the pneumotricipital fossae varies in the distance it extends distally towards the distal margin of the bicipital crest. In some species (e.g., *Pinguinus impennis*) this crest terminates proximal to the distal edge of the bicipital crest. In some species (e.g., *Alle alle*) this crest extends to the distal edge of the bicipital crest.

**119. Humerus, primary pneumotricipital fossa, excavation for insertion of humerotriceps muscle:** (0) absent; (1) present. The interior (i.e., anterior wall) of the ventral pneumotricipital fossa (fossa pneumotricipitalis ventralis; Baumel and Witmer, 1993) in most alcids (e.g., *Alca torda*) is smooth. In *Fratercula cirrhata* this area is characterized by a small 'eye shaped' excavation.

**120. Humerus, primary pneumotricipital fossa, ridge:** (0) absent; (1) present. The interior (i.e., anterior wall) of the ventral pneumotricipital fossa in most alcids (e.g., *Alca torda*) is smooth. In some Fraterculini (e.g., *Cerorhinca monocerata*) this area is characterized by a small ridge.

**121. Humerus, primary pneumotricipital fossa, depth:** (0) deeply pneumatic; (1) moderately deep; (2) shallow. In contrast to the deeply pneumatic (i.e., deeper than wide) primary pneumotricipital fossa of most charadriiforms (e.g., *Larus marinus*), the primary pneumotricipital fossa of most alcids (e.g., *Uria aalge*) is moderate in depth (i.e., ~ as deep as wide). In true auks (e.g., *Alca torda*) the primary pneumotricipital fossa is very shallow and constricted (i.e., less deep than wide). **Ordered**

**122. Humerus, primary pneumotricipital fossa, shape:** (0) round; (1) oval. The first pneumotricipital fossa varies in shape from rounded (e.g., *Pinguinus impennis*) to oval (e.g., *Cerorhinca monocerata*).



**123. Humerus, ‘mancalline scar’ on posterior side of proximal humerus extending distal to the primary pneumotricipital fossa:** (0) absent; (1) present. In *Mancalla* a deep scar extends along the humeral shaft distal to the primary pneumotricipital fossa. This distinct scar, hereafter referred to as the ‘mancalline scar’, is absent in all other charadriiforms. And its homology is, therefore, uncertain. Although it is possible that this scar may represent an additional insertion point of m. humerotriceps (see Baumel and Witmer, 1993:99).

**124. Humerus, ‘mancalline scar’ on posterior side of proximal humerus, conformation:** (0) excavated; (1) raised. The dorsal and ventral borders of the scar on the posterior side of the proximal humerus of *Mancalla* extend parallel to one another in some species (e.g., *Mancalla californiensis*). In other species (e.g., *Miomancalla wetmorei*) these borders converge proximally, giving this scar a more triangular shape.

**125. Humerus, ‘mancalline scar’ on posterior side of proximal humerus, proximal extension relative to the primary pneumotricipital fossa:** (0) extends within the first pneumotricipital fossa; (1) scar terminates near the distal margin of the primary pneumotricipital fossa. The proximal extent of this scar varies from a condition in which the scar extends well within the primary pneumotricipital fossa (e.g., *Mancalla californiensis*) to a condition in which this scar terminates near the distal margin of the primary pneumotricipital fossa (e.g., *Miomancalla wetmorei*).

**126. Humerus, ‘mancalline scar’ on posterior side of proximal humerus, shape:** (0) ridges parallel; (1) ridges converge proximally. The dorsal and ventral borders of the scar on the posterior side of the proximal humerus of *Mancalla* extend parallel to one another in some species (e.g., *Mancalla californiensis*). In other species (e.g., *Miomancalla wetmorei*) these borders converge proximally, giving this scar a more triangular shape.

**127. Humerus, attachment of m. subcoracoideus, position:** (0) dorsal; (1) ventral. The insertion point of m. subcoracoideus in many alcids (e.g., *Cephus columba*) is restricted to the posterior surface of the ventral tubercle. This fossa extends anteroventrally along the ventral margin of the primary pneumotricipital fossa in other alcids (e.g., *Alca torda*).

**128. Humerus, m. subcoracoideus scar, depth:** (0) flat or slightly concave; (1) a deep pit. As noted by Olson and Rasmussen (2001), in alcids the attachment point of m. subcoracoideus on the posterior surface of the ventral tubercle varies from a basically flat or slightly concave surface (e.g., *Alca torda*) to a more deeply excavated accessory fossa (e.g., *Fratercula arctica*).

**129. Humerus, primary pneumotricipital fossa, shape of distal edge:** (0) convex; (1) straight; (2) concave. The distal edge of the pneumotricipital fossa is concave (e.g., *Aethia pusilla*) or straight (e.g., *Alca torda*) in alcids. This feature is convex in most other charadriiforms (e.g., *Charadrius wilsonia*).

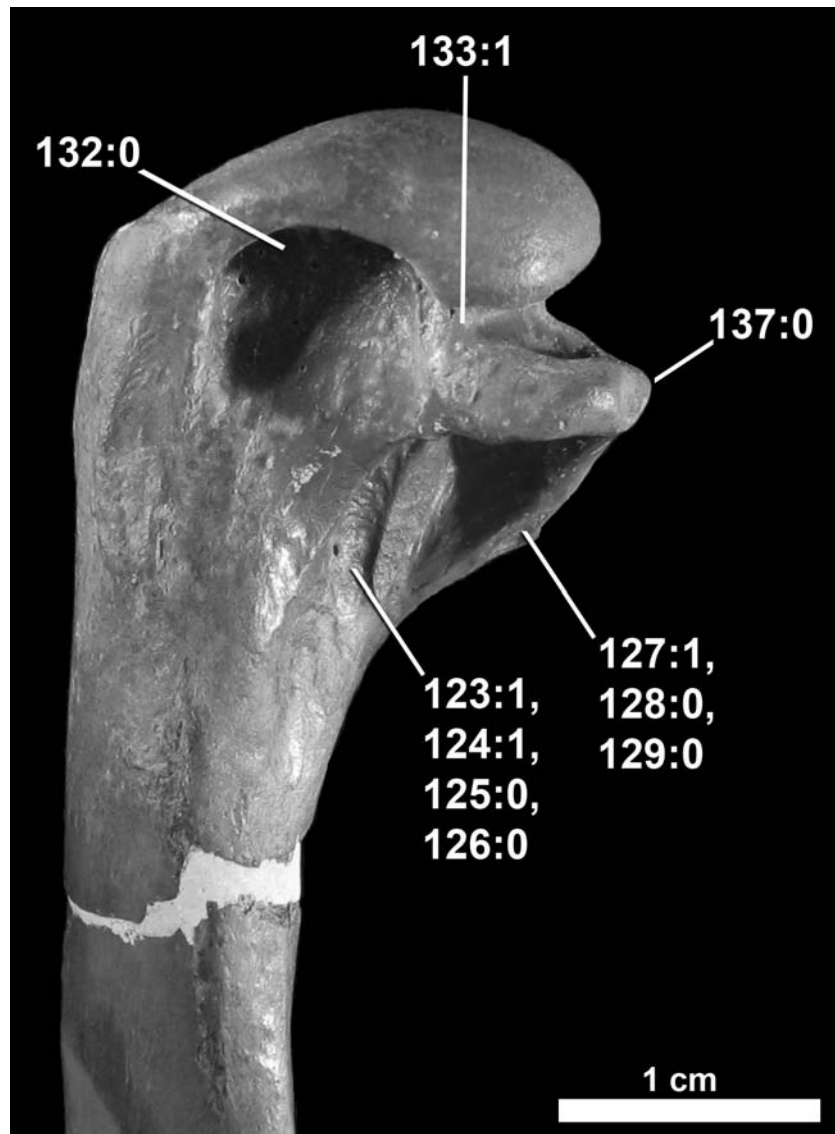


Figure A2.24- Proximal end of holotype left humerus of *Mancalla californiensis* (USNM 4976) in posterior view.

**130. Humerus, secondary pneumotricipital fossa**, (fossa pneumotricipitalis dorsalis; Baumel and Witmer, 1993; modified from Strauch, 1985, character 17): (0) absent; (1) present. The Lari and most other charadriiforms (e.g., *Larus marinus*) have a well-developed secondary pneumotricipital fossa of the humerus. However, in many alcids (e.g., *Alca torda*), it is poorly developed or absent (Strauch, 1985).

**131. Humerus, secondary pneumotricipital fossa, depth** (fossa pneumotricipitalis; Baumel and Witmer, 1993; modified from Strauch, 1985, character 17): (0) a deep

excavation; (1) a shallow excavation. Among alcids, only the puffins (e.g., *Cerorhinca monocerata*) possess an excavated secondary pneumotricipital fossa.

**132. Humerus, secondary pneumotricipital fossa, division:** (0) absent; (1) present. The secondary pneumotricipital fossa of some alcids (e.g., *Aethia pygmaea*) is divided by a medial crest, creating two separate points for muscle insertion. This feature is absent in most alcids (e.g., *Cerorhinca monocerata*).

**133. Humerus, ridge between ventral tubercle and secondary pneumotricipital fossa:** (0) absent; (1) present. On the posterior side of the humerus in *Brachyramphus* a slight ridge extends distally from underneath the distally overturned head of the humerus and contacts dorsal margin of the ventral tubercle, thus dividing the secondary pneumotricipital fossa from the capital groove.

**134. Humerus, ventral tubercle, shape:** (0) long and thin; (1) short and thick. In ventral view the ventral tubercle of some species of alcids (e.g., *Fratercula arctica*) is fairly thin and extends posteriorly to a point roughly level with the posterior extent of the caput. In other alcids (e.g., *Alca torda*) this feature does not extend as far posteriorly, and is more robust.

**135. Humerus, ventral tubercle, lateral margin curvature:** (0) single concavity; (1) double concavity. When viewed ventrally the lateral margin of the ventral tubercle of all alcid species other than *Cerorhinca monocerata* is a single concave curve. This feature in *Cerorhinca monocerata* is characterized by two concave curves. This character is the result of the crus ventrale fossae of *Cerorhinca monocerata* being divided into two sections.

**136. Humerus, ventral tubercle, shape of posterior tip:** (0) rounded or oval; (1) elongate. In *Brachyramphus* the posterior-most extension/point of the ventral tubercle is dorsally expanded into an elongate shape. In other alcids (e.g., *Fratercula arctica*) this feature is rounded or oval in shape.

**137. Humerus, ventral tubercle, ventral margin curvature:** (0) not deeply grooved; (1) deeply grooved. In anterior or posterior view the point at which the ventral tubercle and the ventral margin of the primary pneumotricipital fossa merge varies in its shape from ventrally convex or flat (e.g., *Fratercula corniculata*) to ventrally concave (e.g., *Pinguinus impennis*).

**138. Humerus, ventral tubercle, orientation of posterior tip:** (0) posteriorly oriented; (1) ventrally downturned. This character was documented by Dyke and Walker (2005), and varies within *Alca*.



Figure A2.25- Proximal end of referred left humerus of *Cerorhinca aurorensis* (USNM 459395) in posterior view.

**139. Humerus, m. latissimus dorsi scar, curvature:** (0) straight; (1) curves dorsally. In posterodorsal view, the m. latissimus dorsi scar in most alcids (e.g., *Fratercula arctica*) extends distally straight down the shaft of the humerus. The m. latissimus dorsi scar of some alcids (e.g., *Cepphus grylle*) curves anteriorly across the dorsal surface of the humeral shaft.

**140. Humerus, capital groove, anterior expression** (modified from Chandler, 1990bb, character 52): (0) curved; (1) notched; (2) deep groove. In anterior view the capital groove of most alcids (e.g., *Alca torda*) is visible as a notch on the mediolateral side of the humeral head. In the auklets (e.g., *Ptychoramphus aleuticus*) the capital groove is not expressed anteriorly, resulting in a convexly curved shaped mediolateral side of the humeral head. In the Mancallinae alcids (e.g., *Mancalla cedrosensis*) the capital groove communicates with the ligamental furrow, and is expressed as a deep groove in the ventral margin of the anterior humeral head. **Ordered**

**141. Humerus, capital groove, width:** (0) wide; (1) constricted. In all alcids (e.g., *Fratercula arctica*) except *Mancalla* the capital groove is an open ‘U’ shaped groove. Only in *Mancalla* does the caput overhang the capital groove, giving the proximal wall of the capital groove a convex shape, and constricting this passageway.

**142. Humerus, capital groove, shape:** (0) ‘U’ shaped; (1) pointed anteriorly. In ventral view the capital groove is ‘U’ shaped in most alcids (e.g., *Aethia psittacula*). In *Mancalla* the capital groove is constricted anteriorly.

**143. Humerus, orientation of head relative to shaft:** (0) in line with shaft; (1) rotated anteriorly. As noted by Miller (1933), the humeral head of most alcids (e.g., *Alca torda*) is in-line with the shaft of the humerus, while the ventral portion of the humeral head of mancalline alcids (e.g., *Mancalla cedrosensis*) is rotated anteriorly.

**144. Humerus, longitudinal shape of shaft:** (0) sigmoidal; (1) arced. As noted by Lucas (1901), the shaft of most alcids (e.g., *Alca torda*), when viewed laterally, is slightly sigmoidal in shape, while the shaft of Mancallinae (e.g., *Mancalla californiensis*) is arced.

**145. Humerus, cross-sectional shape of shaft:** (0) rounded; (1) semi-rounded; (2) flattened. As noted by Howard (1978, 1982), the humeral shaft of most alcids (e.g., *Alca torda*) is flattened in cross-section (flattened oval). The shaft of some alcids (e.g., *Cephus grylle*) is more rounded (i.e., semi-rounded) in cross-section. The humeral shaft of other charadriiforms (e.g., *Larus marinus*) is rounded in cross-section. **Ordered**

**146. Humerus, shaft thickness:** (0) robust; (1) gracile. The thickness of the humeral shaft varies from robust (i.e., width of shaft in anterior view greater than or equal to half the width of the humeral head; e.g., *Brachyramphus marmoratus*) to gracile (i.e., width of shaft in anterior view less than or equal to half the width of the humeral head; e.g., *Alle alle*).

**147. Humerus, dorsal supracondylar process, shape:** (0) large dorsally pointing projection; (1) small dorsally pointing projection; (2) smoothly transitioning; (3) square; (4) rounded knob. The attachment point for M. extensor carpi along the dorsal margin of the distal humerus projects dorsally away from the shaft in many charadriiforms (e.g.,

*Larus marinus*; state 0) while in all alcids this feature is elongated along the shaft of the humerus medially and does not project as far dorsally. States within Alcidae include: (1) a small dorsally projecting point (e.g., *Alca torda*), (2) square, ~ 90° contact with shaft (e.g., *Fratercula arctica*) (3) smoothly transitioning to the shaft (e.g., *Pinguinus impennis*). In *Mancalla* this process is a rounded knob that is separated from the distal extent of the dorsal supracondylar prominence (crest) by a gap.  
Figure A2.24-

**148. Humerus, dorsal supracondylar process, length:** (0) short; (1) long. The dorsal supracondylar process of most alcids (e.g., *Aethia pygmaea*) is short (i.e., the proximodistal length measured from the distal end of the humerus to the proximal termination of the crest on the humeral shaft is shorter than the greatest distal width of the humerus measured from the entepicondyle to the dorsal condyle). The dorsal supracondylar process of some alcids (e.g., *Mancalla lucasi*) extends further proximally onto the humeral shaft.

**149. Humerus, sulcus between dorsal condyle and dorsal supracondylar process:** (0) continuous; (1) divided. The sulcus for passage of m. extensor metacarpi radialis, which runs between the dorsal supracondylar process and the dorsal condyle is continuous in all alcids (e.g., *Pinguinus impennis*) except the Fraterculini (e.g., *Fratercula arctica*), in which this sulcus is divided by a bony crest, forming a round pit on the posterior edge of the dorsal condyle.

**150. Humerus, ventral epicondyle, orientation relative to shaft:** (0) flared ventrally; (1) nearly straight. As noted by Olson and Rasmussen (2001), in anterior view the ventral margin of the ventral epicondyle is flared ventrally in *Fratercula arctica*, but is nearly straight in *Cepphus grylle*.

**151. Humerus, tricipital sulci, width** (modified from Chandler, 1990b, character 54): (0) scapulotricipital sulcus narrower than humerotricipital sulcus; (1) sulci of equal width; (2) scapulotricipital sulcus broader than humerotricipital sulcus. The scapulotricipital sulcus of Fraterculini species (e.g., *Cerorhinca monocerata*) is narrower than humerotricipital sulcus. In most other alcid taxa (e.g., *Alca torda*) these sulci are of roughly equal width. *Alle alle* is the only species of extant alcid in which the scapulotricipital sulcus is broader than the humerotricipital sulcus.

**152. Humerus, crest between tricipital, shape:** (0) straight, projects posteriorly; (1) curved dorsally over scapulotricipital sulcus; (2) bifurcated. The crest that divides the tricipital sulci (humerotricipital and scapulotricipital sulci) is a low posteriorly projecting ridge in most alcids (e.g., *Uria aalge*). In *Mancalla* this ridge veers dorsally and merges with the dorsal margin of the scapulotricipital sulcus on its lateral side. The crest that divides the tricipital sulci is bifurcated in *Bisulca demerei*.

**153. Humerus, humerotricipital sulcus, shape in distal view:** (0) flattened; (1) ‘U’ shaped or curved. In distal view the humerotricipital sulcus of all alcids other than *Alle alle* and *Uria aalge* is curved or ‘U’ shaped.

**154. Humerus, fossae in tricipital sulci:** (0) absent; (1) present. The scapulotricipital and humerotricipital sulci of Mancallinae are characterized by fossae positioned at the proximal end of the sulci. The sulci of other alcids transition smoothly onto the posterior face of the humeral shaft.

**155. Humerus, relative distal extension of condyles** (Chandler, 1990b, character 61): (0) level; (1) distal extent of dorsal condyle proximal to distal extent of ventral condyle. The dorsal condyles of all extant alcids (e.g., *Alca torda*) are situated slightly proximal to the ventral condyle. The condyles of most other charadriiforms (e.g., *Gygis alba*) extend distally an equal distance.

**156. Humerus, ventral condyle in distal view, posterior trochlear process:** (0) absent; (1) present. As noted by Marsh (1870) in the original description of *Cataractes antiquus* a posterodorsally-projecting tubercle is present on the ventral condyle; projecting into the sulcus between the ventral condyle and the saddle that defines the distal extent of the humerotricipital sulcus. This characteristic is also present in *Pinguinus*, but is lacking in all other alcids (e.g., *Alca torda*). This character has also been noted in penguins and plotopterids (Marples, 1952; Ksepka et al. 2006).

**157. Humerus, ventral condyle, shape** (Chandler, 1990b, character 59): (0) rounded; (1) flattened. The anterior face of the ventral humeral condyle is flattened in most alcids (e.g., *Pinguinus impennis*), while the ventral condyle is rounded in all other charadriiforms examined during this study (e.g., *Larus argentatus*).

**158. Humerus, separation of humeral condyles:** (0) absent; (1) present. In distal view the humeral condyles of *Brachyramphus* are separated, whereas the ventral margin of the dorsal condyle and the dorsal margin of the ventral condyle of other alcids (e.g., *Synthliboramphus antiquus*) contact one another.

**159. Humerus, tubercle adjacent to dorsal condyle:** (0) absent; (1) present. As noted by Howard (1982), a small rounded tubercle lies ventral to the dorsal condyle along the ventral margin of the brachial impression in some alcids (e.g. *Mancalla californiensis*), but is absent in most species of alcids (e.g., *Alca torda*).

**160. Humerus, tubercle(s) dorsal to scapulotricipital groove:** (0) absent; (1) present. Many alcids (e.g., *Brachyramphus perdix*) possess a tubercle along the dorsal border of the scapulotricipital sulcus. In alcids this tubercle is located distal to paired fossae that lie between the raised dorsal margin of the scapulotricipital sulcus and the dorsal sulcus.

**161. Humerus, tubercle(s) dorsal to scapulotricipital groove, quantity:** (0) a single tubercle; (1) paired tubercles. Rather than a single tubercle, some alcids (e.g., *Mancalla cedrosensis*) possess two tubercles dorsal to the scapulotricipital sulcus.

**162. Humerus, ventral supracondylar tubercle (anterior ligament scar), shape in anterior view:** (0) triangular; (1) rounded. On the anterior surface of the distal shaft of the humerus ventral to the brachialis scar, the ventral supracondylar tubercle, which is the attachment for the ventral collateral ligament, varies in its shape from triangular (e.g., *Brachyramphus marmoratus*), to an oval/rounded pit (e.g., *Alca torda*).

**163. Humerus, scar associated with ventral supracondylar tubercle:** (0) absent; (1) present. A small scar on the distal humerus marks the attachment point of the m. pronator sublimis in some species of alcids (e.g., *Alca torda*), but is absent in many species (e.g., *Uria aalge*).

**164. Humerus, position of scar adjacent to ventral supracondylar tubercle:** (0) proximal; (1) ventral; (2) detached. The position of the small scar, which marks the origination point of the m. pronator sublimis varies in its position. In some species (e.g., *Aethia pygmaea*) this feature is located at the proximal tip of the anterior ligament scar, while in other species of alcids (e.g., *Aethia psittacula*) it is located along the dorsal margin of this scar. In some other charadriiforms (e.g., *Phaetusa simplex*) this scar is detached from the anterior ligament scar.

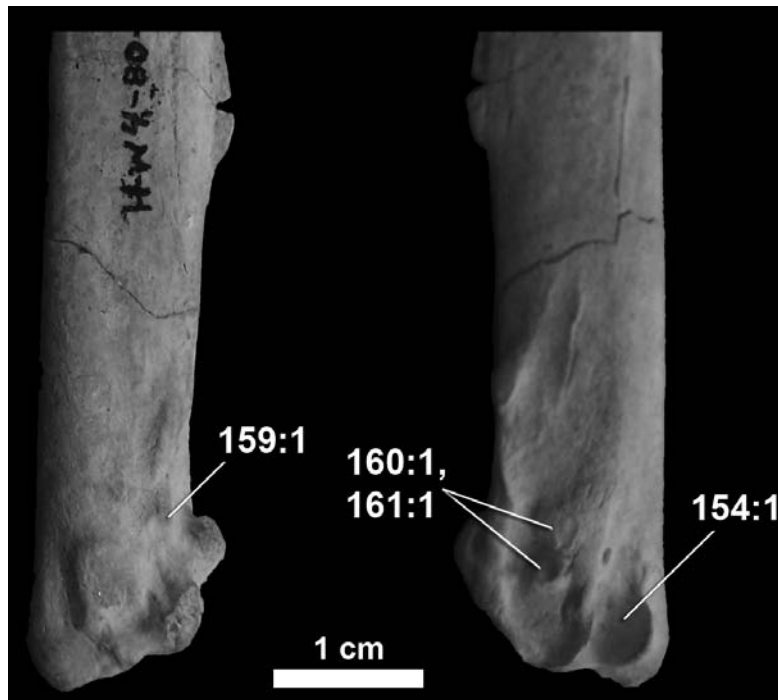


Figure A2.26- Distal end of left humerus of *Mancalla lucasi* (SDSNH 25237) in anterior (left) and posterior (right) views.



## RADIUS

**165. Radius, bicipital tubercle:** (0) reduced; (1) distinct. The auklets (e.g., *Ptychoramphus aleuticus*) and murrelets (e.g., *Synthliboramphus antiquus*) lack the distinct bicipital tubercle found in other alcids (e.g., *Alca torda*).

**166. Radius, bicipital tubercle, shape:** (0) a crest; (1) a round tubercle. The shape of the bicipital tubercle in Alcidae (e.g., *Alca torda*) is an elongated crest-like structure, rather than the rounded tubercle of other charadriiforms (e.g., *Larus marinus*).

**167. Radius, bicipital tubercle, position:** (0) contacts papilla; (1) separate. The bicipital tubercle of most alcids (e.g., *Uria lomvia*) is a swollen area along the distal margin of what Howard (1929) termed the ligamental papilla. In a few alcids (e.g., *Cephus columba*) the bicipital tubercle is a separate structure, positioned distally and separated from the ligamental papilla.

**168. Radius, tendinal sulcus** (Chu, 1998, character 102): (0) not divided; (1) divided lengthwise by a crest. The tendinal groove located on the dorsal side of the distal radius is divided by a crest in some species of alcids (e.g., *Synthliboramphus antiquus*). This feature is lacking in the charadriiform outgroup taxa examined and also in the auklets (e.g., *Aethia pusilla*).

**169. Radius, notch in distal end:** (0) absent; (1) present. In anterior view, the crest associated with the scapho-lunar facet of some alcids (e.g., *Aethia pygmaea*) extends far enough distally so that a notch is formed between that crest and the ventral-most articulation surface of the distal radius with the radiale. In other alcids (e.g., *Alle alle*) the crest on the anterior surface of the radius transitions smoothly into the distal end of the radius.

## ULNA

**170. Ulna, olecranon, length:** (0) long; (1) short; (2) truncate. The olecranon of most alcids (e.g., *Alca torda*), is a long (i.e., projects well past the medial extent of the ventral cotyla) medially projecting point. In some species (e.g., *Pinguinus impennis*) the olecranon is truncated (i.e., does not extend past the medial extent of the ventral cotyla), while the condition in other alcids (i.e., *Aethia pusilla*) is intermediate (i.e., olecranon short). **Ordered**

**171. Ulna, olecranon, curvature:** (0) flares posteriorly; (1) curves anteriorly. In dorsal view the posterior margin of the ulnar head of most alcids (e.g., *Pinguinus impennis*) flares posteriorly to form the posterior edge of the olecranon, while in some species (e.g., *Alca torda*) this margin curves anteriorly.

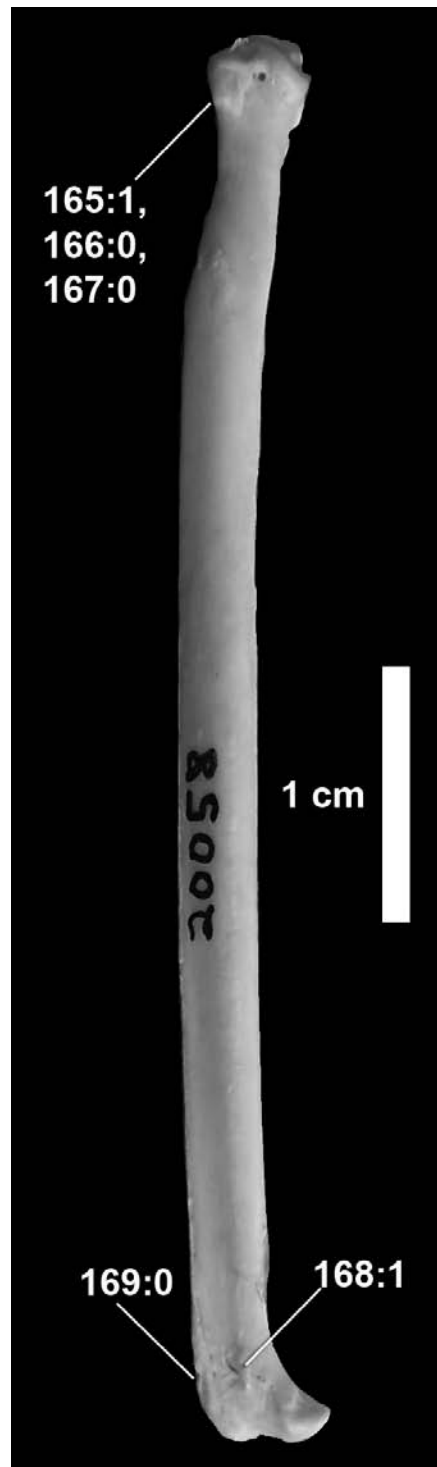


Figure A2.27- Left radius of *Alca torda* (NCSM 20058) in dorsal view.

**172. Ulna, ventral collateral ligament tubercle, shape:** (0) triangular; (1) rounded. The scar for the attachment of the ventral collateral ligament is triangular in some alcids (e.g., *Alca torda*) and more rounded in others (e.g., *Aethia psittacula*).

**173. Ulna, crest extending from the ventral cotyla to the anterior margin of the ventral collateral ligament tubercle** (modified from Chandler, 1990b, character 63): (0) absent; (1) present. The ventral cotyla of the proximal ulna is separate from the scar for the attachment of the ventral collateral ligament in some species of alcids (e.g., *Cepphus grylle*). In other alcids (e.g., *Alle alle*) a crest extends laterally from the ventral cotyla and contacts the anterior margin of the collateral ligament scar.

**174. Ulna, crest extending from the ventral cotyla to the posterior margin of the ventral collateral ligament tubercle:** (0) absent; (1) present. Although most alcids (e.g., *Alca torda*) lack a crest, which extends from the ventral cotyla to contact the posterior margin of the ventral collateral ligament scar, several alcids (e.g., *Brachyramphus brevirostris*) possess this character.

**175. Ulna, dorsal cotylar process, anterior margin shape:** (0) rounded; (1) straight. The dorsal condyle of alcids is bordered on the posterior margin by a posteriorly projecting blade-like process for attachment of m. scapulotriceps. The anterior margin of this feature in dorsal view can be either rounded (e.g., *Alca torda*) or straight (e.g., *Fratercula cirrhata*).

**176. Ulna, dorsal cotylar process, development** (Chu, 1998, character 98): (0) poorly developed; (1) well developed. The dorsal cotylar process of all alcids (e.g., *Alca torda*) is a distinct anteriorly expanded structure when compared to the less developed condition observed in other charadriiforms (e.g., *Larus marinus*).

**177. Ulna, proximal radial depression, shape:** (0) a round pit; (1) a triangular pit; (2) broad and flat. In contrast to the distinctly triangular shape of the proximal radial depression of most charadriiforms (e.g., *Larus marinus*), the proximal radial depression of all extant alcids (e.g., *Uria aalge*) is a round pit situated distal to the ulnar cotylae. In some charadriiforms not closely related to Alcidae (e.g., *Bartramia longicauda*) the radial depression is broad and flat. In *Miomancalla wetmorei* the proximal radial depression is a broad flat space bordered dorsally and ventrally by distinct crests that occupies the entire anterior surface of the ulna (Howard, 1982). **Ordered**

**178. Ulna, brachial impression, breadth:** (0) thin; (1) broad. As noted by Howard (1982) the brachial impression on the proximal ulna of some alcids (e.g., *Alca torda*) is a relatively thin scar (i.e., does not comprise more than half the width of the ulnar shaft), while in some species (e.g., *Fratercula arctica*) this feature is broader (i.e., comprises more than half of the width of this proximal portion of the ulna).

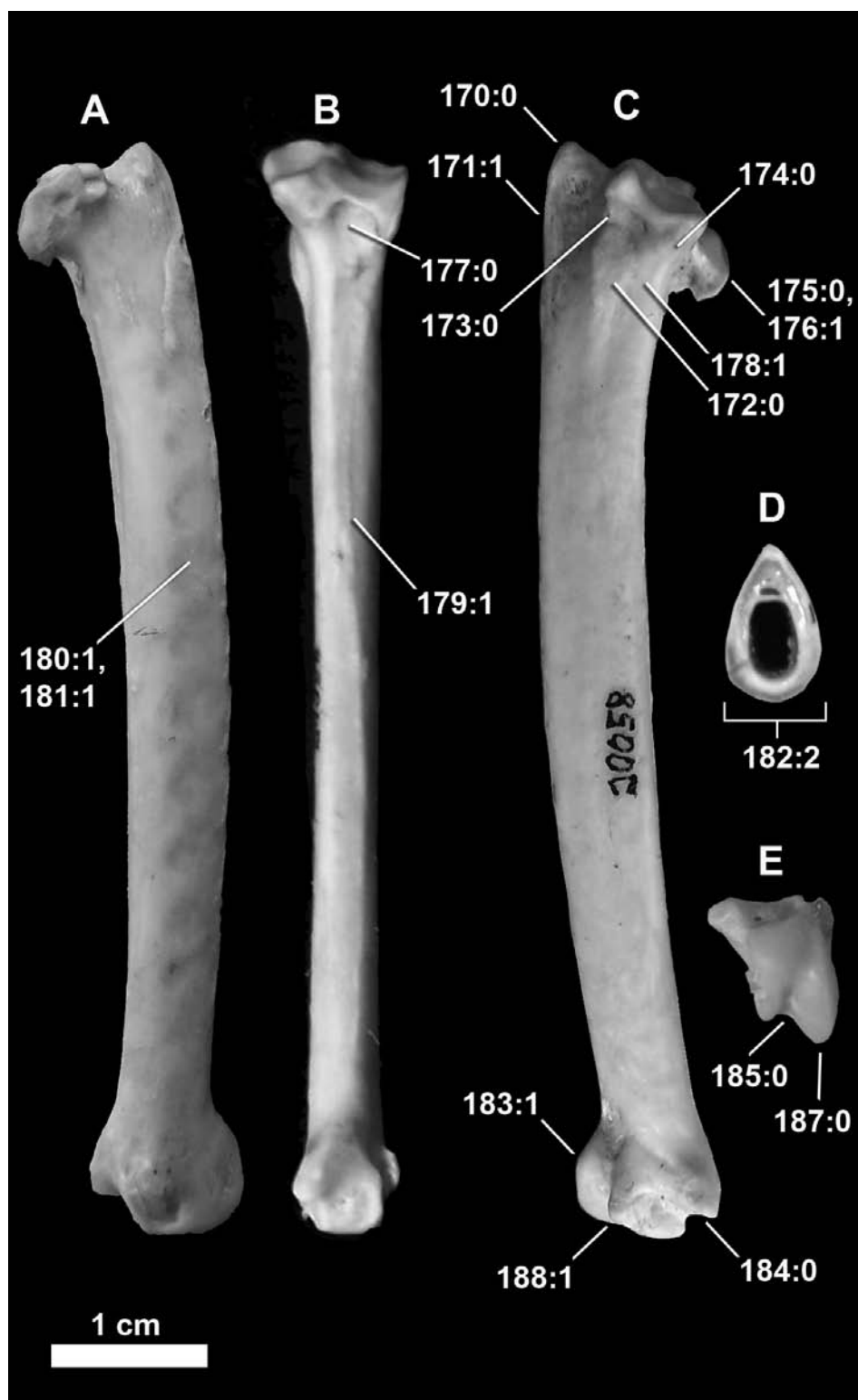


Figure A2.28- Left ulna of *Alca torda* (NCSM 20058) in dorsal (A); anterior (B); ventral (C); and distal (E) views. Cross-sectional view (D) of *Alca* fossil ulna (NCSM 8854).

**179. Ulna, intramuscular line:** (0) non-distinct; (1) distinct, raised ridge. As noted by Olson (1981), an inter-muscular line runs between the proximal radial depression and the nutrient foramen. This inter-muscular line is non-distinct and often barely visible in many species of alcids (e.g., *Alle alle*), while in others this feature is distinct and raised (e.g., *Pinguinus impennis*).

**180. Ulnar quill knobs or impressions:** (0) absent; (1) present. Although ulnar quill knobs that mark insertion points for secondary feathers are present in most charadriiforms (e.g., *Alca torda*), they are absent in some species (e.g., *Pinguinus impennis*).

**181. Ulnar quill knobs, form:** (0) distinct knobs; (1) reduced to impressions. The form of quill ‘knobs’ varies in charadriiforms, with some species (e.g., *Alca torda*) having quill impressions rather than the projected knobs that characterize other species (*Charadrius vociferus*).

**182. Ulna, shaft, shape:** (0) rounded; (1) semi-flattened; (2) flattened. As noted by Howard (1978) the ulnae of most alcids (e.g., *Alca torda*) exhibit the flattening typical of the pectoral elements of wing-propelled divers, while the ulnae of some alcids (e.g., *Cephus grylle*) are more rounded (i.e., semi-flattened) in cross section. The ulnae of other charadriiforms (e.g., *Larus marinus*) are rounded in cross section. **Ordered**

**183. Ulna, dorsal condyle, shape:** (0) rounded; (1) angular. The entire posterior margin of the dorsal ulnar condyle of some alcids (e.g., *Pinguinus impennis*) is rounded, while in other alcids (e.g., *Alca torda*) the dorsal condyle has an angular bend distal to the contact with the ulnar shaft.

**184. Ulna, carpal tubercle, shape:** (0) flat or angled distally; (1) concave. The distal margin of the carpal tubercle of some alcids (e.g., *Alca torda*) is flat or angles slightly distally in some specimens. In *Cephus* this surface is concave, giving the distal surface of the carpal tubercle a hooked appearance.

**185. Ulna, intercondylar sulcus:** (0) concave; (1) flat. In distal view the groove between the ulnar condyles is a concave ‘U’ shaped depression in some species (e.g., *Alca torda*). In other species (e.g., *Pinguinus impennis*) the posterior surface of the ventral condyle angles anteriorly from the sulcus towards the ventral surface of the ulna, forming a flat almost 90° angle between the condyles (i.e., ‘stairstep-like’).

**186. Ulna, length:** (0) longer than carpometacarpus; (1) shorter than carpometacarpus. The ulnae of most alcids (e.g., *Cephus grylle*) are longer than their carpometacarpi, while the ulnae of Mancallinae are shorter (e.g., *Mancalla cedrosensis*). This condition is not known in other flightless birds, but interestingly, is found in some hummingbirds.

**187. Ulna, ventral condyle, orientation** (Chandler, 1990b, character 64: (0) directed posteriorly; (1) directed posteroventrally. The ventral condyle of *Mancalla* species (e.g.,

*Mancalla cedrosensis*) is directed posteroventrally, while in all other charadriiform taxa examined during this study, the ventral condyle is directed posteriorly.

**188. Ulna, dorsal condyle, distal extension** (Chandler, 1990b, character 65): (0) dorsal condyle extends distal to ventral condyle; (1) level. The dorsal condyle of most alcids (e.g., *Alca torda*) extends distally the same distance as the ventral condyle. In *Mancalla* (e.g., *Mancalla cedrosensis*) the dorsal condyle extends further distally than the ventral condyle.

## CARPOMETACARPUS

**189. Carpometacarpus, extensor process of metacarpal 1:** (0) present; (1) absent. The carpometacarpus of all alcids except *Mancalla* (e.g., *Mancalla cedrosensis*) have an extensor process on the anterior margin of metacarpal 1.

**190. Carpometacarpus, metacarpal I, length** (modified from Chandler, 1990b, character 67): (0) short; (1) long. The first metacarpal of most alcids (e.g., *Alca torda*) extends distally about one third of the length of metacarpal 2, while in *Mancalla* species (e.g., *Mancalla cedrosensis*) metacarpal I terminates approximately at the midpoint of metacarpal 2.

**191. Carpometacarpus, anterior margin of metacarpal 1, shape** (modified from Strauch, 1985, character 18; Chandler, 1990b, character 69): (0) rounded knob; (1) flat. The anterior margin of metacarpal 1 is a short, rounded knob in the Lari and most other charadriiforms (e.g., *Fratercula arctica*). In the Alcini (e.g., *Alca torda*) the anterior margin of metacarpal 1 is flat in comparison with other extant alcids (yet still slightly anteriorly convex).

**192. Carpometacarpus, proximal intermetacarpal spatium, position relative to the distal extent of metacarpal 1** (modified from Chandler, 1990b, character 71): (0) symphysis distal to MC1; (1) symphysis level with MC1; (2) symphysis proximal to MC1. In relation to the pollical facet, the symphysis can be either distal to it (e.g., *Aethia cristatella*), ~level with it (e.g., *Cephus carbo*), or proximal to it (e.g., *Synthliboramphus antiquus*).

**193. Carpometacarpus, posterior extension of ventral trochlear margin relative to metacarpal III** (modified from Chandler, 1990b, character 70): (0) ventral trochlear margin of carpometacarpus extends posteriorly to metacarpal III (e.g., *Alca torda*); (1) ventral trochlear margin and metacarpal III extend an equal distance posteriorly (e.g., *Fratercula arctica*); (2) ventral trochlear margin does not extend as far posteriorly as metacarpal III (e.g., *Aethia pusilla*).

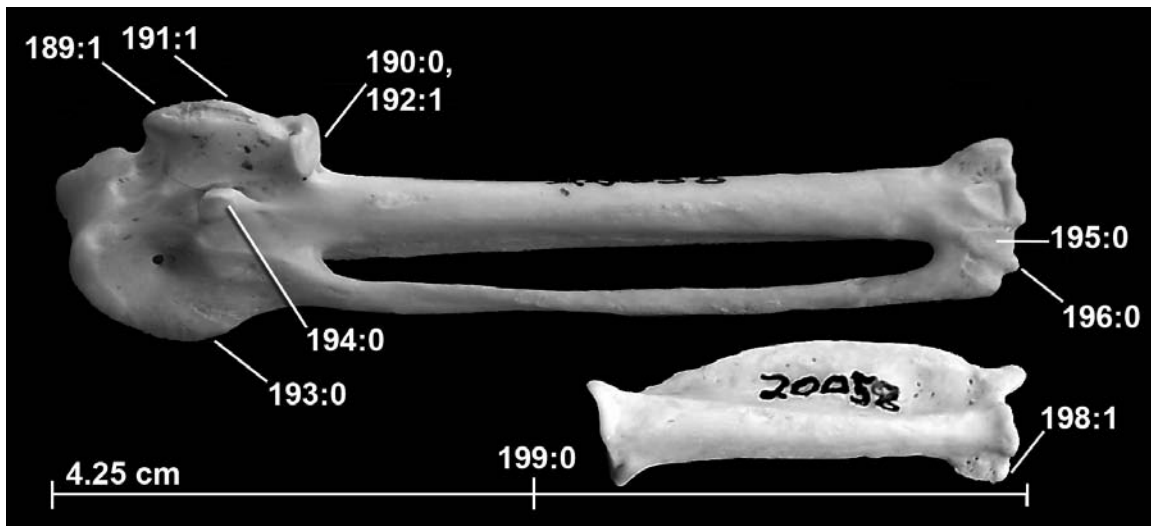


Figure A2.29- Left carpometacarpus (top; ventral view) and digit II phalanx 1 (bottom; dorsal view) of *Alca torda* (NCSM 20058).

**194. Carpometacarpus, pisiform process, development:** (0) distinct; (1) reduced. The Pisiform process of most alcids (e.g., *Miomancalla wetmorei*) is a distinct ventral projection. The Pisiform process of *Mancalla cedrosensis* is reduced to a small scar. Similar to the condition observed in penguins, the reduction of this feature in *Mancalla* may be related to the stiffening of the wing that is associated with the lack of these highly specialized wing propelled divers need to flex the manus.

**195. Carpometacarpus, distal end of tendinal groove** (i.e., sulcus interosseous; Baumel and Witmer, 1993): (0) a sulcus; (1) a bony canal. The sulcus occupied by the tendons of the interossei muscle on the distal end of the dorsal carpometacarpus varies from a distally open-ended groove (e.g., *Uria lomvia*), to a partially or fully roofed bony canal (e.g., *Aethia pusilla*).

**196. Carpometacarpus, minor digit articulation:** (0) level with facies articularis digitalis major; (1) proximal to facies articularis digitalis major. The articulation surface of the minor digit (III:1) is located proximally to the articulation surface for the major digit (II:1) in some species (e.g., *Pinguinus impennis*), whereas in other species (e.g., *Alca torda*) the articulation surfaces are approximately level.

## MAJOR PHALANX

**197. Manual digit II, phalanx 1, fenestration:** (0) absent; (1) present. The major phalanx of many charadriiforms (e.g., *Larosterna inca*) is penetrated by two fenestrae. These fenestrae are absent in all alcids.

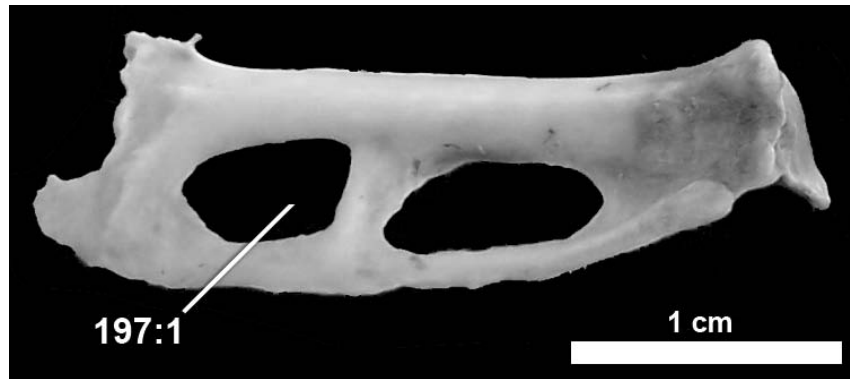


Figure A2.29- Left digit II phalanx 1 of *Sterna maxima* (NCSM 10248) in dorsal view.

**198. Manual digit II, phalanx 1, shape of process on dorsal surface of the distal end:** (0) rounded; (1) rectangular. A bladelike process projects posteriorly from the distal end of the first phalanx of the second digit. In dorsal view this process varies from rounded (e.g., *Aethia pusilla*) to rectangular (e.g., *Alca torda*).

**199. Manual digit II, phalanx 1, length:** (0)  $<1/2$  length of carpometacarpus; (1)  $>1/2$  length of carpometacarpus. The greatest length of the major phalanx of some charadriiforms (e.g., *Sterna maxima*) is  $>1/2$  the greatest length of the carpometacarpus. The length of the major phalanx is  $<1/2$  the length of the carpometacarpus in all alcids except *Pinguinus impennis*, in which the relative length of the wing elements has been reduced in association with flightlessness.

## PELVIS

**200. Ilium, pre-acetabular ilium, lateral expansion:** (0) not expanded, narrow; (1) expanded laterally, spatulate. As noted by Kuroda (1954) the anterior ends of the pre-acetabular blades of the ilium are laterally expanded (i.e., wider) in some species of alcids (e.g., *Uria lomvia*) than others (e.g., *Synthliboramphus antiquus*).

**201. Symsacral strut extending to acetabulum** (Strauch, 1985, character 15; Chandler, 1990b, character 47): (0) absent; (1) present. In most charadriiforms (e.g., *Aethia pygmaea*) a strut or brace extends from the fused sacral-caudal vertebrae towards the acetabulum. In alcids this strut may be well developed (contra Strauch, 1978), it may be reduced to a very slight ridge, or it may be completely absent (e.g., *Alca torda*; Strauch, 1985).

**202. Renal depression** (Chandler, 1990b, character 44): (0) broad; (1) narrows posteriorly. The renal depression on the ventral side of the ilium maintains a relatively constant width in some alcids (e.g., *Aethia pusilla*) while in other alcid species (e.g., *Uria aalge*) the renal depression narrows posteriorly.



**203. Antitrochanteral sulcus, distal extension:** (0) terminates at antitrochanter; (1) extends past antitrochanter. The antitrochanteral sulcus (sulcus antitrochantericus, Baumel and Witmer, 1993) is bordered medially by a crest that extends distal to the acetabulum in some alcids (e.g., *Alca torda*). This crest curves laterally and ends at, or just past, the distal extent of the antitrochanter in other species of alcids (e.g., *Cepphus grylle*).

**204. Iliosynsacral suture:** (0) fused; (1) perforated. The contact between the lateral processes of the sacral vertebrae and the ilium, termed the iliosynsacral suture (sutura iliosynsacralis, Baumel and Witmer, 1993), is fused along its entire margin in some alcids (e.g., *Cepphus columba*), while in other species (e.g., *Alca torda*) this suture is non-continuous (i.e., perforated by spaces between the lateral processes of the sacral vertebrae). This feature is distinct from the foramina intertransversaria of Baumel and Witmer (1993), which are located medially to the iliosynsacral suture.

**205. Ilium, post acetabular dorsal ilium, width:** (0) broadens; (1) narrows. The dorsal ilium crest broadens posterior to the acetabulum and angles posterolaterally in some species of alcids (e.g., *Uria aalge*), whereas in other species of alcids (e.g., *Alca torda*) the post acetabular area of the ilium is narrower (i.e., tapers posteriorly).

**206. Ilium, dorsolateral iliac spine orientation:** (0) dorsal; (1) dorsolateral. The dorsolateral iliac spine (spina dorsolateralis ilii, Baumel and Witmer, 1993) is oriented so that its surface faces much more dorsally in some species of alcids (e.g., *Cepphus columba*) than in others (e.g., *Uria aalge*).

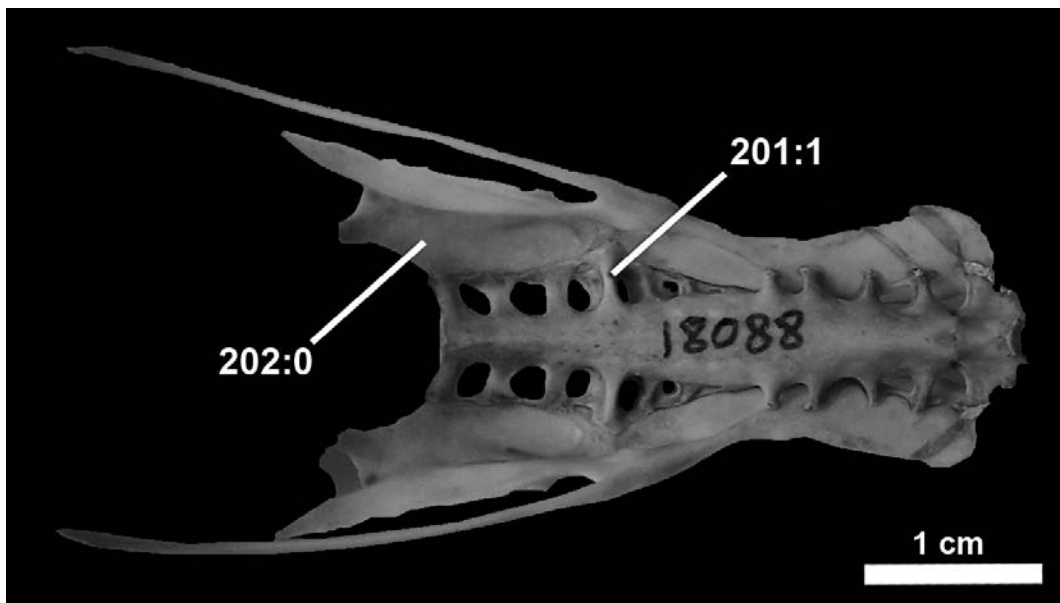


Figure A2.30- Pelvis of *Ptychoramphus aleuticus* (NCSM 18088) in ventral view.

**207. Ilium, dorsolateral iliac spine shape:** (0) pointed; (1) square. The dorsolateral iliac spine (spina dorsolateralis ilii, Baumel and Witmer, 1993) is pointed in all alcids (e.g., *Cepphus columba*) except *Aethia* (e.g., *Aethia pygmaea*).

**208. Ischium, relative length of ischial angle and posterior projection** (Strauch, 1985, character 16; Chandler, 1990b, character 46): (0) ischial angle much longer; (1) both structures about the same length. In the Lari and most other charadriiforms (e.g., *Alca torda*) the ischial angle is much longer than the posterior projection of the ilium; in the auklets (e.g., *Aethia pusilla*) the length of the ischial angle is much reduced, and the structures are almost the same length. These differences also are indicated by Storer's (1945a) measurements of alcid skeletons (Strauch, 1985).

**209. Pelvis, width:** (0) broad; (1) narrow. In contrast to the broad (i.e., length of pelvis from anterior-most ilium to distal point of the dorsal iliac spine  $\leq 2 \times$  width across pelvis at antitrochanter) pelvis of many other charadriiforms (e.g., *Sterna maxima*), the pelvis of all alcids are narrow (i.e., length of pelvis from anterior-most ilium to distal point of the dorsal iliac spine  $> 2 \times$  width across pelvis at antitrochanter).

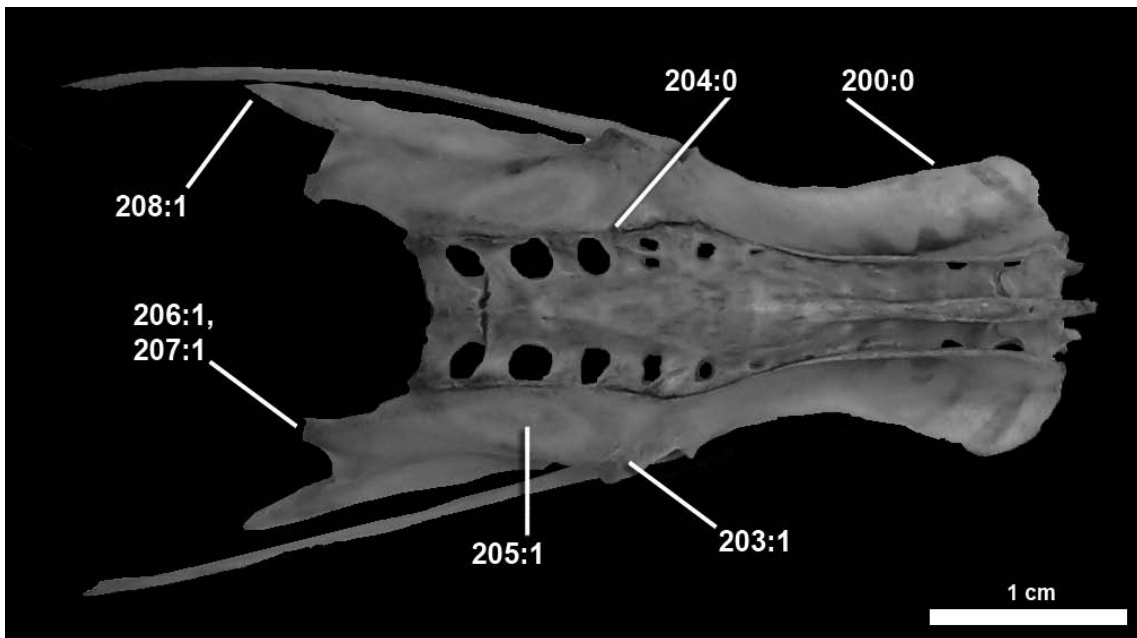


Figure A2.31- Pelvis of *Ptychoramphus aleuticus* (NCSM 18088) in dorsal view.

## FEMUR

**210. Femur, trochanteric ridge, shape:** (0) convex; (1) straight; (2) concave. In most alcids the anterior margin of the femoral trochanter in lateral or medial view is straight (e.g., *Alca torda*) or convex (e.g., *Alle alle*). In puffins (e.g., *Fratercula arctica*) the trochanter is slightly concave.

**211. Femur, trochanteric ridge, length:** (0) long; (1) short. As noted by Miller (1937) the trochanteric crest of the femur varies in the extent to which it extends distally down the lateral shaft of the proximal femur from short (i.e., extends distally  $< 2\times$  width of the lateral surface of femoral head; e.g., *Synthliboramphus hypoleucus*) to long (i.e., extends distally  $\geq 2\times$  width of the lateral surface of femoral head; e.g., *Alca torda*).



Figure A2.32- Right femur of *Alca torda* (NCSM 20058) in medial view.

## TIBIOTARSUS

**212. Tibiotarsus, cnemial crests, shape in proximal view:** (0) 'T' shaped; (1) 'L' shaped. In some alcids (e.g., *Aethia cristatella*) the medial cnemial crest extends posteriorly along the medial margin of the femoral articulation surface. This gives this feature a 'T' shape in proximal view. Some alcids (e.g., *Uria lomvia*) lack this posterior extension and as a result the cnemial crests appear 'L' shaped in proximal view.

**213. Tibiotarsus, cnemial crests, distal extent** (Chandler, 1990b, character 74): (0) anterior crest extends further distally than lateral cnemial crest; (1) both extend distally about equal. The distal extent of the cnemial crests is roughly equal in some alcids (e.g., *Alle alle*) while the anterior cnemial crest extends further distally in some alcids (e.g., *Aethia psittacula*).

**214. Tibiotarsus, lateral cnemial crest orientation:** (0) directed anterolaterally; (1) directed laterally. In proximal view the external cnemial crest of some alcids (e.g., *Alca torda*) is directed anterolaterally, while the lateral cnemial crest of other alcids (e.g., *Aethia psittacula*) is directed laterally, which results in a more constricted incisura tibialis.

**215. Tibiotarsus, notch in lateral margin of medial condyle** (Chandler, 1990b, character 75): (0) absent; (1) present. The distal most portion of the medial condyle of many alcids (e.g., *Pinguinus impennis*) is notched in lateral view. Other alcids (e.g., *Alca torda*) lack this feature. This notch is a common feature in many charadriiforms (e.g., *Larus marinus*) and its absence is therefore considered derived among alcids.

**216. Tibiotarsus, lateral projection of crest lateral to the groove for peroneus profundus tendon, posterior view:** (0) a distinct projection; (1) not visible in posterior view. The lateral edge of the groove for the peroneus profundus tendon projects far enough laterally in some species of alcids (e.g., *Alca torda*) to be visible in posterior view.

**217. Tibiotarsus, supratendinal bridge:** (0) not fully ossified; (1) fully ossified. The supratendinal bridge of all alcids (e.g., *Alle alle*) except *Pinguinus* is ossified.

**218. Tibiotarsus, relative length:** (0) <2X greatest length of tarsometatarsus; (1) >2X greatest length of tarsometatarsus. The greatest length of the tibiotarsus is greater than two times the greatest length of the tarsometatarsus in most alcids (e.g., *Alca torda*), but in some species of alcids (e.g., *Synthliboramphus antiquus*) the tibiotarsus is less than twice the length of the tarsometatarsus.

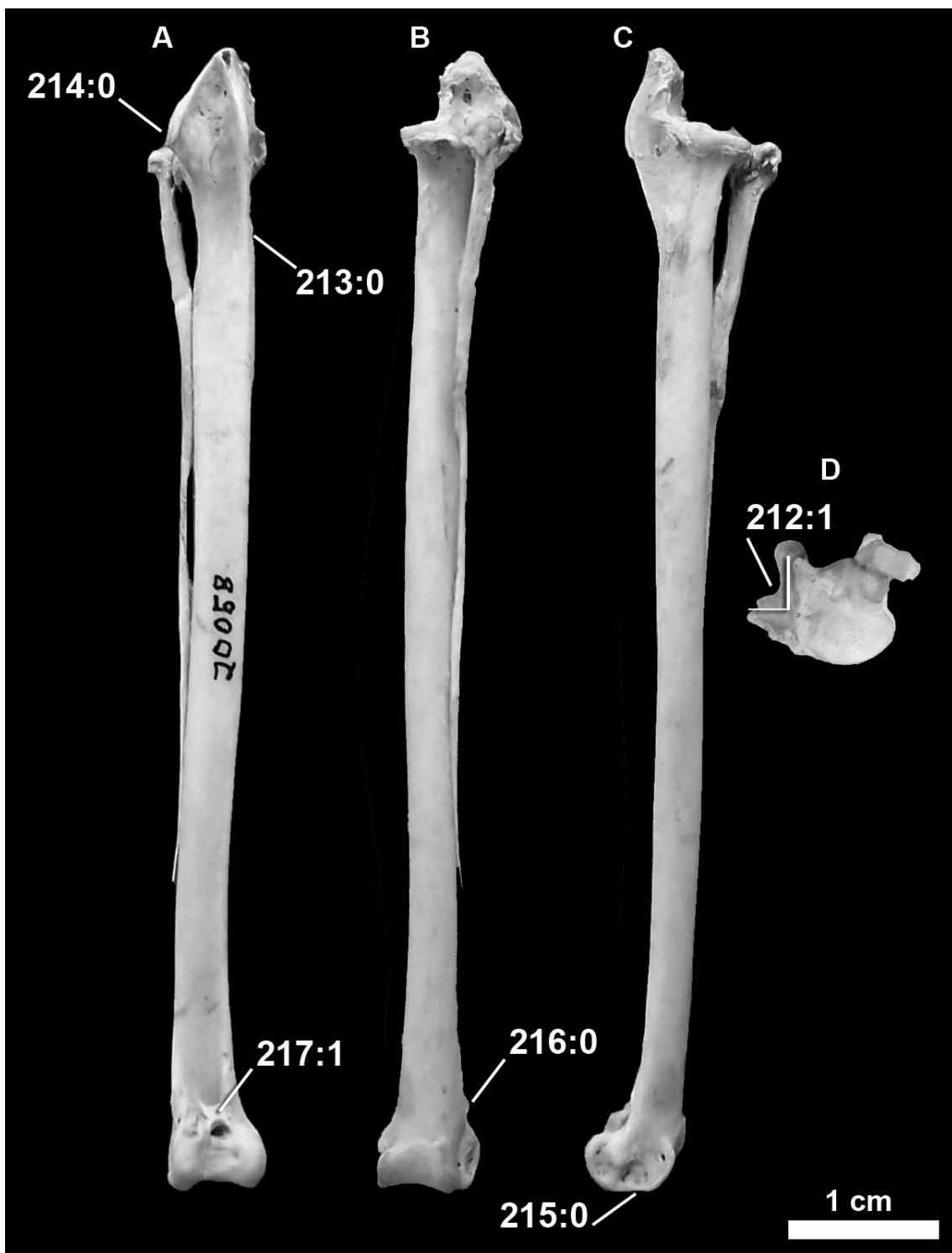


Figure A2.33- Right tibiotarsus and fibula of *Alca torda* (NCSM 20058) in anterior (A); posterior (B); medial (C); and proximal (D) views.

## TARSOMETATARSUS

**219. Tarsometatarsus, tendinal canal No. 1 of hypotarsus, conformation** (Strauch, 1978, character 64; Chandler, 1990b, character 82): (0) deep channel; (1) bony canal. The pattern of the canals in the hypotarsus of charadriiforms is discussed by Strauch (1978). In most charadriiforms canal No. 1 is a bony canal; in the Lari it is either a bony canal or a deep channel. In the Alcidae it may be a bony canal (e.g., *Aethia pusilla*), or a deep channel (e.g., *Alca torda*). The bony canal in charadriiforms is hypothesized to be primitive (Strauch, 1978). More open canals in the hypotarsus have been linked with greater specialization and probably represent derived states (Harrison 1976 in Strauch, 1985). In charadriiforms, tendinal canal No. 1 provides passage for m. flexor digitorum longus (Strauch, 1978).

**220. Tarsometatarsus, tendinal canal No. 2 of hypotarsus, position** (Strauch, 1978, character 65): (0) posterior to tendinal canal 1; (1) confluent with tendinal canal 1; (2) posteromedial to tendinal canal 1, bordered medially by medial hypotarsal crest. In alcids that have an enclosed tendinal canal 1, this canal is positioned anterior to tendinal canal 2 (e.g., *Alle alle*). In alcids that do not have an enclosed tendinal canal 1 (e.g., *Alca torda*), the tendons for M. flexor digitorum longus, and M. flexor perforatus digit IV and/or M. flexor perforans et et perforatus digiti II, presumably run within what has been designated tendinal canal 1 (Strauch, 1978). The second tendinal canal of some other charadriiforms (e.g., *Charadrius wilsonia*) is located posteromedial to tendinal canal 1 along the medial border of the medial hypotarsal crest.

**221. Tarsometatarsus, tendinal canal No. 3 of hypotarsus, conformation** (Strauch, 1978, character 66): (0) open groove; (1) mostly or completely enclosed bony channel. In the taxa examined, the third tendinal canal of the hypotarsus varies from a shallow groove (e.g., *Alca torda*) to a partially or fully enclosed bony canal (e.g., *Cephus grylle*). In charadriiforms, the tendinal canal No. 3 provides passage for m. flexor hallicus longus (Strauch, 1978).

**222. Tarsometatarsus, calcaneal ridges of hypotarsus, distal extension:** (0) short; (1) long. The calcaneal ridges of the hypotarsus extend further distally (i.e., proximodistally longer than mediolaterally wide) in some species of alcids (e.g., *Synthliboramphus wumizusume*) while in others (e.g., *Ptychoramphus aleuticus*), the calcaneal ridges are shorter (i.e., proximodistally shorter than mediolaterally wide).

**223. Tarsometatarsus, medial crest of hypotarsus:** (0) reduced; (1) prominent. The medial crest of the hypotarsus in many charadriiforms (e.g., *Sterna maxima*) is a well-developed posteriorly projecting and distally extending structure. In all alcids (e.g., *Alca torda*) the medial hypotarsal crest is reduced (i.e., relatively the same size as other hypotarsal crests).

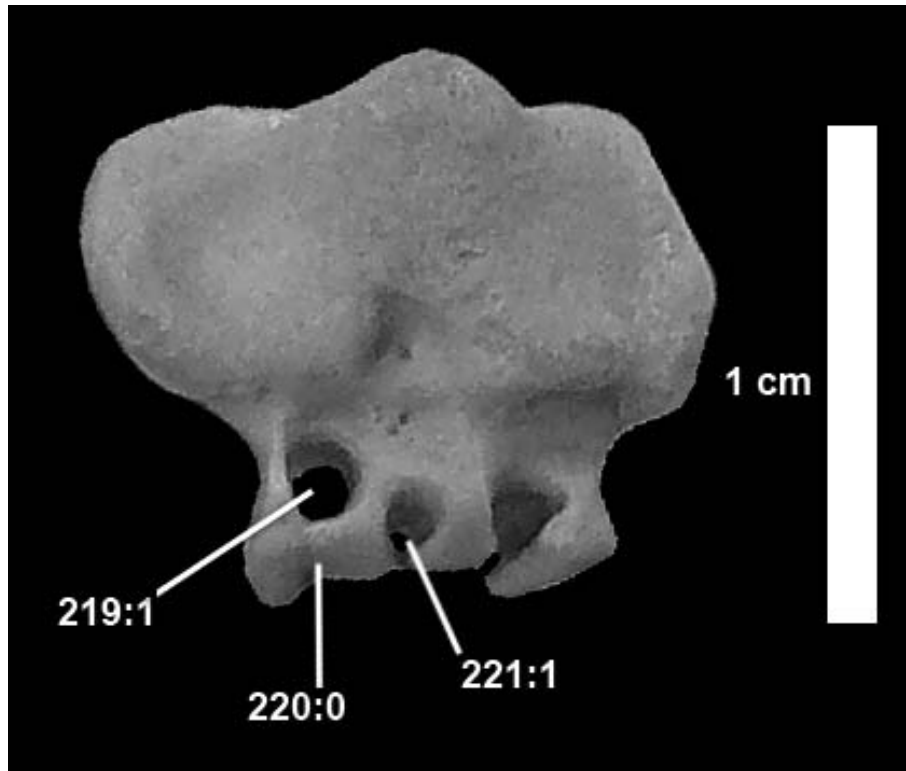


Figure A2.34- Right tarsometatarsus of *Cephus grylle* (USNM 344759) in proximal view.

**224. Tarsometatarsus, proximal vascular foramina, penetration of medial calcaneal ridge:** (0) absent; (1) present. There are two proximal vascular foramina in alcids. The medial foramina penetrates the medial calcaneal ridge all species (e.g., *Alca torda*) except (e.g., *Ptychoramphus aleuticus*) in which this foramina is positioned distal to the distal extent of the medial calcaneal ridge.

**225. Tarsometatarsus, anterior groove, conformation** (Chandler, 1990b, character 79): (0) deep groove; (1) shallow groove. The anterior surface of the shaft of the tarsometatarsus is relatively flat in some alcids (e.g., *Alca torda*) and a deep groove in others (e.g., *Cerorhinca monocerata*).

**226. Tarsometatarsus, cross-sectional shape:** (0) square; (1) rectangular. The tarsometatarsus of many alcids at mid-shaft is much wider than it is deep (e.g., *Fratercula cirrhata*), while in other alcids (e.g., *Cephus columba*) the tarsometatarsus is approximately as wide as it is deep.

**227. Tarsometatarsus, distal vascular foramen, size:** (0) small; (1) large. The distal vascular foramen is small (i.e., constitutes less than 1/3 of width of distal tarsometatarsus)

in most charadriiforms ((e.g., *Synthliboramphus antiquus*). In a few charadriiforms (e.g., *Hydrophasianus chirurgus*) the distal vascular foramen is a large and deeply excavated.

**228. Tarsometatarsus, distal vascular foramen, position:** (0) proximal; (1) distal. The distal border of the distal vascular foramen is continuous with proximal margin of the fourth trochlea in *Hydrophasianus*, whereas the distal vascular foramen is positioned more proximally in other species (e.g., *Alca torda*).

**229. Tarsometatarsus, distal vascular foramen, placed in a groove:** (0) not in a groove; (1) in a groove. The distal vascular foramen is positioned at the distal end of a distinct groove that tapers proximally to a point in some species (e.g., *Hydrophasianus chirurgus*). This groove is distinct from the anterior groove of the tarsometatarsus, which extends over a broader area of the shaft.

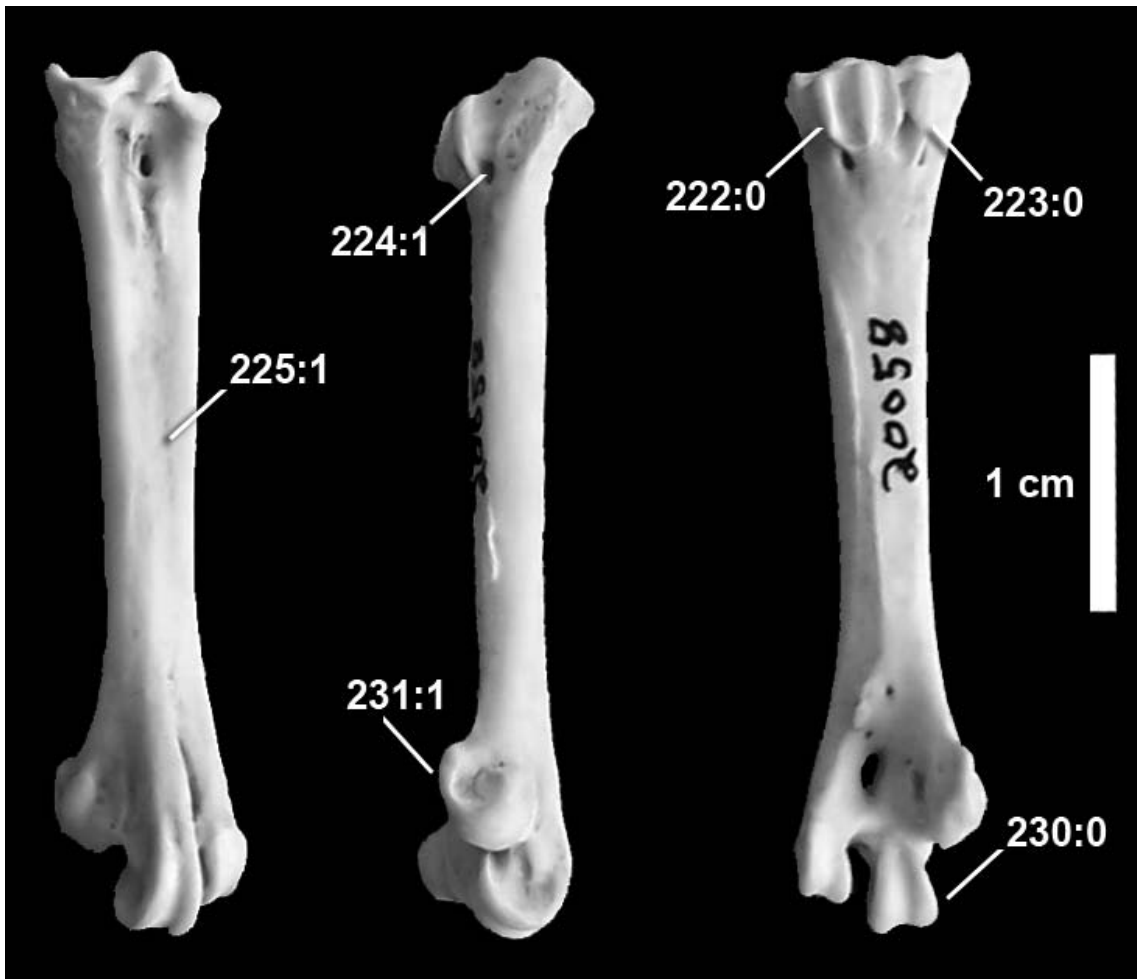


Figure A2.35- Left tarsometatarsus of *Alca torda* (NCSM 20058) in anterior (left), medial (middle), and posterior (right) views.



**230. Tarsometatarsus, trochlear proportions** (Strauch, 1985, character 20): (0) fairly robust (i.e., "normal") proportions for charadriiforms; (1) long and slender. In the Lari and most alcids (e.g., *Alca torda*) the proportions of the trochlea are similar. In some murrelets (e.g., *Synthliboramphus antiquus*) the trochleae are relatively long and somewhat compressed and give the tarsometatarsus a slender appearance (Storer 1945b in Strauch, 1985).

**231. Tarsometatarsus, trochlea II in lateral view, overlap of trochlea III** (Chandler, 1990b, character 81): (0) trochlea 2 does not overlap trochlea 3; (1) trochlea 2 overlaps trochlea 3. The distal extension of the second trochlea of the tarsometatarsus relative to the third trochlea is variable in Alcidae. In most alcids (e.g., *Alca torda*) trochlea 2 partially overlaps trochlea 3 in medial view, while in some alcids (e.g., *Synthliboramphus antiquus*) there is no overlap at all.

**232. Tarsometatarsus, length:** (0) tarsometatarsus longer than femur; (1) tarsometatarsus shorter than femur. The tarsometatarsi of a few alcids (e.g., *Synthliboramphus antiquus*) are longer than their femurs. Most alcids have femurs that are longer than their tarsometatarsi (e.g., *Alca torda*).

## INTEGUMENT

**233. Maxillary rhamphotheca, color of tip** (modified from Chandler, 1990b, character 95): (0) black or very dark brown; (1) red, orange or yellow; (2) white. In some alcids the tip of the beak varies in color from the rest of the rhamphothecum. The distal tip of the maxillary rhamphothecum varies in color from black or very dark brown (e.g., *Alca torda*), to shades of red, orange and yellow (e.g., *Aethia psittacula*), to white or light colored (e.g., *Aethia pusilla*).

**234. Maxillary rhamphotheca, color** (modified from Chandler, 1990b, character 92): (0) primarily red, yellow or orange; (1) primarily black; (2) horn or grey. The maxillary rhamphothecum varies in color from black only (e.g., *Uria aalge*), to horn or grey colored (e.g., *Synthliboramphus wumizusume*), to shades of red, yellow or orange (e.g., *Fratercula arctica*).

**235. Maxillary rhamphotheca, lateral surface ornamentation** (modified from Chandler, 1990b, character 98): (0) smooth; (1) **vertically grooved**. The rhamphothecum of some alcids have dorsoventrally oriented grooves (e.g., *Alca torda*), although this feature is not present in all alcids (e.g., *Alle alle*).

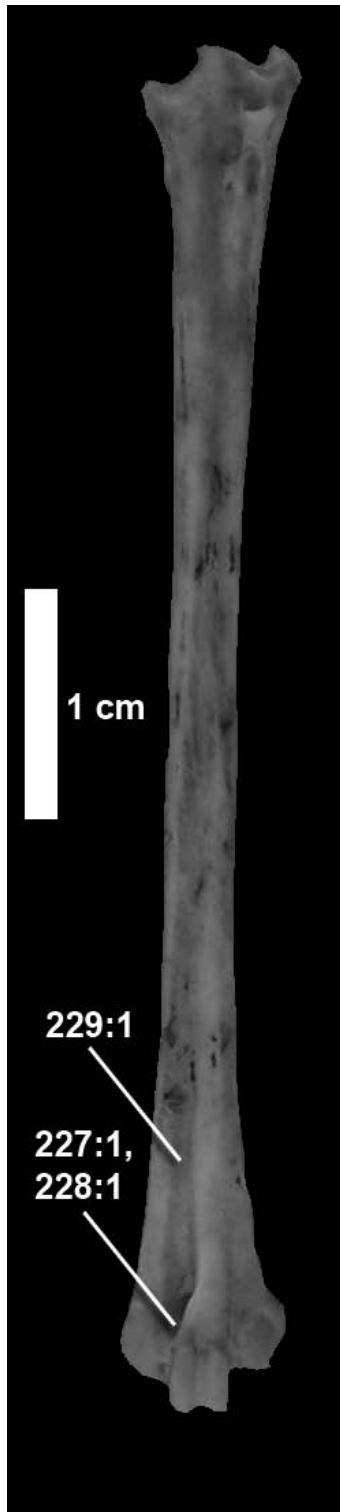


Figure A2.36- Left tarsometatarsus of *Hydrophasianus chirurgus* (USNM 490566) in anterior view.

**236. Maxillary rhamphotheca, horn at base of maxilla:** (0) absent; (1) present. A dorsally projecting horn is present on the base of the posterior maxillary rhamphotheca of *Cerorhinca monocerata* and *Aethia pusilla*. This feature is absent in all other alcids (e.g., *Alle alle*) and the nearest outgroups to Alcidae.

**237. Maxillary rhamphotheca, seasonal change** (Chu, 1998, character 121): (0) absent; (1) present. The bill structure of most alcids (e.g., *Alle alle*) does not change once they reach adulthood, while the bills of some species (e.g., *Fratercula arctica*) undergo dramatic changes associated with the breeding season.

**238. Mouth tissue color** (modified from Chandler, 1990b, character 93): (0) yellow; (1) red or orange; (2) white. The lining inside the mouth varies in color from shades of red (e.g., *Cepphus grylle*), orange (e.g., *Fratercula corniculata*) and yellow (e.g., *Alca torda*) to white (e.g., *Aethia psittacula*; Ridgway, 1919).

**239. External nares, orientation:** (0) laterally or dorsally directed oval or slit; (1) ventrally directed, medially oriented slit. Most alcids (e.g., *Cepphus grylle*) have oval shaped dorsally oriented nares. A few alcids (e.g., *Fratercula arctica*) have nares in the form of long, ventrally opening, medially oriented slits.

**240. Nostril feathering** (Strauch, 1985, character 22; Chandler, 1990b, character 89): (0) nostrils bare; (1) partially feathered; (2) fully feathered. The nostrils of the Lari, some alcids (e.g., *Cerorhinca monocerata*), and most other charadriiforms are bare. Some alcids (e.g., *Cepphus grylle*) have partially feathered nostrils, and others have completely feathered ones (e.g., *Alca torda*). It is hypothesized that increasing feathering represents progressively derived states. This character was first used by Brandt (1837) to classify the alcids (Strauch, 1985). **Ordered**

**241. Eye color:** (0) darkly colored; (1) lightly colored. The eye color of most alcids (e.g., *Alca torda*) is brown, although a few alcids (e.g., *Aethia pygmaea*) have yellow or grey colored eyes.

**242. Eye scales** (Strauch, 1985, character 24; Chandler, 1990b, character 90): (0) absent; (1) present. The Lari and most other charadriiforms have no eye scales (e.g., *Aethia psittacula*); they are present in some puffins (e.g., *Fratercula corniculata*; Strauch, 1985). These dermal structures, although they change color during the breeding season and are undoubtedly used for mating display purposes, are also present year round and even on nestlings. This suggests that these ‘horns’ may have another purpose, possibly hydrodynamic. The evolution of a hardened horn solely for mating purposes seems unlikely given that a simple mating display could be achieved via feather coloration.

**243. Plume in front of eye** (Chandler, 1990b, character 86): (0) absent; (1) present. *Aethia pygmaea* is unique in possessing a plume that originates anterior to the eye. All other alcids lack this feature.

**244. Plume behind eye** (Chandler, 1990b, character 87): (0) absent; (1) present. While most alcids (e.g., *Alca torda*) lack this feature, some alcids (e.g., *Aethia pusilla*) possess a plume that originates posterior to the eye.

**245. Plume on forehead** (Chandler, 1990b, character 85): (0) absent; (1) present. Although lacking in most alcids (e.g., *Alle alle*), some species (e.g., *Aethia psittacula*) possess a head plume that originates on the forehead (in addition to plumes behind and in front of the eye).

**246. Head plumage** (Strauch, 1985, character 23): (0) typical feathering; (1) velvety plumage. The head plumage of the Lari and most other charadriiforms consists of typical feathers (e.g., *Aethia psittacula*); in some alcids (e.g., *Alca torda*) the head plumage is distinctly velvety (Strauch, 1985).

**247. Neck plumage** (Chandler, 1990b, character 101): (0) not notched; (1) notched. The neck plumage of some alcids (e.g., *Uria lomvia*) is notched in anterior view.

**248. White tips on secondaries** (Strauch, 1985, character 26; Chandler, 1990b, character 88): (0) absent; (1) present. In the Lari the secondaries may be solid-colored or white-tipped. The condition in the Lari thus does not indicate the primitive state in the Alcidae. Since dark-tipped secondaries (e.g., *Aethia pusilla*) are found in three of the four major groups of alcids ["widespread" according to the principles of Kluge and Farris (1969)], white tips (e.g., *Uria aalge*) are hypothesized to be a derived state (Strauch, 1985).

**249. White wing patch** (Chandler, 1990b, character 105): (0) absent; (1) present. Although absent in most alcids (e.g., *Alle alle*), some alcids possess a white wing patch (e.g., *Cephus grylle*).

**250. Number of primaries:** (0) eleven; (1) nine. All alcids (e.g., *Cephus grylle*) and many other charadriiforms have 10 functional primary flight feathers and an eleventh reduced primary, while some charadriiforms (e.g., *Charadrius wilsonia*) have 9 primaries.

**251. Number of retrices** (Strauch, 1985, character 27; Chandler, 1990b, character 96): (0) ten; (1) twelve; (2) fourteen; (3) sixteen or more. The Lari have 12 retrices. Alcid species may have 12 (e.g., *Alca torda*), 14 (e.g., *Cephus columba*), 16, or 18 retrices (e.g., *Fratercula arctica*). The number appears to be constant within a species except for *Cerorhinca monocerata*, which may have 16 or 18. It is hypothesized that an increasing number of retrices represents increasingly derived states (Strauch, 1985). Some other charadriiforms (e.g., *Anous tenuirostris*) only have ten retrices. **Ordered**

**252. Shape of retrices** (Strauch, 1985, character 28; Chandler, 1990b, character 97): (0) rounded at tips; (1) pointed at tips. The retrices of the Lari and most other charadriiforms

(e.g., *Cephus columba*) have rounded tips. In some auks (e.g., *Alca torda*) the retrices are distinctly pointed at the tips (Strauch, 1985).

**253. Winter plumage** (Chandler, 1990b, character 83): (0) contrasting dark mantle and white underparts; (1) mantle and underparts dark. While some species of alcids (e.g., *Aethia pygmaea*) remain darkly colored above and below year-round, many alcids (e.g., *Alca torda*) display white underparts during the winter months.

**254. Juvenile plumage:** (0) resembles winter adults; (1) resembles summer adults. The juvenile plumage of all alcids (e.g., *Uria lomvia*) except *Alca torda* and *Alle alle* resembles the winter plumage of adults, in which the juvenile plumage resembles the summer plumage of adults (Kozlova, 1957).

**255. Molt:** (0) simultaneous; (1) gradual. Most alcids (e.g., *Uria lomvia*) moult their flight feathers simultaneously, resulting in a roughly 45-day period of flightlessness. Only the auklets (e.g., *Aethia pygmaea*) moult their flight feathers gradually, maintaining the ability of flight year-round (Kozlova, 1957).

**256. Tail shape** (modified from Chandler, 1990b, character 99): (0) rounded; (1) central notched; (2) pointed; (3) forked. Variation in the tail shape of alcids includes rounded (e.g., *Uria lomvia*), central notched (e.g., *Fratercula arctica*) and pointed (e.g., *Alca torda*).

**257. Foot color** (modified from Chandler, 1990b, character 94): (0) red, orange, or pink; (1) white or grey; (2) black or dark brown; (3) buff or tan. Foot color in the Alcidae varies from red (e.g., *Cephus columba*), to grey (e.g., *Aethia pygmaea*), to black (e.g., *Alca torda*; Ridgway, 1919).

**258. Scutellation** (modified from Strauch, 1985, character 29; Chandler, 1990b, character 106): (0) scutellate; (1) reticulate. The scutellation on the dorsal podotheca (i.e., acrotarsium) of the Lari is scutellate. In alcids it may be either scutellate (e.g., *Alca torda*) or reticulate (e.g., *Aethia pygmaea*; Strauch, 1985).

**259. Ungual (claw) of inner toe, shape** (modified from Strauch, 1985, character 21): (0) gracile, gently curving; (1) stout and strongly recurved. The second claw of most charadriiforms (e.g., *Aethia pygmaea*) is moderately arched, compressed, and acute (Coues, 1868). In puffins that dig their own burrows (e.g., *Fratercula arctica*), the inner (second) toe is usually stout and strongly recurved (Strauch, 1985).

**260. Foot webbing:** (0) absent; (1) present. All alcids (e.g., *Alca torda*) have webbing between the second, third and fourth toes. Some charadriiforms (e.g., *Charadrius wilsonia*) lack this characteristic.

**261. Hallux** (Chandler, 1990b, character 80): (0) absent; (1) present. Alcids (e.g., *Uria lomvia*) differ from many other charadriiforms (e.g., *Larus marinus*) in that they lack a first toe or hallux.

**262. White face color in breeding plumage** (Chandler, 1990b, character 91): (0) absent; (1) present. During the breeding season the face color of some alcids (e.g., *Fratercula arctica*) changes to white in color. The face color of most alcids (e.g., *Alca torda*) is not white during the reproductive phase.

**263. Belly color during breeding plumage** (Chandler, 1990b, character 84): (0) white; (1) black; (2) mottled brown; (3) grey. The belly-color of alcids during the breeding season varies from white (e.g., *Alca torda*), to black (e.g., *Fratercula cirrhata*), to mottled brown (e.g., *Brachyramphus marmoratus*), to grey (e.g., *Aethia pygmaea*).

**264. Barred breeding plumage** (Chandler, 1990b, character 104): (0) absent; (1) present. The breeding plumage of some alcids (e.g., *Brachyramphus marmoratus*) is barred.

## REPRODUCTION

**265. Incubation patches** (Strauch, 1985, character 25; Chandler, 1990a, character 103): (0) two; (1) one. Paired lateral incubation patches are found in shorebirds, Lari, and some alcids (e.g., *Alle alle*; Bailey 1952). Some alcids (e.g., *Alca torda*) have only one patch (Strauch, 1985).

**266. Nest sites** (modified from Strauch, 1985, character 32): (0) bare rock or scrape; (1) natural crevices; (2) burrows; (3) built of sticks, grass, feathers, etc... The Lari nest in the open, as do some alcids (*Ptychoramphus aleuticus*). Other alcids (e.g., *Fratercula arctica*) nest in crevices or in burrows. Kozlova (1961) thought that the original nest sites of alcids were on open rocks or coastal cliffs (e.g., *Alca torda*). It is hypothesized that nesting in crevices or in burrows represents increasingly derived conditions (Strauch, 1985).

**267. Nesting dispersion** (Strauch, 1985, character 33): (0) colonial; (1) solitary. The Lari and most of the alcids (e.g., *Alca torda*) nest in colonies. Some species of alcids (e.g., *Brachyramphus marmoratus*), however, nest solitarily (Strauch, 1985).

**268. Nesting proximity to shore:** (0) near-shore; (1) inland. Although most alcids (e.g., *Alca torda*) nest on sea-cliffs or rocky beaches near-shore, a few alcids (e.g., *Brachyramphus marmoratus*) are known to nest further inland.

**269. Clutch size** (Strauch, 1985, character 30; Chandler, 1990a, character 102): (0) one; (1) two or more. The Lari and almost all other charadriiforms lay a clutch of two or more.

Although some alcids (e.g., *Cepphus grylle*) lay two eggs, most species lay only one (e.g., *Alca torda*; Strauch, 1985).

**270. Egg shape** (modified from Chandler, 1990a, character 100): (0) ovate; (1) pyriform; (2) elliptical; (3) sub-elliptical/ovate. Alcid eggs display considerable variety of shape. The eggs of the majority of alcid species (e.g., *Cepphus grylle*) are characterized as sub-elliptical/ovate in shape. The second most common alcid egg shape is ovate (e.g., *Alle alle*). Other shapes include pyriform (e.g., *Pinguinus impennis*) and elliptical (e.g., *Synthliboramphus hypoleucus*).

**271. Egg markings, scribbling:** (0) absent; (1) present. The eggs of some alcids (e.g., *Pinguinus impennis*) display complex "scribbles", although the eggs of most alcids (e.g., *Aethia cristatella*) lack this feature.

**272. Egg texture:** (0) smooth; (1) granular. The eggs of some alcids (e.g., *Alca torda*) have a rough, granular texture. The eggs of other alcids (e.g., *Cepphus grylle*) and most charadriiforms have a smooth texture.

**273. Egg luster:** (0) non-glossy; (1) glossy. The luster of murrelet (e.g., *Synthliboramphus antiquus*) eggs varies from all other alcids (e.g., *Alca torda*) in having a glossy luster.

**274. Color of downy chicks:** (0) variable; (1) primarily brown; (2) primarily black; (3) primarily grey; (4) primarily buff or white. The down feathering of charadriiform chicks is predictably colored in most species (e.g., black in *Cepphus grylle*), although the color of the down feathers in some terns (e.g., *Sterna maxima*) is variable (i.e., sometimes black, sometimes buff).

**275. Post-hatching development pattern** (Strauch, 1985, character 31): (0) semi-precocial; (1) intermediate; (2) precocial. Alcids have three distinct post-hatching development patterns: precocial, intermediate, and semi-precocial (Sealy 1973). The pattern for *Pinguinus* is unknown. Bengtson (1984), in a review of the literature on *Pinguinus*, estimated that chicks leave the nest at about 10 days old, which would agree with an intermediate pattern. In the Lari the pattern is semi-precocial; it is hypothesized that shortening of the nestling period in alcids represents a derived condition (Strauch, 1985). **Ordered**

## DIET

**276. Adult prey preference:** (0) primarily invertebrates; (1) primarily vertebrates; (2) significant amounts of invertebrates and vertebrates. Many of the smaller alcids (e.g., *Alle alle*) are specialized feeders on small invertebrates, while some larger alcids (i.e., *Fratercula arctica*) subsist on a diet of mostly fish (del Hoyo et al., 1996).

**277. Chick diet:** (0) primarily invertebrates; (1) primarily vertebrates; (2) significant amounts of invertebrates and vertebrates. The diet that alcids feed to their chicks varies from primarily invertebrates such as copepods, amphipods, and euphausiids (del Hoyo et al., 1996; e.g., *Alle alle*), to primarily vertebrates such as fish and eels (del Hoyo et al., 1996; e.g., *Uria lomvia*). Many close outgroup taxa to Alcidae are more generalized feeders (i.e., a combination of both invertebrates, vertebrates, carrion, trash; del Hoyo et al., 1996; e.g., *Larus marinus*).

#### MUSCULATURE

(see Hudson et al., 1969 for detailed character descriptions)

**278. M. pectoralis abdominalis insertion on** (Hudson, 1969): (0) tendon of M. pectoralis thoracica; (1) humerus.

**279. Anterior head of M. subcoracoideus** (Hudson, 1969): (0) small or absent; (1) short or long.

**280. M. propatagialis longus dilation at wrist** (Hudson, 1969): (0) unossified; (1) ossified.

**281. M. propatagialis** (Hudson, 1969): (0) two tendons; (1) one tendon.

**282. Patagial fan sesamoid** (Hudson, 1969) : (0) present; (1) absent.

**283. M. deltoideus minor dorsal head** (Hudson, 1969): (0) present; (1) absent.

**284. Swelling in M. triceps tendons** (Hudson, 1969): (0) unossified; (1) ossified.

**285. Swelling in humero-ulnar pulley** (Hudson, 1969): (0) ossified; (1) unossified.

**286. M. biceps brachii** (Hudson, 1969): (0) divided lengthwise; (1) divided distally; (2) undivided.

**287. M. flexor digitorum sublimis dilation at base of phalanx 1** (Hudson, 1969): (0) ossified; (1) unossified.

**288. M. ulnometacarpalis dorsalis ventral head** (Hudson, 1969): (0) present; (1) absent.

**289. M. ambiens** (Hudson, 1969): (0) present; (1) absent.

**290. Pars iliofemoralis of M. piriformis** (Hudson, 1969): (0) absent; (1) present.



- 291. Pars interna of *M. gastrocnemius*** (Hudson, 1969): (0) extends around anterior surface of knee; (1) does not extend around anterior surface of knee.
- 292. Pars interna of *M. gastrocnemius*** (Hudson, 1969): (0) no extra head from tibia; (1) extra head from tibia.
- 293. Pars medialis of *M. gastrocnemius*** (Hudson, 1969): (0) present; (1) absent.
- 294. *M. plantaris*** (Hudson, 1969): (0) present; (1) absent.
- 295. Sesamoid of *M. scapulotriceps*** (Hudson, 1969): (0) absent; (1) present.
- 296. Sesamoid of *M. humerootriceps*** (Hudson, 1969): (0) absent; (1) present.
- 297. Sesamoid of humero-ulnar pulley** (Hudson, 1969): (0) absent; (1) present.
- 298. Sesamoid of propatagialis longus at wrist** (Hudson, 1969): (0) absent; (1) present.
- 299. Sesamoid of flexor digitorum profundus in hand** (Hudson, 1969): (0) absent; (1) present.
- 300. Sesamoid of flexor digitorum sublimis at base of phalanx 1** (Hudson, 1969): (0) absent; (1) present.
- 301. Sesamoid of flexor digitorum longus** (Hudson, 1969): (0) absent; (1) present.

#### FEATHER MICROSTRUCTURE

(see Dove, 2000 for complete character descriptions)

- 302. Subpennaceous region** (modified from Dove, 2000 character 1): (0) absent; (1) present.
- 303. Subpennaceous region pigmentation** (modified from Dove, 2000 character 2): (0) absent, both vanules unpigmented (1) present, both vanules pigmented.
- 304. Subpennaceous region pigmentation position** (modified from Dove, 2000 character 2): (0) distal vanule more pigmented; (1) both vanules equally pigmented.
- 305. Subpennaceous length** (modified from Dove, 2000 character 3): (0) short; (1) long; (2) very long.
- 306. Barbule base pigmentation** (modified from Dove, 2000 character 4): (0) absent; (1) present.

- 307. Barbule base length** (modified from Dove, 2000 character 5): (0) short; (1) long; (2) continuous with pennulum.
- 308. Barbule base cells** (modified from Dove, 2000 character 6): (0) not visible; (1) visible.
- 309. Barbule base cell composition** (modified from Dove, 2000 character 6): (0) single cell; (1) multiple cells; (2) both single and multiple.
- 310. Barb length** (modified from Dove, 2000 character 7): (0) short; (1) long; (2) both short and long.
- 311. Barb pigmentataion** (modified from Dove, 2000 character 8): (0) absent, not pigmented; (1) present, pigmented.
- 312. Barb pigmentation position** (modified from Dove, 2000 character 8): (0) pigmented base to tip; (1) proximally pigmented; (2) both fully pigmented and unpigmented; (3) both fully pigmented and half-pigmented.
- 313. Barbule pigmentation** (modified from Dove, 2000 character 11): (0) absent, no pigmented nodes; (1) present, all nodes pigmented.
- 314. Barbule pigmentation position** (modified from Dove, 2000 character 11): (0) proximal nodes pigmented; (1) all nodes pigmented.
- 315. Node expansion** (modified from Dove, 2000 character 12): (0) unexpanded; (1) expanded.
- 316. Node expansion location** (modified from Dove, 2000 character 12): (0) uniform; (1) proximal.
- 317. Density of nodes per barbule** (modified from Dove, 2000 character 13): (0) sparse; (1) dense.
- 318. Proximal node shape** (modified from Dove, 2000 character 14): (0) normal; (1) flared; (2) oblong; (3) straight.
- 319. Midsection nodes shape** (modified from Dove, 2000 character 15): (0) normal; (1) flared; (2) oblong; (3) straight.
- 320. Distal nodes** (modified from Dove, 2000 character 16): (0) indistinct, not visible; (1) distinct, visible.

- 321. Distal node shape** (modified from Dove, 2000 character 16): (0) normal; (1) oblong.
- 322. Nodal spines** (modified from Dove, 2000 character 17): (0) absent; (1) present.
- 323. Nodal spine position** (modified from Dove, 2000 character 17): (0) present at all nodes; (1) present at basal nodes; (3) with and without spines.
- 324. Nodal prongs** (modified from Dove, 2000 character 18): (0) absent; (1) present.
- 325. Nodal points** (modified from Dove, 2000 character 19): (0) absent; (1) present.
- 326. Nodal point position** (modified from Dove, 2000 character 19): (0) present at all nodes; (1) present at basal nodes; (2) present at distal nodes; (3) nodes with and without points.
- 327. Proximal node pigment** (modified from Dove, 2000 character 20): (0) absent or only a few pigment granules; (1) many pigment granules present.
- 328. Proximal node pigment shape** (modified from Dove, 2000 character 20): (0) long and constricted; (1) diamond shaped; (2) short and constricted; (3) round; (4) diffuse.
- 329. Mid-node pigment** (modified from Dove, 2000 character 21): (0) absent or only a few pigment granules; (1) many pigment granules present.
- 330. Mid-node pigment shape** (modified from Dove, 2000 character 21): (0) long and constricted; (1) diamond shaped; (2) short and constricted; (3) round; (4) diffuse.
- 331. Distal node pigmentation** (modified from Dove, 2000 character 22): (0) unpigmented nodes; (1) nodes pigmented.
- 332. Distal pigment distribution** (modified from Dove, 2000 character 22): (0) continuous pigmentation; (1) distal pigmentation; (2) trailing pigment; (3) node clear, internode pigmented.
- 333. Nodal pigment intensity at basal nodes** (modified from Dove, 2000 character 23): (0) absent; (1) present.
- 334. Nodal pigment intensity at basal nodes** (modified from Dove, 2000 character 23): (0) lightly pigmented; (1) heavily pigmented.
- 335. Nodal pigment at distal nodes** (modified from Dove, 2000 character 24): (0) absent; (1) present.

**336. Nodal pigment intensity at distal nodes** (modified from Dove, 2000 character 24): (0) lightly pigmented; (2) heavily pigmented.

**337. Pigment color** (modified from Dove, 2000 character 25): (0) brown; (1) black; (2) light reddish-brown.

**338. Morphology of first node** (modified from Dove, 2000 character 26): (0) reduced; (1) similar to other nodes; (2) both reduced and expanded first nodes.

**339. Internode pigmentation** (modified from Dove, 2000 character 27): (0) absent; (1) present.

**340. Internode pigmentation** (modified from Dove, 2000 character 27): (0) stippled; (1) heavily pigmented; (2) uniformly pigmented.

**341. True down pigmentation** (modified from Dove, 2000 character 30): (0) absent; (1) present.

**342. True down pigmentation** (modified from Dove, 2000 character 30): (0) proximal; (1) present throughout.

**343. True down nodes** (modified from Dove, 2000 character 31): (0) node indistinct, not visible (1) distinct, visible.

**344. True down nodes** (modified from Dove, 2000 character 31): (0) flared; (1) normal; (2) both flared and normal.

**345. True down pigment shape** (modified from Dove, 2000 character 32): (0) long and constricted; (1) diamond shaped; (2) short and constricted; (3) round; (4) diffuse.

**346. True down pigmented like contour down** (modified from Dove, 2000 character 33): (0) no; (1) yes.

**347. True down pigmented like afterfeather down** (modified from Dove, 2000 character 34): (0) no; (1) yes.

**348. Afterfeather pigmentation** (modified from Dove, 2000 character 35): (0) absent; (1) present.

**349. Afterfeather pigmentation** (modified from Dove, 2000 character 35): (0) proximal; (1) throughout; (2) distal.

**350. Afterfeather down pigmented like contour feather down** (modified from Dove, 2000 character 36): (0) no; (1) yes.

**351. Villi** (modified from Dove, 2000 character 37): (0) absent; (1) present.

**352. Distal prongs** (modified from Dove, 2000 character 38): (0) absent; (1) present.

**353. Distal prong morphology** (modified from Dove, 2000 character 38): (0) unequal length; (2) equal length.

REJECTED CHARACTERS: The following characters from the data of Chandler (1990a) were rejected due to intraspecies variability: 15, 32, 48, 55, 72, 73, 77, 78; or because they were parsimony uninformative (i.e., they did not vary among taxa examined): 27, 31, 34, 45, 54, 56, 57, 66, 68, 76.

The following characters of Dove (2000) were not included the matrix because they did not vary in any taxa examined in this study: 9, 10, 28, 29. Several characters of Dove (2000) were split into two separate characters following the philosophy of character independence with respect to absence of character states outlined by Hawkins et al. (1997).

All the characters of Strauch (1985) and Chandler (1990a) were rescored for this analysis using multiple specimens (see Appendix 2, comparative material). Many of the characters of Strauch (1985) and Chandler (1990a) were modified to describe variability not originally noted by those authors (see notations in character list).

Characters from Hudson et al. (1969) were not rescored, although scorings for *Uria aalge*, *Alle alle*, *Fratercula corniculata*, *Cepphus columba*, *Aethia psittacula*, and *Synthliboramphus antiquus* were confirmed through dissections (see comparative material for specimen #'s).

Contra Koslova 1958, a patella is present in *Uria aalge*, *Alle alle*, *Cepphus columba*, *Synthliboramphus antiquus*, *Aethia psittacula*, and *Fratercula corniculata*. However, this character was not included in the phylogenetic analysis because its distribution among other taxa is unknown.

### APPENDIX 3.

#### MORPHOLOGICAL CHARACTER MATRIX

Morphological character scorings for extant and extinct taxa included in the phylogenetic analyses or referred to in the text. Polymorphic scorings are represented by capital letters (A:0&1; B:0&2; C:1&2). Non-applicable scorings (e.g., the position of a tubercle in a taxon that does not possess that tubercle) are represented by a dash ‘-’.

Scorings for the *Fratercula* aff. *arctica* terminal were compiled based upon the following specimens: USNM 183471, 177800, 192901, 206640, 181103, 192894, 193070, 206517, 210475, 215617, 215677, 215720, 181031, 206639, 193243, 241402, 24855, and scorings for the *Fratercula* aff. *cirrhata* terminal were compiled based upon the following specimens: USNM 490887, 368496, 206324, 256229, 275800, 459394, 460789, 193131, 215678, 250704, 430958, 177996, 192813, 178023, 192053, 192726.

	10	20	30	40	50	60
Aethia storeri	?	?	?	?	?	?
Aethia cristatella	?	?	?	?	?	?
Aethia psittacula	?	?	?	?	?	?
Aethia pusilla	?	?	?	?	?	?
Aethia pygmaea	?	?	?	?	?	?
Aethia barnesi	?	?	?	?	?	?
Aethia rossmoori	?	?	?	?	?	?
Brachyramphus brevirostris	?	?	?	?	?	?
Brachyramphus dunkeli	?	?	?	?	?	?
Brachyramphus marmoratus	?	?	?	?	?	?
Brachyramphus perdix	?	?	?	?	?	?
Brachyramphus pliocenum	?	?	?	?	?	?
Brachyramphus sp. SDSNH 24865	?	?	?	?	?	?
Brachyramphus sp. SDSNH 24866	?	?	?	?	?	?
Alca ausonia holotype	?	?	?	?	?	?
Alca ausonia USNM 446692	?	?	?	?	?	?
Alca ausonia SST	?	?	?	?	?	?
Alca carolinensis	?	?	?	?	?	?
Alca grandis holotype	?	?	?	?	?	?
Alca grandis USNM 215454	?	?	?	?	?	?
Alca grandis USNM 236802	?	?	?	?	?	?
Alca grandis USNM 336379	?	?	?	?	?	?
Alca grandis USNM 495616	?	?	?	?	?	?
Alca grandis SST	?	?	?	?	?	?
Alca olsoni holotype	?	?	?	?	?	?
Alca olsoni USNM 495613	?	?	?	?	?	?
Alca stewarti types	?	?	?	?	?	?
Alca stewarti USNM 242238	?	?	?	?	?	?
Alca stewarti SST	?	?	?	?	?	?
Alca minor hypodigm	?	?	?	?	?	?
Alca torda	?	?	?	?	?	?
Alca aff. torda USNM 321314	?	?	?	?	?	?
ACPM 01 Alca skull	?	?	?	?	?	?
Alca USNM 419708	?	?	?	?	?	?
Alca USNM 495612	?	?	?	?	?	?
Alca USNM 336380	?	?	?	?	?	?





















61 70 80 90 100 110 120 . . . . .

????  
 ????  
 0210-1001101000001110101110210100-10101000131101121101120100  
 0111100000-0010000001100100010001102000-00020001000001102000  
 ????  
 011111010-101000000101100110010-02000-00000001010101102000  
 ????  
 ????  
 0110-10011101000111010011021011110101100110001110101111100  
 0210-10011101000111010010021011110101100111001110101111100  
 0210-10011101000111010010111011110101100111001110101111100  
 ????  
 ????  
 ????  
 ????  
 1211100111111000111101111210001010101101021001111010011101  
 ????  
 ????  
 ????  
 ????  
 ????  
 0111100000-110000000100000110011102000-00100001100101102000  
 0111000000-100000000100000110011102000-00100001100101102000  
 0111000000-001000000000010010011102000-00020001000001102000  
 0111000001000100000010010011011102000-00110001000111102000  
 011100?000-101000000100000?010-02000-00?10001?20?0102100  
 12111001111110001111011112100010101101121001111010010001  
 ????  
 12111001111110001111011112100010101101121001111010010010  
 ????  
 11111001111110001111011112100010101101121001111010010100  
 121?0011?111000111?000112100010101101?20?0111100?010000  
 ????  
 001100?000-000000000101100?010-02000-00?10001?10?0102000  
 0111000000-001000000100011001101100100100001000100102000  
 0010-01000-111000000000000010010-02100-00110001020001102000

Alca USNM 192101  
 Alcides ulnulus  
 Alle alle  
 Anous tenuirostris  
 Australca grandis holotype  
 Bartramia longicauda  
 SDSNH 25358  
 Boutersemia belgica  
 Cepphus carbo  
 Cepphus columba  
 Cepphus grylle  
 Cepphus olsoni  
 Cepphus storeri  
 Cerorhinca dubia  
 Cerorhinca minor  
 Cerorhinca moncerata  
 Cerorhinca reali  
 Cerorhinca sp. LACM 18274  
 Cerorhinca sp. LACM 18275  
 Cerorhinca sp. SDSNH 23079  
 Cerorhinca aurorensis  
 Charadrius vociferus  
 Charadrius wilsonia  
 Chlidonias leucoptera  
 Creagrus furcatus  
 Cusorius temminckii  
 Fratercula arctica  
 Fratercula aff. arctica  
 Fratercula cirrhata  
 Fratercula aff. cirrhata  
 Fratercula corniculata  
 Fratercula dowi  
 Fratercula sp. NHMUK PV A 9034  
 Glareola maldivarum  
 Gygis alba  
 Hydrophasianus chirurgus



121 130 140 150 160 170 180  
. . . . .  
210---1120-101000001000020100110101?100??110??01??????11  
??  
110---0010-10100000100002110012000101001000-11-00000010101  
010---0100-01100000000000000000000000101010-0111100002111  
??  
010---01111000000010000010000010100001011010-0010000002111  
??  
??  
110---0110-01100001100001130010010101001000-11011001010101  
110---0110-01101001100001130010010101000-01011210001000101  
110---0110-01101001100001130010010101000-01011011001000101  
110---0110-0110000?100001130010010101000-??22222222222222  
??  
??  
200---1121101000001000020222222222222222222222222222222  
210---112110001000000002020100010101000-111112011001010101  
210---01?110100001100002020100010101001001122222222222222  
??  
??  
??  
210---110110001000010000202000000101001001122222222222222  
010---0100-0010000010000010000001010000-11010-0011100001001  
010---0100-0010000010000010000001010000-10-10-0011100001101  
010---01110001000010000001010000000000101010-0110000001111  
010---01010001000001000000000000000000-11010-0011100001111  
170---0000-0?00?010?000?0000000?000?0?10-10-0011100001111  
110?--112110000000100002020100010101000-111112011001010101  
110?--112110000000100002020100010101000-111222222222222222  
110---112110000000100002020100010101000-111110011001010101  
110---112110000000100002020100010101000-111222222222222222  
110---112110000000100002020100010101000-111112011001010101  
110---11211000000010000202010001010100101?110011100110101  
??  
170---0100-0?10?000?000?010000?000?0?1122220011100001111  
010---011100010000110000010000000000001000-10-0101000001111  
010---0110--1001000000000010000000000000-11010-0101100001101

Alca USNM 192101  
Alcodes ulnulus  
Alle alle  
Anous tenuirostris  
Australca grandis holotype  
Bartramia longicauda  
SDSNH 25358  
Boutersemia belgica  
Cepphus carbo  
Cepphus columba  
Cepphus grylle  
Cepphus olsoni  
Cepphus storeri  
Cerorhinca dubia  
Cerorhinca minor  
Cerorhinca monocerata  
Cerorhinca reali  
Cerorhinca sp. LACM 18274  
Cerorhinca sp. LACM 18275  
Cerorhinca sp. SDSNH 23079  
Cerorhinca auroreensis  
Charadrius vociferus  
Charadrius wilsonia  
Chlidonias leucoptera  
Creagrus furcatus  
Cusorius temminckii  
Fratricula arctica  
Fratricula aff. arctica  
Fratricula cirrhata  
Fratricula aff. cirrhata  
Fratricula corniculata  
Fratricula dowi  
Fratricula sp. NHMUK PV A 9034  
Glareola maldivarum  
Gygis alba  
Hydrophasianus chirurgus

181	190	200	210	220	230	240
Alca USNM 192101	.	.	.	.	.	.
Alcodes ulinulus						
Alle alle						
Anous tenuirostris						
Australca grandis holotype						
Bartramia longicauda						
SDSNH 25358						
Boutersemia belgica						
Cephus carbo						
Cephus columba						
Cephus grylle						
Cephus olsoni						
Cephus storeri						
Cerorhinca dubia						
Cerorhinca minor						
Cerorhinca monocerata						
Cerorhinca reali						
Cerorhinca sp. LACM 18274						
Cerorhinca sp. LACM 18275						
Cerorhinca sp. SDSNH 23079						
Cerorhinca auroreensis						
Charadrius vociferus						
Charadrius wilsonia						
Chlidonias leucoptera						
Creagrus furcatus						
Cusorius temminckii						
Fratercula arctica						
Fratercula aff. arctica						
Fratercula cirrhata						
Fratercula aff. cirrhata						
Fratercula corniculata						
Fratercula dowi						
Fratercula sp. NHMUK PV A 9034						
Glareola maldivarum						
Gygis alba						
Hydrophasianus chirurgus						





301 . 310 . 320 . 330 . 340 . 350  
 ???? ???? ???? ???? ???? ???? ???? ???? ???? ???? ???? ???? ???? ???? ????  
 ???? ???? ???? ???? ???? ???? ???? ???? ???? ???? ???? ???? ???? ???? ????  
 ?1112120-010110-033110-10-1010121110111110-211111011  
 ???? ???? ???? ???? ???? ???? ???? ???? ???? ???? ???? ???? ???? ???? ????  
 ???? ???? ???? ???? ???? ???? ???? ???? ???? ???? ???? ???? ???? ???? ????  
 ?11111100101110000101000-1010101111001111101111100-  
 ???? ???? ???? ???? ???? ???? ???? ???? ???? ???? ???? ???? ???? ???? ????  
 ???? ???? ???? ???? ???? ???? ???? ???? ???? ???? ???? ???? ???? ???? ????  
 ???? ???? ???? ???? ???? ???? ???? ???? ???? ???? ???? ???? ???? ???? ????  
 ?1111120-210110-033110-10-1111121010011110-211111010  
 1??  
 1??  
 ???? ???? ???? ???? ???? ???? ???? ???? ???? ???? ???? ???? ???? ???? ????  
 ???? ???? ???? ???? ???? ???? ???? ???? ???? ???? ???? ???? ???? ???? ????  
 ???? ???? ???? ???? ???? ???? ???? ???? ???? ???? ???? ???? ???? ???? ????  
 ???? ???? ???? ???? ???? ???? ???? ???? ???? ???? ???? ???? ???? ???? ????  
 ???? ???? ???? ???? ???? ???? ???? ???? ???? ???? ???? ???? ???? ???? ????  
 ???? ???? ???? ???? ???? ???? ???? ???? ???? ???? ???? ???? ???? ???? ????  
 ?110120-010110-033110-10-11111210100110110-211111010  
 ???? ???? ???? ???? ???? ???? ???? ???? ???? ???? ???? ???? ???? ???? ????  
 ???? ???? ???? ???? ???? ???? ???? ???? ???? ???? ???? ???? ???? ???? ????  
 ???? ???? ???? ???? ???? ???? ???? ???? ???? ???? ???? ???? ???? ???? ????  
 ???? ???? ???? ???? ???? ???? ???? ???? ???? ???? ???? ???? ???? ???? ????  
 ???? ???? ???? ???? ???? ???? ???? ???? ???? ???? ???? ???? ???? ???? ????  
 ?110011101011101001010012121111100101112111110-  
 ???? ???? ???? ???? ???? ???? ???? ???? ???? ???? ???? ???? ???? ???? ????  
 ???? ???? ???? ???? ???? ???? ???? ???? ???? ???? ???? ???? ???? ???? ????  
 ?10-0011210---1000010120130-0-0-0-10-1010000-100-  
 ???? ???? ???? ???? ???? ???? ???? ???? ???? ???? ???? ???? ???? ???? ????  
 1111120-010110-033110-10-11111210100110110-211111010  
 ???? ???? ???? ???? ???? ???? ???? ???? ???? ???? ???? ???? ???? ???? ????  
 1111120-210110-033110-10-1111121110011110-211111010  
 ???? ???? ???? ???? ???? ???? ???? ???? ???? ???? ???? ???? ???? ???? ????  
 1??  
 ???? ???? ???? ???? ???? ???? ???? ???? ???? ???? ???? ???? ???? ???? ????  
 ???? ???? ???? ???? ???? ???? ???? ???? ???? ???? ???? ???? ???? ???? ????  
 ???? ???? ???? ???? ???? ???? ???? ???? ???? ???? ???? ???? ???? ???? ????  
 ?10-1011200---10000101000-0-0-0-0-10-11-110-100-  
 ???? ???? ???? ???? ???? ???? ???? ???? ???? ???? ???? ???? ???? ???? ????

Alca USNM 192101  
 Alcodes ulnulus  
 Alle alle  
 Anous tenuirostris  
 Australca grandis holotype  
 Bartramia longicauda  
 SDSNH 25358  
 Boutersemia belgica  
 Cepphus carbo  
 Cepphus columba  
 Cepphus grylle  
 Cepphus olsoni  
 Cepphus storeri  
 Cerorhinca dubia  
 Cerorhinca minor  
 Cerorhinca monocerata  
 Cerorhinca reali  
 Cerorhinca sp. LACM 18274  
 Cerorhinca sp. LACM 18275  
 Cerorhinca sp. SDSNH 23079  
 Cerorhinca aurorensis  
 Charadrius vociferus  
 Charadrius wilsonia  
 Chlidonias leucoptera  
 Creagrus furcatus  
 Cusorius temminckii  
 Fratercula arctica  
 Fratercula aff. arctica  
 Fratercula cirrhata  
 Fratercula aff. cirrhata  
 Fratercula corniculata  
 Fratercula dowi  
 Fratercula sp. NHMUK PV A 9034  
 Glareola maldivarum  
 Gygis alba  
 Hydrophasianus chirurgus





































## APPENDIX 4.

### MOLECULAR SEQUENCE AUTHORSHIP

Genbank accession numbers and authorship of molecular sequences used in this analysis. Key to lowercase letters in parentheses following accession numbers which denote authorship of sequences: **a**, Baker et al. 2007; **b**, Pereira and Baker 2008; **c**, Paton and Baker 2006; **d**, Bridge et al. 2005; **e**, Moum et al. 2002; **f**, Whittingham et al. 2000; **g**, Yamamoto et al. 2005; **h**, Moum et al. 1994; **i**, Hebert et al. 2004; **j**, Kerr et al. 2007; **k**, Friesen et al. 1996; **l**, Liebers et al. 2004; **m**, Cohen et al. 1997; **n**, Fain and Houde 2007; **o**, Paton et al. 2003; **p**, Groth and Barrowclough 1999; \*, unpublished sequence deposited in Genbank by Chen, X.-F. and Li, Q.-W., August 20, 2001.

Taxa	ND2	ND5	ND6	CO1
<i>Aethia cristatella</i>	EF373219 (a)	---	X73928 (h)	EF380315 (b)
<i>Aethia psittacula</i>	EF373235 (a)	---	X73925 (h)	EF380327 (b)
<i>Aethia pusilla</i>	EF380337 (b)	---	X73926 (h)	EF380316 (b)
<i>Aethia pygmaea</i>	EF380338 (b)	---	X73927 (h)	EF380317 (b)
<i>Alca torda</i>	EF373220 (a)	AJ242683 (e)	X73916 (h)	EF380318 (b)
<i>Alle alle</i>	EF373221 (a)	AJ242684 (e)	X73915 (h)	EF380319 (b)
<i>Anous tenuirostris</i>	EF373223 (a)	---	---	---
<i>Bartramia longicauda</i>	EF373226 (a)	---	---	AY666283 (i)
<i>Brachyramphus brevirostris</i>	EF373227 (a)	---	X73922 (h)	EF380321 (b)
<i>Brachyramphus marmoratus</i>	EF380340 (b)	---	X73923 (h)	EF380322 (b)
<i>Brachyramphus perdix</i>	EF380341 (b)	---	---	EF380323 (b)
<i>Cephus carbo</i>	EF380342 (b)	---	---	EF380324 (b)
<i>Cephus columba</i>	EF373229 (a)	---	X73918 (h)	EF380325 (b)
<i>Cephus grylle</i>	---	AJ242688 (e)	X73917 (h)	DQ433470 (j)
<i>Cerorhinca monocerata</i>	EF373230 (a)	---	---	EF380326 (b)
<i>Charadrius alexandrinus</i>	---	---	AF411407.1*	---
<i>Charadrius vociferous</i>	DQ385082 (c)	DQ385150 (c)	---	DQ385167 (c)
<i>Charadrius wilsonia</i>	---	---	---	AY666175 (j)
<i>Chidonias leucopterus</i>	EF373231 (a)	---	---	---
<i>Creagrurus furcatus</i>	EF373234 (a)	---	---	---
<i>Cursorius temminckii</i>	DQ385090 (c)	DQ385158 (c)	---	DQ385175 (c)
<i>Fratercula arctica</i>	DQ385092 (c)	DQ385160 (c)	X73929 (h)	DQ385177 (c)
<i>Fratercula cirrhata</i>	EF380343 (b)	---	X73931 (h)	EF380329 (b)
<i>Fratercula corniculata</i>	EF380344 (b)	---	X73930 (h)	EF380328 (b)
<i>Gelochelidon nilotica</i>	AY631383 (d)	---	---	DQ434167 (j)
<i>Glareola maldivarum</i>	EF373241 (a)	---	---	---
<i>Gygis alba</i>	EF373242 (a)	---	---	---
<i>Hydrophasianus chirurgis</i>	EF373243 (a)	AF146627 (f)	---	---
<i>Larosterna inca</i>	AY631364 (d)	---	---	---
<i>Larus argentatus</i>	---	---	---	DQ433743 (j)
<i>Larus marinus</i>	EF373246 (a)	---	---	DQ433757 (j)
<i>Numenius minutus</i>	EF373253 (a)	---	---	---

<b>Taxa</b>	<b>cyt b</b>	<b>12S rDNA</b>	<b>16S rDNA</b>	<b>RAG-1</b>
<i>Aethia cristatella</i>	U37087 (k)	EF373064 (b)	EF380278 (b)	EF373165 (a)
<i>Aethia psittacula</i>	U37296 (k)	EF373077 (a)	EF380290 (b)	EF373179 (a)
<i>Aethia pusilla</i>	U37104 (k)	EF380303 (b)	EF380279 (b)	EF380266 (b)
<i>Aethia pygmaea</i>	U37286 (k)	EF380304 (b)	EF380280 (b)	EF380267 (b)
<i>Alca torda</i>	U37288 (k)	EF373065 (a)	EF380281 (b)	AY228788 (o)
<i>Alle alle</i>	U37287 (k)	AJ242684 (e)	EF380282 (b)	EF373166 (a)
<i>Anous tenuirostris</i>	EF373119 (a)	EF373066 (a)	---	EF373168 (a)
<i>Bartramia longicauda</i>	EF373122 (a)	EF373069 (a)	---	EF373171 (a)
<i>Brachyramphus brevirostris</i>	U37289 (k)	EF380306 (b)	EF380284 (b)	EF373172 (a)
<i>Brachyramphus marmoratus</i>	U37290 (k)	EF380306 (b)	EF380285 (b)	EF380269 (b)
<i>Brachyramphus perdix</i>	U37291 (k)	EF380307 (b)	EF380286 (b)	EF380270 (b)
<i>Cepphus carbo</i>	U37292 (k)	EF380308 (b)	EF380287 (b)	EF380271 (b)
<i>Cepphus columba</i>	U37293 (k)	X76349 (h)	DQ674610 (n)	EF373173 (a)
<i>Cepphus grylle</i>	U37294 (k)	AJ242688 (e)	---	---
<i>Cerorhinca monocerata</i>	U37295 (k)	EF373072 (a)	EF380289 (b)	EF373174 (a)
<i>Charadrius vociferous</i>	DQ385218 (c)	DQ385269 (c)	DQ385286 (c)	AF143736 (p)
<i>Charadrius wilsonia</i>	---	---	---	---
<i>Chidonias leucopterus</i>	EF373124 (a)	EF373073 (a)	---	EF373175 (a)
<i>Creagrus furcatus</i>	EF373127 (a)	EF373076 (a)	---	EF373178 (a)
<i>Cursorius temminckii</i>	DQ385226 (c)	DQ385277 (c)	DQ385294 (c)	AY228780 (o)
<i>Fratercula arctica</i>	U37297 (k)	DQ385279 (c)	DQ385296 (c)	AY228787 (o)
<i>Fratercula cirrhata</i>	U37298 (k)	EF380309 (b)	EF380291 (b)	EF380273 (b)
<i>Fratercula corniculata</i>	U37299 (k)	EF380310 (b)	EF380292 (b)	EF380272 (b)
<i>Gelochelidon nilotica</i>	AY631311 (d)	AY631347 (d)	---	EF373184 (a)
<i>Glareola maldivarum</i>	EF373133 (a)	EF373083 (a)	---	---
<i>Gygis alba</i>	AY631290 (d)	EF373084 (a)	---	EF373185 (a)
<i>Hydrophasianus chirurgus</i>	EF373135 (a)	EF373085 (a)	---	EF373186 (a)
<i>Larosterna inca</i>	AY631292 (d)	AY631328 (d)	---	EF373190 (a)
<i>Larus argentatus</i>	AJ508101 (l)	---	---	---
<i>Larus marinus</i>	AJ508140 (l)	EF373088 (a)	---	AY228799 (o)
<i>Numenius minutus</i>	EF373145 (a)	EF373095 (a)	---	EF373195 (a)



Taxa	ND2	ND5	ND6	CO1
<i>Pagophila eburnea</i>	EF373255 (a)	---	---	DQ433862 (j)
<i>Phaetusa simplex</i>	AY631365 (d)	---	---	---
<i>Pinguinus impennis</i>	---	AJ242685 (e)	AJ242685 (e)	---
<i>Ptychoramphus aleuticus</i>	EF373261 (a)	---	X73924 (h)	EF380330 (b)
<i>Rhinoptilus chalcopterus</i>	EF373263 (a)	---	---	---
<i>Rhodostethia rosea</i>	EF373264 (a)	---	---	DQ434048 (j)
<i>Rissa tridactyla</i>	DQ385093 (c)	DQ385161 (c)	---	DQ385178 (c)
<i>Rynchops niger</i>	DQ385094 (c)	DQ385162 (c)	---	DQ385179 (c)
<i>Stercorarius longicaudus</i>	EF373267 (a)	---	---	DQ434147 (j)
<i>Stercorarius skua</i>	DQ385091 (c)	DQ385159 (c)	---	DQ385176 (c)
<i>Sterna anaethetus</i>	AY631368 (d)	---	---	DQ433203 (j)
<i>Sterna maxima</i>	AY631381 (d)	---	---	DQ434165 (j)
<i>Sternula superciliaris</i>	AY631388 (d)	---	---	---
<i>Stiltia isabella</i>	EF373268 (a)	---	---	---
<i>Synthliboramphus antiquus</i>	EF373269 (a)	AP009042 (g)	X73920 (h)	EF380331 (b)
<i>Synthliboramphus craveri</i>	EF380345 (b)	---	---	EF380332 (b)
<i>Synthliboramphus hypoleucus</i>	---	---	X73921 (h)	DQ434184 (j)
<i>Synthliboramphus wumizusume</i>	EF380346 (b)	---	X73919 (h)	EF380333 (b)
<i>Tryngites subruficollis</i>	EF373272 (a)	---	---	AY666178 (i)
<i>Uria aalge</i>	EF380348 (b)	AJ242686 (e)	X73913 (h)	EF380334 (b)
<i>Uria lomvia</i>	EF373273 (a)	AJ242687 (e)	X73914 (h)	EF380336 (b)
<i>Xema sabini</i>	EF373275 (a)	---	---	---

Taxa	cyt b	12S rDNA	16S rDNA	RAG-1
<i>Pagophila eburnea</i>	EF373147 (a)	EF373097 (a)	---	EF373198 (a)
<i>Phaetusa simplex</i>	AY631293 (d)	AY631329 (d)	---	EF373200 (a)
<i>Pinguinus impennis</i>	AJ242685 (e)	AJ242685 (e)	---	---
<i>Ptychoramphus aleuticus</i>	U37302 (k)	EF373103 (a)	EF380293 (b)	EF373204 (a)
<i>Rhinoptilus chalcopterus</i>	EF373154 (a)	EF373105 (a)	---	EF373205 (a)
<i>Rhodostethia rosea</i>	EF373155 (a)	EF373106 (a)	---	EF373206 (a)
<i>Rissa tridactyla</i>	DQ385229 (c)	DQ385280 (c)	DQ385297 (c)	AY228785 (o)
<i>Rynchops niger</i>	DQ385230 (c)	DQ385281 (c)	DQ385298 (c)	AY228784 (o)
<i>Stercorarius longicaudus</i>	U76820 (m)	EF373109 (a)	---	EF373208 (a)
<i>Stercorarius skua</i>	DQ385227 (c)	DQ385278 (c)	DQ385295 (c)	AY228783 (o)
<i>Sterna anaethetus</i>	AY631296 (d)	AY631332 (d)	---	---
<i>Sterna maxima</i>	AY631309 (d)	DQ674571 (n)	DQ674609 (n)	---
<i>Sternula superciliaris</i>	AY631316 (d)	AY631352 (d)	---	EF373210 (a)
<i>Stiltia isabella</i>	EF373159 (a)	EF373110 (a)	---	EF373211 (a)
<i>Synthliboramphus antiquus</i>	U37303 (k)	EF373111 (a)	EF380294 (b)	EF373212 (a)
<i>Synthliboramphus craveri</i>	U37304 (k)	EF380311 (b)	EF380295 (b)	EF380274 (b)
<i>Synthliboramphus hypoleucus</i>	U37305 (k)	---	---	---
<i>Synthliboramphus wumizusume</i>	U37306 (k)	EF380312 (b)	EF380296 (b)	EF380275 (b)
<i>Tryngites subruficollis</i>	EF373162 (a)	EF373114 (a)	---	EF373215 (a)
<i>Uria aalge</i>	U37307 (k)	DQ485794 (n)	DQ485832 (n)	EF380276 (b)
<i>Uria lomvia</i>	U37308 (k)	AJ242687 (e)	EF380299 (b)	EF373216 (a)
<i>Xema sabini</i>	EF373164 (a)	EF373116 (a)	---	EF373217 (a)

## APPENDIX 5.

### EXTANT OSTEOLOGICAL MEASUREMENT DATA

Measurements of extant alcid species (in mm). “---” denotes measurements missing due to damage or missing elements. All measurements were taken according to Von den Driesch (1976). Abbreviations (in order of usage): gbs, greatest breadth of skull; gls, greatest length of skull; cblS, condylobasal length of skull; ghS, greatest height of skull; gbF, greatest breadth of frontal; glR, greatest length of rostrum; glM, greatest length of mandible; lsM, length of mandibular symphysis; lFa, length from articular to apex of mandible; mlS, maximum length of sternum; dlS, dorsal length of sternum; lcS, length of sternal carina; SBF, smallest breadth between costal rib facets; glC, greatest length of coracoid; mlC, medial length of coracoid; bbC, basal breadth of coracoid; diS, diagonal of proximal scapula; glH, greatest length of humerus; bpH, breadth of proximal humerus; scH, smallest dorsoventral breadth of humeral corpus (shaft); dpH, depth of proximal humerus; bdH, breadth of distal humerus; ddH, distal diagonal of humerus; bdH, breadth of distal humerus; ddH, diagonal of distal humerus; dpH, diagonal of proximal humerus; glR, greatest length of radius; bpR, breadth of proximal radius; scR, greatest width of radial shaft at midpoint; bdR, breadth of distal radius; glU, greatest length of ulna; bpU, breadth of proximal ulna; scU, width of ulnar shaft; bdU, breadth of distal ulna; ddU, diagonal of distal ulna; glC, greatest length of carpometacarpus; lMC1, length of metacarpal 1; bpC, breadth of proximal carpometacarpus; ddC, diagonal of distal carpometacarpus; glD, greatest length of digit 2 phalanx 1; lD, articular length of digit 2 phalanx 1; glP, greatest length of pelvis; lsP, length to dorsal iliac spine of pelvis; lvP, length of synsacrum; cbP, greatest breadth of ilium; sbP, smallest breadth of ilium; aaP, distance between acetabulae; dA, diameter of acetabulum; bA, breadth across antitrochanters; glF, greatest length of femur; mlF, medial length of femur; bpF, breadth of proximal femur; dpF, depth of proximal femur; scF, breadth of femoral shaft; bdF, breadth of distal femur; ddF, depth of distal femur; glT, greatest length of tibiotarsus; laT, axial length of tibiotarsus; dpT, diagonal of proximal tibiotarsus; scT, breadth of tibial shaft; bdT, breadth of distal tibiotarsus; ddT, depth of distal tibiotarsus; glTm, greatest length of tarsometatarsus; bpTm, breadth of proximal tarsometatarsus; scTm, breadth of tarsal shaft; bdTm, breadth of distal tarsometatarsus. *P. aleuticus* refers to the species *Ptychoramphus aleuticus*.

Taxa	Catalog #	Sex	gbS	glS	cbLS	ghS	gbF	glR	ghR	glM	lsM	IFa
<i>Aethia cristatella</i>	USNM 561934	FEMALE	20	50.7	45.8	17.6	4.5	20	5.1	38.4	3.1	9.1
<i>Aethia cristatella</i>	USNM 223707	?	22.1	52.6	46.7	17.9	4.6	23.2	5.6	42.5	4.2	9.2
<i>Aethia cristatella</i>	USNM 610941	MALE	21.1	50.3	45.1	17.1	4.9	20.9	6	41.6	3.8	9
<i>Aethia cristatella</i>	USNM 498282	FEMALE	20.9	50.2	45.1	17.3	4.9	20.5	5.3	40	4.3	11.7
<i>Aethia cristatella</i>	NCSM 17749	MALE	22	52.8	47.7	17.9	5.1	22.7	6.7	43.2	3.7	9.8
<i>Aethia psittacula</i>	NCSM 14804	?	20	52.8	48.8	17.5	4.3	23.1	9	42.8	4.2	10.1
<i>Aethia psittacula</i>	NCSM 18387	?	21.2	55.9	49	19.5	3.7	24.5	9.2	46	4	10.5
<i>Aethia psittacula</i>	NCSM 14147	MALE	22	---	---	19.6	---	---	---	---	4.3	10.6
<i>Aethia psittacula</i>	NCSM 20177	?	20.9	56.1	50.1	16.4	4.3	25.2	9.8	46.2	4.3	9.9
<i>Aethia psittacula</i>	USNM 610513	?	21.3	54.8	49.2	18.5	3.7	23.7	8.3	43.9	4.6	10.4
<i>Aethia psittacula</i>	USNM 610514	?	20.9	54.3	48.5	18.4	3.8	23.5	7.9	42.4	4	10
<i>Aethia psittacula</i>	USNM 610937	MALE	21.3	53.6	48.2	18.4	3.7	25	8.4	39.5	3.9	10.3
<i>Aethia pusilla</i>	NCSM 17737	?	15.5	---	---	15.2	---	---	---	---	2.2	5.9
<i>Aethia pusilla</i>	NCSM 17736	FEMALE	18.5	---	---	14.7	---	---	---	---	2.5	6.2
<i>Aethia pusilla</i>	NCSM 17734	FEMALE	15.5	39.3	34.4	15.2	2.5	15.9	3.4	30.7	2.4	6.7
<i>Aethia pusilla</i>	NCSM 224009	FEMALE	16.4	39.9	34.6	14.5	2.8	15.8	3.2	31		8.3
<i>Aethia pusilla</i>	USNM 498285	MALE	15.7	39.7	35.4	15	2.8	16.7	3.2	31.7	3.1	6.1
<i>Aethia pusilla</i>	USNM 224010	MALE	18.8	41.6	36.8	15.2	2.8	17.1	3.6	31.7	2.3	6
<i>Aethia pygmaea</i>	UMMZ 204592	FEMALE	16.9	42.4	36.4	15.9	2.6	17.1	4	32.2	2.2	6.6
<i>Aethia pygmaea</i>	UMMZ 224882	MALE	16.8	43.4	37.3	16	2.4	18.5	4.1	32	2.5	8.7
<i>Aethia pygmaea</i>	UMMZ 224883	FEMALE	16.8	42.6	36.4	16.4	3	18	4.2	32.6	2.2	6.6
<i>Aethia pygmaea</i>	USNM 344544	?	16	41.1	36	15.5	2.6	17.8	3.4	30.2	2	7.2
<i>Alca torda</i>	USNM 555666	MALE	33.9	95.6	88.6	29.1	6.5	51.2	11.3	82	8.4	25.6
<i>Alca torda</i>	USNM 502378	MALE	33.4	94.6	87.5	27.9	5.9	50.4	12.2	78.3	8.6	22.6
<i>Alca torda</i>	USNM 502387	MALE	33.6	91.1	85.1	27.7	5.9	47.6	12	80.3	7.1	22.8
<i>Alca torda</i>	USNM 502389	FEMALE	31.3	93.9	86.3	28.5	6.2	50.5	11	79	8.6	25.5
<i>Alca torda</i>	USNM 18062	FEMALE	35.3	94.7	87.3	27.1	6.8	51.2	12.7	82.6	7.1	23
<i>Alle alle</i>	USNM 560932	MALE	19.8	50.4	45.6	19.3	2.5	22.1	5	41.8	3.4	11.2

Taxa	Catalog #	Sex	gbS	glS	cbIS	ghS	gbF	glR	ghR	glM	lsM	IFa
<i>Alle alle</i>	USNM 560927	MALE	20.2	48.7	43.2	16.3	3.2	23	4.6	41.7	3	10.9
<i>Alle alle</i>	USNM 560926	FEMALE	22.1	49.9	43.6	16.3	3.1	23.9	4.9	42.2	3.5	11.2
<i>Alle alle</i>	USNM 344748	MALE	19.5	48.8	43.9	18.1	2.9	20.7	4.6	41.1	2.6	11.5
<i>Alle alle</i>	USNM 502391	FEMALE	18.9	47.7	43.3	18.7	3	22.5	4.7	39.7	2.7	11.2
<i>Cephus columba</i>	USNM 610936	MALE	24.9	79.4	74.0	22.7	4.3	41.2	6.8	68.7	6.3	16.3
<i>Cephus columba</i>	USNM 612989	MALE	24.8	81.3	76.7	22.9	4.1	43.6	6.4	69.6	6.2	17.8
<i>Cephus columba</i>	USNM 498423	MALE	25.2	78.3	74.2	22.8	4.4	41.6	6.5	67.8	4.3	17.2
<i>Cephus columba</i>	USNM 498422	FEMALE	24.8	80.8	75.5	22.4	4.3	41.4	7.0	69.5	4	15.1
<i>Cephus columba</i>	USNM 612988	FEMALE	25.0	80.2	75.7	22.8	3.8	43.1	6.2	71.4	5.3	17.3
<i>Cephus grylle</i>	USNM 344753	FEMALE	24.1	69.0	64.0	21.0	3.7	35.6	5.4	59.6	4.5	15
<i>Cephus grylle</i>	USNM 344760	MALE	23.5	71.8	66.6	20.4	4.0	36.6	5.7	60.8	5.1	15.9
<i>Cephus grylle</i>	USNM 344758	MALE	23.7	71.7	67.2	21.0	3.7	35.5	6.0	61.3	5.7	15.6
<i>Cephus grylle</i>	USNM 347071	FEMALE	22.3	72.1	68.1	19.8	3.8	36.2	5.3	62.9	3.3	15.7
<i>Cephus grylle</i>	USNM 344754	FEMALE	21.4	73.7	68.3	21.1	3.7	36.3	6.1	61.3	5.5	17.3
<i>Fratrercula arctica</i>	USNM 292346	?	31.6	81.1	72.7	26.3	5.5	46.8	17.2	66.1	5.1	15.6
<i>Fratrercula arctica</i>	USNM 225762	?	30.1	76.2	67.0	25.2	5.1	43.1	17.2	63.5	4.1	14.5
<i>Fratrercula arctica</i>	USNM 292344	?	33.7	84.8	75.4	27.7	5.9	47.5	20.1	70.7	5.5	15.8
<i>Fratrercula arctica</i>	USNM 292347	?	30.5	78.8	70.8	25.7	4.9	43.4	17.2	65.1	4.4	15
<i>Fratrercula arctica</i>	USNM 224189	MALE	31.6	79.6	71.6	26.5	5.3	45.4	17.8	64.8	4.2	16.6
<i>Pinguinus impennis</i>	USNM no #	?	46.5	161.4	155.0	---	8.6	99.2	24.5	142.3	12.7	31.8
<i>Pinguinus impennis</i>	USNM no #	?	46.1	158.1	151.2	---	8.1	100.1	21.6	143.2	11.2	31.6
<i>Pinguinus impennis</i>	USNM no #	?	46.3	160.3	153.7	---	8.9	103.5	23.8	145.9	10.9	37.8
<i>Pinguinus impennis</i>	USNM no #	?	48.0	156.3	149.0	---	7.8	96.2	20.8	139.1	11.8	33.9
<i>Pinguinus impennis</i>	USNM no #	?	44.4	155.5	146.5	---	9.2	94.4	22.7	135.7	13.1	33.1
<i>P. aleuticus</i>	USNM 557611	MALE	19.1	52.2	46.5	16.5	2.9	27.5	4.6	42.2	3.1	8.1
<i>P. aleuticus</i>	USNM 491305	MALE	20.9	53.1	46	16.4	3.4	27	4.9	43.2	3.3	9.4
<i>P. aleuticus</i>	USNM 557607	FEMALE	17.8	48.4	43.7	15.9	2.8	23.9	4.3	38.8	3.7	7.8
<i>P. aleuticus</i>	USNM 557609	FEMALE	18	49	43.3	16.9	3.1	24.4	4.5	36.6	3.4	8.6



Taxa	Catalog #	Sex	gbS	glS	cbIS	ghS	gbF	glR	ghR	glM	lsM	IFa
<i>P. aleuticus</i>	NCSM 18088	FEMALE	18.2	50	44.5	16	2.9	25.2	3.6	41.3	3.1	7.8
<i>Uria aalge</i>	USNM 502349	MALE	31.8	103.7	98.7	29.3	6.0	55.5	9.2	94.0	9.5	22.6
<i>Uria aalge</i>	USNM 502355	MALE	30.9	104.1	98.1	28.8	6.3	56.9	9.3	90.3	10.7	24.7
<i>Uria aalge</i>	USNM 502348	MALE	31.4	102.6	96.6	28.5	6.0	56.3	8.6	90.3	8.8	25.4
<i>Uria aalge</i>	USNM 557539	FEMALE	30.3	103.3	96.8	28.7	6.8	55.9	8.9	90.6	10	24.1
<i>Uria aalge</i>	USNM 18066	FEMALE	31.1	102.5	97.9	28.0	6.3	57.3	9.1	92.6	9.2	24.2
<i>Uria lomvia</i>	USNM 502358	MALE	32.0	89.1	82.6	26.9	6.3	47.6	8.6	79.0	7.9	21.8
<i>Uria lomvia</i>	USNM 502361	MALE	32.7	92.2	86.3	27.1	5.9	49.4	8.7	82.1	8.7	24.5
<i>Uria lomvia</i>	USNM 502372	FEMALE	32.4	89.1	85.8	27.8	5.8	47.8	8.0	80.2	8.4	23.6
<i>Uria lomvia</i>	USNM 502369	FEMALE	31.9	92.1	86.2	27.2	6.0	49.1	8.7	81.5	6.5	24.6
<i>Uria lomvia</i>	USNM 502374	FEMALE	30.4	87.5	81.6	26.0	4.9	45.7	8.4	75.5	6	22.4

Taxa	Catalog #	mlS	dlS	lcS	SBF	glC	mlC	bbC	bfC	dlS	glH	bpH	scH
<i>Aethia cristatella</i>	USNM 561934	62.6	57.9	66.9	3.1	28.3	26.2	8.7	7.1	7.9	50.6	11.3	3.8
<i>Aethia cristatella</i>	USNM 223707	63.5	59.0	69.9	3.5	30.9	28.9	8.7	8.4	8.0	54.3	11.2	4.3
<i>Aethia cristatella</i>	USNM 610941	61.2	56.9	65.9	3.7	29.2	26.8	8.8	7.7	8.2	51.3	11.2	4.0
<i>Aethia cristatella</i>	USNM 498282	65.3	61.1	71.0	3.4	30.1	27.7	10.4	8.0	8.6	51.6	11.7	4.1
<i>Aethia cristatella</i>	NCSM 17749	63.4	59.7	69.1	3.0	29.5	28.6	8.9	8.1	8.5	53.8	12.3	4.2
<i>Aethia psittacula</i>	NCSM 14804	72.8	65.8	74.9	3.5	27.1	25.6	9.8	7.8	9.1	53.3	12.1	4.1
<i>Aethia psittacula</i>	NCSM 18387	74.5	70.6	77.7	3.2	27.9	27.1	9.8	8.4	8.2	53.9	11.8	4.0
<i>Aethia psittacula</i>	NCSM 14147	75.5	71.2	80.4	3.1	28.9	27.8	10.5	8.6	8.8	53.9	12.8	4.4
<i>Aethia psittacula</i>	NCSM 20177	70.9	64.3	75.3	3.2	27.6	26.9	10.2	7.9	8.1	54.5	11.6	4.1
<i>Aethia psittacula</i>	USNM 610513	55.0	51.6	57.3	3.0	26.2	25.1	9.9	7.7	8.2	54.6	11.8	4.4
<i>Aethia psittacula</i>	USNM 610514	56.2	51.8	56.3	2.8	27.9	26.4	10.3	8.5	7.8	55.5	11.9	4.6
<i>Aethia psittacula</i>	USNM 610937	57.8	52.8	58.3	3.5	27.2	24.9	9.4	7.9	8.3	54.2	11.6	4.4
<i>Aethia pusilla</i>	NCSM 17737	42.9	40.9	38.5	1.4	18.1	17.9	6.4	5.2	5.4	34.0	7.8	2.4
<i>Aethia pusilla</i>	NCSM 17736	45.0	42.1	39.9	1.9	18.6	17.9	6.1	5.0	5.5	35.3	7.8	2.5
<i>Aethia pusilla</i>	NCSM 17734	37.0	34.6	39.1	1.7	18.4	18.1	6.0	5.0	5.5	35.2	7.8	2.5

Taxa	Catalog #	mLS	dLS	lcS	SBF	gIC	mLC	bbC	bFC	diS	gIH	bpH	scH
<i>Aethia pusilla</i>	NCSM 224009	38.3	35.3	40.0	2.3	19.4	17.9	6.9	5.3	5.8	35.6	7.7	2.5
<i>Aethia pusilla</i>	USNM 498285	35.9	33.1	38.7	2.1	18.6	17.2	6.3	4.9	5.6	33.9	7.5	2.5
<i>Aethia pusilla</i>	USNM 224010	38.3	35.3	40.0	1.8	18.8	17.5	6.7	5.2	6.0	35.2	7.6	2.5
<i>Aethia pygmaea</i>	UMMZ 204592	46.9	43.2	47.6	2.9	20.5	18.8	6.7	5.2	6.0	37.8	8.0	2.8
<i>Aethia pygmaea</i>	UMMZ 224882	44.5	41.2	48.3	2.6	20.8	19.0	6.2	5.3	6.8	38.0	8.4	2.6
<i>Aethia pygmaea</i>	UMMZ 224883	45.0	42.3	47.0	2.6	19.9	18.5	6.6	5.0	6.2	37.4	8.2	2.7
<i>Aethia pygmaea</i>	USNM 344544	42.8	40.9	42.0	2.5	20.6	19.5	6.0	5.5	6.1	38.3	7.6	2.9
<i>Alca torda</i>	USNM 555666	104.5	98.0	113.2	4.6	38.8	36.9	19.7	14.7	10.6	79.9	16.7	7.4
<i>Alca torda</i>	USNM 502378	99.1	93.9	108.2	5.5	39.0	36.9	19.9	15.0	10.6	76.3	16.8	7.2
<i>Alca torda</i>	USNM 502387	98.6	91.6	108.6	4.1	38.5	36.2	19.0	14.7	11.1	77.0	16.3	7.1
<i>Alca torda</i>	USNM 502389	92.6	85.1	100.5	4.4	39.1	37.5	19.6	14.4	11.0	82.8	16.9	7.0
<i>Alca torda</i>	USNM 18062	96.8	91.1	104.9	5.7	40.6	38.5	19.4	15.0	10.5	77.2	16.2	7.0
<i>Alle alle</i>	USNM 560932	52.4	48.8	54.0	2.4	21.8	18.9	10.4	6.8	7.0	41.6	9.9	3.3
<i>Alle alle</i>	USNM 560927	54.0	49.6	54.0	1.8	22.9	19.8	10.3	7.2	6.4	40.3	9.8	3.2
<i>Alle alle</i>	USNM 560926	53.4	49.8	56.3	2.0	21.5	19.3	10.1	6.8	6.7	41.1	9.7	3.2
<i>Alle alle</i>	USNM 344748	53.0	49.7	55.5	2.1	22.1	20.5	9.6	6.7	6.2	41.2	9.7	3.3
<i>Alle alle</i>	USNM 502391	52.4	49.0	56.8	2.0	22.5	19.7	10.9	6.9	6.3	43.4	9.6	3.1
<i>Cephus columba</i>	USNM 610936	84.2	76.4	90.8	4.0	36.9	33.7	19.3	13.0	9.3	68.8	15.9	5.0
<i>Cephus columba</i>	USNM 612989	75.8	69.7	84.1	4.0	35.6	31.9	16.4	12.1	8.6	64.6	14.6	4.9
<i>Cephus columba</i>	USNM 498423	78.3	72.5	79.1	3.4	34.2	31.4	17.2	11.3	9.3	65.9	15.0	5.4
<i>Cephus columba</i>	USNM 498422	82.2	76.1	86.3	3.2	35.4	32.2	17.7	12.2	8.6	67.1	15.3	5.5
<i>Cephus columba</i>	USNM 612988	82.5	75.6	88.2	3.1	35.9	32.2	17.6	12.9	9.0	66.5	15.7	4.8
<i>Cephus grylle</i>	USNM 344753	76.2	69.5	84.0	3.5	31.5	28.2	14.8	11.2	8.6	57.8	13.5	4.1
<i>Cephus grylle</i>	USNM 344760	76.2	69.5	81.0	3.9	31.1	28.0	15.8	10.9	8.8	59.5	14.0	4.4
<i>Cephus grylle</i>	USNM 344758	76.6	70.4	82.8	3.5	32.8	29.6	15.5	11.8	9.1	60.4	14.5	4.5
<i>Cephus grylle</i>	USNM 347071	71.7	71.5	86.3	3.3	32.5	29.8	15.2	11.6	9.5	60.5	14.2	4.5
<i>Cephus grylle</i>	USNM 344754	76.3	71.1	81.3	3.6	33.9	30.2	16.9	11.8	8.3	61.7	14.2	4.3
<i>Fratercula arctica</i>	USNM 292346	73.3	66.1	85.2	3.7	37.1	35.2	10.5	9.6	8.5	67.2	14.0	4.8

Taxa	Catalog #	mLS	dlS	lcS	SBF	glC	mIC	bbC	bfC	diS	glH	bpH	scH
<i>Fratercula arctica</i>	USNM225762	71.9	64.4	80.2	3.4	35.5	33.7	13.3	10.5	9.2	63.3	14.5	4.9
<i>Fratercula arctica</i>	USNM 292344	79.6	76.9	90.0	3.8	38.3	36.1	13.8	10.9	9.6	68.9	15.4	5.7
<i>Fratercula arctica</i>	USNM 292347	71.4	66.6	79.8	3.7	34.8	34.1	13.3	11.0	8.6	61.2	14.5	4.9
<i>Fratercula arctica</i>	USNM 224189	69.5	64.9	78.8	3.4	37.5	34.5	11.9	9.4	9.4	68.2	13.8	4.9
<i>Pinguinus impennis</i>	USNM no #	176.5	165.5	193.5	8.4	66.3	60.5	33.7	24.8	16.7	106.3	24.8	10.5
<i>Pinguinus impennis</i>	USNM no #	180.5	167.7	184.0	6.1	63.2	58.6	37.3	26.9	17.6	105.8	24.8	11.0
<i>Pinguinus impennis</i>	USNM no #	170.7	161.6	185.9	6.0	62.6	59.1	34.1	26.3	16.1	105.2	24.1	10.0
<i>Pinguinus impennis</i>	USNM no #	178.7	166.7	199.2	9.8	61.7	57.6	28.7	24.3	17.1	103.7	24.6	10.2
<i>Pinguinus impennis</i>	USNM no #	187.2	177.1	201.5	7.6	65.0	61.0	34.1	28.0	17.9	101.8	24.7	10.8
<i>P. aleuticus</i>	USNM 557611	48.8	45.8	50.2	2.6	23.7	21.5	7.7	6.1	6.7	44.8	9.3	3.4
<i>P. aleuticus</i>	USNM 491305	48.1	46.0	49.9	1.8	24.5	22.7	8.8	6.9	6.7	47.3	9.8	3.4
<i>P. aleuticus</i>	USNM 557607	46.8	43.9	49.5	2.3	23.0	21.6	7.8	6.2	6.3	44.3	9.2	3.5
<i>P. aleuticus</i>	USNM 557609	47.3	44.1	49.0	2.0	23.3	21.4	8.4	6.7	7.0	43.5	9.4	3.2
<i>P. aleuticus</i>	NCSM 18088	49.3	45.4	51.0	1.8	23.4	22.5	8.3	6.5	6.6	45.6	9.4	3.7
<i>Uria aalge</i>	USNM 502349	119.6	110.8	129.0	4.2	40.7	38.3	22.3	16.2	11.8	84.1	17.0	7.2
<i>Uria aalge</i>	USNM 502355	125.8	117.1	137.4	4.8	40.1	38.0	21.4	16.3	12.7	85.5	17.5	7.5
<i>Uria aalge</i>	USNM 502348	121.1	112.3	133.5	5.1	39.8	38.6	21.6	16.1	12.0	84.9	17.8	7.6
<i>Uria aalge</i>	USNM 557539	112.3	102.5	123.4	4.0	39.1	37.1	20.5	14.8	11.1	81.9	16.4	7.5
<i>Uria aalge</i>	USNM 18066	126.0	116.9	135.9	5.1	42.5	39.7	23.8	17.1	12.5	89.2	19.0	7.8
<i>Uria lomvia</i>	USNM 502358	110.2	102.8	119.8	5.0	41.4	39.0	21.4	16.2	11.5	87.6	17.1	6.8
<i>Uria lomvia</i>	USNM 502361	116.0	108.1	125.3	5.3	41.9	39.4	22.3	16.8	11.8	87.7	17.9	7.6
<i>Uria lomvia</i>	USNM 502372	113.0	104.8	123.3	4.1	44.0	41.0	21.5	16.5	11.9	88.3	17.5	7.3
<i>Uria lomvia</i>	USNM 502369	111.4	103.6	120.4	3.6	40.9	37.8	21.9	17.1	12.0	87.5	18.3	7.2
<i>Uria lomvia</i>	USNM 502374	110.2	102.1	117.6	3.2	39.5	36.6	21.5	16.0	11.9	89.4	17.4	6.9

Taxa	Catalog #	BdH	ddH	dpH	glR	bpR	scR	bdR	glU	bpU	scU	bdU	ddU	glC
<i>Aethia cristatella</i>	USNM 561934	8.1	5.6	11.1	41.5	3.3	1.7	3.6	43.9	7.8	6.3	5.7	4.7	29.0
<i>Aethia cristatella</i>	USNM 223707	8.7	6.0	11.5	44.4	3.2	2.2	3.9	46.8	7.8	6.3	6.0	4.8	30.6



Taxa	Catalog #	BdH	ddH	dpH	gIR	bpR	scR	bdR	gIU	bpU	scU	bdU	ddU	gIC
<i>Aethia cristatella</i>	USNM 610941	8.5	5.8	11.5	41.6	3.5	2.2	3.6	52.4	10.6	7.5	7.7	6.1	27.8
<i>Aethia cristatella</i>	USNM 498282	8.5	6.0	11.1	42.4	3.4	2.1	3.7	44.4	8.5	6.8	6.1	4.5	29.2
<i>Aethia cristatella</i>	NCSM 17749	8.4	6.0	11.8	---	---	---	---	48.7	9.2	7.3	6.5	5.2	---
<i>Aethia psittacula</i>	NCSM 14804	8.4	6.3	11.2	46.5	3.5	2.0	3.8	48.5	8.2	6.7	6.2	5.0	30.0
<i>Aethia psittacula</i>	NCSM 18387	8.9	6.4	11.3	46.6	3.5	2.1	3.7	48.6	8.7	6.9	6.3	5.4	---
<i>Aethia psittacula</i>	NCSM 14147	9.0	6.6	11.6	46.4	3.9	2.2	3.9	46.9	8.3	6.7	6.1	5.3	---
<i>Aethia psittacula</i>	NCSM 20177	8.7	6.1	11.3	45.5	3.7	2.0	3.4	47.1	8.8	6.7	6.2	5.1	30.0
<i>Aethia psittacula</i>	USNM 610513	8.6	6.2	11.3	46.9	3.5	2.2	3.7	49.2	8.4	6.3	6.0	4.9	30.8
<i>Aethia psittacula</i>	USNM 610514	8.8	6.1	10.9	47.5	3.6	2.3	4.0	49.7	8.6	6.8	6.0	4.3	31.8
<i>Aethia psittacula</i>	USNM 610937	8.8	6.3	11.5	46.7	3.8	2.3	3.7	49.1	8.5	6.4	6.1	4.8	31.0
<i>Aethia pusilla</i>	NCSM 17737	5.5	4.1	7.4	27.2	2.2	1.3	2.2	28.8	5.4	4.3	4.0	2.8	---
<i>Aethia pusilla</i>	NCSM 17736	5.6	4.0	7.1	28.8	2.1	1.4	2.5	30.1	5.6	4.3	4.0	3.2	---
<i>Aethia pusilla</i>	NCSM 17734	5.4	3.9	7.5	29.2	2.1	1.3	2.6	30.2	5.3	4.3	4.2	3.1	---
<i>Aethia pusilla</i>	NCSM 224009	5.6	4.1	7.1	29.1	2.2	1.3	2.7	30.5	5.8	4.7	4.4	3.3	20.0
<i>Aethia pusilla</i>	USNM 498285	5.4	3.9	7.1	27.7	2.2	1.3	2.5	29.2	5.2	4.1	3.9	3.0	19.1
<i>Aethia pusilla</i>	USNM 224010	5.5	4.1	7.6	28.3	2.3	1.5	2.6	29.8	5.7	4.4	4.2	3.3	19.8
<i>Aethia pygmaea</i>	UMMZ 204592	5.8	4.3	7.8	30.5	2.5	1.3	2.7	32.2	5.9	4.6	4.4	3.3	21.2
<i>Aethia pygmaea</i>	UMMZ 224882	6.1	4.4	8.3	30.5	2.5	1.4	2.9	32.2	6.0	4.6	4.5	3.3	20.9
<i>Aethia pygmaea</i>	UMMZ 224883	5.9	4.2	7.7	30.5	2.5	1.4	2.8	32.0	5.6	4.5	4.3	3.5	20.5
<i>Aethia pygmaea</i>	USNM 344544	5.8	4.3	7.4	31.3	2.5	1.4	2.7	32.8	5.6	4.4	4.4	3.3	20.8
<i>Alca torda</i>	USNM 555666	11.2	7.9	16.7	61.5	5.1	3.4	5.3	63.6	12.3	7.7	8.5	5.9	42.6
<i>Alca torda</i>	USNM 502378	11.2	8.1	15.2	59.4	5.4	3.3	5.4	61.6	12.4	7.8	8.2	6.3	41.0
<i>Alca torda</i>	USNM 502387	11.3	8.3	15.6	60.4	5.3	3.4	5.2	62.8	12.1	7.2	8.3	6.0	41.4
<i>Alca torda</i>	USNM 502389	11.0	7.8	16.0	62.5	4.9	3.3	5.3	65.1	11.8	7.8	8.6	6.2	41.8
<i>Alca torda</i>	USNM 18062	11.1	8.0	16.5	59.5	5.3	3.5	5.7	61.5	12.4	7.8	8.4	7.4	40.8
<i>Alle alle</i>	USNM 560932	6.8	4.8	8.6	31.8	2.7	1.8	2.7	34.1	7.0	4.8	4.8	3.3	21.8
<i>Alle alle</i>	USNM 560927	6.4	4.6	8.9	31.9	2.6	1.9	3.2	34.2	7.2	4.3	4.9	3.8	21.9
<i>Alle alle</i>	USNM 560926	6.7	4.6	8.6	31.7	2.8	1.7	3.2	33.8	5.8	4.5	5.0	3.3	21.7



Taxa	Catalog #	BdH	ddH	dpH	gIR	bpR	scR	bdR	gIU	bpU	scU	bdU	ddU	gIC
<i>Alle alle</i>	USNM 344748	6.6	4.6	8.8	31.8	2.9	1.7	3.2	34.2	7.4	4.4	4.9	3.2	22.6
<i>Alle alle</i>	USNM 502391	6.5	4.5	9.1	32.5	2.7	1.8	3.1	34.4	6.8	4.4	4.7	3.4	22.2
<i>Cephus columba</i>	USNM 610936	10.0	8.0	14.2	55.2	4.5	2.7	5.1	58.2	10.7	7.7	8.0	6.6	39.3
<i>Cephus columba</i>	USNM 612989	9.5	7.1	13.5	51.7	4.4	2.7	4.7	54.4	10.2	6.3	7.7	6.3	36.2
<i>Cephus columba</i>	USNM 498423	9.9	7.7	13.7	53.1	4.7	2.9	5.0	56.0	10.7	7.1	7.8	5.9	37.1
<i>Cephus columba</i>	USNM 498422	9.9	7.7	14.2	54.2	4.5	3.2	4.9	57.1	10.6	7.4	7.7	5.7	38.3
<i>Cephus columba</i>	USNM 612988	9.3	7.4	14.0	53.6	4.7	2.8	4.6	56.5	10.4	7.6	7.6	5.4	38.2
<i>Cephus grylle</i>	USNM 344753	8.6	6.4	12.6	47.0	4.2	2.2	4.2	49.4	9.1	6.4	6.7	5.5	33.0
<i>Cephus grylle</i>	USNM 344760	8.5	6.3	12.5	49.3	3.9	2.6	4.4	52.0	9.2	6.4	6.9	5.5	34.2
<i>Cephus grylle</i>	USNM 344758	9.0	7.0	13.1	49.3	4.1	2.5	4.6	52.8	9.9	7.2	7.5	6.0	34.2
<i>Cephus grylle</i>	USNM 347071	9.1	6.9	12.8	49.2	4.1	2.6	4.6	51.4	9.6	6.3	7.0	6.1	33.9
<i>Cephus grylle</i>	USNM 344754	9.1	7.2	13.4	51.1	4.9	2.8	4.8	53.1	9.7	7.1	7.4	5.7	36.0
<i>Fratrula arctica</i>	USNM 292346	9.8	6.8	13.1	51.2	4.3	2.8	4.3	52.9	9.7	6.5	7.3	4.9	35.5
<i>Fratrula arctica</i>	USNM 225762	9.4	6.5	13.4	48.5	4.0	2.6	4.5	50.8	9.4	6.4	7.1	5.0	33.5
<i>Fratrula arctica</i>	USNM 292344	10.6	7.2	14.7	51.7	4.5	3.2	5.0	54.0	10.3	6.9	8.1	5.8	37.3
<i>Fratrula arctica</i>	USNM 292347	9.9	6.5	12.7	46.6	4.1	2.9	4.8	48.3	9.2	6.4	7.0	5.3	32.5
<i>Fratrula arctica</i>	USNM 224189	10.0	7.4	13.5	52.3	4.5	3.0	4.9	54.1	9.5	6.9	7.8	6.2	36.3
<i>Pinguinus impennis</i>	USNM no #	16.3	10.7	22.6	58.1	6.7	5.7	6.5	58.1	16.9	10.2	9.7	6.9	43.6
<i>Pinguinus impennis</i>	USNM no #	16.5	9.9	22.7	55.2	6.9	5.8	6.5	55.2	16.5	10.8	10.0	7.1	43.0
<i>Pinguinus impennis</i>	USNM no #	15.6	10.8	22.5	56.3	6.8	5.9	6.2	56.3	15.8	10.0	10.9	7.2	45.2
<i>Pinguinus impennis</i>	USNM no #	15.7	10.8	22.4	56.7	6.4	6.0	6.3	59.7	16.9	10.8	10.3	6.9	41.7
<i>Pinguinus impennis</i>	USNM no #	15.4	10.7	23.0	55.9	7.1	6.1	7.1	55.8	16.4	10.3	10.2	6.6	42.7
<i>P. aleuticus</i>	USNM 557611	7.2	4.9	9.1	36.8	2.9	1.9	3.2	38.5	7.1	5.5	5.2	4.2	25.5
<i>P. aleuticus</i>	USNM 491305	7.4	5.2	9.6	38.3	2.8	1.7	3.3	40.1	7.2	5.7	5.2	4.1	25.8
<i>P. aleuticus</i>	USNM 557607	6.6	4.8	8.8	37.1	2.7	1.9	3.0	38.8	6.7	5.4	4.9	3.6	24.5
<i>P. aleuticus</i>	USNM 557609	6.8	4.9	9.6	36.3	2.9	1.7	2.9	38.2	6.8	5.4	5.0	3.8	24.4
<i>P. aleuticus</i>	NCSM 18088	7.1	5.0	9.3	37.5	2.9	2.0	3.0	39.4	6.9	5.4	5.0	3.8	25.5
<i>Uria aalge</i>	USNM 502349	12.1	8.5	15.4	61.4	5.5	3.5	5.6	64.3	13.1	8.3	8.8	6.4	43.6

Taxa	Catalog #	BdH	ddH	dpH	gIR	bpR	scR	bdR	glU	bpU	scU	bdU	ddU	glC
<i>Uria aalge</i>	USNM 502355	12.4	8.6	16.8	62.2	5.8	3.4	5.9	64.0	13.0	8.2	8.9	6.4	43.9
<i>Uria aalge</i>	USNM 502348	12.4	8.7	15.9	60.7	5.8	3.7	5.9	62.7	12.9	8.6	9.1	6.5	43.9
<i>Uria aalge</i>	USNM 557539	11.9	8.4	16.0	58.6	5.4	3.7	5.6	61.0	12.4	8.0	8.3	6.2	42.4
<i>Uria aalge</i>	USNM 18066	12.7	8.8	18.2	65.2	5.9	3.7	6.0	67.8	14.1	8.6	9.6	6.9	44.9
<i>Uria lomvia</i>	USNM 502358	12.1	9.3	16.3	66.6	5.7	3.4	5.5	69.4	12.9	9.9	9.4	7.2	44.3
<i>Uria lomvia</i>	USNM 502361	12.3	8.9	16.6	65.0	5.4	3.8	5.8	67.7	13.2	8.6	9.3	8.0	44.6
<i>Uria lomvia</i>	USNM 502372	11.6	8.3	16.2	65.7	5.0	3.4	5.4	68.5	12.9	9.3	8.9	7.1	45.9
<i>Uria lomvia</i>	USNM 502369	12.6	9.1	16.8	65.7	5.7	3.5	5.6	67.8	13.2	8.8	9.3	7.2	44.8
<i>Uria lomvia</i>	USNM 502374	12.2	8.6	15.3	65.9	5.5	3.3	5.4	68.1	12.7	8.2	8.7	6.5	43.4

Taxa	Catalog #	IMC1	bpC	ddC	gID	ID	glP	lsP	lvP	cbP	sbP	aaP	dA	bA
<i>Aethia cristatella</i>	USNM 561934	4.3	4.8	4.4	14.1	13.1	45.1	41.9	35.3	15.7	10.7	14.6	3.1	16.7
<i>Aethia cristatella</i>	USNM 223707	5.1	4.6	4.5	14.8	13.0	49.5	45.3	37.5	17.0	11.3	16.4	3.0	18.2
<i>Aethia cristatella</i>	USNM 610941	4.4	4.7	3.0	13.7	12.6	45.3	42.4	40.0	15.6	11.9	16.0	3.4	17.2
<i>Aethia cristatella</i>	USNM 498282	5.0	4.9	4.3	13.8	12.7	46.8	44.8	36.2	17.9	11.3	16.6	3.5	18.5
<i>Aethia cristatella</i>	NCSM 17749	---	---	---	---	---	45.4	42.4	32.0	17.2	11.8	15.7	3.3	17.7
<i>Aethia psittacula</i>	NCSM 14804	4.3	5.2	4.5	14.2	13.2	45.3	41.4	32.4	15.0	12.2	18.0	3.1	20.3
<i>Aethia psittacula</i>	NCSM 18387	---	---	---	---	---	45.0	41.9	35.2	17.0	13.0	18.0	3.3	20.9
<i>Aethia psittacula</i>	NCSM 14147	---	---	---	---	---	44.9	41.1	33.5	15.5	12.3	17.8	3.5	21.2
<i>Aethia psittacula</i>	NCSM 20177	5.1	4.8	3.8	13.7	12.5	46.1	42.2	36.1	16.7	12.0	16.4	3.4	19.9
<i>Aethia psittacula</i>	USNM 610513	4.3	5.0	3.0	13.3	12.2	---	---	33.1	---	---	---	3.7	---
<i>Aethia psittacula</i>	USNM 610514	5.3	4.8	4.2	14.1	13.0	---	---	35.3	---	---	---	3.4	---
<i>Aethia psittacula</i>	USNM 610937	5.1	4.5	4.4	13.8	12.6	47.7	42.6	35.9	15.6	12.7	16.1	3.7	19.9
<i>Aethia pusilla</i>	NCSM 17737	---	---	---	---	---	26.5	25.0	20.6	10.2	9.1	12.9	1.8	13.3
<i>Aethia pusilla</i>	NCSM 17736	---	---	---	---	---	28.8	26.4	21.8	11.2	9.7	13.7	2.0	14.1
<i>Aethia pusilla</i>	NCSM 17734	---	---	---	---	---	28.2	26.4	22.2	11.2	9.2	12.2	2.1	14.0
<i>Aethia pusilla</i>	NCSM 224009	3.0	3.1	3.0	9.5	8.7	29.4	26.7	22.6	12.2	9.6	13.2	2.1	14.6
<i>Aethia pusilla</i>	USNM 498285	3.1	3.1	3.2	9.4	8.6	28.4	27.3	22.5	11.5	10.3	13.9	1.8	15.0

Taxa	Catalog #	IMC1	bpC	ddC	gLD	ID	gIP	lsP	lvP	cbP	sbP	aaP	dA	bA
<i>Aethia pusilla</i>	USNM 224010	3.3	3.3	2.9	9.3	8.3	29.4	27.6	22.9	12.5	9.8	13.8	2.1	14.6
<i>Aethia pygmaea</i>	UMMZ 204592	3.3	3.5	3.2	10.1	9.3	33.2	30.3	27.5	13.1	9.2	13.1	2.5	15.0
<i>Aethia pygmaea</i>	UMMZ 224882	3.5	3.3	3.3	10.4	9.6	35.2	31.7	26.0	13.9	9.4	13.3	2.6	15.0
<i>Aethia pygmaea</i>	UMMZ 224883	3.1	3.5	3.3	9.6	8.8	31.8	29.2	27.8	11.9	9.2	12.5	2.5	13.9
<i>Aethia pygmaea</i>	USNM 344544	3.8	3.2	2.4	10.6	9.7	31.6	28.7	25.6	11.8	9.0	12.3	2.2	13.4
<i>Alca torda</i>	USNM 555666	7.9	10.7	7.0	21.1	18.8	76.6	66.3	54.4	24.2	16.7	20.4	4.8	23.7
<i>Alca torda</i>	USNM 502378	7.1	10.7	6.7	20.6	18.4	72.4	66.6	56.6	22.5	15.6	19.5	4.8	21.6
<i>Alca torda</i>	USNM 502387	7.2	10.8	6.8	20.8	19.3	73.3	64.3	53.7	21.2	15.0	18.7	4.6	21.8
<i>Alca torda</i>	USNM 502389	7.2	10.4	7.1	20.9	18.8	79.7	64.6	52.2	23.5	17.1	18.1	4.7	23.7
<i>Alca torda</i>	USNM 18062	7.7	10.2	7.1	21.0	18.9	74.0	66.7	54.7	23.0	16.0	18.5	4.6	22.0
<i>Alle alle</i>	USNM 560932	3.6	6.1	3.8	10.6	10.2	40.2	33.7	27.8	13.8	12.4	15.1	2.1	17.1
<i>Alle alle</i>	USNM 560927	3.7	6.3	4.3	11.1	9.8	41.7	31.9	27.1	14.9	11.9	14.3	2.2	16.3
<i>Alle alle</i>	USNM 560926	2.7	6.3	4.1	10.7	9.9	40.4	31.3	25.0	14.5	12.8	15.5	2.1	16.4
<i>Alle alle</i>	USNM 344748	4.0	6.3	4.4	11.7	10.6	39.1	32.9	28.8	14.4	12.1	15.3	2.2	17.1
<i>Alle alle</i>	USNM 502391	3.8	6.0	4.3	11.3	10.3	41.3	32.4	28.4	13.7	11.7	14.2	2.2	15.7
<i>Cepphus columba</i>	USNM 610936	6.0	9.8	6.3	17.4	15.6	72.8	56.2	54.5	22.9	16.3	21.8	4.3	24.0
<i>Cepphus columba</i>	USNM 612989	5.1	9.3	6.2	15.9	14.2	67.8	51.5	46.7	21.5	16.3	19.4	3.9	23.0
<i>Cepphus columba</i>	USNM 498423	6.1	9.5	6.3	16.5	14.5	69.4	54.0	47.1	19.3	15.6	21.3	3.8	24.2
<i>Cepphus columba</i>	USNM 498422	6.6	9.4	6.3	17.9	15.9	66.7	51.3	49.7	20.8	16.7	21.9	4.6	24.1
<i>Cepphus columba</i>	USNM 612988	6.7	9.3	6.1	18.3	16.4	71.6	52.9	48.3	23.7	17.8	22.5	4.3	24.9
<i>Cepphus grylle</i>	USNM 344753	5.0	7.9	5.3	14.7	13.1	61	45.1	41.2	17.9	14.2	17.3	3.4	21.0
<i>Cepphus grylle</i>	USNM 344760	5.3	7.8	5.5	16.1	14.2	60.7	46.8	38.9	17.3	14.0	17.9	3.2	20.8
<i>Cepphus grylle</i>	USNM 344758	5.1	8.7	5.7	16.4	15.1	59.1	48.3	43.8	20.7	14.0	18.6	3.4	20.8
<i>Cepphus grylle</i>	USNM 347071	5.5	8.4	5.8	16.0	14	62.1	49.2	38.8	21.6	15.0	18.8	3.5	21.6
<i>Cepphus grylle</i>	USNM 344754	5.7	8.6	6.2	16.2	14.8	67	49.3	41.3	20.0	15.1	19.2	3.9	23.0
<i>Fratrula arctica</i>	USNM 292346	6.2	8.3	5.1	18.2	16.1	66.6	53.3	38.0	18.2	13.6	19.2	4.1	22.8
<i>Fratrula arctica</i>	USNM 225762	6.0	8.4	5.7	16.3	14.9	61.7	48.8	40.5	16.6	14.8	20.4	3.6	24.3
<i>Fratrula arctica</i>	USNM 292344	6.8	9.0	6.3	18.3	15.8	71.3	55.4	43.6	18.1	14.9	20.7	4.3	26.0



Taxa	Catalog #	IMC1	bpC	ddC	gID	ID	glP	lsP	lvP	cbP	sbP	aaP	dA	bA
<i>Fratercula arctica</i>	USNM 292347	5.6	8.4	5.7	16.5	14.7	66.2	52.7	44.4	17.9	16.2	21.8	4.0	26.2
<i>Fratercula arctica</i>	USNM 224189	6.4	9.1	6.2	18.5	16.8	68.9	53.9	45.2	15.9	14.3	21.3	4.4	24.3
<i>Pinguinus impennis</i>	USNM no #	12.5	12.6	9.2	22.5	21.9	---	---	98.8	---	---	---	9.1	---
<i>Pinguinus impennis</i>	USNM no #	12.5	13.3	9.4	23.0	21.4	---	---	100.7	---	---	---	9.0	---
<i>Pinguinus impennis</i>	USNM no #	12.4	12.9	8.6	22.4	20.8	---	---	95.3	---	---	---	9.3	---
<i>Pinguinus impennis</i>	USNM no #	11.5	12.8	9.2	21.2	20.6	---	---	94.2	---	---	---	9.1	---
<i>Pinguinus impennis</i>	USNM no #	11.5	13.2	8.5	22.0	20.5	---	---	94.1	---	---	---	9.4	---
<i>P. aleuticus</i>	USNM 557611	4.0	3.8	4.2	11.7	10.9	36.0	32.5	26.1	11.7	10.1	13.8	2.3	15.8
<i>P. aleuticus</i>	USNM 491305	4.2	4.5	4.5	12.5	11.5	38.5	36.1	28.5	---	---	---	2.8	---
<i>P. aleuticus</i>	USNM 557607	4.0	3.7	3.5	11.4	10.5	37.1	33.4	26.8	14.8	10.6	13.7	2.1	15.2
<i>P. aleuticus</i>	USNM 557609	4.1	3.8	3.9	11.4	10.8	36.8	34.7	28.2	12.9	10.1	13.8	2.5	16.1
<i>P. aleuticus</i>	NCSM 18088	4.0	4.0	3.1	12.2	11.6	38.4	25.4	30.4	14.2	10.6	14.3	2.6	16.0
<i>Uria aalge</i>	USNM 502349	8.0	10.6	7.1	21.1	19.4	88.2	72.9	62.1	22.9	17.2	22.0	5.2	22.5
<i>Uria aalge</i>	USNM 502355	8.6	10.7	8.0	20.3	18.6	86.7	75.5	57.9	26.4	16.5	21.6	4.6	22.9
<i>Uria aalge</i>	USNM 502348	8.9	10.4	7.8	21.2	19.3	90	73.6	55.5	27.2	17.4	22.1	5.0	23.4
<i>Uria aalge</i>	USNM 557539	7.6	9.6	6.9	19.4	18.2	84.8	70.8	62.2	23.3	15.9	19.5	4.9	22.0
<i>Uria aalge</i>	USNM 18066	8.5	10.6	7.9	21.7	19.7	91.4	78.8	60.8	25.9	18.0	22.4	5.7	24.7
<i>Uria lomvia</i>	USNM 502358	7.6	10.5	7.6	20.5	19.2	81.3	68.6	54.1	26.0	16.6	20.3	4.6	22.7
<i>Uria lomvia</i>	USNM 502361	9.0	10.5	7.5	21.5	19.7	82.6	68.7	54.5	23.3	16.9	20.1	5.1	21.2
<i>Uria lomvia</i>	USNM 502372	8.6	10.4	7.6	22.2	20.1	84.5	71.1	59.4	28.2	18.2	22.3	4.9	23.8
<i>Uria lomvia</i>	USNM 502369	8.5	10.8	7.7	21.0	19.1	82.7	67.3	53.1	24.6	17.8	22.7	5.1	23.0
<i>Uria lomvia</i>	USNM 502374	7.2	10.3	7.2	20.6	19.4	78.1	65.6	54.2	23.0	15.5	20.4	4.3	21.7

Taxa	Catalog #	glF	mlF	bpF	dpF	scF	bdF	ddF	glT	laT	dpT	scT	bdT	ddT
<i>Aethia cristatella</i>	USNM 561934	34.8	33.0	6.1	4.0	2.8	5.5	5.2	58.4	54.3	6.7	2.6	4.9	4.7
<i>Aethia cristatella</i>	USNM 223707	36.9	35.3	6.5	4.0	3.0	5.9	5.4	63.8	59.6	7.7	2.8	4.8	5.2
<i>Aethia cristatella</i>	USNM 610941	33.8	32.1	6.5	4.2	2.8	5.5	5.3	58.7	55.1	7.0	2.8	5.1	5.0

Taxa	Catalog #	glF	mlF	bpF	dpF	scF	bdF	ddF	glT	laT	dpT	scT	bdT	ddT
<i>Aethia cristatella</i>	USNM 498282	34.7	33.6	6.3	4.4	3.2	6.1	5.4	61.4	56.9	7.0	2.8	5.3	5.0
<i>Aethia cristatella</i>	NCSM 17749	36.0	34.2	6.8	4.3	2.9	5.8	5.8	63.7	59.7	7.2	2.7	5.5	5.1
<i>Aethia psittacula</i>	NCSM 14804	32.5	31.9	6.6	4.9	3.0	5.9	5.5	58.1	53.6	7.7	2.4	5.4	5.2
<i>Aethia psittacula</i>	NCSM 18387	34.7	33.0	6.6	4.5	3.0	6.3	5.9	60.2	55.4	7.8	2.9	4.8	5.4
<i>Aethia psittacula</i>	NCSM 14147	34.0	32.8	6.6	4.5	2.8	6.5	5.9	60.6	55.9	7.1	3.0	5.9	5.7
<i>Aethia psittacula</i>	NCSM 20177	35.1	33.3	6.9	4.5	2.7	6.0	5.6	59.0	54.9	7.4	2.8	5.7	5.5
<i>Aethia psittacula</i>	USNM 610513	34.8	33.4	6.8	4.4	3.2	6.0	5.5	59.4	55.8	7.5	2.8	5.2	5.2
<i>Aethia psittacula</i>	USNM 610514	34.1	32.5	6.2	4.9	3.2	5.8	5.8	59.3	54.0	7.2	2.9	5.4	5.4
<i>Aethia psittacula</i>	USNM 610937	33.9	32.7	6.3	4.7	2.9	5.9	5.9	58.8	54.3	7.2	3.0	5.7	5.5
<i>Aethia pusilla</i>	NCSM 17737	21.9	21.0	3.9	2.6	2.0	3.8	3.4	36.8	35.6	4.8	1.7	2.8	3.3
<i>Aethia pusilla</i>	NCSM 17736	23.0	22.1	4.3	2.8	1.9	4.1	3.5	40.1	37.3	4.8	1.8	3.3	3.3
<i>Aethia pusilla</i>	NCSM 17734	22.7	21.8	4.0	2.6	1.9	3.9	3.4	39.9	37.2	4.9	1.7	3.4	3.4
<i>Aethia pusilla</i>	NCSM 224009	22.4	21.4	4.1	3.1	2.1	3.9	3.5	41.1	38.2	4.9	1.6	3.4	3.3
<i>Aethia pusilla</i>	USNM 498285	22.7	21.7	3.8	2.9	2.0	3.8	3.7	40.1	37.2	4.5	1.8	3.2	3.3
<i>Aethia pusilla</i>	USNM 224010	23.0	21.9	4.5	3.0	2.0	3.9	3.7	40.9	37.4	5.0	1.8	3.4	3.5
<i>Aethia pygmaea</i>	UMMZ 204592	26.9	25.6	5.2	3.0	2.3	4.1	4.1	45.3	42.4	4.9	1.8	3.6	3.6
<i>Aethia pygmaea</i>	UMMZ 224882	25.6	24.5	4.7	2.8	2.1	4.3	3.7	43.8	41.4	5.0	1.8	3.6	3.6
<i>Aethia pygmaea</i>	UMMZ 224883	24.4	23.4	4.2	3.1	2.0	4.1	3.8	43.7	41.2	4.8	2.0	3.8	3.4
<i>Aethia pygmaea</i>	USNM 344544	25.6	24.4	4.9	2.9	2.3	4.0	4.0	45.6	43.1	4.4	1.7	3.7	3.3
<i>Alca torda</i>	USNM 555666	43.0	41.4	9.1	6.7	4.0	8.0	7.4	79.8	73.8	9.6	4.0	6.7	6.8
<i>Alca torda</i>	USNM 502378	42.9	41.1	8.0	6.5	3.9	8.0	7.4	76.1	71.0	10.6	3.6	6.8	6.1
<i>Alca torda</i>	USNM 502387	41.9	40.8	8.1	6.4	4.1	7.7	6.8	76.1	71.4	9.5	3.7	6.3	6.1
<i>Alca torda</i>	USNM 502389	45.5	44.0	8.6	7.1	3.8	7.6	7.1	81.6	76.5	9.5	3.6	6.6	6.4
<i>Alca torda</i>	USNM 18062	41.7	40.6	8.8	6.9	3.9	7.9	7.2	78.4	72.7	9.4	4.0	6.7	6.3
<i>Alle alle</i>	USNM 560932	26.8	26.1	4.8	3.3	2.4	4.5	3.5	47.5	44.0	5.6	2.0	4.0	4.0
<i>Alle alle</i>	USNM 560927	26.9	25.8	4.8	3.3	2.1	4.3	4.1	46.9	43.4	5.7	1.8	3.9	4.2
<i>Alle alle</i>	USNM 560926	25.9	24.8	4.5	3.6	2.1	4.5	4.1	45.9	42.5	5.2	2.0	4.1	4.1
<i>Alle alle</i>	USNM 344748	27.4	26.5	5.1	3.4	2.1	4.7	3.9	46.9	43.6	5.3	1.9	4.2	3.8

Taxa	Catalog #	gIF	mIF	bpF	dpF	scF	bdF	ddF	gIT	laT	dpT	scT	bdT	ddT
<i>Alle alle</i>	USNM 502391	26.1	25.2	4.6	3.1	2.0	4.4	3.7	45.9	42.7	5.3	1.8	3.8	3.6
<i>Cephus columba</i>	USNM 610936	40.4	38.6	8.2	5.9	3.8	8.3	6.8	75.6	69.2	9.4	4.0	6.3	6.5
<i>Cephus columba</i>	USNM 612989	38.7	37.2	7.5	5.6	3.7	7.4	6.7	73.9	68.0	8.8	3.8	5.9	6.0
<i>Cephus columba</i>	USNM 498423	39.8	37.5	7.7	5.8	3.8	7.8	6.8	72.6	66.4	9.5	4.7	6.2	6.2
<i>Cephus columba</i>	USNM 498422	39.3	37.6	7.3	5.7	3.9	7.6	6.9	74.8	68.8	9.0	4.1	6.6	6.2
<i>Cephus columba</i>	USNM 612988	39.8	38.3	7.6	5.6	3.5	7.5	6.1	74.9	68.7	9.3	4.0	6.2	6.2
<i>Cephus grylle</i>	USNM 344753	35.0	32.8	6.7	5.0	2.9	6.1	5.7	62.8	58.0	7.1	2.8	5.4	5.2
<i>Cephus grylle</i>	USNM 344760	35.7	34.2	6.4	4.4	3.3	6.4	5.7	62.7	58.1	7.9	3.0	5.6	5.3
<i>Cephus grylle</i>	USNM 344758	36.5	34.5	7.0	5.2	3.2	6.7	6.0	65.2	60.3	8.4	2.9	6.1	5.6
<i>Cephus grylle</i>	USNM 347071	35.3	33.8	6.8	4.8	3.6	6.4	6.2	62.9	58.3	8.2	3.1	5.7	5.3
<i>Cephus grylle</i>	USNM 344754	37.6	35.9	7.2	5.6	3.3	7.1	6.5	66.6	61.4	8.8	3.1	6.4	5.8
<i>Fratercula arctica</i>	USNM 292346	40.3	38.9	7.1	5.3	3.3	6.8	6.3	67.9	63.4	8.3	3.4	6.4	6.4
<i>Fratercula arctica</i>	USNM 225762	37.7	36.5	7.5	5.7	3.1	7.2	6.2	66.5	62.3	8.2	3.5	5.6	6.1
<i>Fratercula arctica</i>	USNM 292344	42.3	41.1	8.8	5.2	3.5	7.8	6.4	73.3	68.8	9.3	3.6	6.4	6.5
<i>Fratercula arctica</i>	USNM 292347	38.1	36.8	7.2	5.5	3.1	7.1	6.1	63.0	59.3	9.0	3.7	5.9	6.2
<i>Fratercula arctica</i>	USNM 224189	41.5	40.2	7.7	5.4	3.2	7.4	7.3	70.4	66.6	9.1	3.6	6.4	6.7
<i>Pinguinus impennis</i>	USNM no #	76.6	73.4	16.2	11.2	9.4	14.6	13.8	133.6	124.6	15.6	7.3	12.6	12.3
<i>Pinguinus impennis</i>	USNM no #	72.4	69.8	14.0	10.0	7.8	13.3	12.6	131.3	122.1	16.7	7.1	12.8	12.3
<i>Pinguinus impennis</i>	USNM no #	71.0	68.3	14.6	10.5	7.3	12.9	12.0	133.5	125.8	16.2	7.1	11.4	11.4
<i>Pinguinus impennis</i>	USNM no #	74.6	72.4	16.2	11.6	9.2	14.8	13.1	129.7	120.8	16.6	7.0	12.1	10.8
<i>Pinguinus impennis</i>	USNM no #	76.5	74.2	15.6	11.0	8.2	14.4	13.5	129.9	121.6	16.1	7.3	12.9	12.8
<i>P. aleuticus</i>	USNM 557611	27.9	26.6	4.8	3.4	2.5	4.7	4.7	50.6	46.5	6.1	2.3	4.3	4.3
<i>P. aleuticus</i>	USNM 491305	29.6	28.2	5.2	3.5	2.3	5.0	4.9	51.6	47.2	5.0	2.3	4.4	4.3
<i>P. aleuticus</i>	USNM 557607	26.7	25.7	4.7	3.0	2.5	4.3	4.4	47.8	43.5	5.6	2.3	4.3	4.0
<i>P. aleuticus</i>	USNM 557609	26.0	25.0	4.7	3.7	2.4	4.5	4.5	47.7	43.9	5.8	2.1	4.2	4.1
<i>P. aleuticus</i>	NCSM 18088	28.1	26.8	5.0	3.7	2.7	4.8	4.5	51.0	46.9	5.8	2.5	4.4	4.3
<i>Uria aalge</i>	USNM 502349	48.2	46.1	9.2	7.4	5.0	8.4	8.0	97.0	90.5	10.1	4.7	8.1	7.7
<i>Uria aalge</i>	USNM 502355	48.4	46.1	9.0	7.6	4.8	8.6	7.9	94.0	87.4	9.9	4.6	7.8	7.3



Taxa	Catalog #	glF	mlF	bpF	dpF	scF	bdF	ddF	glT	laT	dpT	scT	bdT	ddT
<i>Uria aalge</i>	USNM 502348	47.7	45.5	9.1	7.3	5.1	8.5	8.5	94.2	87.2	10.1	5.0	8	7.8
<i>Uria aalge</i>	USNM 557539	45.0	43.4	8.9	7.4	4.8	7.8	7.2	88.4	82.4	9.6	4.5	7.6	7.0
<i>Uria aalge</i>	USNM 18066	47.1	45.3	9.0	7.3	5.0	8.2	7.8	92.4	85.9	9.4	4.2	7.4	7.4
<i>Uria lomvia</i>	USNM 502358	45.7	43.6	8.3	6.9	4.6	8.0	7.8	86.8	80.9	9.6	3.7	7.3	7.0
<i>Uria lomvia</i>	USNM 502361	45.9	44.1	8.6	7.2	5.0	7.8	7.5	88.2	82.4	9.8	3.9	7.5	6.8
<i>Uria lomvia</i>	USNM 502372	47.8	45.5	8.3	7.1	4.7	7.8	7.6	87.7	82.1	9.1	3.7	7.3	6.9
<i>Uria lomvia</i>	USNM 502369	46.2	43.8	8.6	6.9	4.5	7.9	7.2	86.8	80.6	8.9	3.7	7.1	6.6
<i>Uria lomvia</i>	USNM 502374	44.9	43.8	7.7	6.4	4.2	7.2	7.0	83.8	78.6	8.3	3.5	6.8	6.1

Taxa	Catalog #	glTm	bpTm	scTm	bdTm
<i>Aethia cristatella</i>	USNM 561934	26.7	5.3	2.3	4.9
<i>Aethia cristatella</i>	USNM 223707	30.7	5.2	2.4	5.0
<i>Aethia cristatella</i>	USNM 610941	25.5	5.3	2.0	5.0
<i>Aethia cristatella</i>	USNM 498282	27.6	5.4	2.2	5.3
<i>Aethia cristatella</i>	NCSM 17749	29.0	5.9	2.3	5.4
<i>Aethia psittacula</i>	NCSM 14804	28.1	6.1	2.8	5.4
<i>Aethia psittacula</i>	NCSM 18387	29.6	6.0	2.5	5.5
<i>Aethia psittacula</i>	NCSM 14147	29.2	6.8	2.7	6.1
<i>Aethia psittacula</i>	NCSM 20177	29.4	6.2	2.8	5.3
<i>Aethia psittacula</i>	USNM 610513	29.2	5.7	2.6	5.3
<i>Aethia psittacula</i>	USNM 610514	29.9	6.0	3.1	5.4
<i>Aethia psittacula</i>	USNM 610937	29.1	6.1	2.6	5.7
<i>Aethia pusilla</i>	NCSM 17737	18.5	3.3	1.4	3.3
<i>Aethia pusilla</i>	NCSM 17736	18.7	3.5	1.5	3.4
<i>Aethia pusilla</i>	NCSM 17734	19.1	3.6	1.4	3.5
<i>Aethia pusilla</i>	NCSM 224009	19.8	3.6	1.5	3.8
<i>Aethia pusilla</i>	USNM 498285	19.1	3.6	1.4	3.2
<i>Aethia pusilla</i>	USNM 224010	19.1	3.7	1.5	3.6

Taxa	Catalog #	gTm	bpTm	scTm	bdTm
<i>Aethia pygmaea</i>	UMMZ 204592	21.8	3.5	1.5	3.0
<i>Aethia pygmaea</i>	UMMZ 224882	20.8	4.1	1.7	3.7
<i>Aethia pygmaea</i>	UMMZ 224883	19.8	4.0	1.9	3.8
<i>Aethia pygmaea</i>	USNM 344544	20.5	3.6	1.7	3.5
<i>Alca torda</i>	USNM 555666	36.0	7.3	3.2	7.2
<i>Alca torda</i>	USNM 502378	33.8	7.5	3.2	7.2
<i>Alca torda</i>	USNM 502387	33.5	6.8	3.7	7.2
<i>Alca torda</i>	USNM 502389	34.9	7.4	3.5	7.3
<i>Alca torda</i>	USNM 18062	34.8	7.3	3.6	7.8
<i>Alle alle</i>	USNM 560932	20.4	4.2	2.2	4.6
<i>Alle alle</i>	USNM 560927	19.7	4.3	2.0	4.5
<i>Alle alle</i>	USNM 560926	20.0	4.4	2.2	3.3
<i>Alle alle</i>	USNM 344748	20.1	4.6	1.9	4.5
<i>Alle alle</i>	USNM 502391	19.6	4.0	1.9	4.0
<i>Cepphus columba</i>	USNM 610936	38.3	7.2	2.9	6.8
<i>Cepphus columba</i>	USNM 612989	35.0	6.5	2.6	6.2
<i>Cepphus columba</i>	USNM 498423	35.6	7.2	3.2	6.5
<i>Cepphus columba</i>	USNM 498422	35.8	7.4	2.7	6.8
<i>Cepphus columba</i>	USNM 612988	35.4	6.9	3.1	6.1
<i>Cepphus grylle</i>	USNM 344753	30.0	6.0	2.1	5.3
<i>Cepphus grylle</i>	USNM 344760	29.8	5.9	2.3	5.6
<i>Cepphus grylle</i>	USNM 344758	31.3	6.9	2.5	6.1
<i>Cepphus grylle</i>	USNM 347071	29.9	6.0	2.3	5.6
<i>Cepphus grylle</i>	USNM 344754	1.7	6.6	2.5	6.1
<i>Fratrercula arctica</i>	USNM 292346	28.7	6.8	3.2	7.1
<i>Fratrercula arctica</i>	USNM 225762	26.9	6.3	3.3	6.6
<i>Fratrercula arctica</i>	USNM 292344	30.7	6.8	4.1	7.7
<i>Fratrercula arctica</i>	USNM 292347	27.0	6.3	3.7	6.7



Taxa	Catalog #	glTm	bpTm	scTm	bdTm
<i>Fratercula arctica</i>	USNM 224189	30.2	6.8	3.2	7.1
<i>Pinguinus impennis</i>	USNM no #	50.3	13.4	7.5	14.8
<i>Pinguinus impennis</i>	USNM no #	55.6	14.4	7.9	15.1
<i>Pinguinus impennis</i>	USNM no #	53.0	14.5	7.4	14.7
<i>Pinguinus impennis</i>	USNM no #	54.1	13.6	7.1	14.4
<i>Pinguinus impennis</i>	USNM no #	52.8	14.9	7.3	14.2
<i>P. aleuticus</i>	USNM 557611	25.6	4.8	1.8	4.1
<i>P. aleuticus</i>	USNM 491305	25.5	4.9	2.3	4.4
<i>P. aleuticus</i>	USNM 557607	24.3	4.6	1.8	4.0
<i>P. aleuticus</i>	USNM 557609	24.6	4.7	2.5	4.0
<i>P. aleuticus</i>	NCSM 18088	25.9	5.0	2.1	4.1
<i>Uria aalge</i>	USNM 502349	40.5	8.9	3.8	7.8
<i>Uria aalge</i>	USNM 502355	38.1	9.0	4.0	8.0
<i>Uria aalge</i>	USNM 502348	40.5	8.5	3.9	8.3
<i>Uria aalge</i>	USNM 557539	36.6	8.2	3.9	7.4
<i>Uria aalge</i>	USNM 18066	37.8	8.3	3.7	7.6
<i>Uria lomvia</i>	USNM 502358	36.6	8.3	3.1	7.0
<i>Uria lomvia</i>	USNM 502361	37.8	8.2	3.2	7.2
<i>Uria lomvia</i>	USNM 502372	37.1	7.8	3.1	7.1
<i>Uria lomvia</i>	USNM 502369	34.8	7.7	3.0	7.1
<i>Uria lomvia</i>	USNM 502374	33.8	7.7	2.8	6.5

## APPENDIX 6.

### FOSSIL MEASUREMENT DATA

#### APPENDIX 6A.

**Measurements and species referrals for humeri used in the final morphometric analysis:** Measurements of *Alca* fossil specimens (in mm). “---” denotes measurements missing due to damage. All measurements according to Von den Driesch (1976).

Abbreviations: glH, greatest length of humerus; bpH, breadth of proximal humerus; dpH, depth of proximal humerus; scH, smallest dorsoventral breadth of humeral corpus (shaft); bdH, breadth of distal humerus; ddH, distal diagonal of humerus.

SPECIMEN #	glH	bpH	dpH	scH	bdH	ddH	Specimen Referral to Species
ANSP 13357	96.2	19.7	18.8	8.2	13.9	9.4	<i>Alca grandis</i> (holotype)
BMNH A 7052	111.2	22.8	21.8	8.9	15.5	12.1	<i>Alca stewarti</i> (paratype)
BMNH A 7055	---	---	---	9.0	13.9	10.4	<i>Alca grandis</i>
BMNH A 7054	---	---	---	7.8	14.1	11.3	<i>Alca carolinensis / olsoni</i>
GCVF 5691	99.6	20.0	19.5	8.5	14.8	10.4	<i>Alca grandis</i>
GCVF 5690	---	---	---	---	13.7	10.0	<i>Alcini incertae sedis</i>
IGF 14875	---	---	---	7.5	12.4	9.1	<i>Alca ausonia</i> (holotype)
NCMNS 13734	102.4	20.8	21.0	9.2	14.9	10.4	<i>Alca carolinensis</i> (holotype)
NCMNS 13001	---	---	---	7.2	12.5	9.0	<i>Alca ausonia</i>
NCMNS 14116	---	---	---	8.1	12.8	9.2	<i>Alca ausonia</i>
NCMNS 15064	97.8	8.5	---	14.4	10.2	19.5	<i>Alca grandis</i>
NCSM 24366	104.3	23.2	23.0	8.8	16.2	11.6	<i>Alca carolinensis / olsoni</i>
UF 61953	---	17.0	16.3	6.6	---	---	<i>Alca torda</i>
UF 61539	---	17.6	16.9	7.0	---	---	<i>Alca torda</i>
UF 61531	---	18.2	16.1	7.7	---	---	<i>Alca torda</i>
UF 21031	---	16.3	15.0	7.2	---	---	<i>Alca torda</i>
UF 61995	---	---	---	7.0	12.0	8.1	<i>Alca ausonia</i>
UF 58456	---	---	---	6.7	11.8	8.3	<i>Alca ausonia</i>
UF 61542	---	---	---	6.6	11.2	8.2	<i>Alca torda</i>
UF 61541	---	---	---	7.2	11.7	8.2	<i>Alca ausonia</i>
UF 61537	---	16.1	15.4	5.7	---	---	<i>Alca torda</i>
UF 57254	---	---	---	5.9	11.2	7.8	<i>Alca torda</i>
UF 12473	---	15.8	15.2	6.3	---	---	<i>Alca torda</i>
UF 12474	---	15.8	14.3	7.1	---	---	<i>Alca torda</i>
UF 21069	---	16.0	14.9	6.8	---	---	<i>Alca torda</i>
UF 21074	---	16.0	14.8	7.2	---	---	<i>Alca torda</i>
UF 61533	---	---	---	9.0	14.4	10.0	<i>Alca grandis</i>
UF 67956	---	---	---	8.8	13.8	9.6	<i>Alca grandis</i>
UF 12477	---	---	---	7.5	13.7	9.5	<i>Alca grandis</i>
UF 21191	---	16.5	15.0	6.9	---	---	<i>Alca torda</i>
UF 21032	---	---	---	5.9	11.0	7.8	<i>Alca torda</i>
UF 21038	---	---	---	6.7	11.5	7.9	<i>Alca torda</i>
UF 21078	---	---	---	7.0	12.2	8.8	<i>Alca ausonia</i>
UF 21114	---	---	---	7.7	13.3	8.6	<i>Alca ausonia</i>
UF 208612	---	16.6	16.0	7.1	---	---	<i>Alca torda</i>

SPECIMEN #	glH	bpH	dpH	scH	bdH	ddH	Specimen Referral to Species
UF 95473	---	14.9	14.9	6.7	---	---	<i>Alca torda</i>
UF 125027	---	---	---	6.5	10.8	7.7	<i>Alca torda</i>
UF 123805	---	---	---	7.1	11.9	8.8	<i>Alca ausonia</i>
UF 117423	---	---	---	6.5	10.5	7.4	<i>Alca torda</i>
UF 49094	---	---	---	8.4	13.7	9.4	<i>Alca grandis</i>
UF 49095	---	15.7	14.6	6.2	---	---	<i>Alca torda</i>
UF 117492	---	16.9	15.5	6.6	---	---	<i>Alca torda</i>
UF 211946	---	---	---	6.3	10.7	8.0	<i>Alca torda</i>
UF 208384	---	---	---	8.6	13.7	9.9	<i>Alca grandis</i>
UF 21145	---	---	---	6.5	11.6	7.9	<i>Alca torda</i>
UF 61954	---	---	---	6.3	11.3	8.0	<i>Alca torda</i>
UF 21107	---	15.7	14.7	6.7	---	---	<i>Alca torda</i>
UF/PB 7948	---	---	---	6.5	11.9	8.3	<i>Alca ausonia</i>
UF/PB 7949	---	---	---	6.6	10.9	7.7	<i>Alca torda</i>
UF/PB 7989	---	---	---	6.5	11.3	7.8	<i>Alca torda</i>
UF/PB 7942	---	15.3	15.2	6.9	---	---	<i>Alca torda</i>
UF/PB 7945	---	---	---	7.3	13.1	9.0	<i>Alca ausonia</i>
UF/PB 7947	---	---	---	6.0	11.1	7.8	<i>Alca torda</i>
UF/PB 7752	---	19.3	18.7	8.2	---	---	<i>Alca grandis</i>
UF/PB 91	---	---	---	6.5	11.7	8.3	<i>Alca ausonia</i>
UF/PB 304	---	---	---	6.2	11.4	8.1	<i>Alca torda</i>
UF/PB 305	---	---	---	7.0	11.6	7.9	<i>Alca ausonia</i>
USNM 192101	---	21.6	21.0	8.9	---	---	<i>Alca carolinensis / olsoni</i>
USNM 419708	---	20.8	20.1	8.6	---	---	<i>Alca grandis</i>
USNM 460786	---	16.7	15.5	7.0	---	---	<i>Alca torda</i>
USNM 178221	---	21.1	20.0	8.6	---	---	<i>Alca grandis</i>
USNM 236802	95.8	20.7	19.7	8.8	14.0	10.1	<i>Alca grandis</i>
USNM 236802	95.9	---	---	8.6	14.0	10.1	<i>Alca grandis</i>
USNM 495613	103.4	21.9	---	8.9	15.1	11.0	<i>Alca carolinensis / olsoni</i>
USNM 242238	111.4	24.1	23.7	10.4	17.0	12.1	<i>Alca stewarti</i>
USNM 177981	94.6	---	---	8.2	13.8	10.2	<i>Alca grandis</i>
USNM 179285	98.9	21.1	---	8.7	14.2	9.8	<i>Alca grandis</i>
USNM 181086	93.6	19.1	18.6	8.0	13.8	10.0	<i>Alca ausonia</i>
USNM 192840	96.9	20.4	19.6	8.6	13.8	10.0	<i>Alca grandis</i>
USNM 206301	104.9	22.2	21.0	9.7	15.0	10.7	<i>Alca carolinensis / olsoni</i>
USNM 242288	95.9	19.6	---	8.5	14.0	9.8	<i>Alca ausonia</i>
USNM 302324	63.7	13.8	---	5.7	---	---	<i>Alca minor</i> (holotype)
USNM 192879	---	13.2	---	---	---	---	<i>Alca minor</i>
USNM 495600	---	---	---	5.8	9.1	7.0	<i>Alca minor</i>
USNM 275787	94.3	20.1	19.1	8.0	13.6	9.6	<i>Alca ausonia</i>
USNM 302358	94.6	19.9	17.9	8.4	---	---	<i>Alca ausonia</i>
USNM 367013	106.4	22.2	21.0	9.2	15.5	10.5	<i>Alca carolinensis / olsoni</i>
USNM 446649	102.9	---	---	8.9	14.8	10.8	<i>Alca carolinensis / olsoni</i>
USNM 446652	105.8	22.7	21.9	9.6	15.7	11.1	<i>Alca carolinensis / olsoni</i>
USNM 446654	89.7	19.0	18.4	7.9	13.2	9.2	<i>Alca ausonia</i>
USNM 446662	92.7	19.5	19.5	8.8	14.0	9.7	<i>Alca ausonia</i>
USNM 446663	97.7	21.4	20.3	8.9	14.4	10.1	<i>Alca grandis</i>

SPECIMEN #	glH	bpH	dpH	scH	bdH	ddH	Specimen Referral to Species
USNM 446664	96.5	20.8	19.9	8.6	13.6	9.3	<i>Alca grandis</i>
USNM 446666	102.0	21.5	21.0	8.8	14.1	9.9	<i>Alca carolinensis / olsoni</i>
USNM 446668	104.7	22.3	21.7	9.2	14.3	10.8	<i>Alca carolinensis / olsoni</i>
USNM 192014	92.3	20.2	19.4	8.5	13.1	8.8	<i>Alca ausonia</i>
USNM 215795	91.0	20.4	19.5	8.3	13.6	9.8	<i>Alca ausonia</i>
USNM 275846	103.1	20.8	---	8.8	14.8	10.4	<i>Alca carolinensis / olsoni</i>
USNM 302320	101.8	21.9	20.3	8.8	14.8	10.4	<i>Alca carolinensis / olsoni</i>
USNM 321235	103.9	20.6	---	8.6	14.2	10.3	<i>Alca carolinensis / olsoni</i>
USNM 366793	100.3	22.4	---	8.8	15.1	10.6	<i>Alca carolinensis / olsoni</i>
USNM 446671	92.0	19.7	19.0	8.2	14.1	10.1	<i>Alca ausonia</i>
USNM 446673	102.1	22.0	20.9	8.8	15.1	11.3	<i>Alca carolinensis / olsoni</i>
USNM 446674	106.5	22.3	---	9.7	14.9	10.6	<i>Alca carolinensis / olsoni</i>
USNM 446675	104.3	21.5	21.2	9.1	15.0	10.2	<i>Alca carolinensis / olsoni</i>
USNM 446676	101.8	21.6	21.3	9.0	15.2	10.8	<i>Alca carolinensis / olsoni</i>
USNM 446677	99.0	21.5	20.7	8.6	14.0	10.6	<i>Alca grandis</i>
USNM 446680	99.3	21.5	21.0	8.9	14.8	10.7	<i>Alca grandis</i>
USNM 446681	104.3	21.6	20.9	9.6	15.0	10.2	<i>Alca carolinensis / olsoni</i>
USNM 446682	102.8	22.2	20.4	9.5	14.7	11.4	<i>Alca carolinensis / olsoni</i>
USNM 446683	98.8	20.7	20.4	9.0	13.8	9.5	<i>Alca grandis</i>
USNM 446687	99.6	20.4	19.3	8.9	---	9.6	<i>Alca grandis</i>
USNM 446688	98.1	20.9	20.3	8.8	13.6	9.9	<i>Alca grandis</i>
USNM 446692	91.0	19.4	18.7	7.7	12.5	8.9	<i>Alca ausonia</i>
USNM 446690	93.9	19.6	19.1	8.4	13.5	9.8	<i>Alca ausonia</i>
USNM 446694	105.9	21.4	21.1	8.8	15.4	10.7	<i>Alca carolinensis / olsoni</i>
USNM 446695	97.7	20.5	20.0	8.5	14.3	10.6	<i>Alca grandis</i>
USNM 446696	101.1	21.2	21.0	9.3	15.2	10.1	<i>Alca carolinensis / olsoni</i>
USNM 446697	101.9	21.7	21.1	9.0	---	10.3	<i>Alca carolinensis / olsoni</i>
USNM 495673	101.0	21.8	21.6	9.3	15.0	11.4	<i>Alca carolinensis / olsoni</i>
USNM 446684	101.7	22.4	21.2	9.2	15.5	10.7	<i>Alca carolinensis / olsoni</i>
USNM 446699	106.8	22.1	21.7	9.6	15.8	11.0	<i>Alca carolinensis / olsoni</i>
USNM 532685	---	21.4	21.6	9.6	---	---	<i>Alca carolinensis / olsoni</i>
USNM 532686	---	20.7	20.2	9.3	---	---	<i>Alca grandis</i>
USNM 532689	90.9	19.4	18.8	8.2	13.9	9.5	<i>Alca ausonia</i>
USNM 532715	---	19.0	18.3	8.4	---	---	<i>Alca ausonia</i>
USNM 532738	---	22.5	22.2	8.8	---	---	<i>Alca grandis</i>
USNM 532741	---	20.4	20.1	9.0	---	---	<i>Alca grandis</i>
USNM 532742	---	16.7	16.0	6.7	---	---	<i>Alca torda</i>
USNM 532858	---	16.3	15.4	6.6	---	---	<i>Alca torda</i>
USNM 532859	---	19.5	18.2	7.9	---	---	<i>Alca grandis</i>
USNM 532860	---	16.5	15.3	6.9	---	---	<i>Alca torda</i>
USNM 532861	---	13.9	13.2	5.6	---	---	<i>Alca minor</i>
USNM 275856	---	18.8	17.8	7.7	---	---	<i>Alca grandis</i>
USNM 366257	---	19.3	19.1	7.8	---	---	<i>Alca ausonia</i>
USNM 366258	---	21.5	20.8	8.8	---	---	<i>Alca carolinensis / olsoni</i>
USNM 181098	---	19.4	18.3	8.3	---	---	<i>Alca ausonia</i>
USNM 368484	---	21.6	20.3	8.5	---	---	<i>Alca grandis</i>
USNM 368485	---	21.0	20.4	8.8	---	---	<i>Alca grandis</i>
USNM 532869	---	21.2	20.4	8.6	---	---	<i>Alca grandis</i>

SPECIMEN #	glH	bpH	dpH	scH	bdH	ddH	Specimen Referral to Species
USNM 532870	---	20.4	19.7	8.3	---	---	<i>Alca carolinensis / olsoni</i>
USNM 532871	---	18.1	17.2	7.3	---	---	<i>Alca torda</i>
USNM 532874	---	17.0	16.6	7.4	---	---	<i>Alca torda</i>
USNM 532878	---	22.1	21.4	8.5	---	---	<i>Alca grandis</i>
USNM 532880	---	21.7	20.6	9.0	---	---	<i>Alca carolinensis / olsoni</i>
USNM 532884	---	21.3	20.6	8.3	---	---	<i>Alca carolinensis / olsoni</i>
USNM 532885	---	21.5	21.3	9.4	---	---	<i>Alca carolinensis / olsoni</i>
USNM 532886	---	21.4	20.2	8.5	---	---	<i>Alca grandis</i>
USNM 532887	---	21.9	21.1	8.9	---	---	<i>Alca carolinensis / olsoni</i>
USNM 532890	---	20.6	19.9	8.6	---	---	<i>Alca grandis</i>
USNM 532896	---	20.7	20.3	8.8	---	---	<i>Alca grandis</i>
USNM 532897	---	21.8	21.5	9.4	---	---	<i>Alca carolinensis / olsoni</i>
USNM 532900	---	17.3	17.1	7.0	---	---	<i>Alca torda</i>
USNM 532908	---	16.6	16.2	6.5	---	---	<i>Alca torda</i>
USNM 275852	---	18.6	18.1	7.6	---	---	<i>Alca ausonia</i>
USNM 533145	---	18.8	19.0	7.4	---	---	<i>Alca grandis</i>
USNM 366558	102.4	20.9	---	8.3	14.7	10.5	<i>Alca carolinensis / olsoni</i>
USNM 446656	83.5	16.8	16.2	6.9	12.0	8.7	<i>Alca torda</i>
USNM 533036	99.4	22.0	20.8	9.1	15.1	10.8	<i>Alca grandis</i>
USNM 533037	96.9	20.6	19.6	8.1	14.6	10.5	<i>Alca grandis</i>
USNM 533038	101.1	21.8	21.0	8.7	15.4	10.7	<i>Alca carolinensis / olsoni</i>
USNM 533039	100.0	21.7	---	8.5	15.0	10.7	<i>Alca grandis</i>
USNM 533040	86.7	19.3	18.4	7.5	13.3	8.8	<i>Alca ausonia</i>
USNM 533041	74.5	16.0	15.6	6.9	10.9	8.0	<i>Alca torda</i>
USNM 533042	71.2	14.7	14.2	6.4	9.8	7.8	<i>Alca torda</i>
USNM 533171	---	---	---	7.1	13.2	9.0	<i>Alca ausonia</i>
USNM 533172	---	---	---	9.2	15.2	10.8	<i>Alca carolinensis / olsoni</i>
USNM 215443	88.8	19.1	18.8	8.4	14.0	9.8	<i>Alca ausonia</i>
USNM 368479	82.7	17.1	16.2	7.3	12.3	8.7	<i>Alca torda</i>
USNM 179220	84.4	19.1	17.9	7.9	12.4	9.1	<i>Alca torda</i>
USNM 275870	78.7	16.2	15.3	6.6	11.5	8.4	<i>Alca torda</i>
USNM 366571	86.4	---	---	7.3	11.9	9.2	<i>Alca ausonia</i>
USNM 181038	82.2	17.7	15.4	6.7	12.1	8.6	<i>Alca torda</i>
USNM 495672	85.3	---	---	7.8	13.0	8.8	<i>Alca ausonia</i>
USNM 366584	81.7	---	---	7.5	12.8	8.9	<i>Alca torda</i>
USNM 183425	87.8	19.9	18.5	8.0	13.9	9.8	<i>Alca ausonia</i>
USNM 368480	87.5	18.2	17.1	7.1	12.9	9.4	<i>Alca ausonia</i>
USNM 495671	89.7	19.5	19.3	8.3	13.8	9.9	<i>Alca ausonia</i>
USNM 446685	86.0	19.7	18.4	7.7	13.0	9.6	<i>Alca ausonia</i>
USNM 446661	82.2	18.9	---	6.8	12.7	9.2	<i>Alca torda</i>
USNM 446670	78.6	17.3	16.6	7.2	12.0	8.3	<i>Alca torda</i>
USNM 495670	81.2	17.3	16.7	7.0	11.4	8.4	<i>Alca torda</i>
USNM 256354	---	---	---	7.0	11.1	8.3	<i>Alca torda</i>
USNM 256361	---	---	---	9.1	13.6	10.5	<i>Alca grandis</i>
USNM 256355	---	15.2	14.9	6.5	---	---	<i>Alca torda</i>
USNM 256358	---	15.6	14.9	6.0	---	---	<i>Alca torda</i>
USNM 447052	---	16.2	15.7	6.8	---	---	<i>Alca torda</i>
USNM 447054	---	16.1	15.7	6.5	---	---	<i>Alca torda</i>

SPECIMEN #	glH	bpH	dpH	scH	bdH	ddH	Specimen Referral to Species
USNM 532557	---	---	---	7.0	11.8	8.6	<i>Alca ausonia</i>
USNM 532559	---	---	---	7.5	13.6	9.7	<i>Alca grandis</i>
USNM 495616	97.9	20.4	---	8.8	14.3	10.3	<i>Alca grandis</i>
USNM 495614	---	20.5	20.8	8.8	---	---	<i>Alca grandis</i>
USNM 459609	---	---	---	8.5	15.0	10.3	<i>Alca carolinensis / olsoni</i>
USNM 454590	104.0	22.8	21.7	8.8	15.4	11.0	<i>Alca olsoni</i> (holotype)
USNM 336379	---	8.8	---	8.8	14.1	10.3	<i>Alca grandis</i>
USNM 215454	---	---	---	8.4	13.9	9.7	<i>Alca grandis</i>
USNM 495613	103.4	21.9	---	8.9	15.1	11.0	<i>Alca carolinensis / olsoni</i>
USNM 495612	---	21.4	20.9	8.6	14.2	10.2	<i>Alca carolinensis / olsoni</i>
USNM 183510	---	19.8	18.6	9.0	---	---	<i>Alca grandis</i>
USNM 237248	---	22.1	20.1	9.1	---	---	<i>Alca carolinensis / olsoni</i>
USNM 237264	---	16.9	15.0	6.2	---	---	<i>Alca torda</i>
USNM 446650	112.0	24.2	22.4	10.0	16.8	12.2	<i>Alca stewarti</i>
USNM 299637	---	---	---	10.6	16.7	11.7	<i>Alca stewarti</i>
USNM 460811	---	---	---	9.9	16.3	11.6	<i>Alca stewarti</i>
USNM 210532	---	---	---	6.0	10.5	7.5	<i>Alca torda</i>
USNM 321314	76.0	16.0	---	6.7	11.2	8.2	<i>Alca torda</i>
USNM 446657	74.0	15.2	14.2	6.2	10.6	7.6	<i>Alca torda</i>
USNM 446686	75.7	15.6	14.1	7.3	11.5	8.0	<i>Alca torda</i>
USNM 446691	76.9	16.0	15.5	6.7	11.1	8.0	<i>Alca torda</i>
USNM 495589	79.0	17.2	13.6	7.3	---	---	<i>Alca torda</i>
USNM 257519	77.6	---	---	6.7	10.0	7.2	<i>Alca torda</i>
USNM 495592	65.4	---	---	5.8	8.8	6.6	<i>Alca minor</i>
USNM 250772	---	---	---	5.7	9.6	6.7	<i>Alca torda</i>
USNM 495591	---	---	---	5.8	9.1	6.4	<i>Alca minor</i>

## APPENDIX 6B

### *ALCA* FOSSIL HUMERI MEASUREMENT DATA

Measurements of *Alca* fossil specimens (in mm). Empty cells denote measurements missing due to damage. All measurements according to Von den Driesch (1976).  
Abbreviations: glH, greatest length of humerus; bpH, breadth of proximal humerus; dpH, depth of proximal humerus; scH, smallest dorsoventral breadth of humeral corpus (shaft); bdH, breadth of distal humerus; ddH, distal diagonal of humerus.

MUSEUM	SPEC. #	glH	bpH	dpH	scH	bdH	ddH
USNM	192101	21	8.9				
USNM	192101			14.9	10.5		
USNM	419708	20.1	8.6				
USNM	460786	15.5	7				
USNM	215717			12.8	9		
USNM	252435			12.9	9.5		
USNM	495610			15.2	10.6		
USNM	215549	18.7					
USNM	178221	20	8.6				
USNM	214919						
USNM	236802	95.8	20.7	19.7	8.8	14	10.1
USNM	236802	94.9			8.6	14	10.1
USNM	215454		8.4	13.9	9.7		
USNM	495613	103.4	21.9		8.9	15.1	11
USNM	495612	20.9	8.6	14.2	10.2		
USNM	495612	20.9					
USNM	237270		6	10.1	7.2		
USNM	237270		6	10.1	7.2		
USNM	242238	111.4	24.1	23.7	10.4	17	12.1
USNM	321314	76	16		6.7	11.2	8.2
USNM	177981	94.6			8.2	13.8	10.2
USNM	179285	98.9	21.1		8.7	14.2	9.8
USNM	181086	93.6	19.1	18.6	8	13.8	10
USNM	192840	96.9	20.4	19.6	8.6	13.8	10
USNM	206301	104.9	22.2	21	9.7	15	10.7
USNM	242288	95.9	19.6		8.5	14	9.8
USNM	275787	94.3	20.1	19.1	8	13.6	9.6
USNM	302358	94.6	19.9	17.9	8.4		
USNM	367013	106.4	22.2	21	9.2	15.5	10.5

MUSEUM	SPEC. #	glH	bpH	dpH	scH	bdH	ddH
USNM	446649	102.9			8.9	14.8	10.8
USNM	446652	105.8	22.7	21.9	9.6	15.7	11.1
USNM	446654	89.7	19	18.4	7.9	13.2	9.2
USNM	446662	92.7	19.5	19.5	8.8	14	9.7
USNM	446663	97.7	21.4	20.3	8.9	14.4	10.1
USNM	446664	96.5	20.8	19.9	8.6	13.6	9.3
USNM	446666	102	21.5	21	8.8	14.1	9.9
USNM	446668	104.7	22.3	21.7	9.2	14.3	10.8
USNM	192014	92.3	20.2	19.4	8.5	13.1	8.8
USNM	215795	91	20.4	19.5	8.3	13.6	9.8
USNM	275846	103.1	20.8		8.8	14.8	10.4
USNM	302320	101.8	21.9	20.3	8.8	14.8	10.4
USNM	321235	103.9	20.6		8.6	14.2	10.3
USNM	366793	100.3	22.4		8.8	15.1	10.6
USNM	446671	92	19.7	19	8.2	14.1	10.1
USNM	446673	102.1	22	20.9	8.8	15.1	11.3
USNM	446674	106.5	22.3		9.7	14.9	10.6
USNM	446675	104.3	21.5	21.2	9.1	15	10.2
USNM	446676	101.8	21.6	21.3	9	15.2	10.8
USNM	446677	99	21.5	20.7	8.6	14	10.6
USNM	446680	99.3	21.5	21	8.9	14.8	10.7
USNM	446681	104.3	21.6	20.9	9.6	15	10.2
USNM	446682	103.8	22.2	20.4	9.5	14.7	11.4
USNM	446683	98.8	20.7	20.4	9	13.8	9.5
USNM	446687	99.6	20.4	19.3	8.9		9.6
USNM	446688	98.1	20.9	20.3	8.8	13.6	9.9
USNM	446692	91	19.4	18.7	7.7	12.5	8.9
USNM	446690	93.9	19.6	19.1	8.4	13.5	9.8
USNM	446694	105.9	21.4	21.1	8.8	15.4	10.7
USNM	446695	97.7	20.5	20	8.5	14.3	10.6
USNM	446696	101.1	21.2	21	9.3	15.2	10.1
USNM	446697	101.9	21.7	21.1	9		10.3
USNM	495673	101	21.8	21.6	9.3	15	11.4
USNM	446684	101.7	22.4	21.2	9.2	15.5	10.7
USNM	446699	106.8	22.1	21.7	9.6	15.8	11
USNM	532685		21.4	21.6	9.6		
USNM	532686		20.7	20.2	9.3		
USNM	532687		19.1	18.4			
USNM	532689	90.9	19.4	18.8	8.2	13.9	9.5
USNM	532690				12.1	18.1	11.5



MUSEUM	SPEC. #	glH	bpH	dpH	scH	bdH	ddH
USNM	532696		20.5	20.1			
USNM	532697				6	12	8.7
USNM	532698				8.1	13.9	9.5
USNM	177931		21	20.1			
USNM	177944		22.6	21			
USNM	177959		21.7	20.5			
USNM	177978		20.3	19.9			
USNM	177993		19	19.4			
USNM	178001		21.6	20.5			
USNM	179298		20.3	18.2			
USNM	179303		19	19			
USNM	181084		20	19.6			
USNM	181111		21.5	20.9			
USNM	181114		20.7	19.9			
USNM	183476		19.1	18.5			
USNM	192015		19.1	18			
USNM	192017		20.4	19.5			
USNM	192024		19.3	19			
USNM	192025		21.2	20.7			
USNM	192490		22.3	21			
USNM	192850		21.2	19.9			
USNM	192851		19.7	18.8			
USNM	275790		21.1	20.7			
USNM	275809		21.1	20.5			
USNM	275871		21.1	20.2			
USNM	275874		20.8	20.3			
USNM	302367		18.9	17.8			
USNM	306337		21.3	19.9			
USNM	308251		15.6	14.5			
USNM	321286		21.6	21.5			
USNM	366421		20.6	20.3			
USNM	366456		18.4	17.2			
USNM	366575		19	17.4			
USNM	366585		18	17			
USNM	366635		20.5	19.5			
USNM	366636		20.2	18.9			
USNM	366734		16.4	16.2			
USNM	366810		16.4	16.1			
USNM	367037		16.7	15			

MUSEUM	SPEC. #	glH	bpH	dpH	scH	bdH	ddH
USNM	367098		19.2	17.8			
USNM	367146		22	21.2			
USNM	193007		17.3	16.2			
USNM	193045		20.8	20			
USNM	193050		19.1	18.1			
USNM	193177		19.9	19.2			
USNM	193183		20.2	18.6			
USNM	193286		19	18.1			
USNM	193347		16	15.2			
USNM	193377		19.3	18.4			
USNM	206379		20.9	19.7			
USNM	206451		14.8	14.1			
USNM	206465		19.3	18.8			
USNM	206494		19.2	18.4			
USNM	206554		16.3	15.6			
USNM	206579		20.2	19.2			
USNM	206637		19.9	19.7			
USNM	215490		20.2	19.4			
USNM	215557		20.9	20.8			
USNM	215595		21.2	20.8			
USNM	215750		20.8	20.2	9.0		
USNM	215776		20.4	19.3			
USNM	215810		20.1	19.4			
USNM	215835		20.1	19.1			
USNM	236855		17.2	16.6			
USNM	241352		20.8	19.4			
USNM	241438		16.9	16.5			
USNM	242214		21.7	21.2			
USNM	242294		20	19.5			
USNM	242321		18.5	18.3			
USNM	248544		15.6	14.6			
USNM	250688		20.1	19.2			
USNM	250718		16.2	14.9			
USNM	250820		20.1	18.8			
USNM	250827		19.6	19.6			
USNM	252367		20.1	20.1			
USNM	252441		17.1	16.8			
USNM	256252		16	15.4			
USNM	257476		19	18			

MUSEUM	SPEC. #	glH	bpH	dpH	scH	bdH	ddH
USNM	532700		19	18.5			
USNM	532701		18.9	17.6			
USNM	532702		20.2	19			
USNM	532703		21.8	20.7			
USNM	532704		19.5	18.8			
USNM	532705		21.2	20.4			
USNM	532706		24.6	23.6			
USNM	532707		21.7	21			
USNM	532708		18.4	18.3	8.3		
USNM	532709		20	19			
USNM	532710		22.6	21.3			
USNM	532712		22.7	21.1			
USNM	532713		19.3	18.5			
USNM	532715		19	18.3	8.4		
USNM	532717		20.3	19.5			
USNM	532723		18.2	17.9			
USNM	532725		18	17			
USNM	532726		22.7	21.7			
USNM	532727		18.9	18			
USNM	532728		19.1	18.4			
USNM	532729		21.5	21.1			
USNM	532731		18.9	18.5			
USNM	532732		21.1	19.8			
USNM	532733		21.1	20.8			
USNM	532734		19.2	18.6			
USNM	532735		22	21.3			
USNM	532736		18.1	17.1			
USNM	532738		22.5	22.2	8.8		
USNM	532741		20.4	20.1	9		
USNM	532742		16.7	16	6.7		
USNM	532743		18.4	17.6			
USNM	532744		15.8	15			
USNM	532745		21.7	21.4			
USNM	532746		19.2	18.8			
USNM	532858		16.3	15.4	6.6		
USNM	532859		19.5	18.2	7.9		
USNM	532860		16.5	15.3	6.9		
USNM	532861		13.9	13.2	5.6		
USNM	532862		17.8	17.1			
USNM	532863		17.6	17.3			
USNM	532864		12.2	11.4	4.4		

MUSEUM	SPEC. #	glH	bpH	dpH	scH	bdH	ddH
USNM	532865		16.2	15.7			
USNM	532866		16.4	16.3			
USNM	532867		17.1	15.9			
USNM	178145		18.8	19			
USNM	178146		19	18.9			
USNM	178147		19.5	18.8			
USNM	366754		20.6	19.3			
USNM	275856		18.8	17.8	7.7		
USNM	425121		18.9	18.1			
USNM	177995		15.2	14.7			
USNM	366943		21.1	20.6			
USNM	366257		19.3	19.1	7.8		
USNM	366258		21.5	20.8	8.8		
USNM	533110		21.2	19.9			
USNM	533111		21.1	20.2			
USNM	533112		16.8	15.4			
USNM	533114		21.7	20.8			
USNM	533115		21.6	20.7			
USNM	533116		19.1	18.6			
USNM	533118		20.8	20.1			
USNM	533119		22.7	21.6			
USNM	533120		22.7	21.3			
USNM	533121		20.7	19.5			
USNM	533122		21.3	20.1			
USNM	533123		12.4	11.6			
USNM	177924		22.9	21.7			
USNM	177946		20.8	19.8			
USNM	177983		19.5	19.4			
USNM	177992		20.1	19.3			
USNM	177997		20.4	20.2			
USNM	178000		20.7	19.8			
USNM	178004		19.3	18.7			
USNM	178058		20.7	20.4			
USNM	178235		20.2	19.2			
USNM	179283		20.5	19.9			
USNM	181023		19.1	18.8			
USNM	181098		19.4	18.3	8.3		
USNM	181104		15.9	15.8			
USNM	181113		19.7	19.7			
USNM	183487		21.9	20.8			
USNM	183493		19.4	19			

MUSEUM	SPEC. #	glH	bpH	dpH	scH	bdH	ddH
USNM	183501		16.8	16.7			
USNM	192112		19.7	19.7			
USNM	192702		19.8	18.9			
USNM	236830		19.7	19.3			
USNM	236831		19.1	19.2			
USNM	236850		19.8	19.5			
USNM	242219		19.9	19.3			
USNM	242220		19.8	19			
USNM	244228		16.9	19	6.6		
USNM	248548		19.4	18.9			
USNM	250734		19.5	19.2			
USNM	252384		19.3	19			
USNM	252425		19.5	18.4			
USNM	257489		19.5	19.3			
USNM	275792		19.2	18.6			
USNM	275869		19	18.4			
USNM	192995		19	18.7			
USNM	193032		19.5	19.2			
USNM	193118		18	17.4			
USNM	193395		21.2	20.9			
USNM	206349		20	20.1			
USNM	206356		21.7	21			
USNM	206387		16.4	15.7			
USNM	210538		19.8	18.9			
USNM	214419		22.6	22.2			
USNM	215566		18.5	18			
USNM	215575		19.5	18.8			
USNM	215577		16.1	15.8			
USNM	215602		19.7	19.5			
USNM	215610		19.3	18.4			
USNM	215642		20.2	19.9			
USNM	215653		17	16.1			
USNM	21758		22.3	21.5			
USNM	302231		21.8	21			
USNM	302332		20.3	20.4			
USNM	306270		21.2	20.4			
USNM	306271		21.6	21.6			
USNM	306273		22.1	21			
USNM	306275		19.8	19.5			
USNM	306304		22.9	21.6			
USNM	321310		21.9	21			

MUSEUM	SPEC. #	glH	bpH	dpH	scH	bdH	ddH
USNM	366419		22.2	21.3			
USNM	366581		18.8	18			
USNM	366586		17.4	17.4			
USNM	366678		19.4	19.1			
USNM	366700		21	21			
USNM	366732		20.1	18.6			
USNM	366832		17.3	17.1			
USNM	368484		21.6	20.3	8.5		
USNM	368485		21	20.4	8.8		
USNM	368489		19.9	18.7			
USNM	532869		21.2	20.4	8.6		
USNM	532870		20.4	19.7	8.3		
USNM	532871		18.1	17.2	7.3		
USNM	532874		17	16.6	7.4		
USNM	532876		20.4	18.8			
USNM	532878		22.1	21.4	8.5		
USNM	532879		22.6	21.8			
USNM	532880		21.7	20.6	9		
USNM	532881		18.7	17.7			
USNM	532882		20.5	20			
USNM	532884		21.3	20.6	8.3		
USNM	532885		21.5	21.3	9.4		
USNM	532886		21.4	20.2	8.5		
USNM	532887		21.9	21.1	8.9		
USNM	532889		19.8	19			
USNM	532890		20.6	19.9	8.6		
USNM	532892		19.5	18.3			
USNM	532893		20.5	20.3			
USNM	532896		20.7	20.3	8.8		
USNM	532897		21.8	21.5	9.4		
USNM	532898		19.5	18.9			
USNM	532899		21.3	20.2			
USNM	532900		17.3	17.1	7		
USNM	532901		20	18.6			
USNM	532902		18.5	18			
USNM	532903		20.7	20			
USNM	532904		23.2	23.2			
USNM	532905		17.2	16.4			
USNM	532906		19.4	18.6			
USNM	532907		19.9	19.1			
USNM	532908		16.6	16.2	6.5		

MUSEUM	SPEC. #	glH	bpH	dpH	scH	bdH	ddH
USNM	532909		18.1	17.5			
USNM	532912		17.9	17			
USNM	532913		19.4	18.4			
USNM	532917		16.2	15.7			
USNM	532919		16.2	16.3			
USNM	532920		15.5	13.8			
USNM	532921		16.4	15.9			
USNM	532922		16.4	16			
USNM	532923		17	16.9			
USNM	366262		19.4	18.9			
USNM	178084		17.3	16.8			
USNM	275852		18.6	18.1	7.6		
USNM	275865		22	21.1			
USNM	366755		20.4	18.3			
USNM	366998		20.7	20			
USNM	367049		24.4	23.6			
USNM	533145		18.8	19	7.4		
USNM	533146		22.3	21.1			
USNM	533147		22.8	22.6			
USNM	533148		21.1	20.5			
USNM	533149		17.4	16.8			
USNM	533150		21.3	20.6			
USNM	533151		22	21.3			
USNM	533152		20.9	20.6			
USNM	533153		14.7	14.2			
USNM	533125					13.7	9.5
USNM	533126					15.6	10.9
USNM	533127				8.6	13.5	9.7
USNM	533128					14.9	10.5
USNM	533129				8.5	13.9	9.8
USNM	533130				9.1	14.9	10.4
USNM	533131				8.8	15.4	10.8
USNM	533132				9.3	15.8	11
USNM	533133				9	15.1	10.7
USNM	533134				7.9	14.9	10.4
USNM	533135				8	13.6	9.3
USNM	533136				6.2	10.5	7.6
USNM	533137				6.2	11.3	7.9
USNM	533138				7.1	12.5	9
USNM	533139				4.5	8.5	6.3
USNM	533140				7.2	12	8.5

MUSEUM	SPEC. #	glH	bpH	dpH	scH	bdH	ddH
USNM	533143				7.4	11.9	8.3
USNM	177892					15.6	11.2
USNM	177956				8.2	13.4	9.7
USNM	177957				7	13.3	9
USNM	177961				8.1	14.5	10.1
USNM	177973				7.9	13.5	9.8
USNM	177977				7.9	13.7	9.6
USNM	177990				8.2	13.8	9.6
USNM	177994				8.7	15.1	10.4
USNM	178008				7.7	13.6	9.2
USNM	178029				7.7	12.7	9.1
USNM	178150				8.2	14.7	10.6
USNM	178166				8.6	14.9	10.6
USNM	181046				8.3	14.1	10.1
USNM	181054				8.8	14.3	10.1
USNM	180181					13.5	9.5
USNM	183454				8.1	13.7	9.7
USNM	183455				8.7	13.9	9.7
USNM	183456				7.9	14	9.5
USNM	183461				7.8	13.4	9.1
USNM	183495				8	13.8	9.5
USNM	192108				7.8	11.8	8.3
USNM	192502				8	13.4	9.7
USNM	192657				8.4	14	9.8
USNM	192669				8.3	15.2	9.9
USNM	192719				8.5	13.6	9.5
USNM	192761				7.4	13.3	9.5
USNM	192807				7.8	13.2	9
USNM	192808				8	13.9	9.9
USNM	192917				8.4	13	9.5
USNM	192918				8.2	13.8	10.1
USNM	192931					15.2	10.4
USNM	192933				8.8	14.2	10
USNM	192941				8.9	15.2	10.6
USNM	192973					15.8	11
USNM	193025				7.3	10.8	7.4
USNM	242283				8.3	13.1	9
USNM	242284					14	9.8
USNM	242297				8.8	14.3	10.1
USNM	242349				8.8	14.3	10
USNM	248502				8.7	13.6	9.3



MUSEUM	SPEC. #	glH	bpH	dpH	scH	bdH	ddH
USNM	248543				8.8	13.6	9.9
USNM	248550				8.2	14.5	10.1
USNM	248554				6.5	11.1	7.9
USNM	250819				8.1	13.4	9.4
USNM	250832				8.1	14.5	9.8
USNM	250847				8.8	15.3	10.7
USNM	250855				6.9	11.1	7.8
USNM	252393				8.1	13.9	9.6
USNM	252394				7.7	13.1	8.8
USNM	256217				6.5	11.2	8
USNM	256232					13.1	9.2
USNM	257479				6.4	11	7.9
USNM	257484				7.8	13.2	9.4
USNM	257516				7.7	13.5	9.4
USNM	275776				8.4	14.2	10.2
USNM	302331				8.7	13.8	10
USNM	302387					15.1	10.7
USNM	302394				5.9	10.8	7.7
USNM	308203				7.2	11.6	8.1
USNM	308214				9.3	16	11.2
USNM	308231				8.8	14.7	10.1
USNM	321262				8	13.7	9.7
USNM	321263				7.4	12.2	8.4
USNM	321309				8.1	13.2	9.4
USNM	193104				7.3	13.5	9.6
USNM	193119				8.5	12.8	9.3
USNM	193263				7.7	13.8	9.9
USNM	193300				8.4	13.7	9.9
USNM	193385					15.8	11
USNM	206336				8.7	15.1	10.5
USNM	206339				6.4	12	8.1
USNM	206441				8.4	14	9.4
USNM	206602				8.1	13.9	10
USNM	206622				8	14.5	10.6
USNM	210428				8.3	14.1	9.7
USNM	210502				7.9	13.4	9.8
USNM	215458				9	15.1	10.6
USNM	215477				6.1	10.4	7.5
USNM	215564				9	14.6	10.1
USNM	215733				8.6	14.2	10
USNM	215813				8.5	13.9	10

MUSEUM	SPEC. #	glH	bpH	dpH	scH	bdH	ddH
USNM	215820				9.6	15.3	10.5
USNM	215857				8.4	14.3	10.2
USNM	215903				8.6	13.5	9.7
USNM	215838				6.5	11	8
USNM	236815				8.3	14	9.9
USNM	241362				8.5	14.6	10.1
USNM	366553				8.7	15	10.4
USNM	366590				9.1	15.1	10.4
USNM	366591				8	14.4	10.3
USNM	366639				8.9	15.4	10.8
USNM	366821				9.6	16	11.4
USNM	366822				8	12.4	8.5
USNM	366854				8.7	14.4	10.1
USNM	366863				9.1	15	10.8
USNM	366864				7.9	14	9.6
USNM	366930				8.3	15.1	10.5
USNM	366974				6.4	11.3	7.8
USNM	367003				9	15.1	10.6
USNM	367119				8.9	15.1	10.8
USNM	367172				8.6	14.7	10.3
USNM	368504				7.8	12.9	9.1
USNM	368506				8.3	14	9.7
USNM	368507				9.6	16.2	11.6
USNM	368509				9.1	14.9	10.5
USNM	532924				8.6	15.8	11.2
USNM	532925				9.8	16.3	11
USNM	532927				7.3	13.1	9.2
USNM	532928				7.3	13.5	9.5
USNM	532929				8.7	14.5	9.8
USNM	532931					15.1	10.5
USNM	532932				8.8	14.5	10.5
USNM	532934				7.6	13.8	9.9
USNM	532936				7.4	12.8	9.3
USNM	532937				7.1	12.5	8.5
USNM	532938				8	14.3	9.8
USNM	532939				9.2	14.6	10.3
USNM	532940				8.5	15.2	10.6
USNM	532942				6.8	11.4	7.6
USNM	532943				7.6	13.8	9.4
USNM	532944				8.2	15	10.6
USNM	532945				9	15.6	11

MUSEUM	SPEC. #	glH	bpH	dpH	scH	bdH	ddH
USNM	532946				8.5	14.9	10.3
USNM	532947				9	15.7	11.1
USNM	532948				7.3	13.3	9.4
USNM	532950					13.8	9.6
USNM	532951				8.6	14.5	9.9
USNM	532953				7.7	14.6	10.8
USNM	532956				8.7	15.6	11.1
USNM	532957				8.5	13.7	10
USNM	532960				8.4	14.9	10.4
USNM	532961				8.4	13.9	9.5
USNM	532963				8.2	13.8	9.6
USNM	532964				8.2	14.3	10.1
USNM	532966				8	13.1	9.3
USNM	532967					12.6	8.7
USNM	532968				6.2	11.8	8.4
USNM	532969				11.3	16.6	10.8
USNM	532970				9.6	16.9	12.1
USNM	532971				8.8	15.1	10.6
USNM	532972				5	9.3	6.5
USNM	532973					12.9	8.9
USNM	532974				6.9	11.8	8.3
USNM	532975				5.7	10.1	6.8
USNM	532976				7.1	11.8	7.9
USNM	193066				6.1	10.9	7.7
USNM	178021				6.8	11	8
USNM	179223				8.6	14.2	10.1
USNM	179217				8.9	14.5	10.1
USNM	179224				8.5	14.7	10.5
USNM	177998				9.1	15.1	10.9
USNM	178003				8.4	13.7	9.1
USNM	178024					13.9	9.9
USNM	179213					14.6	10.1
USNM	179221				8.7	13.8	9.8
USNM	179284				7	11.6	8
USNM	179287				7.9	13.2	9.1
USNM	179294				7.8	13.3	9.5
USNM	179308				8.5	14	10.1
USNM	181033				9	14.2	10.7
USNM	181066				7.9	12.9	9
USNM	181107				8.3	13.7	9.5
USNM	183450				8.1	13.7	9.6

MUSEUM	SPEC. #	glH	bpH	dpH	scH	bdH	ddH
USNM	192521				8.3	13.6	9.8
USNM	192528				6.9	11.7	9
USNM	192546					12.3	8.7
USNM	192556				8.6	14	10.5
USNM	192628				8.6	14.5	10.7
USNM	192780				8.6	13.8	10.2
USNM	215768				8	13.7	10
USNM	236809					13.8	9.7
USNM	236863					14.3	10.1
USNM	241404					12.2	8.7
USNM	241432					15.8	11.7
USNM	242163				8.7	13.9	9.7
USNM	242188					13	9.1
USNM	242190				9.2	15	10.5
USNM	242218				8.4	14.2	10
USNM	242289				7.7	13.9	9.9
USNM	242293				8.6	13.8	9.7
USNM	248568					13.4	9.6
USNM	250684				8	14.5	10
USNM	250835				9.7	16.1	11.5
USNM	252365				8.5	14.6	10.4
USNM	252375				8.2	13.9	9.6
USNM	252399				8.1	13.7	9.7
USNM	252443				9.5	14.8	10.3
USNM	256213				8.8	14.7	10.4
USNM	256218				8.3	15.5	11.4
USNM	256239				7.7	12	8.7
USNM	257467					13.8	9.4
USNM	257470				9.3	15.4	10.8
USNM	257527				8.4	14.7	10.4
USNM	192815				7.7	13.2	9.4
USNM	192963				8.5	14.1	10
USNM	193042				8.6	14.5	10.3
USNM	193093					11.7	8.7
USNM	193106				8.2	13.5	9.4
USNM	193108				8.9	14.7	10.6
USNM	193139				8.2	14	9.9
USNM	193143				8.9	14.2	10
USNM	193280				8.9	14.9	10.6
USNM	193434				7.3	13.4	10
USNM	193435					14.4	10.3

MUSEUM	SPEC. #	glH	bpH	dpH	scH	bdH	ddH
USNM	206316				8.8	13.4	9.5
USNM	206400				6.7	11.7	8
USNM	206409					13.9	9.7
USNM	206456				8	13.7	9.6
USNM	206505				8.9	15	10.9
USNM	206507				8.7	13.9	10.1
USNM	206519				8	13.3	9.6
USNM	206522				8.3	14.4	10.3
USNM	206530				7.9	13.9	9.9
USNM	206580					14.2	10.2
USNM	206601				8.7	14.5	10
USNM	206624				8.8	14.3	10.2
USNM	210445					14.8	10.4
USNM	210486				8.9	15	10.5
USNM	210490				8.5	14.4	9.9
USNM	210518				8.5	15.3	10.7
USNM	215427				7.3	12.3	
USNM	215464				8.3	14	10
USNM	215495				9.1	15.8	11.1
USNM	215545				8.3	13.9	9.9
USNM	215630				8.7	15.1	10.8
USNM	215639					14.1	9.7
USNM	215654				8.1	14.2	10.2
USNM	215671				8.7	14.1	9.8
USNM	299636				8	14.8	10.5
USNM	302302				8.5	15.1	11.1
USNM	306264				7.3	13.3	9.3
USNM	302343				6.5	11.5	
USNM	302412				6.4	11.5	8.1
USNM	306307				7.1	12.7	8.9
USNM	321298				8.6	14.9	10.1
USNM	366232				5.5	9	6.3
USNM	366574				7.7	12.8	9.8
USNM	366641				7	12.3	8.5
USNM	366710				9.2	15.3	11
USNM	366738				7.2	12.6	9
USNM	366739				7.8	13.8	9.8
USNM	366828				8.5	14.4	10.2
USNM	366842				8.6	15.4	11
USNM	366853				9.1	16.2	11.4
USNM	366899				8.5	14.7	10.9

MUSEUM	SPEC. #	glH	bpH	dpH	scH	bdH	ddH
USNM	367046				8.5	14.6	10.4
USNM	368500				7.7	13.6	9.9
USNM	532977				9.1	14.8	10.1
USNM	532978				8.1	15.4	11
USNM	532979				9.8	15.3	10.9
USNM	532980				7.3	13.2	9.6
USNM	532981				8.6	14.5	10.2
USNM	532983				8.9	15.1	10.6
USNM	532984				8.5	13.7	9.9
USNM	532985				7.8	13.4	9.1
USNM	532986				6.9	12.5	9
USNM	532988				8.8	15.1	10.8
USNM	532989					14.8	10.6
USNM	532990				8.2	13.5	9.8
USNM	532991				8.5	15	11.2
USNM	532994				8.4	15.2	10.9
USNM	532996				8.9	15.8	11.8
USNM	532997				7.8	13.9	9.7
USNM	532998				7.7	13.1	9.1
USNM	533000				7.6	13.4	9.5
USNM	533002				6.8	11.2	7.8
USNM	533003				7.3	12.4	8.5
USNM	533004				8.6	15.2	11.1
USNM	533005				8.8	15.3	11.7
USNM	533006				8.5	14.9	10.5
USNM	533007				7	12.2	8.7
USNM	533008				7.7	13.6	9.8
USNM	533009				6.3	11.6	8
USNM	533010				7.4	13	9.3
USNM	533012					14.4	10.3
USNM	533013				8.2	14	9.8
USNM	533014				6.4	11.5	8.4
USNM	533015				8.4	14.2	10.3
USNM	533016				7.6	13.1	9.2
USNM	533017				8.5	14.7	10.7
USNM	533018				7.9	13.6	9.6
USNM	533019				7.7	13.9	10
USNM	533020				7.8	14.1	10.3
USNM	533021				8.1	14	10.1
USNM	533022				8.5	14.1	9.9
USNM	533023				8.5	15.5	11.3

MUSEUM	SPEC. #	glH	bpH	dpH	scH	bdH	ddH
USNM	533024				7.2	12.1	8.4
USNM	533025					13.6	9.6
USNM	533026				8.1	13.4	9.3
USNM	533027				8	14.5	10.3
USNM	533028				8.6	15.1	10.6
USNM	533029					15.5	10.3
USNM	192477				6.4	10.6	7.4
USNM	192472				5.8	11.2	7.8
USNM	181117				6.1	11	7.8
USNM	193180				7.2	12.9	8.9
USNM	533031				6.3	9.9	7.6
USNM	533033				6.4	12	8.5
USNM	533034				6.3	11.9	8.6
USNM	533035				6.4	12.4	8.7
USNM	366558	102.4	20.9		8.3	14.7	10.5
USNM	446656	83.5	16.8	16.2	6.9	12	8.7
USNM	366386	101.1			8.7	15.2	10.6
USNM	533036	99.4	22	20.8	9.1	15.1	10.8
USNM	533037	96.9	20.6	19.6	8.1	14.6	10.5
USNM	533038	101.1	21.8	21	8.7	15.4	10.7
USNM	533039	100	21.7		8.5	15	10.7
USNM	533040	86.7	19.3	18.4	7.5	13.3	8.8
USNM	533041	74.5	16	15.6	6.9	10.9	8
USNM	533042	71.2	14.7	14.2	6.4	9.8	7.8
USNM	533043		22.9	21.8	9		
USNM	533044		12.5	12.1			
USNM	533045		21.4	20.2			
USNM	533046		22.6	21.7			
USNM	533047		20.6	19.6			
USNM	533048		17.6	15.9			
USNM	533049		17.1	16.1			
USNM	533050				7.6	14	9.8
USNM	533051				8.4	15.6	10.5
USNM	533052				9.1	14.6	10.2
USNM	533053				7.6	13.7	10.1
USNM	533054				7.2	12	8.6
USNM	533156				8.8	15.2	10.8
USNM	533157				7.4	15.5	10.3
USNM	533158				8.6	14.6	10.3
USNM	533160				7.6	11.6	8.5
USNM	533161				7.7	12.5	8.9

MUSEUM	SPEC. #	glH	bpH	dpH	scH	bdH	ddH
USNM	533162					15.7	11.5
USNM	533163				7.3	13.5	9.4
USNM	533164				6.8	12.4	8.9
USNM	533165				8.5	14.4	10.2
USNM	533166				8.9	14.7	10.6
USNM	533167				8.5	15.2	11
USNM	533168				8.1	15	10.5
USNM	533169				7	11.6	8.2
USNM	533170				8.8	15.1	11.2
USNM	533171				7.1	13.2	9
USNM	533172				9.2	15.2	10.8
USNM	533172				6.4	10.9	7.9
USNM	533055		24.2	23			
USNM	533056		21.4	20.6			
IGF	14875				7.5	12.4	9.1
USNM	215443	88.8	19.1	18.8	8.4	14	9.8
USNM	368479	82.7	17.1	16.2	7.3	12.3	8.7
USNM	179220	84.4	19.1	17.9	7.9	12.4	9.1
USNM	275870	78.7	16.2	15.3	6.6	11.5	8.4
USNM	366571	86.4			7.3	11.9	9.2
USNM	181038	82.2	17.7	15.4	6.7	12.1	8.6
USNM	495672	85.3			7.8	13	8.8
USNM	366584	81.7			7.5	12.8	8.9
USNM	183425	87.8	19.9	18.5	8	13.9	9.8
USNM	368480	87.5	18.2	17.1	7.1	12.9	9.4
USNM	495671	89.7	19.5	19.3	8.3	13.8	9.9
USNM	446685	86	19.7	18.4	7.7	13	9.6
USNM	446661	82.2	18.9		6.8	12.7	9.2
USNM	446698	78.1	16.4		6.8		
USNM	446670	78.6	17.3	16.6	7.2	12	8.3
USNM	495670	81.2	17.3	16.7	7	11.4	8.4
USNM	256354				7	11.1	8.3
USNM	256361				9.1	13.6	10.5
USNM	256356					10.9	8
USNM	256360		18.7	17.5			
USNM	256357		16.6	14.9			
USNM	256355		15.2	14.9	6.5		
USNM	256359		15.4	14.9			
USNM	256358		15.6	14.9	6		
USNM	447052		16.2	15.7	6.8		
USNM	447054		16.1	15.7	6.5		



MUSEUM	SPEC. #	glH	bpH	dpH	scH	bdH	ddH
USNM	256421		15.8	14.9			
USNM	447055					11.2	7.7
USNM	532557				7	11.8	8.6
USNM	532559				7.5	13.6	9.7
USNM	192101	21.6	21	8.9			
USNM	192101				14.9	10.5	
USNM	495616	97.9	20.4		8.8	14.3	10.3
USNM	495614	20.5	20.8	8.8			
USNM	459609			8.5	15	10.3	
USNM	495624						
USNM	454590	104	22.8	21.7	8.8	15.4	11
USNM	454590			8.9	15.2	11.2	
USNM	336379	8.8		8.8	14.1	10.3	
USNM	236802	95.8	20.7	19.7	8.8	14	10.1
USNM	236802	94.9			8.6	14	10.1
USNM	215454			8.4	13.9	9.7	
USNM	495613	103.4	21.9		8.9	15.1	11
USNM	495612	21.4	20.9	8.6	14.2	10.2	
USNM	495612	21.3	20.9				
USNM	237212		21.7	21.1			
USNM	183510		19.8	18.6	9		
USNM	237248		22.1	20.1	9.1		
USNM	237158				5.4	8.8	6.4
USNM	237264		16.9	15	6.2		
USNM	446650	112	24.2	22.4	10	16.8	12.2
USNM	299643		25.3	24.4			
USNM	299637				10.6	16.7	11.7
USNM	460811				9.9	16.3	11.6
USNM	210532				6	10.5	7.5
USNM	321314	76	16		6.7	11.2	8.2
USNM	446653	75.2			6.7		8.1
USNM	446657	74	15.2	14.2	6.2	10.6	7.6
USNM	446658	80.9			6.8		8.1
USNM	446686	75.7	15.6	14.1	7.3	11.5	8
USNM	446691	76.9	16	15.5	6.7	11.1	8
USNM	495589	79	17.2	13.6	7.3		
USNM	495668	76.6			6.6		8.2
USNM	257519	77.6			6.7	10	7.2
USNM	495592	65.4			5.8	8.8	6.6
USNM	250772				5.7	9.6	6.7
USNM	495591				5.8	9.1	6.4

MUSEUM	SPEC. #	glH	bpH	dpH	scH	bdH	ddH
ANSP	13357	96.2	19.7	18.8	8.2	13.9	9.4
NCSM	13734	102.4	20.8	21	9.2	14.9	10.4
NCSM	7677		16.2				
NCSM	7980		21.7				
NCSM	7982				9	15.2	10.7
NCSM	8102	93.9	21	18.9	8.5	13.8	9.8
NCSM	8180					12	
NCSM	8583					11.7	
NCSM	8599		19				
NCSM	8600					12.9	8.7
NCSM	8609					13.4	9.2
NCSM	8612					13.5	
NCSM	8864					13.3	9.2
NCSM	8868					12.9	
NCSM	8872		16.6				
NCSM	8874		18.8				
NCSM	8878					11.9	8.3
NCSM	8879					13.3	
NCSM	8882					13.9	9.5
NCSM	8883		21.1				
NCSM	8885					12	
NCSM	8886					13.7	9.5
NCSM	8906					11.6	8.4
NCSM	12990					10.5	7.4
NCSM	12991		18.7				
NCSM	12992					13.7	
NCSM	13001				7.2	12.5	9
NCSM	13002					12.7	8.8
NCSM	13147					12.8	
NCSM	13211		20.1				
NCSM	13216					12	
NCSM	13232					9	
NCSM	13254					14.5	
NCSM	13257					11.4	8.2
NCSM	13327					11.2	
NCSM	13332		17.7				
NCSM	13582					15.3	11.1
NCSM	13734	102.4	20.8	21	9.2	14.9	10.4
NCSM	13771					14.6	10.4
NCSM	13773					9	
NCSM	13862					12.3	

MUSEUM	SPEC. #	glH	bpH	dpH	scH	bdH	ddH
NCSM	14107		17.6				
NCSM	14108		20.1				
NCSM	14113					10.2	
NCSM	14116				8.1	12.8	9.2
NCSM	15064	97.8	8.5		14.4	10.2	19.5
NCSM	15543		18.5				
NCSM	16585		20.1				
NCSM	17914		19.8				
NCSM	18240					9.7	
NCSM	18954		23.1				
NCSM	18955		16				
NCSM	18956					11.8	8.3
NCSM	18957					10.4	7.4
NCSM	18985					13.4	
NCSM	20322		16.5				
NCSM	21470					12.5	
NCSM	18987-1					11.6	
UF/PB	7948				6.5	11.9	8.3
UF/PB	7949				6.6	10.9	7.7
UF/PB	7989				6.5	11.3	7.8
UF/PB	7942		15.3	15.2	6.9		
UF/PB	7945				7.3	13.1	9
UF/PB	7947				6	11.1	7.8
UF/PB	7752		19.3	18.7	8.2		
UF/PB	91				6.5	11.7	8.3
UF/PB	304				6.2	11.4	8.1
UF/PB	305				7	11.6	7.9
UF	21148		15.7	15.2			
UF	61953		17	16.3	6.6		
UF	61539		17.6	16.9	7		
UF	61531		18.2	16.1	7.7		
UF	21193		19.9	19.2			
UF	21031		16.3	15	7.2		
UF	61995				7	12	8.1
UF	58456				6.7	11.8	8.3
UF	61542				6.6	11.2	8.2
UF	61541				7.2	11.7	8.2
UF	61537		16.1	15.4	5.7		
UF	57254				5.9	11.2	7.8
UF	12473		15.8	15.2	6.3		
UF	12474		15.8	14.3	7.1		

MUSEUM	SPEC. #	glH	bpH	dpH	scH	bdH	ddH
UF	21064		16.5	15.4			
UF	21069		16	14.9	6.8		
UF	21074		16	14.8	7.2		
UF	61533				9	14.4	10
UF	58379				7.4	14	
UF	67956				8.8	13.8	9.6
UF	123804					15.1	10.3
UF	12477				7.5	13.7	9.5
UF	21191		16.5	15	6.9		
UF	21032				5.9	11	7.8
UF	21038				6.7	11.5	7.9
UF	21078				7	12.2	8.8
UF	21114				7.7	13.3	8.6
UF	208612		16.6	16	7.1		
UF	95473		14.9	14.9	6.7		
UF	125027				6.5	10.8	7.7
UF	123805				7.1	11.9	8.8
UF	117423				6.5	10.5	7.4
UF	49094				8.4	13.7	9.4
UF	49095		15.7	14.6	6.2		
UF	117492		16.9	15.5	6.6		
UF	211946				6.3	10.7	8
UF	208384				8.6	13.7	9.9
UF	21145				6.5	11.6	7.9
UF	61954				6.3	11.3	8
UF	21107		15.7	14.7	6.7		
GCVP	5691	99.6	20	19.5	8.5	14.8	10.4
GCVP	5690					13.7	10
BMNH	7052	111.2	22.8	21.8	8.9	15.5	12.1
BMNH	7053		~25.6		10.6		
BMNH	7055				9	13.9	10.4
BMNH	7054				7.8	14.1	11.3
BMNH	9030		13.9	13.3			
BMNH	9029		17.8	16.2	7.1		
NCSM	24366	104.3	23.2	23	8.8	16.2	11.6
USNM	555666	79.9	16.7	16.7	7.4	11.2	7.9
USNM	502378	76.3	16.8	15.2	7.2	11.2	8.1
USNM	502387	77	16.3	15.6	7.1	11.3	8.3
USNM	502389	82.8	16.9	16	7	11	7.8
USNM	18062	77.2	16.2	16.5	7	11.1	8
USNM	502388	77.1	15.9	15.1	6.7	11.2	8.1

MUSEUM	SPEC. #	glH	bpH	dpH	scH	bdH	ddH
USNM	502382	77.6	16.4	15.7	7	11.3	8.1
USNM	501644	81.3	17.6	16.5	7.3	11.8	8.4
NCSM	20058	80.9	16.5	15.6	6.9	11.5	8.1
NCSM	20502	78.9	16.2	15.4	7.4	11	7.8
USNM	347946	81.7	16.3	16.1	7.2	11.7	8.6
USNM	502549	75.9	15.5	14.9	6.7	10.9	7.8
USNM	555668	72.9	15.6	14.7	6.6	10.6	7.7
USNM	495584				5.9	8.3	5.7
USNM	302324	63.7	13.7		5.7	8.4	5.9
USNM	495600				5.8	9.3	7.3
USNM	242178				5.9	9.5	7
USNM	215499				5.7	9.1	6.4
USNM	192879		13.8	13	5.4		
USNM	430948				5.7	8.4	6.6
USNM	178015		13.2	12.1			
USNM	192691				5.4		
USNM	242316				5.1	8.4	6.6
USNM	192698				5.5		

## APPENDIX 6C.

### *ALCA* ULNAE MEASUREMENT DATA

Measurements of *Alca* fossil specimens (in mm). Blank cells denote measurements missing due to damage. All measurements according to Von den Driesch (1976). Abbreviations: gdbU, greatest distal breadth of ulna; gpwU, greatest proximal width of ulna; glU, greatest length of ulna; bpU, breadth of proximal ulna; ddU, distal diagonal of ulna; scU, greatest width of ulnar shaft at midpoint.

MUSEUM	SPEC. #	glU	gpwU	bpU	scU	gdbU	ddU
USNM	366294	78	15.3	12.1	7.1	10.5	7.7
USNM	366944	83.3	15.9	11.9	7	10.8	8.1
USNM	446555	85.3	14.5	11.5	6.8	10.5	8.2
USNM	446558	81.5	15.4	12.2	6.9	11	8.2
USNM	446651	79	15.5	11.4	6.9	9.6	7.7
USNM	446562	79.5	15.4	11.9	6.6	10.4	7.7
USNM	446566	81.6	15.8	12	6.8	10.8	8.2
USNM	446567	77.8	15.2	11.7	7	10.6	7.9
USNM	446571	80.8	15.6	12.2	7	10.9	8.1
USNM	446580	82.1	16.4	12.2	7	10.7	7.9
USNM	446582	81.2	14.3	11.2	6.4	9.9	7.5
USNM	446609	87	15.9	11.8	7.4	10.7	7.8
USNM	446614	79.5	15.7	11.9	7.1	10.6	8.3
USNM	446630	73.6	13.1	10.3	6.3	9	6.3
USNM	446629	87.2	15.3	12.3	7.3	11.1	9
USNM	446632	78.3	14.3	11	6.2	10	7.7
USNM	446643	79.2	15.3	11.8	6.5	10.2	8.1
USNM	446645	79.1	15	11.1	6.6	9.8	7.1
USNM	495618	89.3	16.9	12.9	7.8	11.4	8.7
USNM	533175		12.3	9.2	5.8		
USNM	533176		12.5	9.4	6		
USNM	533178		15.1	11.8			
USNM	533179		14.3	10.8	6.5		
USNM	533180		16.1	12.7	7.5		
USNM	533181		17.6	13.2			
USNM	533182		15.7	12.1	7.7		
USNM	533183		16.1	11.9	8.2		
USNM	533184		15.4	12.2	7.7		
USNM	533185		16.5	12.8	7.7		
USNM	533186		14.8	11.4	7.5		

MUSEUM	SPEC. #	glU	gpwU	bpU	scU	gdbU	ddU
USNM	533188		12.8	9.8	6.1		
USNM	533189		11	8.1	5.5		
USNM	533190		15.1	11.7			
USNM	533191		13.6	10.7			
USNM	533192		13.2	10.4			
USNM	533193		15.7	12.4	7.1		
USNM	533194		16.6	12.3	8		
USNM	533195		16.9	12.7	7.9		
USNM	533196		17.3	13.2			
USNM	533197		13.7	10	6.3		
USNM	533198		13.2	10.3	6.6		
USNM	366949		14.3	11.1	6.7		
USNM	178081		14.5	11.7	7		
USNM	178096		13.9	11.2	6.8		
USNM	178097		15.5	11.6	7.4		
USNM	178206		15.1	11.3	7.5		
USNM	177834		14.8	10.6			
USNM	177835		15.2	11.5	7.3		
USNM	177842		15.1	11.1	7		
USNM	177844		15.1	11.5			
USNM	177848		15.9	11.8	7.3		
USNM	178156		15	11.3	7.2		
USNM	178195		15.3	11.3			
USNM	179306		15.2	11.3	7		
USNM	181061		15.4	11.5	7.3		
USNM	192461		14.5	10.9	6.9		
USNM	192516		15.9	12.3	7.6		
USNM	192621		14.4	11.6	7		
USNM	192630		14.3	11.1	7.3		
USNM	192906		11.7	9.5	6		
USNM	192923		14.4	11.6	6.7		
USNM	192946		16.1	11.8	7.4		
USNM	193090		13	10.1	6.8		
USNM	193103		15.4	11.5	7		
USNM	193125		14.5	11.3			
USNM	193213		15.2	12.2	7.4		
USNM	193329		14	11.1			
USNM	206343		14.1	11.1			
USNM	206474		14.5	11.5	6.7		

MUSEUM	SPEC. #	glU	gpwU	bpU	scU	gdbU	ddU
USNM	215618		15.2	11.3	7.3		
USNM	215632		15	12	7.3		
USNM	215821		13.6	11.2			
USNM	236842		14.3	11.4	7.7		
USNM	241371		14.5	11.1			
USNM	241360		16	11.8			
USNM	241373		14.1	11.6	6.8		
USNM	241405		13.1	9.8	6.4		
USNM	242208		13.7	10.8			
USNM	242301		15.3	11.7	7.2		
USNM	242305		15.6	11.3			
USNM	242367		14.3	10.9			
USNM	248551		14.1	11.5	7.1		
USNM	250788		14.6	11.5	7.1		
USNM	252328		15.9	12.2	7.5		
USNM	252333		10.6	8.7	5		
USNM	256256		16.1	12.6	8		
USNM	257508		14.2	11.1			
USNM	302379		15.4	11.4			
USNM	306244		16.5	12.8	7.7		
USNM	366555		14	10.6	6.3		
USNM	366691		16	12			
USNM	366747		14.1	11.2	6.7		
USNM	366749		10.7	7.8	4.8		
USNM	366750		15.1	12.2	7.6		
USNM	366775		14.2	11.1	7.1		
USNM	366838		14.4	10.3			
USNM	366868		13.4	10.7			
USNM	367079		14.6	11.5			
USNM	177836		15.5	11.6	6.5		
USNM	177838		11.7	8.8			
USNM	177845		13.9	11.2			
USNM	177847		15.1	11.3			
USNM	177866		15.7	11.7	7.1		
USNM	178117		15.3	11.3	7		
USNM	178164		15.8	12.3	6.8		
USNM	181036		14.6	11.4	7.1		
USNM	181041		14	11.4	6.8		
USNM	181071		14.4	11.4	6.6		



MUSEUM	SPEC. #	glU	gpwU	bpU	scU	gdbU	ddU
USNM	192444		15.2	11.4	6.7		
USNM	192495		15.1	11	6.5		
USNM	192639		15	11.4			
USNM	192998		15.8	12.1	7.5		
USNM	193065		14.2	10.7			
USNM	193097		15.7	11.5			
USNM	193271		14.5	11.3	7		
USNM	193328		14.7	10.6	6.6		
USNM	193332		13.6	10.9	7.2		
USNM	206380		14.6	11	6.6		
USNM	206453		14.7	10.9	7.2		
USNM	206549		14.7	11.3	7.4		
USNM	210455		13.7	10.3	6.9		
USNM	215428		14.8	11.7	7.2		
USNM	215494		14.9	11.8			
USNM	215839		14.7	10.9			
USNM	236813		15.7	11.9	7.6		
USNM	236839		14.4	10.7	7		
USNM	250675		15.4	11.6	7		
USNM	252329		14.9	11.2	7.3		
USNM	252336		15.8	12.3	7.1		
USNM	302348		15.8	12.7	7.3		
USNM	306308		11.9	9			
USNM	306245		14.3	11.3	6.9		
USNM	306265		15	11.4	7.1		
USNM	306330		15.6	11.9			
USNM	308209		14.2	10.7			
USNM	366568		15.3	12.2	7.7		
USNM	366699		10.5	8	4.8		
USNM	366776		11.4	8.4	5		
USNM	367018		16.3	12.6			
USNM	178130				6.6	10.1	7.6
USNM	178167				7	10.2	7.5
USNM	179236				6.7	9.9	7
USNM	179278				6.7	10	7.4
USNM	192658				7.2	9.9	7.4
USNM	192637					9.7	7.4
USNM	192697					10.1	7.5
USNM	192758				7.2	10.1	7.2
USNM	192778				6.6	10.1	7.9

MUSEUM	SPEC. #	glU	gpwU	bpU	scU	gdbU	ddU
USNM	192806				6.6	9.2	7.2
USNM	192870				5.8	9	6.4
USNM	192896				6.2	9.3	6.9
USNM	193053				6.1	9.9	7.3
USNM	193179				6.7	9.6	7.2
USNM	193207				7.1	9.3	6.9
USNM	193215				7.1	9.9	7.3
USNM	193221				7.1	9.9	7.6
USNM	193294				6.5	9.8	7.4
USNM	193337					11.2	8.7
USNM	193357				5.4	8	6
USNM	193363				7.1	10.2	7.4
USNM	193382				7.5	10.8	8.1
USNM	206300				6.9	9.4	7.4
USNM	206467					10.7	8.2
USNM	206553				7.1	10.2	7.6
USNM	206633				7.3	10.1	7.6
USNM	210427					10.6	8
USNM	210434				6.8	9.9	7.5
USNM	210436				6.8	9.5	7
USNM	215042					9.5	7.5
USNM	215604				6.4	9.6	7.7
USNM	215694				6.9	9.8	7.3
USNM	236849				7.4	10.5	7.5
USNM	236859				7.1	10.5	7.6
USNM	241359				7.2	9.6	7.7
USNM	242189				7.2	9.8	7.6
USNM	242217				7.4	10.2	7.7
USNM	242328				7.3	11.1	8.4
USNM	248509				4.6	7.9	5.4
USNM	248553				5.5	8	5.6
USNM	248591				6.2	9.2	7
USNM	2506955				7.2	10.2	7.6
USNM	250727				5	7.8	5.8
USNM	252343				6	9.4	7
USNM	257448				6.7	10.1	7.7
USNM	257449					9.7	7.3
USNM	256259				6.6	10.4	7.5
USNM	302307				7.3	10.7	8.3
USNM	302351				7.8	10.5	7.9
USNM	302393				4.5	7.4	5.5

MUSEUM	SPEC. #	glU	gpwU	bpU	scU	gdbU	ddU
USNM	306257				7.4	10.6	8.2
USNM	308160				7.8	11.5	8.8
USNM	321251				5	7.9	6
USNM	321295				6.2	9.9	7.2
USNM	321296				7.9	11.5	8.7
USNM	321299				7.6	10.8	7.8
USNM	366235				5.4	8.2	6.3
USNM	366569				7.9	13.2	9.6
USNM	366778				7.9	12.2	9.2
USNM	366938					10	7.8
USNM	367090				7.4	11	8
USNM	366278				7.2	10.4	7.5
USNM	177868				7.1	9.7	7.2
USNM	192475				5.9	9.2	6.8
USNM	192539				6.2	9.4	6.5
USNM	192855				6.4	9.4	7.1
USNM	192050				6.8	9.6	6.9
USNM	533199				5.2	7.8	6.4
USNM	533200				6.4	10.5	7.8
USNM	533201				7.2	11.4	8.6
USNM	533202				6.8	10.9	8.1
USNM	533203				6.9	9.7	7.6
USNM	533204				6	9.1	7.2
USNM	533206				7	10.3	7.6
USNM	533207				7.4	11.1	8.2
USNM	533208				7.2	10.7	8.2
USNM	533209				7.1	10.9	8.1
USNM	533210				7.5	11.3	8.4
USNM	533212				5.4	7.6	5.8
USNM	533213				7.6	10.4	7.3
USNM	533214				6.8	10.2	7.8
USNM	533215				7.5	10.6	8.3
USNM	533216				7.2	10.9	8.2
USNM	533217				6.9	10.4	7.8
USNM	533218				8.1	11.4	8.8
USNM	533219				6.2	9.3	7.1
USNM	533220				6.5	10.1	7.3
USNM	533221				7.8	11.8	8.9
USNM	533222				7.5	11.3	8.4
USNM	533223				7.7	11.2	8.5
USNM	533224				7.7	11.2	7.7

MUSEUM	SPEC. #	glU	gpwU	bpU	scU	gdbU	ddU
USNM	533225				7.3	10.1	7.8
USNM	533226				6.7	10.9	7.9
USNM	533227				5.4	8.4	6.1
USNM	177937					10.2	7.6
USNM	179302				7.5	10.3	8
USNM	192606				7.4	10.5	8
USNM	192626					10.7	8.1
USNM	192810				8.4	11.3	8.5
USNM	533228		15.5	11.8			
USNM	533229		16.1	11.3			
USNM	533230		15.8	11.8	7.2		
USNM	533232		15.2	11.2	7.2		
USNM	533233		14.2	11	6.5		
USNM	533234		16.1	12.2			
USNM	533235		16.8	13			
USNM	533236		12.9	9.9	6.2		
USNM	533237		13.5	10	6.3		
USNM	533238		16.4	12.6			
USNM	533239		14.9	11			
USNM	533240		14.7	10.7	7.3		
USNM	533241		13	9.9			
USNM	533242		14.9	11.1			
USNM	533243		17.5	13.6			
USNM	533244		15.2	11.8	6.8		
USNM	533245		16.1	11.9			
USNM	533246		12.5	9.5	6.2		
USNM	533247		11.2	9.2			
USNM	533248				6.8	10.6	7.7
USNM	533249				7.5	10.4	8
USNM	533251				7.4	10.6	7.8
USNM	533252				6.9	10.8	7.7
USNM	533253				8.3	12.3	8.9
USNM	533254				8.3	12.4	9.3
USNM	533255				6.9	10.8	8.2
USNM	533257				6.8	10.7	8
USNM	533258				7.7	11.4	8.6
USNM	533259				7.5	10.3	7.7
USNM	533260					10.4	8.1
USNM	533261					10.6	7.5
USNM	533262				6.2	9.6	7.1
USNM	533263				7.9	10.9	8.5

MUSEUM	SPEC. #	glU	gpwU	bpU	scU	gdbU	ddU
USNM	533264				7	10.9	8.4
USNM	533265				7	9.7	7.3
USNM	533266				4.8	8.1	5.8
USNM	177862				6.5	9.7	7.4
USNM	177864				7.6	10.8	8.4
USNM	177870					10.3	7.5
USNM	188871				5.7	8.6	6.7
USNM	177872				7	10.2	7.1
USNM	177874				6.7	10.3	7.7
USNM	178093				7.2	10.3	7.7
USNM	192057				6	9.5	7
USNM	192523				6.7	8.7	6.1
USNM	192600				7.1	9.9	7.3
USNM	192631				7.7	11.1	8.4
USNM	193071				5.6	8.3	6.3
USNM	193117				7.8	12	8.5
USNM	193324				6.1	10.5	7.7
USNM	193339				6.4	9.8	7.6
USNM	193344				6.6	9.7	7.3
USNM	210534					10.3	7.5
USNM	210539				7	9.7	7.4
USNM	215498				6.7	10.6	7.9
USNM	215692					10.1	7.8
USNM	215916				7.3	10.8	8.1
USNM	241357				7.5	10.5	7.9
USNM	241378				6.5	9.7	7.2
USNM	241399				6.5	9.6	7.1
USNM	250730				5.9	10.2	7.4
USNM	250822				5.7	8.7	6.5
USNM	252349				7.2	10.7	8
USNM	275820				5.7	8.9	6.7
USNM	308163				7.9	11.9	8.9
USNM	321293				7.6	11.4	8.4
USNM	366005				6.5	8.9	6
USNM	366746				7.3	10.4	7.9
USNM	367083				7.6	11.1	8.5
USNM	181089	59.9	10.9	8.1	5.1	7.8	5.8
USNM	302366	64.6	11.7	9	5.6	8.3	6.4
USNM	177885	58.7	10.6	8.3	5.1	7.7	5.5
USNM	275788	63.7			5.6	7.6	6.2
USNM	308218	68.9	13.6	10.7	7.1	9.1	6.9

MUSEUM	SPEC. #	glU	gpwU	bpU	scU	gdbU	ddU
USNM	446587	80	14.8	11.5	7	9.8	7.9
USNM	446590	76.5	15.4	11.8	7.5	10.6	7.6
USNM	446642	72.1	12.6	10.4	6.6	9.3	7.2
USNM	446628	79.4	14.8	11.4	6.9	10.1	7.3
USNM	446616	71	13.9	10.1	6.6	9	6.6
USNM	446636	77.5	14.6	11.7	7.1	10.6	7.2
USNM	446633	71.7	13.4	10.5	6.5	9.2	6.7
USNM	446608	76	14	11.4	6.7	9.7	7.4
USNM	446625	70.3	12.6	9.6	6.1	8.8	6.5
USNM	446634	75.8	14.2	11.4	6.6	10.1	7.6
USNM	446594	78.8	15	12	6.9	10.1	7.4
USNM	446624	66.1	13.2	10.5	6.4	8.8	6.7
USNM	446601	69.5	12.1	10.2	6	8.9	6.6
USNM	366718	70	13	9.5	5.5	8.4	6.5
USNM	448906	63.1			6.1	8.3	6.4
USNM	448911	61.2	10.7	9.3	5.9	8.4	6.3
USNM	446592	78	14.5	10.8	7.1	9.5	
USNM	446598	72.3			6.4	9	7.1
USNM	446550	77.8	15.2	11.7	7.2	10.8	7.8
USNM	446551	68.4	12.9	9.6	6.2	8.9	6.9
USNM	533269	61.9	12.4	9.5	6	8.1	6.1
USNM	192902	72.6	13.6	10.8	6.8	8.7	6.3
USNM	215695	72.9	14.4	11	6.5	9.1	6.8
USNM	183497	73.1	15	11.2	7.3	9.7	6.4
USNM	308229	74	14.7	10.8	7.1		
USNM	368511	75.6			6.7	9.1	6.6
USNM	241376	74.7	15.1	11.9	7	10.4	8.1
USNM	193157	72.3	14.7	11.5	8	9.5	7.3
USNM	193094	75.6	14.2	11.6	7.3	9.7	7.2
USNM	177841	73.2	13.9	11	7.1	10.2	7.2
USNM	533267	72.4	14.2	10.4	6	8.9	6.9
USNM	533268	65.8	122.5	8.9	6.2	7.9	6.1
USNM	256258	73.3	13.7	10.8	7.2	9.9	7
USNM	250780	74	13.8	10.7	6.8	9.1	7.1
USNM	446604	81.8	15.2	12.2	7.6	10.7	8
USNM	446605	67.6			6.7	9.8	7.3
USNM	446641	79.3	15.3	12.1	7.6	11.1	8
USNM	446638	75	14.7	10.6	6.7	10.1	7.8
USNM	446639	78.5	16.5	12.5	8	10.9	8
USNM	446635	79.1	15.4	11.5	7.7	10.4	7.8
USNM	446613	81.5	14.6	11.5	7.4	10.8	7.9

MUSEUM	SPEC. #	glU	gpwU	bpU	scU	gdbU	ddU
USNM	336181	85.4	15.8	12.2	8	10.8	8.4
USNM	446611	73.9	14.5	11.4	6.7	10	7.4
USNM	446612	70.6	14.7	10.8	7	10	7.7
USNM	257504	79.2	16.1	12.1	7.1	10.5	7.8
USNM	193110	75.3	14.2	11.2	6.9	9.8	7.9
USNM	366308	82.2	15.1	12.2	7.8		
USNM	533271	80.7	15	11.4	7.5	10.7	7.7
USNM	193362	78.9	14.2	11.1	6.5	9.6	7.3
USNM	192737	79.5	15	11.4	7.3	9.8	7.9
USNM	250703	80.1	14.2	12	7	10.4	7.5
USNM	366647	80.9	14.7	12.5	7.8	10.8	8.3
USNM	181028	77.4	15.7	11.8	7.9	10.8	7.7
USNM	252448	75.5	14.6	11.5	7.5	9.6	7.1
USNM	302375	80.7	14.4	11.5	7.4	10.7	7.9
USNM	366598	78.3	14.5	11.3	7	10.5	8
USNM	366742	87.3	15.5	11.8	7.6	10.9	7.8
USNM	366984	85.5	15.6	12.1	7.7	11.2	8.5
USNM	446570	90.1	16.3	12.9	8	11.5	8.3
USNM	446584	88.5	16.9	13.2	8.1	11.7	9.1
USNM	446565	87.8	16.1	12.8	8.1	11.1	8.4
USNM	446572	82.4	15.4	12.5	7.5	11.2	8.3
USNM	446554	80.8	14.8	10.8	7	10	7.5
USNM	446586	79.4	14	10.7	7.2	9.9	7.3
USNM	446575	81.6	15.7	12.3	7.4	10.7	7.9
USNM	446579	72.3	14	10.7	6.4	8.9	6.9
USNM	533272	86.7	15.8	12.1	8	11.2	8.1
USNM	533273	79	15.2	11	8.1	10.6	7.8
USNM	533274	75.9	13.9	10.8	6.7	9.7	7.1
USNM	533275	66.4	13.2	10.3	6.3	9.2	7.2
USNM	533276	64	12.6	9.6	6.3	8.7	6.5
USNM	533277	81	16.4	12.4	7.8	11.7	8.4
USNM	533278	88.7	16	12.2	7.7	11.2	8.5
USNM	533280	85.1	16.4	12.7	7.5	11	8.2
USNM	533281	80.4	15.8	12.8	7.8	10.7	7.8
USNM	533282	68.4	12.9	9.5	6.1	8.7	6.2
USNM	533283	72.3	14.1	10.4	6.5	9.6	7.1
USNM	533284	82.8	16.1	12.3	8.2	11.3	8.1
USNM	533285	69.6	13.8	11	7.1	10	7.7
USNM	533286	79.2	15	12	7.1	10.1	7.9
USNM	533287	81.1	14.6	10.9	7.4	10.7	7.7
USNM	533288	74	13.5	11.3	6.2	10.3	7.4

MUSEUM	SPEC. #	glU	gpwU	bpU	scU	gdbU	ddU
USNM	533289	82.6	14.4	12	7.2	10.1	7.1
USNM	533290	78.2	14.9	11.7	6.8	14.8	11.6
USNM	533291		15.4	11.7			
USNM	533292		13.2	10.5	5.9		
USNM	533293		14.6	10.9	7.1		
USNM	533294		14.1	10.4	6.2		
USNM	533295		14	10.4	6.5		
USNM	533296		14.7	11.1	7.3		
USNM	533297		15.5	11.4			
USNM	533298		16	12.3	7.7		
USNM	533300		15.5	12.2			
USNM	533301		14.1	10.8	6.5		
USNM	533302		15.4	12			
USNM	533303		16.3	12.3	7.9		
USNM	533304				6	8	6.3
USNM	533305				7.8	11.5	8.3
USNM	533306				7.1	10.4	7.8
USNM	533307				5.6	9.2	6.9
USNM	533308				8	11	8.6
USNM	306340	91.5	16.4	11.4	8	11.7	9.1
USNM	181090		19.2	12.4			
USNM	321314	62.1	11.9	9.1	5.1	8	5.7
USNM	193184	59.2	10.8	8.5	5.4	6.9	5.3
USNM	215809	55.1	11.1	8.4	4.8	7.7	5.9
USNM	448898	61	11.3	9.5	5.8		
USNM	448904	68.9	12.1	9.3	5.5	6.9	5.5
USNM	448908	68.1	11.4	9.4	5.4	8.2	6.1
USNM	448909	59.1	11.8	9.5	5.5	8.1	6.3
USNM	368515	59.9	12.4	9.1	5.7	7.3	5.7
USNM	446644	64.1	12.3	10	5.7	8.4	6
USNM	495594				5.5	8.1	5.2
USNM	252435	13.5	8.6				
USNM	215791			8.7	9.6	6.9	
USNM	215792	14.2	9.2				
USNM	192101			7.6	10.6	8	
USNM	192101			7.6	10.6	8	
USNM	495616	79.9	14.2	11.5	6.9	10.3	7.6
USNM	454590	87.5	16.4	11.1	7	11.1	8.7
USNM	367907			7	10.7	8.1	
USNM	336380	83.5	16.2	8.6	7.4	10.7	8.5
USNM	336379	71.9	15.3	9.7	7.2	10.1	



MUSEUM	SPEC. #	glU	gpwU	bpU	scU	gdbU	ddU
USNM	495613	84.4	16.3	11.1	7	10.9	8.5
USNM	495612			7.3	11.1	8.2	
USNM	495612	13.9	10.5				
USNM	237270	55.5	10.4	8.3	4.7	7.5	5.7
USNM	242238	93.2	18.2	13.6	8	12.6	9.8
USNM	321314	62.1	11.9	9.1	5.1	8	5.7

## APPENDIX 6D.

### *ALCA* CARPOMETACARPI MEASUREMENT DATA

Measurements of *Alca* fossil specimens (in mm). Blank cells denote measurements missing due to damage. All measurements according to Von den Driesch (1976). Abbreviations: glC, greatest length of carpometacarpus; bpC, breadth of proximal carpometacarpus; ddH, distal diagonal of carpometacarpus; Lmc1, length of the first metacarpal.

MUSEUM	SPEC. #	SIDE	<u>glC</u>	<u>lmc1</u>	<u>bpC</u>	<u>ddC</u>
USNM	419708	R				7.5
USNM	214920	L		8.5	13	
USNM	192101	L				8.7
USNM	336379	R				9.2
USNM	495612	L	54.1	9.6	10.6	
USNM	446520	L	57.6	10.1	10.9	10
USNM	446525	R	57.5	10.3	10.5	8
USNM	446528	R	57.8	10.2	10.7	8
USNM	367107	R		7	7.8	
USNM	178072	R	43	7.7	7.9	7.1
USNM	368532	R	39.4	6.8	8.1	7
USNM	193292	R	36.7	6.7	7.7	6
USNM	495593	R	36.8	7	7.7	
USNM	183421	R		7.1	7.3	
USNM	215836	L		7.8	7.5	
USNM	177782	R	52.2	9.7	10.2	7.8
USNM	177785	R	50.8	9.4	9.4	8.2
USNM	181097	R	50.1	8.9	10.2	7.4
USNM	192020	R	49.9	10.1	9.6	6.7
USNM	192448	R	51	9.5	9.5	7
USNM	236803	R	51.5	10.1	10.1	6.8
USNM	308157	R	50.1	9.5	9.3	6
USNM	308219	R	54.9	9.8	9	7.5
USNM	178106	L	51.3	9.1	9.7	7.3
USNM	178172	L	54.2	11.3	10.9	7.4
USNM	183447	L	52	10.3	9.9	7.5
USNM	275875	L	53	9.8	10.4	7.6
USNM	302371	L	49.3	8.8	9.6	6.2
USNM	366428	L	54.7	10.4	10.3	7.5
USNM	366622	L	52.1	9.1	9.2	7.5

MUSEUM	SPEC. #	SIDE	<u>glC</u>	<u>lmc1</u>	<u>bpC</u>	<u>ddC</u>
USNM	275872	L	51.8	9.3	10.1	6.9
USNM	446509	R	55.8	9.4	10	
USNM	446510	R	46.3	8.4	8.6	7.2
USNM	446511	R	54.8	9.7	10.1	7.9
USNM	446512	R	51.8	9.7	9.9	8
USNM	446513	R	55.2	9.1	9.9	7.7
USNM	446514	R	52	10	10.2	
USNM	446515	R	51.6	9.2	9.8	7.6
USNM	446516	R	46.9	7.8	9	6.8
USNM	446519	R	52.4	8.6	9.6	7.3
USNM	446521	R	53.8	9.1	11.1	7.8
USNM	446522	R	54.8	9.8		6.8
USNM	446523	R	56.5	11.4	10.8	7.4
USNM	446535	R	46.3	7.9	9.3	6.6
USNM	532560	R	48.4	7.9	9.6	6.5
USNM	532561	R	53.1	9.8	10.1	7.6
USNM	532562	R	56.4	10	10.4	6.5
USNM	532565	R	54.4	10.1	9.8	7.6
USNM	532564	R	53	9.7	9.9	7.8
USNM	446526	L	50.9	10.2	9.3	6.9
USNM	446527	L	53.6	10	10.7	7.5
USNM	446532	L	54.9	9.8	10.3	7.9
USNM	446533	L	54.4	9.2	9.9	6.8
USNM	446538	L	48.9	8.4	9.8	6.8
USNM	446530	L	51.2	9.9	9.5	6.9
USNM	446539	L	52.4	9.8	9.7	7.6
USNM	446540	L	52.8	10.1	9.8	7
USNM	446541	L	48.9	8.6	9.4	6.1
USNM	446542	L	49.7	9.4	9.8	6.6
USNM	446543	L	52.7	9.4	10.8	7.1
USNM	446544	L	51.5	8.8	9.9	7.1
USNM	532563	L	51.9	9.3	11.3	7.7
USNM	532566	L	48.9	8.2	9	6.9
USNM	178108	R		10.6	9.2	
USNM	193044	R		8.8	9.1	
USNM	181100	R		10	9.5	
USNM	178087	R		9.6	9.7	
USNM	179280	R		9.4	9.1	
USNM	248499	R		8.8	9.6	
USNM	181058	R		9.8	8.5	
USNM	248584	R		8.8	10	
USNM	206406	R		8.5	9.4	

MUSEUM	SPEC. #	SIDE	glC	lmc1	bpC	ddC
USNM	210523	R		8.7	9	
USNM	366455	R		8.6	9.3	
USNM	210495	R		10.3	9.9	
USNM	215457	R		9.8	9.4	
USNM	206616	R		11.2	10	
USNM	215667	R		9.2	9.4	
USNM	275818	R		9.5	10.4	
USNM	306306	L		10	9.1	
USNM	215859	L		11.1	9.2	
USNM	366784	L		9.4	9	
USNM	215587	L		9.4	8.7	
USNM	215470	L		8.8	9	
USNM	210499	L		10	9.5	
USNM	368531	L		9.7	9.8	
USNM	256221	L		9.4	10.2	
USNM	366942	L		8.3	9.5	
USNM	242354	L		9.9	10	
USNM	241382	L		10.4	9.1	
USNM	215485	L		10.9	9.1	
USNM	252439	L		9.4	9.9	
USNM	236887	L		9.4	9.5	
USNM	242209	L		7.3	9.7	
USNM	178107	L		10.1	8.9	
USNM	193021	L		10.1	9.1	
USNM	192992	L		10.7	9.2	
USNM	193079	L		9.7	8.9	
USNM	193315	L		8.6	9.2	
USNM	179290	L		9.5	9.4	
USNM	192028	L		9.8	9	
USNM	178125	L		9	9.3	
USNM	193010	R				6.5
USNM	206488	R				6.7
USNM	206342	R				7.3
USNM	215853	R				7.7
USNM	366673	R				6.9
USNM	193167	L				7.3
USNM	210528	L				6.6
USNM	210533	L				6.6
USNM	192514	L				6.5
USNM	250711	L				7.7

USNM	210453	L				7
MUSEUM	SPEC. #	SIDE	<u>glC</u>	<u>lmc1</u>	<u>bpC</u>	<u>ddC</u>
USNM	193049	L				7.7
USNM	250794	L				7
USNM	206590	L				7.3
USNM	532682	R	52.1	9.7	9.8	7.2
USNM	532683	L	49.2	8.8	9.2	6
USNM	532684	L	49.9	8.2	8.1	
USNM	532694	L	53.3	9.5	9.3	7
USNM	532695	L	53.1	9.5	10.4	7.5

## APPENDIX 6E.

### *ALCA* CORACOID MEASUREMENT DATA

Measurements of *Alca* fossil specimens (in mm). Blank cells denote measurements missing due to damage. All measurements according to Von den Driesch (1976). Abbreviations: glC, greatest length of coracoid; bbC, basal breadth of coracoid; mlC, medial length of coracoid; bfC, breadth of sternal facet of coracoid.

MUSEUM	SPEC. #	glC	mlC	bbC	bfC
USNM	193349	44.4			18.6
USNM	206492	46.5	44.4	22.5	18.3
USNM	206515	43	41.3		16.6
USNM	250790	43.2			18.9
USNM	252288	46.8	45.7		19.1
USNM	366366	45.5	43.9		20.3
USNM	366367	49.5	47.6	23.7	19.8
USNM	366999	47.9	45.6	22.2	19
USNM	367008	43.5	44.4		17.6
USNM	367109	43.5			18.6
USNM	177764	47.9			20.9
USNM	181092	47.6	45.7		18.5
USNM	183473	45	44.4		18.4
USNM	206532	44.6	43.7		18.7
USNM	241366	47.2	46.3		18.6
USNM	248540	48.6	46.7		22.1
USNM	488862	50.5	49.4		21.7
USNM	448824	42.9	42.3		18.3
USNM	448825	38.1	36.7		16.4
USNM	448826	47.9	44.6		20.3
USNM	448827	38.4	37.6		15.3
USNM	448828	48.7	45.5		19.7
USNM	448829	48.7	46.9	21	18.7
USNM	448830	45.8	43.5		20.5
USNM	448831	38.9	36.8		14
USNM	448832	37	36.5		14.6
USNM	448834	47.7	46.4	20.4	18.6
USNM	448836	48.4	45.9	23	20.9
USNM	448837	45.2	44.2		19
USNM	448839	47.3	45.7		18.3

MUSEUM	SPEC. #	glC	mlC	bbC	bfc
USNM	448842	47.4	46.1	19.5	18.2
USNM	448845	47.2	47.3	21.4	19.9
USNM	448846	37.4	35.5	16.3	14.4
USNM	448848	45.9	44.7		20.5
USNM	448849	41.4			15.7
USNM	448851	49.5	46.2		19.7
USNM	448852	38.6			13.1
USNM	448853	34.2	33.1		13
USNM	448854	46.3	45		19.8
USNM	448856	46.5	45	20.8	19
USNM	448857	34.6			14
USNM	448858	42.6	40.6		17.7
USNM	448860	49.9	46.5		20.1
USNM	448861	45.1	42.8	18.9	17.1
USNM	448863	47.7			19.6
USNM	448864	42.4	41.9	18.8	17.4
USNM	448865	40.7	40.1	18.4	17.4
USNM	448866	34.7	33.9		13.3
USNM	448867	43.8	43.7	19.6	18.2
USNM	448869	46.9	45.8	22.2	18.8
USNM	448870	47.7	46.1	21.5	19.8
USNM	448871	46.6	45.5	21.4	19.3
USNM	448872	44.7	42.1		17
USNM	448873	43.8			17.3
USNM	448874	39.8	37.3		15.8
USNM	448876	40.6	39.2		16.1
USNM	448878	43.7	40.9		18.5
USNM	448879	48.8	47.5		20.6
USNM	448882	38.7			15.1
USNM	448883	44.3	43.7		18.2
USNM	448884	38.2			15
USNM	448885	44.8	43.8		18.4
USNM	448886	41.2			14.9
USNM	448888	41.1	39.6		16.6
USNM	448889	41.7	39.4		16.7
USNM	448890	44	41.5		18.2
USNM	448891	42.6	41.1		18.3
USNM	448892	41.6	40.2	20.6	17.2
USNM	448893	47.7	46.2	22.9	19.2
USNM	448894	50.5	47.8	26.7	21
USNM	448895	48.1	46.9	22.2	20.2



MUSEUM	SPEC. #	<u>glC</u>	<u>mlC</u>	<u>bbC</u>	<u>bfC</u>
USNM	448896	47.2			18.8
USNM	177766	44.5	42.8		18.9
USNM	192675	44.6	42.4		18.9
USNM	206521	44.8			18.8
USNM	367117	48.3	46.7		17.6
USNM	368527	47.5	45.3		19.6
USNM	179251	49.7	47.8	22.3	20.3
USNM	532650	43.4	42.9		17.9
USNM	532651	47.7	45.7		19.4
USNM	532652	45.8	45	22.8	19.9
USNM	532653	44.5	43.6		18.3
USNM	532654	47.5			20.2
USNM	532655	50.7	48.9		20
USNM	532656	42.5	41.2		17.5
USNM	532657	48.6	46.2		20.3
USNM	532658	40.7	38.6		15.5
USNM	532659	38.7	37.3	15.5	11.5
USNM	532660	43.2			15.4
USNM	532663	48.4	46.4		19.6
USNM	532664	50.6			21.1
USNM	532665	39.2	38		15.2
USNM	532666	40.4	37.2		15.4
USNM	532667	43.6	42.5	18.9	16.3
USNM	532668	45.9	43.6		19.4
USNM	532669	43.2	42.8	20	18
USNM	532670	43.3	42.4	22.3	17.2
USNM	532672	46.5	45.9		18.7
USNM	532673	50.4	48.8		19.8
USNM	532674	43.6			17.9
USNM	532675	48.3	46.6		21.8
USNM	532688	46.7	44.8	25.4	19.8
USNM	532691	46.4	45	20.6	18
USNM	495620	55.1	53.8		23.2
USNM	308210	53.1	49.9		21.2
USNM	308221	52.9	50.6		21.4
USNM	177758	38.4	37.3		14.5
USNM	495629	32.1	31		11.5
USNM	495628	36.2	35	17	14.7
USNM	321264	35.5	33.5		14
USNM	495626	38			15.2
USNM	181070	36.7	35.8		15.3

---



MUSEUM	SPEC. #	glC	mlC	bbC	bfC
USNM	419708				16.8
USNM	495610	42.5	41.3		15.7
USNM	459609	47.3	46.1	23	19.8
USNM	495624	48.2			19.3
USNM	454590	48.5	46.8		20.3
USNM	215454	46	43.6		17.9
USNM	242238	57.1	53.4	26.5	23.2

## APPENDIX 7.

### A CRITIQUE OF PREVIOUSLY APPLIED CHARADRIIFORM FOSSIL CALIBRATIONS

The fossil calibration used by Baker et al. (2007) to date the *Larus-Rissa* split at 15.9 Ma is listed as 4 spp. of *Larus* and corresponds in Brodkorb (1967) to *Larus elegans*, *Larus totanoides*, and *Larus desnoyersii* from the Early Miocene of France and *Larus pristinus* from the early Miocene of Oregon. *Larus elegans*, *Larus totanoides*, and *Larus desnoyersii* were described by Milne-Edwards (1863, 1867-1871) based on isolated and fragmentary remains. The holotype specimen of *Larus pristinus* Shufeldt, 1915 (Yale Peabody Museum 935) is an isolated proximal tibiotarsus. In addition to the fact that these taxa may or may not be coeval, the referral of *Larus desnoyersii* and *Larus pristinus* to Laridae was questioned on the basis of osteological characteristics (Olson, 1985). Although the systematic position of *Larus elegans* and *Larus totanoides* has not been previously questioned, the age of these species is estimated at somewhere between 20-23Ma (Aquatanian; Gradstein et al., 2004) based on biostratigraphic correlations with other Miocene deposits in Europe (Hugueney et al., 2003).

The fossil calibration used to date the split between *Uria* and *Alca* + *Alle* by Baker et al. (2007) is listed as *Uria antiqua*. The name of this taxon was changed to *Alca antiqua* by Olson and Rasmussen (2001) to reflect its affinities with that clade, and subsequently amended to *Alca grandis* by Olson (2007) because the name *Alca antiqua* was unavailable according to the International Code of Zoological Nomenclature (ICZN, 2000). Although the holotype specimen of *Alca grandis* cannot be definitively assigned an age because its exact provenience is not known, the age of *Alca grandis* is now

considered to be Early Pliocene (~4.4 Ma) rather than middle Miocene (11.6 Ma) based on the abundant remains of this taxon from the Pliocene Yorktown Formation of Beaufort County, North Carolina (Olson and Rasmussen, 2001).

*Brachyramphus pliocenium* Howard, 1949 was used by Baker et al. (2007) to date the split between *Brachyramphus* and the remainder of Alcinae. Remains of this taxon are known from Middle Pliocene sediments of the San Diego Formation of southern California. The fossil bearing units in this formation, from which remains of this taxon were recovered, have been assigned an age of ~3.6 Ma (Wagner et al., 2001).

The fossil calibration used to date the *Aethia-Ptychoramphus* split by Baker et al. (2007) is the enigmatic alcid fossil taxon *Ptychoramphus tenuis* Miller and Bowman, 1958. The holotype specimen of this taxon (UCMP 45562) is a single weathered tarsometatarsus from the Middle to Late Pliocene San Diego Formation that does not retain sufficient characteristics to confidently assign it to *Ptychoramphus* (see Chapter 5). As the name "*tenuis*" suggests, the systematic position of this fossil is doubtful, and it is therefore inappropriate as a fossil calibration.

The fossil calibration used to date the *Cerorhinca-Fratercula* split by Baker et al. (2007) is another poorly known fossil taxon, *Cerorhinca dubia* Miller, 1925. The holotype specimen of this taxon (UCMP 26546) consists of impressions of leg bones (femur, tibiotarsus, tarsometatarsus, and pedal phalanges) from the Middle to late Miocene diatomite deposits exposed at Lompoc, California. The original diagnosis of this taxon (Miller, 1925) was based primarily on the ratio of limb bones, as the specimen does not preserve sufficient diagnostic features to place it systematically (see Chapter 4). As

the name "*dubia*" suggests, the systematic position of this fossil is doubtful, and it is therefore inappropriate as a fossil calibration.

The fossil calibration used to date the *Calidris-Aphriza* split by Baker et al. (2007) is constrained by the fossil species *Calidris pacis*, and was assigned an age of 3.6 Ma. The early Pliocene section of the Bone Valley Formation in which *Calidris pacis* was discovered has been assigned an age of ~4.5Ma (Dodd and Morgan, 1992).

The fossil calibrations for nodes H, J, and K of Baker et al. (2007), *Limosa gypsum*, *Charadrius sheppardianus*, and *Vanellus selysii* respectively, are all taxa of uncertain phylogenetic affinity (i.e., Aves incertae sedis; Olson, 1985) and are therefore inappropriate for use as fossil calibrations. Furthermore, Baker et al. (2007) purport to use *Limosa gypsum* to date the split between *Limosa* and *Prosobonia*; however, molecular sequences for *Prosobonia* are not listed by Baker et al. (2007; supplementary table 1) and are not available from GenBank as of this writing.

*Numenius antiquus* was used to date the split between *Numenius* and *Bartramia* by Baker et al. (2007) and was assigned an age of 11.6 Ma. The middle Miocene deposits have been assigned to magnetopolarity zone MN6, which corresponds with an age of 14.3-16 Ma (Sen and Ginsburg, 2000).

Baker et al. (2007) used specimens referred to the Late Cretaceous to Early Paleocene taxon *Paleotringa* to date the minimum age of the Lari-Scolopaci split. Specimens referred to *Paleotringa* include isolated partial tibiotarsi, tarsometatarsi, and humeri (Brodkorb, 1967) and do not preserve any apomorphies that would allow their referral to Charadriiformes (Hope, 2002). Accordingly the use of *Paleotringa* to date the

divergence of Charadriiformes from its nearest sister group, or to date the split between scolopacid and larid lineages is inadvisable.

The list of fossil taxa used to constrain the age of the split of Charadriiformes from its nearest outgroup by Baker et al. (2007) includes three species of *Paleotringa* (addressed above), three species of *Cimolopteryx*, and *Ceramornis major* from the Late Cretaceous or Early Paleocene. *Ceramornis* is considered to be Neornithes incertae sedis (Hope, 2002), and is therefore inappropriate for use as a charadriiform fossil calibration. The systematic position of *Cimolopteryx* within Charadriiformes is by no means certain (Hope, 2002). Accordingly, *Cimolopteryx* should not be used as a calibration point to date the basal divergence among charadriiforms.

Although fossils of Turnipacidae Mayr, 2000 (i.e., stem buttonquail) are known from the Early Oligocene (~32 Ma) of France and Germany (Mayr, 2000; Mayr and Knopf, 2007), these fossils were not used by Baker et al. to date the minimum time of divergence between Turnicidae and other charadriiforms. The systematic placement of *Turnix* remains an issue of contention (Baker et al., 2007; Hackett et al., 2008; Livezey, 2009, 2010). *Turnix* was not included in the combined analysis and Turnipacidae fossils were not used as calibrations in the divergence time analysis because of the unusually long branch-lengths associated with this taxon in the results of previous analyses (Baker et al., 2007; Hackett et al., 2008; Livezey, 2009, 2010) and the potential for extremely long branch lengths to effect the estimation of rates of nucleotide change, and associated estimates of phylogeny and node ages (Rambaut and Bromham, 1998; Thorne and Kishino, 2002; Yang and Rannala, 2005).

## APPENDIX 8.

### PHYLOGENETIC CLASSIFICATION OF PAN-ALCIDAE

In compliance with the International Code of Phylogenetic Nomenclature (Cantino and de Queiroz, 2010) the following clade names (annotated [P]) and phylogenetic definitions are proposed (Reference cladogram Fig. 8.8).

**Pan-Alcidae [P] *nomen cladi novum*.** Definition: The most inclusive clade containing the internal specifier *Alca torda* Linnaeus 1758 but not *Stercorarius longicaudus* Vieillot 1819 or *Larus marinus* Linnaeus 1758. This branch-based definition is adopted so that pan-alcids recovered outside of the crown clade (e.g., *Bisulca demerei*) and potential discoveries of stem alcids (i.e., pan-alcids) will not require alteration of the definition of the clade Pan-Alcidae. Although the monophyly of Pan-Alcidae is strongly supported, the sister taxon of Pan-Alcidae is an issue of contention (Pereira and Baker, 2008; Chu et al., 2009). Accordingly, *Stercorarius longicaudus* and *Larus marinus* are both specified as outgroup taxa to maintain stability of this clade definition of Pan-Alcidae. The current contents of this clade at the species-level include:

*Aethia cristatella* (Pallas, 1769)

*Aethia psittacula* (Pallas, 1769)

*Aethia pusilla* (Pallas, 1811)

*Aethia pygmaea* (Gmelin, 1789)

*Aethia barnesi* Smith, 2011 †  
*Aethia rossmoori* Howard, 1968 †  
*Aethia storeri* Smith, 2011 †  
*Brachyramphus brevirostris* (Vigors, 1829)  
*Brachyramphus dunkeli* Chandler, 1990 †  
*Brachyramphus marmoratus* (Gmelin, 1789)  
*Brachyramphus perdix* (Pallas, 1811)  
*Brachyramphus pliocenium* Howard, 1949 †  
*Alca ausonia* (Portis, 1888) †  
*Alca carolinensis* Smith and Clarke, 2011 †  
*Alca grandis* (Marsh, 1870) †  
*Alca minor* Smith and Clarke, 2011 †  
*Alca olsoni* Smith and Clarke, 2011 †  
*Alca stewarti* Martin et al., 2001 †  
*Alca torda* Linnaeus, 1758  
*Alcodes ulnulus* Howard, 1968 † (Pan-Alcidae *insertae sedis*)  
*Alle alle* (Linnaeus, 1758)  
*Cepphus carbo* Pallas, 1811  
*Cepphus columba* Pallas, 1811  
*Cepphus grylle* (Linnaeus, 1758)  
*Cepphus olsoni* Howard, 1982 †  
*Cerorhinca auroreensis* Smith, 2011 †  
*Cerorhinca minor* Howard, 1971 †

*Cerorhinca monocerata* Pallas, 1811  
*Cerorhinca reai* Chandler, 1990 †  
*Fratercula arctica* Linnaeus, 1758  
*Fratercula cirrhata* (Pallas, 1769)  
*Fratercula corniculata* (Naumann, 1821)  
*Fratercula dowi* Guthrie et al., 1999 †  
*Mancalla californiensis* Lucas, 1901 †  
*Mancalla cedrosensis* Howard, 1971 †  
*Mancalla diegensis* (Miller, 1937) † (Pan-Alcidae *insertae sedis*)  
*Mancalla emlongi* Olson, 1981 † (Mancallinae *insertae sedis*)  
*Mancalla milleri* Howard, 1970 † (Pan-Alcidae *insertae sedis*)  
*Mancalla lucasi* Smith, 2011 †  
*Mancalla vegrandis* Smith, 2011 †  
*Miomancalla howardi* Smith, 2011 †  
*Miomancalla wetmorei* (Howard, 1976) †  
*Miocepphus blowi* Wijnker and Olson, 2009 †  
*Miocepphus bohaski* Wijnker and Olson, 2009 †  
*Miocepphus mcclungi* Wetmore, 1940 †  
*Miocepphus mergulellus* Wijnker and Olson, 2009 †  
*Pinguinus alfrednewtoni* Olson, 1977 †  
*Pinguinus impennis* (Linnaeus, 1758) †  
*Praemancalla lagunensis* Howard, 1966 † (Mancallinae *insertae sedis*)



*Pseudocepheus teres* Wijnker and Olson, 2009 †

*Ptychoramphus aleuticus* (Pallas, 1811)

*Synthliboramphus antiquus* (Gmelin, 1789)

*Synthliboramphus craveri* (Salvadori, 1867)

*Synthliboramphus hypoleucus* (Xántus de Vesey, 1860)

*Synthliboramphus wumizusume* (Temminck, 1835)

*Synthliboramphus rineyi* Chandler, 1990

*Uria aalge* Pontoppidan, 1763

*Uria affinis* Marsh, 1872 †

*Uria brodkorbi* Howard, 1981 †

*Uria lomvia* (Linnaeus, 1758)

*Uria paleohesperis* Howard, 1982 †

**Alcidae [P] *converted clade name*.** Alcidae (ex Alcadae Leach, 1820) is converted to a node-based name (de Queiroz and Gauthier, 1992) that refers to the alcid crown-clade.

Clade Alcidae is defined as the most recent common ancestor of internal specifiers *Alca torda* Linnaeus, 1758 and *Fratercula arctica* Linnaeus, 1758 and all of its descendants.

The contents of this clade are consistent with the Linnaean Family Alcidae (*sensu* American Ornithologists' Union, 1998).

**Alcinae [P] *converted clade name*.** Alcinæ (Bonaparte, 1831) is converted to a node-based name (de Queiroz and Gauthier, 1992) that refers to the most inclusive clade containing the internal specifier *Alca torda* Linnaeus, 1758 but not *Fratercula arctica*

Linnaeus, 1758. (i.e., contents = *Alca* Linnaeus, 1758, *Pinguinus* Bonaterre, 1790, *Uria* Brisson, 1760, *Alle* Link, 1806, *Brachyramphus* Brandt, 1837, *Cepphus* Moehring, 1758, and *Synthliboramphus* Brandt, 1837). The contents of this clade are consistent with the Linnaean subfamily Alcinae.

**Fraterculinae [P] *converted clade name*.** Fraterculinae (American Ornithologists' Union, 1886) is converted to a node-based name (de Queiroz and Gauthier, 1992) that refers to most recent common ancestor of internal specifiers *Fratercula arctica* Linnaeus, 1758 and *Aethia psittacula* Pallas, 1769, and all of its descendants (i.e., contents = *Fratercula* Brisson, 1760, *Cerorhinca* Bonaparte, 1831, *Aethia* Merrem, 1788, and *Ptychoramphus* Brandt, 1837). The contents of this clade are consistent with the Linnaean subfamily Fraterculinae.

**Mancallinae [P] *converted clade name*.** Mancallinae Brodkorb 1967 is converted to a node-based name (de Queiroz and Gauthier, 1992) that refers to the most recent common ancestor of internal specifiers *Mancalla californiensis* Lucas, 1901 and *Miomancalla howardi* Smith, 2011, and all of its descendants (i.e., contents = *Mancalla* Lucas, 1901 and *Miomancalla* Smith, 2011). The contents of this clade are consistent with the Linnaean subfamily Mancallinae Brodkorb, 1967.

**Alcini [P] *converted clade name*.** Alcini Storer 1960 is converted to a node-based name (de Queiroz and Gauthier, 1992) that refers to the most recent common ancestor of internal specifiers *Alca torda* Linnaeus, 1758 and *Uria aalge* Pontoppidan, 1763, and all

of its descendants (i.e., contents = *Alca* Linnaeus, 1758, *Pinguinus* Bonaterre, 1790, *Miocepphus* Wetmore, 1940, *Alle* Link, 1806, and *Uria* Pontoppidan, 1763. The contents of this clade are consistent with the Linnaean Tribe Alcini Storer, 1960.

**Fraterculini [P] *converted clade name*.** Fraterculini Storer 1960 is converted to a node-based name (de Queiroz and Gauthier, 1992) that refers to the most recent common ancestor of internal specifiers *Fratercula arctica* Linnaeus, 1758 and *Cerorhinca monocerata* (Pallas, 1811), and all of its descendants (i.e., contents = *Fratercula* Brisson, 1760 and *Cerorhinca* Bonaparte, 1831). The contents of this clade are consistent with the Linnaean Tribe Fraterculini Storer, 1960.

**Aethiini [P] *converted clade name*.** Aethiini Storer, 1960 is converted to a branch-based name (de Queiroz and Gauthier, 1992) that refers to the most inclusive clade containing the internal specifier *Aethia psittacula* Pallas, 1769 but not *Fratercula arctica* Linnaeus, 1758 (i.e., contents = *Aethia* Merrem, 1788 and *Ptychoramphus* Brandt, 1837). This branch-based definition is adopted to include extinct auklet species such as *Aethia storeri* that are recovered outside the auklet crown clade (see Fig. 8.8). The contents of this clade are consistent with the Linnaean Tribe Aethiini Storer, 1960.

**Cepphini [P] *converted clade name*.** Cepphini Storer, 1960 is converted to a branch-based name (de Queiroz and Gauthier, 1992) that refers to the most inclusive clade containing the internal specifier *Cepphus grylle* (Linnaeus, 1758) but not *Brachyramphus marmoratus* (Gmelin, 1789) or *Synthliboramphus antiquus* (Gmelin, 1789; i.e., contents

include *Cepphus* Moehring, 1758 and *Pseudocepphus* Wijnker and Olson, 2009). This branch-based definition is adopted to include extinct guillemot species such as *Pseudocepphus teres* that are recovered outside the guillemot crown clade (see Fig. 8.8). The contents of this clade are consistent with the Linnaean Tribe Cepphini Storer, 1960.

***Mancalla* [P] converted clade name.** *Mancalla* Lucas, 1901 is converted to a branch-based name (de Queiroz and Gauthier, 1992) that refers to the most inclusive clade containing the internal specifier *Mancalla californiensis* Lucas, 1901, but not *Miomancalla howardi* Smith, 2011. This branch-based definition is adopted so that any potential discoveries of stem *Mancalla* will not require alteration of the definition of the clade *Mancalla*. The contents of this clade are consistent with the Linnaean Genus *Mancalla* (*sensu* Brodkorb, 1967).

***Miomancalla* [P] converted clade name.** *Miomancalla* Smith, 2011 is converted to a branch-based name (de Queiroz and Gauthier, 1992) that refers to the most inclusive clade containing the internal specifier *Miomancalla howardi* Smith, 2011, but not *Mancalla californiensis* Lucas, 1901. This branch-based definition is adopted so that any potential discoveries of stem *Miomancalla* will not require alteration of the definition of the clade *Miomancalla*. The contents of this clade are consistent with the Linnaean Genus *Miomancalla* (*sensu* Smith, 2011).

***Alca* [P] converted clade name.** *Alca* Linnaeus, 1758 is converted to a branch-based name (de Queiroz and Gauthier, 1992) that refers to the most inclusive clade containing

the internal specifier *Alca torda* Linnaeus, 1758, but not *Pinguinus impennis* (Linnaeus, 1758). This branch-based definition is adopted so that any potential discoveries of stem *Alca* will not require alteration of the definition of the clade *Alca*. The contents of this clade are consistent with the Linnaean Genus *Alca* (*sensu* American Ornithologists' Union, 1998).

***Pinguinus* [P] converted clade name.** *Pinguinus* Bonaterre, 1790 is converted to a branch-based name (de Queiroz and Gauthier, 1992) that refers to the most inclusive clade containing the internal specifier *Pinguinus impennis* (Linnaeus, 1758), but not *Alca torda* Linnaeus, 1758. This branch-based definition is adopted so that any potential discoveries of stem *Pinguinus* will not require alteration of the definition of the clade *Pinguinus*. The contents of this clade are consistent with the Linnaean Genus *Pinguinus* (*sensu* American Ornithologists' Union, 1998).

***Uria* [P] converted clade name.** *Uria* Pontoppidan, 1763 is converted to a branch-based name (de Queiroz and Gauthier, 1992) that refers to the most inclusive clade containing the internal specifier *Uria aalge* Pontoppidan, 1763, but not *Alle alle* Link, 1806. This branch-based definition is adopted so that any potential discoveries of stem *Uria* will not require alteration of the definition of the clade *Uria*. The contents of this clade are consistent with the Linnaean Genus *Uria* (*sensu* American Ornithologists' Union, 1998).

***Cephus* [P] converted clade name.** *Cephus* Moehring, 1758 is converted to a branch-based name (de Queiroz and Gauthier, 1992) that refers to the most inclusive clade

containing the internal specifier *Cepphus grille* (Linnaeus, 1758), but not *Alle alle* Link, 1806, *Brachyramphus marmoratus* (Gmelin, 1789), or *Synthliboramphus antiquus* (Gmelin, 1789). These external specifiers are chosen because of the uncertain systematic position of *Cepphus* in Alcidae. This branch-based definition is adopted so that any potential discoveries of stem *Cepphus* will not require alteration of the definition of the clade *Cepphus*. The contents of this clade are consistent with the Linnaean Genus *Cepphus* (*sensu* American Ornithologists' Union, 1998).

***Synthliboramphus* [P] converted clade name.** *Synthliboramphus* Brandt, 1837 is converted to a branch-based name (de Queiroz and Gauthier, 1992) that refers to the most inclusive clade containing the internal specifier *Synthliboramphus antiquus* (Gmelin, 1789), but not *Brachyramphus marmoratus* (Gmelin, 1789). This branch-based definition is adopted so that any potential discoveries of stem *Synthliboramphus* will not require alteration of the definition of the clade *Synthliboramphus*. The contents of this clade are consistent with the Linnaean Genus *Synthliboramphus* (*sensu* American Ornithologists' Union, 1998).

***Brachyramphus* [P] converted clade name.** *Brachyramphus* Brandt, 1837 is converted to a branch-based name (de Queiroz and Gauthier, 1992) that refers to the most inclusive clade containing the internal specifier *Brachyramphus marmoratus* (Gmelin, 1789), but not *Synthliboramphus antiquus* (Gmelin, 1789). This branch-based definition is adopted so that any potential discoveries of stem *Brachyramphus* will not require alteration of the

definition of the clade *Brachyramphus*. The contents of this clade are consistent with the Linnaean Genus *Brachyramphus* (*sensu* American Ornithologists' Union, 1998).

***Fratercula* [P] converted clade name.** *Fratercula* Brisson, 1760 is converted to a branch-based name (de Queiroz and Gauthier, 1992) that refers to the most inclusive clade containing the internal specifier *Fratercula arctica* Linnaeus, 1758, but not *Cerorhinca monocerata* Pallas, 1811. This branch-based definition is adopted so that any potential discoveries of stem *Fratercula* will not require alteration of the definition of the clade *Fratercula*. The contents of this clade are consistent with the Linnaean Genus *Fratercula* (*sensu* American Ornithologists' Union, 1998).

***Cerorhinca* [P] converted clade name.** *Cerorhinca* Bonaparte, 1831 is converted to a branch-based name (de Queiroz and Gauthier, 1992) that refers to the most inclusive clade containing the internal specifier *Cerorhinca monocerata* Pallas, 1811, but not *Fratercula arctica* Linnaeus, 1758. This branch-based definition is adopted so that any potential discoveries of stem *Cerorhinca* will not require alteration of the definition of the clade *Cerorhinca*. The contents of this clade are consistent with the Linnaean Genus *Cerorhinca* (*sensu* American Ornithologists' Union, 1998).

## LITERATURE CITED

- Addicot, W. O. 1972. Provincial middle and late Tertiary molluscan stages, Temblor Range, California. pgs. 1-26 *in* Proceedings of the Pacific Coast Miocene Biostratigraphic Symposium. E. H. Stinemeyer (Ed.). Society of Economic Paleontologists and Mineralogists.
- Ainley, D. G. 1990. Farallon seabirds: patterns at the community level. pgs. 349-380 *in* Seabirds of the Farallon Islands: ecology, dynamics, and structure of an upwelling-system community. D.G. Ainley and R. J. Boekelheide (Eds.). Stanford University Press, Stanford.
- Ainley, D. G., S. H. Morrell, and R. J. Boekelheide. 1990a. Rhinoceros Auklet and Tufted Puffin. pgs. 339-348 *in* Seabirds of the Farallon Islands: ecology, dynamics, and structure of an upwelling-system community. D.G. Ainley and R. J. Boekelheide (Eds.). Stanford University Press, Stanford.
- Ainley, D. G., C. S. Strong, T. M. Penniman, and R. J. Boekelheide. 1990b. The feeding ecology of of Farallon seabirds. pgs. 51-127 *in* Seabirds of the Farallon Islands: ecology, dynamics, and structure of an upwelling-system community. D.G. Ainley and R. J. Boekelheide (Eds.). Stanford University Press, Stanford.
- American Ornithologists' Union. 1886. The Code of Nomenclature and Check-list of North American Birds, 1<sup>st</sup> ed. American Ornithologists' Union, New York.
- American Ornithologists' Union. 1895. Check-list of North American Birds, 2<sup>nd</sup> ed. American Ornithologists' Union, New York.
- American Ornithologists' Union. 1944. Nineteenth supplement to the American Ornithologists' Union check-list of North American birds. *Auk* 61:441-464.
- American Ornithologists' Union. 1983. Check-list of North American Birds: the species of birds of North America from the Arctic through Panama, including the West Indies and Hawaiian Islands. 6th ed. American Ornithologists' Union, Washington, DC.
- American Ornithologists' Union. 1998. Check-list of North American Birds: the species of birds of North America from the Arctic through Panama, including the West Indies and Hawaiian Islands. 7th ed. American Ornithologists' Union, Washington, DC.



- American Ornithologists' Union. 2008. North American check-list committee proposals 2008-A-06. Adopt a new English name for *Cerorhinca monocerata* (Charadriiformes, Alcidae). [http://www.aou.org/committees/nacc/proposals/2008\\_A\\_votes\\_web.php#2008-A-6](http://www.aou.org/committees/nacc/proposals/2008_A_votes_web.php#2008-A-6).
- Arbogast, B. S., and J. B. Slowinsky. 1998. Pleistocene Speciation and the Mitochondrial DNA Clock. *Science* 282:1955a.
- Arnold, R. 1906. Tertiary and Quaternary Pectens of California. United States Geological Survey Professional Paper no. 47, 264pp.
- Awise, J. C., and D. Walker. 1998. Pleistocene phylogeographic effects on avian populations and the speciation process. *Proceedings of the Royal Society of London B*, 265:457-463.
- Baichich, P. J., and C. J. O. Harrison. 1997. A Guide to the Nests, Eggs, and Nestlings of North American Birds, 2<sup>nd</sup> ed. Academic Press, San Diego, 347pp.
- Bailey, R. E. 1952. The incubation patch of passerine birds. *Condor* 54:121-136.
- Baker, A. J., S. L. Pereira, and T. A. Paton. 2007. Phylogenetic relationships and divergence times of Charadriiformes genera: multigene evidence for the Cretaceous origin of 14 clades of shorebirds. *Biology Letters* 3:205-209.
- Ballmann, P. 1979. Fossile Glareolidae aus dem Miozän des Nördlinger Ries (Aves: Charadriiformes). *Bonner Zoologische Beiträge* 30:51-101.
- Barnes, L. G., H. Howard, J. H. Hutchison, and B. J. Welton. 1981. The vertebrate fossils of the marine Cenozoic San Mateo Formation at Oceanside, California. pgs. 53-70 *in* Geologic Investigations of the Coastal Plain. P. L. Abbott and S. O'Dunn (Eds.). San Diego County, California. San Diego Association of Geologists.
- Barrett, R. T., T. Anker-Nielsen, and Y. V. Krasov. 1997. Can Norwegian and Russian Razorbills *Alca torda* be identified by their measurements? *Marine Ornithology* 25:5-8.
- Barron, J. A. 1986. Updated biostratigraphy for the Monterey Formation of California. pgs. 105-119 *in* Siliceous Microfossil and Microplankton Studies of the Monterey Formation and Modern Analogs. R. E. Casey and J. A. Barron (Eds.). Pacific Section SEPM, Book 45.
- Bartoli, G., M. Sarnthein, M. Weinelt, H. Erlenkeuser, D. Garbe-Schönberg, and D. W. Lea. 2005. Final closure of Panama and the onset of northern hemisphere glaciation. *Earth and Planetary Science Letters* 237:33-44.

- Baumel, J., and L. Witmer. 1993. Osteologica. pgs. 45-132 in *Handbook of Avian Anatomy: nomina anatomica avium*, 2<sup>nd</sup> ed. J. J. Baumel, A. S. King, J. E. Breazile, H. E. Evans, and J. C. Vanden Berge (Eds.). Publications of the Nuttall Ornithology Club, 23.
- Becker, J. J. 1987. *Neogene Avian Localities of North America*. Smithsonian Institution Press, Washington, D.C., 171pp.
- Bédard, J. 1969. Adaptive radiation in the Alcidae. *Ibis* 111:189-198.
- Bédard, J. 1985. Evolution and characteristics of the Atlantic Alcidae. pgs. 1-50 in *The Atlantic Alcidae: the evolution, distribution, and biology of the auks inhabiting the Atlantic Ocean and adjacent water areas*. D. N. Nettleship and T. R. Birkhead (Eds.). Academic Press, London.
- Beddard, F. E. 1898. *Structure and Classification of Birds*. Longmans Green and Co., New York. 548pp.
- Bell, C. J., J. A. Gauthier, and G. S. Bever. 2010. Covert biases, circularity, and apomorphies: a critical look at the North American Quaternary herpetofaunal stability hypothesis. *Quaternary International* 217:30-36.
- Bengston, S. A. 1984. Breeding ecology and extinction of the Great Auk. *Auk* 101:1-12.
- Benton, M. J., and P. C. J. Donoghue. 2007. Paleontological evidence to date the tree of life. *Molecular Biology and Evolution* 24:26-53.
- Benvenuti, S., F. Bonadonna, L. Dall'Antonia, and G. A. Gudmundsson. 1998. Foraging flight of breeding Thick-billed Murres (*Uria lomvia*) as revealed by bird-borne direction recorders. *Auk* 115:57-66.
- Berggren, W. A., F. J. Hilgen, C. G. Langereis, D. V. Kent, J. D. Obradovich, I. Raffi, M. E. Raymo, and N. J. Shackleton. 1995. Late Neogene chronology: new perspectives in high-resolution stratigraphy. *Geological Society of America Bulletin* 107:1272-1287.
- Björklund, M. 1994. Phylogenetic relationships among Charadriiformes: reanalysis of previous data. *Auk* 111:825-832.
- Binford L. C., B. G. Elliot, and S. W. Singer. 1975. Discovery of a nest and the downy young of the Marbled Murrelet. *Wilson Bulletin* 87:303-440.

- Bock W. J. 1958. A generic review of the plovers (Charadriinae, Aves). Bulletin of the Museum of Comparative Zoology 118:27-97.
- Boessenecker, R. W. 2011. New records of the fur seal *Callorhinus* (Carnivora: Otariidae) from the Plio-Pleistocene of the Rio Dell Formation of Northern California and comments on otarid dental evolution. Journal of Vertebrate Paleontology 31:454-467.
- Boessenecker, R. W., and N. A. Smith. 2011. Latest Pacific basin record of a bony-toothed bird (Aves, Pelagornithidae) from the Pliocene Purisima Formation of California, U.S.A. Journal of Vertebrate Paleontology 31:652-657.
- Bonaparte, C. L. 1831. Saggio di una distribuzione metodica degli animali vertebrati. Principe di Musignano, Presso Antonio Boulzaler, Roma.
- Bonaterre, P. J. 1790. Tableau encyclopedique et methodique des trois regnes de la nature. Ophiologie. Chez Panckoucke, Librairie, Paris.
- Bradstreet, M. S. W., and R. G. B. Brown. 1985. Feeding ecology of the Atlantic Alcidae. pgs. 263-318 in The Atlantic Alcidae: the evolution, distribution, and biology of the auks inhabiting the Atlantic Ocean and adjacent water areas. D. N. Nettleship and T. R. Birkhead (Eds.). Academic Press, London.
- Brandt, J. F., von. 1837. Rapport sur une monographie de la famille des Alcades. Bulletin Scientifique, l'Académie Impériale des Sciences de Saint Pétersbourg, v2:344-349.
- Bridge, E. S., A. W. Jones, and A. J. Baker. 2005. A phylogenetic framework for the terns (Sternini) inferred from mtDNA sequences: implications for taxonomy and plumage evolution. Molecular Phylogenetics and Evolution 35:459-469.
- Briggs, J. C. 1970. A faunal history of the North Atlantic Ocean. Systematic Zoology 19:19-34.
- Briggs, K. T., W. B. Tyler, D. B. Lewis, and D. R. Carlson. 1987. Bird communities at sea off California:1975-1983. Studies in Avian Biology 11:1-74.
- Brisson, M -J. 1760. Ornithologie ou méthode contenant la division des oiseaux en ordres, sections, genres, especes and leurs varieties, v6. Imprimeur du Roi, Paris.
- Britton, T., C. L. Anderson, D. Jacquet, S. Lundqvist, and K. Bremer. 2007. Estimating divergence times in large phylogenetic trees. Systematic Biology 56: 741-752.

- Brodkorb, P. 1955. The avifauna of the Bone Valley Formation. Florida Geological Survey Report of Investigations 14.
- Brodkorb, P. 1967. Catalogue of fossil birds: Part 3 (Ralliformes, Ichthyornithiformes, Charadriiformes). Bulletin of the Florida State Museum, Biological Sciences 11:99-220.
- Brown, J. W., R. B. Payn, and D. P. Mindell. 2007. Nuclear DNA does not reconcile 'rocks' and 'clocks' in Neoaves: a comment on Ericson *et al.* Biology Letters 3:257-259.
- Brown, R. W. 1956. Composition of Scientific Words. Smithsonian Institution Press, Washington and London, 850pp.
- Bull, J. J., J. P. Huelsenbeck, C. W. Cunningham, D. L. Swofford, and P. J. Waddell. 1993. Partitioning and combining data in phylogenetic analysis. Systematic Biology 42:384.
- Burness, G. P., and W. A. Montevecchi. 1992. Oceanographic-related variation in the bone sizes of Great Auks. Polar Biology 11:545-551.
- Butzin, M., G. Lohmann, and T. Bickert. 2011. Miocene ocean circulation inferred from marine carbon cycle modeling combined with benthic isotope records. Paleoceanography 26:doi:10.1029/2009PA001901.
- Cantino, P. D., and K. de Queiroz. 2010. International Code of Phylogenetic Nomenclature, v4c. <http://www.ohio.edu/phylocode/>.
- Chai, P. 1997. Hummingbird hovering energetics during moult of primary flight feathers. Journal of Experimental Biology 200:1527-1536.
- Chandler, R. M. 1985. Two new species of the flightless auk, *Mancalla*, from the Late Miocene San Mateo Formation of Oceanside, San Diego County, California. Abstracts from the Society of Vertebrate Paleontology Annual Meeting, 1985.
- Chandler, R. M. 1990a. Phylogenetic analysis of the alcids. Doctoral Dissertation, University of Kansas, Lawrence Kansas, 133 pp.
- Chandler, R. M. 1990b. Fossil birds of the San Diego Formation, Late Pliocene, Blencoe, San Diego County California. Ornithological Monographs 44:73-161.
- Chandler, R. M., and D. Parmley. 2002. The earliest North American record of an auk (Aves: Alcidae) from the Late Eocene of central Georgia. Oriole 68:7-9.

- Chang, M. M., and Y. Y. Chen. 2000. Late Mesozoic and Tertiary ichthyofaunas from China and some puzzling patterns of distribution. *Vertebrata Palasiatica* 38:161-175.
- Chapman, W. L. 1965. Appearance of ossification centers and epiphyseal closures as determined by radiographic techniques. *Journal of the American Veterinary Medical Association* 147:138-141.
- Cheetham, A., and L. C. Hayek. 1988. Phylogeny reconstruction in the Neogene bryozoan *Metrarabdotus*: a paleontological evaluation of methodology. *Historical Biology* 1:65-83.
- Chiappe, L. M., and L. M. Witmer (Eds.). 2002. *Mesozoic Birds: above the heads of dinosaurs*. University of California Press, 520pp.
- Chippendale P. T., and J. J. Wiens. 1994. Weighting, partitioning, and combining characters in phylogenetic analysis. *Systematic Biology* 43:278-287.
- Christian, P., D. L. Christidis, and R. Schodde. 1992. Biochemical systematics of the Charadriiformes (shorebirds): relationships between Charadrii, Scolopaci, and Lari. *Australian Journal of Zoology* 40:225-233.
- Chu, P. C. 1995. Phylogenetic reanalysis of Strauch's data set for the Charadriiformes. *Condor* 97:174-196.
- Chu, P. C. 1998. A Phylogeny of the Gulls (Aves: Larinae) inferred from osteological and integumentary characters. *Cladistics* 14:1-53.
- Chu, P. C., S. K. Eizenschenk, and S. Zhu. 2009. Skeletal morphology and the phylogeny of skuas (Aves: Charadriiformes, Stercorariidae). *Zoological Journal of the Linnean Society* 157:612-621.
- Churchill, S. P., E. O. Wiley, and L. A. Hauser. 1984. A critique of Wagner groundplan-divergence studies and a comparison with other methods of phylogenetic analysis. *Taxon* 33:212-233.
- Clark, G. A. Jr. 1993. Termini situm et directionum partium corporis indicantes. pgs. 1-5 in *Handbook of Avian Anatomy: nomina anatomica avium*, 2<sup>nd</sup> ed. J. J. Baumel, A. S. King, J. E. Breazile, H. E. Evans, and J. C. Vanden Berge (Eds.). Cambridge, MA: Publications of the Nuttall Ornithological Club 23.
- Clarke, J. A. 2004. Morphology, phylogenetic taxonomy, and systematics of *Ichthyornis* and *Apatornis* (Avialae: Ornithurae). *Bulletin of the American Museum of Natural History* 286: 1-179.

- Clarke, J. A., D. T. Ksepka, M. Stucchi, N. Gianninni, S. Bertelli, Y. Narváez, and C. A. Boyd. 2007. Paleogene equatorial penguins challenge the proposed relationship between biogeography, diversity, and Cenozoic climate change. *Proceedings of the National Academy of Sciences of the USA* 104:11545-11550.
- Clarke, J. A., and M. A. Norell. 2002. The morphology and phylogenetic position of *Apsaravis ukhaana* from the Late Cretaceous of Mongolia. *American Museum Novitates* 3387:1-46.
- Clarke, J. A., and K. M. Middleton. 2008. Mosaicism, modules, and the evolution of birds: results from a Bayesian approach to the study of morphological evolution using discrete character data. *Systematic Biology* 57:185-201.
- Clarke, J. A., C. P. Tambussi, J. I. Noriega, G. M. Erickson, and R. A. Ketchum. 2005. Definitive fossil evidence for the extant avian radiation in the Cretaceous. *Nature* 433:305-308.
- Clyde, W. C., and P. D. Gingerich. 1998. Mammalian community response to the latest Paleocene thermal maximum: an isotaphonomic study in the northern Bighorn Basin, Wyoming. *Geology* 26:1011-1014.
- Cohen, B. L., A. J. Baker, K. Blechschmidt, D. L. Dittman, R. W. Furness, J. A. Gerwin, A. J. Helbig, J. de Korte, H. D. Marshall, R. L. Palma, H. -U. Peter, R. Ramli, I. Siebold, M. S. Willcox, R. H. Wilson, and R. M. Zink. 1997. Enigmatic phylogeny of skuas (Aves: Stercorariidae). *Proceedings of the Royal Society of London B* 264:181-190.
- Coues, E. 1868. A monograph of the Alcidae. *Proceedings of the Academy of Natural Sciences of Philadelphia* 13:215-257.
- Coues, E. 1872. Key to North American Birds containing a concise account of every species of living and fossil bird at present known from the continent north of the Mexican and United States boundary. *Naturalists' Agency*, Salem.
- Cracraft, J. 1968. The lacrimal-ectethmoid bone complex in birds: a single character analysis. *American Midland Naturalist* 80:316-359.
- Cracraft, J., F. K. Barker, M. Braun, J. Harshman, G. J. Dyke, J. Feinstein, S. Stanley, A. Cibois, P. Schikler, and P. Beresford. 2004. Phylogenetic relationships among modern birds (Neornithes). pgs. 468-489 *in* *Assembling The Tree of Life*. J. Cracraft and M. J. Donoghue (Eds.). Oxford University Press, USA.
- Croll, D. A., A. J. Gaston, A. E. Burger, and D. Konnoff. 1992. Foraging behavior and

- physiological adaptations for diving in Thick-billed Murres. *Ecology* 73:344-356.
- Dawson, W. 1920. An oological revision of the Alciformes. *Journal of the Museum of Comparative Oology* 1:7-14.
- Dayrat, B., P. D. Cantino, J. A. Clarke, and K. de Queiroz. 2008. Species names in the *Phylocode*: the approach adopted by the International Society for Phylogenetic Nomenclature. *Systematic Biology* 57:507-514.
- del Hoyo, J., A. Elliot, and J. Sargatal (Eds.) 1996. *Handbook of the Birds of the World. Vol 3. Hoatzins to Auks*. Lynx Edicions, Barcelona, Spain. 821pp.
- Deméré, T. A. 1982. Review of the lithostratigraphy, biostratigraphy, and age of the San Diego Formation. *Geologic Studies in San Diego* 1982:127-134.
- Deméré, T. A. 1983. The Neogene San Diego basin: a review of the marine Pliocene San Diego Formation. pgs. 187-195 *in* *Cenozoic Marine Sedimentation, Pacific Margin U.S.A.*. D. K. Larue and R. J. Steel (Eds.). Society of Economic Paleontologists and Mineralogists.
- Deméré, T. A., and A. Berta. 2005. New skeletal material of *Thalassoleon* (Otariidae: Pinnipedia) from the Late Miocene-Early Pliocene (Hemphillian) of California. *Bulletin of the Florida Museum of Natural History* 45:379-411.
- Deméré, T. A., A. Berta, and P. J. Adam. 2003. Pinnipedimorph evolutionary biogeography. *Bulletin of the American Museum of Natural History* 279:32-76.
- Deméré, T. A., M. A. Roeder, R. M. Chandler, and J. A. Minch. 1984. Paleontology of the Middle Miocene Los Indios Member of the Rosarito Beach Formation, Northwestern Baja California, Mexico. pgs. 47-56 *in* *Miocene and Cretaceous Depositional Environments, Northwestern Baja California, Mexico*. J. A. Minch and J. R. Ashby (Eds.). Pacific Section AAPG 54.
- Depaolo, D. P., and K. L. Finger. 1991. High-resolution strontium-isotope stratigraphy and biostratigraphy of the Miocene Monterey Formation, central California. *Geological Society of America Bulletin* 103:112-124.
- de Queiroz, K. 1993. For consensus (sometimes). *Systematic Biology* 42:368-372.
- de Queiroz, K., M. J. Donoghue, and J. Kim. 1995. Separate versus combined analysis of phylogenetic evidence. *Annual Review of Ecology and Systematics* 26:657-681.
- de Queiroz, K., and J. A. Gauthier. 1992. Phylogenetic taxonomy. *Annual Review of*

Ecology and Systematics 23:449-480.

- De Santo, T. L., and K. Nelson. 1995. Reproductive ecology of the auks (Family Alcidae) with emphasis on the Marbled Murrelet. pgs. 33-47 *in* USDA Forest Service General Technical Report, PSW-152.
- Dingus, L., and T. Rowe. 1998. The Mistaken Extinction: Dinosaur Evolution and the Origin of Birds. W. H. Freeman and Company, New York, 332 pp.
- Dodd, C. K., and G. S. Morgan. 1992. Fossil sea turtles from the early Pliocene Bone Valley Formation, Central Florida. *Journal of Herpetology* 26:1-8.
- Dolphin, W. F., and D. McSweeney. 1982. Incidental ingestion of Cassin's Auklets by humpback whales. *Auk* 100:214.
- Domning, D. P. 2001. Sirenians, seagrasses, and Cenozoic ecological change in the Caribbean. *Palaeogeography, Palaeoclimatology, Palaeoecology* 166:27-50.
- Domning, D. P., and T. A. Deméré. 1984. New material of *Hydrodamilis cuestae* (Mammalia: Dugonidae) from the Miocene and Pliocene of San Diego County, California. *Transactions of the San Diego Society of Natural History* 20:169-188.
- Donoghue, M. J., J. A. Doyle, J. Gauthier, A. G. Kluge, and T. Rowe. 1989. The importance of fossils in phylogeny reconstruction. *Annual Review of Ecology and Systematics* 20:431-460.
- Dove, C. J. 2000. A descriptive and phylogenetic analysis of plumulaceous feather characters in Charadriiformes. *Ornithological Monographs* 51:1-163.
- Dowsett, H. J., J. Barron, and R. Poore. 1992. Middle Pliocene sea surface temperatures: a global reconstruction. *Marine Micropaleontology* 27:13-26.
- Drummond, A. J., S. Y. W. Ho, M. J. Phillips, and A. Rambaut. 2006. Relaxed phylogenetics and dating with confidence. *Plos Biology* 4:699-710.
- Drummond, A. J., A. Rambaut, and M. Suchard. 2010. BEAST v1.6.1 Bayesian evolutionary analysis sampling trees. Available from <http://evolve.zoo.ox.ac.uk/beast/>.
- Duffy, D. C., W. E. Arntz, H. T. Serpa, P. D. Boersma, and R. L. Norton. 1988. A comparison of the effects of El Niño and the southern oscillation on birds in Peru and the Atlantic Ocean. *Acta XIX Congressus Internationalis Ornithologici* 2:1740-1746.



- Duffy, D. C., F. S. Todd, and W. R. Siegfried. 1987. Submarine foraging behavior of alcids in an artificial environment. *Zoological Biology* 6:373-378.
- Dumont, M. P., and Barron, J. A., 1995. Diatom biochronology of the Sisquoc Formation in the Santa Maria Basin, California, and its paleoceanographic and tectonic implications. *in* Evolution of sedimentary basins/offshore oil and gas investigations Santa Maria province. M. A. Keller (Ed.), U.S. Geological Survey Bulletin 1995K:K1-K17.
- Dyke, G. J., and C. A. Walker. 2005. New records of fossil birds from the Pliocene of Kallo, Belgium, *Nues Jahrbuch für Geologie und Paläontologie* 200:233-247.
- Elliott, W. J. 1975. Stratigraphic correlation chart for western San Diego County and southern Orange County, California. pgs. 48-50 in *Studies of Camp Pendleton and Western San Diego County, California Fieldtrip Guidebook*. A. Ross and R. J. Dowlen (Eds.). San Diego Association of Geologists.
- Emslie, S. D. 1998. Avian community, climate, and sea-level changes in the Pliocene of the Florida peninsula. *Ornithological Monographs* 50.
- Emslie, S. D., W. D. Allmon, F. J. Rich, J. H. Wren, and S. D. deFrance. 1996. Integrated taphonomy of an avian death assemblage in marine sediments from the late Pliocene of Florida. *Palaeogeography, Palaeoclimatology, Palaeoecology* 124:107-136.
- Emslie, S. D., and G. S. Morgan. 1994. A catastrophic death assemblage and paleoclimatic implications of Pliocene seabirds of Florida. *Science* 264:684-685.
- Ericson, P. G. P., C. J. Anderson, T. Britton, A. Elzanowski, U. S. Johansson, M. Kallersjö, J. I. Ohlson, T. J. Parsons, D. Zuccon, and G. Mayr. 2006. Diversification of Neoaves: integration of molecular sequence data and fossils. *Biology Letters* 2:543-547.
- Ericson, P. G. P., I. Envall, M. Irestedt, and J. A. Norman. 2003. Inter-familial relationships of the shorebirds (Aves: Charadriiformes) based on nuclear DNA sequence data. *BMC Evolutionary Biology* 3:doi:10.1186/1471-2148-3-16.
- Estabrook, G. F., C. S. Johnson Jr., and F. R. McMorris. 1976. A mathematical foundation for the analysis of cladistic character compatibility. *Mathematical Biosciences* 29:181-187.
- Fain, M. G., and P. Houde. 2004. Parallel radiations in the primary clades of birds.

Evolution 58:2558-2573.

- Fain, M. G., and P. Houde. 2007. Multilocus perspectives on the monophyly and phylogeny of the order Charadriiformes (Aves). *BMC Evolutionary Biology* 7:35.
- Feduccia, A. 1995. Explosive evolution in Tertiary birds and mammals. *Science* 267:637-638.
- Feduccia, A. 1996. The origin and evolution of birds, 2nd ed. Yale University Press, New Haven, 466pp.
- Feduccia, A., and P. O. McGrew. 1974. A flamingo-like wader from the Eocene of Wyoming. *University of Wyoming Contributions to Geology* 13:49-61.
- Felsenstein, J. 1985. Phylogenies and the comparative method. *American Naturalist* 125:1-15.
- Fisher, J., and R. M. Lockley. 1954. *Sea Birds*. Collins, London, 320pp.
- Fitzgerald, E. M. G. 2005. Pliocene marine mammals from the Whalers Bluff Formation of Portland, Victoria, Australia. *Memoirs of Museum Victoria* 62:67-89.
- Fleagle, J. G., T. M. Bown, J. D. Obradovich, and E. L. Simons. 1986. Age of the earliest african anthropoids. *Science* 234:1247-1249.
- Flower, B. P., and J. P. Kennett. 1994. The Middle Miocene climatic transition: east antarctic ice sheet development, deep ocean circulation and global carbon cycling. *Palaeogeography, Palaeoclimatology, Palaeoecology* 108:537-555.
- Ford, D., and J. Golonka. 2003. Phanerozoic paleogeography, paleoenvironment and lithofacies maps of the circum-Atlantic margins. *Marine and Petroleum Geology* 20:249-285.
- Fraser, N. C., and M. Benton. 1989. The Triassic reptiles *Brachyrhinodon* and *Polysphenodon* and the relationships of the spheodontids. *Zoological Journal of the Linnean Society* 96:413-445.
- Friedmann, H. 1934. Bird bones from eskimo ruins on St. Lawrence Island, Bering Sea. *Journal of the Washington Academy of Sciences* 24:83-96.
- Friedmann, H. 1937. Bird bones from archaeological sites in Alaska. *Journal of the Washington Academy of Sciences* 27:431-438.

- Friedmann, H. 1941. Bird bones from eskimo ruins at Cape Prince of Whales, Alaska. *Journal of the Washington Academy of Sciences* 31:404-409.
- Friesen, V., A. Baker, and J. Piatt. 1996. Phylogenetic relationships within the Alcidae (Charadriiformes: Aves) inferred from total molecular evidence. *Molecular Biology and Evolution* 13:359-367.
- Friesen, V., J. Piatt. and A. Baker. 1996b. Evidence from cytochrome *b* sequences and allozymes for a new species of alcid: the Long-Billed Murrelet (*Brachyramphus perdix*). *Condor* 98:681-690.
- Fuller, E. 1987. *Extinct Birds*. Cornell University Press, Ithaca, NY. 399 pp.
- Fuller, E. 1999. *The Great Auk*. Errol Fuller, Kent, England, 448pp.
- Fürbringer, M. 1888. *Untersuchungen zur Morphologie und Systematic der Vogel*. T.J. Van Holkema, Amsterdam.
- Furness, R. W., and A. E. Burger. 1988. Effects of energy constraints on seabirds breeding at high latitudes. pgs. 1205-1217 *in* *Acta XIX Congressus Internationalis Ornithologici* v.1 Ottawa. H. Ouellet (Ed.). National Museum of Natural Sciences and University of Ottawa Press.
- Furness, R. W., and D. N. Nettleship (Eds.). 1991. Seabirds as monitors of changing marine environments. *Proceedings of the International Ornithological Congress Symposium* 41.
- Gadow, H. 1892. On the classification of birds. *Proceedings of the Zoological Society of London* 1892:229-256.
- Gao, K., and M. Norell. 1998. Taxonomic review of *Carusia* (Reptilia: Squamata) from the late Cretaceous of the Gobi Desert and phylogenetic relationships of anguimorph lizards. *American Museum Novitates* 3230:1-51.
- Gaston, A. J. 1990. Population parameters of the Ancient Murrelet. *Condor* 92:998-1011.
- Gaston, A. J., H. G. Gilchrist, and J. M. Hipfner. 2005. Climate change, ice conditions and reproduction in an Arctic nesting marine bird: Brunnich's Guillemot (*Uria lomvia* L.). *Journal of Animal Ecology* 74:832-84.
- Gaston, A. J., and K. Woo. 2008. Razorbills (*Alca torda*) follow subarctic prey into the Canadian Arctic: colonization results from climate change. *Auk* 125:939-942.
- Gauthier, J., and K. de Queiroz. 2001. Feathered dinosaurs, flying dinosaurs, crown

dinosaurs, and the name “*Aves*”. pgs. 7-41 *in* New Perspectives on the Origin and Early Evolution of Birds: proceedings of the international symposium in honor of John H. Ostrom. J. Gauthier and L. F. Gall (Eds.). Yale University Peabody Museum of Natural History, New Haven.

Gauthier, J., A. G. Kluge, and T. Rowe, 1988. Amniote phylogeny and the importance of fossils. *Cladistics* 4:105-209.

Gibbard, P. L., M. J. Head, M. J. C. Walker, and the Subcommittee on Quaternary Stratigraphy. 2010. Formal ratification of the Quaternary System/Period and the Pleistocene Series/Epoch with a base at 2.58 Ma. *Journal of Quaternary Science* 25:96-102.

Gibson, T. G. 1967. Stratigraphy and paleoenvironment of the phosphatic Miocene strata of North Carolina. *Bulletin of the Geological Society of America* 78:631-649.

Gibson, T. G. 1983. Stratigraphy of Miocene through lower Pleistocene strata of the United States central Atlantic coastal plain. *Smithsonian Contributions to Paleobiology* 53:35-80.

Gmelin, J. F. 1789. *Systema Naturae, per regna tria natura: secundum classes, ordines, genera, species, cum characteribus, differentiis, synonymis, locis*. 13th edition. Tome 1, pars II: 501-1032- Lyon.

Gradstein, F. M., J. G. Ogg, and A. G. Smith (Eds.). 2004. *A Geologic Timescale 2004*. Cambridge University Press, Cambridge, Mass., USA, 589pp.

Graur, D., and W. Martin. 2004. Reading the entrails of chickens: molecular timescales of evolution and the illusion of precision. *Trends in Genetics* 20:80-86.

Groth, J. G., and G. F. Barrowclough. 1999. Basal divergences in birds and the phylogenetic utility of the nuclear RAG-1 gene. *Molecular Phylogenetics and Evolution* 12:115-123.

Guthrie, D. 1992. A late Pleistocene avifauna from San Miguel Island, California. pgs. 319-327 *in* Papers in Avian Paleontology Honoring Pierce Brodkorb. K. E. Campbell (Ed.). Science Series no. 36, Natural History Museum of Los Angeles County, Los Angeles, CA.

Guthrie, D., H. Thomas, and G. Kennedy. 1999. A new species of extinct Late Pleistocene puffin (Aves: Alcidae) from the southern California Channel Islands. *Proceedings of the Fifth California Islands Symposium*. US Dept. of Interior, Minerals Management Service, Pacific OCS Region (published as CD) MMS 99-0038.

- Gysels, H., and M. Rabaey. 1964. Taxonomic relationships of *Alca torda*, *Fratercula arctica*, and *Uria aalge* as revealed by biochemical methods. *Ibis* 106:536-540.
- Habib, M. 2010. The structural mechanics and evolution of aquaflying birds. *Biological Journal of the Linnean Society* 99:687-698.
- Habib, M., and C. B. Ruff. 2008. The effects of locomotion on the structural characteristics of avian limb bones. *Zoological Journal of the Linnean Society* 153:601-624.
- Hackett, S. J., R. T. Kimball, S. Reddy, R. C. K. Bowie, E. L. Braun, M. J. Braun, J. L. Chojnowski, W. A. Cox, K. Han, J. Harshman, C. J. Huddleston, B. D. Marks, K. J. Miglia, W. S. Moore, F. H. Sheldon, D. W. Steadman, C. C. Witt, and T. Yuri. 2008. A phylogenomic study of birds reveals their evolutionary history. *Science* 320:1763-1768.
- Hamilton, J. L. 2006. Alcid swimming: kinematics, muscle activity patterns, and pelagic diving behaviour. Doctoral Dissertation, Brown University, 180pp.
- Haug, G. H., and R. Tiedemann. 1998. Effect of the formation of the Isthmus of Panama on Atlantic Ocean thermohaline circulation. *Nature* 393:673-676.
- Haq, B. U., J. Hardenbol, and P. R. Vail. 1988. Mesozoic and Cenozoic chronostratigraphy and cycles of sea-level change. pgs. 71-108 *in* Sea-level Changes: an integrated approach, C. K. Wilgus, B. S. Hastings, C. A. Ross, H. Posamentier, J. Van Wagoner, and C. G. Kendall (Eds.). SEPM Special Publication 42.
- Hardin, G. 1960. The competitive exclusion principle. *Science* 131:1292-1297.
- Harris, M. P., and T. R. Birkhead. 1985. Breeding ecology of the Atlantic Alcidae. pgs. 155-204 *in* The Atlantic Alcidae: the evolution, distribution, and biology of the auks inhabiting the Atlantic Ocean and adjacent water areas. D. N. Nettleship and T. R. Birkhead (Eds.). Academic Press, London.
- Harrison, C. J. O. 1977, A new guillemot, *Cepphus* species, from the lower Pleistocene. *Suffolk Natural History* 238-239.
- Harrison, C. J. O., and J. R. Stewart. 1999. The bird remains. pgs. 187-196 *in* The Middle Pleistocene Site at ARC Earham Quarry, Boxgrove, West Sussex. U.K., M.B. Roberts and S.A. Parfitt (Eds.). English Heritage Monograph Series 16, London.
- Harrison, C. J. O., and C. A. Walker. 1972. The affinities of *Halcyornis* from the lower

- Eocene. *Bulletin of the British Museum (Geology)* 21:153-170.
- Harrison, C. J. O., and C. A. Walker. 1977. Birds of the British lower Eocene. *Tertiary Research Special Paper* 3:1-32.
- Hasegawa, Y., Y. Tomida, N. Kohno, K. Ono, H. Nokariya, and T. Uyeno. 1988. Quaternary vertebrates from Shiriya area, Shimokita Peninsula, northeastern Japan. *Memoirs of the National Science Museum* 21:17-36.
- Hatch, S. A. 1987. Did the 1982-1983 El Niño-Southern Oscillation affect seabirds in Alaska? *Wilson Bulletin* 468-474.
- Hawkins, J. A., C. E. Hughes, and R. W. Scotland. 1997. Primary homology assessment, characters and character states. *Cladistics* 13:275-283.
- Hazel, J. 1983. Age and correlation of the Yorktown (Pliocene) and Croatan (Pliocene and Pleistocene) Formations at the Lee Creek Mine. *Smithsonian Contributions to Paleobiology* 53:81-200.
- Head, M. J., P. Gibbard, and A. Salvador. 2008. The Quaternary: its character and definition. *Episodes* 31:234-238.
- Heath, T. A., S. M. Hedtke, and D. M. Hillis. 2008. Taxon sampling and the accuracy of phylogenetic analyses. *Journal of Systematics and Evolution* 46:239-257.
- Hebert, P. D., M. Y. Stoeckle, T. S. Zemlak, and C. M. Francis. 2004. Identification of birds through DNA barcodes. *PloS Biology* 2:E312.
- Hedd, A., P. M. Regular, W. A. Montevecchi, A. D. Buren, C. M. Burke, and D. A. Fifield. 2009. Going deep: Common Murres dive into frigid water for aggregated, persistent and slow-moving capelin. *Marine Biology* 156:741-751.
- Heimberg, A. M., L. F. Sempere, V. N. Moy, P. C. Donoghue, and K. J. Peterson. 2008. MicroRNAs and the advent of vertebrate morphological complexity. *Proceedings of the National Academy of Sciences* 105:2946-2950.
- Herman, J., M. Crochard, and M. Giradot. 1974. Quelques restes de sélaciens récoltés dans les sables du Kattendijk á Kalló. *Bulletin de la Société Belge de Géologie de Paléontologie et d'Hydrologie (Bruxelles)* 83:15-31.
- Hipfner, M. J. 2008. Matches and mismatches: ocean climate, prey phenology and breeding success in a zooplanktivorous seabird. *Marine Ecology Progress Series* 368:295-304.

- Hipfner, M. J., and J. L. Greenwood. 2008. Breeding biology of the Common Murre at Triangle Island, British Columbia, Canada, 2002–2007. *Northwestern Naturalist* 89:76-84.
- Ho, S. Y. W. 2009. An examination of phylogenetic models of substitution rate variation among lineages. *Biology Letters* 5:421-424.
- Ho, S. Y. W., and M. J. Phillips. 2009. Accounting for calibration uncertainty in phylogenetic estimation of evolutionary divergence times. *Systematic Biology* 58:367-380.
- Holder, M., and P. O. Lewis. 2003. Phylogeny estimation: traditional and Bayesian approaches. *Nature Reviews* 4:275-284.
- Hope, S. 2002. The Mesozoic radiation of neornithes. pgs. 339-388 *in* Mesozoic Birds: above the heads of dinosaurs, L. M. Chiappe, and L. M. Witmer (Eds.). University of California Press.
- Hou, L., and P. G. P. Ericson. 2002. A Middle Eocene shorebird from China. *Condor* 104:896-899.
- Howard, H. 1929. The avifauna of Emeryville shellmound. University of California Publications in Zoology 32:301-394.
- Howard, H. 1949. New avian records for the Pliocene of California. Carnegie Institute of Washington Publications, Contributions to Paleontology 584:177-199.
- Howard, H. 1953. An early bird. *Los Angeles County Museum Quarterly* 10:12-13.
- Howard, H. 1966. A possible ancestor of the Lucas Auk (Family: Mancallidae) from the Tertiary of Orange County, California. *Los Angeles County Museum Contributions in Science* 101:1-8.
- Howard, H. 1968. Tertiary birds from Laguna Hills, Orange County, California. *Los Angeles County Museum Contributions to Science* 142:1-21.
- Howard, H. 1970. A review of the extinct avian genus *Mancalla*. *Los Angeles County Museum Contributions in Science* 203:1-12.
- Howard, H. 1971. Pliocene avian remains from Baja California. *Los Angeles County Museum Contributions to Science* 217:1-17.
- Howard, H. 1976. A new species of flightless auk from the Miocene of California

- (Alcidae: Mancallinae). pgs.141-146 in *Collected Papers in Avian Paleontology Honoring the 90<sup>th</sup> Birthday of Alexander Wetmore*. S. L. Olson (Ed.). Smithsonian Contributions to Paleobiology 27.
- Howard, H. 1978. Late Miocene marine birds from Orange County, California. *Natural History Museum of Los Angeles County Contributions to Science* 290:1-26.
- Howard, H. 1981. A new species of murre, genus *Uria*, from the Late Miocene of California. *Bulletin of the Southern California Academy of Science* 80:1-12.
- Howard, H. 1982. Fossil birds from the Tertiary marine beds at Oceanside, San Diego County, California, with descriptions of two new species of the genera *Uria* and *Cepphus* (Aves: Alcidae). *Natural History Museum of Los Angeles County Contributions to Science* 341:1-15.
- Howard, H., and L. G. Barnes. 1987. Middle Miocene marine birds from the foothills of the Santa Ana Mountains, Orange County, California. *Natural History Museum of Los Angeles County Contributions to Science* 383:1-9.
- Huddelstun, P. F., and J. H. Hetrick. 1986. Upper Eocene stratigraphy of central and eastern Georgia. *Georgia Geologic Survey Bulletin* 95:1-78.
- Hudson, G. E., K. M. Hoff, J. Vanden-Berge, and E. C. Trivette. 1969. A numerical study of the wing and leg muscles of the Lari and Alcae. *Ibis* 111:459-524.
- Huelsenbeck, J. P. 1991. When are fossils better than extant taxa in phylogenetic analysis? *Systematic Zoology* 40:458-469.
- Huelsenbeck, J. P., J. J. Bull, and C.W. Cunningham. 1996. Combining data in phylogenetic analysis. *Trends in Ecology & Evolution* 11:152-158.
- Huelsenbeck J. P., B. Larget, R. E. Miller, and F. Ronquist. 2002. Potential applications and pitfalls of Bayesian inference of phylogeny. *Systematic Biology* 51:673-688.
- Huelsenbeck J. P., F. Ronquist, R. Nielsen, and J. P. Bollback. 2001. Bayesian inference of phylogeny and its impact on evolutionary biology. *Science* 294:2310.
- Hug, L. A., and A. J. Roger. 2007. The impact of fossils and taxon sampling on ancient molecular dating analyses. *Molecular Biology and Evolution* 24:1889-1897.
- Hugueney, M., D. Berthet, A. Boderat, F. Escuillié, C. Mourer-Chauviré, and A. Wattinne. 2003. The Oligocene-Miocene boundary in Limagne: faunal changes in the mammals, birds and ostracods from the different levels of Billy-Créchy



- (Allier, France). *Geobios* 36:719-731.
- Huxley, T. 1867. On the classification of birds: and on the taxonomic value of the modifications of certain of the cranial bones observable in the class. *Proceedings of the Zoological Society of London* 1867:415-472.
- Hyrenbach, D. K., and R. R. Veit. 2003. Ocean warming and seabird communities of the southern California current system (1987-98): response at multiple temporal scales. *Deep Sea Research II* 50:2537-2565.
- Inc. SPSS. 2007. SPSS v16. Available at <http://www.spss.com>.
- Ingle, J. C. Jr., 1979. Biostratigraphy and paleoecology of Early Miocene through Early Pleistocene benthonic and planktonic foraminifera, San Joaquin Hills-Newport Bay-Dana Point area, Orange County, California. pgs. 53-77 in *Miocene Lithofacies and Depositional Environments, Coastal Southern California and Northwestern Baja California*. C. J. Stuart (Ed.). Pacific Section SEPM.
- International Commission on Zoological Nomenclature. 1977. Notices prescribed by the International Congress of Zoology. *The Bulletin of Zoological Nomenclature* v4, part 1:1-64.
- International Commission on Zoological Nomenclature. 2000. *International Code of Zoological Nomenclature*, 4th ed., International Trust For Zoological Nomenclature, 306pp.
- International Union for Conservation of Nature. 2010. Red list of threatened species v2101.4. [www.iucnredlist.org/](http://www.iucnredlist.org/).
- Johansson, L. C., and B. S. W. Aldrin. 2002. Kinematics of diving Atlantic Puffins (*Fratercula arctica* L.): evidence for an active upstroke. *Journal of Experimental Biology* 205:371-378.
- Jones, I. L., F. M. Hunter, and G. J. Robertson. 2002. Annual adult survival of Least Auklets (Aves, Alcidae) varies with large-scale climatic conditions of the North Pacific Ocean. *Oecologia* 133:38-44.
- Kameo, K., and T. Sato. 2000. Biogeography of Neogene calcareous nannofossils in the Caribbean and the eastern equatorial Pacific - floral response to the emergence of the Isthmus of Panama. *Marine Micropaleontology* 39:201-218.
- Kearney, M. 2002. Fragmentary taxa, missing data, and ambiguity: mistaken assumptions and conclusions. *Systematic Biology* 51:369-381.

- Kearney, M., and J. M. Clark. 2003. Problems due to missing data in phylogenetic analyses including fossils: a critical review. *Journal of Vertebrate Paleontology* 23:263-274.
- Kelley, D. C., T. J. Bralower, and J. C. Zachos. 1998. Evolutionary consequences of the latest Paleocene thermal maximum for tropical planktonic foraminifera. *Palaeogeography Palaeoclimatology Palaeoecology* 141:139-161.
- Kennett, J. P., and L. D. Scott. 1991. Abrupt deep-sea warming, palaeoceanographic changes and benthic extinctions at the end of the Paleocene. *Nature* 353:225-229.
- Kern, J. P., and E. R. Wicander. 1974. Origin of bathymetrically displaced marine invertebrate fauna in the upper part of the Capistrano Formation (lower Pliocene), southern California. *Journal of Paleontology* 48:495-505.
- Kerr, K. C. R., M. Y. Stoeckle, C. J. Dove, L. A. Weigt, C. M. Francis, and P. D. N. Hebert. 2007. Comprehensive DNA barcode coverage of North American birds. *Molecular Ecology Notes* 7:535-543.
- Kidd, M. G., and V. Friesen. 1998. Sequence variation in the guillemot (*Alcidae: Cepphus*) mitochondrial control region and its nuclear homolog. *Molecular Biology and Evolution* 15:61-70.
- Kitaysky, A. S., and E. G. Golubova. 2000. Climate change causes contrasting trends in reproductive performance of planktivorous and piscivorous alcids. *Journal of Animal Ecology* 69:248-262.
- Klicka, J. and R. M. Zink. 1997. The importance of recent ice ages in speciation: a failed paradigm. *Science* 277:1666-1669.
- Kluge, A. G., 1989. A concern for evidence and a phylogenetic hypothesis of relationships among *Epicrates* (Boidae, Serpentes). *Systematic Zoology* 38:7-25.
- Kluge, A. G. 1998. Total evidence or taxonomic congruence: cladistics or consensus classification. *Cladistics* 14:151-158.
- Kluge, A. G., and J. S. Farris. 1969. Quantitative phyletics and the evolution of the anurans. *Systematic Zoology* 18:1-32.
- Köenig, E. 1825. *Icones fossilium sectiles. Centuria prima*, London.
- Kohl, R. F. 1974. A new Late Pleistocene fauna from Humboldt County, California.

Veliger 17:211-219.

- Kohno, N. 1997. Latest Miocene vertebrate fauna from Sendai, Japan. *Journal of Vertebrate Paleontology Supplement* 17:57.
- Konyukhov, N. B. 2002. Possible ways of spreading and evolution in the alcids. *Biology Bulletin* 29:447-454.
- Kovacs, E. C., and R. A. Meyers. 2000. Anatomy and histochemistry of flight muscles in a wing-propelled diving bird, the Atlantic Puffin, *Fratercula arctica*. *Journal of Morphology* 244:109-125.
- Kozlova, E. V. 1957. Fauna of USSR birds, v2, no.3, Charadriiformes, Suborder Alcae. *Zoological Institute of the Academy of Sciences, new series* 65:1-140.
- Krantz, D. E. 1991. A chronology of Pliocene sea-level fluctuations: the U.S. middle Atlantic coastal plain record. *Quaternary Science Review* 10:163-174.
- Krijgsman, W., C. G. Langereis, R. Daams, and A. J. van der Meulen. 1994. Magnetostratigraphic dating of the Middle Miocene climate change in the continental deposits of the aragonian type area in the Calatayud-Teruel basin (Central Spain). *Earth and Planetary Science Letters* 128:513-526.
- Ksepka, D. T., S. Bertelli, and N. Giannini. 2006. The phylogeny of the living and fossil Sphenisciformes (penguins). *Cladistics* 22:412-441.
- Ksepka, D. T., and J. A. Clarke. 2010. The basal penguin (Aves: Sphenisciformes) *Perudyptes devriesi* and a phylogenetic evaluation of the penguin fossil record. *Bulletin of the American Museum of Natural History* 337:1-77.
- Kuroda, N. 1954. On some osteological and anatomical features of Japanese Alcidae (Aves). *Japanese Journal of Zoology* 11:311-327.
- Kuroda, N. 1955. Additional notes on the osteology of the Alcidae (Aves). *Annotationes Zoologicae Japonenses* 28:110-113.
- Lambrecht, K. 1933. *Handbuch der Palaeornithologie*. Verlag von gerbrüder borntraeger in Berlin W 35. Reprinted by Neudruck A Asher and Company, Amsterdam, 1964.
- Lariviere J., C. Ravelo, P. B. Talmage, M. W Lyle, and A. Olivarez-Lyle. 2009. Sea surface temperatures of the subtropical north Pacific since the Late Miocene: cooling trends and mid-Pliocene warmth. *American Geophysical Union Fall Meeting 2009*, abstract #PP41A-1500.

- Lawrence, K. T., Z. Liu, and T. D. Herbert. 2006. Evolution of the eastern tropical Pacific through Plio-Pleistocene glaciation. *Science* 312:79-83.
- Leach W. E., 1820. Eleventh Room. pgs. 65-68 *in* Synopsis of the Contents of the British Museum, 17<sup>th</sup> ed. Richard and Arthur Taylor, London.
- Lear, C. H., H. Elderfield, and P. A. Wilson. 2000. Cenozoic deep-sea temperatures from Mg/Ca in benthic foraminiferal calcite. *Science* 287:269-272.
- Lee, D. S. 2009. Species Profiles of Western North Atlantic Seabirds. Prepared for the Pelagic Longline Observer Program, Southeast Fisheries Science Center, Miami, FL., NOAA Fisheries National Seabird Program. 84pp.
- Legendre, S., and F. L  v  que. 1997. Etalonnage de l'  chelle biochronologique mammalienne du Pal  og  ne d'Europe occidentale: vers une integration    l'  chelle globale. pgs. 461-473 *in* Actes du Congr  s Biochro-M'97. J. -P. Aguilar, S. Legendre, and J. Michaux (Eds.). M  moires et Travaux de l'Ecole Pratique des Hautes Etudes, Institut de Montpellier 21.
- Levin, S. A. 1970. Community equilibria and stability, and an extension of the competitive exclusion principle. *American Naturalist* 104:413-423.
- Lewis, P. O. 2001a. A likelihood approach to estimating phylogeny from discrete morphological character data. *Systematic Biology* 50:913-925.
- Lewis, P. O. 2001b. Phylogenetic systematics turns over a new leaf. *Trends in Ecology and Evolution* 16:30-37.
- Liebers, D., P. de Knijff, and A. J. Helbig. 2004. The herring gull complex is not a ring species. *Proceedings Biological Sciences* 271:893-901.
- Link, H. F. 1806. *Uber Naturphilosophie*. In der Stillerschen Buchhandlung.
- Linnaeus, C. 1758. *Systema naturae per regna tria naturae, secundum classes, ordines, genera, species, cum characteribus, differentiis, synonymis, locis*. Editio decima, reformata. Holmiae. Laurentii Salvii. [1-4], 1-824.
- Liu, Z., M. Pagani, D. Zinniker, R. DeConto, M. Huber, H. Brinkhuis, S. R. Shah, R. M. Leckie, and A. Pearson. 2009. Global cooling during the Eocene-Oligocene climate transition. *Science* 323:1187-1190.
- Livezey, B. C. 1988. Morphometrics of flightlessness in the Alcidae. *Auk* 105:681-698.
- Livezey, B. C. 1989. Morphometric patterns in recent and fossil penguins (Aves,

- Sphenisciformes). *Journal of the Zoological Society of London* 219:269-307.
- Livezey, B. C. 2009. Phylogenetics of modern shorebirds (Charadriiformes) based on phenotypic evidence: I, characterization. *Bulletin of the Carnegie Museum of Natural History* 40:1-96.
- Livezey, B. C. 2010. Phylogenetics of modern shorebirds (Charadriiformes) based on phenotypic evidence: II, analysis and discussion. *Zoological Journal of the Linnean Society* 160:567-618.
- Livezey, B. C., and P. S. Humphrey. 1986. Flightlessness in steamer ducks (Anatidae: *Tachyeres*): its morphological bases and probable evolution. *Evolution* 40:540-558.
- Livezey, B. C., and R. L. Zusi. 2006. Higher-order phylogeny of modern birds (Theropoda, Aves: Neornithes) based on comparative anatomy: I. methods and characters. *Bulletin of the Carnegie Museum of Natural History* 37.
- Livezey B. C., and R. L. Zusi. 2007. Higher-order phylogeny of modern birds (Theropoda, Aves: Neornithes) based on comparative anatomy: II. analysis and discussion. *Zoological Journal of the Linnean Society* 149:1-95.
- Lovvorn, J. R. 2001. Upstroke Thrust, Drag Effects, and Stroke-glide Cycles in Wing-propelled Swimming by Birds. *American Zoologist* 41:154-165.
- Lowe, P. R. 1931. On the relationships of the Gruimorphae to the Charadriimorphae and Rallimorphae, with special reference to the taxonomic position of Rostratulidae, Jacanidae, and Burnhinidae (Oedienemidae *olim*): with a suggested new order (Telmatomorphae). *Ibis* 1931:491-534.
- Lucas, F. A. 1890. The expedition to Funk Island, with observations upon the history and anatomy of the Great Auk. pgs. 493-529 *in* Report of the United States National Museum for 1887-1888.
- Lucas, F. A. 1901. A flightless auk, *Mancalla californiensis*, from the Miocene of California. *Proceedings of the United States National Museum* 24:113-134.
- Lunt, D. J., P. J. Valdes, A. Haywood, and I. C. Rutt. 2008. Closure of the Panama Seaway during the Pliocene: implications for climate and Northern Hemisphere glaciation. *Climate Dynamics* 30:1-18.
- Maddison, W. P. 2000. Testing character correlation using pairwise comparisons on a phylogeny. *Journal of Theoretical Biology* 202:195-204.

- Maddison D. R., and W. P. Maddison. 2005. MacClade v4.08. Sinauer Associates, Sunderland, Massachusetts.
- Marlow, J. R., C. B. Lange, G. Wefer, and A. Rosell-Melé. 2000. Upwelling intensification as part of the Pliocene-Pleistocene climate transition. *Science* 290:2288-2291.
- Marples, B. J. 1952. Early Tertiary penguins of New Zealand. *New Zealand Geological Survey Paleontological Bulletin* 20:1-66.
- Marsh, O. C. 1870. Exhibition of a series of specimens of the remains of birds from the Cretaceous and Tertiary of the United States. *Proceedings of the Academy of Natural Sciences of Philadelphia* 1870:204-217.
- Marsh, O. C. 1872. Notice of some new Tertiary and post-Tertiary birds. *American Journal of Science* s3 4:256-262.
- Martin, J. W. R., C. A. Walker, R. Bonser, and G. J. Dyke. 2001. A new species of large auk from the Pliocene of Belgium. *Oryctos* 3:53-60.
- May, R. M., J. H. Lawton, and N. E. Stork. 1995. Assessing extinction rates. pgs. 1-24 *in* *Extinction Rates*. J. H. Lawton and R. M. May (Eds.). Oxford University Press, New York.
- Mayr, G. 2000. Charadriiform birds from the Early Oligocene of Céreste (France) and the Middle Eocene of Messel (Hessen, Germany). *Geobios* 33:625-636.
- Mayr, G. 2004. Old world fossil record of modern-type hummingbirds. *Science* 304:861-864.
- Mayr, G. 2005. The Paleogene fossil record of birds in Europe. *Biological Review* 80:515-542.
- Mayr, G. 2007. New specimens of Eocene stem-group psittaciform bird may shed light on the affinities of the first named fossil bird, *Halcyornis toliapicus*. *Nues Jahrbuch für Geologie und Paläeontologie* 244: 207-213.
- G. Mayr. 2008. Phylogenetic affinities and morphology of the Late Eocene anseriform bird *Romainvillia stehlini* Lebedinsky, 1927. *Nues Jahrbuch für Geologie und Paläeontologie* 248:365-380.
- Mayr, G. 2009. *Paleogene Fossil Birds*. Springer-Verlag, Heidelberg, 262pp.
- Mayr, G. 2011. The phylogeny of charadriiform birds (shorebirds and allies) - reassessing

- the conflict between morphology and molecules. *Zoological Journal of the Linnean Society* DOI: 10.1111/j.1096-3642.2010.00654.x.
- Mayr, G., and J. Clarke. 2003. The deep divergences of neornithine birds: a phylogenetic analysis of morphological characters. *Cladistics* 19:527-553.
- Mayr, G., and C. W. Knopf. 2007. A stem lineage representative of buttonquails from the lower Oligocene of Germany - fossil evidence for a charadriiform origin of the Turnicidae. *Ibis* 149:774-782.
- Mayr, G., and R. Smith. 2001. Ducks, rails, and limicoline waders (Aves: Anseriformes, Gruiformes, Charadriiformes) from the lowermost Oligocene of Belgium. *Geobios* 34:547-561.
- McNab, B. K. 1994. Energy conservation and the evolution of flightlessness in birds. *American Naturalist* 144:628-642.
- Merrem, B. 1788. Versuch eines Grundrisses zur allgemeinen Geschichte und natürlichen Eintheilung der Vogel. *Tentamen Naturalis Systematis Avium* 1:7,13,20.
- Mickevich, M. F. 1978. Taxonomic congruence. *Systematic Biology* 27:143.
- Mickevich, M. F., and L. R. Parenti. 1980. *Review of* The phylogeny of the Charadriiformes (Aves): a new estimate using the method of character compatibility analysis. J.G. Strauch, Jr. 1978. *Transactions of the Zoological Society of London* 34:263-345. *Systematic Zoology* 29:108-113.
- Miller, A. H. 1931. An auklet from the Eocene of Oregon. University of California Publications, *Bulletin of the Department of Geological Sciences* 20:23-26.
- Miller, K. G., J. D. Wright, and J. V. Browning. 2005. Visions of ice sheets in a greenhouse world. *Marine Geology* 217:215-231.
- Miller, K. G., J. D. Wright, M. E. Katz, B. S. Wade, J. V. Browning, B. S. Cramer, and Y. Rosenthal. 2009. Climate threshold at the Eocene-Oligocene transition: Antarctic ice sheet influence on ocean circulation. *Geological Society of America Special Paper* 452:169-178.
- Miller, L. 1925. Avian remains from the Miocene of Lompoc, California. *Carnegie Institution of Washington, Contributions to Paleontology* 349:107-117.
- Miller, L. 1933. The Lucas auk of California. *Condor* 35:34-35.

- Miller, L. 1937. An extinct puffin from the Pliocene of San Diego, California. Transactions of the San Diego Society of Natural History 8:375-378.
- Miller, L. 1946. The Lucas auk appears again. Condor 48:32-36.
- Miller, L. 1956. A collection of bird remains from the Pliocene of San Diego California. Proceedings of the California Academy of Sciences 28:615-621.
- Miller, L., and R. I. Bowman. 1958. Further bird remains from the San Diego Pliocene. Los Angeles County Museum Contributions in Science 20:4-15.
- Miller, L., and H. Howard, 1949. The flightless Pliocene bird *Mancalla*. Carnegie Institution of Washington Publications, Contributions to Paleontology 584:203-228.
- Milne-Edwards, A., 1863. Sur la distribution géologique des oiseaux fossiles et description de quelques espèces nouvelles. Comptes Rendus Hebdomadaires des Séances de l'Académie des Sciences Paris 56:1219-1222.
- Milne-Edwards, A., 1867-1871. Recherches anatomiques et paléontologiques pour servir à l'histoire des oiseaux fossiles de la France. Victor Masson et Fils, Paris 1, 474 p., 2 ; 627 p., atlas.
- Mlikovsky, J., and J. Kovar. 1987. Eine neue alkenart (Aves:Alcidae) aus dem ober-Oligozän osterreichs. Annalen des Naturhistorischen Museums in Wien (A) 88:131-147.
- Moe, B., L. Stempniewicz, D. Jakubas, F. Angelier, O. Chaste, F. Dinussen, G. W. Gabrielsen, F. Hanssen, N. J. Karnovsky, B. Rønning, J. Welcker, K. Wojczulanis-Jakubas, C. Bech. 2009. Climate change and phenological responses of two seabird species breeding in the high-Arctic. Marine Ecology Progress Series 393:235-246.
- Moehring, P. H. G. 1758. Aviumgenera [Latin MS in 1752, 58pp. Bremen]. Published Dutch translation, C.Nozeman and A.Vosmaer (Eds.). Geslachten der Vogelen. Pieter Meijer, Amsterdam.
- Moen, S. M. 1991. Morphologic and genetic variation among breeding colonies of the Atlantic Puffin (*Fratercula arctica*). Auk 108:755-763.
- Molnar, P. 2008. Closing of the Central American Seaway and the ice age: a critical review. Paleooceanography 23:doi: 10.1029/2007PA001574.
- Montevecchi, W. A. 1993. Birds as indicators of change in marine prey stocks. pgs. 217-



266 *In* Birds as Indicators of Environmental Change. Furness R. W and J. J. D. Greenwood (Eds.), Chapman and Hall, London.

- Moum, T., U. Årnason, and E. Årnason. 2002. Mitochondrial DNA sequence evolution and phylogeny of the Atlantic Alcidae, including the extinct Great Auk (*Pinguinus impennis*). *Molecular Biology and Evolution* 19:1434-1439.
- Moum, T., S. Johansen, K. E. Erikstad, and J. F. Piatt. 1994. Phylogeny and evolution of the auks (subfamily Alcinae) based on mitochondrial DNA sequences. *Proceedings of the National Academy of Sciences* 91:7912-7916.
- Mourer-Chauvire, C., D. Berthet, and M. Hugueney. 2004. The Late Oligocene birds of the Cr  chy quarry (Allier, France) with a description of two new genera (Aves: Pelicaniformes: Phalacrocoracidae, and Anseriformes: Anseranatidae). *Senckenbergiana Lethaea* 84:303-315.
- Mourer-Chauvir  , C., and D. Geraads. 2008. The Struthionidae and Pelagornithidae (Aves: Struthioniformes, Odontopterygiformes) from the late Pliocene of Ahl Al Oughlam, Morocco. *Oryctos* 7:169-187.
- Mourer-Chauvir  , C., and D. Geraads. 2010. The upper Pliocene avifauna of Ahl al Oughlam, Morocco: systematics and biogeography. *Records of the Australian Museum* 62:157-184.
- M  ller, J., and R. R. Reisz. 2005. Four well-constrained calibration points from the vertebrate fossil record for molecular clock estimates. *BioEssays* 27:1069-1075.
- Naafs, B. D. A., R. Stein, J. Hefter, N. Kh  lifi, S. De Schepper, and G. H. Haug. 2010. Late Pliocene changes in the north Atlantic current. *Earth and Planetary Science Letters* 298:434-442.
- Naumann, J. 1821. *Isis*. 781pp.
- Near, T. J., and M. J. Sanderson. 2004. Assessing the quality of molecular divergence time estimates by fossil calibrations and fossil-based model selection. *Philosophical Transactions of the Royal Society of London B* 359:1477-1483.
- Nettleship, D. N., and T. R. Birkhead (Eds.). 1985. *The Atlantic Alcidae: the evolution, distribution, and biology of the auks inhabiting the Atlantic Ocean and adjacent water areas*. Academic Press, London and Orlando, 574pp.
- Nesbitt, S. J., and M. R. Stocker. 2008. The vertebrate assemblage of the Late Triassic Canjilon Quarry (northern New Mexico, USA), and the importance of apomorphy-based assemblage comparisons. *Journal of Vertebrate Paleontology*

28:1063-1072.

- Nixon, K. C., and Q. D. Wheeler. 1992. Extinction and the origin of species. pgs. 119-143 *in* Extinction and Phylogeny. M. J. Novacek and Q. D. Wheeler (Eds.). Columbia University Press, New York, 253pp.
- National Oceanic and Atmospheric Association. 2011. Ocean Service Education. [http://oceanservice.noaa.gov/educational/kits/currents/media/supp\\_cur04a.html](http://oceanservice.noaa.gov/educational/kits/currents/media/supp_cur04a.html).
- Norell, M. A. 1989. Late Cenozoic lizards of the Anza Borrego Desert, California. Natural History Museum of Los Angeles County Contributions in Science 414:1-31.
- Norell, M. A. 1992. The effect of phylogeny on temporal diversity and evolutionary tempo. pgs. 89-118 *in* Extinction and Phylogeny, M. J. Novacek and Q. D. Wheeler (Eds.), Columbia University Press, New York.
- Nunes, F. and R. D. Norris. 2006. Abrupt reversal in ocean overturning during the Palaeocene/Eocene warm period. Nature 439:60-63.
- Nylander, J. A. 2008. MrModeltest v2.3. Program distributed by the author. Evolutionary Biology Centre, Uppsala University.
- Nylander J. A., F. Ronquist, J. P. Huelsenbeck, and J. L. Nieves-Aldrey. 2004. Bayesian phylogenetic analysis of combined data. Systematic Biology 53:47-67.
- Ogg, J. G., G. Ogg, and F. M. Gradstein. 2008. The Concise Geologic Timescale. Cambridge University Press, 184pp.
- Olson, S. L. 1977. A Great Auk, *Pinguinis* (sic), from the Pliocene of North Carolina (Aves:Alcidae). Proceedings of the Biological Society of Washington 90:690-697.
- Olson, S. L. 1981. A third species of *Mancalla* from the Late Pliocene San Diego Formation of California (Aves: Alcidae). Journal of Vertebrate Paleontology 1:97-99.
- Olson, S. L. 1984. A brief synopsis of the fossil birds from the Pamunkey River and other Tertiary marine deposits in Virginia. pgs. 217-223 *in* Stratigraphy and Paleontology of the Outcropping Tertiary Beds in the Pamunkey River Region, Central Virginia Coastal Plain. Guidebook for Atlantic Coastal Plain Geological Association 1984 Field Trip, L. W. Ward and K. Krafft, (Eds.). Atlantic Coastal Plain Geological Association, Norfolk, Virginia.

- Olson, S. L. 1985. The fossil record of birds. pgs. 79-252 *in* Avian Biology vol. 8. D. S. Farmer and A. King, (Eds.). Academic Press. Orlando, Florida.
- Olson, S. L. 1999. Early Eocene birds from eastern North America: a faunule from the Nanjemoy Formation of Virginia. pgs. 123-132 *in* Early Eocene Vertebrates and Plants From the Fisher/Sullivan Site (Nanjemoy Formation) Stafford County, Virginia. R. E. Weems and G. J. Grimsley (Eds.). Virginia Division of Mineral Resources Publication 152.
- Olson, S. L. 2007. *Alca antiqua* (Marsh, 1870), an invalid combination for a fossil auk (Alcidae). Bulletin of the British Ornithological Club 127:225.
- Olson S. L., and J. N. Lund. 2007. Whalers and woggins: a new vocabulary for interpreting some early accounts of the Great Auk and penguins. Archives of Natural History 34:69-78.
- Olson, S. L., and D. C. Parris. 1987. The Cretaceous birds of New Jersey. Smithsonian Contributions to Paleobiology 63:1-22.
- Olson, S. L., and P. Rasmussen. 2001. Miocene and Pliocene Birds from the Lee Creek Mine, North Carolina. Smithsonian Contributions to Paleobiology 90:233-365.
- Ono, K., and Y. Hasegawa. 1991. Vertebrate fossils of the Iwaki Formation, 1; avian fossils. pgs. 6-8, 15-16 *in* The Excavation Research Report of the Animal Fossils of the Iwaki Formation, Iwaki City, Japan. Y. Koda et al. (Eds.).
- Pagel, M. 1994. Detecting correlated evolution on phylogenies: a general method for the comparative analysis of discrete characters. Proceedings of the Royal Society B 255:37-45.
- Pallas, P. S. 1769. Spicilegia zoological quibus novae imprimis et obscurae animalium species iconibus, descriptionibus atque commentariis illustrantur.
- Pallas, P. S. 1811. Zoographia rosso-asiatica: sistens omnium animalium in extenso Imperio rossico, et adjacentibus maribus observatorum recenssionem, domicilia, mores et descriptions, anatomen atque icons plurimorum.
- Parmley, D., and J. A. Holman. 2003. *Nebraskophis* HOLMAN from the late Eocene of Georgia (USA), the oldest known North American colubrid snake. Acta Zoologica Cracoviensia 46:1-8.
- Paton, T. A., and A. J. Baker. 2006. Sequences from 14 mitochondrial genes provide a well-supported phylogeny of the charadriiform birds congruent with the nuclear RAG-1 tree. Molecular Phylogenetics and Evolution 39:657-667.

- Paton, T. A., A. J. Baker, J. G. Groth, and G. F. Barrowclough. 2003. RAG-1 sequences resolve phylogenetic relationships within charadriiform birds. *Molecular Phylogenetics and Evolution* 29:268-278.
- Paton, T. A., O. Haddrath, and A. J. Baker. 2002. Complete mitochondrial DNA genome sequences show that modern birds are not descended from transitional shorebirds. *Proceedings of the Royal Society of London B* 269:839-846.
- Pennycuik, C. J. 1975. Mechanics of flight. pgs.1-75 in *Avian Biology* v5. D. S. Farner and J. R. King (Eds.), Academic Press, New York.
- Pennycuik, C.J. 1987. Flight of auks (Alcidae) and other northern Pacific seabirds compared with southern Procellariiformes: ornithodolite observations. *Journal of Experimental Biology* 128:335-347.
- Pereira, S. L., and A. J. Baker. 2006. A mitogenic timescale for birds detects variable phylogenetic rates of molecular evolution and refutes the standard molecular clock. *Molecular Biology and Evolution* 23:1731-1740.
- Pereira, S. L., and A. J. Baker. 2008. DNA evidence for a Paleocene origin of the Alcidae (Aves: Charadriiformes) in the Pacific and multiple dispersals across northern oceans. *Molecular Phylogenetics and Evolution* 46:430-455.
- Piat, J. F., and D. N. Nettleship. 1985. Diving depth of four alcids. *Auk* 102:293-297.
- Pontoppidan, 1763. Den Danske atlas eller Konge-Riget Dannemark, med dets naturlige egenskaber, elementer, indbyggere, værter, dyr og andre affødninger, dets gamle tildragelser og nærværende omstændigheder i alle provintzer, stæder, kirker, slotte og herre-gaarde. Forestillet ved en udførlig lands-beskrivelse, saa og oplyst med dertil forfærdigede land-kort over enhver provintz, samt ziret med stædernes prospector, grund-ridser, og andre merkværdige kaabber-stykker. Efter Søy-kongelig allernaadigst befalning. Tomus I. - pp. [1-6], I-XL [= 1-40], [1-4], 1-723, Tab. I-XXX [= 1-30], Kiøbenhavn. (Godiche).
- Popenoe, P. 1985. Cenozoic depositional and structural history of the North Carolina margin from seismic-stratigraphic analyses. pgs. 125-187 in *Geologic Evolution of the United States Atlantic Margin*. C. Wylie Poag (Ed.). Van Nostrand Reinhold Company, New York.
- Portis, A. 1888. Contribuzioni alla ornitologica italiana, parte II. *Memorie della Reale Accademia delle Scienze di Torino*, series 2 38:181-203.

- Portis, A. 1891. Gli ornitoliti del vardonio superiore e di alcune altre localita plioceniche di Toscana. Memorie del Istituto Superiore de Perfeziamento (Firenze) 1891:1-20.
- Post, W., and S. Bogart. 2007. A specimen of the Common Murre (*Uria aalge*) from South Carolina: southernmost Atlantic coast occurrence since the Late Pleistocene. *Chat* 71:127-129.
- Prince, P. A., and M. P. Harris. 1988. Food and feeding ecology of breeding Atlantic alcids and penguins. pgs. 1195-1204 *in* Proceedings of the 19<sup>th</sup> International Ornithological Congress. University of Ottawa Press, Ottawa, Canada.
- Prothero, D. A. 1994. The Eocene-Oligocene transition: paradise lost. Columbia University Press, New York. 291pp.
- Prothero, D. A., and W. A. Berggren (Eds.). 1992. Eocene-Oligocene Climatic and Biotic Evolution. Princeton University Press, Princeton, NJ. 568pp.
- Purdy, R., V. P. Schneider, S. P. Applegate, J. H. McLellan, R. L. Meyer, and B. H. Slaughter. 2001. The Neogene sharks, rays, and bony fishes from Lee Creek Mine, Aurora, North Carolina. *Smithsonian Contributions to Paleobiology* 90:71-202.
- Raikow, R. J., L. Bicanovsky, and A. H. Bledsoe. 1988. Forelimb joint mobility and the evolution of wing-propelled diving in birds. *Auk* 105:446-451.
- Rambaut, A. 2002. Se-AI v2.0a11. Available from <http://tree.bio.ed.ac.uk/software/seal>.
- Rambaut, A. 2009. FigTree v1.3.1. available at <http://tree.bio.ed.ac.uk/software/>.
- Rambaut, A., and L. Bromham. 1998. Estimating divergence dates from molecular sequences. *Molecular Biology and Evolution* 15:442-448.
- Rambaut, A., and A. J. Drummond. 2009. Tracer v1.5 MCMC Trace Analysis Package. available at <http://tree.bio.ed.ac.uk/software/>.
- Rambaut, A., and A. J. Drummond. 2010. TreeAnnotator v1.6.1. available at <http://tree.bio.ed.ac.uk/software/>.
- Rannala, B., and Z. Yang. 1996. Probability distribution of molecular evolutionary trees: a new method of phylogenetic inference. *Journal of Molecular Evolution* 43:304-311.
- Rasmussen, D. T., S. L. Olson, and E. L. Simons. 1987. Fossil birds from the Oligocene

- Jebel Qatrani Formation, Fayum Province, Egypt. Smithsonian Contributions to Paleobiology 62.
- Ray, C. E. (Ed.). 1983 Geology and Paleontology of the Lee Creek Mine, North Carolina, I. Smithsonian Contributions to Paleobiology 53, 529pp.
- Ray, C. E. (Ed.). 1987 Geology and Paleontology of the Lee Creek Mine, North Carolina, II. Smithsonian Contributions to Paleobiology 61, 283pp.
- Ray, C. E., and D. J. Bohaska (Eds.). 2001. Geology and Paleontology of the Lee Creek Mine, North Carolina, III. Smithsonian Contributions to Paleobiology 90, 365 pp.
- Ray, C. E., and D. J. Bohaska, I. A. Koretsky, L. W. Ward, and L. G. Barnes (Eds.). 2008. Geology and Paleontology of the Lee Creek Mine, North Carolina, IV. Virginia Museum of Natural History Special Publication 14, 517 pp.
- Ravelo, A. C., D. H. Andreasen, M. Lyle, A. O. Lyle, and M. W. Wara. 2004. Regional climate shifts caused by gradual global cooling in the Pliocene epoch. *Nature* 429:263-267.
- Ravelo, A. C., P. S. Dekens, and M. McCarthy. 2006. Evidence for El niño-like conditions during the Pliocene. *GSA Today* 16:4-11.
- Reisz, R. R., and J. Müller. 2004. Molecular timescales and the fossil record: a paleontological perspective. *Trends in Genetics* 20:237-241.
- Repenning, C. A., and R. H. Tedford. 1977. Otariid seals of the Neogene. Geological Survey Professional Paper 992. United States Government Printing Office, Washington, DC.
- Ridgway, R. 1919. The birds of north and middle America. United States National Museum Bulletin 50:700-797.
- Riggs, S. R. 1984. Paleooceanographic model of Neogene phosphorite deposition, U.S. continental margin. *Science* 223:123-131.
- Roger, A. J., and L. A. Hug. 2006. The origin and diversification of eukaryotes: problems with molecular phylogenetics and molecular clock estimation. *Philosophical Transactions of the Royal Society B* 362:1039-1054.
- Rokas, A., B. L. Williams, N. King, and S. B. Carroll. 2003. Genome approaches to resolving incongruence in molecular phylogenies. *Nature* 425:798-804.

- Ronquist, F., and J. P. Huelsenbeck. 2003. Mr. Bayes 3: Bayesian phylogenetic analysis under mixed models. *Bioinformatics* 19:1572-1574.
- Rowe, T. 1988. Definition, diagnosis and origin of Mammalia. *Journal of Vertebrate Paleontology* 8:241-264.
- Rutschmann, F. 2006. Molecular dating of phylogenetic trees: a brief review of current methods that estimate divergence times. *Diversity and Distributions* 12:35-48.
- Salomonsen, F. 1944. The Atlantic Alcidae. Göteborgs Kungl. Vetenskaps-och Vitterhets-Samhälles Handlingar. Sjätte Följden, Ser. B., Band 3, No. 5:1-138.
- Savadori, 1867. Descrizione di altre nuove specie di Uccelli esistenti nel Museo di Torino. Estratto dagli Atti della Società Italiana di Scienze Naturali, vol. viii.
- Sanchez-Marco, A. 2003. A paleospecies of *Alca* (Aves, Charadriiformes) in the Pliocene of Spain. *Nues Jahrbuch für Geologie und Paläeontologie* 5:314-320.
- Sanderson, M. J. 2002. Estimating absolute rates of molecular evolution and divergence times: a penalized likelihood approach. *Molecular Biology and Evolution* 19: 101-109.
- Sanderson, M. J., A. Purvis, and C. Henze. 1998. Phylogenetic supertrees: assembling the trees of life. *Trends in Ecology & Evolution* 13:105-109.
- Sandvik, H., K. E. Erikstad, R. T. Barrett, and N. G. Yoccoz. 2005. The effect of climate on adult survival in five species of north Atlantic seabirds. *Journal of Animal Ecology* 74:817-831.
- Sarnthein, M., M. Prange, A. Schmittner, B. Schneider, and M. Weinelt. 2009. Mid-Pliocene shifts in ocean overturning circulation and the onset of Quaternary-style climates. *Climates of the Past* 5:251-285.
- Schoell, M., S. Schouten, J. S. Sinninghe Damste, J. W. de Leeuw, and R. E. Summons. 1994. A molecular organic carbon isotope record of Miocene climate changes. *Science* 263:1122-1124.
- Schroeder, I. D., W. J. Sydeman, N. Sarkar, S. A. Thompson, S. J. Bograd, F. B. Schwing. 2009. Winter pre-conditioning of seabird phenology in the California Current. *Marine Ecology Progress Series* 393:211-223.
- Scotese, C. R. 2004. Cenozoic and Mesozoic palaeogeography: changing terrestrial biogeographic pathways. pgs. 9-26 in *Frontiers of Biogeography: new directions*

- in the geography of nature. M.V. Lomolino & L. R. Heaney (Eds.) Sinauer and Associates, Sunderland, Mass.
- Sealy, S. G. 1973. Adaptive differences in the breeding biology of the Alcidae. University of Michigan, PhD Dissertation, 283 pp.
- Sealy, S. G. (Ed.). 1990. Auks At Sea. Studies in Avian Biology, 14, 180pp.
- Sen, S., and L. Ginsburg. 2000. La magnetostratigraphie du site de Sansan pgs. 69-82 in La Faune Miocene de Sansan et son Environnement. L. Ginsburg (Ed.). Memoires du Museum National D'Histoire Naturelle, Tome 183, Publications Scientifiques du Museum, Paris, France.
- Shaul, S., and D. Graur. 2002. Playing chicken (*Gallus gallus*): methodological inconsistencies of molecular divergence date estimates due to secondary calibration points. Gene 300:59-61.
- Shufeldt, R. W. 1888. Contributions to the comparative osteology of arctic and sub-arctic waterbirds, Part 1. Journal of Anatomy and Physiology 23:1-39.
- Shufeldt, R. W. 1889. Contributions to the comparative osteology of arctic and sub-arctic waterbirds, Part 5. Journal of Anatomy and Physiology 23:165-186.
- Shufeldt, R. W. 1901. On the osteology and systematic position of the Alcae. American Naturalist 35:541-551.
- Shufeldt, R. W. 1915. Fossil birds in the Marsh collection of Yale University. Transactions of the Connecticut Academy of Science 19:1-110.
- Sibley, C. G., and J.E. Ahlquist. 1972. A comparative study of the egg white proteins of non-passerine birds. Peabody Museum of Natural History Bulletin 39, 322pp.
- Sibley C. G. and J. E. Ahlquist. 1990. Phylogeny and Classification of Birds: a study in molecular evolution. Yale University Press, New Haven, 976 pp.
- Simpson G. G. 1946. Fossil penguins. Bulletin of the American Museum of Natural History 87:1-99.
- Smith A. B., and K. J. Peterson. 2002. Dating the time of origin of major clades: molecular clocks and the fossil record. Annual Review of Earth and Planetary Sciences 30:65-88.
- Smith, A. G., Smith, D. G. and B. M. Funnell. 1994. Atlas of Mesozoic and Cenozoic Coastlines. Cambridge University Press, Cambridge, 99pp.



- Smith, N. A. 2007. Taxonomic revision of the Pliocene genus *Alca* (Aves, Alcidae): and a novel approach for assessing diversity among taxa known from isolated specimens. *Journal of Vertebrate Paleontology*, Supplement 27:148-149.
- Smith, N. A. 2008. A new species of auk from the Miocene of California reveals morphological trends related to flightlessness within Alcidae. *Journal of Vertebrate Paleontology* Supplement 28:145.
- Smith, N. A. 2011. Taxonomic revision and phylogenetic analysis of the flightless Mancallinae (Aves, Pan-Alcidae). *Zookeys* 91:1-116.
- Smith, N. A. and J. A. Clarke. *In press*. An alphataxonomic revision of extinct and extant razorbills (Aves, Alcidae): a combined morphometric and phylogenetic approach. *Ornithological Monographs* 72.
- Smith, N. A., S. L. Olson, and J. A. Clarke. 2007. First Atlantic record of the puffin *Cerorhinca* (Aves, Alcidae) from the Pliocene of North Carolina. *Journal of Vertebrate Paleontology* 27:1039-1042.
- Snyder, S. W. 2001. Benthic foraminifera and paleoecology of the Pliocene Yorktown and Chowan River Formations, Lee Creek Mine, North Carolina, USA. *Journal of Foraminiferal Research* 31:244-274.
- Sole, C. L., A. D. S. Bastos, and C. H. Scholtz. 2007. Do individual and combined data analyses of molecules and morphology reveal the generic status of '*Pachysoma*' MacLeay (Coleoptera: Scarabaeidea)? *Insect Systematics and Evolution* 38:311-330.
- Sparks J., and T. Soper. 1987. *Penguins*, 2<sup>nd</sup> ed. David and Charles, Newton Abbott and London, 246 pp.
- Spring, L. 1971. A comparison of functional and morphological adaptations in the Common Murre (*Uria aalge*) and Thick-billed Murre (*Uria lomvia*). *Condor* 73:1-27.
- Springer, A. M., A. Y. Kondratyev, H. Ogi, Y. V. Shibaev, and G. B. van Vliet. 1993. Status, ecology, and conservation of *Synthliboramphus* murrelets and auklets. pgs. 187-201 *In* The Status, Ecology, And Conservation Of Marine Birds Of The North Pacific, Vermeer, K., Briggs, K. T., Morgan, K. H., and Siegel-Causey, D (Eds.), Canadian Wildlife Service.

- Stempniewicz, L. 1994. Predator-prey interaction between Glaucous Gull *Larus hyperboreus* and Little Auk *Alle alle* in Spitsbergen. *Acta Ornithologica* 29:155-170.
- Stewart, J. R. 2002. Sea-birds from coastal and non-coastal, archaeological and “natural” Pleistocene deposits or not all unexpected deposition is of human origin. *Acta Zoologica Cracoviensia* 45:167-178.
- Stewart, J. R. 2007. The Evolutionary study of some archaeologically significant avian taxa in the Quaternary of the western palaeartic. BAR International Series 1653. Hadrian Books Ltd, Oxford.
- Storer, R. W. 1945a. Structural modifications in the hind limb in the Alcidae. *Ibis* 87:433-456.
- Storer, R. W. 1945b. The systematic position of the murrelet genus *Endomychura*. *Condor* 47:154-160.
- Storer, R. W. 1952. A comparison of variation, behavior and evolution in the sea bird genera *Uria* and *Cepphus*. University of California Publications in Zoology 52:121-222.
- Storer, R. W. 1960. Evolution in the diving birds. pgs. 694-707 in *Proceedings of the Twelfth International Ornithological Congress*. G. Bergman, K. O. Donner, and L. v. Haartman (Eds.). Tilgmannin Kirjapaino, Helsinki.
- Storer, R. W. 2001. A new Pliocene grebe from the Lee Creek deposits. *Smithsonian Contributions to Paleobiology* 90:227-231.
- Strauch, J. G. 1978. The phylogeny of the Charadriiformes (Aves): a new estimate using the method of character compatibility analysis. *Transactions of the Zoological Society of London* 34:263-345.
- Strauch, J. G. 1985. The phylogeny of the Alcidae. *Auk* 102:520-539.
- Swainson, W. 1837. On the natural history and classification of birds, v2. The Cabinet Encyclopedia. Longman, Rees, Orme, Brown, Green and Longman, London.
- Swofford, D. L. 2002. PAUP\* Phylogenetic analysis using parsimony (\*and other methods). Version 4.0, Sinauer Associates, Sunderland.
- Swofford, D. L., G. J. Olsen, P. J. Waddell, and D. M. Hillis. 1990. Phylogeny reconstruction. *Molecular Systematics* 411-501.

- Szekely, T., J. D. Reynolds, and J. Figuerola. 2000. Sexual size dimorphism in shorebirds, gulls, and alcids: the influence of sexual and natural selection. *Evolution* 54:1404-1413.
- Tan, S. S., and M. P. Kennedy. 1996. Geologic maps of the northwestern part of San Diego County, California. California Division of Mines and Geology Open File Report 96-02.
- Temminck, C. J., 1835. Manuel d'Ornithologie ou Tableau Systematique des Oiseaux qui se Trouvent en Europe, 2nd ed. v.3: i-lxxxiv, Paris, 305pp.
- Thomas, E. 1998. The biogeography of the Late Paleocene benthic foraminiferal extinction. pgs. 214-243 *in* Late Paleocene-Early Eocene Biotic and Climatic Events in the Marine and Terrestrial Records. M. P. Aubry, et al. (Eds.), Columbia University Press, New York.
- Thomas, G., M. A. Wills, and T. Szekely. 2004. Phylogeny of shorebirds, gulls and alcids (Aves: Charadrii) from the cytochrome-*b* gene: parsimony, Bayesian inference, minimum evolution and quartet puzzling. *Molecular Phylogenetics and Evolution* 30:516-526.
- Thompson, J. D., T. J. Gibson, F. Plewniak, F. Jeanmougin, and D. G. Higgins. 1997. The ClustalX windows interface: flexible strategies for multiple sequence alignment aided by quality analysis tools. *Nucleic Acids Research* 24:4876-4882.
- Thoresen, A. C. 1985. Diurnal activity and social displays of Rhinoceros Auklets on Teuri Island, Japan. *Condor* 85:373-375.
- Thorne, J. L., and H. Kishino. 2002. Divergence time and evolutionary rate estimation with multilocus data. *Systematic Biology* 51:689-702.
- Thorne, J. L., H. Kishino, and I. S. Painter. 1998. Estimating the rate of evolution of the rate of molecular evolution. *Molecular Biology and Evolution* 15:1647-1657.
- Tyrberg, T. 1998. Pleistocene Birds of the Palearctic. Publications of the Nuttall Ornithology Club 27, 720pp.
- Vedder, J. G. 1960. Previously unreported Pliocene Mollusca from the southeastern Los Angeles Basin. United States Geological Survey Professional Paper 400B:B326-B328.
- Vedder, J. G. 1972. Review of stratigraphic names and megafaunal correlation of Pliocene rocks along the southeast margin of the Los Angeles basin, California.

- pgs. 158-172 *in* Pacific Coast Miocene Biostratigraphic Symposium, E. H. Stinmeyer (Ed.). Society of Economic Paleontologists and Mineralogists.
- Verheyen, R. 1958. Contribution a la systematique des Alciformes. Bulletin de l' Institut Royal des Sciences Naturelles de Belgique 34:1-15.
- Vermeij, G. J. 1991. When biotas meet: understanding biotic interchange. *Science* 253:1099-1104.
- Versteegh, G. J. M. 1997. The onset of major northern hemisphere glaciation and their impact on dinoflagellate cysts and acritarchs from the Singa section Calabria (southern Italy) and DSDP Holes 607/607A (North Atlantic). *Marine Micropaleontology* 30:319-343.
- Via, R. K., and D. J. Thomas. 2006. Evolution of Atlantic thermohaline circulation: Early Oligocene onset of deep-water production in the north Atlantic. *Geology* 34:441-444.
- Vieillot, J. P. 1819. Nouveau Dictionnaire d'Histoire Naturelle Appliquée aux Arts (nouveau ed.) 32:157pp.
- Vigors, N. 1825. Observations on the natural affinities that connect the families of birds. *Transactions of the Linnean Society of London* 14:395-517.
- Volterra, V. 1926. Variazione e fluttuazione del numero d'individui in specie animali conviventi. *Memoirs of the Academe Nazionale Lincei Serial 6* 2:31-113.
- von den Driesch, A. 1976. A guide to the measurement of animal bones from archaeological sites. *Peabody Museum Bulletin* 1:103-129.
- Wagner, H. M., B. O. Riney, T. A. Deméré, and D. R. Prothero. 2001. Magnetic stratigraphy and land mammal biochronology of the nonmarine facies of the Pliocene San Diego Formation, San Diego County, California. pgs. 359-368 *in* Magnetic Stratigraphy of the Pacific Coast Cenozoic. Pacific Section SEPM, Book 91.
- Walsh, H. E., and V. L. Friesen. 2003. A comparison of intraspecific patterns of DNA sequence variation in mitochondrial DNA,  $\alpha$ -enolase, and MHC class II B loci in auklets (Charadriiformes: Alcidae). *Journal of Molecular Evolution* 57:681-693.
- Walsh, H. E., I. L. Jones, and V. L. Friesen. 2005. A test of founder effect speciation using multiple loci in the auklets (*Aethia* spp.). *Genetics* 171:1885-1894.

- Warheit, K. I. 1992a. The role of morphometrics and cladistics in the taxonomy of fossils: a paleornithological example. *Systematic Biology* 41:345-369.
- Warheit, K. I. 1992b. A review of the fossil seabirds from the Tertiary of the north Pacific: plate tectonics, paleoceanography, and faunal change. *Paleobiology* 18:401-424.
- Warheit, K. I. 2002. The seabird fossil record and the role of paleontology in understanding seabird community structure. pgs.17-55 *in* *Biology of Marine Birds*. E.A. Schrieber and J. Burger (Eds.). CRC Press, Boca Raton, Florida.
- Warheit, K. I., and D. R. Lindberg. 1988. Interactions between seabirds and marine mammals through time: interference competition at breeding sites. pgs. 292-328 *in* *Seabirds and Other Marine Vertebrates: competition, predation, and other interactions*. J. Burger (Ed.). Columbia University Press, New York.
- Watada, M., R. Kakizawa, N. Kuroda, and S. Utida. 1987. Genetic differentiation and phylogenetic relationships of an avian family, Alcidae (auks). *Journal of the Yamashina Institute of Ornithology* 19:79-88.
- Watanuki, Y. 2010. Climate induced phenological mismatch: an implication from a long-term monitoring study of seabirds. *Japanese Journal of Ecology* 60:1-11.
- Watanuki, Y., and A. E. Burger. 1999. Body mass and dive duration in alcids and penguins. *Canadian Journal of Zoology* 77:1838-1842.
- Watanuki, Y., Y. Nizuma, G. Gabrielsen, K. Sato, and Y. Naito. 2003. Stroke and glide of wing propelled divers: deep diving seabirds adjust surge frequency to buoyancy change with depth. *Proceedings of the Royal Society of London* 270: 483-488.
- Watanuki, Y., W. Wanless, M. Harris, J. R. Lovvorn, M. Miyazaki, H. Tanaka, and K. Sato. 2006. Swim speeds and stroke patterns in wing-propelled divers: a comparison among alcids and a penguin. *Journal of Experimental Biology* 209:1217-1230.
- Westerhold, T., T. Bickert, and U. Röhl. 2005. Middle to Late Miocene oxygen isotope stratigraphy of ODP site 1085 (SE Atlantic): new constraints on Miocene climate variability and sea-level fluctuations. *Palaeogeography, Palaeoclimatology, Palaeoecology* 217:205-222.
- Westgate, J. W. 2001. Paleoeology and biostratigraphy of marginal marine gulf coast Eocene vertebrate localities. pgs. 263-297 *in* *Eocene Biodiversity: unusual occurrences and rarely sampled habitats*. G. F. Gunnell (Ed.). Kluwer

Academic/Plenum Press, New York.

- Wetmore, A. 1926. Fossil birds from the Green River deposits of eastern Utah. *Annals of the Carnegie Museum* 16:391-402.
- Wetmore, A. 1940. Fossil bird remains from Tertiary deposits in the United States. *Journal of Morphology* 66:25-37.
- Wheeler, W. C. 1992. Extinction, sampling, and molecular phylogenetics. pgs. 205-215 *in* *Extinction and Phylogeny*. M. J. Novacek and Q. D. Wheeler (Eds.). Columbia University Press, New York.
- Whittingham, L. A., F. H. Sheldon, and S. T. Emlen, 2000. Molecular phylogeny of jacanas and biogeographical implications. *Auk* 117:22-32.
- Whitworth, D. L., J. Y. Takekawa, H. R. Carter, S. H. Newman, T. W. Keeney, and P. R. Kelly. 2000. Distribution of Xantus' Murrelet *Synthliboramphus hypoleucus* at sea in the southern California bight, 1995-97. *Ibis* 142:268-279.
- Wiens, J. J. 1998. Combining data sets with different phylogenetic histories. *Systematic Biology* 47:568-581.
- Wiens, J. J. 2003. Missing data, incomplete taxa, and phylogenetic accuracy. *Systematic Biology* 52:528.
- Wiens, J. J. 2005. Can incomplete taxa rescue phylogenetic analyses from long-branch attraction? *Systematic Biology* 54:731-742.
- Wiens, J. J. 2009. Paleontology, genomics, and combined-data phylogenetics: can molecular data improve phylogeny estimation for fossil taxa? *Systematic Biology* 58:87-99.
- Wiens, J. J., and P. T. Chippendale. 1994. Combining and weighting characters and the prior agreement approach revisited. *Systematic Biology* 43:564-566.
- Wiens, J. J., C. A. Kuczynski, T. Townsend, T. W. Reeder, D. G. Mulcahy, and J. W. Sites. 2010. Combining phylogenomics and fossils in higher-level squamate reptile phylogeny: molecular data change the placement of fossil taxa. *Systematic Biology* 59:674-688.
- Wiese, F. K., G. J. Robertson, A. J. Gaston. 2004. Impacts of chronic marine oil pollution and the murre hunt in Newfoundland on Thick-billed Murre *Uria lomvia* populations in the eastern Canadian arctic. *Biological Conservation* 116:205-216.

- Wijnker, E., and S. L. Olson. 2009. A revision of the fossil genus *Miocepphus* and other Miocene Alcidae (Aves: Charadriiformes) of the western north Atlantic Ocean. *Journal of Systematic Paleontology* 7:471-487.
- Wilkinson, M. 1995. Arbitrary resolutions, missing entries, and the problem of zero-length branches in parsimony analysis. *Systematic Biology* 44:109-111.
- Wing, S. L., G. J. Harrington, F. A. Smith, J. I. Bloch, D. M. Boyer, and K. H. Freeman. 2005. Transient floral change and rapid global warming at the Paleocene-Eocene boundary. *Science* 310:993-996.
- Wojczulanis-Jakubas, K., D. Jakubas, J. Welcker, A. M. A. Harding, N. J. Karnovsky, D. Kidawa, H. Steen, L. Stempniewicz, and C. J. Camphuysen. Body size variation of a high-Arctic seabird: the dovekie (*Alle alle*). *Polar Biology* 34:847-854.
- Woodburne, M. O., and C. C. Swisher III. 1995. Land mammal high-resolution geochronology, intercontinental overland dispersals, sea level, climate, and vicariance. Society for Sedimentary Geology (SEPM) Special Publication 54:335-364.
- Xántus de Vesey, J. 1860. Descriptions of supposed new species of birds from Cape St. Lucas, lower California. *Proceedings of the Academy of Natural Sciences of Philadelphia* 11:297-299.
- Yamamoto, Y., R. Kakizawa, and S. Yamagishi. 2005. Mitochondrial Genome Project of Endangered Birds in Japan. Hyogo College of Medicine, Department of Genetics.
- Yang, Z., and B. Rannala. 1997. Bayesian phylogenetic inference using DNA sequences: a markov chain monte carlo method. *Molecular Biology and Evolution* 14:717.
- Yang, Z., and B. Rannala. 2005. Branch-length prior influences Bayesian posterior probability of phylogeny. *Systematic Biology* 54:455-470.
- Yang, Z., and B. Rannala. 2006. Bayesian estimation of species divergence times under a molecular clock using multiple fossil calibrations with soft bounds. *Molecular Biology and Evolution* 23:212-226.
- Yen, P. P.W., W. J. Sydeman, and K. D. Hyrenbach. 2004. Marine bird and cetacean associations with bathymetric habitats and shallow-water topographies: implications for trophic transfer and conservation. *Journal of Marine Systems* 50:79-99.

- You, Y., M. Huber, D. Muller, C. J. Poulson, and J. Ribbe. 2009. Simulation of the Middle Miocene climate optimum. *Geophysical Research Letters* 36: doi:10.1029/2008GL036571.
- Zachos, J. C., G. R. Dickens, and R. E. Zeebe. 2008. An early Cenozoic perspective on greenhouse warming and carbon-cycle dynamics. *Nature* 451:279-283.
- Zachos J. C., M. Pagani, L. Sloan, E. Thomas, K. and Billups. 2001. Trends, rhythms, and aberrations in global climate 65 Ma to present. *Science* 292:686-693.
- Zachos, J. C., M. W. Wara, S. Bohaty, M. L. Delaney, M. R. Petrizzo, and A. Brill. 2003. A transient rise in tropical sea surface temperature during the Paleocene-Eocene thermal maximum. *Science* 302:1551-1554.
- Zink, R. M., J. Klicka, and B. R. Barber. 2004. The tempo of avian diversification during the Quaternary. *Philosophical Transactions of the Royal Society of London B* 359:215-220.
- Zusi, R. L., and J. R. Jehl, Jr. 1970. The systematic relationships of *Aechmorrhynchus*, *Prosobonia*, and *Phegornis* (Charadriiformes: Charadrii). *Auk* 87:760-780.
- Zwickl, D. J., and D. M. Hillis. 2002. Increased taxon sampling greatly reduces phylogenetic error. *Systematic Biology* 51:588.